

Michael R. Hughes
Kelly M. McNagny *Editors*

Mast Cells

Methods and Protocols

Second Edition

METHODS IN MOLECULAR BIOLOGY

Series Editor

John M. Walker

School of Life Sciences

University of Hertfordshire

Hatfield, Hertfordshire, AL10 9AB, UK

For further volumes:
<http://www.springer.com/series/7651>

Mast Cells

Methods and Protocols

Second Edition

Edited by

Michael R. Hughes and Kelly M. McNagny

*Department of Medical Genetics, The Biomedical Research Centre, University of British Columbia,
Vancouver, BC, Canada*

 **Humana Press**

Editors

Michael R. Hughes
Department of Medical Genetics
The Biomedical Research Centre
University of British Columbia
Vancouver, BC, Canada

Kelly M. McNagny
Department of Medical Genetics
The Biomedical Research Centre
University of British Columbia
Vancouver, BC, Canada

ISSN 1064-3745 ISSN 1940-6029 (electronic)
ISBN 978-1-4939-1567-5 ISBN 978-1-4939-1568-2 (eBook)
DOI 10.1007/978-1-4939-1568-2
Springer New York Heidelberg Dordrecht London

Library of Congress Control Number: 2014948203

© Springer Science+Business Media New York 2015

This work is subject to copyright. All rights are reserved by the Publisher, whether the whole or part of the material is concerned, specifically the rights of translation, reprinting, reuse of illustrations, recitation, broadcasting, reproduction on microfilms or in any other physical way, and transmission or information storage and retrieval, electronic adaptation, computer software, or by similar or dissimilar methodology now known or hereafter developed. Exempted from this legal reservation are brief excerpts in connection with reviews or scholarly analysis or material supplied specifically for the purpose of being entered and executed on a computer system, for exclusive use by the purchaser of the work. Duplication of this publication or parts thereof is permitted only under the provisions of the Copyright Law of the Publisher's location, in its current version, and permission for use must always be obtained from Springer. Permissions for use may be obtained through RightsLink at the Copyright Clearance Center. Violations are liable to prosecution under the respective Copyright Law.

The use of general descriptive names, registered names, trademarks, service marks, etc. in this publication does not imply, even in the absence of a specific statement, that such names are exempt from the relevant protective laws and regulations and therefore free for general use.

While the advice and information in this book are believed to be true and accurate at the date of publication, neither the authors nor the editors nor the publisher can accept any legal responsibility for any errors or omissions that may be made. The publisher makes no warranty, express or implied, with respect to the material contained herein.

Printed on acid-free paper

Humana Press is a brand of Springer
Springer is part of Springer Science+Business Media (www.springer.com)

Dedication

I would like to dedicate this book to my mother in memory of her love and courage.

Michael R. Hughes

Preface

In selecting the topics for this latest edition of *Mast Cells: Methods and Protocols* we quickly realized that the previous edition editors, Drs. Guha Krishnaswamy and David S. Chi, had established an exceptionally high standard in their 2006 edition (Vol. 315). Their edition remains a vibrant, valuable, and highly relevant compendium of essential mast cell methods and techniques with little need for modification. For that reason, we encourage readers to add this newest addition to their undoubtedly well-worn first edition. We consider this volume to be an *extension*, rather than a replacement, of their excellent first edition and have deliberately attempted to avoid duplication of their earlier work.

In the current edition we have invited some of the top investigators in mast cell biology to share their latest techniques, methods, and opinions. Importantly, we also asked for the authors to share their tips, tricks, and details that are often omitted in the materials and methods sections of original publications. Many of the participating authors herein present techniques and methods that take advantage of the technical innovations in primary cell isolation and analysis, the commercial availability of specialty reagents for immunobiology research, and the proliferation of transgenic animal strains and increasingly sophisticated animal models of human disease. Although the ethical debate of expanding the use of experimental animals is frequently contentious we feel the data gleaned from the behavior of mast cells *in situ* provide insights that are unattainable from studying cells *in vitro*. In addition, the accessibility of methods for the isolation of primary cells from ever-smaller quantities of tissue (human, rodent and other) permits more data to be obtained from fewer animals. Taken together, these innovations and the proliferation of specialty reagents are serving to expand the breadth and quality of information researchers can collect from each experiment. The challenge of so much information then becomes deciding which data are biologically relevant and assembling the relevant data into an explanatory model.

Mast Cells: Methods and Protocols follows the popular format of the *Methods in Molecular Biology* series by providing step-by-step instructions to the reader that can be directly applied or easily adapted to the design of their own experiments. In addition, we have solicited a broad selection of reviews that cover topics of interest to mast cell neophytes and *cognoscenti* alike. *Part I* consists of reviews aimed at the history of developments in the mast cell field, the phylogenetic profile of mast cells and their developmental ontology. In addition, Part I provides methods for the enumeration of tissue mast cells and isolation of mature mast cells and mast cell progenitors from mammalian tissues including lung, intestine, and peripheral blood. New to this edition, we are very pleased to include a chapter on the versatile and powerful *Danio rerio* (zebrafish) model in the study of mast cell development and function. In *Part II*, we present chapters covering the functions of mast cells in human health and disease and methods for the isolation, derivation, and activation of mast cells from primary human tissue. Methods for the investigation of the molecular mechanisms of mast cell activation and their effector functions are provided in *Part III*. Assays for the detection and analysis of mast cell secretory and cell surface phenotype and mast cell activation state (including high-throughput approaches) are presented in *Part IV*. The concluding and largest section of this volume, *Part V*, is dedicated to experimental mouse

models of disease that have been deemed useful for the assessment of mast cell functions in the regulation of innate and adaptive immune response in cancer, tissue fibrosis, auto-inflammation, and allergic disease. Clearly there are many more methods that merit inclusion in this volume and many additional experts in mast cell biology that we, regrettably, have not been able to include in this text. We therefore encourage the readers to view this volume as a “sampler” of useful methods and techniques and we hope that those experienced and new to the field will find this volume to be a well-rounded cross section of useful approaches in the study of mast cell biology.

Finally, we are very grateful to all authors who participated in this volume for sharing their methods, ideas, and scientific insights and generously giving their valuable time to this effort. We also wish to thank Humana Press and the Series Editor, Dr. John Walker, for the invitation to participate in this project as editors and for their patience awaiting the completed work. Finally, we greatly appreciate the helpful advice and encouragement of Dr. Guha Krishnaswamy, editor of the first edition, who graciously provides the introductory chapter for this volume.

Vancouver, BC, Canada

*Michael R. Hughes
Kelly M. McNagny*

Contents

<i>Preface</i>	<i>vii</i>
<i>Contributors</i>	<i>xiii</i>

PART I ONTOLOGY, PHYLOGENY, AND TISSUE DISTRIBUTION OF MAST CELLS

1 Paul Ehrlich's Mastzellen: A Historical Perspective of Relevant Developments in Mast Cell Biology	3 <i>Jack Ghaby, Hana Saleh, Harsha Vyas, Emma Peiris, Niva Misra, and Guha Krishnaswamy</i>
2 The Phylogenetic Profile of Mast Cells	11 <i>Enrico Crivellato, Luciana Travan, and Domenico Ribatti</i>
3 Mast Cell Development and Function in the Zebrafish	29 <i>Sabar I Da'as, Tugce B. Balci, and Jason N. Berman</i>
4 Human Mast Cell and Basophil/Eosinophil Progenitors	59 <i>Gail M. Gauvreau and Judah A. Denburg</i>
5 Methods for the Study of Mast Cell Recruitment and Accumulation in Different Tissues	69 <i>Tatiana G. Jones and Michael F. Gurish</i>
6 Notch2 Signaling in Mast Cell Development and Distribution in the Intestine	79 <i>Mamiko Sakata-Yanagimoto and Shigeru Chiba</i>

PART II MAST CELLS IN HUMAN HEALTH AND DISEASE

7 Mast Cells in Human Health and Disease	93 <i>Erin J. DeBruin, Matthew Gold, Bernard C. Lo, Kimberly Snyder, Alissa Cai, Nikola Lasic, Martin Lopez, Kelly M. McNagny, and Michael R. Hughes</i>
8 The Emerging Prominence of the Cardiac Mast Cell as a Potent Mediator of Adverse Myocardial Remodeling	121 <i>Joseph S. Janicki, Gregory L. Brower, and Scott P. Levick</i>
9 The Parasympathetic Nervous System as a Regulator of Mast Cell Function	141 <i>Paul Forsythe</i>
10 Growth of Human Mast Cells from Bone Marrow and Peripheral Blood-Derived CD34 ⁺ Pluripotent Hematopoietic Cells	155 <i>Geethani Bandara, Dean D. Metcalfe, and Arnold S. Kirshenbaum</i>
11 Isolation and Characterization of Human Intestinal Mast Cells	163 <i>Axel Lorentz, Gernot Sellge, and Stephan C. Bischoff</i>

12 Human Mast Cell Activation with Viruses and Pathogen Products 179
Ian D. Haidl and Jean S. Marshall

PART III MOLECULAR MECHANISMS OF MAST CELL FUNCTION

13 Basic Techniques to Study Fc ϵ RI Signaling in Mast Cells 205
Yuko Kawakami and Toshiaki Kawakami

14 Membrane-Cytoskeleton Dynamics in the Course of Mast Cell Activation 219
Pavel Dráber and Petr Dráber

15 Fc ϵ RI Expression and Dynamics on Mast Cells 239
Eon J. Rios and Janet Kalesnikoff

16 Regulation of Mast Cell Survival and Apoptosis 257
Christine Möller Westerberg, Maria Ekoff, and Gunnar Nilsson

17 Protein Tyrosine Phosphatases in Mast Cell Signaling 269
Alexander Geldman and Catherine J. Pallen

18 MicroRNA Function in Mast Cell Biology: Protocols to Characterize and Modulate MicroRNA Expression 287
Steven Maltby, Maximilian Plank, Catherine Ptaschinski, Joerg Mattes, and Paul S. Foster

PART IV MAST CELL PRODUCTS AND MEDIATORS

19 Assay of Mast Cell Mediators 307
Madeleine Rådinger, Bettina M. Jensen, Emily Swindle, and Alasdair M. Gilfillan

20 Induction of Mast Cell Apoptosis by a Novel Secretory Granule-Mediated Pathway 325
Fabio R. Melo, Sara Wernersson, and Gunnar Pejler

21 Measurement of Nitric Oxide in Mast Cells with the Fluorescent Indicator DAF-FM Diacetate 339
Chris D. St. Laurent, Tae Chul Moon, and A. Dean Befus

22 Real-Time Imaging of Ca $^{2+}$ Mobilization and Degranulation in Mast Cells 347
Roy Cohen, David A. Holowka, and Barbara A. Baird

23 Flow Cytometry-Based Monitoring of Mast Cell Activation 365
Glenn Cruse, Alasdair M. Gilfillan, and Daniel Smrz

24 Measurement of Mast Cell Surface Molecules by High-Throughput Immunophenotyping Using Transcription (HIT) 381
D. James Haddon, Justin A. Jarrell, Michael R. Hughes, Kimberly Snyder, Kelly M. McNagny, Michael G. Kattab, and Paul J. Utz

PART V MOUSE MODELS OF DISEASE TO STUDY MAST CELL FUNCTION

25 Cre/loxP-Based Mouse Models of Mast Cell Deficiency and Mast Cell-Specific Gene Inactivation 403
Katrin Peschke, Anne Dudeck, Anja Rabenhorst, Karin Hartmann, and Axel Roers

26	Evaluation of Synovial Mast Cell Functions in Autoimmune Arthritis	423
	<i>Peter A. Nigrovic and Kichul Shin</i>	
27	Methods for the Study of Mast Cells in Cancer	443
	<i>Nichole R. Blatner, FuNien Tsai, and Khashayarsha Khazaie</i>	
28	Studying Mast Cells in Peripheral Tolerance by Using a Skin Transplantation Model	461
	<i>Victor C. de Vries, Isabelle Le Mercier, Elizabeth C. Nowak, and Randolph J. Noelle</i>	
29	The Function of Mast Cells in Autoimmune Glomerulonephritis	487
	<i>Renato C. Monteiro, Walid Beghdadi, Lydia Celia Madjene, Maguelonne Pons, Michel Peuchmaur, and Ulrich Blank</i>	
30	A Mouse Model of Atopic Dermatitis	497
	<i>Yuko Kawakami and Toshiaki Kawakami</i>	
31	Mouse Models of Allergic Asthma	503
	<i>Matthew Gold, David Marsolais, and Marie-Renee Blanchet</i>	
32	Methods in Assessment of Airway Reactivity in Mice	521
	<i>Matthew Gold and Marie-Renee Blanchet</i>	
	<i>Index</i>	529

Contributors

BARBARA A. BAIRD • *Department of Chemistry and Chemical Biology, Cornell University, Ithaca, NY, USA*

TUGCE B. BALCI • *IWK Health Centre, Dalhousie University, Halifax, NS, Canada; Department of Medical Genetics, University of Ottawa, Ottawa, ON, Canada*

GEETHANI BANDARA • *Laboratory of Allergic Diseases, Mast Cell Biology Section, NIH/National Institute of Allergy and Infectious Diseases, Bethesda, MD, USA*

A. DEAN BEFUS • *Pulmonary Research Group, Department of Medicine, University of Alberta, Edmonton, AB, Canada*

WALID BEGHDADI • *Faculté de Médecine, Université Paris-Diderot, Inserm UMRS-699 et Sorbonne Paris Cite, Paris, France*

JASON N. BERMAN • *IWK Health Centre, Dalhousie University, Halifax, NS, Canada*

STEPHAN C. BISCHOFF • *Department of Nutritional Medicine, University of Hohenheim, Stuttgart, Germany*

MARIE-RENÉE BLANCHET • *Centre de Recherche, Institut Universitaire de Cardiologie et de Pneumologie de Québec, Québec City, QC, Canada*

ULRICH BLANK • *Faculté de Médecine, Université Paris-Diderot, Paris, France*

NICHOLE R. BLATNER • *Robert H. Lurie Comprehensive Cancer Center, Northwestern University, Chicago, IL, USA*

GREGORY L. BROWER • *Department of Cell Biology and Anatomy, School of Medicine, University of South Carolina, Columbia, SC, USA*

ALISSA CAIT • *Department of Microbiology and Immunology, The University of British Columbia, Vancouver, BC, Canada*

SHIGERU CHIBA • *Department of Hematology, University of Tsukuba, Tsukuba, Ibaraki, Japan*

ROY COHEN • *Baker Institute for Animal Health, Cornell University College of Veterinary Medicine, Ithaca, NY, USA*

ENRICO CRIVELLATO • *Section of Anatomy, Department of Experimental and Clinical Medicine, University of Udine Medical School, Udine, Italy*

GLENN CRUSE • *Laboratory of Allergic Diseases, National Institute of Allergy and Infectious Diseases, National Institutes of Health, Bethesda, MD, USA*

SAHAR I. DA'AS • *IWK Health Centre, Dalhousie University, Halifax, NS, Canada*

VICTOR C. DE VRIES • *Laboratory of Allergy and Inflammation, Singapore Immunology Network (SIgN), Agency for Science, Technology and Research (A*STAR), Singapore, Singapore*

ERIN J. DEBRUIN • *Department of Experimental Medicine, The Biomedical Research Centre, The University of British Columbia, Vancouver, BC, Canada*

JUDAH A. DENBURG • *McMaster University, Hamilton, ON, Canada*

PAVEL DRÁBER • *Laboratory of Biology of Cytoskeleton, Institute of Molecular Genetics, Academy of Sciences of the Czech Republic, v.v.i., Prague, Czech Republic*

PETR DRÁBER • *Laboratory of Signal Transduction, Institute of Molecular Genetics, Academy of Sciences of the Czech Republic, v.v.i., Prague, Czech Republic*

ANNE DUDECK • *Medical Faculty "Carl-Gustav Carus", Institute for Immunology, Technische Universität Dresden, Dresden, Germany*

MARIA EKOFF • *Clinical Immunology and Allergy Unit, Department of Medicine, Karolinska Institutet, Stockholm, Sweden*

PAUL FORSYTHE • *Department of Medicine, The Brain-Body Institute, St. Joseph's Healthcare, McMaster University, Hamilton, ON, Canada*

PAUL S. FOSTER • *Priority Research Centre for Asthma and Respiratory Diseases, School of Biomedical Sciences and Pharmacy, Faculty of Health, University of Newcastle, NSW, Australia; Hunter Medical Research Institute, NSW, Australia*

GAIL M. GAUVREAU • *McMaster University, Hamilton, ON, Canada*

JACK GHABLY • *Division of Allergy, Asthma and Clinical Immunology, Department of Internal Medicine, East Tennessee State University, Johnson City, TN, USA; James H. Quillen VA Medical Center and Quillen College of Medicine, East Tennessee State University, Johnson City, TN, USA*

ALEXANDER GELDMAN • *Department of Medicine, Child and Family Research Institute, University of British Columbia, Vancouver, BC, Canada*

ALASDAIR M. GILFILLAN • *Laboratory of Allergic Diseases, National Institute of Allergy and Infectious Diseases, National Institutes of Health, Bethesda, MD, USA*

MATTHEW GOLD • *Department of Experimental Medicine, The Biomedical Research Centre, The University of British Columbia, Vancouver, BC, Canada*

MICHAEL F. GURISH • *Division of Rheumatology, Immunology, and Allergy, Department of Medicine, Brigham and Women's Hospital, Harvard Medical School, Boston, MA, USA*

D. JAMES HADDON • *Division of Immunology and Rheumatology, Stanford University School of Medicine, Stanford, CA, USA*

IAN D. HAIDL • *Dalhousie Inflammation Group, Department of Microbiology and Immunology, Dalhousie University, Halifax, NS, Canada*

KARIN HARTMANN • *Department of Dermatology, University of Cologne, Cologne, Germany*

DAVID HOLOWKA • *Department of Chemistry and Chemical Biology, Cornell University, Ithaca, NY, USA*

MICHAEL R. HUGHES • *Department of Medical Genetics, The Biomedical Research Centre, The University of British Columbia, Vancouver, BC, Canada*

JOSEPH S. JANICKI • *Department of Cell Biology and Anatomy, School of Medicine, University of South Carolina, Columbia, SC, USA*

JUSTIN A. JARRELL • *Division of Immunology and Rheumatology, Stanford University School of Medicine, Stanford, CA, USA*

BETTINA M. JENSEN • *Allergy Clinic, Copenhagen University Hospital, Gentofte, Denmark*

TATIANA G. JONES • *Division of Rheumatology, Immunology, and Allergy, Department of Medicine, Brigham and Women's Hospital, Harvard Medical School, Boston, MA, USA*

JANET KALESNIKOFF • *Department of Epithelial Biology, Stanford University, Palo Alto, CA, USA; Department of Pathology, Stanford Cardiovascular Institute, Stanford, CA, USA*

MICHAEL G. KATTAH • *Division of Gastroenterology, Department of Medicine, University of California San Francisco, San Francisco, CA, USA*

TOSHIAKI KAWAKAMI • *Division of Cell Biology, La Jolla Institute for Allergy and Immunology, San Diego, CA, USA*

YUKO KAWAKAMI • *Division of Cell Biology, La Jolla Institute for Allergy and Immunology, San Diego, CA, USA*

KHASHAYARSHA KHAZAEI • *Departments of Immunology and Surgery, Mayo Clinic College of Medicine, Mayo Clinic, Rochester, MN, USA*

ARNOLD S. KIRSHENBAUM • *Laboratory of Allergic Diseases, Mast Cell Biology Section, NIH/National Institute of Allergy and Infectious Diseases, Bethesda, MD, USA*

GUHA KRISHNASWAMY • *Pulmonary, Critical Care, Allergic and Immunological Diseases, Department of Medicine, Wake Baptist Medical Center and Brenner Childrens Hospital and Wake Forrest University, Bottom of Form, Inston-Salem, NC, USA*

CHRIS D. ST. LAURENT • *Pulmonary Research Group, Department of Medicine, University of Alberta, Edmonton, AB, Canada*

NIKOLA LASIC • *Department of Medical Genetics, The Biomedical Research Centre, The University of British Columbia, Vancouver, BC, Canada*

SCOTT P. LEVICK • *Department of Pharmacology and Toxicology and the Cardiovascular Center, Medical College of Wisconsin, Milwaukee, WI, USA*

BERNARD C. LO • *Department of Experimental Medicine, The Biomedical Research Centre, The University of British Columbia, Vancouver, BC, Canada*

MARTIN LOPEZ • *Department of Medical Genetics, The Biomedical Research Centre, The University of British Columbia, Vancouver, BC, Canada*

AXEL LORENTZ • *Department of Nutritional Medicine, University of Hohenheim, Stuttgart, Germany*

LYDIA CELIA MADJENE • *Faculté de Médecine, Université Paris-Diderot, Inserm UMRS-699 et Sorbonne Paris Cite, Paris, France*

STEVEN MALTBY • *Priority Research Centre for Asthma and Respiratory Diseases, School of Biomedical Sciences and Pharmacy, Faculty of Health, University of Newcastle, NSW, Australia; Hunter Medical Research Institute, NSW, Australia*

JEAN S. MARSHALL • *Dalhousie Inflammation Group, Department of Microbiology and Immunology, Dalhousie University, Halifax, NS, Canada*

DAVID MARSOLAIS • *Centre de Recherche, Institut Universitaire de Cardiologie et de Pneumologie de Québec, Québec City, QC, Canada*

JOERG MATTES • *Priority Research Centre for Asthma and Respiratory Diseases, School of Biomedical Sciences and Pharmacy, Faculty of Health, University of Newcastle, NSW, Australia*

KELLY M. McNAGNY • *Department of Medical Genetics, The Biomedical Research Centre, The University of British Columbia, Vancouver, BC, Canada*

FABIO R. MELO • *Department of Anatomy, Physiology and Biochemistry, Swedish University of Agricultural Sciences, Uppsala, Sweden*

ISABELLE LE MERCIER • *Department of Microbiology and Immunology, Dartmouth Medical School and Norris Cotton Cancer Center, Lebanon, NH, USA*

DEAN D. METCALFE • *Laboratory of Allergic Diseases, Mast Cell Biology Section, NIH/National Institute of Allergy and Infectious Diseases, Bethesda, MD, USA*

NIVA MISRA • *Division of Allergy, Asthma and Clinical Immunology, Department of Internal Medicine, East Tennessee State University, Johnson City, TN, USA; James H. Quillen VA Medical Center and Quillen College of Medicine, East Tennessee State University, Johnson City, TN, USA*

RENATO C. MONTEIRO • *Faculté de Médecine, Université Paris-DiderotInserm, UMRS-699 et Sorbonne Paris Cite, Paris, France*

TAE CHUL MOON • *Pulmonary Research Group, Department of Medicine, University of Alberta, Edmonton, AB, Canada*

PETER A. NIGROVIC • *Division of Rheumatology, Immunology and Allergy, Brigham and Women's Hospital, Boston, MA, USA; Division of Immunology, Boston Children's Hospital, Boston, MA, USA*

GUNNAR NILSSON • *Clinical Immunology and Allergy Unit, Department of Medicine, Karolinska Institutet, Stockholm, Sweden*

RANDOLPH J. NOELLE • *Department of Microbiology and Immunology, Dartmouth Medical School and Norris Cotton Cancer Center, Lebanon, NH, USA; King's Health Partners, Medical Research Council (MRC) Centre of Transplantation, King's College London, Guy's Hospital, London, UK; Norris Cotton Cancer Center, Lebanon, NH, USA*

ELIZABETH C. NOWAK • *Department of Microbiology and Immunology, Dartmouth Medical School and Norris Cotton Cancer Center, Lebanon, NH, USA*

CATHERINE J. PALLEN • *Departments of Pediatrics, Child and Family Research Institute, University of British Columbia, Vancouver, BC, Canada*

EMMA PEIRIS • *Division of Allergy, Asthma and Clinical Immunology, Department of Internal Medicine, East Tennessee State University, Johnson City, TN, USA; James H. Quillen VA Medical Center and Quillen College of Medicine, East Tennessee State University, Johnson City, TN, USA*

GUNNAR PEJLER • *Department of Anatomy, Physiology and Biochemistry, Swedish University of Agricultural Sciences, Uppsala, Sweden*

KATRIN PESCHKE • *Medical Faculty "Carl-Gustav Carus", Institute for Immunology, Technische Universität Dresden, Dresden, Germany*

MICHEL PEUCHMAUR • *Faculté de Médecine, Service de Pathologie, Hôpital Robert Debré, Sorbonne Paris Cité et APHP, Université Paris-Diderot, Paris, France*

MAXIMILIAN PLANK • *Priority Research Centre for Asthma and Respiratory Diseases, School of Biomedical Sciences and Pharmacy, Faculty of Health, University of Newcastle, NSW, Australia*

MAGUELONNE PONS • *Faculté de Médecine, Université Paris-Diderot, Inserm UMRS-699 et Sorbonne Paris Cité, Paris, France*

CATHERINE PTASCHINSKI • *Department of Pathology, University of Michigan, Ann Arbor, MI, USA*

ANJA RABENHORST • *Department of Dermatology, University of Cologne, Cologne, Germany*

MADELEINE RÄDINGER • *Krefting Research Centre, The Sahlgrenska Academy, University of Gothenburg, Gothenburg, Sweden*

DOMENICO RIBATTI • *Department of Basic Medical Sciences, Neurosciences and Sensory Organs, University of Bari Medical School, National Cancer Institute "Giovanni Paolo II", Bari, Italy*

EON J. RIOS • *Department of Epithelial Biology, Stanford University, Palo Alto, CA, USA*

AXEL ROERS • *Medical Faculty "Carl-Gustav Carus", Institute for Immunology, Technische Universität Dresden, Dresden, Germany*

MAMIKO SAKATA-YANAGIMOTO • *Department of Hematology, University of Tsukuba, Tsukuba, Ibaraki, Japan*

HANA SALEH • *Division of Clinical Immunology, Department of Internal Medicine, University of Iowa Hospitals and Clinic, Iowa City, IA, USA*

GERNOT SELLGE • *Department of Medicine III, University hospital (UKA), University of Aachen (RWTH), Aachen, Germany*

KICHUL SHIN • *Division of Rheumatology, SMG-SNU Borame Medical Center, Seoul, South Korea*

DANIEL SMRZ • *Laboratory of Allergic Diseases, National Institute of Allergy and Infectious Diseases, National Institutes of Health, Bethesda, MD, USA; Institute of Immunology, 2nd Faculty of Medicine and University Hospital Motol, Charles University in Prague, Czech Republic, EU*

KIMBERLY SNYDER • *Department of Experimental Medicine, The Biomedical Research Centre, The University of British Columbia, Vancouver, BC, Canada*

EMILY SWINDELL • *Faculty of Medicine, Academic Unit of Clinical and Experimental Sciences, University of Southampton, Southampton, UK*

LUCIANA TRAVAN • *Section of Anatomy, Department of Experimental and Clinical Medicine, University of Udine Medical School, Udine, Italy*

FUNIEN TSAI • *Robert H. Lurie Comprehensive Cancer Center, Northwestern University, Chicago, IL, USA*

PAUL J. UTZ • *Division of Immunology and Rheumatology, Stanford University School of Medicine, Stanford, CA, USA*

HARSHA VYAS • *Hematology and Medical Oncology, Georgia Regents University, Medical College of Georgia, Augusta, GA, USA; Hematology and Medical Oncology, Cancer Center of Middle Georgia LLC, Dublin, GA, USA*

SARA WERNERSSON • *Department of Anatomy, Physiology and Biochemistry, Swedish University of Agricultural Sciences, Uppsala, Sweden*

CHRISTINE MÖLLER WESTERBERG • *Clinical Immunology and Allergy Unit, Department of Medicine, Karolinska Institutet, Stockholm, Sweden*

Part I

Ontology, Phylogeny, and Tissue Distribution of Mast Cells

Chapter 1

Paul Ehrlich's Mastzellen: A Historical Perspective of Relevant Developments in Mast Cell Biology

Jack Ghably, Hana Saleh, Harsha Vyas, Emma Peiris, Niva Misra, and Guha Krishnaswamy

Abstract

Following the discovery of mast cells (or mastzellen) by the prolific physician researcher, Paul Ehrlich, many advances have improved our understanding of these cells and their fascinating biology. The discovery of immunoglobulin E and receptors for IgE and IgG on mast cells heralded further *in vivo* and *in vitro* studies, using molecular technologies and gene knockout models. Mast cells express an array of inflammatory mediators including tryptase, histamine, cytokines, chemokines, and growth factors. They play a role in many varying disease states, from atopic diseases, parasitic infections, hematological malignancies, and arthritis to osteoporosis. This review will attempt to summarize salient evolving areas in mast cell research over the last few centuries that have led to our current understanding of this pivotal multifunctional cell.

Key words Mast cells, Immunoglobulin E, Cytokine, Gene expression, Host defense, Inflammation, History

1 Ehrlich's "Mastzellen"

Paul Ehrlich (Fig. 1) is credited with the initial discovery of mast cells (Fig. 2) as we know them today. He was born near Breslau, now called Wroclaw Poland, in 1854. He studied to become a medical doctor at the university there and attended universities in Strasbourg, Freiburg, and Leipzig [1]. Ehrlich was greatly influenced by his cousin Karl Weigert, an eminent histopathologist who pioneered the use of aniline dyes for staining bacteria and tissue sections [1]. Weigert had a strong and positive influence throughout Ehrlich's life [2]. As a result, even as a medical student, Ehrlich had an extensive knowledge of structural organic chemistry and a

I would like to dedicate this chapter to my father, Dr. Narayanaswamy Krishnaswamy, M.B.B.S., an immunologist and clinician extraordinaire, who encouraged me to enter academic medicine and who continues to inspire me with his clinical acumen, his wide-armed compassion, and his practical yet gentle wisdom. By Guha Krishnaswamy, M.D.



Fig. 1 Picture of Paul Ehrlich from the Nobel Archives. *Source:* © Nobelstiftelsen

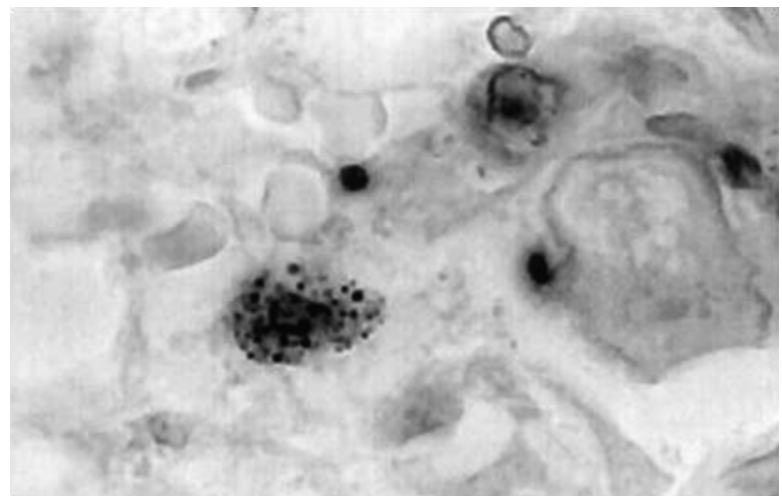


Fig. 2 Mast cell in atherosomatous plaque (Courtesy Dr. George Youngberg, M.D., East Tennessee State University)

fascination for dyes as probes of cellular structure [2]. He was quite excited by the idea that organic chemicals can have differential and specific reactions with various tissues and bacteria.

On June 17, 1878, Paul Ehrlich, a 24-year-old medical student at the time, presented his doctoral thesis “Contributions to the theory and practice of histological staining” to the Medical Faculty of Leipzig. The medical student divided his thesis into two halves. In the first part he talked about the chemical basis of many important histological reactions, while in the second he presented a detailed discussion about aniline dyes [1]. The first description of the mast cell comes in the portion of the thesis dedicated to the histological applications of the aniline dyes. He presented his point of view that

“aniline dyes displayed an absolutely characteristic behavior towards protoplasmic deposits of certain cells” which he referred to as “mastzellen,” now known as mast cells. He sought to distinguish these cells from “plasmazellen” cells previously described by Waldeyer [1].

Ehrlich said that these anilophilic cells from, the descriptive point of view, should be most conveniently described as “granular cells of the connective tissue.” From a physiological standpoint, these cells, according to Ehrlich, might represent a “further development of the fixed cells of the connective tissue.” To support his theory, Ehrlich explained that aniline-reactive cells indeed “have a tendency to collect around developing preformed structures in the connective tissue.” He also stated that “granular cells are characterized by an ‘undetermined chemical substance’ in the protoplasm with which the aniline dye reacts to give a typical metachromasia” [1]. To this day, although by no means absolute, mast cells are recognized by the presence of metachromatic granules when fixed and stained with toluidine blue.

Further in his dissertation, Ehrlich provided an accurate description of the microscopic features of mast cells. He described that the typical aspect of these “granular cells” is mostly unstained protoplasm filled with numerous granules of varying size with a nucleus not stainable even in samples that otherwise displayed beautiful nuclear staining. He strived to classify these cells using specific histochemical reactions rather than histology, a forward-looking concept for his time.

A historically interesting aspect is why Ehrlich decided to call these cells the “mastzellen” or mast cell as these were plump-appearing cells (well-fed cells). The name for these new cells was probably derived from the Greek “mast” (or breast) or the German “mastung” (masticate). In today’s research, mast cells are being increasingly recognized for their role in connective tissue remodeling and repair [1]. We now know that their granules contain many proteases and cytokines that are known to exert far-reaching effects on other cell types like the smooth muscle, fibroblasts, and endothelial cells.

Ehrlich also recognized that mast cells sometimes localize far from the blood vessels and express a series of biological functions not related to vascular functions. He also noted that these cells could be found around developing tissues. The close relationship between mast cell and tumor growth stems from this very same idea. Unfortunately, the original text of this remarkable work was destroyed in an air raid on Leipzig in 1943. In the same year, Ehrlich moved to the Charité Hospital in Berlin, where he continued his work and wrote an influential thesis on the oxygen requirement of cells. In January of 1879, the Physiological Society of Berlin reviewed the remarkable paper by Paul Ehrlich wherein he first described the mast cells that he had discovered as a medical student several years earlier. Ehrlich, in these papers, pointed out that mast cells exhibit a great avidity to basic dyes and characteristically altered the shade of the dye [1].

In 1891 along with Westphal, one of his pupils, Ehrlich showed another characteristic feature of mast cell granules in many species, namely their water solubility. Almost 50 years later, Michels wrote that “uncounted pages of useless and misleading research have been a result of failure on the part of many investigators to heed admonition originally given by Ehrlich and Westphal that mast cell granules are soluble in water and that to preserve them, tissues must be fixed in 50 % alcohol and stained in alcoholic thionine [1].”

Ehrlich then studied the special affinity of leucocytes for various dyes. In 1891, he had discovered basophilic granular cells in blood from a patient with myeloid leukemia and was quick to infer with his characteristic insight that, in higher species especially humans, the mast cells are actually leucocytes arising from precursor cells in the bone marrow. He believed that there were two types of mast cells: the first is often located in connective tissue and the second, of bone marrow origin, localized in the peripheral blood. In 1900, Jolly had established the bone marrow origin for the mast cells. Hence, by the time his textbook (Die Anaemie by Ehrlich and Lazarus, 1898) was revised in 1909, human mast cell origins were better understood. It is now accepted that mast cells arise from a pluripotent cell in the bone marrow that expresses CD34, *c-kit*, and CD13.

Ehrlich also led the way in observing mast cells in two pathological situations of utmost importance—chronic inflammation and neoplasia. He felt that in both of these situations, the tissue was “over nourished” due to lymph stasis, and hence, there was an accumulation of tissue fluid rich in nutriments. This led the mast cells to convert some of this abundant extracellular fluid to specific intracellular granules [1]. Thus, according to Ehrlich, mast cells served as an “indices for the nutritional status of the connective tissue,” whose activity increased and decreased during periods of hypernutrition and starvation. Ehrlich and his pupil Westphal found that mast cells accumulated in many tumors, more in the periphery of carcinomatous tumors than the substance of the tumor. Besides the discovery of the mast cell, Ehrlich made pioneering contributions to the method of staining the bacillus that causes tuberculosis, to the development of a therapeutic antiserum against diphtheria, and to the concepts of antibodies and chemotherapy. Some typical features of Paul Ehrlich’s colorful personality included his habits of smoking 25 cigars a day, carrying around a pocketful of colored precisely sharpened pencils with which he would write daily instructions to his research team, and his exceptional clinical knowledge and acumen. On the 150th anniversary of his birth, we cannot help but admire the invaluable contribution he made to the science of immunology.

A chronology of developments in mast cell and immediate hypersensitivity research is provided below (Table 1). This includes Paul

Ehrlich's initial description, culminating in immunological, molecular, and genomic technologies that have accelerated our understanding of the mechanisms underlying immediate hypersensitivity and relevant mast cell biology in diverse inflammatory processes.

Table 1
Chronology of developments in immediate hypersensitivity and relevant mast cell research

Year(s)	Major development in the understanding of mast cell biology
3300–3640 (BCE)	Allergic reaction to bee sting in a pharaoh is documented historically
1878	Paul Ehrlich describes mast cells in his doctoral thesis at the University of Leipzig and coins the term “mastzellen” derived from German word “mast” (breast) [1]
1879	Paul Ehrlich describes metachromasia [1]
1891	Water solubility of mast cells demonstrated by Paul Ehrlich [1]
1891	Description of cells with basophilic granules in leukemia by Paul Ehrlich [1]
1898	Paul Ehrlich describes two types of cells with basophilic granules. One localized to tissue (tissue mast cells) and another derived from bone marrow and localized to blood (blood mast cell, basophil, mast leukocyte) [1]
1900	Demonstration of bone marrow origin of mast cells by Jolly [1]
1900	Paul Ehrlich describes antibody formation theory [1]
1902	Description of “anaphylaxis” is made by Paul Portier and Charles Richet [3]
1906	The term “allergy” is coined by Clemens von Pirquet
1907	Histamine is synthesized by Windaus and Vogt [4]
1908	Paul Ehrlich receives the Nobel Prize in Physiology or Medicine along with Ilya Ilyich Mechnikov for discoveries in immunology
1910	Physiological functions of histamine described by Dale and Laidlaw [4]
1913	Nobel Prize awarded to Charles Richet for discovery of “anaphylaxis” [3, 5–7]
1913	Schultz and Dale describe smooth muscle contraction in sensitized animals; Schultz used intestinal muscle, while Dale used uterine muscle of guinea pigs [8–10]
1921	Description of passive transfer of hypersensitivity with serum by Prausnitz, popularly known as the Prausnitz-Kustner reaction (P-K reaction) [11–13]
1948	Description of passive cutaneous anaphylaxis (PCA) by Ovary [10]
1952	Discovery of “histamine” in mast cells by James Riley and Geoffrey West [14]
1961	Ovary demonstrates the release of slow-reacting substance of anaphylaxis (SRS-A) from mast cells when activated by allergen [10]
1961	Mast cells identified in the bronchial tissue in asthma
1973	Putative receptor on mast cells for IgE recognized [15]

(continued)

Table 1
(continued)

Year(s)	Major development in the understanding of mast cell biology
1979	Slow-reacting substance of anaphylaxis (SRS-A) identified in mast cells as a “leukotriene” [16]
1988	Sir James Black awarded the Nobel Prize for the discovery of histamine (H2) receptor antagonist [17]
1967	Kimishige Ishizaka recognizes immunoglobulin E as reaginic antibody [18, 19]
1985	Susumu Tonegawa receives the Nobel Prize for identification of immunoglobulin genes [20–22]
1989	Plaut and Paul show mast cells are capable of secreting multiple lymphokines [23]
1989	Cloning of canine mast cell tryptase is reported [24]
1990	Cloning of human mast cell tryptase is reported [25]
1990	Steel locus kit ligand (KL) is identified as ligand for <i>c-kit</i> and reported to be involved in mast cell proliferation [26, 27]
1990	Cloning of canine mast cell chymase is reported [28]
1991	Cloning of human mast cell chymase is reported [29]
1994	Ability of mast cells to phagocytose bacteria is shown [30]
1994	Murine mast cells are shown to present antigen to T cells [31]
1994–1996	Dominant role for mast cells in the Arthus reaction is demonstrated [31–33]
1996	Mast cells are shown to be important in defense against <i>E. coli</i> infection [34]
2001	Transcriptome of human mast cells is analyzed [35, 36]
2001–2003	Toll-like receptors are described on mast cells [37–39]
2003	Toll-like receptor and high-affinity IgE signaling shown to induce distinct gene profiles in mast cells [40]
2003	Histamine deficiency induced by histidine decarboxylase gene targeting in mice reveals lower mast cell numbers and defective mast cell degranulation [41]
2004	Expression of nitric oxide synthase and nitric oxide in human mast cells demonstrated [42]
2006	Genomic profiling of mast cells and transcriptome analysis show a wide range of inflammatory responses [43, 44]
2009–2010	Molecular involvement of mast cells in diverse gastrointestinal tract diseases such as Crohn’s disease and eosinophilic esophagitis demonstrated [45, 46]
2011	Mast cell targeting shown to hamper development of prostate carcinoma [47]
2012	Siglec-8 expressed in mast cells and eosinophils may be a target for asthma therapy [48]
2012	Mast cells may link eczema to airway reactivity in a mouse model [49]
2012	Pimecrolimus, a calcineurin inhibitor, may be an effective treatment for mast cell-related disease processes [50]

References

1. Crivellato E, Beltrami C, Mallardi F, Ribatti D (2003) Paul Ehrlich's doctoral thesis: a milestone in the study of mast cells. *Br J Haematol* 123:19–21
2. Kasten FH (1996) Paul Ehrlich: pathfinder in cell biology. 1. Chronicle of his life and accomplishments in immunology, cancer research, and chemotherapy. *Biotech Histochem* 71:2–37
3. Kemp SF, Lockey RF (2002) Anaphylaxis: a review of causes and mechanisms. *J Allergy Clin Immunol* 110:341–348
4. Hill SJ, Ganellin CR, Timmerman H, Schwartz JC, Shankley NP et al (1997) International union of pharmacology. XIII. Classification of histamine receptors. *Pharmacol Rev* 49:253–278
5. Ring J, Brockow K, Behrendt H (2004) History and classification of anaphylaxis. *Novartis Found Symp* 257:6–16
6. Richet G, Estingoy P (2003) The life and times of Charles Richet. *Hist Sci Med* 37:501–513
7. Estingoy P (2003) On the creativity of the researcher: the work of Charles Richet. *Hist Sci Med* 37:489–499
8. Geiger WB, Alpers HS (1959) The mechanism of the Schultz-Dale reaction. *J Allergy* 30:316–328
9. Coulson EJ (1953) The Schultz-Dale technique. *J Allergy* 24:458–473
10. Ovary Z (1994) Immediate hypersensitivity. A brief, personal history. *Arerugi* 43:1375–1385
11. Saint-Paul M, Millot P (1960) The Prausnitz-Kuestner reaction in experimental immunology. Its application to the study of tissue antigens and antibodies and in particular to autoantibodies in man and animal. *Pathol Biol (Paris)* 8:2223–2231
12. Pisani S, Poiron JM, De Poir P, Bocciolosi L (1953) Attempted passive transmission of food sensitivity; Prausnitz-Kustner technic. *Sem Med* 102:527–535
13. Dogliotti M (1954) Prausnitz-Kuestner's passive transfer and gamma globulin. *Minerva Dermatol* 29:383–387
14. Riley JF, West GB (1952) Histamine in tissue mast cells. *J Physiol* 117:72P–73P
15. Bach MK, Brashler JR (1973) On the nature of the presumed receptor for IgE on mast cells. II. Demonstration of the specific binding of IgE to cell-free particulate preparations from rat peritoneal mast cells. *J Immunol* 111:324–330
16. Murphy RC, Hammarstrom S, Samuelsson B (1979) Leukotriene C: a slow-reacting substance from murine mastocytoma cells. *Proc Natl Acad Sci U S A* 76:4275–4279
17. Black J (1989) Nobel lecture in physiology or medicine: 1988. Drugs from emasculated hormones—the principle of syntopic antagonism. *In Vitro Cell Dev Biol* 25:311–320
18. Kishimoto T (2000) Immunology in the 20th century: progress made in research on infectious and immunological diseases. *Kekkaku* 75:595–598
19. Woolcock AJ (1976) Immediate hypersensitivity: a clinical review. *Aust N Z J Med* 6: 158–167
20. Tonegawa S (1993) The nobel lectures in immunology. The nobel prize for physiology or medicine, 1987. Somatic generation of immune diversity. *Scand J Immunol* 38:303–319
21. Weltman JK (1988) The 1987 nobel prize for physiology or medicine awarded to molecular immunogeneticist Susumu Tonegawa. *Allergy Proc* 9:575–576
22. Newmark P (1987) Nobel prize for Japanese immunologist. *Nature* 329:570
23. Plaut M, Pierce JH, Watson CJ, Hanley-Hyde J, Nordan RP, Paul WE (1989) Mast cell lines produce lymphokines in response to cross-linkage of Fc epsilon RI or to calcium ionophores. *Nature* 339:64–67
24. Vanderslice P, Craik CS, Nadel JA, Caughey GH (1989) Molecular cloning of dog mast cell tryptase and a related protease: structural evidence of a unique mode of serine protease activation. *Biochemistry* 28:4148–4155
25. Miller JS, Westin EH, Schwartz LB (1989) Cloning and characterization of complementary DNA for human tryptase. *J Clin Invest* 84:1188–1195
26. Copeland NG, Gilbert DJ, Cho BC, Donovan PJ, Jenkins NA et al (1990) Mast cell growth factor maps near the steel locus on mouse chromosome 10 and is deleted in a number of steel alleles. *Cell* 63:175–183
27. Huang E, Nocka K, Beier DR, Chu TY, Buck J et al (1990) The hematopoietic growth factor KL is encoded by the Sl locus and is the ligand of the c-kit receptor, the gene product of the W locus. *Cell* 63:225–233
28. Caughey GH, Raymond WW, Vanderslice P (1990) Dog mast cell chymase: molecular cloning and characterization. *Biochemistry* 29:5166–5171
29. Caughey GH, Zerweck EH, Vanderslice P (1991) Structure, chromosomal assignment, and deduced amino acid sequence of a human gene for mast cell chymase. *J Biol Chem* 266:12956–12963

30. Malaviya R, Ross EA, MacGregor JI, Ikeda T, Little JR et al (1994) Mast cell phagocytosis of FimH-expressing enterobacteria. *J Immunol* 152:1907–1914
31. Fox CC, Jewell SD, Whitacre CC (1994) Rat peritoneal mast cells present antigen to a PPD-specific T cell line. *Cell Immunol* 158:253–264
32. Smith EL, Hainsworth AH (1998) Acute effects of interleukin-1 beta on noradrenaline release from the human neuroblastoma cell line SH-SY5Y. *Neurosci Lett* 251:89–92
33. Sylvestre DL, Ravetch JV (1996) A dominant role for mast cell Fc receptors in the Arthus reaction. *Immunity* 5:387–390
34. Malaviya R, Ikeda T, Ross E, Abraham SN (1996) Mast cell modulation of neutrophil influx and bacterial clearance at sites of infection through TNF-alpha. *Nature* 381:77–80
35. Iida M, Matsumoto K, Tomita H, Nakajima T, Akasawa A et al (2001) Selective down-regulation of high-affinity IgE receptor (Fc epsilon RI) alpha-chain messenger RNA among transcriptome in cord blood-derived versus adult peripheral blood-derived cultured human mast cells. *Blood* 97:1016–1022
36. Nakajima T, Matsumoto K, Suto H, Tanaka K, Ebisawa M et al (2001) Gene expression screening of human mast cells and eosinophils using high-density oligonucleotide probe arrays: abundant expression of major basic protein in mast cells. *Blood* 98:1127–1134
37. Supajatura V, Ushio H, Nakao A, Akira S, Okumura K et al (2002) Differential responses of mast cell Toll-like receptors 2 and 4 in allergy and innate immunity. *J Clin Invest* 109:1351–1359
38. McCurdy JD, Lin TJ, Marshall JS (2001) Toll-like receptor 4-mediated activation of murine mast cells. *J Leukoc Biol* 70:977–984
39. McCurdy JD, Olynich TJ, Maher LH, Marshall JS (2003) Cutting edge: distinct Toll-like receptor 2 activators selectively induce different classes of mediator production from human mast cells. *J Immunol* 170:1625–1629
40. Okumura S, Kashiwakura J, Tomita H, Matsumoto K, Nakajima T et al (2003) Identification of specific gene expression profiles in human mast cells mediated by Toll-like receptor 4 and Fc epsilon RI. *Blood* 102:2547–2554
41. Kozma GT, Losonczy G, Keszei M, Komlosi Z, Buzas E et al (2003) Histamine deficiency in gene-targeted mice strongly reduces antigen-induced airway hyper-responsiveness, eosinophilia and allergen-specific IgE. *Int Immunol* 15:963–973
42. Gilchrist M, McCauley SD, Befus AD (2004) Expression, localization, and regulation of NOS in human mast cell lines: effects on leukotriene production. *Blood* 104:462–469
43. Jaypal M, Tay HK, Reghunathan R, Zhi L, Chow KK et al (2006) Genome-wide gene expression profiling of human mast cells stimulated by IgE or Fc epsilon RI-aggregation reveals a complex network of genes involved in inflammatory responses. *BMC Genomics* 7:210
44. Liu SM, Xavier R, Good KL, Chtanova T, Newton R et al (2006) Immune cell transcriptome datasets reveal novel leukocyte subset-specific genes and genes associated with allergic processes. *J Allergy Clin Immunol* 118:496–503
45. Okumura S, Yuki K, Kobayashi R, Okumura S, Ohmori K et al (2009) Hyperexpression of NOD2 in intestinal mast cells of Crohn's disease patients: preferential expression of inflammatory cell-recruiting molecules via NOD2 in mast cells. *Clin Immunol* 130:175–185
46. Abonia JP, Blanchard C, Butz BB, Rainey HF, Collins MH et al (2010) Involvement of mast cells in eosinophilic esophagitis. *J Allergy Clin Immunol* 126:140–149
47. Pittoni P, Tripodo C, Piconese S, Mauri G, Parenza M et al (2011) Mast cell targeting hampers prostate adenocarcinoma development but promotes the occurrence of highly malignant neuroendocrine cancers. *Cancer Res* 71:5987–5997
48. Farid SS, Mirshafiey A, Razavi A (2012) Siglec-8 and Siglec-F, the new therapeutic targets in asthma. *Immunopharmacol Immunotoxicol* 34:721–726
49. Hershko AY, Charles N, Olivera A, Alvarez-Errico D, Rivera J (2012) Cutting edge: persistence of increased mast cell numbers in tissues links dermatitis to enhanced airway disease in a mouse model of atopy. *J Immunol* 188:531–535
50. Ma Z, Jiao Z (2011) Mast cells as targets of pimecrolimus. *Curr Pharm Des* 17:3823–3829

Chapter 2

The Phylogenetic Profile of Mast Cells

Enrico Crivellato, Luciana Travan, and Domenico Ribatti

Abstract

Mast cells (MCs) are tissue-based immune cells that participate to both innate and adaptive immunities as well as to tissue-remodelling processes. Their evolutionary history appears as a fascinating process, whose outline we can only partly reconstruct according to current remnant evidence. MCs have been identified in all vertebrate classes, and a cell population with the overall characteristics of higher vertebrate MCs is identifiable even in the most evolutionarily advanced fish species. In invertebrates, cells related to vertebrate MCs have been recognized in ascidians, a class of urochordates which appeared approximately 500 million years ago. These comprise the granular hemocyte with intermediate characteristics of basophils and MCs and the “test cell” (see below). Both types of cells contain histamine and heparin, and provide defensive functions. The test cell releases tryptase after stimulation with compound 48/80. A leukocyte ancestor operating in the context of a primitive local innate immunity probably represents the MC phylogenetic progenitor. This cell was likely involved in phagocytic and killing activity against pathogens and operated as a general inducer of inflammation. This early type of defensive cell possibly expressed concomitant tissue-reparative functions. With the advent of recombinase activating gene (RAG)-mediated adaptive immunity in the Cambrian era, some 550 million years ago, and the emergence of early vertebrates, MC progenitors differentiated towards a more complex cellular entity. Early MCs probably appeared in the last common ancestor we shared with hagfish, lamprey, and sharks about 450–500 million years ago.

Key words Mast cells, Vertebrates, Ascidians, Granular hemocytes, Innate immunity, Adaptive immunity, Tissue regeneration

1 Introduction

Mast cells (MCs) are bone-marrow-derived tissue-homing leukocytes, which express versatile functions in a vast assortment of immunological and non-immunological settings [1]. They have recently been recognized as crucial effectors in both innate and adaptive immunities. Furthermore, there is mounting evidence that MCs may exert relevant functions in tissue homeostasis, remodelling, repair, fibrosis, and angiogenesis.

Comparative studies have identified MCs in all vertebrate classes [2]. In the last few years, interest has expanded in the functional profile of MCs in a phylogenetic perspective. A crucial question has

emerged from these studies: who is the ancestor of current MCs and what kind of functional activity did this cell provide? In all vertebrates, MCs appear as granulated cells which share some common characteristics. Their cytoplasm is filled with plentiful metachromatic granules which store secretory compounds such as histamine—also serotonin in rodents and fish—and proteases embedded in a glycosaminoglycan matrix. Remarkably, tryptase and histamine have also been recognized in MCs of teleost fish [3, 4]. Upon immunoglobulin E (IgE)-dependent and IgE-independent stimulations, MCs in mammals release a vast array of cytokines and growth factors. Some of them appear to exist preformed within granules but the majority are synthesized de novo. All mammalian MCs express on their surface high levels of the stem cell factor (SCF) receptor KIT and the tetrameric $\alpha\beta\gamma_2$ form of the high-affinity receptor (Fc ϵ RI) for IgE [1]. Both surface molecules are of basic relevance in MC biology, and, remarkably, KIT-like and Fc ϵ RI-like receptors have been recognized even in fish MCs [4, 5]. Thus, a cell population with the overall characteristics of higher vertebrate MCs is identifiable in the most evolutionarily advanced fish species. Fc ϵ RI is the first recognized and most important receptor for MC activation [6], but, in mammals, MCs may also be activated by “alternative,” IgE-independent pathways, such as aggregation of Fc γ RIII by IgG/antigen complexes, KIT and Toll-like receptor (TLR) mechanisms, exposure to chemokines, anaphylatoxins C3a and C5a, fragments of fibrinogen, and fibronectin [7–11].

Comparative studies have also identified some important distinguishing features among vertebrate MCs, which led investigators to shape the concept of “MC heterogeneity” [12–15]. Cell dimension, granule number, granule chemical content, and distinctive substructural pattern may differ significantly according to the species examined [16]. In addition, MC subtypes may be recognized at specific anatomical sites even in the same species and may respond to different inducers and express fairly distinct functional profiles. MCs in rodents can be differentiated in two broad subtypes, namely, connective tissue MCs and mucosal MCs [17], and in man three MC subtypes have conventionally been identified according to their protease content: (1) MCs which contain tryptase only; (2) MCs that contain both tryptase and chymase, along with other proteases such as carboxypeptidase A and cathepsin G; and (3) MCs which express chymase without tryptase [18]. MC heterogeneity for histamine content as well as chymotrypsin-like and trypsin-like activity has been recognized in avian, reptile and amphibian MCs [19–22].

MC persistence throughout vertebrate evolution indicates a strong selective pressure in favor of their survival and suggests that these cells may have beneficial and important roles. In humans, MCs collectively comprise a substantial cell population, and it has been estimated that if all tissue MCs were amassed

together in a single organ, it would equal the size of a normal spleen [23]. An enormous cell mass that hardly reconciles with the pure detrimental role in IgE-mediated allergic reactions initially attributed to these cells and suggests for them significant and positive functions. In all vertebrates, MCs normally reside in proximity to surfaces that interface the external environment which are common portals for pathogen, allergen, and toxin entry. Thus, MCs are likely to be among the first inflammatory cells to interact with invading microorganisms and initiate immune responses [24]. Since ancient times, MCs have probably been part of protective mechanisms. A leukocyte ancestor operating in the context of a primitive local innate immunity and involved in phagocytic and killing activity against pathogens probably represented the MC phylogenetic progenitor. Its original function was most likely to be found in parasite and bacterial defense of the host and as a general inducer of inflammation. This early type of defensive cell possibly differentiated towards a more complex cellular entity—which was incorporated with success into the networks of recombinase activating genes (RAG)-mediated adaptive immunity in the Cambrian era, some 550 million years ago—and progressively evolved into a tissue regulatory cell involved in different processes, such as immunomodulation, wound healing, tissue regeneration, and remodelling after injury, fibrosis, angiogenesis, and possibly other biological functions.

2 Mast Cells in Fish

Studies on MC equivalents in fish have elucidated some aspects of MC phylogenesis and have increased our understanding of MC functional profile in lower vertebrates. In the most advanced teleost fish, MCs comprise a cell population with the overall characteristics of higher vertebrate MCs. Thus, comparative studies in fish MCs are of great value in an attempt to reconstruct the evolutionary process accomplished by these immune and tissue-remodelling cells. In general terms, fish MCs represent a heterogeneous entity. They express different morphology, variable granule content, erratic sensitivity to fixatives, and unequal response to drugs. In salmonids, cyprinids, and erythrinids—all teleostean fish—plentiful granular cells have been identified in the mucosa lining the intestinal tract, the dermis, and the gills. It must be noted that gill, like the intestinal tract and the skin, is one of the tissues first exposed to pathogenic and environmental challenges. Cells with the overall structural and histochemical features of MCs have been identified even in primitive jawless fish (Agnatha: hagfish, lamprey) and cartilaginous fish (Chondrichthyes: sharks). However, granular cells have not been identified in all examined fish species. Remarkably, secretory granules in fish MCs show different staining

properties. In many species, they appear as either basophilic or eosinophilic. For this reason, MC equivalents in fish have frequently been referred to as basophilic granular cells or acidophilic/eosinophilic granule cells (EGCs) [25]. The nomenclature MC/EGCs has persisted in the literature in reference of these cells due probably to a failure of certain fixation techniques to consistently demonstrate metachromatic staining in a subpopulation of these cells stained with toluidine blue [25]. Interestingly, erratic staining responsiveness has been recognized also in some amphibian and reptile MCs [26].

The functional properties of fish MCs have recently been investigated by several authors. The picture that emerges is that of a cell involved in defensive mechanisms against parasite and bacteria infections. This cell may act directly by killing pathogen microorganisms, but the bulk of evidence suggests a more complex defensive function. Zebra fish (*Danio rerio* H.) MCs, for instance, participate in innate and adaptive immune responses [5]. In the gill and intestine of this teleost, cells regarded as analogous to mammalian MCs contain an ovoid eccentric nucleus and toluidine blue-positive metachromatic granules. Under electron microscopy, they closely approximate the appearance of murine MCs [4]. Intraperitoneal injection of compound 48/80—a well-known MC secretagogue in mammals—or live *Aeromonas salmonicida* results in a rapid and significant degranulation of intestinal MCs, which is recognizable histologically and by increased plasma tryptase levels [5]. This response is abrogated by the H₁ histamine antagonist and MC stabilizing agent ketotifen. In addition, whole mount in situ hybridization procedures indicate that *myd88*, a Toll-like receptor adaptor, is expressed in a subset of mature MC equivalents, suggesting conservation of innate immune responses mediated through TLRs [5]. Notably, zebra fish MCs possess an analogous Fc ϵ RI that results in reproducible systemic anaphylactic responses after stimulation [5]. Histochemically, these cells demonstrate a positive reaction to polyclonal antihuman KIT and monoclonal antihuman MC tryptase antibodies [4]. A carboxypeptidase A (CPA) 5 protein, which shares 38 % identity with CPA3 expressed in human MCs, has been identified in zebra fish MCs. The *cpa5*-expressing MCs represent a unique myeloid subpopulation arising from a cell with both granulocyte and monocyte potential [4]. MCs belonging to the Perciformes, the largest and most evolutionarily advanced order of teleosts, have been found to contain histamine [3]. Remarkably, histamine is biologically active in these fish and is able to regulate the inflammatory response by acting on professional phagocytic granulocytes. Thus, in the most phylogenetically developed teleostean species, a cell type with the basic structure-function profile of mammalian MC counterpart is recognizable. In addition, many studies have shown that fish MC equivalents contain serotonin instead of histamine.

In general terms, fish MCs undergo cell degranulation after inoculation of certain substances, such as *Aeromonas salmonicida* and *Vibrio anguillarum* toxins, compound 48/80, substance P, and capsaicin. In addition, their number has been shown to increase after parasitic infection. Of note, migration and accumulation of neutrophils has often been observed at the site of MC degranulation [27], suggesting that MC secretion may have a role in attracting other types of cells involved in the inflammatory process, especially during initial pathogenic challenge. Thus, fish MCs are supposed to contain or generate a variety of mediators that induce neutrophil chemotaxis, as observed in mammals.

Fish MCs store in their granules different components which are common to mammalian counterparts: alkaline and acid phosphatases, leucine aminopeptidase, arylsulphatase and 5'-nucleotidase, lysozyme, and met-enkephalin. Notably, the granules of MCs in teleosts contain piscidins, a class of 22-amino-acid antimicrobial peptides that have potent, broad-spectrum antibacterial activity against fish pathogens [28, 29]. Piscidins are thought to inhibit the synthesis of the cell wall, nucleic acids, and proteins or even inhibit enzymatic activity [30]. Piscidin-immunoreactive MCs are most common at sites of pathogen entry, including the skin, gill, and gastrointestinal tract. Remarkably, not all fish MCs are piscidin-positive. Piscidins 3 and 4, for instance, have been identified only in MCs of fish belonging to the orders of Perciformes and Gadiformes. A related family of antimicrobial peptides, called pleurocidins, are synthesized in MCs of the Atlantic halibut (*Pseudopleuronectes americanus*), a flatfish belonging to the order Pleuronectiformes [31].

3 Mast Cell-Like Cells in Invertebrates

Potential MC progenitors have been identified in ascidians, marine invertebrates commonly known as sea squirts. Ascidians belong to the subphyla of invertebrate chordates Urochordates which appeared approximately 500 million years ago. The hemolymph of ascidians contains different types of circulating cells. Some of these cells migrate from hemolymph to tissues, where they carry out several immunologic actions, such as phagocytosis of self and non-self molecules, expression of cytotoxic agents, encapsulation of foreign antigens, and also reparation of damaged tissues. In 2007, de Barros and co-workers reported that circulating granular hemocytes in the hemolymph of the ascidia *Styela plicata* expressed intermediate characteristics of basophils and MCs [32]. Viewed by transmission electron microscopy, these cells appeared as mono-nuclear cells of 3.5–6 μm diameter, characterized by a cytoplasm filled with spherical granules of uniform size and variable density. The general morphology was closely related to that of mammalian

MCs and basophils. Unlike the hemocytes of any other invertebrate species, the granules of these cells contained both heparin and histamine. These molecules are major components of MC granules in mammals. Heparin is a highly sulfated glycosaminoglycan (GAG) made up of a mixture of polymers with a similar backbone of repeating hexuronic acid linked to 1,4 to α -d-glucosamine units. It represents the dominant GAG in human MCs and constitutes some 75 % of the total, with a mixture of chondroitin sulfates making up the remainder [33]. In man, the heparin content in tryptase- and tryptase/chymase-containing MCs is roughly the same. In the mouse, the proteoglycan content of MC granules varies in the different MC subtypes. Connective tissue MCs contain heparin, which is largely absent in mucosal MCs. Heparin proteoglycan is thought to form the granule matrix that binds histamine, neutral proteases, and carboxypeptidases primarily by ionic interactions, and, therefore, it contributes to the packaging and storage of these molecules in the granules. Mice that lack the enzyme *N*-deacetylase/*N*-sulfotransferase-2 (NDST-2), which are unable to produce fully sulfated heparin, exhibit severe defects in the granule structure of MCs, with impaired storage of certain proteases and reduced content of histamine [34, 35]. Histamine was the first discovered mediator in MCs. In human MCs, histamine is present at a concentration of 1–4 pg/cell [33]. Mammalian and avian MCs contain high concentrations of histamine in their secretory granules [36, 37]. In poikilothermic vertebrates, reports of MC histamine content are contradictory. Various amounts of this biogenic amine were found in reptilian MCs using the o-phthalaldehyde fluorescence method [36–38]. In the granules of frog (*Rana catesbeiana*) MCs, the presence of very low amounts of histamine was revealed using a double fluorometric and ultrastructural approach [20]. The histamine content per frog MC (about 0.1 pg/cell) was approximately 30 times lower than that of human MCs isolated from various tissues. Histamine has also been recognized in MCs belonging to the Perciformes [3]. Remarkably, histamine is biologically active in these fish and is able to regulate the inflammatory response by acting on professional phagocytic granulocytes. The presence of histamine has been reported in several classes of invertebrates, such as Cnidaria, Mollusca, Arthropoda, and Echinodermata. In invertebrates, histamine is involved in defense mechanisms. It is present in the venom of the jumper ant (*Myrmecia pilosula*), in the tentacles of anemones (Actiniaria), and in the toxin of the sea urchin (Echinoida, Diadematoida). In this perspective, the identification of histamine in the granules of the hemocyte found in the hemolymph of *Styela plicata* further supports the notion that it may represent an ancient effector cell of the innate immunity [39].

Being the positions of ascidians at the top of the invertebrate phylogenetic tree, close to vertebrate chordates, these granular

hemocytes might well represent the primitive counterparts of mammalian MCs. They provide defensive functions and are involved in different immunological actions, such as migration from the blood vessels to perform activities like phagocytosis, liberation of antimicrobial peptides, triggering of the complement system, encapsulation of foreign organisms, and regeneration of tissues.

Another cell type in *Styela plicata*, the test cell, shares some structural and functional characteristics with vertebrate MCs [40]. Similarly to the granular hemocyte, this type of cell contains histamine and heparin in cytoplasmic granules and appears metachromatic under light microscopy. Test cells are accessory cells that reside in the periviteline space of oocytes [39]. Their origin is controversial. It has been proposed that they can derive from amoeboid cells migrating to the surface of young oocytes. Therefore, they may represent ancient effector cells of the innate immunity involved in protection of the oocyte, which in this species is in contact with the external environment, against invasion of microorganisms [41, 42]. Viewed under transmission electron microscopy, these cells appear as mononuclear cells endowed with circular, membrane-bound granules composed by electron-dense filaments [42]. Remarkably, these cells contain heparin and histamine, and both molecules co-localize inside granules. Most remarkably, incubation of test cell-rich preparations with the MC secretagogue compound 48/80 causes tryptase release in the supernatant accompanied by loss of metachromasia and the ultrastructural organization of granules in the test cells. Thus, these cells share some morphological, biochemical and functional characteristics with vertebrate MCs.

4 Mast Cells and Innate Immunity

The innate immunity represents the first line of host responses to pathogen invasion. Innate immunity depends on germ line-encoded receptors that have evolved to recognize highly conserved pathogen-associated molecular patterns. These receptors are termed pattern recognition receptors [43]. MCs likely evolved from an ancestral defensive cell. Mammalian MCs still retain some residual functions of this ancient MC progenitor presumably implicated in defense from parasites by pathogen seclusion and direct killing. In mammals, both human and mouse MCs are capable of eliminating bacteria *in vitro* through an intracellular killing system similar to that of professional phagocytes [44]. Although the physiological significance of the phagocytic activity exerted by MCs in higher vertebrates remains undetermined, mucosal MCs in mice are known to play a role in the expulsion of the nematode *Trichinella spiralis* *in vivo* [45], and indirect evidence of MC degranulation has been provided in the intestine and muscles of

rats infected with nematodes [46]. MCs in mice can kill opsonized bacteria. *Salmonella typhimurium* coated with the C3b fragment of complement is recognized through complement receptor 3 (CR3) on the MC membrane [47]. Mammalian MCs express other complement receptors: C3aR, C5aR CR2, CR4, and C1qR [11, 48]. The CR3 was first recognized in ascidians [49]. It represents an essential ancestral component of the primordial complement system that functioned in an opsonic manner. Indeed, the C3 complement factor—the central component of the complement system—has also been recognized in the horseshoe crab *Carcinoscorpius rotundicauda*, a protostome considered a “living fossil” originating over 500 million years ago [50]. These animals, which lack adaptive immunity, mount an effective antimicrobial defense in response to pathogens. The C3 protein has been identified in jawless vertebrates, the lamprey and hagfish, as well as in deuterostome invertebrates, ascidians, amphioxus, and sea urchins (echinoderm). Interestingly, MC equivalents have been recognized in jawless fish, and a possible MC precursor has been identified in ascidians. MCs in mice can also recognize parasites, bacteria, and viruses in the absence of opsonins [11]. This trait is likely mediated through the cell surface pattern recognition receptors, such as the TLRs and the FimH receptor CD48 [48]. TLRs are widely distributed throughout the evolutionary scale. TLR genes are absent from non-animal phyla but are recognizable in most eumetazoans, from cnidarians to vertebrates. In humans, MCs may exert bactericidal activity via a recently identified extracellular phagocytosis-independent mechanism consisting of the production of extracellular structures similar to neutrophil extracellular traps (NETs) [51]. In a phylogenetic perspective, these network structures provide similarities with the process of nodule formation by invertebrate granular hemocytes. Nodules are multicellular hemocytic aggregates that may entrap a large number of bacteria in an extracellular material. Bacterial killing by MC extracellular traps might represent retention of an early ability expressed by MC phylogenetic precursors to promote pathogen seclusion and removal by nodule formation.

Several lines of evidence indicate that MCs produce antimicrobial peptides, which are host defense effector molecules. Fish MCs contain antimicrobial peptides of the class of piscidins and pleurocidins and therefore are presumed to be directly involved in killing microbes. Piscidins are the prototype of antimicrobial peptides found in fish MCs. They have strong, broad-spectrum antibacterial, antifungal, and antiparasitic activities. Studies in mammals reveal that human and murine MCs contain antimicrobial peptides as well. MCs in mice express abundant amounts of cathelin-related antimicrobial peptide, while human skin MCs have been shown to contain the cathelicidin peptide LL-37 [52]. Thus, mammalian MCs, like fish MCs, are endowed with the defensive machinery provided by the class of antimicrobial peptides.

Besides their possible participation in direct killing of invading pathogens, MCs are regarded as sentinels of innate immunity due to their capacity to orchestrate efficient antibacterial responses by recruiting other inflammatory cells at the site of pathogen entry. This mechanism is sufficiently known in the MC-deficient mice model. Here, MCs have been shown to protect against bacteria, fungi, and protozoa through the release of proinflammatory and chemotactic mediators [44]. Upon contact with invading microorganisms, MCs release a variety of molecules—including tumor necrosis factor (TNF)- α , interleukin (IL)-4 and IL-8, and leukotriene B₄ (LTB₄)—which are crucial effectors in promoting the influx of neutrophils and other inflammatory cells. Although the relevant molecular machinery remains unidentified, stimulation of neutrophil recruitment has also been recognized at the site of MC degranulation in fish. Here, migration and accumulation of neutrophils have often been observed which suggests that fish MCs may contain or generate mediators capable of inducing neutrophil chemotaxis, as observed in mammals [27]. Histamine has been identified in MCs of perciform fish, the largest and most evolutionarily advanced order of teleosts. Functional studies indicate that fish professional phagocyte function may be regulated by the release of histamine from MCs upon H₁ and H₂ receptor engagement [3]. Interestingly, the cathelicidin antimicrobial peptide LL-37 recognized in human MCs is active as a leukocyte chemoattractant through binding of human formyl peptide receptor like 1/lipoxin-A receptor [53]. In addition, human LL-37 influences the expression of chemokines, such as IL-8, and chemokine receptors, such as CCR2 and IL8RB, in macrophages [54]. Thus, cathelicidin antimicrobial peptides may contribute to attract neutrophils and expand the inflammatory response at the site of pathogen entry. In a similar way, antimicrobial peptides released by fish MCs might be partly responsible for the accumulation of neutrophils at sites of MC degranulation.

5 Mast Cells and Adaptive Immunity

This is perhaps the most difficult aspect of MC function to be analyzed and interpreted in an evolutionary perspective because virtually nothing is known about MC participation to adaptive immunity in nonmammalian species. Thus, its reconstruction is absolutely conjectural.

Experimental evidence in mammals indicates that MCs are crucially involved in adaptive immunity. These cells have been increasingly implicated in different aspects of immune regulation, influencing the outcome of both physiological and pathological T cell responses [55–58]. MC involvement in adaptive immunity is broad. They coordinate responses to pathogens, by orchestrating

migration, maturation, and function of dendritic cells, T cells, and B cells [59–61]. They interact with T cells, being capable of expressing major histocompatibility complex (MHC) class II moieties and co-stimulatory molecules, travelling from the activation site to regional lymph nodes like dendritic cells and thereby becoming potential antigen presenting cells for T cells [62, 63]. They contribute to the initiation of the primary immune responses to allergens and amplify exacerbations of allergic diseases [64]. They exert an important role in generating immune tolerance and primarily affect certain autoimmune diseases [65].

When did these MC functions emerge during evolution? We have too limited information about MC participation to adaptive immunity in nonmammalian species to provide a plausible answer to such a question. In addition to innate defense mechanisms, jawed vertebrates (gnathostomes) have evolved an adaptive immune system mediated primarily by lymphocytes. Adaptive immunity made its appearance some 550 million years ago during the Cambrian era with the emergence of the Ig-based RAG-mediated immune system that coincided with the coming out of early vertebrates [66, 43]. By rearrangement of IgV, D, and J gene segments—the Ig domains are an ancient protein superfamily involved in pathogen recognition or self/nonself discrimination in invertebrates—the jawed vertebrates generated a lymphocyte receptor repertoire of sufficient diversity to recognize the antigenic component of any potential pathogen or toxin [43]. At the dawn of vertebrate evolution, cartilaginous fish first rearranged their V(D)J gene segments to assemble complete genes for the cell surface antigen receptors expressed by T and B lymphocytes, whose triggering initiates specific cell-mediated or humoral-immune responses. This Ig-based recombinatorial system generated anticipatory receptors in T and B lymphocytes that enabled these cells to work together and, with other cells, to mediate effective adaptive immunity. The appearance of RAG-mediated immunity within a relatively short evolutionary period of about 40 million years represents a stunning enigma for immunologists. In this evolutionary scenario, it might be speculated that phylogenetic progenitors of MCs were transmitted from invertebrates to their vertebrate descendants and incorporated into the networks of the new defensive system. Vertebrate MCs acquired key elements of adaptive immunity, such as MHC class I and II molecules, becoming involved in co-stimulatory activity [67]. Interestingly, even in vertebrates innate immunity provides the first line of defense against pathogens because it takes at least several days to orchestrate an efficient adaptive immune response. In this way, the modern MC may represent the pivotal cell that links primitive schemes of surveillance to more evolved and versatile defensive strategies.

Clonal B cell activation and production of specific antibodies represent a crucial aspect of adaptive immunity. The IgE molecule,

and its interaction with the Fc ϵ RI, is the critical MC triggering factor of anaphylaxis in mammalian MCs [64]. IgE and its receptors are believed to have evolved as a mechanism for protection against parasites [68, 69]. In vertebrates other than mammals, IgE molecules are not recognizable and the low molecular weight isotype characteristic of birds, reptiles, and amphibians is the IgY molecule [70]. In an evolutionary scale, it is believed that IgY is the precursor of both mammalian IgE and IgG classes [70]. Some indirect proof is available for the expression of receptors for IgY on MCs in birds [71], which suggests a functional relevance of IgE-like molecules in avian MC activation as well. Teleost fish produce both IgM-like and IgD-like molecules but not IgE molecules [72]. In general terms, the Fc ϵ RI appears to be a relatively recent acquisition in MC evolution if IgE originated first with the emergence of mammalian species. Thus, it is of great interest that a polyclonal antibody directed to the γ subunit of the human Fc ϵ RI recognizes a specific determinant on the surface of zebra fish intestinal MCs and that reproducible passive systemic anaphylactic responses can be elicited in this fish species, likely as a result of the stimulation of such Fc ϵ RI analogues [5]. This finding provides evidence for a conserved IgE-like receptor throughout vertebrate evolution.

6 Linking Defensive and Tissue-Remodelling Activities

Modern MCs are tissue-based immune cells involved in innate and adaptive immunities as well as the preservation of tissue homeostasis. Probably, the key structures which provided an effective connection between protective and reparative functions in the hypothetical MC ancestor were enzymes belonging to the class of serine proteases. Tryptase and chymase are the major types of serine proteases stored in MC granules and seemingly well conserved among vertebrate species [73]. Serine proteases are important effector molecules in the immune system of mammals and have been found not only in MC granules but also in the granules of neutrophils, T cells, and NK cells [74]. MC tryptase and chymase are phylogenetically related to neutrophil cathepsin G and T cell granzymes. These proteases show a large distribution through the evolutionary scale. Serine proteases related to the mammalian hematopoietic serine protease family have been identified in teleost fish [75]. Tryptase has also been recognized in zebra fish MCs [4]. This protease is designed for exocytosis as compound 48/80-mediated degranulation of zebrafish MCs leads to elevation of plasma tryptase level [4]. Interestingly, test cells from the urochordate *Styela plicata*, a potential MC phylogenetic progenitor, also release tryptases after incubation with compound 48/80 [42].

MC proteases play an important role in innate host defense. In the mouse, at least five different granule-associated chymases (mMCP-1, mMCP-2, MMCP-3, MMCP-4, MMCP-5) and three different granule-associated tryptases (mMCP-6, mMCP-7, mMMP-11/transmembrane tryptase (mTMT)) have been described at the protein level [76]. There appear to be multiple forms of human tryptases as well (tryptases α I, α II, β I, β II, β III, γ I, and γ II and transmembrane tryptase) [77–79]. In mice, MC-stored proteases are endowed with the capacity to generate important defensive as well as tissue-remodelling responses. MC tryptase mMCP-6, for instance, has a critical protective function in bacterial and parasite infection. mMCP-6-deficient mice are less able to clear *Klebsiella pneumoniae* injected into their peritoneal cavities, probably because of less recruitment of neutrophils [80]. mMCP-6 is also important for the clearance of the chronic *Trichinella spiralis* infection [81]. MC chymase mMCP-1 as well is important for expulsion of the adult helminth and the larvae of *Trichinella spiralis* in infected mice [45]. MC chymase mMCP-2 contributes to neutrophil recruitment and host survival in the “cecal ligation and puncture” model [82]. The human tryptase β I, the predominant form stored in secretory granules of all human MCs, is also capable to stimulate the influx of neutrophils at site of pathogen entry [44].

Serine proteases, in addition, provide fundamental role in various aspects of tissue homeostasis and tissue remodelling after injury. Tryptases are potent activators of fibroblast migration and proliferation [83] and can stimulate the synthesis and release of type collagen I from fibroblasts in culture, as well as provoke secretion of collagenase [84]. Tryptases cleave fibronectin and type VI collagen. They activate the pre-enzyme forms of some metalloproteases (MMPs) and urinary plasminogen activators (uPA) which are implicated in tissue degradation. Tryptases cleave various bronchial and intestinal neuropeptides and may also have a role in tissue repair processes as a growth factor for epithelial and muscle cells [85]. A number of studies have demonstrated the angiogenic potential of tryptase and its important role in neovascularization, stimulating endothelial cell activation, proliferation, migration, and tube formation [86]. Chymases may contribute to tissue remodelling by cleaving type IV collagen and by splitting the dermal-epidermal junction. They may also express a proangiogenic activity. Chymases degrade some neuropeptides and cleave angiotensin I to angiotensin II more effectively than the angiotensin-converting enzyme [33].

Genetic analysis of tryptases in different species suggests that these proteases proliferated and changed rapidly during mammalian evolution, arising from ancestral membrane-anchored peptidases, which are present in a variety of vertebrate genomes such as reptiles, amphibians, and fish [87]. We have seen that two potential

MC ancestors have been identified in ascidians, namely, the granular hemocyte and the test cell. Both cell types are supposed to be involved in defensive functions and provide tissue-reparative activity. Interestingly, a third type of ascidia cell called the large-granule tunic cell has been found to contain granules with tessellated substructures [88]. This cell too seems to have originated from granulocytes that migrate in the tunic from the hemolymph. Granulated tunic cells have been found to infiltrate the integumentary matrix, the inner layer of the tunic—a protective envelop wholly covering the outside of the epidermis—during tissue reconstitution taking place after experimentally induced wounds of the integumentum, suggesting a direct or indirect participation of these cells in the process of tunic healing [89]. In addition, some tissue manipulations can be accomplished by granular cells in insects during metamorphosis. Thus, cells possibly belonging (or close) to MC phylogenetic lineage appear as blood-derived, tissue-homing elements involved in both protective actions and restoration of damaged structures. Since primordial times, these two aspects of tissue homeostasis—namely, defense and repair—seem to be closely related. It is most likely that a repair function would have been acquired well before the development of an adaptive immune response. During evolution, vertebrate MCs have retained and further exploited such fundamental properties, growing into highly versatile tissue sentinels capable to sense the microenvironment and to coordinate sophisticated defensive strategies as well as multifaceted tissue-remodelling actions.

7 Conclusions

In evolutionary terms, MCs appear as ancient cells. They have been identified in all classes of vertebrates, and comparative analysis has suggested possible MC analogues in invertebrates. Current MCs may derive from a leukocyte ancestor, which probably displayed functional features similar to those expressed by present invertebrate granular hemocytes. This archaic cell was probably an effector cell, chiefly providing tissue defense in the context of a primitive local innate immunity. It was involved in protective functions, such as phagocytosis of self and nonself molecules, expression of cytotoxic agents, nodule formation, and encapsulation of microorganisms. Besides immunity actions, the MC ancestor probably engaged in restoration of damaged structures. Thus, MC phylogenetic progenitors were probably involved in both aspects of tissue homeostasis—namely, defense and repair—since primordial times. In invertebrates, two types of possible MC progenitor cells have been recognized, namely, the basophil/MC-like cell and the test cell. They have been identified in ascidians, chordates which appeared approximately 500 million years ago. Both cell types

contain histamine and heparin in their secretory granules. Test cells also contain tryptase and are induced to degranulate by the well-known mast cell secretagogue compound 48/80.

In the Cambrian period, some 550 million years ago, an Ig-based RAG-mediated immune system appeared together with the emergence of early vertebrates. During the transition from invertebrates to vertebrates, the ancient MC precursor evolved into a novel cell type. It continued to perform innate immune and protective functions concomitantly with the stepwise acquisition of acquired immune functions. Vertebrate MCs added new molecular strategies to their functional arsenal without losing many of the properties accumulated during million years of invertebrate evolution. Archaic MCs were integrated into the complex networks of adaptive immune responses, and current MCs probably appeared in the last common ancestor we shared with hagfish, lamprey, and shark about 450–500 million years ago.

Acknowledgments

This study was supported by MIUR local funds to the Department of Experimental and Clinical Medicine, Anatomy Section, University of Udine.

References

1. Galli SJ, Kalesnikoff J, Grimaldston MA, Piliponsky AM, Williams CMM, Tsai M (2005) Mast cells as “tunable” effector and immuno-regulatory cells: recent advances. *Annu Rev Immunol* 23:749–786
2. Baccari GC, Pinelli C, Santillo A, Minucci S, Rastogi RK (2011) Mast cells in nonmammalian vertebrates: an overview. *Int Rev Cell Mol Biol* 290:1–53
3. Mulero I, Sepulcre MP, Meseguer J, Garcia-Ayala A, Mulero V (2007) Histamine is stored in mast cells of most evolutionarily advanced fish and regulates the fish inflammatory response. *Proc Natl Acad Sci U S A* 104:19434–19439
4. Dobson JT, Seibert J, The EM, Da'as S, Fraser RB, Paw BH, Lin TJ, Berman JN (2008) Carboxypeptidase A5 identified a novel mast cell lineage in the zebrafish providing new insight into mast cell fate determination. *Blood* 112:2969–2972
5. Da'as S, The EM, Dobson JT, Nasrallah GK, McBride ER, Wang H, Neuberg DS, Marshall JS, Lin T-J, Berman JN (2011) Zebrafish mast cells possess an Fc ϵ RI-like receptor and participate in innate and adaptive immune responses. *Dev Comp Immunol* 35:125–134
6. Blank U, Rivera J (2004) The ins and outs of IgE-dependent mast-cell exocytosis. *Trends Immunol* 25:266–273
7. Johnson AR, Hugli TE, Müller-Eberhard HJ (1975) Release of histamine from rat mast cells by the complement peptides C3a and C5a. *Immunology* 28:1067
8. Wojtecka-Lukasik E, Maslinski S (1992) Fibronectin and fibrinogen degradation products stimulate PMN-leukocytes and mast-cell degranulation. *J Physiol Pharmacol* 43:173–181
9. Prodeus AP, Zhou X, Maurer M, Galli SJ, Carroll MC (1997) Impaired mast cell-dependent natural immunity in complement C3-deficient mice. *Nature* 390:172–175
10. Gommerman JL, Oh DY, Zhou X, Tedder TF, Maurer M, Galli SJ, Carroll MC (2000) A role for CD21/CD35 and CD19 in responses to acute septic peritonitis: a potential mechanism for mast cell activation. *J Immunol* 165:6915–6921
11. Marshall JS (2004) Mast-cell responses to pathogens. *Nat Rev Immunol* 4:787–799
12. Enerbäck L (1966) Mast cells in rat gastrointestinal mucosa. 1. Effects of fixation. *Acta Pathol Microbiol Scand* 66:289–302

13. Enerbäck L (1966) Mast cells in rat gastrointestinal mucosa. 2. Dye-binding and metachromatic properties. *Acta Pathol Microbiol Scand* 66:303–312
14. Bienenstock J, Befus AD, Denburg J, Goodacre R, Pearce F, Shanahan F (1983) Mast cell heterogeneity. *Monogr Allergy* 18:124–128
15. Galli SJ (1990) Biology of disease. New insights into “the riddle of mast cells”: microenvironmental regulation of mast cell development and phenotypic heterogeneity. *Lab Invest* 62:5–33
16. Dvorak AM (2005) Ultrastructural studies of human basophils and mast cells. *J Histochem Cytochem* 53:1043–1070
17. Enerbäck L (1986) Mast cell heterogeneity: the evolution of the concept of a specific mucosal mast cell. In: Befus AD, Bienenstock J, Denburg JA (eds) *Mast cell differentiation and heterogeneity*. Raven, New York, NY, pp 1–26
18. Irani AM, Schechter NM, Craig SS, De Blois G, Schwartz LB (1986) Two types of human mast cells that have distinct neutral protease composition. *Proc Natl Acad Sci U S A* 83: 4464–4468
19. Chiu H, Lagunoff D (1971) Histochemical comparison of frog and rat mast cells. *J Histochem Cytochem* 19:369–375
20. Chieffi Baccari G, De Paulis A, Di Matteo L, Gentile M, Marone G, Minacci S (1998) In situ characterization of mast cells in the frog *Rana esculenta*. *Cell Tissue Res* 292:151–162
21. Izzo Vitiello I, Chieffi Baccari G, Di Matteo L, Rusciani A, Chieffi P, Minucci S (1997) Number of mast cells in the Harderian gland of the lizard *Podarcis sicula sicula* (Raf): the annual cycle and its relation to environmental factors and estradiol administration. *Gen Comp Endocrinol* 107:394–400
22. Baccari GC, Chieffi G, Di Matteo L, Dafnis D, De Rienzo G, Minucci S (2000) Morphology of the Harderian gland of the Gecko, *Tarentola mauritanica*. *J Morphol* 244:137–142
23. Sayed BA, Christy A, Quirion MR, Brown MA (2008) The master switch: the role of mast cells in autoimmunity and tolerance. *Annu Rev Immunol* 26:705–739
24. Metz M, Siebenhaar F, Maurer M (2008) Mast cell functions in the innate skin immune system. *Immunobiology* 213:251–269
25. Reite OB, Evensen O (2006) Inflammatory cells of teleostean fish: a review focusing on mast cells/eosinophilic granule cells and rodlet cells. *Fish Shellfish Immunol* 20:192–208
26. Sottovia-Filho D (1974) Morphology and histochemistry of the mast cells of snakes. *J Morphol* 142:109–116
27. Matsuyama T, Iida T (1999) Degranulation of eosinophilic granular cells with possible involvement in neutrophil migration to site of inflammation in tilapia. *Dev Comp Immunol* 23:451–457
28. Silphaduang U, Noga EJ (2001) Antimicrobials: peptide antibiotics in mast cells of fish. *Nature* 414:268–269
29. Silphaduang U, Colorni A, Noga EJ (2006) Evidence for widespread distribution of piscidin antimicrobial peptides in teleost fish. *Dis Aquat Organ* 72:241–252
30. Campagna S, Saint N, Molle G, Aumelas A (2007) Structure and mechanism of action of the antimicrobial peptide piscidin. *Biochemistry* 46:1771–1778
31. Murray HM, Gallant JW, Douglas SE (2003) Cellular localization of pleurocidin gene expression and synthesis in winter flounder gill using immunohistochemistry and in situ hybridization. *Cell Tissue Res* 312:197–202
32. De Barros CM, Andrade LR, Allodi S, Viskov C, Mourier PA, Cavalcante MCM, Straus AH, Tahahashi HK, Pomin VH, Carvalho VF, Martins MA, Pavão MSG (2007) The hemolymph of the ascidian *Styela plicata* (Chordata-Tunicata) contains heparin inside basophil-like cells and a unique sulfated galactoglucomannan in the plasma. *J Biol Chem* 282:1615–1626
33. Church M, Levi-Schaffer F (1997) The human mast cell. *J Allergy Clin Immunol* 99:155–160
34. Humphries DE, Wong GW, Friend DS, Gurish MF, Qiu WT, Huang C, Sharpe AH, Stevens RL (1999) Heparin is essential for the storage of specific granule proteases in mast cells. *Nature* 400:769–772
35. Forsberg E, Pejler G, Ringvall M, Lunderius C, Tomasini-Johansson B, Kusche-Gullberg M, Eriksson I, Ledin J, Hellman L, Kjellen L (1999) Abnormal mast cells in mice deficient in a heparin-synthesizing enzyme. *Nature* 400:773–776
36. Reite OB (1965) A phylogenetic approach to the functional significance of tissue mast cell histamine. *Nature* 206:1034–1035
37. Takaya K (1969) The relationship between mast cells and histamine in phylogeny with special reference to reptiles and birds. *Arch Histol Jpn* 30:401–420
38. Takaya K, Fujito T, Endo K (1967) Mast cells free of histamine in *Rana catesbeiana*. *Nature* 215:776–777
39. Cavalcante MCM, De Aandrade LR, Du Bocage Santos-Pinto C, Straus AH, Takahashi HK, Allodi S, Pavão MSG (2002) Colocalization of heparin and histamine in the intracellular granules of test cells from the invertebrate *Styela plicata* (chordata-tunicata). *J Struct Biol* 137:313–321

40. Cavalcante MCM, Mourão PA, Pavão MS (1999) Isolation and characterization of a highly sulfated heparin sulfate from ascidian test cells. *Biochim Biophys Acta* 1428:77–87

41. Gianguzza M, Dolcemascolo G (1978) On the ultrastructure of the follicle cells of *Ascidia malaca* during oogenesis. *Acta Embryol Exp* 2:197–211

42. Cavalcante MCM, Allodi S, Valente AP, Straus AH, Takahashi HK, Mourão PAS, Pavão MSG (2000) Occurrence of heparin in the invertebrate *Styela plicata* (Tunicata) is restricted to cell layers facing the outside environment. *J Biol Chem* 275:36189–36196

43. Pancer Z, Cooper MD (2006) The evolution of adaptive immunity. *Annu Rev Immunol* 24: 497–518

44. Féger F, Varadaradjalou S, Gao Z, Abraham SN, Arock M (2002) The role of mast cells in host defense and their subversion by bacterial pathogens. *Trends Immunol* 23:151–157

45. Knight PA, Wright SH, Lawrence CE, Paterson YY, Miller HR (2000) Delayed expulsion of the nematode *Trichinella spiralis* in mice lacking the mucosal mast cell-specific granule chymase, mouse mast cell protease-1. *J Exp Med* 192:1849–1856

46. Terenina NB, Asatrian AM, Movsessian SO (1997) Neurochemical changes in rats infected with *Trichinella spiralis* and *T. pseudospiralis*. *Dokl Biol Sci* 355:412–413

47. Sher A, Hein A, Moser G, Caulfield JP (1979) Complement receptors promote the phagocytosis of bacteria by rat peritoneal mast cells. *Lab Invest* 41:490–499

48. Gilfillan AM, Tkaczyc C (2006) Integrated signalling pathways for mast-cell activation. *Nat Rev Immunol* 6:218–230

49. Miyazawa S, Azumi K, Nonaka M (2001) Cloning and characterization of integrin alpha subunits from the solitary ascidian, *Halocynthia roretzi*. *J Immunol* 166:1710–1715

50. Zhu Y, Thangamani S, Ho B, Ding JL (2005) The ancient origin of the complement system. *EMBO J* 24:382–394

51. Von Köckritz-Blickwede M, Goldmann O, Thulin P, Heinemann K, Norrby-Teglund A, Rohde M, Medina E (2008) Phagocytosis-independent antimicrobial activity of mast cells by means of extracellular trap formation. *Blood* 111:3070–3080

52. Di Nardo A, Vitiello A, Gallo RL (2003) Cutting edge: mast cell antimicrobial activity is mediated by expression of cathelicidin antimicrobial peptide. *J Immunol* 170:2274–2278

53. De Y, Chen Q, Schmidt AP, Anderson GM, Wang JM, Wooters J, Oppenheim JJ, Chertov O (2000) LL-37, the neutrophil granule- and epithelia cell-derived cathelicidin, utilizes formyl peptide receptor-like 1 (FPRL1) as a receptor to chemoattract human peripheral blood neutrophils, monocytes, and T cells. *J Exp Med* 192:1069

54. Scott MG, Davidson DJ, Gold MR, Bowdish D, Hancock RE (2002) The human antimicrobial peptide LL-37 is a multifunctional modulator of innate immune responses. *J Immunol* 169:3883–3891

55. Galli SJ, Nakae S, Tsai M (2005) Mast cells in the development of adaptive immune responses. *Nat Immunol* 6:135–142

56. Galli SJ, Grimaldeston M, Tsai M (2008) Immunomodulatory mast cells: negative, as well as positive, regulators of immunity. *Nat Rev Immunol* 8:445–454

57. Sayed BA, Brown MA (2007) Mast cells as modulators of T-cell responses. *Immunol Rev* 217:53–64

58. Frossi B, Gri G, Tripodo C, Pucillo C (2010) Exploring a regulatory role for mast cells: 'MCregs'? *Trends Immunol* 31:97–102

59. Ritter U, Meissner A, Ott J, Kömer H (2003) Analysis of the maturation process of dendritic cells deficient for TNF and lymphotoxin- α reveals an essential role for TNF. *J Leukoc Biol* 74:216–222

60. Merluzzi S, Frossi B, Gri G, Parusso S, Tripodo C, Pucillo C (2010) Mast cells enhance proliferation of B lymphocytes and drive their differentiation toward IgA-secreting plasma cells. *Blood* 115:2810–2817

61. Hershko AY, Rivera J (2010) Mast cell and T cell communication; amplification and control of adaptive immunity. *Immunol Lett* 128: 98–104

62. Nakae S, Suto H, Iikura M, Kakurai M, Sedgwick JD, Tsai M, Galli SJ (2006) Mast cells enhance T cell activation: importance of mast cell costimulatory molecules and secreted TNF. *J Immunol* 176:2238–2248

63. Kambayashi T, Allenspach EJ, Chang JT, Zou T, Shoag JE, Reiner SL, Caton AJ, Koretzky GA (2009) Inducible MHC class II expression by mast cells supports effector and regulatory T cell activation. *J Immunol* 182:4686–4695

64. Galli SJ, Tsai M, Piliponski AM (2008) The development of allergic inflammation. *Nature* 454:445–454

65. Nakae S, Suto H, Kakurai M, Sedgwick JD, Tsai M, Galli SJ (2005) Mast cells enhance T cell activation: importance of mast cell-derived TNF. *Proc Natl Acad Sci U S A* 102:6467–6472

66. Laird DJ, De Tomaso AW, Cooper MD, Weissman IL (2000) 50 million years of chordate evolution: seeking the origins of adaptive

immunity. Proc Natl Acad Sci U S A 97: 6924–6926

67. Bachelet I, Levi-Schaffer F (2007) Mast cells as effector cells: a costimulating question. Trends Immunol 28:360–365

68. Rihet P, Demeure CE, Bourgois A, Prata A, Dessein AJ (1991) Evidence for an association between human resistance to *Schistosoma mansoni* and high anti-larval IgE levels. Eur J Immunol 21:2679–2686

69. King CL, Xianli J, Malthotra I, Liu S, Mahmoud AA, Oettgen HC (1997) Mice with a targeted deletion of the IgE gene have increased worm burdens and reduced granulomatous inflammation following primary infection with *Schistosoma mansoni*. J Immunol 158:294–300

70. Warr GW, Magon KE, Higgins DA (1995) IgY: clues to the origins of modern antibodies. Immunol Today 16:392–398

71. Caldwell DJ, Danforth HD, Morris BC, Ameiss KA, McElroy AP (2004) Participation of the intestinal epithelium and mast cells in local mucosal immune responses in commercial poultry. Poult Sci 83:591–599

72. Bengtén E, Clem LW, Miller NW, Warr GW, Wilson M (2006) Channel catfish immunoglobulins: repertoire and expression. Dev Comp Immunol 30:77–92

73. McNeil HP, Adachi R, Stevens RI (2007) Mast cell-restricted tryptase: structure and function in inflammation and pathogen disease. J Biol Chem 282:20785–20789

74. Woodbury RG, Neurath H (1980) Structure, specificity and localization of the serine proteases of connective tissues. FEBS Lett 114: 189–196

75. Wernersson S, Reimer JM, Poorafshar M, Karlson U, Wermenstam N, Bengtén E, Wilson M, Pilström L, Hellman L (2006) Granzyme-like sequences in bony fish shed light on the emergence of hematopoietic serine proteases during vertebrate evolution. Dev Comp Immunol 30:901–918

76. Huang C, Sali A, Stevens RL (1998) Regulation and function of mast cell proteases in inflammation. J Clin Immunol 18:169–183

77. Vanderslice P, Ballinger SM, Tam EK, Glodstein SM, Crail CS, Caughey GM (1990) Human mast cell tryptase: multiple cDNAs and genes reveal a multigene serine protease family. Proc Natl Acad Sci U S A 87:3811–3815

78. Miller JS, Westin EH, Schwartz LB (1989) Cloning and characterization of complementary DNA for human tryptase. J Clin Invest 84:1188–1195

79. Miller JS, Moxley G, Schwartz LB (1990) Cloning and characterization of a second complementary DNA for human tryptase. J Clin Invest 86:864–870

80. Thakurdas SM, Melicoff E, Sansores-Garcia L, Moreira DC, Petrova Y, Stevens RL, Adachi R (2007) The mast cell-restricted tryptase mMCP-6 has a critical immunoprotective role in bacterial infections. J Biol Chem 282: 20809–20815

81. Shin K, Watts GF, Oettgen HC, Friends DS, Pemberton AD, Gurish MF, Lee DM (2008) Mouse mast cell tryptase mMCP-6 is a critical link between adaptive and innate immunity in the chronic phase of *Trichinella spiralis* infection. J Immunol 180:4885–4891

82. Orinska Z, Maurer M, Mirghomizadeh F, Bulanova E, Metz M, Nashkevich N, Schiemann F, Schulmistrat J, Budagian V, Giron-Michel V, Brandt E, Paus R, Bulfone-Paus S (2007) IL-15 constrains mast cell-dependent antibacterial defences by suppressing chymase activities. Nat Med 13:927–934

83. Ruoss SJ, Hartmann T, Caughey GH (1991) Mast cell tryptase is a mitogen for cultured fibroblasts. J Clin Invest 88:493–499

84. Cairns JA, Walls AF (1997) Mast cell tryptase stimulate the synthesis of type I collagen in human lung fibroblasts. J Clin Invest 99: 1313–1321

85. Gruber BL, Kew RR, Jelaska A, Marchese MJ, Garlick J, Ren S, Schwartz WB, Korn JH (1997) Human mast cells activate fibroblasts. J Immunol 158:2310–2317

86. Blair RJ, Meng H, Marchese MJ, Ren S, Schwartz LB, Tonnesen MG, Gruber BL (1997) Tryptase is a novel, potent angiogenic factor. J Clin Invest 99:2691–2700

87. Trivedi NN, Tong Q, Raman K, Bhagwandin VJ, Caughey GH (2007) Mast cell α and β tryptases changed rapidly during primate speciation and evolved from γ -like transmembrane peptidases in ancestral vertebrates. J Immunol 179:6072–6079

88. Hirose E, Shirae M, Saito Y (2003) Ultrastructures and classification of circulating hemocytes in 9 botryllid ascidians (Chordata: Ascidiacea). Zoolog Sci 20:647–656

89. Hirose E, Taneda Y, Ishii T (1997) Two modes of tunic cuticle formation in a colonial ascidian *Aplidium yamazii*, responding to wounding. Dev Comp Immunol 21:25–34

Chapter 3

Mast Cell Development and Function in the Zebrafish

Sahar I Da'as, Tugce B. Balci, and Jason N. Berman

Abstract

The many advantages of the zebrafish model provide a unique opportunity to integrate the tools of developmental embryology, transgenesis, and functional assays to elucidate the molecular pathways underlying hematopoiesis and for modeling human blood diseases. These methodologies have recently been applied to the zebrafish mast cell lineage and have resulted in a better understanding of vertebrate mast cell biology. By employing whole-mount *in situ* hybridization alone and in combination with co-localization approaches, fluorescence-activated cell sorting (FACS), and morpholino gene knockdown studies, new insights into early mast cell transcriptional regulation and ontogeny have been exposed *in vivo*. Transgenic strategies have permitted the modeling of human mast cell diseases, like systemic mastocytosis in zebrafish, which can subsequently be exploited for high-throughput chemical screens to identify potential therapies in these conditions. Mast cell functional assays have been adapted to zebrafish providing the opportunity to utilize this model for interrogating the cellular players in innate and adaptive immunity and as a live animal readout for drug responses in allergic and inflammatory reactions. These techniques are detailed in the following chapter.

Key words Zebrafish, Mast cells, Carboxypeptidase A5, Flow cytometry, Morpholino, Cardiac puncture, *In situ* hybridization, Transgenesis, Fc ϵ R, KIT, Tryptase, Mastocytosis

1 Introduction

The zebrafish has emerged as a robust and versatile model system for studying vertebrate hematopoiesis, by virtue of conserved genetics and the accessibility provided by large numbers of transparent embryos that are produced externally [1, 2]. Recently, we have shown that the opportunities afforded by the zebrafish for studying other hematopoietic lineages can be effectively applied to studying mast cell biology [3, 4]. This discovery is timely with the continued growth of this model for better understanding of the complexity of both innate and adaptive immune responses [5–7]. The zebrafish is amenable to a number of genetic manipulations that provide rapid phenotypic *in vivo* data that have greatly contributed to our understanding of mast cell development and the factors underlying mast cell fate determination. By optimizing whole-mount RNA *in situ*

hybridization (WISH) and innovatively combining this approach with fluorescence-activated cell sorting (FACS), we identified carboxypeptidase A5 (*cpa5*) as a zebrafish mast cell-specific marker [3, 33]. We subsequently employed this marker as a readout for mast cells in embryos in combination with other analytical techniques including WISH co-localization, morpholino oligonucleotide gene knockdown studies, and chemical inhibition assays. These approaches enabled us to establish *gata2* and *pu.1* as the key transcription factors necessary for early mast cell development, with upstream regulation directed through notch signaling and particularly *notch1b*. Definitive mast cells were also found to arise from the transient erythromyeloid progenitor (EMP) population followed by a gradual transition to hematopoietic stem cells (HSCs), which serve as the cells of mast cell origin for the duration of the life of the zebrafish [8]. These experiments set the stage for using the zebrafish model as a platform for further detailed characterization of the development of the mast cell lineage in vertebrates.

Systemic mastocytosis is a human myeloproliferative neoplasm that can arise from perturbed mast cell development and proliferation [9]. While systemic mastocytosis encompasses a wide spectrum of clinical phenotypes, aggressive forms of the disease include visceral organ involvement with the potential to evolve into mast cell leukemia. These more severe manifestations are currently without curative therapy. As has been demonstrated for other human hematopoietic malignancies, the zebrafish holds tremendous potential to serve as an efficient *in vivo* tool for use in high-throughput chemical screens [10–13] to identify novel therapies effective in mast cell diseases. We have been modeling systemic mastocytosis in two ways: Given the roles we have identified for the notch signaling pathway in mast cell development, we have employed notch overexpressing transgenic fish lines by breeding *hsp70::GAL4* or *mitfa::GAL4* and *UAS::nicd1a* together and activating notch transcription by heat shock. These fish have been found to have an abundance of *cpa5*-labeled mast cells [8] (and unpublished data). We have also employed the Gateway cloning system (Invitrogen, Carlsbad, CA) to generate stable transgenic lines expressing the human *KIT* D816V mutation, found commonly in human systemic mastocytosis, under the control of the zebrafish ubiquitous β -*actin* promoter together with an *eGFP* reporter [34]. These transgenic embryos display an apparent block in G2/M phase transition by phosphohistone H3 labeling and decreased expression of DNA methyltransferase 1 (*dnmt1*), as well as reduced expression of epithelial cell adhesion molecule (*epcam*), and decreased neuromast numbers. Adult fish succumb at only several months of age, developing skin and visceral lesions, some containing an abundance of mast cells. Both these models are amenable to targeted (e.g., notch inhibitor) and unbiased small-molecule screens for agents that restore a wild-type embryonic phenotype.

To evaluate phenotypes in adult zebrafish, we have adapted and established the utility of a number of histochemical (hematoxylin and eosin, periodic acid–Schiff, toluidine blue) and immunohistochemical (KIT, tryptase, antihuman Fc ϵ RI γ) stains to identify mast cells in zebrafish tissues, such as the gastrointestinal mucosa and gills, which are abundant in mast cells like their mammalian counterparts [3, 4]. The chromogenic tryptase assay is the most reliable technique for measuring mast cell degranulation, and we have used this approach to document response to direct mast cell stimulants such as Compound 48/80, as well as innate immune responses to *Aeromonas salmonicida* infection and adaptive immune responses to passive systemic anaphylaxis employing matched di- and trinitrophenyl-specific antibodies and substrates administered by intraperitoneal injection [4]. Transmission electron microscopy can be employed to examine intracellular structures, including the composition of granules in both resting and activated mast cells [3, 4]. These assays provide the basis for characterizing the phenotype in adult zebrafish models of diseases of perturbed mast cell development and proliferation, as described above. In addition, evidence for conserved components of the mast cell functional “apparatus” in zebrafish, such as an analogous high-affinity immunoglobulin E (IgE)-like receptor and the ability to abrogate responses to irritant and infectious stimuli using clinically relevant agents like ketotifen [4], highlight the feasibility of this model system as a novel *in vivo* tool for elucidating mechanisms underlying the role of mast cells in allergic and inflammatory reactions.

The zebrafish model provides a unique opportunity to integrate the tools of transgenesis, experimental embryology, and functional studies to allow a considerably broad understanding of mast cell biology. Amenable to diverse transgenic approaches, the zebrafish can be exploited in different ways to create fluorescent reporter lines and models of human diseases. In our efforts to use zebrafish as a tool for studying human systemic mastocytosis, the ultimate goal is to employ these transgenic lines for high-throughput small-molecule chemical screens. The zebrafish is inherently suited for these types of screens on account of their small size, large numbers, and robust phenotypic readouts, permitting a more rapid and cost-effective methodology than is possible in mammalian model systems. These screens can easily identify compounds specifically affecting signaling pathways, development, or disease processes. The zebrafish has increasingly been used as this type of platform and has produced promising results in several disease models [10, 11], including hematopoietic malignancies [13].

Reporter lines provide the advantage of labeling individual cell populations and monitoring them during specific activities throughout their life span. These cells can subsequently be sorted by FACS-based approaches, and these lines can be crossed with

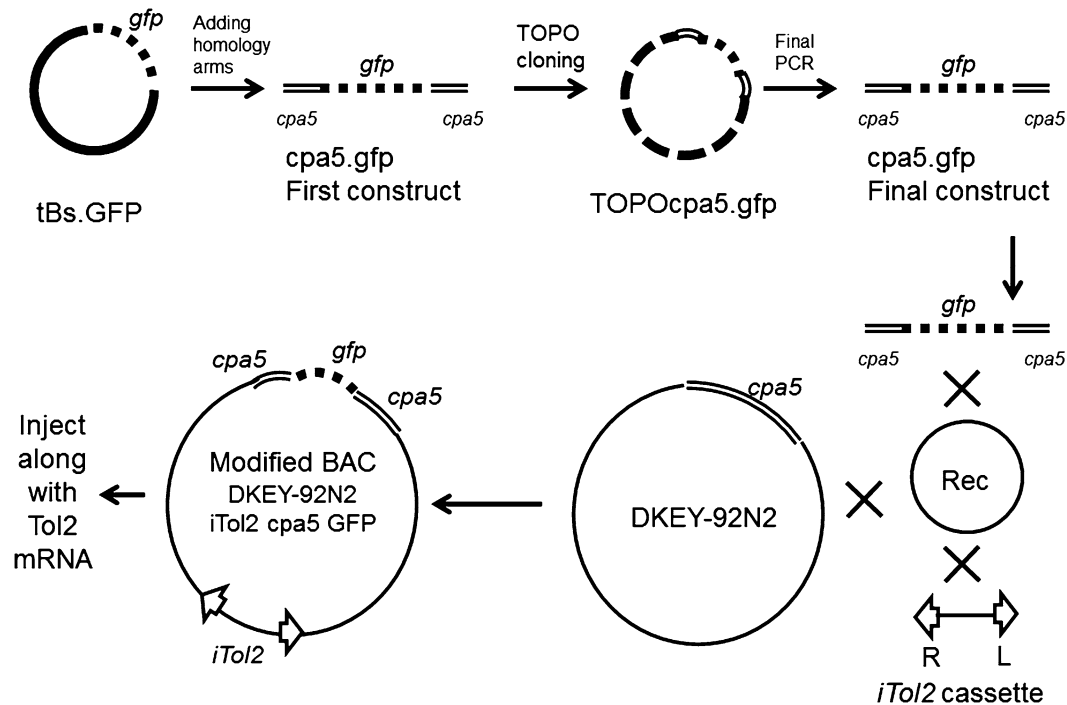


Fig. 1 BAC transgenesis approach for carboxypeptidase A5 promoter (*cpa5*)

other reporter lines to facilitate studies of cellular ontogeny, migration, and interaction [14–17]. With the zebrafish genome sequencing project almost complete and several bacterial artificial chromosome (BAC) libraries available, BAC transgenesis techniques are now being applied to complement more traditional approaches. In order to generate a mast cell reporter line, a BAC-based strategy that has been gaining popularity in the zebrafish field [18, 19] is currently being employed. The technique is based on modifying the BACs using targeting cassettes followed by a recombination step which places *GFP* or *Gal4* reporters under the control of the zebrafish mast cell-specific *cpa5* promoter and BAC regulatory elements (Fig. 1) [19, 20]. More recently, strategies involving the clustered, regularly interspaced, short palindromic repeat (CRISPR) - Cas9 system have facilitated the insertion of fluorescent tags at specific sites in the genome, providing an alternative approach to generating a mast cell reporter lines [35]. A zebrafish mast cell reporter line could eventually be used to specifically show interactions of mast cells with other cell types in immunological or neoplastic processes. Xenotransplantation of human cancer cells into zebrafish has demonstrated the utility of this model for rapid analysis of tumor cell proliferation and response to drugs [36]. In our laboratory, we have established the xenotransplantation of leukemia cell lines and developed a robust cell proliferation assay demonstrating *in vivo* targeted therapeutic inhibition.

of these xenografted cells in zebrafish embryos [21]. This method is readily being applied to solid tumors, such as sarcomas, to provide insight into tumor cell invasion and metastatic behavior [22]. A mast cell reporter line has the potential to be incorporated into the xenotransplantation model to reveal the contributions of mast cells during invasion and metastasis, which in turn may shed light on the intricate relations at play in the inflammatory niche of a tumor. In support of this contention, previous studies using reporter lines in zebrafish embryos have already provided new insights into the response of tumor cells to other myeloid cells and drawn parallels between tumor- and wound-mediated inflammation [23]. Additionally, the mast cell reporter line would also make possible the isolation, culturing, and clonal analysis of zebrafish mast cells [24], providing further potential for the exploration of mast cell biology by enabling the application of established mast cell *in vitro* assays to zebrafish mast cell cultures.

2 Materials

All solutions listed in this section are prepared in distilled and deionized water (ddH₂O) or were purchased as manufacturer-prepared solutions or reagents unless otherwise indicated.

2.1 Equipment

1. 28.5 °C incubator (humidified air).
2. 65 °C incubator.
3. Micropipette.
4. Microcentrifuge.
5. Centrifuge.
6. Hybridization oven (65 °C).
7. Benchtop vortex mixer.
8. Gentle shaker.
9. Humidified chamber.
10. Stereomicroscope.
11. Inverted microscope.
12. Fluorescence-activated cell sorting (FACS) instrument (e.g., FACSaria, BD Biosciences, Canada).
13. 96-well microplate ELISA reader (e.g., BIO-RAD 680 microplate reader).
14. Western blot apparatus.
15. Electron microscope.

2.2 Adult Zebrafish and Embryos

1. Adult wild-type, transgenic, and mutant zebrafish were maintained in tanks with 28.5 °C water (pH 6–8) with a salinity of 1,100–1,300 mS. Fish are exposed to 14 h light per day.

2. Mating tanks with dividers.
3. Egg water: 5 mM NaCl, 0.17 mM KCl, 0.4 mM CaCl₂, 0.16 mM MgSO₄.
4. 0.003 % PTU: 1-phenyl-2-thiourea (Sigma-Aldrich, St. Louis, MO).
5. 10 mg/mL pronase (Roche, Indianapolis, IN, USA).
6. Phosphate-buffered saline (PBS).
7. 4 % paraformaldehyde (PFA) prepared in PBS.
8. PBS-T: 0.1 % Tween-20 (v/v) in PBS.
9. Transfer pipettes (wide opening).
10. Injection plate (*see* Subheading 3.19.)
11. Thin-wall glass microinjection capillaries with filaments (dimensions: 100 mm length, 1.0 mm outer diameter, 0.75 mm inner diameter (e.g., TW100F-4 World Precision Instruments, Inc. Sarasota, FL)).
12. 10 mg/mL Proteinase K (Sigma-Aldrich, St. Louis, MO).
13. Fish anesthesia: 4 mg/mL ethyl 3-aminobenzoate methanesulfonate (Tricaine-MS-222) (Sigma-Aldrich, St. Louis, MO).

2.3 RNA Probe Labeling

1. Plasmid DNA.
2. Restriction enzymes.
3. QIAquick PCR Purification Kit (Qiagen, Toronto, ON, Canada).
4. T7 RNA Polymerase (Roche, Indianapolis, IN, USA).
5. RNase Inhibitor 2,000 U (Roche, Indianapolis, IN, USA).
6. Digoxigenin (DIG) and fluorescein (FITC) RNA labeling mix (Roche, Indianapolis, IN, USA).
7. NucAway spin columns (Ambion, Applied Biosystems, Streetsville, ON, Canada).
8. RNase- and DNase-free sterile distilled water.

2.4 Whole-Mount *In Situ* Hybridization (WISH)

1. 5× SSC (saline sodium citrate buffer): 43.8 g sodium chloride, 22 g sodium citrate (dihydrate) in ~950 mL ddH₂O. Adjust to pH 7 with concentrated HCl and add ddH₂O to 1 L.
2. SSC-T: 1× SSC, 0.1 % Tween-20.
3. Hyb(−) solution: 50 % formamide, 5× SSC-T. Store at −20 °C.
4. Hyb(+) solution: 50 % formamide, 5× SSC-T, 500 mg/mL torula yeast RNA type IV, 50 µg/mL heparin. Store at −20 °C.
5. Maleic acid buffer-Tween (MAB-T): 100 mM maleic acid, 150 mM NaCl, 10 % Tris base, 0.1 % Tween-20.
6. Blocking solution: 10 % FBS, 2 % blocking reagent for nucleic-acid hybridization (Roche, Indianapolis, IN, USA) prepared in MAB-T.

7. Anti-DIG or anti-FITC Fab fragments from sheep coupled to peroxidase (POD) (Roche, Indianapolis, IN, USA).
8. Fast Red tablets (Roche, Indianapolis, IN, USA).
9. Alkaline phosphate substrate: BCIP/NBT (5-bromo-4-chloro-3-indolyl phosphate/nitroblue tetrazolium) (Vector Laboratories, Inc. CA, USA).

2.5 Embryo Dissociation

1. 10 mM dithiothreitol (DTT) in egg water.
2. Embryo dissociation buffer: 0.28 Wünsch U/mL Blendzyme 3 (Roche, Indianapolis, IN, USA) in 1× Hank's buffered saline (HBSS) with 5 mM CaCl₂.
3. 40 µm strainer (BD Falcon, Becton Dickinson, NJ, USA).
4. 0.9× PBS supplemented with 5 % heat-inactivated fetal bovine serum (HI-FBS).

2.6 Morpholinos

1. We use oligonucleotides designed and purchased from Gene Tools, LLC (Philomath, OR).

2.7 Chemical Treatment of Embryos

1. Gamma-secretase inhibitor. Prepare a 1 mM stock of Compound E (Alexis Biochemicals, San Diego, CA) in DMSO. Store at -20 °C.

2.8 Cloning (Gateway®)

1. Multisite Gateway® Pro cloning kit (Invitrogen, Burlington, ON, Canada).

2.9 Histochemical Staining

1. 10 % neutral buffered formalin.
2. 5 µm sections of zebrafish intestine or gills.
3. 1 % (w/v) toluidine blue stock solution: 1 g toluidine blue O dissolved in 100 mL of 70 % EtOH (in water).
4. 1 % sodium chloride (NaCl) solution: 0.5 g NaCl in 50 mL of ddH₂O. Make this solution fresh every time. Adjust pH to 2.0–2.5.
5. Toluidine blue working solution: 5 mL toluidine blue stock solution in 45 mL 1 % NaCl solution (pH 2.0–2.5). Mix well and discard after use.
6. Hematoxylin staining solution: Accustain® Harris' hematoxylin solution.
7. Eosin solution: 2 g of eosin Y disodium salt in 200 mL ddH₂O, 4 mL glacial acetic acid, 600 mL 95 % EtOH.
8. Xylene.
9. 100, 95, and 70 % ethanol (EtOH) diluted in MilliQ water.
10. Gill's hematoxylin (Surgipath Leica, Wetzlar, Germany).
11. Scott's tap water substitute: Add 3.1 g NaHCO₃ and 17.8 g MgSO₄ to 1 L tap water. Add a crystal of thymol (2-isopropyl-5-methylphenol) to prevent the growth of mold and bacteria.

12. 1 % alcoholic eosin (Surgipath, Leica, Wetzlar, Germany).
13. Glycerol Gelatin (Sigma-Aldrich, St. Louis, MO).
14. McManus periodic acid-Schiff (PAS).
 - (a) 1 % periodic acid.
 - (b) *Cold* Schiff's reagent: 1 % (w/v) basic fuchsin, 3.8 % (w/v) sodium metabisulfite in 0.25 N HCl. Shake vigorously and dissolve overnight, add several teaspoons of activated charcoal. Shake well for 2 min, let stand for 5 min, filter, and refrigerate.
15. Fast Red stain: Add one Fast Red tablet to 2 mL of 0.1 M Tris (pH 8.5). Full dissolution requires vigorous vortex mixing.
16. BCIP/NBT stain: Add two drops of reagent 1–5 mL of 0.1 M Tris (pH 9.5), invert to mix. Then add two drops of reagent 2 (invert to mix) followed by two drops of reagent 3 (invert to mix).

2.10 Immunohisto-chemistry

1. 0.01 M sodium citrate buffer (pH 6.1): 2.58 g sodium citrate (dihydrate) in 1 L ddH₂O.
2. 3 % hydrogen peroxide in PBS: 3 mL (30 % H₂O₂) in 27 mL of PBS.
3. 5 % (v/v) normal goat serum in PBS.
4. Antihuman Fc ϵ RI γ polyclonal rabbit IgG (Millipore, Billerica, MA) diluted to 1:400 in PBS.
5. Biotinylated goat anti-rabbit IgG diluted in PBS (1:600).
6. Diaminobenzidine (DAB) (Vectastain ABC Kit, Vector Laboratories, Burlingame, CA).
7. Mayer's hematoxylin (Sigma-Aldrich, St. Louis, MO).
8. Isotype control consisting of non-immunized rabbit IgG (Cedarlane Laboratories, Hornby, ON, Canada).
9. Cytoseal (Richard-Allan Scientific, Kalamazoo, MI).

2.11 Electron Microscopy

1. 0.1 M sodium cacodylate buffer: 1.78 g sodium cacodylate trihydrate ((CH₃)₂AsO₂Na · 3H₂O) in ddH₂O.
2. 2.5 % glutaraldehyde prepared in 0.1 M sodium cacodylate buffer.
3. 1 % osmium tetroxide.
4. 100 % epon araldite resin.
5. 2 % aqueous uranyl acetate.
6. 0.25 % uranyl acetate.
7. 0.3 % lead citrate.

2.12 Mast Cell Responses to Stimuli

1. 0.07 % bromophenol blue in isotonic saline.
2. Compound 48/80.
3. Live *Aeromonas salmonicida* in a final concentration of 5×10^9 cfu/mL.
4. 1× PBS.
5. Ketotifen fumarate salt (Sigma-Aldrich, St. Louis, MO).
6. $\text{Na}^{\alpha}\text{-Benzoyl-DL-arginine } p\text{-nitroanilide}$ (BAPNA) [25].
7. Human LAD2 mast cell line.

2.13 Protein Extraction and Immunoblotting

1. Ringer's solution: 5 mM HEPES (pH 7.2), 116 mM NaCl, 2.9 mM KCl, 1.8 mM CaCl₂ in 0.5 L ddH₂O.
2. Lysis buffer #1: 1 % Nonidet P-40, 0.1 % SDS, 100 mM NaCl, 50 mM Tris (pH 7.4–7.7) in 25 mL H₂O. Prepare in advance and store at 4 °C.
3. Lysis buffer #2: 50 mM NaF, 1 mM Na₃VO₄, one tablet complete mini protease inhibitor with EDTA (Roche, Indianapolis, IN, USA). Add lysis buffer #1 to a total volume of 5 mL.

3 Methods

3.1 Embryo Dechorionation

1. Reduce the egg or PTU water to a minimal volume where embryos can still move freely in the dish when swirled.
2. Add 0.5 µg of pronase (warmed to 28.5 °C) into the Petri dish and incubate for 10–15 min at 28.5 °C. Gentle pronase treatment progressively softens the chorion without damaging the embryos (see Note 1). Embryos can be dechorionated by gentle pipetting using 2.5 mL transfer pipette. Alternatively, embryos can be dechorionated by hand using sharpened forceps, but this is a slow process, which can be used only for a small quantity of embryos.
3. After the incubation, gently rinse the embryos at least five times with egg or PTU water.
4. Let the embryos develop at 28.5 °C until they reach the required stage.

3.2 Embryo Fixation

1. Stage the zebrafish embryos according to Westerfield [26].
2. Transfer dechorionated embryos into 1.5 mL microfuge tubes.
3. Wash embryos with PBS-T. Do one quick wash and then wash once for 5 min on shaker. Replace with 1 mL fresh PBS-T.
4. Treat the embryos with Proteinase K (10 mg/mL stock solution) as appropriate for the developmental stage as shown in Table 1.

Table 1
Recommended Proteinase K concentrations and treatment times appropriate for developmental stage of zebrafish embryos

Embryo stage	Proteinase K treatment
<30 hpf	Not needed or 10 µg/mL, 10 min (1 µL stock in 1 mL PBST)
30 hpf	30 µg/mL, 10 min (3 µL stock in 1 mL PBST)
35–52 hpf	50 µg/mL, 20 min (5 µL stock in 1 mL PBST)
53 hpf+	100 µg/mL, 20 min (10 µL stock in 1 mL PBST)
5 dpf+	100 µg/mL, 30 min (10 µL stock in 1 mL PBST)
7 dpf+	100 µg/mL, 45 min (10 µL stock in 1 mL PBST)

hpf=hours postfertilization, dpf=days postfertilization

5. Wash embryos with PBS-T. Do one quick wash and then wash once for 5 min on shaker. Replace with 1 mL fresh PBS-T.
6. Add 1.5 mL of 4 % PFA and fix on the shaker overnight at 4 °C (embryos can be stored in 4 % PFA up to 6 weeks).
7. Wash embryos by aspirating the PFA.
8. Wash embryos with PBS-T. Do one quick wash and then wash once for 5 min on shaker. Replace with 1 mL fresh PBS-T.
9. Add enough 100 % methanol (MeOH) to cover embryos. Cap and mix gently.
10. Incubate at -20 °C for at least 30 min.
11. Aspirate and replace with fresh 100 % MeOH.
12. Embryos can be stored indefinitely in 100 % MeOH at -20 °C.

3.3 RNA Probe Preparation

Plasmid Linearization

The following example methods are for generation of a probe to detect expression of zebrafish mast cell-specific marker, carboxypeptidase A5 (*cpa5*) *in situ*.

1. Linearize 2–5 µg plasmid DNA using appropriate restriction enzyme. Mix 2–5 µg of linear DNA (e.g., pBK-CMV-*cpa5* plasmid) with 2 µL 10x restriction enzyme buffer and 2 µL restriction enzyme (e.g., *Bam*HI). Add DEPC-treated or DNase/RNase-free water for a total reaction volume of 20 µL. Let the digestion reaction incubate for 2 h at 37 °C.
2. Clean the linear DNA product using QIAquick PCR Purification Kit according to manufacturers' protocol.
3. Resuspend DNA in 30 µL of DEPC-treated, RNase-free water. Let it sit for 1 min.
4. Run 1–2 µL of digested DNA on agarose gel to make sure the DNA is linear.

3.3.1 Probe Labeling Reaction

1. Prepare a DIG- or FITC-labeled probe using the linearized DNA template. Mix 1–3 μ L linearized DNA (2 μ g) with 1 μ L RNase inhibitor, 2 μ L 10 \times DIG or FITC RNA labeling mix (see Note 2), 2 μ L 10 \times transcription buffer and 2 μ L T7 (or SP6) DNA polymerase. Add nuclease free water for a total reaction volume of 20 μ L. Incubate at 37 °C for 4 h.
2. Optional: Add 1 μ L 10 \times Turbo DNase I and incubate for 15 min at 37 °C.
3. Purify probe using Ambion NucAway spin columns according to manufacturers' protocol.
4. Check 2 μ L of the probe on an agarose gel.
5. Add 1 μ L of RNase Inhibitor (40 U/ μ L) to the completed probe.
6. Store labeled probes at -20 or -80 °C.

3.4 Whole-Mount *In Situ* Hybridization (WISH) (See Fig. 2)

Day 1: Hybridization

1. Gently wash embryos (steps 2–7 below) before performing the *in situ* hybridization (see Note 3). During these washes preheat the Hyb(–) and Hyb(+) solutions in the 65 °C incubator.
2. For embryos stored in 100 % MeOH (see Subheading 3.2), aspirate MeOH and replace with 75 % MeOH/PBS-T, wash for 5 min at room temperature (RT).
3. Repeat step 3 with 50 % MeOH/PBS-T and then again with 25 % MeOH/PBS-T.
4. Aspirate and wash twice for 5 min with PBS-T.
5. For embryos stored in paraformaldehyde (4 % PFA) (see Subheading 3.2), wash briefly but carefully in PBS-T at RT. Embryos should be kept in PFA at 4 °C at least overnight for best results.
6. Prehybridize in 1 mL of Hyb(–) for at least 15 min in a 65 °C incubator with gentle rocking.
7. Replace Hyb(–) with 300 μ L Hyb(+) and incubate in a 65 °C incubator with gentle rocking for 1 h.
8. Add labeled probe to Hyb(+) (4 μ L or more if the probe is weak) and incubate overnight in 65 °C incubator with gentle shaking (see Note 4).

Day 2: Washing, Blocking, and 2° Antibody

9. Collect the probe solution, and store at -20 °C for a later use (probes in Hyb(+) solution can be used for a total of three times).

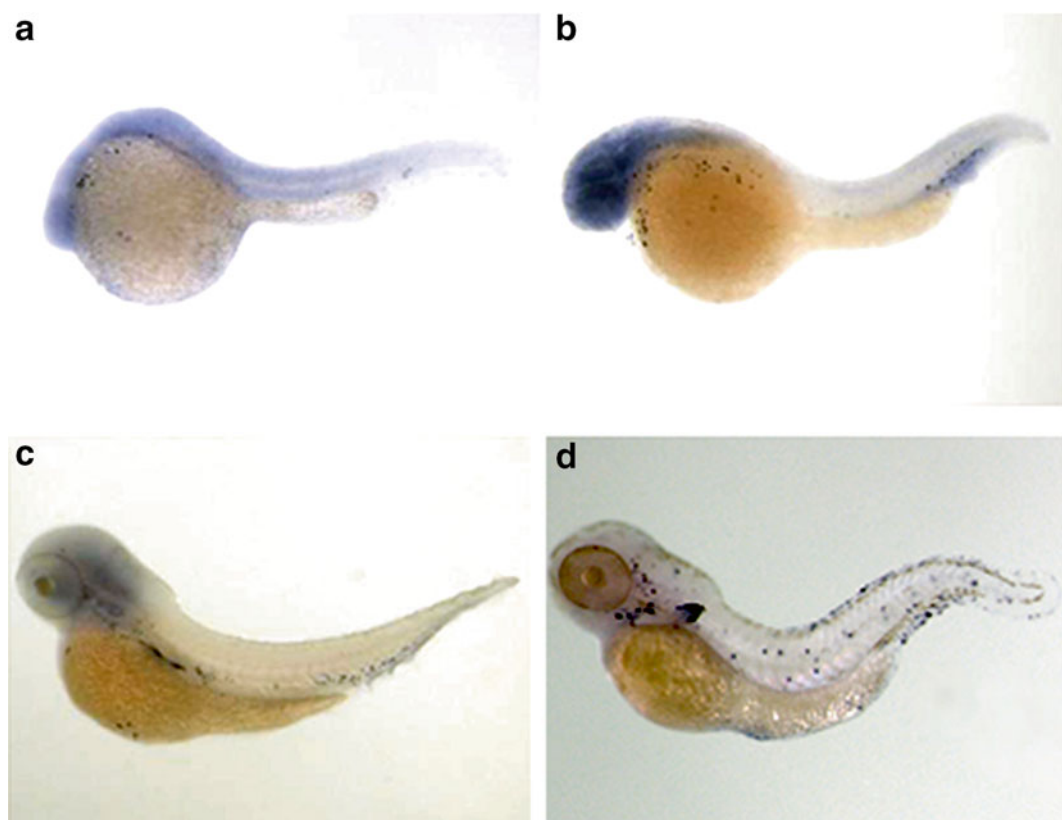


Fig. 2 A time course of *cpa5* expression from 24 hpf to 5 dpf. Expression is observed in white blood cells at the sites of primitive embryonic hematopoiesis (anterior paraxial mesoderm (ALPM) and intermediate cell mass (ICM)) and in circulation. *cpa5* expression begins at 24 hpf (a), peaks at 28 hpf (b) and then remains present through to 72 hpf (c) and 5 dpf (d) (Objective 5 \times). This research was originally published in *Blood*. Dobson, J.T., Seibert, J., Teh, E.M., Da'as, S., Fraser, R.B., Paw, B.H., Lin, T.J., and Berman, J.N. Carboxypeptidase A5 identifies a novel mast cell lineage in the zebrafish providing new insight into mast cell fate determination. *Blood* 112:2969–2972. © The American Society of Hematology

10. Wash embryos in 65 °C incubator as follows:
 - (a) Wash twice with 1 mL of 2 \times SSC-T in 50 % formamide (15 min each wash).
 - (b) Wash once with 2 \times SSC-T (15 min).
 - (c) Wash twice with 0.2 \times SSC-T (15 min each wash).
11. Wash embryos at RT on a gentle shaker three times with MAB-T (5 min per wash).
12. Prepare the blocking solution: 10 mL of 10 % blocking medium, 5 mL of heat-inactivated FBS, 35 mL of MAB-T. Store any unused blocking solution at 4 °C for washes on day 3.
13. Block in 1 mL of in situ blocking solution. Shake gently at RT for 1 h.

14. Add 0.5 μ L 2° antibody (POD-coupled anti-DIG or anti-FITC Fab) to blocking solution and incubate 2° antibody overnight at 4 °C on a gentle shaker.

Day 3: Detection

15. The following steps are performed at RT with gentle shaking (*see Note 5*).
16. Wash once with *in situ* blocking solution (15 min).
17. Coat transfer pipette in MAB-T to be sure that the embryos will not stick into the transfer pipette. Carefully transfer embryos to new wells in 12-well plate.
18. Wash twice with MAB-T (15 min each).
19. Wash four times (5 min each) with the appropriate buffer. For example, if staining with BCIP/NBT wash with 0.1 M Tris (pH 9.5). If staining with Fast Red, wash with 0.1 M Tris (pH 8.2).
20. Embryo staining
 - (a) BCIP/NBT stain: For two groups of embryos; mix 5 mL of 0.1 M Tris pH 9.5. Add two drops reagent 1, invert to mix. Add two drops reagent 2, invert to mix. Add two drops reagent 3, invert to mix. Develop at RT with gentle shaking in the dark (cover with aluminum foil). Examine after 1.5 h and, if necessary, every 30 min thereafter.
 - (b) Fast Red stain: Add 3 tablets per 6 mL to 0.1 M Tris (pH 8.5) and mix vigorously to dissolve. This is sufficient volume for staining two groups of embryos. Add Fast Red staining solution to the embryos and develop at 37 °C for 2 h then replace with fresh Fast Red and let it shake overnight at 4 °C. Alternatively, incubate at 37 °C for 4 h, then check for staining (this will save you 1 day).
21. Stop the reaction by washing with PBS-T at RT for 5 min (*see Note 6*).
22. Stained embryos (e.g., Fig. 2) are now ready to view under the microscope (*see Note 7*).

3.5 Co-Localization Studies Using Double WISH

Perform all steps as previously mentioned in Subheading 3.4 except for the following modifications:

Day 1: Hybridization

1. Add both DIG- and FITC-labeled probes to Hyb(+) (4 μ L each or more if the probe is weak) and incubate overnight at 65 °C with gentle shaking.

Day 2: Washing, Blocking, and 2° Antibody

2. Add 0.5 μ L 2° antibody of the first probe (e.g., anti-DIG or anti-FITC) to the 1 mL blocking solution.

Day 3: Detection of the First Probe

3. Use Fast Red stain as in Subheading 3.4.

Day 4: Washing, Blocking, and 2° Antibody

4. Incubate in 1 \times MAB with 10 mM EDTA at 60 °C for 10 min (inactivation).
5. Wash three times (5 min each wash) with MAB-T at RT with gentle shaking.
6. Block in 1 mL in situ blocking solution (as in Subheading 3.4, step 20). Shake gently at RT for 1 h.
7. Add 0.5 μ L 2° antibody of the second probe, anti-DIG or anti-FITC to the 1 mL blocking solution.

Day 5: Detection of the Second Probe

8. Stain with BCIP/NBT as in Subheading 3.4.

3.6 Co-localization Studies Using Double Fluorescent Whole-Mount RNA In Situ Hybridization (WISH)

Perform all steps as previously mentioned in the section of double WISH except for the following modifications:

Day 2: Washing, Blocking, and 2° Antibody

1. Add 0.5 μ L 2° antibody of the first probe, anti-DIG to the 1 mL blocking solution.

Day 3: Detection for the First Probe

2. Use Fast Red stain as in Subheading 3.4.

Day 4: Washing, Blocking, and 2° Antibody

3. Incubate in 1 \times MAB with 10 mM EDTA in a 60 °C incubator for 10 min (inactivation).
4. Washes at RT on a gentle shaker.
5. Wash three times with MAB-T (5 min each wash).
6. Blocking: Add 0.5 μ L 2° antibody of the second probe, anti-FITC to the 1 mL blocking solution.

Day 5: Imaging

7. Wash once with in situ blocking solution for 15 min.
8. Coat transfer pipette in MAB-T to be sure that the embryos will not stick into the transfer pipette. Carefully transfer embryos to net wells in 12-well plate.
9. Wash twice with MAB-T (15 min each wash).

10. Wash once with PBS-T (5 min).
11. View under the microscope for imaging.
12. Embryos can be stored in 4 % PFA at 4 °C.

3.7 Combination Fluorescence-Activated Cell Sorting (FACS) and WISH Fig. 3

Perform all steps as previously mentioned in the section of WISH except for the following modifications:

Day 1: Hybridization

1. Add FITC-labeled probe to Hyb(+) (4 µL or more if the probe is weak) and incubate overnight in 65 °C incubator with gentle shaking.

Day 2: Washing, Blocking, and 2° Antibody

2. Add 0.5 µL 2° anti-FITC antibody to the 1 mL blocking solution.

Day 3: Detection for the First Probe

3. Use Fast Red stain as in Subheading 3.4.

Day 4: Dissociation of Embryos for FACS

4. Incubate approximately 100 embryos in 10 mM dithiothreitol (DTT) in egg water for 30 min at RT with gentle shaking.
5. Dissociate in embryo dissociation buffer (Subheading 2.5, step 2) for 2–3 h on shaker in 37 °C incubator, vortex every 30 min.
6. Prepare ice-cold 0.9× PBS supplemented with 5 % HI-FBS in pre-coated 50 mL tubes.
7. Pour coating buffer 0.9× PBS with 5 % FBS into two tubes (15 mL): one tube for sorting and one tube (5 mL) for cell suspension.
8. Filter the cell suspension using 40 µM cell strainer into coated 50 mL tube.
9. Centrifuge 10 min at 4,500×*g* speed.
10. Discard supernatant and resuspend pellet in 1,000 µL 0.9× PBS with 5 % FBS.
11. Store at 4 °C wrapped with foil for FACS sorting.
12. Sort and collect desired cell population (Fig. 3) into prelabeled tubes containing 1 mL 0.9× PBS with 5 % FBS (see Note 8).

Cytospins of FACS-Sorted Cells

13. Spin down sorted cells in refrigerated centrifuge (5 min, 470×*g*, 4 °C). Resuspend in appropriate volume (~400 µL) of buffer (0.9× PBS with 5 % FBS).

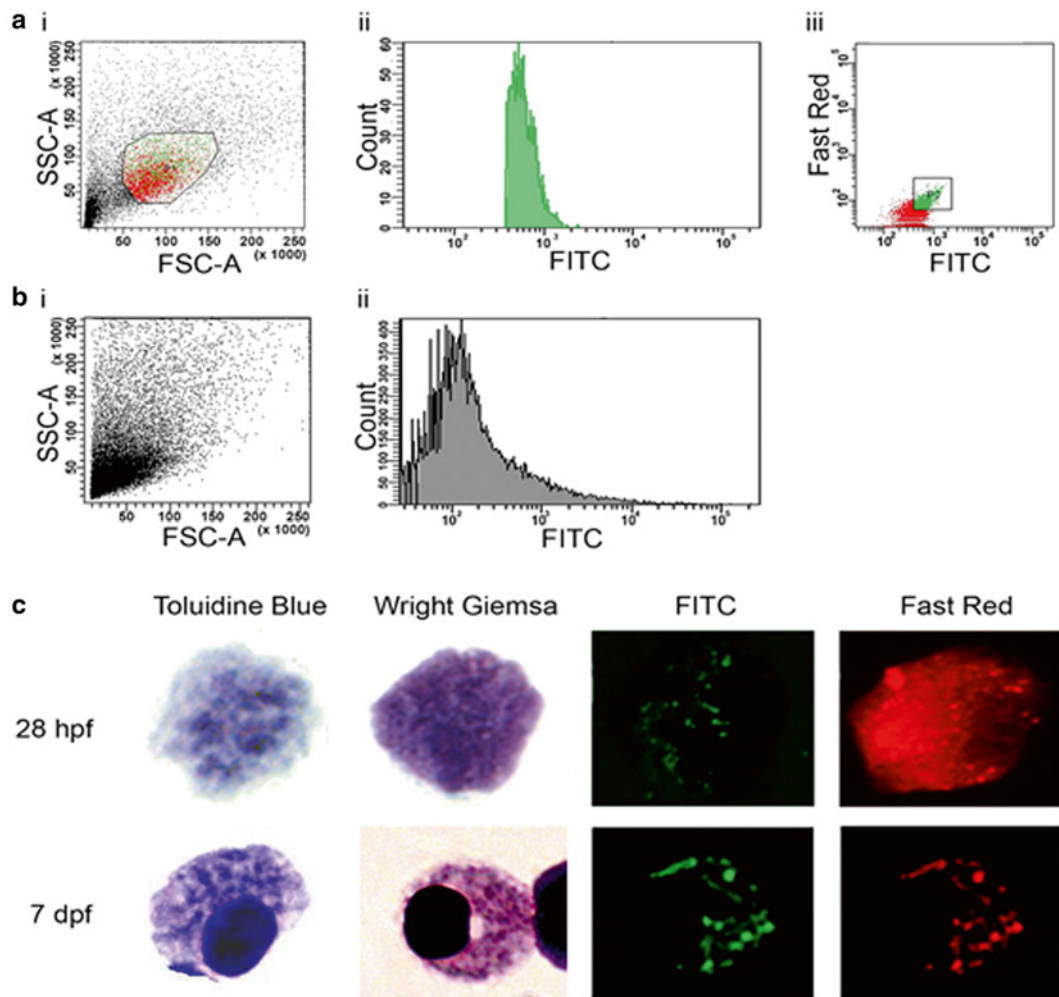


Fig. 3 WISH-FACS isolation technique can identify a specific mast cell population. Cells were isolated based on mRNA expression of *cpa5* labeled by WISH. FACS data for the *cpa5*⁺ cell population isolated from 7 dpf embryos is shown in (a). Cell suspensions were gated based on forward scatter (FSC-A) and side scatter (SSC-A) (a, i) to exclude cellular debris and nonspecific cells and sorted on the basis of FITC fluorescence (a, ii) and subsequently FITC and Fast Red fluorescence together (a, iii). Negative control data from embryos that were subjected to WISH conditions in the absence of an RNA probe is shown in (b). This population was also gated based on FSC-A and SSC-A (b, i), but the resulting population reveals no FITC fluorescence as expected (b, ii). Isolated cell populations were fixed onto slides by cytopsin, stained by Wright Giemsa to examine morphology, or toluidine blue, a mast cell-specific stain. The *first row of panel c* shows an immature mast cell harvested at 28 hpf. The *second row* shows a morphologically mature mast cell isolated from embryos at 7 dpf. Toluidine blue staining shows characteristic metachromatic granules. The last two panels in each row demonstrate that the cells shown are both FITC and Fast Red fluorescent, which confirms the presence of *cpa5* mRNA (Objective 100 \times). This research was originally published in *Blood*. Dobson, J.T., Seibert, J., Teh, E.M., Da's, S., Fraser, R.B., Paw, B.H., Lin, T.J., and Berman, J.N. Carboxypeptidase A5 identifies a novel mast cell lineage in the zebrafish providing new insight into mast cell fate determination. *Blood* 112:2969–2972. © The American Society of Hematology and in Dobson, J.T., Da's, S., McBride, E.R., and Berman, J.N. 2009. Fluorescence-activated cell sorting (FACS) of whole-mount *in situ* hybridization (WISH) labelled haematopoietic cell populations in the zebrafish. *Br J Haematol* 144:732–735

14. Assemble the following parts of the cytopspin rig in this order: Bracket (metal, comes with the sealed head), glass microscope slide (frosted side toward outside of rotation), filter card, and then cytofunnel (hole should line up with hole in filter card, funnel points up/out).
15. Pre-wet: Load 100 μ L of coating buffer into the funnels and spin at $470 \times g$ for 3 min.
16. Cytospin: Load 100 μ L of cells into cytofunnel after pre-wetting. Spin at $470 \times g$ for 5 min. Carefully dismantle rig (see Note 9).

3.8 Morpholino Oligonucleotides

Morpholino oligos are short chains of about 25 nucleotides. Morpholino subunits can inhibit translation, redirect splicing, or inhibit activity, maturation, or target access of a miRNA (see Note 10)

3.9 Preparation of Stock Solution

1. Each oligo is delivered as a pre-quantified, sterile, salt-free, lyophilized solid in a glass vial.
2. We recommend making a 2 mM stock solution in distilled water (morpholinos can be damaged by diethyl pyrocarbonate (DEPC)).
3. Store morpholino stock solutions and working stocks at RT, when stored cold or frozen, morpholinos can come out of solution. Before using, heat the solution 10 min at 65 °C and cool to RT before use. If that does not recover full oligo activity, autoclave the solution to dissolve oligo.

3.10 Embryo Collection

1. Set up mating of wild-type or transgenic fish pairs using mating tanks with dividers to separate males and females.
2. Pull the dividers the following morning. One hour later, collect embryos using embryo strainer and place embryos in a Petri dish with PTU water.

3.11 Zebrafish Morpholino Injection

1. Mix 2 % agarose in egg water.
2. Bring to boil in microwave then pour in the Petri dish, insert mold slide, and get rid of bubbles and let it cool down before pulling the mold out.
3. Line the collected embryos in the injection plate.
4. Inject the desired concentration of morpholino with 0.05 % phenol red (a nontoxic injection tracer) into the yolk of 1–4 cell stage embryos (it will be transported into the forming cells).
5. Transfer injected embryos to a clean Petri dish and allow recovering at 28.5 °C incubator until required age before fixation.

3.12 Chemical Inhibitors

Gamma (γ)-Secretase Inhibitor (Compound E) Treatment

1. Dilute Compound E stock (1 mM in DMSO) in egg water and apply to dechorionated zebrafish embryos at 28.5 °C at final concentrations of 50 and 75 μ M from 22 h postfertilization (hpf) to 48 hpf.
2. Fix embryos with 4 % PFA.
3. Treat control embryo groups with (a) egg water and (b) egg water with 0.5 % DMSO.

3.13 Transgenic Mast Cell Disease Models

In our efforts to use the zebrafish as a tool for human systemic mastocytosis (SM), we generated a transgenic line expressing the human KIT gene harboring the specific mutation (D816V) that is seen in SM patients [34]. We used the Multisite Gateway® Pro Technology to express this mutated gene under the ubiquitous zebrafish promoter, beta actin, with a reporter gene. The advantages of the Multisite Gateway system with the flanking Tol2 sites have been well documented in the zebrafish field to provide ease and convenience in generating different constructs to serve various purposes [27–29]:

1. Design primers flanking your gene of interest (in this case, human *KIT D816V*) with attB1 and attB2 sites added to the ends and produce your attB1 and attB4-flanked PCR product.
2. Perform a BP recombination reaction, according to manufacturers' instructions, between the attB1 and attB2-flanked PCR product and pDONR P1-P2 to generate the middle entry clone (pME).
3. Confirm the structure of the cloned DNA by sequencing.
4. Repeat steps for the p5E (5' entry clone, in this case zebrafish β -actin (*actb1*)) and p3E (3' entry clone, in this case enhanced green fluorescent protein (eGFP) with the viral 2A linker) using appropriate att sites.
5. Perform LR reaction and combine the three clones giving rise to pTol2- β -*actin*-*hKIT D816V*-2AeGFP.
6. Inject along with Tol2 mRNA into the cell of the embryos at 1-cell stage as described above.
7. Screen embryos for ubiquitous expression of GFP and grow them up.
8. When GFP+ fish reach maturity, mate them to wild-type line and screen offspring to identify a founder.
9. Once founders are identified, continue mating and screen for stable reporter expression in the embryos to generate a stable transgenic line.

3.14 RNA (Carboxypeptidase A5) In Situ Hybridization on Tissue Sections

Day 1: Hybridization

1. Use 5 μ m sections of paraffin-embedded intestine tissue and mounted on glass slides.
2. Deparaffinize the sections with xylene twice (10 min each). Perform in a fume hood.
3. Rehydrate the tissue sections using serial washes with EtOH as follows:
 - (a) Wash twice with 100 % EtOH (5 min each).
 - (b) Wash once with 95 % EtOH in PBS for 2 min.
 - (c) Wash once with 85 % EtOH in PBS for 2 min.
 - (d) Wash once with 60 % EtOH in PBS for 2 min.
 - (e) Wash once with 30 % EtOH in PBS for 1 min.
 - (f) Wash once with distilled water for 2 min.
 - (g) Wash once with PBS for 5 min.
4. Pre-hybridize sections by immersing in Hyb(+) buffer for 1 h at 37 °C.
5. Add DIG-labeled antisense *cpa5* probe to Hyb(+) 1:150 (enough volume to overlay the sections) and incubate overnight in 37 °C incubator with gentle shaking in a humidified container.

Day 2: Washing, Blocking, and 2° Antibody

6. Collect the probe solution, and store at -20 °C for a later use (solution can be used twice again).
7. Wash tissue section in a 37 °C incubator as follows:
 - (a) Wash twice with 2 \times SSC-T, 50 % formamide (15 min each wash).
 - (b) Wash once with 2 \times SSC-T (15 min).
 - (c) Wash twice with 0.2 \times SSC-T (15 min each).
8. Wash tissue sections at RT on a gentle shaker for 5 min with Buffer A: 100 mM Tris-HCl (pH 7.5), 150 mM NaCl.
9. Prepare the blocking solution: 10 mL of 10 % blocking medium, 5 mL of heat-inactivated FBS, 35 mL MAB-T. Store the blocking solution at 4 °C to use for the washes on day 3.
10. Block in 1 mL *in situ* blocking solution, shake gently at RT for 1 h.
11. Add 0.5 μ L of the secondary (2°) antibody (anti-DIG or anti-FITC) to the 1 mL blocking solution. Incubate overnight at 4 °C on a gentle shaker.

Day 3: Detection

12. Perform the following detection steps at RT on a gentle shaker.
13. Wash with in situ blocking solution (15 min).
14. Wash twice with Buffer A (5 min each).
15. Wash twice with 0.1 M Tris (pH 9.5) (5 min each wash).
16. BCIP/NBT stain: Add two drops reagent #1 to 5 mL of 0.1 M Tris (pH 9.5) and invert to mix. Then add two drops reagent #2, invert to mix followed by two drops reagent #3, invert to mix. Finally, add 400 µg/mL levamisole.
17. Develop at RT with gentle shaking in the dark (cover with aluminum foil). Examine after 1.5 h and, if necessary, every 30 min thereafter.
18. Counterstain with methyl green for 30 s.
19. Stop the reaction by washing with PBS-T at RT for 5 min.
20. Mount the slide with Glycerol Gelatin (Sigma-Aldrich, St. Louis, MO).
21. View under the microscope.

3.15 Histochemical Stains

Standard protocols were used for staining 5 µm sections of zebrafish intestine. Slides are visualized using Zeiss Z1 microscope and Axiocam Rev 3.0 camera, Wetzlar, Germany (*see Note 11*).

3.15.1 Toluidine Blue Staining (Metachromasia)

This stain is specifically used to visualize mast cells by demonstrating metachromasia (red, pink, or purple) in tissue sections, whereas nuclei and other components will appear as shades of blue (Modified from Carleton's Histological Technique).

1. Deparaffinize and hydrate sections in distilled water.
2. Stain sections in toluidine blue working solution for 3 min.
3. Wash well with three changes of distilled water.
4. Dehydrate rapidly through 95 % and then two changes of 100 % EtOH.
5. Clear in xylene with two changes (3 min each).
6. Mount with Cytoseal (Richard-Allan Scientific) mounting media and a coverslip.

3.15.2 Hematoxylin and Eosin

Reference: Histotechnology: A Self Instructional Text, 3rd Edition, Freida L Carson and Christa Hladik, 2009 [30].

1. Deparaffinize in xylene with three changes (5 min each).
2. Serially hydrate using 100, 95, and 70 % EtOH (2 min each).
3. Rinse 30 s in running tap water.
4. Stain with hematoxylin (2.5 min).

5. Rinse 2 min in running tap water.
6. Blue in Scott's tap water substitute for 1 min.
7. Rinse 1 min in running tap water.
8. Dip in 0.2 % nitric acid to differentiate slide.
9. Rinse 1 min in running tap water.
10. Dip (20 times) in eosin Y solution.
11. Dehydrate through serial washes in 70, 95, and 100 % EtOH (20 dips in each solution).
12. Clear in xylene with three changes (20 dips each).
13. Mount with coverslip using Cytoseal mounting media (Richard-Allan Scientific) (*see Note 12*).

3.15.3 McManus

Periodic Acid-Schiff (PAS)

Carleton's Histological Technique

PAS-positive material stains reddish purple or magenta
Nuclei stains blue

1. Deparaffinize sections in xylene and rehydrate through alcohol series as in Subheading "Hematoxylin and Eosin", **steps 1 and 2**.
2. Incubate in 1 % periodic acid for 5–10 min.
3. Wash in tap water for 10 min.
4. Incubate in Schiff reagent 15 min.
5. Wash in tap water 20 min.
6. Incubate in Gill's hematoxylin for 3–5 min.
7. Rinse 1 min in running tap water.
8. Blue in Scott's tap water substitute.
9. Rinse 1 min in running tap water.
10. Dehydrate through serial rinses in 70, 95, and 100 % EtOH.
11. Clear twice in xylene (20 dips each).
12. Cover using Tek® Glas coverslipper.

3.16 Immunohistochemistry (Fig. 4)

Day 1: Washing, Blocking, and 1° Antibody

1. Use 5 μ m sections of paraffin-embedded intestine tissue and mounted on positive-charged glass slides.
2. Deparaffinize with xylene (three changes, 5 min each).
3. Serial hydrate in EtOH 100, 95, and 70 % (2 min each step).
4. Wash in PBS three times (30 s each).
5. Endogenous peroxidase activity is quenched in 3 % H_2O_2 in PBS for 10 min.
6. Wash in PBS three times (30 s each).
7. Antigen retrieval: 0.01 M sodium citrate buffer (pH 6.1) in a decloaking chamber (Biocare Medical).

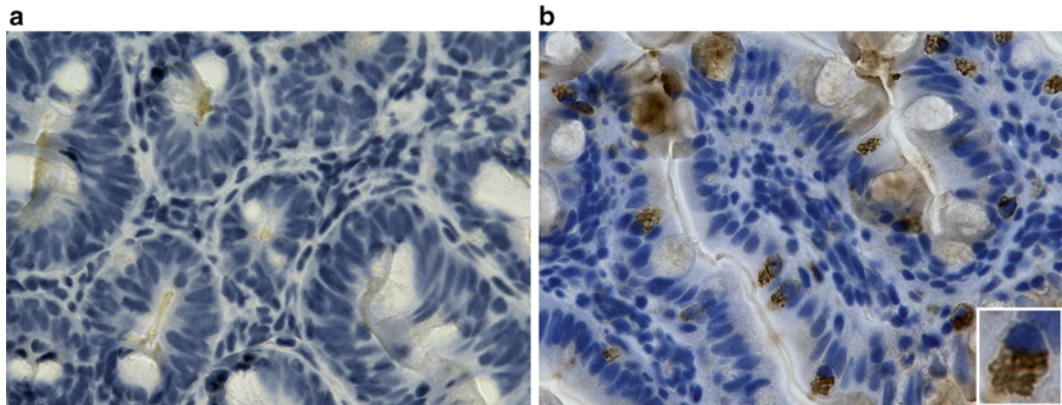


Fig. 4 Zebrafish mast cells express an Fc ϵ RI-like receptor and antibody. Immunohistochemistry of wild-type adult zebrafish intestine using antihuman Fc ϵ RI γ demonstrates specific staining in intestinal mast cells (**b**, and inset) compared with human IgG isotype control (**a**). This figure is reproduced from Da'as, S., Teh, E.M., Dobson, J.T., Nasrallah, G.K., McBride, E.R., Wang, H., Neuberg, D.S., Marshall, J.S., Lin, T.J., and Berman, J.N. 2011. Zebrafish mast cells possess an Fc ϵ RI-like receptor and participate in innate and adaptive immune responses. *Dev Comp Immunol* 35:125–134

8. Wash slides in PBS three times (2 min each).
9. Block by incubating slides in a humidified chamber with 1:20 normal goat or horse serum diluted in PBS for 30 min at RT.
10. Add polyclonal rabbit immunoglobulin G (IgG), antihuman Fc ϵ RI γ (Millipore, Billerica, MA) antibody to one slide and add the isotype control consisting of non-immunized rabbit IgG (Cedarlane Laboratories, Hornby, ON, Canada) to the second slide, each diluted at 1:400 in 1 \times PBS and incubate overnight at 4 °C in a humid chamber.

Day 2: Washing, Blocking, and 2° Antibody

1. Wash slides with PBS (three times, 2 min each).
2. Add secondary antibody, biotinylated goat anti-rabbit IgG diluted in 1:600 in PBS and incubate for 30 min at RT in a humid chamber.
3. Prepare the staining solution. Vectastain ABC kit (Vector Laboratories, Burlingame, CA): To 5 mL of PBS add one drop of solution A. Mix and then add one drop of solution B. Mix and then let sit for 30 min before use.
4. Wash slides with PBS (three times, 2 min).
5. Add the staining solution and incubate for 30 min at RT on a shaker.
6. Wash slides three times with PBS (2 min each wash) (*see Note 13*).

7. Add the DAB (diaminobenzidine) solution (add one drop of DAB and two drops of H_2O_2 to 5 mL of PBS) and incubate for 5 min at RT on a shaker.
8. Rinse slides with running tap water.
9. Counterstain slides with Mayer's hematoxylin (Sigma-Aldrich, St. Louis, MO).
10. Blue in Scott's tap water substitute.
11. Rinse slides with running tap water.
12. Dehydrate through EtOH series: 70, 95, and 100 % (twice in each solution, 20 dips each).
13. Clear in xylene (three changes, 20 dips).
14. Mount with Cytoseal mounting media (Richard-Allan Scientific).
15. Zebrafish intestine labeled with anti-Fc ϵ RI is provided as sample data in Fig. 4.

3.17 Electron Microscopy (EM)

1. Collect zebrafish intestine immediately following cardiac puncture and fix with 2.5 % glutaraldehyde in 0.1 M sodium cacodylate buffer at 4 °C overnight.
2. Move samples to 1 % osmium tetroxide and 0.25 % uranyl acetate and embed in 100 % epon araldite resin for further fixation.
3. Cut thin sections (100 nm) and place on 300 mesh copper grids.
4. Stain the sections with 2 % aqueous uranyl acetate followed by 0.3 % lead citrate.
5. View the samples using a Transmission Electron Microscope at 80 kV (e.g., JEOL JEM 1230 (Tokyo, Japan)).
6. Capture images using digital camera (e.g., Hamamatsu ORCA-HR (Bridgewater, NJ)).

3.18 Embryo Protein Immunoblotting

The following protocol is modified from Sidi et al. [31]

1. Dechorionate embryos (*see Note 14*).
2. Transfer embryos to ice-cold Ringer's solution to de-yolk if required (*see Note 15*).
3. Transfer embryos to a 2 mL microcentrifuge tube and remove all residual Ringer's solution.
4. Add lysis buffer #2 (1 μ L per embryo).
5. Homogenize embryos with a plunger from 1 mL syringe or homogenize for 20–40 s with rotor-stator in 5 mL round bottom tube.

6. Centrifuge $800 \times g$, 10 min at 4 °C.
7. Transfer the supernatant to a fresh 1.5 mL microcentrifuge tube and store at -80 °C.

Protein Quantification

8. To quantify protein concentration of embryo lysates, use BIO-RAD DC™ Protein Assay for 96-well plate with the following modifications of the manufacturers' instructions.
9. Dilute 2 μ L lysate sample in 20 μ L total lysis buffer #2.
10. Use 2 mg/mL BSA to generate standard curve by serial dilution (see Note 16).
 - (a) Add 25 μ L of reagent A.
 - (b) Add 200 μ L of reagent B.
11. Incubate for 15 min at RT.
12. Read on plate reader at 655 nm.
13. Plot standard curve to calculate lysate protein concentration.

Western Blot

14. Extract protein from zebrafish embryos 7 days postfertilization (7 dpf).
15. Treat protein extract with or without 5 % 2-mercaptoethanol.
16. Load a total of 50 μ g of protein for Western blot.
17. Add 1:1,000 dilution of the polyclonal rabbit antihuman IgE that reacts with the epsilon-chain of human IgE (A009402, Dako, Denmark) for the detection of the zebrafish Ig heavy chain.
18. Add the secondary antibody.
19. Detect the protein by chemiluminescence detection by using Image Kodak.

3.19 Intraperitoneal Injection and Cardiac Puncture

1. Anesthetize wild-type adult zebrafish in pairs with 100 μ g/mL tricaine (MS-222) in a “treatment tank.”
2. Inject fish by intraperitoneal (IP) route with 4 μ L volume of test treatment or saline control (see Subheading 3.17) mixed with 1 μ L of 0.07 % bromophenol blue (i.e., a total volume of 5 μ L). The bromophenol blue is a marker dye used to ensure correct anatomical location.
3. Allow the zebrafish to recover and monitor for desired postinjection time.
4. At the experimental endpoint, euthanize fish with 2 mg/mL tricaine.
5. Lay the fish on a fitted platform immediately postmortem.
6. Make a small ventral slit using microdissection scissors to reveal the heart.

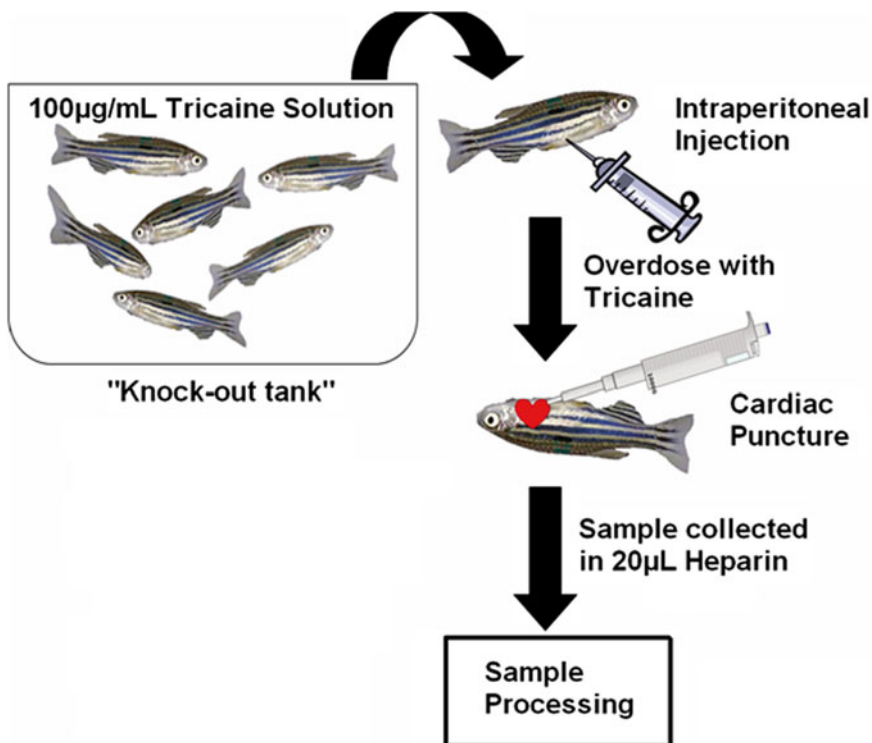


Fig. 5 Method of intraperitoneal injections and blood collection via cardiac puncture from adult zebrafish

7. Use a fine pipette tip (e.g., SDS-PAGE gel-loading tips) preloaded with 10 μ L heparin to puncture the heart (see procedure illustration in Fig. 5).
8. Dispense the 10 μ L heparin around the heart and collect the blood into a 1.5 mL microcentrifuge tube containing 20 μ L heparin (see Notes 17 and 18).
9. Centrifuge collected samples at 855 $\times g$ for 5 min at 4 °C.
10. Remove plasma (~20 μ L) into a clean microfuge tube.

3.20 Mast Cell Treatments

3.20.1 Activation of Mast Cells

3.20.2 Infectious Stimuli

1. Inject (IP) fish with 10 μ g of compound 48/80 as described in Subheading 3.19, steps 1–3.
2. Use saline injections for the control group.
3. Allow fish to recover for 5 min prior to blood sampling by cardiac puncture.
1. Inject fish with live *A. salmonicida* using technique described in Subheading 3.16, steps 1–3. Use a final concentration of 3×10^7 cfu/adult fish.
2. Use saline injections for the control group.
3. Allow fish to recover for 10–60 min prior to blood sampling by cardiac puncture.

3.20.3 Mast Cell Stabilization

1. Add ketotifen fumarate salt (Sigma-Aldrich, St. Louis, MO) directly to the tank water at 400 µg/mL final concentration, 1 h prior to IP injection of compound 48/80 or *A. salmonicida* (or other treatments) (see Notes 19 and 20).

3.20.4 Antigen-IgE Stimulation

1. Sensitize adult zebrafish by IP injection with 5 µL containing 20 ng of mouse monoclonal anti-DNP (dinitrophenyl) IgE (Sigma-Aldrich, St. Louis, MO) or anti-TNP IgE (trinitrophenyl) (Biosearch Technologies, USA).
2. Saline is used for the control group.
3. Allow fish to recover for 24 h.
4. Challenge fish with IP injections of 20 µg of DNP-BSA (bovine serum albumin; Sigma-Aldrich, St. Louis, MO) or 40 µg of TNP-BSA (Biosearch Technologies, USA) prior to blood sampling by cardiac puncture.

3.21 Tryptase Assay

1. Tryptase is a glycoprotein released from mast cells during degranulation (see Note 21).
2. Add 20 µL of BAPNA to an equal volume of plasma.
3. Incubate tubes in a humidified incubator at 37 °C for 48 h.
4. Add 60 µL of PBS and mix (by vortex).
5. Centrifuge briefly at high speed.
6. Load 60 µL of the BAPNA/PBS/plasma mixture into a 96-well plate.
7. Read the tryptase activity (proportional to absorbance at $\lambda=415$ nm) using a 96-well microplate reader (see Note 22).

4 Notes

1. Once dechorionated, the embryos are very fragile and should be manipulated gently.
2. Generally, DIG-labeled probes are much stronger than FITC-labeled probes.
3. Use 15–20 embryos per in situ labeling reaction and be gentle with the embryos because they are fragile.
4. Label the tube with the probe whether it is DIG- or FITC-labeled probe.
5. Detection at RT on a gentle shaker.
6. To eliminate diffuse background stain, wash embryos with 100 % MeOH at RT for 5–10 min then wash with PBS-T.
7. Embryos can be stored in 4 % PFA at 4 °C.
8. We perform cell sorting (FACS) using a FACSaria machine (BD Biosciences). Cells were gated by forward and side scatter

and subsequently by FITC fluorescence at 515–545 nm. The population with the highest fluorescent signal was then gated using FITC and Fast Red (600–620 nm) to provide a more intense fluorescent signal before sorting.

9. Take apart rig, making sure to lift the filter card off the slide rather than sliding it off. If cytospins are to be stained later, store them in 10 % buffered formalin.
10. Types of morpholinos:
 - (a) *Translation Blocking*: By blocking the translation initiation complex, morpholinos can knockdown protein expression sufficiently such that the band corresponding to that protein is eliminated on Western blot. Inhibition of translation by a morpholino should be assayed by immunoblotting as the mRNA is not rapidly degraded. RT-PCR will not provide an accurate readout.
 - (b) *Splice Blocking*: Used to block sites involved in splicing pre-mRNA, morpholinos can modify splicing, usually causing targeted exon deletions or intron insertions. This activity can be assayed by RT-PCR, with successful splice-modification visualized on electrophoretic gels as either shifts in the size of cDNA or disappearance of the RT-PCR product.
 - (c) *miRNA Blocking*: A morpholino bound to the guide strand of a miRNA can inhibit its activity (Modified from Gene Tools, LLC, Philomath, OR, USA).
11. Use 5 μ m sections of paraffin-embedded intestine tissue and mounted on glass slides.
12. Look at slides regularly under the microscope to be sure that nuclear detail is sufficient and that eosinophilic staining is well differentiated—not too pale or pale darkly stained.
13. The avidin–biotin complex (ABC) method is used, and the peroxidase reaction with diaminobenzidine (DAB) will be employed for visualization (Vectastain ABC Kit).
14. To obtain sufficient yields of protein, use at least 50 embryos chilled on ice for 60 min in egg water; if younger than 48 hpf we recommend using 100 embryos.
15. If younger than 36 hpf, embryos should be de-yolked by mechanical shearing using gel-loading tips.
16. Use serial dilutions of 0, 1, 2, 5, 7, and 10 μ g.
17. Heparin is required for proper RBC processing to prevent sample clotting.
18. All tubes should be kept on ice through the collection and processing.

19. Ketotifen fumarate is an H1 histamine receptor antagonist and mast cell-stabilizing agent used in the treatment of asthma and other allergic diseases [32]. It is used here to prevent mast cell degranulation.
20. *A. salmonicida* can be used as an infectious agent to show accumulation and activation of mast cells.
21. Tryptase activity is measured by the release of *p*-nitroanilide from Na^+ -Benzoyl-DL-arginine *p*-nitroanilide (BAPNA), a tryptase substrate [25].
22. Relative levels of tryptase activity in zebrafish samples were normalized by using a standard curve generated from a human LAD2 mast cell line.

Acknowledgments

The authors would like to thank Patricia Colp for assistance with histology and immunohistochemistry methodologies, Mary Ann Trevors for assistance with the electron microscopy protocol, and Chansey Veinotte for editing this manuscript.

References

1. Berman JN, Kanki JP, Look AT (2005) Zebrafish as a model for myelopoiesis during embryogenesis. *Exp Hematol* 33:997–1006
2. Carradice D, Lieschke GJ (2008) Zebrafish in hematatology: sushi or science? *Blood* 111:3331–3342
3. Dobson JT, Seibert J, Teh EM, Da'as S, Fraser RB, Paw BH, Lin TJ, Berman JN (2008) Carboxypeptidase A5 identifies a novel mast cell lineage in the zebrafish providing new insight into mast cell fate determination. *Blood* 112:2969–2972
4. Da'as S, Teh EM, Dobson JT, Nasrallah GK, McBride ER, Wang H, Neuberg DS, Marshall JS, Lin TJ, Berman JN (2011) Zebrafish mast cells possess an Fc ϵ RI-like receptor and participate in innate and adaptive immune responses. *Dev Comp Immunol* 35:125–134
5. Meeker ND, Trede NS (2008) Immunology and zebrafish: spawning new models of human disease. *Dev Comp Immunol* 32:745–757
6. Trede NS, Langenau DM, Traver D, Look AT, Zon LI (2004) The use of zebrafish to understand immunity. *Immunity* 20:367–379
7. Traver D, Herbomel P, Patton EE, Murphey RD, Yoder JA, Litman GW, Catic A, Amemiya CT, Zon LI, Trede NS (2003) The zebrafish as a model organism to study development of the immune system. *Adv Immunol* 81:253–330
8. Da'as SI, Coombs AJ, Balci TB, Grondin CA, Ferrando AA, Berman JN (2012) The zebrafish reveals dependence of the mast cell lineage on Notch signaling *in vivo*. *Blood* 119:3585–3594
9. Metcalfe DD (2008) Mast cells and mastocytosis. *Blood* 112:946–956
10. Peal DS, Mills RW, Lynch SN, Mosley JM, Lim E, Ellinor PT, January CT, Peterson RT, Milan DJ (2011) Novel chemical suppressors of long QT syndrome identified by an *in vivo* functional screen. *Circulation* 123:23–30
11. Bowman TV, Zon LI (2010) Swimming into the future of drug discovery: *in vivo* chemical screens in zebrafish. *ACS Chem Biol* 5:159–161
12. Yeh JR, Munson KM (2010) Zebrafish small molecule screen in reprogramming/cell fate modulation. *Methods Mol Biol* 636:317–327
13. Yeh JR, Munson KM, Elagib KE, Goldfarb AN, Sweetser DA, Peterson RT (2009) Discovering chemical modifiers of oncogene-regulated hematopoietic differentiation. *Nat Chem Biol* 5:236–243
14. Bertrand JY, Kim AD, Violette EP, Stachura DL, Cisson JL, Traver D (2007) Definitive hematopoiesis initiates through a committed erythromyeloid progenitor in the zebrafish embryo. *Development* 134:4147–4156

15. Renshaw SA, Loynes CA, Trushell DM, Elworthy S, Ingham PW, Whyte MK (2006) A transgenic zebrafish model of neutrophilic inflammation. *Blood* 108:3976–3978
16. Hsu K, Traver D, Kutok JL, Hagen A, Liu TX, Paw BH, Rhodes J, Berman JN, Zon LI, Kanki JP et al (2004) The pu.1 promoter drives myeloid gene expression in zebrafish. *Blood* 104:1291–1297
17. Lin HF, Traver D, Zhu H, Dooley K, Paw BH, Zon LI, Handin RI (2005) Analysis of thrombocyte development in CD41-GFP transgenic zebrafish. *Blood* 106:3803–3810
18. Yang Z, Jiang H, Lin S (2009) Bacterial artificial chromosome transgenesis for zebrafish. *Methods Mol Biol* 546:103–116
19. Gray C, Loynes CA, Whyte MK, Crossman DC, Renshaw SA, Chico TJ (2011) Simultaneous intravital imaging of macrophage and neutrophil behaviour during inflammation using a novel transgenic zebrafish. *Thromb Haemost* 105:811–819
20. Lee EC, Yu D, Martinez de Velasco J, Tessarollo L, Swing DA, Court DL, Jenkins NA, Copeland NG (2001) A highly efficient *Escherichia coli*-based chromosome engineering system adapted for recombinogenic targeting and subcloning of BAC DNA. *Genomics* 73:56–65
21. Corkery DP, Dellaire G, Berman JN (2011) Leukaemia xenotransplantation in zebrafish: chemotherapy response assay *in vivo*. *Br J Haematol* 153:786–789
22. Veinotte CJ, Corkery D, Dellaire G, El-Naggar A, Sinclair K, Bernstein ML, Sorensen PB, Berman JN (2012) Using zebrafish xenotransplantation to study the role of Y-Box binding protein (YB-1) in the metastasis of Ewing family tumors. American Academy of Cancer Research Annual Meeting, Abstract 1398
23. Feng Y, Santoriello C, Mione M, Hurlstone A, Martin P (2010) Live imaging of innate immune cell sensing of transformed cells in zebrafish larvae: parallels between tumor initiation and wound inflammation. *PLoS Biol* 8:e1000562
24. Stachura DL, Svoboda O, Lau RP, Balla KM, Zon LI, Bartunek P, Traver D (2011) Clonal analysis of hematopoietic progenitor cells in the zebrafish. *Blood* 118:1274–1282
25. Lavens SE, Proud D, Warner JA (1993) A sensitive colorimetric assay for the release of tryptase from human lung mast cells *in vitro*. *J Immunol Methods* 166:93–102
26. Westerfield M (2000) The zebrafish book. A guide for the laboratory use of zebrafish (*Danio rerio*). University of Oregon Press, Eugene
27. Villefranc JA, Amigo J, Lawson ND (2007) Gateway compatible vectors for analysis of gene function in the zebrafish. *Dev Dyn* 236:3077–3087
28. Kwan KM, Fujimoto E, Grabher C, Mangum BD, Hardy ME, Campbell DS, Parant JM, Yost HJ, Kanki JP, Chien CB (2007) The Tol2kit: a multisite gateway-based construction kit for Tol2 transposon transgenesis constructs. *Dev Dyn* 236:3088–3099
29. Fisher S, Grice EA, Vinton RM, Bessling SL, Urasaki A, Kawakami K, McCallion AS (2006) Evaluating the biological relevance of putative enhancers using Tol2 transposon-mediated transgenesis in zebrafish. *Nat Protoc* 1:1297–1305
30. Carson F, Hladik C (2009) Histotechnology: a self instructional text. American Society for Clinical Pathology, Chicago
31. Sidi S, Sanda T, Kennedy RD, Hagen AT, Jette CA, Hoffmans R, Pascual J, Imamura S, Kishi S, Amatruda JF et al (2008) Chk1 suppresses a caspase-2 apoptotic response to DNA damage that bypasses p53, Bcl-2, and caspase-3. *Cell* 133:864–877
32. Schwarzer G, Bassler D, Mitra A, Ducharme FM, Forster J (2004) Ketotifen alone or as additional medication for long-term control of asthma and wheeze in children. *Cochrane Database Syst Rev*. CD001384, PMID 14973969
33. Dobson JT, Da'as S, McBride ER, Berman JN (2009) Fluorescence-activated cell sorting (FACS) of whole mount *in situ* hybridization (WISH) labelled haematopoietic cell populations in the zebrafish. *Br J Haematol* 144:732–735
34. Balci TB, Prykhozhiy SV, Teh EM, Da'as SI, McBride E, Liwski R, Chute IC, Leger D, Lewis SM, Berman JN (2014) A transgenic zebrafish model expressing KIT-D816V recapitulates features of aggressive systemic mastocytosis. *Br J Haematol* 167(1):48–61. doi:10.1111/bjh.12999
35. Auer TO, Duroure K, De Cian A, Concorde JP, Del Bene F (2013) Highly efficient CRISPR/Cas9-mediated knock-in in zebrafish by homology-independent DNA repair. *Genome Res* 24:142–153
36. Veinotte CJ, Dellaire G, Berman JN (2014) Hooking the big one: the potential of zebrafish xenotransplantation to reform cancer drug screening in the genomic era. *Dis Model Mech* 7(7):745–54

Chapter 4

Human Mast Cell and Basophil/Eosinophil Progenitors

Gail M. Gauvreau and Judah A. Denburg

Abstract

Mast cell, basophil, and eosinophil lineages all derive from CD34⁺ hemopoietic stem cells; however, mast cells are derived from a distinct, nonmyeloid progenitor, while eosinophils and basophils share a common myeloid progenitor. These progenitors likely evolved from an ancestral leukocyte population involved in innate immunity and currently play a central role in the pathology of allergic disease. Advances in isolation and analysis of mast cell and basophil/eosinophil progenitor populations have been critical to understanding lineage commitment, differentiation, function, and transcriptional regulation of these cells and have provided a way of monitoring the effect of novel investigational therapies on these cell populations in samples of blood, bone marrow, and airway secretions.

Key words Mast cell, Basophil, Eosinophil, Progenitor, Tissue culture, Flow cytometry, Cord blood, Bone marrow, Blood, Sputum

1 Introduction

While nonneoplastic human mast cells and basophils perform many similar functions and share a high-affinity IgE receptor, these cells do not share a common progenitor, as opposed to myeloid basophil and eosinophil leukocytes, which do [1]. All three lineages derive from a CD34⁺ hemopoietic stem cell, in response to various differentiation stimuli. CD34 can be found on some differentiated mast cells and eosinophils, as a contributor to cell migration in tissue inflammatory responses [2, 3]. Mast cells are derived from a distinct, nonmyeloid progenitor [4], which likely evolved, along with basophils and eosinophils, from an ancestral leukocyte population involved in innate immunity [5–7]. Major recent advances in mapping human basophil/eosinophil and mast cell growth and differentiation pathways have come from rodent models [8–11], which have underscored key roles of epithelial factors such as TSLP, IL-33, IL-25, and toll-like receptors (TLRs) [12, 13].

The mast cell differentiation-specific stem cell factor (SCF) and its receptor, *c-kit*, and mutations leading to changes in their

expression have guided much recent research into the specific roles of mast cells in a variety of biological processes, including allergic inflammation, angiogenesis and tumor growth, tissue remodeling, graft tolerance, and some autoimmune diseases [14–21]. Advances in isolation and analysis of mast cell and basophil/eosinophil progenitor populations [22–25] have been critical to understanding lineage commitment, differentiation, function, and transcriptional regulation of these cells.

1.1 Mast Cell and Basophil/Eosinophil Progenitors

Human mast cell differentiation proceeds from an immature CD34⁺, CD38⁺, CD13⁺, c-kit⁺, Fc ϵ RI⁻, Fc γ RII/III⁺ cell [4, 26, 27] which can give rise to both mucosal and serosal mast cell phenotypes (Fig. 1). Phenotypic alterations of mast cell populations depend on the tissue milieu and derivation [5, 28]; indeed, cord blood CD34⁺ c-kit⁺ progenitors respond differently to differentiative stimuli than mature Fc ϵ RI⁺, c-kit⁺ cells [4, 29], indicating that progenitor and phenotypic maturation are both tissue dependent [30]. Mast cell as well as basophil/eosinophil progenitors can be identified in blood, bone marrow, and various other tissues [31–35].

The recent identification of a novel antigenic marker of mast cells, basophils, and their progenitors [36] has again raised the hypothesis that these cell types may share some lineage characteristics; nonetheless, there is much more solid evidence that human basophils and eosinophils share a common lineage.

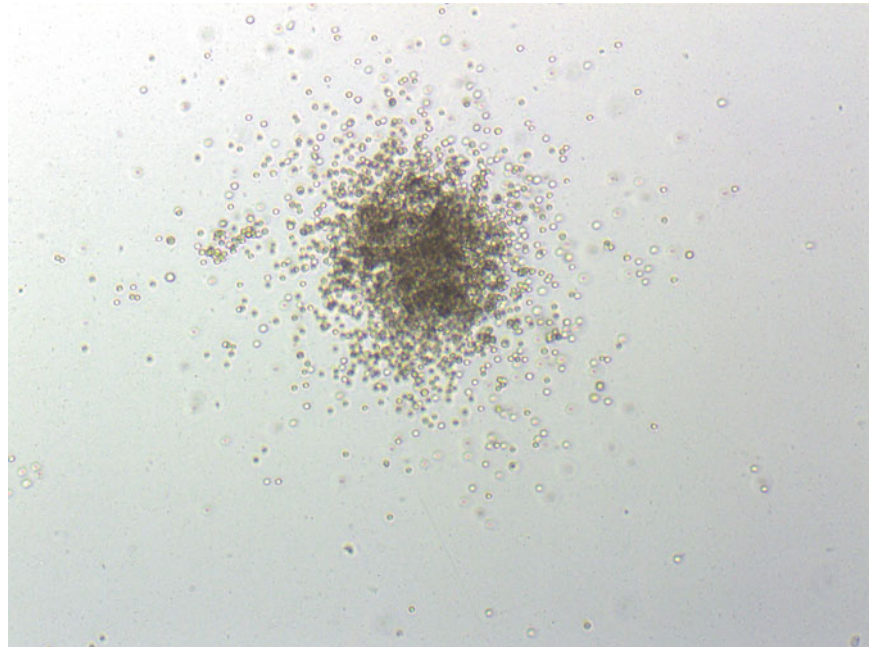


Fig. 1 Eosinophil/basophil colony-forming unit, $\times 400$ magnification, appearing as tightly packed granulated cells

New studies have shown the role of gut microbiota in regulating tissue basophilopoiesis and Th2-dependent IgE responses [37]. Normal and atopic human blood, marrow, and tissues can be used to identify pure or mixed basophil/eosinophil colonies in semi-solid cultures [1, 31, 38] (termed “CFU-baso/eo”) [1, 39].

1.2 Basophil/ Eosinophil Differentiation- Inducing Cytokines

While IL-3 alone is probably involved in human basophil growth and differentiation [40], granulocyte-macrophage colony-stimulating factor (GM-CSF) [1, 31, 38, 41] and IL-5 [39, 42] are directly involved in basophil/eosinophil differentiation. Studies on basophil crisis in chronic myeloid leukemia and the suppressive role of retinoic acid on basophil/eosinophil differentiation support this notion and have further elaborated on these common myeloid pathways [43]. Factors that modulate basophil/eosinophil or mast cell differentiation are listed in Table 1.

Allergic disease is manifested through elevated levels of activated mast cells, eosinophils, and basophils in the affected tissue [44]. In subjects with allergic asthma following allergen challenge, we have observed increased levels of basophils and eosinophils [45] and their progenitors in blood and bone marrow [46–48], and also in the airways [46–49], where these cells may differentiate *in situ* under the influence of local growth factors. More traditional therapies for treatment of allergic asthma, such as glucocorticoids, have been shown to reduce the level of basophil and eosinophil progenitor cells in bone marrow and blood [46], likely through inhibition of growth factors including IL-3, IL-5, and GM-CSF [50]. Investigational therapies are now emerging which target mast cells, basophils, and eosinophils through pathways critical for cell differentiation. Administration of antibodies to IL-5 has been

Table 1
Cytokines and other factors involved in basophil and mast cell growth and differentiation

Cytokine	Effect
GM-CSF	Basophil/eosinophil growth and differentiation; may downregulate human mast cell differentiation
IL-3	Human basophil growth and differentiation; basophil activation/survival; promotes <i>in vivo</i> basophilia (in primates)
IL-5	Basophil and eosinophil growth and differentiation, activation, and survival
SCF	Primary human mast cell growth and differentiation factor
NGF	A cofactor in human mast cell and basophil/eosinophil differentiation <i>in vitro</i>
RA	RA receptor mutation permits basophil/eosinophil differentiation
Stat5	A regulator <i>in vivo</i> of mast cell differentiation

GM-CSF granulocyte-macrophage colony-stimulating factor, *IL-3* interleukin 3, *IL-5* interleukin 5, *SCF* stem cell factor, *NGF* nerve growth factor, *RA* retinoic acid, *Stat5* signal transducer and activator of transcription 5

shown to reduce the number of eosinophils in circulation [51], presumably by preventing the differentiation of progenitor cells into mature cells, while inhaled antisense therapy targeting the IL-3/5/GM-CSF receptor common beta chain effectively reduced the level of eosinophil progenitors in the airways [52]. Measures of progenitor cells in blood, bone marrow, and tissue are valuable outcome markers of drug efficacy and can be measured using tissue culture or through measurements of cell surface markers by flow cytometry.

2 Materials

2.1 Methylcellulose Colony Assay

For peripheral blood (PB), cord blood (CB), and bone marrow (BM):

1. 6 % dextran (w/v) in PBS (phosphate-buffered saline).
2. McCoy's 5A media.
3. McCoy's 3⁺ media: McCoy's 5A, 10 % fetal bovine serum (FBS), 1 % penicillin-streptomycin, 50 μ M 2-mercaptoethanol.
4. Iscove's 2⁺ media: Iscove's medium (IMDM), 1 % penicillin-streptomycin, 50 μ M 2-mercaptoethanol.
5. Fetal bovine serum (FBS) (sterile and heat inactivated) (*see Note 1*).
6. Lymphoprep (Accurate Chemical & Scientific).
7. Methylcellulose media (2.1 %) or MethoCultTM (Stem Cell Technologies).
8. Cytokines: hIL-3 (100 ng/mL), hIL-5 (100 ng/mL), and hGM-CSF (1,000 ng/mL) all reconstituted or diluted with PBS + 1 % BSA (bovine serum albumin).
9. Sterile distilled water.
10. Trypan blue (0.4 %).

2.2 Sputum Processing

1. Dulbecco's Phosphate-Buffered Saline (D-PBS).
2. 0.1 % dithiothreitol (DTT) prepared in D-PBS.
3. Trypan blue (0.4 %).
4. Nylon mesh with 48 μ m pore size.
5. Funnel.
6. Bench rocker.

2.3 Flow Cytometry for Surface Staining IL-5R α , IL-3R α , and GM-CSFR α in Cord Blood, Peripheral Blood and Bone Marrow

Store the following solutions and reagents at 4 °C:

1. FACS buffer: D-PBS containing 0.1 % sodium azide and 0.5 % bovine serum albumin (BSA).
2. 1 % paraformaldehyde (PFA) in D-PBS or CytofixTM (BD Biosciences).
3. PerCP-mouse antihuman CD34.

4. FITC-mouse antihuman CD45.
5. PE-mouse antihuman IL-3R α /IL-5R α /GM-CSFR α .
6. Isotype control mouse IgG₁.
7. Fc blocking buffer: FACS buffer with 5 % mouse serum and 5 % human serum.

2.4 Flow Cytometry for Surface Staining of IL-5R α on Progenitor Cells in Sputum

Store the following solutions and reagents at 4 °C:

1. 1 % paraformaldehyde (PFA) in D-PBS (or use Cytofix™).
2. FACS buffer: D-PBS containing 0.1 % sodium azide and 0.5 % BSA.
3. Fc blocking buffer (FACS buffer with 5 % mouse serum, 5 % human serum).
4. PE-mouse antihuman IL-5R α .
5. APC-mouse antihuman CD34.
6. FITC-mouse antihuman CD45.
7. PE-mouse IgG₁ (isotype control).
8. 0.1 % sodium azide in D-PBS.

3 Methods

3.1 Methylcellulose Colony Assay (See Note 2)

Cord blood (see Note 3), peripheral blood and bone marrow (see Note 4):

1. Dilute sample with McCoy's 5A media (see Note 5).
2. Layer up to 25 mL of diluted sample on top of 15 mL of Lymphoprep in a 50 mL conical tube.
3. Centrifuge at 800 $\times g$ at room temperature (RT) for 20 min without brake (see Note 6).
4. Using a sterile transfer pipette, remove the mononuclear cell layer at the white interface and transfer to a new 50 mL tube.
5. Top up to 50 mL with McCoy's 5A and mix well.
6. Perform viability count by diluting 1:1 with trypan blue.
7. Wash the cells by centrifuging at 500 $\times g$ at RT for 10 min.
8. Decant supernatant and resuspend the cell pellet in McCoy's 3+ at a concentration of $<1 \times 10^6$ cells/mL.
9. Transfer to a 150 cm² culture flask, and incubate with flask on its side, cap loosened for 2 h at 37 °C in 5 % CO₂ (see Note 7).
10. Transfer the nonadherent mononuclear cells from the flask to 50 mL tube(s), and centrifuge at 500 $\times g$ at RT for 10 min.
11. Resuspend the cell pellet in 1–3 mL of Iscove's 2+.

12. Check cell viability by trypan blue exclusion (*see Note 8*).
13. Adjust viable CB and BM cells to a concentration of $1.25 \times 10^6/\text{mL}$ and PB to a concentration of $2.5 \times 10^6/\text{mL}$ in Iscove's 2+.
14. Set up the following conditions to make a total volume of 3 mL per tube:
 - Tube 1 (negative control): 1,200 μl methylcellulose, 600 μl FBS, 600 μl Iscove's 2+, 600 μl cells
 - Tube 2 (IL-3): 1,200 μl methylcellulose, 600 μl FBS, 570 μl Iscove's 2+, 600 μl cells, 30 μl IL-3
 - Tube 3 (IL-5): 1,200 μl methylcellulose, 600 μl FBS, 570 μl Iscove's 2+, 600 μl cells, 30 μl IL-5
 - Tube 4 (GM-CSF): 1,200 μl methylcellulose, 600 μl FBS, 570 μl Iscove's 2+, 600 μl cells, 30 μl GM-CSF
15. Prepare one 10 cm Petri plate (Falcon #3003), containing three 35 mm Petri dishes (Falcon #3001).
16. Using a 3 mL syringe and a 16-gauge needle for each sample, mix gently by drawing methylcellulose/cell mixture up and down. Allow bubbles to settle.
17. Draw up 2 mL of the mixture in the syringe and deliver 1 mL to each of 2–35 mm dishes. Tilt gently to spread evenly over dish bottom. Place the 2 dishes (covered) in the 10 cm dish. Add an open 35 mm dish filled with sterile water.
18. Replace the lid on the 10 cm plate and incubate cell cultures for 14 days (CB and PB) or 10 days (BM) at 37 °C in a 5 % CO₂ incubator.
19. On the final day, assess colony morphology and numbers (1 colony = minimum 40 cells; Eo/B are granulated and clump together (Fig. 1), GM are un-granulated and smaller than Eo/B).

3.2 Sputum Processing

1. Select portions of sputum free from saliva (*see Note 9*).
2. Add a volume of 0.1 % DTT equal to 4 times the weight of the sputum (*see Note 10*).
3. Vortex 15 s, then mix for 15 min at RT on a bench rocker.
4. Add a volume of D-PBS equal to 4 times the weight of the cell plug and mix for 5 additional min on a bench rocker.
5. Filter the solution through 48 μm nylon mesh.
6. Centrifuge the sample at $500 \times g$ at RT for 10 min and remove the supernatant.
7. Resuspend the cell pellet in the volume of D-PBS to achieve the required cell concentration.

3.3 Flow Cytometry for Surface Staining of IL-5R α , IL-3R α , and GM-CSFR α in CB, PB, and BM

1. Resuspend 0.5×10^6 cells in 2.5 mL FACS buffer.
2. Wash by centrifugation at $500 \times g$ at 4 °C for 5 min.
3. Remove supernatant and resuspend cell pellet in Fc blocking buffer and vortex for a few seconds.
4. Incubate samples at 4 °C in the dark for 15 min.
5. Add antibodies to each tube and vortex for a few seconds:
 - Tube 1 (compensation): 100 μ l Fc blocking buffer
 - Tube 2 (CD45): 80 μ l Fc blocking buffer, 20 μ l FITC-CD45
 - Tube 3 (CD45): 80 μ l Fc blocking buffer, 20 μ l PE-CD45
 - Tube 4: (CD34): 80 μ l Fc blocking buffer, 20 μ l PerCP-CD34
 - Tube 5: (CD45/CD34/IgG₁): 40 μ l Fc blocking buffer, 20 μ l FITC-CD45, 20 μ l PERCP-CD34, 20 μ l PE IgG₁
 - Tube 6: (CD45/CD34/GM-CSFR α): 40 μ l Fc blocking buffer, 20 μ l FITC-CD45, 20 μ l PERCP-CD34, 20 μ l PE GM-CSFR α
 - Tube 7: (CD45/CD34/IL-3R α): 40 μ l Fc blocking buffer, 20 μ l FITC-CD45, 20 μ l PERCP-CD34, 20 μ l PE-IL-3R α
 - Tube 8: (CD45/CD34/IL-5R α): 40 μ l Fc blocking buffer, 20 μ l FITC-CD45, 20 μ l PerCP-CD34, 20 μ l PE-IL-5R α
6. Incubate at 4 °C in the dark for 30 min.
7. Wash with 2.5 mL FACS buffer. Vortex sample quickly.
8. Centrifuge at $500 \times g$ at 4 °C for 5 min.
9. Discard supernatant and add 350–500 μ l 1 % PFA (or Cytofix™) to all tubes.
10. Cap tubes and wrap in aluminum foil. Store in fridge until sample can be acquired on flow cytometry (see Note 11).

3.4 Flow Cytometry for Surface Staining of IL-5R α on Progenitor Cells in Sputum

1. Distribute at least 0.5×10^6 cells per FACS tube over 3 tubes.
2. Add 2 mL of 0.1 % sodium azide in D-PBS to each FACS tube and centrifuge at $500 \times g$ at 4 °C for 10 min.
3. Pour off the supernatant and blot on tissue. Vortex.
4. Add Fc blocking buffer, incubate 10 min, then add antibodies as follows:
 - Tube 1 (D-PBS): 50 μ l Fc blocking buffer
 - Tube 2 (APC-CD34): 45 μ l Fc blocking buffer, 5 μ l APC-CD34
 - Tube 3 (PE-IL-5R): 45 μ l Fc blocking buffer, 5 μ l PE-IL-5R
 - Tube 4 (FITC-CD45): 45 μ l Fc blocking buffer, 5 μ l FITC-CD45
 - Tube 5 (CD34/CD45/PE-IgG₁): 35 μ l Fc blocking buffer, 5 μ l APC-CD34, 5 μ l FITC-CD45, 5 μ l PE-IgG₁

Tube 6 (CD34/CD45/PE-IL-5R): 35 μ L Fc blocking buffer, 5 μ L APC-CD34, 5 μ L FITC-CD45, 5 μ L PE-IL-5R

5. Vortex. Incubate in the dark, on ice for 30 min.
6. Wash with 0.1 % sodium azide in D-PBS (2 mL) and centrifuge at $500 \times g$ at 4 °C for 10 min.
7. Pour off supernatant and blot on tissue. Vortex.
8. Resuspend the cells in 350–500 μ L of 1 % PFA (or Cytofix™).
9. Cap, vortex, wrap in aluminum foil and store in refrigerator.
10. Samples are ready for analysis by flow cytometry.

4 Notes

1. FBS is heated to 56 °C for 1 h to inactivate complement.
2. The work is carried out in a class II laminar flow hood to ensure sterility of the sample. All reagents/media (except Lymphoprep which is used at RT) are pre-warmed to 37 °C in water bath before use. Collect samples into sodium heparin (1,000 U/mL) anticoagulant.
3. *Cord blood only:* Add 1 volume cord blood to 5 volumes of 6 % dextran, mix well and incubate in a 37 °C water bath for 20–30 min to separate red blood cells (RBCs) from the sample by sedimentation. Using a transfer pipette, transfer the top (clear) layer to a new 50 mL tube before proceeding.
4. Before diluting BM, gently pass up and down through a 16–18-gauge needle to break up any spicules or clumps.
5. PB and CB are diluted 1:1. BM is diluted 1:5.
6. For density gradients it is necessary to use a swinging bucket rotor rather than a fixed angle rotor. The brake is turned off to allow buckets to come to a more gradual stop, minimizing disruption to the cell layers.
7. Monocytes will adhere to the plastic flask. Cells remaining in suspension are nonadherent mononuclear cells.
8. Using a small aliquot of cells, prepare a 1:1 dilution of cell suspension with 0.4 % trypan blue. Load into a hemocytometer and read after 5 min. Cells that take up the blue stain are considered to be nonviable.
9. The weight of the saliva-free sputum that is selected for processing should be 70–200 mg.
10. For example, sputum weighing 100 mg would require 400 μ L of 0.1 % DTT solution.
11. For best results, sample should be analyzed within a few days.

References

1. Denburg JA et al (1985) Heterogeneity of human peripheral blood eosinophil-type colonies: evidence for a common basophil-eosinophil progenitor. *Blood* 66:312–318
2. Drew E et al (2005) CD34 and CD43 inhibit mast cell adhesion and are required for optimal mast cell reconstitution. *Immunity* 22:43–57
3. Drew E et al (2005) CD34 expression by mast cells: of mice and men. *Blood* 106: 1885–1887
4. Chen CC et al (2005) Identification of mast cell progenitors in adult mice. *Proc Natl Acad Sci U S A* 102:11408–11413
5. Selye H (1965) The mast cells. Butterworths, Washington, DC
6. Crivellato E, Nico B, Ribatti D (2011) The history of the controversial relationship between mast cells and basophils. *Immunol Lett* 141:10–17
7. Crivellato E, Ribatti D (2010) The mast cell: an evolutionary perspective. *Biol Rev Camb Philos Soc* 85:347–360
8. Siracusa MC et al (2011) TSLP promotes interleukin-3-independent basophil haematopoiesis and type 2 inflammation. *Nature* 477:229–233
9. Ziegler SF, Artis D (2010) Sensing the outside world: TSLP regulates barrier immunity. *Nat Immunol* 11:289–293
10. Saenz SA, Taylor BC, Artis D (2008) Welcome to the neighborhood: epithelial cell-derived cytokines license innate and adaptive immune responses at mucosal sites. *Immunol Rev* 226:172–190
11. Taylor BC et al (2009) TSLP regulates intestinal immunity and inflammation in mouse models of helminth infection and colitis. *J Exp Med* 206:655–667
12. Reece P et al (2011) Maternal allergy modulates cord blood hematopoietic progenitor Toll-like receptor expression and function. *J Allergy Clin Immunol* 127:447–453
13. Nagai Y et al (2006) Toll-like receptors on hematopoietic progenitor cells stimulate innate immune system replenishment. *Immunity* 24:801–812
14. Coussens LM et al (1999) Inflammatory mast cells up-regulate angiogenesis during squamous epithelial carcinogenesis. *Genes Dev* 13:1382–1397
15. Soucek L et al (2007) Mast cells are required for angiogenesis and macroscopic expansion of Myc-induced pancreatic islet tumors. *Nat Med* 13:1211–1218
16. Gounaris E et al (2007) Mast cells are an essential hematopoietic component for polyp development. *Proc Natl Acad Sci U S A* 104: 19977–19982
17. Maltby S, Khazaie K, McNagny KM (2009) Mast cells in tumor growth: angiogenesis, tissue remodelling and immune-modulation. *Biochim Biophys Acta* 1796:19–26
18. Lee DM et al (2002) Mast cells: a cellular link between autoantibodies and inflammatory arthritis. *Science* 297:1689–1692
19. Secor VH et al (2000) Mast cells are essential for early onset and severe disease in a murine model of multiple sclerosis. *J Exp Med* 191:813–822
20. Heissig B et al (2005) Low-dose irradiation promotes tissue revascularization through VEGF release from mast cells and MMP-9-mediated progenitor cell mobilization. *J Exp Med* 202:739–750
21. Lu LF et al (2006) Mast cells are essential intermediaries in regulatory T-cell tolerance. *Nature* 442:997–1002
22. Leslie M (2010) Immunology. Mouse studies challenge rare immune cell's powers. *Science* 329:1595
23. Sokol CL, Medzhitov R (2010) Emerging functions of basophils in protective and allergic immune responses. *Mucosal Immunol* 3: 129–137
24. Ohnmacht C et al (2010) Basophils orchestrate chronic allergic dermatitis and protective immunity against helminths. *Immunity* 33:364–374
25. Hammad H et al (2010) Inflammatory dendritic cells—not basophils—are necessary and sufficient for induction of Th2 immunity to inhaled house dust mite allergen. *J Exp Med* 207:2097–2111
26. Gurish MF, Boyce JA (2006) Mast cells: ontogeny, homing, and recruitment of a unique innate effector cell. *J Allergy Clin Immunol* 117:1285–1291
27. Franco CB et al (2010) Distinguishing mast cell and granulocyte differentiation at the single-cell level. *Cell Stem Cell* 6:361–368
28. Nakano T et al (1985) Fate of bone marrow-derived cultured mast cells after intracutaneous intraperitoneal and intravenous transfer into genetically mast cell-deficient W/W^v mice. Evidence that cultured mast cells can give rise to both connective tissue type and mucosal mast cells. *J Exp Med* 162:1025–1043
29. Kitamura Y, Ito A (2005) Mast cell-committed progenitors. *Proc Natl Acad Sci U S A* 102:11129–11130

30. Moon TC et al (2012) Microenvironmental regulation of inducible nitric oxide synthase expression and nitric oxide production in mouse bone marrow-derived mast cells. *J Leukoc Biol* 91:581–590
31. Denburg JA et al (1983) Basophil/mast cell precursors in human peripheral blood. *Blood* 61:775–780
32. Denburg JA, van Eeden SF (2006) Bone marrow progenitors in inflammation and repair: new vistas in respiratory biology and pathophysiology. *Eur Respir J* 27:441–445
33. Gauvreau GM, Denburg JA (2005) Hemopoietic progenitors: the role of eosinophil/basophil progenitors in allergic airway inflammation. *Expert Rev Clin Immunol* 1:87–101
34. Gauvreau GM, Ellis AK, Denburg JA (2009) Haemopoietic processes in allergic disease: eosinophil/basophil development. *Clin Exp Allergy* 39:1297–1306
35. Rodewald HR et al (1996) Identification of a committed precursor for the mast cell lineage. *Science* 271:818–822
36. Buhring HJ et al (1999) The monoclonal antibody 97A6 defines a novel surface antigen expressed on human basophils and their multipotent and unipotent progenitors. *Blood* 94:2343–2356
37. Hill DA et al (2012) Commensal bacteria-derived signals regulate basophil hematopoiesis and allergic inflammation. *Nat Med* 18:538–546
38. Leary AG, Ogawa M (1984) Identification of pure and mixed basophil colonies in culture of human peripheral blood and marrow cells. *Blood* 64:78–83
39. Denburg JA, Silver JE, Abrams JS (1991) Interleukin-5 is a human basophilopoietin: induction of histamine content and basophilic differentiation of HL-60 cells and of peripheral blood basophil-eosinophil progenitors. *Blood* 77:1462–1468
40. Valent P et al (1989) Interleukin-3 is a differentiation factor for human basophils. *Blood* 73:1763–1769
41. Hutt-Taylor SR et al (1988) Sodium butyrate and a T lymphocyte cell line-derived differentiation factor induce basophilic differentiation of the human promyelocytic leukemia cell line HL-60. *Blood* 71:209–215
42. Denburg JA (1992) Basophil and mast cell lineages in vitro and in vivo. *Blood* 79:846–860
43. Denburg JA, Wilson WEC, Bienenstock J (1982) Basophil production in myeloproliferative disorders: increases during acute blastic transformation of chronic myeloid leukemia. *Blood* 60:113–120
44. Djukanovic R et al (1990) Mucosal inflammation in asthma. *Am Rev Respir Dis* 142:434–457
45. Gauvreau GM et al (2000) Increased numbers of both airway basophils and mast cells in sputum after allergen inhalation challenge of atopic asthmatics. *Am J Respir Crit Care Med* 161:1473–1478
46. Wood LJ et al (1999) An inhaled corticosteroid, budesonide, reduces baseline but not allergen-induced increases in bone marrow inflammatory cell progenitors in asthmatic subjects. *Am J Respir Crit Care Med* 159:1457–1463
47. Sehmi R et al (1997) Allergen-induced increases in IL-5 receptor α -subunit expression on bone marrow-derived CD34 $^{+}$ cells from asthmatic subjects. A novel marker of progenitor cell commitment toward eosinophilic differentiation. *J Clin Invest* 100:2466–2475
48. Gauvreau GM et al (1998) Enhanced expression of GM-CSF in differentiating eosinophils of atopic and atopic asthmatic subjects. *Am J Respir Cell Mol Biol* 19:55–62
49. Dorman SC et al (2004) Sputum CD34+IL-5R α + cells increase after allergen: evidence for in situ eosinophilopoiesis. *Am J Respir Crit Care Med* 169:573–577
50. Gauvreau GM et al (2000) The effects of inhaled budesonide on circulating eosinophil progenitors and their expression of cytokines after allergen challenge in subjects with atopic asthma. *Am J Respir Crit Care Med* 162:2139–2144
51. Flood-Page P et al (2007) A study to evaluate safety and efficacy of mepolizumab in patients with moderate persistent asthma. *Am J Respir Crit Care Med* 176:1062–1071
52. Imaoka H et al (2011) TPI ASM8 reduces eosinophil progenitors in sputum after allergen challenge. *Clin Exp Allergy* 41:1740–1746

Chapter 5

Methods for the Study of Mast Cell Recruitment and Accumulation in Different Tissues

Tatiana G. Jones and Michael F. Gurish

Abstract

Mast cells (MC) are important effector cells involved in a wide range of inflammatory diseases. The lineage-committed, tissue-localized progenitor (MCp) is not easily identified histochemically like the mature MC because they lack the distinctive cytoplasmic granules. However, they can be identified by their unique cell surface phenotype and by their ability to be expanded in culture using selective growth factors. Here we describe the methods that allow evaluation of MCp and mature MC in peripheral tissues under basal and inflammatory conditions. Thus, one can enumerate mature MC as well as immature committed progenitors in order to study basal homing, inflammatory recruitment, maturation, and life span. We also provide an analysis of difficulties that could emerge during these procedures.

Key words Mast cell, Progenitors, Limiting dilution analysis, Chloroacetate esterase, Protease

1 Introduction

In contrast to other lineages of hematopoietic cells, mast cells (MC) are rare in peripheral blood. The mature highly granulated MC are found in most tissues where they are classified into at least two distinct subpopulations, mucosal MC (MMC) and CTMC, based on tissue localization, staining characteristics, and/or their expression of certain MC-specific proteases. The large concentration of protease complexed to serglycin proteoglycan stored in their secretory granules provides the unique staining characteristic of these cells. We principally use two stains to identify the mature highly granulated cells in the tissues; metachromasia in the presence of toluidine blue and the enzymatic reaction for chloroacetate esterase (CAE) reactivity, which reliably identifies all murine MC [1]. For human, the most reliable identification relies on immunostaining for the human MC tryptase as all classes of MC described to date express tryptase.

Following initial lineage commitment in the bone marrow or spleen, the committed progenitors move into the vasculature and

then into tissues as agranular cells that can be defined by specific cell surface markers. Enumeration of these cells was first described following the observation that they could be expanded in vitro with interleukin (IL)-3, and we routinely use a limiting dilution analysis with both stem cell factor (SCF) and IL-3 to monitor the number of progenitors in various tissues [2, 3]. This requires the initial isolation of a mononuclear cell (MNC) population from the tissues, and we typically isolate the MNC by density gradient to reduce the contamination with mature granulated MC.

2 Materials

2.1 Complete Medium

1. Complete RPMI 1640 medium (filter sterilized): 10 % heat-inactivated fetal calf serum (FCS), 0.1 mM nonessential amino acids (NEAA), 1 mM sodium pyruvate, 2 mM L-glutamine, 10 mM 4-(2-hydroxyethyl)-1-piperazineethanesulfonic acid (HEPES), 10^{-5} M β -mercaptoethanol, penicillin/streptomycin, 10 μ g/mL gentamicin.

2.2 Enzymes and Reagents for Isolation of Tissue Mononuclear Cells

1. DNase I, grade II powder: 100 mg bottle (Roche, NJ). Store at 4 °C.
2. 1 M CaCl₂. Store at RT.
3. 1 M Tris-HCl (pH 7.5). Store at RT.
4. Glycerol, anhydrous (American Bioanalytical). Store at RT.
5. DNase I stock: 10 mg/mL DNase I, 5 mM CaCl₂, 10 mM Tris-HCl (pH 7), 50 % glycerol (v/v). Store at -20 °C.
6. Collagenase type IV (e.g., Worthington # LS004188). Dilute in Ca²⁺- and Mg²⁺-free Hank's Balanced Salt Solution (HBSS).
7. Digestive Enzyme Mix: Final concentration is 500 U/mL collagenase IV and 10 μ g/mL DNase I, diluted in complete RPMI. This is made fresh (preferred) or stored at -70 °C. 1 mM dithiothreitol can be added as an option to break up mucus.

2.3 Percoll Gradient for Isolation of Mononuclear Cells

1. Percoll: For the stock 100 % Percoll (Sigma-Aldrich # P-1644), mix 10 mL of 10× RPMI, 1 mL of 1 M HEPES, 0.5 mL of 7.5 % sodium bicarbonate, and 90 mL of Percoll. Alternatively, mix 10 mL 10× PBS and 90 mL Percoll. Dilute with complete medium for working concentrations of 44 % and 67 %.

2.4 Reagents for Histology and Immunohistochemistry

1. 4 % paraformaldehyde for fixation.
2. Glycolmethacrylate (JB-4, Polysciences, Inc, Niles, IL) or paraffin for embedding.
3. 1 g New Fuchsin dissolved in 25 mL 2 N HCl.

4. 4 % sodium nitrite in ddH₂O.
5. 0.1 M phosphate buffer (pH 7.6).
6. Chloroacetate stock: 10 mg naphthol AS-D chloroacetate in 5 mL *N,N*-dimethyl formamide. Store at -20 °C.
7. Chloroacetate esterase (CAE) solution for staining of mature MC (make fresh each time): mix 2.5 µl New Fuchsin with 2.5 µl 4 % sodium nitrite, then add 1 mL phosphate buffer and mix. Finally, add 50 µl of chloroacetate stock and mix well.
8. Gill's hematoxylin II for counterstaining.
9. 3 % hydrogen peroxide (H₂O₂) with 0.1 % sodium azide.
10. Target Retrieval Solution (Dako, Carpinteria, CA).
11. Monoclonal anti-mMCP-1 from R&D Systems (Minneapolis, MN).
12. Rat on Mouse HRP-Polymer Kit (Biocare, Concord, CA) for mMCP-1 detection.
13. Envision System-HRP (DAB) kit (Dako #205) for mMCP-2, -4, -5, -6, -7, and CPA3 detection.

2.5 Antibodies and Reagents Useful for Identification of Cells by FACS

1. Mature lineage marker antibody mix to exclude other more common cell types: anti-CD3, anti-CD4, anti-CD8, anti-CD19, anti-B220, anti-Gr1 (all conjugated to same fluorochrome or other detectable marker (e.g., biotin)).
2. To define MCp and mature MC: anti-CD34, anti-CD117 (c-Kit), anti-β7-integrin, anti-FcεRIα [4–6].
3. Sterile Ca²⁺-/Mg²⁺-free HBSS (filter sterilize and store at 4 °C).
4. FACS buffer: 2 % sterile heat-inactivated FCS (10 mL) in Ca²⁺-/Mg²⁺-free HBSS (500 mL).
5. 70 % Ethanol.
6. 70 µm cell strainers (Fisher Scientific # 22-363-548).
7. 5 mL Falcon tubes 12×75 mm.

2.6 Antibodies for Identification of Mast Cells by Immuno-histochemistry

1. Anti-mMCP-1 is a monoclonal Ab available from R&D Systems (Minneapolis, MN).
2. Anti-mMCP-2, -4, -5, -6 -7 and CPA3 Ab are polyclonal anti-peptide antibodies prepared in rabbits [7–12].

2.7 Limiting Dilution Assay

1. γ-irradiated splenocytes (30 Gy) for feeder cells.
2. Murine IL-3 and SCF from PeproTech, Inc. (Rocky Hill, NJ). The final concentration will be 10 ng/mL each per well.
3. Flat-bottomed tissue culture microtiter plates (Corning #3596, Corning, NY). Use 2 plates per tissue.

3 Methods

3.1 Isolation of Mononuclear Cells from Mouse Tissues

Small Intestine

1. Excise the small intestine and place in cold complete RPMI medium. Keep on ice while the remaining samples are collected.
2. Flush the lumen 2–3 times with 30–40 mL cold Ca^{2+} -/ Mg^{2+} -free HBSS using a rat oral gavage needle (3", 20 gauge) affixed to a 60 mL syringe. Run the needle the length of the intestine while flushing.
3. After 2–3 flushes, open the intestine lengthwise either with scissors or by tearing the intestine away from the gavage needle sideways.
4. Wash the splayed small intestine three more times by swirling in Petri plates with 50 mL of Ca^{2+} -/ Mg^{2+} -free HBSS.
5. Transfer the tissue to a clean Petri plate and finely chop the tissue with scalpels until homogenous. The finer the tissue is diced, the better the yield of MNC (see Notes 1 and 2).
6. Transfer tissue to 50 mL tubes with 20 mL of complete RPMI 1640 containing collagenase type IV/DNAse I.
7. Perform a series of three enzymatic digestions for ~20 min each on a shaker at 37 °C. Use enough motion to prevent tissue from settling at the bottom but do not shake too vigorously.
8. Fill tubes to the top and allow the undigested tissue to settle for 5–10 min after each digestion round and then collect the supernatant.
9. Perform the next enzymatic digestion on the settled, undigested tissue as in steps 7 and 8. Repeat once more for a total of three digestion rounds.
10. Harvest the liberated cells from the supernatant by centrifugation ($300 \times g$ for 10 min).
11. Isolate the MNC using Percoll gradients as described in Subheading 3.2.

Lungs

1. Perfuse mouse lung vasculature with 10 mL of Ca^{2+} -/ Mg^{2+} -free HBSS administered via the right ventricle of the heart (see Notes 1 and 3).
2. Harvest lung tissue and place in 20 mL of complete RPMI 1640 on ice while all samples are collected.
3. Finely chop the lung tissue using scalpels (as described in Subheading “Small Intestine”, step 5).
4. Perform a series of three enzymatic digestion for ~20 min each at 37 °C and isolate MNCs as described for the intestine (as in Subheading “Small Intestine”, steps 7–11).

Spleen

1. Harvest spleens aseptically.
2. Place spleens in a sterile cell strainer (70 μm) seated in a sterile Petri dish or 24-well plate containing complete RPMI.
3. Liberate splenocytes by grinding the spleen with the flat end of a 1 mL syringe plunger.
4. Discard strainer containing spleen capsule and transfer cell suspension into 50 mL tubes and pellet splenocytes by centrifugation (300 $\times g$ for 10 min).
5. Isolate tissue MNC using Percoll gradients as described in Subheading 3.2.

Bone Marrow

1. Harvest bone marrow (BM) MNC by flushing the cells from the femora and tibias.
2. Flush BM cells by trimming the end of the bone and flushing with complete RPMI using a 25G needle attached to a 10 mL syringe.
3. Aspirate the isolated BM through an 18G needle to disaggregate cell clumps or triturate in a serological pipette.
4. Collect the BM cells by centrifugation (300 $\times g$ for 10 min).
5. Obtain MNC using a Percoll gradient as described in Subheading 3.2.

3.2 Isolation of MNC by Percoll Gradient

1. For the intestine that undergoes multiple enzymatic digestions, a Percoll gradient is run after each digestion and the cells are pooled at the end of the procedure.
2. To isolate MNC from each tissue, cells are pelleted by centrifugation, the supernatant discarded, the pellet disrupted by agitation and then resuspended in 5 mL of 44 % Percoll.
3. Transfer the cell suspension to a 15 mL conical tube, and underlay with 1.5 mL of 67 % Percoll. Centrifuge the Percoll gradient for 20 min (500 $\times g$ at RT).
4. At the end of the centrifugation, you should see cells at the interface. These are MNC, whereas the pellet contains the majority of erythrocytes, mature mast cells, granulocytes, dead cells, and any undigested tissue pieces.
5. Use a 5 mL pipette to first carefully remove and discard most of the upper layer (~2–2.5 mL). Collect cells at the interface without disturbing the bottom pellet.
6. Transfer collected cells into new 15 mL conical tube and fill it with complete RPMI.
7. Mix to dilute the Percoll and harvest MNC by centrifugation at 300 $\times g$ for 10 min.
8. Discard the supernatant and resuspend the MNC pellet in complete RPMI. Determine the number of viable cells by trypan blue dye exclusion using a hemacytometer.

3.3 Assessment of MCp by Limiting Dilution Analysis (Fig. 1)

1. Prepare feeder cells by resuspending γ -irradiated splenocytes at a concentration of 10^6 /mL. Add IL-3 and stem cell factor (20 ng/mL each cytokine) (see Note 4). Approximately 20×10^6 γ -irradiated splenocytes cells in 20 mL media are required per tissue assayed (two plates per tissue).
2. Serially dilute the MNC in complete RPMI (e.g., 8 twofold dilutions).
3. Plate 24 wells for each cell concentration in duplicate 96-well flat-bottomed microtiter tissue culture plates. Lung and spleen MNC are plated at a starting concentration of 20,000 cells/well; intestine and bone marrow MNC at 10,000 cells/well.
4. Use 100 μ l volume per well of each MNC dilution.
5. Next, add 100 μ l of feeder cells to each well (includes added cytokines).
6. Wrap the plates in Parafilm to reduce dehydration and place in a humidified, 5 % CO₂ incubator at 37 °C for 10–12 days.

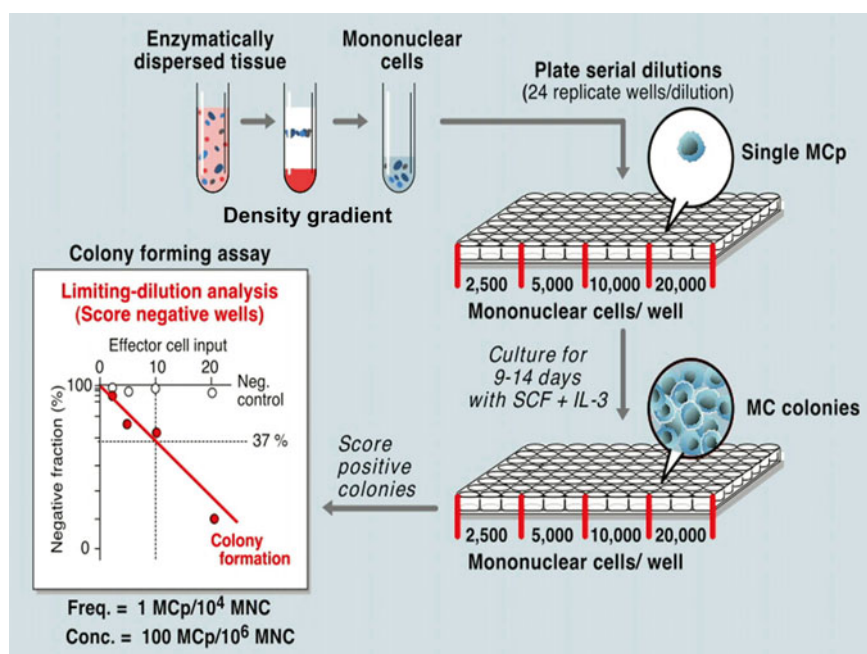


Fig. 1 Limiting dilution analysis (clonogenic assay). Solid tissues are chopped up and enzymatically digested, and the isolated cells run over a density gradient to obtain the mononuclear cells (MNC). Cells are counted and eight serial dilutions are made and plated into two 96-well flat-bottom trays giving 24 replicate wells/dilution. Cells are supplemented with 10 ng/mL each of stem cell factor and IL-3 plus feeder cells and cultured for 10–14 days. Each well is inspected and marked as negative or positive for a MC colony. The number of negative wells versus the number of MNC plated is plotted and the frequency (MCp/MNC) determined by the Poisson distribution

7. Monitor for MCp colonies with an inverted microscope. The MCp colonies appear as large nonadherent colonies consisting of at least 20 small- to medium-sized round cells [2, 13, 14].
8. Calculate the number of MNC plated to find 1 MCp based on a Poisson distribution model. This can be done in a spreadsheet as follows: In column A, list the number of MNC plated per well at each dilution. In Column B, list the negative natural log (-Ln) of the fraction of wells that were negative for any MC colonies (i.e., calculated the -Ln of number in column F) at this dilution. In column C, list number of wells at this dilution that had a least one MC colony. In column D, list total number of wells evaluated at this dilution (this might not be 24 if there was contamination or dehydration). In column E, list the number of negative wells at this dilution (column D minus column C). In column F, list the fraction of wells that were negative for MC growth at this dilution (column E divided by column D). A scatter plot (graph) of the values in column A versus column B will show where the linear relationship is. To calculate the number of MNC plated to find one MCp, calculate a trend line over the linear range and find the number of MNC plated that give a value of 0.994 for the -Ln of the fraction of negative wells. For example, if the linear slope occurred between rows 11 and 14, then the number of MNC plated to find one MCp would be determined by the formula: $f(x) = \text{TREND}(\text{A11:A14}, \text{B11:B14}, 0.994)$. This gives the average number of MNC that needed to be plated to find one MCp over the dilutions listed in rows 11 through 14. Then, the concentration of MCp per 10^6 MNC in the tissue is 10^6 divided by that average number of MNC. An alternative way of estimating the frequency of MCp within the isolated MNC can be obtained by dividing the value in column B by the value in column A. We express the MCp concentration as the number of MCp per 10^6 MNC isolated from the tissue.
9. The total number of MCp/tissue is derived by multiplying the concentration of MCp by the MNC yield (in millions of cells) from the tissue (see Note 5).

3.4 Assessment of MC Numbers in Tissue by Flow Cytometry

1. To evaluate the number of committed MCp in a tissue by cell surface phenotype using FACS analysis, obtain MNC from the various tissues as described in Subheadings 3.1 and 3.2.
2. MCp are characterized as lineage marker negative (Lin^-), CD34^+ , c-Kit^+ , $\beta 7$ integrin^{high}, $\text{Fc}\epsilon\text{RI}\alpha^+$ cells, while myeloid cells not yet committed to the MC lineage are c-Kit^+ but low or no $\text{Fc}\epsilon\text{RI}\alpha$ [4–6]. In instances where high levels of circulating IgE are present, detect $\text{Fc}\epsilon\text{RI}\alpha$ expression by using anti-IgE to avoid loss of sensitivity due to competition by IgE binding to $\text{Fc}\epsilon\text{RI}$.

3. For FACS analysis, filter MNC (resuspended in 1 mL) through 70 μ m mesh into 5 mL Falcon tubes and add 2 mL of cold FACS buffer to a sample tube.
4. Split cells between an experimental tube, a “no stain” control tube, a single stain control tube (need one single stain control for each Ab used in FACS setting), and an Ig isotype control tube.
5. Spin cells down ($300 \times g$ for 5 min) and resuspend in 100 μ L of cold FACS buffer.
6. Block nonspecific Fc binding using anti-CD16/CD32 (BD Pharmingen): Use 2 μ L per 100 μ L of FACS buffer per sample ($\sim 10^6$ cells).
7. Incubate in the dark on ice for 15 min.
8. Without washing, centrifuge the tubes at $300 \times g$ for 5 min and aspirate supernatant.
9. Resuspend cells in 100 μ L of fresh cold FACS buffer and add 1 μ g/100 μ L of specific Ab or isotype control.
10. Incubate in a dark on ice for 20 min, periodically vortexing the tubes.
11. Fill tubes with cold FACS buffer, centrifuge at $300 \times g$ for 5 min, aspirate supernatant.
12. Resuspend in 2 mL of cold FACS buffer, centrifuge again.
13. Aspirate supernatant and resuspend in 0.5 mL of cold FACS buffer.
14. Analyze within a few hours.

3.5 Assessment of Mature MC by Histology

1. For the histochemical evaluation of mature MC in mouse tissues, fix tissues for 8–24 h in 4 % paraformaldehyde and then transfer to PBS for another 8–24 h.
2. Embed tissues in glycolmethacrylate or paraffin (glycolmethacrylate provides finer detail) and prepare slides with 3 or 5 μ m sections, respectively.
3. For detection of mature MC by CAE reactivity, cover sections with CAE staining solution (Subheading 2.3, item 3) for 20 min at RT. Wash with running tap water and counter stain with Gill’s hematoxylin II for 2 min (alternatively, can use methyl green for 30 s). Wash with warm tap water until blue color appears; longer wash times result in darker blue. Dry and mount with mounting medium. MC appear as red stained cells, while PMN are lighter in color with a distinct nuclear morphology [5, 15].
4. MC numbers are counted in a standard area (e.g., 9 high power fields) and expressed as cells per cm^2 for comparison to the literature [16].

5. In the lung, we evaluate MC in 15 large broncho-vascular bundles (bronchi with >200 μm cross section) in each sample. Tissue areas can be determined using Image J (from the National Institutes of Health) image analysis software [15].
6. For evaluation of MC in the trachea, divide the trachea into three transverse sections and embed so that each slide contains a cross section from each area of the trachea. The three sections representing the different areas are examined and expressed as the number of MC per three tracheal rings.
7. Quantify the MCs in the intestine per villus-crypt unit [17, 18].

3.6 Assessment of MC by Immuno-histochemistry

1. For immunohistochemical evaluation of the proteases expressed by MC in various tissues, the tissue is fixed in 10 % neutral buffered formalin for 8–24 h, rinsed in PBS for another 8–24 h, and then embedded in paraffin. Cut and mount 5 μm sections on slides.
2. Deparaffinize and rehydrate the tissue sections.
3. Incubate the sections with freshly prepared 3 % H_2O_2 with 0.1 % sodium azide to inhibit endogenous peroxidase activity.
4. Perform antigen retrieval procedure with Target Retrieval Solution at 97 °C for 30 min as per manufacturer's instructions.
5. Incubate sections with primary antibodies for 1 h at RT.
6. Visualize Ab binding using the Rat on Mouse HRP-Polymer Kit for mMCP-1, and the Envision System-HRP (DAB) for mMCP-2, -4, -5, -6, -7, and CPA3.
7. Immunohistochemical detection of mMCP-1 is done at a final concentration of 5 $\mu\text{g}/\text{mL}$. The appropriate concentration and specificity of each rabbit Ab must be individually determined as the highest concentration that gave a substantial signal with minimal background [15].
8. Counterstain with hematoxylin, dehydrate, and mount.

4 Notes

1. *Mincing tissues.* The numbers of collected MNC and thus the results of limiting dilutions assay are to a high degree dependent on the quality of the tissue processing. Well-prepared tissue must be completely homogeneous.
2. *Isolation of MNC from the intestine.* To obtain as many MNC as possible from small intestine, it is important to first rinse the intestine very well. Secondly, the finer the tissue is chopped before enzymatic digestion, the better.
3. *Lung perfusion.* To limit contamination of lung MNC with cells from circulating blood, the lung must be perfused.

If perfusion is done correctly, lung color changes to white or light pink.

4. *Growth factors (IL-3 and SCF)*. Murine IL-3 and stem cell factor are two major cytokines necessary for performing the limiting dilution MCp assay as well as for culturing bone marrow-derived MC (BMMC). Adequate concentration of these cytokines in culture medium is very important [19]. These cytokines are commercially available. We have had good results using these cytokines from PeproTech, Inc.
5. *Intensity of inflammation*. The recruitment of MCp to inflamed tissues and accumulation of mature MC in the tissues depend, at least in part, on the type and severity of inflammation. Therefore, it is recommended to evaluate dose, duration, and frequency of challenges as well as time of assessment.

References

1. Friend DS, Ghildyal N, Austen KF, Gurish MF, Matsumoto R, Stevens RL (1996) *J Cell Biol* 135:279–290
2. Gurish MF, Tao H, Abonia JP, Arya A, Friend DS, Parker CM, Austen KF (2001) *J Exp Med* 194:1243–1252
3. Abonia JP, Hallgren J, Jones T, Shi T, Xu Y, Koni P, Flavell RA, Boyce JA, Austen KF, Gurish MF (2006) *Blood* 108:1588–1594
4. Arinobu Y, Iwasaki H, Gurish MF, Mizuno S, Shigematsu H, Ozawa H, Tenen DG, Austen KF, Akashi K (2005) *Proc Natl Acad Sci U S A* 102:18105–18110
5. Hallgren J, Jones TG, Abonia JP, Xing W, Humbles A, Austen KF, Gurish MF (2007) *Proc Natl Acad Sci U S A* 104: 20478–20483
6. Liu AY, Dwyer DF, Jones TG, Bankova LG, Shen S, Katz HR, Austen KF, Gurish MF (2013) *J Immunol* 190:1758–1766
7. Ghildyal N, Friend DS, Freelund R, Austen KF, McNeil HP, Schiller V, Stevens RL (1994) *J Immunol* 153:2624
8. Ghildyal N, Friend DS, Nicodemus CF, Austen KF, Stevens RL (1993) *J Immunol* 151:3206
9. Ghildyal N, Friend DS, Stevens RL, Austen KF, Huang C, Penrose JF, Sali A, Gurish MF (1996) *J Exp Med* 184:1061
10. Gurish MF, Pear WS, Stevens RL, Scott ML, Sokol K, Ghildyal N, Webster MJ, Hu X, Austen KF, Baltimore D (1995) *Immunity* 3: 175
11. McNeil HP, Reynolds DS, Schiller V, Ghildyal N, Gurley DS, Austen KF, Stevens RL (1992) *Proc Natl Acad Sci U S A* 89:11174
12. Forsberg E, Pejler G, Ringvall M, Lunderius C, Tomasini-Johansson B, Kusche-Gullberg M, Eriksson I, Ledin J, Hellman L, Kjellen L (1999) *Nature* 400:773–776
13. Crapper RM, Schrader JW (1983) *J Immunol* 131:923–928
14. Dillon SB, MacDonald TT (1986) *Parasite Immunol* 8:503–511
15. Xing W, Austen KF, Gurish MF, Jones TG (2011) *Proc Natl Acad Sci U S A* 108: 14210–14215
16. Yu M, Tsai M, Tam SY, Jones C, Zehnder J, Galli SJ (2006) *J Clin Investig* 116:1633–1641
17. Knight PA, Wright SH, Lawrence CE, Paterson YY, Miller HR (2000) *J Exp Med* 192: 1849–1856
18. Scudamore CL, McMillan L, Thornton EM, Wright SH, Newlands GF, Miller HR (1997) *Am J Pathol* 150:1661
19. Ohnmacht C, Voehringer D (2009) *Blood* 113:2816–2825

Chapter 6

Notch2 Signaling in Mast Cell Development and Distribution in the Intestine

Mamiko Sakata-Yanagimoto and Shigeru Chiba

Abstract

Notch signaling controls cell-fate specification events in various types of blood cells, and it further regulates the function of particular blood cells. Recent studies have identified the role of Notch signaling as a determinant of mast cell fate from bone marrow progenitors and mast cell maturation towards mucosal type rather than connective tissue type. Furthermore, Notch2 has functional properties for immune defense against *Strongyloides venezuelensis* through properly distributing intestinal mast cells. The goal of this chapter is to provide the researchers with the comprehensive protocols to examine the functions of Notch signaling in mast cells both in vitro and in vivo.

Key words Notch, Mast cells, Mucosal-type mast cells, mMCP-1

1 Introduction

Mast cells are generated by culturing mouse bone marrow cells for more than 4 weeks in an appropriate condition as it was first developed by Kitamura Y in the 1970s [1]. These mast cells (cultured mast cells, CMCs) are very useful for investigation of mast cell function and maturation. In recent years, we and others have developed culture systems using Notch ligands for various developmental stages of blood cells. These experimental systems are shown to be effective to clarify the role of Notch signaling in hematopoietic cell differentiation. Among examples are hematopoietic stem cell expansion [2] and promotion of T and NK cell development at the expense of B cells and macrophages [3, 4]. Activation of Notch signaling is also effective for CMC generation, wherein it instructs bone marrow progenitors towards mast cells at the expense of neutrophil/macrophage differentiation [5].

Mast cells are classified into two types dependent on their residual tissue: connective tissue-type mast cells (CTMCs) and mucosal-type mast cells (MMCs) [6]. Each type of mouse mast cells is usually distinguished by the histochemical staining patterns

and the expression profiles of mast cell proteases (mMCPs). CTMCs express mMCP-4, mMCP-5, mMCP-6, and mMCP-7, while MMCs express mMCP-1 and mMCP-2. CMCs show various mMCP expression patterns dependent on cytokine conditions, often recapitulating those of mast cells, present in the tissues. For example, CMCs cultured with interleukin (IL)-9 and/or transforming growth factor beta 1 (TGF- β 1) augment mMCP-1 expression, a marker of intestinal mast cells [7]. Stimulation with Notch ligands upregulates mMCP-1 expression markedly and enhances mMCP-2 expression to some extent, without providing any effects on either mMCP-5 or mMCP-6 (unpublished data). This observation suggests that Notch signaling skews CMCs towards MMCs rather than CTMCs.

To examine the function of Notch2 signaling in mast cells *in vivo*, *Notch2* conditional knockout mice is useful. We clarified that Notch2 is required for proper mast cell distribution in the small intestine and for expulsion of *Strongyloides venezuelensis* using *Notch2* conditional knockout mice [8].

In this chapter, we describe the methods to generate mast cells using Notch ligands and to evaluate the effect of Notch signaling on mast cell maturation *in vitro*. We also describe how to examine Notch2 signaling in mast cells *in vivo* by using *Notch2* conditional knockout mice.

2 Materials

2.1 Vectors

1. pLAT-E and pMYS ires-GFP (*see Note 1*).
2. pGCDNsam ires-human nerve growth factor receptor (NGFR) (*see Note 2*).
3. GATA3 and Hes1 cDNA (*see Note 3*).

2.2 Notch Ligands

1. Recombinant mouse Dll1-Fc from R&D Systems (Catalog Number, 5026DL) or Enzo Life Sciences (Catalog Number, ALX-201-455-C05) (*see Note 4*).
2. Recombinant mouse Jagged-1-Fc from Enzo Life Sciences (Catalog Number, ALX-201-463-C05).
3. Fc portion of human IgG₁ (Fc protein), which is useful as a control, from Jackson ImmunoResearch Laboratories.

2.3 Buffers

1. MACS buffer: 1× phosphate buffered saline (PBS), 0.5 % bovine serum albumin (BSA), and 2 mM ethylenediaminetetraacetic acid (EDTA).
2. Staining buffer: 1× PBS, 2 % fetal bovine serum (FBS), and 0.05 % sodium azide (NaN₃).

3. 0.5 % toluidine blue solution: dilute 0.5 g toluidine blue O (Sigma-Aldrich, Catalog Number, T0394) in 99.5 mL 0.5 N HCl. Final pH is ~0.3.
4. Carnoy's solution: 100 % ethanol, chloroform, and acetic acid at a ratio of 6:3:1.
5. Iodide solution (I₂/KI): 1 g iodine crystals and 2 g potassium iodide in 100 mL water.

2.4 Plates, Medium, and Cytokines

1. 24-well non-tissue culture plate.
2. RPMI-1640 medium.
3. Iscove's modified Dulbecco's medium (IMDM).
4. MethoCult M3231 (STEMCELL Technologies).
5. Cytokines including stem cell factor (SCF), interleukin (IL)-3, IL-4, IL-6, IL-9, IL-10, and thrombopoietin (TPO).
6. Transforming growth factor beta 1 (TGF- β 1) (R&D Systems).

2.5 MACS Cell Separation Kit

1. Streptavidin MicroBeads, LS Columns, and MidiMACS Separator (Miltenyi Biotec).

2.6 Antibodies

1. Biotinylated hamster anti-Notch2 antibody (clone 35.2) (*see Note 5*).
2. Purified mouse immunoglobulin E (IgE) isotype control, fluorescein isothiocyanate (FITC)-conjugated rat anti-IgE, biotinylated rat anti-IgE, and phycoerythrin (PE)-conjugated mouse antihuman nerve growth factor receptor (NGFR) antibodies (BD Biosciences).
3. Purified rabbit antihuman IgG antibody, specific for gamma chain (DAKO).
4. Other fluorescence-conjugated antibodies described here from eBioscience.
5. For a full list of antibodies described in this protocol, *see Table 1*.

2.7 Mice

1. Conditional *Notch2* knockout mice (*see Note 6*).
2. Mx1-*cre* mice (*see Note 7*).

2.8 Instruments

1. Cytospin centrifuge.
2. AutoMACS or equivalent.
3. FACS Aria cell sorter or similar instrument.

Table 1
Specific antibodies described in this protocol

Name	Conjugate	Vendor	Application in this protocol
Biotinylated hamster anti-Notch2 antibody	Biotin	See Note 5	Flow cytometry
Purified mouse immunoglobulin E isotype control	Unconjugated	BD Biosciences	Flow cytometry
FITC-conjugated rat anti-IgE	FITC	BD Biosciences	Flow cytometry
Biotinylated rat anti-IgE	Biotin	BD Biosciences	Flow cytometry
PE-conjugated mouse antihuman nerve growth factor receptor (NGFR)	PE	BD Biosciences	Flow cytometry
Purified rat anti-CD16/32 antibody	Unconjugated	eBioscience	Flow cytometry
APC-conjugated rat anti-c-Kit antibody	APC	eBioscience	Flow cytometry
PE-conjugated rat anti-Ly-6G (Gr-1) antibody	PE	eBioscience	Flow cytometry
PE-conjugated rat anti-CD11b (Mac1) antibody	PE	eBioscience	Flow cytometry
Biotinylated rat anti-CD3e antibody	Biotin	eBioscience	Lin ⁻ selection
Biotinylated rat anti-CD4 antibody	Biotin	eBioscience	Lin ⁻ selection
Biotinylated rat anti-CD8a antibody	Biotin	eBioscience	Lin ⁻ selection
Biotinylated rat anti-B220 antibody	Biotin	eBioscience	Lin ⁻ selection
Biotinylated rat anti-TER-119 antibody	Biotin	eBioscience	Lin ⁻ selection
Biotinylated rat anti-Ly-6G (Gr-1) antibody	Biotin	eBioscience	Lin ⁻ selection
Purified rabbit antihuman IgG antibody	Unconjugated	DAKO	Plate coating

3 Methods

3.1 Induction of Mast Cell Differentiation from Myeloid Progenitors by Notch Ligands

Separation of Lineage-Negative Cells and Myeloid Progenitors (See Note 8)

1. Harvest approximately 2×10^8 mononuclear cells (MNCs) from C57BL/6 mouse bone marrow (BM).
2. Add 16 μ L of biotinylated rat anti-lineage antibodies in 80 μ L of MACS buffer (concentration of each antibody is 14 μ g/mL) and incubate for 30 min at 4 °C (see Note 9).
3. Wash the mixture twice with MACS buffer.
4. Add 28 μ L of streptavidin MicroBeads in 140 μ L of MACS buffer and stand for 15 min at 4 °C.
5. Collect lineage-negative (Lin⁻) cells using either autoMACS or manual separation using LS column and MidiMACS Separator according to the manufacturer's instructions (see Note 10).

6. Separate Lin⁻c-Kit^{+Scal⁻}Fc γ R^{low}CD34⁺ and Lin⁻c-Kit^{+Scal⁻}Fc γ R^{high}CD34⁺ cells using FACS Aria cell sorter as common myeloid progenitors (CMPs) and granulocyte -macrophage progenitors (GMPs), respectively [9].

*Immobilization
of Dll1-Fc or Jagged1-Fc*

1. Coat a 24-well non-tissue culture plate with 10 μ g/mL rabbit antihuman IgG antibody and shake at 60 rpm for 30 min at 37 °C.
2. Remove the antibody, block the plate with RPMI-1640 medium containing 20 % FBS for 30 min at 37 °C, and wash once with PBS.
3. Cover the plate with PBS-diluted Dll1-Fc (3.5 μ g/mL), Jagged1-Fc (5 μ g/mL), or Fc protein (2 μ g/mL) and shake at 60 rpm for 30 min at 37 °C.
4. Remove the protein and wash with PBS once.

*Culture of Myeloid
Progenitors with Delta1-Fc
or Jagged1-Fc*

1. Seed the sorted CMPs, GMPs, or Lin⁻ cells, in Dll1-Fc-, Jagged1-Fc-, or Fc protein-fixed plates in 400 μ L of IMDM supplemented with 20 % FBS, 50 ng/mL SCF, 20 ng/mL IL-3, 20 ng/mL IL-6, and 20 ng/mL TPO. Incubate the cells for 7 days at 37 °C with 5 % CO₂ (see Note 11).
2. Harvest and analyze the cells by flow cytometry on Day 7 as follows:
 - (a) Harvest the cells, wash with staining buffer once, and resuspend the cells in 50 μ L of staining buffer.
 - (b) Add 0.5 μ L of purified rat anti-CD16/32 (Fc γ receptor III/II) antibody to block Fc-mediated interactions.
 - (c) Add 2 μ L of purified mouse IgE isotype control.
 - (d) Wash once with staining buffer.
 - (e) Add FITC-conjugated rat anti-IgE, PE-conjugated rat anti-Gr-1 and anti-Mac1, and allophycocyanin (APC)-conjugated rat anti-c-Kit antibodies.
 - (f) Wash twice with staining buffer and resuspend the cells in 200 μ L of staining buffer. Add 5 μ L of the 7-AAD Viability Dye Solution (Beckman coulter) for each test tube for detection of dead cells.
 - (g) Analyze the cells by flow cytometry.
3. Analyze the cells by toluidine blue stain of cytopsin slide on Day 7 (see Note 12):
 - (a) Cytospin the harvested cells at 28 \times g for 5 min in a cytopsin centrifuge.
 - (b) Air-dry.

- (c) Cover the films with toluidine blue solution and let them stand for 30–45 min.
- (d) Rinse with water and air-dry.

3.2 Induction of Mast Cells by Retrovirus-Mediated Gene Transfer into Myeloid Progenitors

Retrovirus-Mediated Gene Transfer into Myeloid Progenitors (See Note 13)

1. Transfect the retrovirus-packaging cell line, PLAT-E, with Hes1 –pGCSDNsam ires-human NGFR and GATA3-pMYS ires-GFP vector, respectively, using FuGENE 6 (Promega).
2. Change the medium at 24 h after transfection.
3. Collect the supernatant at 96 h after transfection and concentrate it by centrifugation at $21,500 \times g$ for 4–6 h at 4 °C. Discard the supernatant.
4. Coat a 24-well non-tissue culture plate with 40 µg/mL of RetroNectin solution, 250 µL/well (Takara Bio), and stand for overnight at 4 °C.
5. Remove the RetroNectin solution and then block with 300 µL of 2 % BSA in PBS for 30 min at room temperature (RT).
6. Wash with PBS once.
7. Cover the plate with the concentrated viral solution, and stand for 4–6 h at 37 °C.
8. Remove the concentrated viral solution and seed the sorted CMPs or GMPs in the presence of 20 % FBS, 50 ng/mL SCF, 20 ng/mL IL-3, 20 ng/mL IL-6, and 20 ng/mL TPO.
9. Incubate the cells at 37 °C with 5 % CO₂. Harvest the cells by pipetting and move them into a new 24-well non-tissue culture plate 48 h after infection. Change the half of medium approximately every other day.
10. On day 8 after the initiation of infection, analyze the cells by flow cytometry. Stain the cells in the method described in Subheading “Culture of Myeloid Progenitors with Delta1-Fc or Jagged1-Fc” with minor modifications as follows:
 - (a) Add purified rat anti-CD16/32 antibody.
 - (b) Add purified mouse IgE isotype control.
 - (c) Wash with staining buffer once.
 - (d) Add PE-conjugated mouse antihuman NGFR, APC-conjugated rat anti-c-Kit antibodies, and biotinylated rat anti-IgE.
 - (e) Wash with staining buffer once.
 - (f) Add streptavidin PE-Cy7.
 - (g) Wash with staining buffer twice, resuspend the cells in staining buffer, and add the 7-AAD Viability Dye Solution.
 - (h) Analyze the stained cells by flow cytometry (see Note 14).

Mast Cell Generation in Methyl-cellulose

1. Culture the sorted CMPs or GMPs with concentrated viral solution in RetroNectin-coated plate as described in Subheading “Retrovirus-Mediated Gene Transfer into Myeloid Progenitors (see Note 13)”.
2. Sort GFP- and NGFR-positive cells as follows:
 - (a) Harvest the cells 48 h after infection.
 - (b) Add PE-conjugated anti-NGFR receptor antibody and wash with PBS.
 - (c) Sort the GFP-positive and NGFR-positive cells by FACS Aria cell sorter.
3. Subject the sorted cells to colony assay using MethoCult M3231, supplemented with 50 ng/mL SCF, 20 ng/mL IL3, 20 ng/mL IL-6, and 20 ng/mL TPO (see Note 15).
4. At days 7 and 10, observe the colonies under a microscope. Pick representative colonies up, transfer the colony-forming cells into 100 μ L of PBS, and subject the cell suspension to cytospin and stain as described in Subheading “Culture of Myeloid Progenitors with Delta1-Fc or Jagged1-Fc” (see Note 16).

3.3 Effects of Notch Signaling on mMCP-1 and mMCP-2 Expression in CMCs

1. Generate CMCs from whole mouse bone marrow cells using IL-3 and SCF, as described [10]. Immobilize Dll1-Fc or Jagged1-Fc as in Subheading “Immobilization of Dll1-Fc or Jagged1-Fc”.
2. Culture 1×10^4 CMCs in a Dll1-Fc- or Jagged1-Fc-immobilized 24-well plate with 50 ng/mL SCF and 1 ng/mL IL-3 or 50 ng/mL SCF, 1 ng/mL IL-3, 5 ng/mL IL-9, and 1 ng/mL TGF- β 1 for 8 h.
3. Harvest the cells and supernatant at a time appropriate for desired analyses. For example:
 - (a) At \sim 8 h prepare total RNA, reverse-transcribe using Superscript III (Invitrogen), and analyze by quantitative real-time PCR using TaqMan Gene Expression Assays (Applied Biosystems) specific for mMCPs. Evaluate the ribosomal RNA levels by TaqMan ribosomal RNA control reagent (Applied Biosystems) as an internal control and use them to standardize the mRNA levels.
 - (b) Collect the supernatant at 24 h to evaluate mMCP-1 protein levels using an ELISA kit (Moredun Scientific).

3.4 Analysis of Notch2-Signaling Effect on Localization of Mast Cells in the Small Intestine

Mast Cells in Conditional Knockout Mice

1. Generate mice with Mx-cre transgene and *Notch2*^{fl/fl} allele (or other floxed gene of interest) by crossbreeding.
2. Administer polyinosinic-polycytidylic acid (poly I:C) intraperitoneally (20 μ g/g body weight) three times in mice between 4 and 6 weeks old (see Notes 17–19).

Staining of Intestinal Mast Cells

1. Fix intestinal tissue with Carnoy's solution for 4 h at RT or overnight at 4 °C, and then keep transfer to 100 % ethanol for storage until processing.
2. Embed the sections in paraffin, prepare slices on slides at the width of 4 µm, and deparaffinize using standard methods.
3. Stain the specimen with 0.5 % toluidine blue solution (pH 0.3) for 24 h at 20–25 °C, followed by eosin counter-staining.
4. Count the mast cells and present as the number per every 10 villus-crypt units (10 vcu) (see Note 20).

Isolation and Analysis of Peritoneal Mast Cells

1. Inject 5 mL of ice-cold PBS into peritoneal cavity of various mice and recover 3 mL from each mouse. Analyze the cells by flow cytometry as described in Subheading "Culture of Myeloid Progenitors with Delta1-Fc or Jagged1-Fc."
2. To see the Notch2 expression in peritoneal mast cells, stain the cells as follows:
 - (a) Add purified rat anti-CD16/32 antibody.
 - (b) Add isotype IgE and biotinylated hamster anti-Notch2 antibody (clone 35.2).
 - (c) Wash with staining buffer once.
 - (d) Add FITC-conjugated rat anti-IgE, streptavidin PE, and APC-conjugated rat anti-c-Kit antibodies. Wash with staining buffer twice and add the 7-AAD Viability Dye Solution.
 - (e) Analyze by flow cytometry.

3.5 Analysis of Anti-parasite Immunity by Mast Cells in the Intestine

Strongyloides venezuelensis (SV) Infection (See Note 21)

1. Collection of third-stage infective larvae of SV as follows:
 - (a) Infect 6-week-old male Wister rat with infective larvae of SV (see Note 22).
 - (b) Collect rat feces 7–8 days after infection. Put the fecal matter into water, and leave for 30–60 min until the feces becomes loose enough for spreading. Paste it onto the top of a sheet of soft paper, roll the paper, and leave it in the water at 27 °C for 3 days (see Note 23).
 - (c) Recover the third-stage infection-patent larvae from the water. Count the number under a microscope (40×).
2. Inject the larvae-suspension solution subcutaneously into mice using a dose of 2,000–5,000 larvae in 200 µL PBS per mouse.
3. Collect and weigh all the fecal pellets from the mice daily.
4. Resuspend feces in 30 mL water per mouse per day. Stain the eggs present in the feces with an iodide solution, and count the number of eggs under a microscope (40× magnification). The number of eggs is often presented as number of eggs observed per gram of feces.

3.6 Rescue Experiment of Mast Cell-Deficient Mice with Notch2-Null or WT Mast Cells (See Note 24)

1. Prepare Th2-conditioned CMCs as follows:
 - (a) Prepare CMC as in Subheading 3.3.
 - (b) Wash CMCs twice with PBS.
 - (c) Culture them with 10 ng/mL IL-4 and 10 ng/mL IL-10 in IMDM with 10 % FCS for 3 days.
2. Harvest the cells (i.e., Th2-conditioned CMCs) and wash twice with PBS.
3. Infect W^{bd}/W^{bd} mice with SV as in Subheading 3.5.
4. Inject 5×10^6 Th2-conditioned CMCs intravenously at 3 and 6 days of infection with SV.

4 Notes

1. pLAT-E and pMYs ires-GFP were established by Kitamura T (University of Tokyo) [11].
Now it is available from Cell Biolabs, Inc.
2. pGCDNsam vector ires-GFP was established by Nakauchi H (Stanford University) and Onodera M (National Center for Child Health and Development) [12].
3. GATA3 and Hes1 cDNA were subcloned into pMYs ires-GFP and pGCDN ires-human NGFR, respectively.
4. Chimeric proteins comprising extracellular domain of mouse Notch ligands, Delta-like-1 (Dll1) and Jagged-1, and the Fc portion of human immunoglobulin G1, named Dll1-Fc and Jagged1-Fc, respectively, were developed in our laboratory [13]. Now, essentially the same products are commercially available.
5. Hamster anti-Notch2 antibody (clone 35.2) was established by Yagita (Juntendo University) [14]. Now, fluorescence-conjugated forms of this antibody can be purchased from BioLegend.
6. Conditional *Notch2* knockout mice were established in our laboratory [15].
7. Mx-*cre* mice were originally established by Kuhn et al. [16].
8. This method, with minor modifications, was originally described in reference [9].
9. Mix equal amount of rat anti-CD3e, CD4, CD8a, B220, TER-119, and Gr-1 antibodies for anti-lineage antibodies.
10. Lin⁻ cells can be used as a source for mast cell differentiation.
11. The number and viability of cells are extremely important. The appropriate numbers are $2-3 \times 10^4$ cells per well for CMPs and GMPs and $2-5 \times 10^5$ per well for Lin-negative cells.
12. Simultaneously cytopspin films are prepared from aliquots of cells and stained with Wright-Giemsa as well as toluidine blue.

13. The original method for retroviral infection of hematopoietic cells is described in detail [17].
14. GFP- and/or human NGFR-positive fractions are used as markers of viral integrated cells. Compensation for flow cytometry should be adjusted carefully.
15. 200–400 cells per 35 mm dish for CMPs and 2,000–4,000 cells per 35 mm dish for GMPs should be appropriate. The lower limit of the cell number is quite important for cell viability.
16. Mock-infected cells form various GM, M, and mixed colonies. Both Hes1- and GATA3-infected cells form mast cell colonies.
17. Mx-*cre* system is effective for *Notch2* gene deletion in intestinal mast cells but ineffective for that in skin or peritoneal mast cells. The reason of this fact could be explained by the difference in the lifespan between the intestinal mast cells and skin/peritoneal mast cells. The Mx-*cre* system is effective to delete genes in bone marrow progenitors, and these gene-deleted progenitors differentiate into mature mast cells *in vivo*. In contrast, the Mx-*cre* system might be ineffective for direct gene deletion in *in vivo* mature mast cells.
18. To ensure deletion in skin or peritoneal mast cells, the authors recommend transplantation of bone marrow cells prepared from Mx-*cre* *Notch2*^{fl/fl} mice after pI:pC administration to mast cell-deficient mice (*W^{sh}/W^{sh}* or *W/W^v*), and analyze the mast cells in a method described in the section.
19. *Tie2-cre* knockin mice are also useful to delete genes in mast cells *in vivo*.
20. Staining efficiency significantly varies dependent on the batches of toluidine blue. Check the incubation time carefully when you purchase a new batch.
21. For infection of *S. venezuelensis*, we recommend consulting the papers by Prof. Maruyama [18].
22. Sex of the rat is a very important factor for establishment of infection.
23. Only the bottom of the paper should be kept in the water to avoid propagation of bacteria.
24. For mast cell rescue experiment, the method originally described [19] can be used with minor modifications.

References

1. Kitamura Y, Shimada M, Hatanaka K, Miyano Y (1977) Development of mast cells from grafted bone marrow cells in irradiated mice. *Nature* 268:442–443
2. Suzuki T, Yokoyama Y, Kumano K et al (2006) Highly efficient *ex vivo* expansion of human hematopoietic stem cells using Delta1-Fc chimeric protein. *Stem Cells* 24: 2456–2465
3. Dallas MH, Varnum-Finney B, Delaney C, Kato K, Bernstein ID (2005) Density of the Notch ligand Delta1 determines generation of B and T cell precursors from hematopoietic stem cells. *J Exp Med* 201:1361–1366

4. Haraguchi K, Suzuki T, Koyama N et al (2009) Notch activation induces the generation of functional NK cells from human cord blood CD34-positive cells devoid of IL-15. *J Immunol* 182:6168–6178
5. Sakata-Yanagimoto M, Nakagami-Yamaguchi E, Saito T et al (2008) Coordinated regulation of transcription factors through Notch2 is an important mediator of mast cell fate. *Proc Natl Acad Sci U S A* 105:7839–7844
6. Gurish MF, Boyce JA (2006) Mast cells: ontogeny, homing, and recruitment of a unique innate effector cell. *J Allergy Clin Immunol* 117:1285–1291
7. Miller HR, Pemberton AD (2002) Tissue-specific expression of mast cell granule serine proteinases and their role in inflammation in the lung and gut. *Immunology* 105: 375–390
8. Sakata-Yanagimoto M, Sakai T, Miyake Y et al (2011) Notch2 signaling is required for proper mast cell distribution and mucosal immunity in the intestine. *Blood* 117:128–134
9. Akashi K, Traver D, Miyamoto T, Weissman IL (2000) A clonogenic common myeloid progenitor that gives rise to all myeloid lineages. *Nature* 404:193–197
10. Yuan Q, Gurish MF, Friend DS, Austen KF, Boyce JA (1998) Generation of a novel stem cell factor-dependent mast cell progenitor. *J Immunol* 161:5143–5146
11. Kitamura T, Koshino Y, Shibata F et al (2003) Retrovirus-mediated gene transfer and expression cloning: powerful tools in functional genomics. *Exp Hematol* 31:1007–1014
12. Iwama A, Oguro H, Negishi M et al (2004) Enhanced self-renewal of hematopoietic stem cells mediated by the polycomb gene product Bmi-1. *Immunity* 21:843–851
13. Shimizu K, Chiba S, Hosoya N et al (2000) Binding of Delta1, Jagged1, and Jagged2 to Notch2 rapidly induces cleavage, nuclear translocation, and hyperphosphorylation of Notch2. *Mol Cell Biol* 20:6913–6922
14. Moriyama Y, Sekine C, Koyanagi A et al (2008) Delta-like 1 is essential for the maintenance of marginal zone B cells in normal mice but not in autoimmune mice. *Int Immunopharmacol* 20:763–773
15. Saito T, Chiba S, Ichikawa M et al (2003) Notch2 is preferentially expressed in mature B cells and indispensable for marginal zone B lineage development. *Immunity* 18:675–685
16. Kuhn R, Schwenk F, Aguet M, Rajewsky K (1995) Inducible gene targeting in mice. *Science* 269:1427–1429
17. Crcareva A, Saito T, Kunisato A et al (2005) Hematopoietic stem cells expanded by fibroblast growth factor-1 are excellent targets for retrovirus-mediated gene delivery. *Exp Hematol* 33:1459–1469
18. Maruyama H, Yabu Y, Yoshida A, Nawa Y, Ohta N (2000) A role of mast cell glycosaminoglycans for the immunological expulsion of intestinal nematode, *Strongyloides venezuelensis*. *J Immunol* 164:3749–3754
19. Fukao T, Yamada T, Tanabe M et al (2002) Selective loss of gastrointestinal mast cells and impaired immunity in PI3K-deficient mice. *Nat Immunol* 3:295–304

Part II

Mast Cells in Human Health and Disease

Chapter 7

Mast Cells in Human Health and Disease

Erin J. DeBruin, Matthew Gold, Bernard C. Lo, Kimberly Snyder, Alissa Cait, Nikola Lasic, Martin Lopez, Kelly M. McNagny, and Michael R. Hughes

Abstract

Mast cells are primarily known for their role in defense against pathogens, particularly bacteria; neutralization of venom toxins; and for triggering allergic responses and anaphylaxis. In addition to these direct effector functions, activated mast cells rapidly recruit other innate and adaptive immune cells and can participate in “tuning” the immune response. In this review we touch briefly on these important functions and then focus on some of the less-appreciated roles of mast cells in human disease including cancer, autoimmune inflammation, organ transplant, and fibrosis. Although it is difficult to formally assign causal roles to mast cells in human disease, we offer a general review of data that correlate the presence and activation of mast cells with exacerbated inflammation and disease progression. Conversely, in some restricted contexts, mast cells may offer protective roles. For example, the presence of mast cells in some malignant or cardiovascular diseases is associated with favorable prognosis. In these cases, specific localization of mast cells within the tissue and whether they express chymase or tryptase (or both) are diagnostically important considerations. Finally, we review experimental animal models that imply a causal role for mast cells in disease and discuss important caveats and controversies of these findings.

Key words Autoimmune disease, Asthma, Allergy, Cancer, Cardiovascular disease, Fibrosis, Inflammatory bowel disease, Mastocytosis, Organ transplant, Pathogen clearance

1 Introduction

Mast cells (MCs) begin as committed bone marrow (BM)-derived MC precursors that circulate in the bloodstream and migrate into peripheral tissues wherein milieu-specific factors subsequently control their terminal differentiation [1, 2]. Maintenance of MCs in peripheral tissues is dependent on soluble and membrane-bound cytokines expressed by stromal cells (e.g., stem cell factor (SCF)) [3, 4]. Mature MCs reside in close proximity to blood and lymph vessels, neurons, and other tissue-resident immune cells (e.g., dendritic cells (DCs)) and are most abundant in tissues at the host-environment interface, such as skin, airways, and the gastrointestinal

and genitourinary tracts (reviewed in refs. 2, 5–7). MCs provide an undisputed sentinel-protective function in innate immunity by directly killing some invading pathogens, degrading toxins, and by recruiting and activating other immune cells. The detrimental consequences of MC activation, namely, pathological allergy and anaphylaxis, are a result of inappropriate or hyperactive MC responses to environmental triggers (reviewed in refs. 5, 8, 9). In humans, MC populations are classified into three subtypes based on protease content—those that contain only tryptase (MC_T) or chymase (MC_c) and those that contain both tryptase and chymase (MC_{TC}) [10]. In rats and mice, MCs are instead classified based on tissue localization: mucosal (MMC) and connective tissue (CTMC) mast cells, respectively.

MCs express several Toll-like receptors (TLRs) and the allergen- and parasite-responsive high-affinity immunoglobulin E (IgE) receptor, F_c-epsilon receptor I (Fc ϵ RI). TLRs sense and activate MCs in response to infectious agents like viruses and bacteria or their components (e.g., lipopolysaccharide or peptidoglycan), and the IgE/Fc ϵ RI axis activates MCs in response to specific allergens [11, 12]. MC stimulation causes, within seconds, the generation of reactive oxygen species and the release of a multitude of preformed mediators such as antimicrobial peptides, histamine, proteoglycans, proteases, and tumor necrosis factor (TNF α) (reviewed in ref. 13). While many of these MC effector molecules have pro-inflammatory roles, they may also limit the damaging effects of toxins. For example, MC proteases have a critical role in degrading some of the toxins present in animal venoms [14]. MCs also synthesize and release de novo products within hours after stimulation including vascular endothelial growth factors (VEGF), eicosanoids, and cytokines (reviewed in ref. 14). Many of the bioactive mediators released by MCs activate other immune cells, tissue-specific epithelia and stromal cells, blood and lymph vessels, and neurons [14]. Some of these products recruit innate and adaptive immune cells to the site of inflammation or infection [5]. Finally, MCs release exosomes, small membrane vesicles of endocytic origin that act as intracellular messengers by delivering cargo such as proteins, lipids, or nucleic acids to other immune cells and endothelia (among other cell targets). Although their physiological importance is not clear, exosomes released from MCs have been reported to carry functional mRNA and miRNA or deliver exogenous antigen to induce phenotypic and functional maturation of DCs [15, 16].

In this review we will examine evidence that MCs contribute to human host defense and disease pathogenesis. Once we have outlined some of the better-known host defense and allergic functions of MCs, we will focus on the contribution of MCs in a variety of non-infectious and nonallergic human disease. We have selected diverse examples to illustrate these lesser-appreciated functions of MCs.

The appearance of abundant MCs within or near affected tissue in autoinflammatory and autoimmune diseases, malignancy, fibrosis, and rejected solid organ transplants suggests that MCs have a clinically important role in the pathophysiology of these conditions. In some cases, successful treatment of patients with MC-targeted therapeutics supports a role for MC in disease pathogenesis or disease symptoms. Where clinical data is lacking, we review important experimental animal models of disease that imply a role for MCs in human disease.

2 Mast Cells in Pathogen Clearance

Several clinical reports have attempted to implicate MCs as important immunological mediators in response to human infectious diseases by histological analysis of patient tissue biopsies [17–20]. For example, in cholera infection, acute shigellosis, and *Helicobacter pylori*-associated gastritis, MCs accumulate at intestinal mucosal barriers, as do elevated levels of MC-derived proteases and bioactive lipids [17–19]. Culture-derived human MCs or MCs isolated from a variety of human tissues have been used to study human MC responses to pathogens, and animal models provide some understanding of the role of MCs in pathogen clearance *in vivo* [5, 8, 21]. MC functions in human infectious disease are largely inferred from these studies. In rodent models of infection, MCs (and some of their products) are clearly indispensable for pathogen clearance through their ability to rapidly detect pathogens, initiate host defense, and modulate adaptive effector cell function (reviewed in refs. 5, 8, 21).

2.1 Parasites

MCs facilitate host clearance of ecto- and endoparasitic infections that include worms, ticks, and protozoa. MC-deficient mice clear *Trichinella spiralis* infection less efficiently, and they are unable to elicit a protective T_H2 inflammatory immune response [22–25]. Successful expulsion of a variety of parasites is mediated by MCs following cross-linking of Fc ϵ RI by parasite-specific IgE in the presence of antigen. Fc ϵ RI cross-linking causes rapid degranulation and is followed by secretion of type 2 cytokines (defined here as T_H2-polarizing response mediators) [5, 8]. MC activation and hyperplasia in the gut is accompanied by an increase in systemic IgE; the release of MC-derived mediators such as interleukin 4 (IL-4), IL-5, and IL-13; and release of MC granule proteases [26–28]. The chymase, mouse mast cell protease 1 (mMCP1)—not to be confused with monocyte chemoattractant protein 1 (MCP-1/CCL2)—is expressed by intraepithelial mucosal MCs and is required for expulsion of helminth parasites. Mice lacking mMCP1 do not eliminate *T. spiralis* infection despite normal intestinal MC hyperplasia and induction of a T_H2 response [22, 24].

In the *T. spiralis* infection model, mMCP1 likely contributes to the clearance of the parasitic burden by degrading epithelial tight junctions and therefore increasing mucosal permeability [29].

MCs also have a role in cutaneous immunity. For example, MCs are involved in the immune response to the protozoan parasite *Leishmania* in cutaneous leishmaniasis. *Leishmania major*-infected MC-deficient mice (Kit^W/Kit^{Wv}, W/W^v strain [30]) develop larger skin lesions than wild-type control mice, and reconstitution of cutaneous MCs in W/W^v mice by adoptive transfer results in normalization of lesion development [31]. Leishmania infection models in mice further reveal that, in the absence of MCs, recruitment of pro-inflammatory neutrophils, macrophages, and DCs is impaired. MC-deficient mice also display a delay in T cell priming, and the response to *L. major* is skewed toward an inappropriate T_H2 polarized response rather than the protective T_H1 and T_H17 immunity observed in MC-replete wild-type mice [32].

Malaria remains the most deadly vector-borne human disease. Severe human malaria is correlated with high serum concentrations of Flt3 ligand (Flt3L) and increased number of circulating CD141 (also known as thrombomodulin/BCDA-3)-positive DCs [33]. In mouse models of malaria infection (e.g., *Plasmodium chabaudi* and *P. berghei* infection) [34], MCs are a major source of Flt3L ligand (Flt3L) detected in mouse serum within 2 days following *Plasmodium* infection [35]. Importantly, Flt3L causes the expansion of circulating CD8 α^+ DCs (correlate of human CD141⁺ DCs). Overall, these data highlights a mechanism whereby MCs participate in DC maturation in the pathogenesis of severe malaria.

2.2 Bacteria

By initiating an immune response through TLRs, MCs are indispensable for protection from infection by some bacterial pathogens [5, 8]. In addition to their ability to phagocytose and eliminate opsonized bacterial pathogens, following exposure to bacterial antigens, MCs release inflammatory mediators resulting in recruitment of other leukocytes [5, 8, 36]. For example, activation of human MCs by bacterial endotoxin induces the release of IL-1 α and β , which recruits neutrophils necessary for bacterial killing [37]. In mouse models of acute infection, the absence of MC-derived TNF α in MC-deficient W/W^v mice causes severely attenuated neutrophil recruitment, impaired bacterial clearance, and significantly higher mortality [36, 38]. In a model of *Escherichia coli*-induced peritonitis, MCs release high levels of leukotriene (LT) B₄ and LTC₄. These eicosanoids induce smooth muscle contraction and capillary permeability and, consequently, cooperatively enhance early neutrophil infiltration [39].

Several MC-derived proteases are important immune modulators involved with host defense to bacteria. For instance, human chymase has potent leukocyte chemotactic properties in vivo, and the

tryptase mMCP6 selectively recruits neutrophils to the peritoneal cavity [40, 41]. Intratracheal administration of human tryptase beta 1 to W/W^v MC-deficient mice restores neutrophil recruitment and improves clearance of pulmonary *Klebsiella* infection [42]. MCs also release reactive oxygen species, bactericidal peptides, and other products with direct antimicrobial activity. One study demonstrated that MCs lacking a mouse cathelicidin-related antimicrobial peptide are severely impaired in their ability to eliminate group A *Streptococcus* [43].

Although MCs can participate in direct killing of bacteria by phagocytosis and reactive oxygen species production, gaining access to an intracellular compartment also may constitute a pathogenic strategy to escape the extracellular antimicrobial activity. It has been shown, for instance, that human mast cell lines and mouse primary skin mast cells internalize *Staphylococcus aureus*. By gaining access to MC cytosol *S. aureus* not only survived but also persisted for long periods of time [44]. This might be of importance for inflammatory disorders such as atopic dermatitis (AD) in which AD patients exhibit significantly higher rates of *S. aureus* in the skin compared with healthy individuals [44]. In chronic lesions of AD, MC numbers are significantly increased [45]. Another in vitro study provided evidence that *Mycobacterium tuberculosis* employs a cholesterol-dependent pathway to invade mast cells, promoting morphological changes in those cells such as raft formation at the sites of contact with mycobacterium [46]. By entering through rafts, bacteria avoid the immune system and intracellular degradation pathway. This mechanism has been associated with intracellular survival and replication of several pathogens within different host cells (reviewed in ref. 47). Thus, MCs may serve as reservoirs of viable bacteria in some diseases.

The importance of MCs in the adaptive immune response in infectious disease is supported primarily by in vitro response to pathogens and some experimental in vivo animal models (reviewed in refs. 5, 21). MCs contribute indirectly to antigen capture after bacterial activation through their release of IL-6 that mobilizes certain subsets of DCs to lymph nodes [48]. MCs influence T cell and B cell migration directly through the release of cytokines and indirectly through mediators, such as TNF α , that increase cell adhesion molecules expressed on vasculature and increase vascular permeability [21]. Finally, MCs also regulate B cell-dependent IgE production by a mechanism that does not require direct physical contact with B and T cells [49].

2.3 Viruses

Following recognition of viruses or viral components such as double-stranded (ds)RNA through TLR3, MCs can release a panel of antiviral response cytokines and chemokines that promote effector cell recruitment [5, 7]. For instance, MC detection of dengue virus or polyinosinic-polycytidylic acid (poly I:C), a synthetic

dsRNA analog, results in the production of type I interferons (IFNs), CC chemokine ligands (CCL3, CCL4, and CCL5), CXC chemokine ligands (CXCL10 and CXCL12), and CXC3 chemokine ligand 1 (CX3CL1). Collectively, these MC-secreted factors promote CD8⁺ T cell, natural killer (NK) T cell, and NK cell recruitment [50, 51]. Consequently, in dengue infection, MC-deficient mice carry a significantly higher viral burden in their lymph nodes compared with wild-type mice. Thus, efficient downstream chemotaxis of effector cells is MC dependent and is evidence for a protective role of MCs against viral diseases [50]. The response to virus highlights a very selective response since type I IFNs are not released by MCs following exposure to bacteria which would inhibit MC-mediated neutrophil recruitment (ref. 52 as cited in review [53]).

Finally, MCs may participate in viral immunity by directly presenting major histocompatibility complex (MHC) class-I antigens to activate CD8⁺ T cells and by inducing DC maturation and enhancing DC-cytokine release leading to downstream activation and proliferation of CD4⁺ T cells [32]. However, MCs may also act as a reservoir for virus. Circulating progenitor mast cells (pMCs) and placental tissue MCs harboring infectious human immunodeficiency virus (HIV) were isolated from HIV-infected pregnant women even during highly active antiretroviral therapy [54].

3 Mast Cells in Protection from Venoms

Several animals and insects possess defensive and offensive venoms capable of inducing pain, severe tissue injury, or death. Envenomation by snakes poses a serious threat to human health in some parts of the world where antisera are scarce and venomous snakes are frequently encountered [55]. Severe reactions and death from bee-stings are a threat due to the high lifetime risk of stings and re-stings and the incidence of severe anaphylaxis [56]. The importance of MCs in bee-sting anaphylaxis is supported by the findings that patients with mastocytosis (*see* Subheading 5.1) also have increased risk of severe reactions to stings (reviewed in refs. 57, 58).

Venoms contain many allergens and toxins [56, 59]. Although allergen-IgE activation of MCs is an important anaphylaxis response mechanism to bites and stings, a variety of venom toxins can activate MCs through Fc ϵ RI-independent pathways [56, 57, 60]. Activation of an MC-triggered inflammatory cascade may contribute to the efficacy of the “intended” potency of venoms. However, MC activation and release of proteases is also important in the neutralization of at least some of these toxins. For example, MC-deficient mice are more susceptible to toxins in the venoms of honeybee, scorpion, Gila monster, and certain snakes [61, 62].

In particular, in mice, the mast cell proteases carboxypeptidase A3 (CPA3) and mast cell protease (mMCP4) enhance the resistance of envenomed mice by degradation of venom toxins structurally similar to endothelin-1 (ET-1) or vasoactive intestinal polypeptide [62]. In the absence of MCs (or when MC degranulation is blocked), mice become hypothermic, exhibit diarrhea, and are likely to die following treatment with exogenous ET-1 [63]. These data support a protective role for MCs in response to endogenous vasoactive peptides and their mimetic toxins in venoms [64].

4 Mast Cells in Inflammatory Disease

4.1 Asthma

MCs have long been implicated in asthma pathogenesis due to their localization near blood vessels, beneath the basement membrane, and near smooth muscle fibers throughout the lung airways (ASM) [9]. Abundant CD4⁺ T_H2 cells, commonly elicited during asthma pathogenesis, produce IL-4, which, in turn, leads to antibody class switching and increased production of IgE by plasma cells. IgE-engagement primes MCs and basophils for activation and release of preformed and newly synthesized mediators. MC preformed mediators recruit eosinophils and T_H2 cells and can have direct and rapid effects on ASM, leading to bronchoconstriction. For example, the prostaglandin (PG) D₂ receptor (CRTH2) is highly expressed on T_H2 CD4⁺ T cells, suggesting an important role for recruitment of T_H2 effectors to the airways in response to release of PGD₂ by MCs. MC accumulation in the ASM of asthmatics correlates with increasing severity of airway hyperresponsiveness, and the number of degranulated MCs is higher in fatal asthma [65, 66].

In severe asthma patients, allergen-induced bronchoconstriction results in a biphasic response and MC activation may have a causal role in both the early and late phases [67, 68]. The rapid release of mediators by IgE-primed MCs and basophils in the airways triggers the early phase response (within 30 min of allergen exposure). The late phase response, occurring 3–8 h after exposure, is attributed to the influx of eosinophils, neutrophils, and lymphocytes [67, 68]. Notably, MC numbers are higher in patients that experience late phase responses, and MC numbers correlate with the magnitude of bronchoconstriction [69].

The clinically important role of MCs in the pathogenesis of allergic asthma is highlighted by the fact that blocking MC activation and interfering with MC products remain important therapeutic strategies. Omalizumab, a human anti-IgE mAb, successfully reduces systemic IgE concentrations: MCs, basophils, and a subset of Fc ϵ RI-positive DCs are its major targets. [70, 71]. Additionally, therapies that interfere with MC tryptase reduce the severity of the late phase response [72]. Surprisingly, chromones (e.g., sodium

cromoglycate), drugs that block MC degranulation (i.e., MC stabilizers), have not been effective in treating symptoms. Due to the success of other agents that target MCs and their products, the lack of chromone efficacy may be due to drug potency rather than the importance of MC granule release in asthma.

Further research into MC-directed therapeutics is hampered by animal studies that question a role for MCs in allergic airway inflammation. It should be noted that there are considerably fewer MCs in murine lungs compared to humans and that the airway architecture and rate of turnover is significantly different in rodents [73, 74]. Murine studies using ovalbumin as a model antigen suggest the participation of MCs in allergic asthma is strain dependent and only apparent in disease models that do not use an adjuvant (such as alum). Thus, at least in mouse models, MCs are often not required and may only play a minor role in amplifying disease [75]. Discrepant data by various investigators may be attributed to the fact that adoptive transfer of cultured MCs (intravenously) into MC-deficient mice results in a nonphysiologically high frequency of lung MC [76]. Thus, while delivery of MCs to MC-deficient mice results in exacerbated allergic asthma in some studies, it is difficult to assess the biological relevance of these findings [76, 77]. Moreover, the most widely used MC-deficient mouse models, W/W^v and Wsh (Kit^{Wsh}/Kit^{Wsh}) mice, have hematological and other abnormalities that may affect the asthma phenotype (reviewed in ref. 78 and references therein).

4.2 Inflammatory Bowel Diseases

Inflammatory bowel diseases (IBD) such as Crohn's disease (CD) and ulcerative colitis (UC) are characterized by uncontrolled inflammation in the gastrointestinal tract. Although CD and UC share many symptoms and underlying causes, they have distinctly different manifestations [79]. UC is defined as a non-transmural (mucosa-limited) inflammatory disease restricted to the colon, whereas CD can manifest throughout the intestinal tract and inflammation often penetrates deep into the tissue [80]. Although MCs are heavily concentrated at the intestinal mucosa and submucosa in healthy individuals [81, 82], IBD patients frequently display an increased number of intestinal MCs when compared to healthy patients [83]. Intestinal MCs from CD patients are functionally different from those isolated from healthy individuals and show increased expression of TNF α , IL-16, and substance P [83–86]. In the context of IBD, MC degranulation is likely triggered by food or commensal bacterial antigens, and their activation exacerbates a pro-inflammatory cascade with detrimental physiological effects [79]. For example, release of mediators such as histamine, prostaglandins, and proteinases increases gastric acid secretion, enhances recruitment of other immune cells, and causes sensorimotor dysfunction [86]. Increased mucosal permeability

allows bacterial or food antigens to breach the mucosal barrier and, potentially, the endothelial barrier, further propagating an immune response and potentiating symptoms. Notably, patients with CD have significantly increased small intestinal permeability, while increased colonic permeability is found in patients with UC [87].

MCs are found in close proximity to intestinal nerves in both healthy and IBD intestinal tissue [88]. Stress signals are transmitted from the brain to the gut via the gut-brain axis, where MCs are thought to serve as the terminal effectors through their release of pro-inflammatory mediators, cytokines, and neurotransmitters [89]. By sensing extracellular ATP through P2X7 purinergic receptors, MCs become activated and mediate inflammatory responses directly and indirectly through their interactions with other immune cells [90]. Correlative data in human UC and CD indicate that human MCs may be acting by a similar mechanism [90]. Psychoneurological induced activation of MCs via the gut-brain axis can affect intestinal motility, increase intestinal permeability, and modulate inflammation [91]. People suffering from IBD may be more sensitive to this cascade due to increased responsiveness of MCs, as shown by response to physically stressful stimuli [92], and by virtue of the overall increase in the number of intestinal MCs [92]. Direct study of the interaction between the brain, intestinal nerve cells, and MCs in humans is difficult. As such, the link between MCs and the effects of stress on the pathogenesis of IBD is limited and indirect, and further studies are needed to provide detailed mechanisms of action.

There are many animal models of intestinal inflammation that recapitulate aspects of IBD. These models use chemical sensitization, cell-transfer induction, or genetic manipulation methods to induce intestinal inflammation [93]. These experimental models have been used to unravel the underlying biology of IBD and to identify potential targets for therapeutics [93, 94].

Case studies have shown variable success in ameliorating symptoms of IBD using drug treatments that target MCs. Historically, IBD has been treated with sulfasalazine, a drug shown to inhibit IgE-mediated MC degranulation [95]. Other common treatments include 5-aminosalicylic acid, an inhibitor of histamine and PGD₂ release; corticosteroids, which reduce the number of MCs in intestinal tissue; and dexamethasone, an inhibitor of growth and differentiation of BM-derived mucosal MCs [96]. Several studies targeting MC degranulation in gastrointestinal diseases show promise as effective therapeutics (reviewed in ref. 97). One study reported that sodium cromoglycate controls patient symptoms [98] and another reported histamine receptor antagonists are potentially effective treatments for a spectrum of functional gastrointestinal diseases [99].

Finally, tricyclic antidepressants, which are well known to function as antihistamines, may target MC function in gastrointestinal disorders [100]. While these MC-targeted therapies suggest that MCs play a role in IBD etiology, further research is needed to understand the role of MCs in healthy and inflamed intestinal mucosa.

4.3 Cardiovascular Disease

MCs are resident in the intimal layer of arteries just below the endothelium. MC frequency in the heart and vessels of healthy patients is low with a range of 1 MC/mm² in cardiac arteries to 30 MC/mm² in the aorta [101, 102]. In humans, it is typical for both MC subtypes to be present within vascular tissues, although the ratio of MC_T and MC_{TC} cells will differ with location and vessel size. Recent reviews have highlighted a deleterious role for MCs in many cardiovascular diseases including atherosclerosis and coronary artery disease [103–106], abdominal aortic aneurysms [106, 107], cardiomyopathy, and heart failure [108]. A pathophysiological role for MCs in human cardiovascular disease is also inferred from experimental animal models and *in vitro* studies. Here we also highlight some of the direct clinical evidence and the potential clinical value of MC mediators as biomarkers and/or therapeutic targets in cardiovascular disease.

Atherosclerosis and Coronary Artery Disease

Atherosclerosis and coronary artery disease are chronic inflammatory diseases, propagated by innate and adaptive immune mechanisms [109, 110]. MCs, which were first identified in human atherosclerotic lesions in the 1950s [111, 112], have the potential to participate in all stages of atherosclerosis. Fatty streaks, the precursors of atherosclerotic lesions, contain significantly more MCs within the intima than normal vessels [101, 112]. MC presence in fatty streaks suggests that they may participate in foam cell formation, likely by releasing histamine and heparin (reviewed in refs. 103, 113). The release of histamine is sufficient to increase endothelial permeability and could facilitate the influx of low-density lipoprotein (LDL) into the intimal layer [103]. Furthermore, *in vitro* studies demonstrate that human chymase and exocytosed heparin granules proteolyze and bind LDL, respectively, to facilitate the formation of “supersaturated LDL granules.” These granules, when engulfed by smooth muscle cells and macrophages, are sufficient to induce the transition to foam cells [113]. MCs are also more numerous in the shoulder regions of well-developed atherosclerotic lesions (ninemfold more MCs), and most of these MCs (85 %) appear to be degranulated [101]. In fact, MC frequency in the shoulder region is predictive of rupture and suggests that MC activation and degranulation is sufficient to destabilize the plaque [101]. Within the plaques, MCs are located in proximity to the microvessels, and the number of MCs correlates with the density of vessels. As a result, atheromatous plaques, which have significant levels of neovascularization, have more than twofold higher

frequency of MCs and are more likely to display intra-plaque hemorrhage than fibrous plaques [114, 115]. A study by Willems et al. found that the number of MCs in neovascularized areas was predictive of secondary coronary events [115]. In addition, the release of basic fibroblast growth factor (bFGF) within the areas of neovascularization is one mechanism through which MCs contribute to plaque destabilization [116].

Abdominal Aortic Aneurysm

Abdominal aortic aneurysm (AAA) is a pathological remodeling and weakening of the vessel wall. MCs are found in higher frequency (five- to 12-fold) in the medial layer of affected vessels in patients with AAA (and also in ascending thoracic aortic aneurysms), and the number of MCs correlates with the diameter of the lesion [117–119]. MCs contain neutral proteases, many of which have been linked to matrix degradation [120]. The level of MC-derived chymase in the aorta is 17-fold higher in patients with AAA and, at least in vitro, human MC chymase is sufficient to convert pro-MMP2 and pro-MMP9 into their active forms leading to matrix degradation [121]. Cathepsins are important cysteine proteases involved in the degradation of collagen and elastin. The majority (70 %) of cathepsin G content found in intraluminal thrombus of AAA patients is associated with the presence of MCs [117]. Patients with AAA have elevated plasma levels of cathepsin L, but are deficient for cystatin C, the primary inhibitor for cathepsins [122, 123]. Together, these data suggests that the granular contents of MCs contribute to the degradation of the aortic wall through several proteolytic systems. As in atherosclerotic lesions, MCs also localize to areas of neovascularization and are associated with sites of AAA rupture [117, 124]. Incubation of coronary samples with chymase and tryptase shows that these MC proteases contribute to desquamation and denudation of endothelial cells from the artery. Moreover, the junctional protein VE-cadherin is also degraded by chymase and cathepsin G [125].

Cardiomyopathy and Chronic Heart Failure

MCs accumulate in the fibrotic cardiac tissue in patients with cardiomyopathy and are present at a frequency fourfold higher than in healthy hearts [126]. A study of patients with dilated cardiomyopathy found a fivefold increase in histamine over healthy controls, and this correlated with increased MC density [126]. Isolated MCs from these patients were also more sensitive to activation by IgE or SCF as measured by enhanced levels of histamine, tryptase, and LTC₄ [126, 127]. Recently, the use of the left ventricular assist device (LVAD) to support patients with heart failure (and heart transplant candidates) has demonstrated a novel role for MCs. Mechanical support provided by the LVAD “unloads” the heart and has been shown to induce remodeling, reduce collagen content, and improve cardiac function [128]. Notably, in patients with long-term LVAD, the overall frequency of MCs *increased*, likely as

a result of enhanced migration due to increased gene expression of SCF and c-Kit [129, 130]. While MC numbers increase in LVAD patients, the overall ratio of MC_{TC} decreases, as does the number of MCs that express cathepsin G and bFGF, suggesting a phenotypic switch in MCs populating the LVAD-supported heart [129, 131]. Although it remains to be determined if this phenotypic switch in MCs is causal or merely correlative, an attractive hypothesis is that MC_{TC} may play a pathogenic role in heart fibrosis, while the MC_T phenotype may provide a protective function that supports the beneficial remodeling and repair associated with LVAD support [132].

Biomarkers and Potential Treatments

A wealth of epidemiology studies has identified MC mediators as biomarkers (and perhaps therapeutic targets) for cardiovascular disease (reviewed in refs. 105, 109, 133, 134). Histamine and IgE are the most promising MC-associated biomarkers for cardiovascular disease. Histamine levels are elevated in patients with atherosclerosis, coronary artery disease, AAA, and chronic heart failure while IgE levels are elevated in patients with coronary artery disease [135–137]. In addition, recent studies have correlated elevated tryptase levels with increased risk of atherosclerosis and secondary cardiac events in patients with atherosclerosis [115, 138–140].

Histamine is the only MC-associated therapeutic target that has been efficacious in clinical trials. The histamine H₂-receptor blocker famotidine ameliorates patient symptoms associated with chronic heart failure [136], and antihistamine has been used to treat AAA surgical patients to mitigate risk of mesenteric traction syndrome [141]. Experimental models have demonstrated that preventing MC degranulation and inhibiting MC proteases may show promise in cardiovascular diseases (reviewed in refs. 109, 133). For example, the MC stabilizers cromolyn and tranilast decrease mortality in animal models of atherosclerosis and myocardial infarction and reduced lesion size in models of AAA. Statins can reduce IgE-mediated histamine release and SCF-induced differentiation of human MCs in vitro [109, 134]. Of the proteases, chymase inhibitors reduce disease severity in animal models of AAA, atherosclerosis, and myocardial infarction, and tryptase inhibitors block foam cell formation in vitro [133]. In addition, given the importance of cathepsins in cardiovascular pathologies, many of the new general and selective cathepsin inhibitors are potential MC-targeted therapeutics [133].

5 Mast Cells in Cancer

5.1 Mast Cell Malignancy

Mastocytosis embodies a group of rare disorders characterized by the accumulation of clonally transformed committed BM-derived MC precursors and terminally differentiated MCs [142]. The most

common forms of the disease include cutaneous mastocytosis (CM) and systemic mastocytosis (SM). CM is a skin-limited disease with higher prevalence in pediatric cases whereas SM is a more aggressive variant that typically affects adults. SM is marked by lesions in the BM, spleen, liver, gastrointestinal tract, lymph nodes, or mucosa [143].

Mastocytosis is a myeloproliferative disease frequently associated with a gain-of-function somatic point mutation (D816V) in c-Kit [144]. The D816V mutation confers ligand-independent activation of c-Kit contributing to increased proliferation and a malignant MC phenotype [3]. A study quantifying MC concentrations in the skin of CM patients demonstrated MC_{TC} numbers 400- and 70-fold higher in the dermis of lesional and non-lesional skin, respectively [145].

Typically, disease symptoms in mastocytosis are associated with release of bioactive MC mediators including histamine and proteases that trigger localized or systemic inflammation. Simple physical abrasion of CM lesions is often sufficient to cause MC degranulation and induce local inflammation. Because tryptase levels typically correlate to the abundance of MCs, tryptase concentration is used as a noninvasive clinical marker to diagnose and monitor the disease [146]. Besides its ability to cleave extracellular substrates, tryptase is implicated in the inflammatory cascade by freeing IL-8 (a neutrophil chemoattractant) from endothelial cells and by stimulating release of histamine from neighboring MCs [147, 148].

Successful treatment of the symptoms caused by MC mediators is sufficient to improve the quality of life for patients with mastocytosis [143]. Common therapies include a variety of MC-stabilizing agents such as sodium cromolyn, leukotriene receptor antagonists, aspirin, antihistamines, and anti-IgE therapy or MC-clearing agents such as interferon alpha (IFN α), 2-chlorodeoxyadenosine, and corticosteroids [149–154]. Tyrosine kinase inhibitors (e.g., imatinib and midostaurin) show promise in the treatment of mastocytosis, presumably by interfering with autoactivation of c-Kit [155–157].

5.2 Solid Tumor Cancers

Inflammatory and immune cells have been shown to play a multifaceted role in the progression of cancer from early tumorigenesis to metastasis [158]. In 1891, Westphal first described the presence of MCs in human tumors and noted that MCs tend to concentrate at the tumor periphery [159]. Subsequent studies have supported Westphal's observations and have shown that MCs are also capable of accumulating within tumors [160] and tumors release a number of factors, like SCF, that encourage recruitment of mast cells [161]. Because MCs likely have the ability to act as both promoters and inhibitors of cancer, the role of MCs in tumorigenesis vastly differs between cancers and is also debated within cancer subtypes. MCs may directly mediate cytotoxic effects, by releasing cytokines such as IL-1,

IL-4, IL-6, and TNF α , thereby initiating an antitumor response. MCs influence tumor growth indirectly through the recruitment and stimulation of other immune cells, including lymphocytes, macrophages, neutrophils, and eosinophils, to mediate an immune response against the tumor. In contrast, MCs may promote tumor development through release of a number of molecules and enzymes such as histamine, VEGF, proteases (MMP9), and leukotrienes that act indirectly to promote tumor proliferation, angiogenesis, invasion, and remodeling of the ECM [160, 162, 163].

In invasive breast carcinoma, MCs accumulate within both the peri-tumoral and intratumoral space and infiltration of MCs into the breast tumor stroma correlates with favorable patient prognosis [164–167]. Several studies, including one assessing the prognostic significance of MCs in a >4,000 case tissue microarray, have shown that abundant MCs in the peri-tumoral space correlates with favorable prognosis in breast carcinoma [168]. Several smaller studies have also cited a possible correlation between MC infiltration and favorable prognostic indicators [164, 169].

In contrast to the anti-tumorigenic role of tissue MCs, the presence of tryptase-positive MCs within the breast tumor stroma correlates with increased tumor angiogenesis [167]. Moreover, the extent of tumor angiogenesis and presence of node micrometastases correlates with the number of tryptase-positive MCs residing in lymph node of breast cancer patients [166]. By release of tryptase and other proteases, MCs may contribute to remodeling of the stroma of primary breast tumors by initiating a phenotypic shift of CD34 $^+$, smooth muscle actin-negative (SMA $^-$) fibroblasts to CD34 $^+$ SMA $^+$ myofibroblasts [167]. Tumor-associated CD34 $^+$ SMA $^+$ myofibroblasts are associated with highly invasive cancers (and fibrotic tissue), and tumors with this phenotype contain a high density of intact tryptase-positive MCs in the peri-tumoral space and high density of degranulated tryptase-positive MCs in the tumor [165, 166, 170].

In pancreatic ductal adenocarcinoma (PDAC), MC frequency positively correlates with higher tumor grade, increased recurrence and decreased overall survival [171–173]. In particular, the presence of tumoral MCs is associated with increased intratumoral vessel density and lymph node metastases [173–174]. Using a spontaneous K-RAS mediated mouse model of PDAC, Chang et al. [173] found that MCs infiltrate the tumor microenvironment very early in disease progression. MC infiltration influences tumor development in the PDAC mouse model, as tumor growth was greatly diminished in MC-deficient Wsh mice and tumor growth was restored upon reconstitution of these mice with bone marrow-derived mast cells (BMMCs) [173].

The presence of MC infiltrates in prostate cancer patients has more variable prognostic value. Nonomura et al. [175] found that the presence of tryptase-positive MCs around prostate tumors

correlates with poor patient prognosis and decreased progression-free survival. However, in another study, the presence of intratumoral MCs correlates positively with favorable outcome, whereas MCs accumulating in nonmalignant tissue surrounding the tumor correlate with poor prognosis [176]. Using a model of transgenic adenocarcinoma of the mouse prostate (TRAMP), Pittoni et al. [177] observed that MCs cluster in areas of highly differentiated, epithelial-like tumor tissue, whereas there were very few MCs in poorly differentiated, mesenchymal-like areas of the tumor. This difference was attributed to the ability of well-differentiated tumor cells to secrete SCF and thus attract MCs. Transplantation of well-differentiated *or* poorly differentiated TRAMP cell lines into Wsh mice revealed that MC-derived MMP9 was required for the development of tumors from well-differentiated TRAMP tumor cell lines. In contrast, development of tumors from poorly differentiated cells was not MC dependent. Strikingly, treatment of TRAMP mice with cromoglycate to stabilize MCs, or crossing TRAMP mice to an MC-deficient strain, resulted in the formation of a highly aggressive and rare neuroendocrine prostate cancer thought to result from dysregulated prostate stem cells [177]. The potential use of MC-targeted therapies in prostate cancer has been recently reviewed by Pittoni and Colombo [178].

6 Mast Cells in Autoimmune and Autoinflammatory Disease

MCs have been implicated in the pathophysiology of several human autoimmune and autoinflammatory diseases including arthritis, multiple sclerosis (MS), autoimmune glomerulonephritis, lupus, scleroderma, pemphigus, pemphigoid, psoriasis, dermatopolymyositis and polymyositis, Sjögren's syndrome, and cryopyrin-associated periodic syndromes (for comprehensive reviews, *see* refs. 14, 179, 180). In addition, MCs are thought to have context-dependent roles in promoting or breaking immune tolerance in allogeneic transplant [179, 181]. In the following sections we outline the prospective roles of MCs in MS, arthritis, glomerulonephritis, and organ transplant. Although most of the evidence for the participation of MCs in these human disease processes is strictly correlative, experimental disease models in mice and other animals have provided direct evidence to support diverse MC functions in autoimmune disease and transplantation. Importantly, the value of experimental mouse models using W/Wv and Wsh strains is controversial.

6.1 Multiple Sclerosis

The first association of MCs with the pathophysiology of an autoimmune disease was noted by Ehrlich and Westphal and confirmed by several others 130 years ago [182]. For example, Neumann described abundant "Mastzellen" in central nervous system (CNS) lesions present in deceased MS patients [182, 183]. MCs only sparsely pop-

ulate the healthy brain, and they are primarily concentrated in the thin leptomeninges surrounding the brain and spinal cord [184]. In CNS tissue derived from MS patients, MCs are found at the border regions of demyelinated lesions, next to vessels with associated immune cell infiltrates and, in some cases, deep within the CNS parenchyma [184–186]. MCs are more common in lesions of patients with “chronic active” or “relapsing-remitting” disease but not prevalent in the case of acute or newly formed lesions [184]. MC-associated transcripts are enriched in plaques of MS patients—but also in “normal” white matter—a hint that the appearance of MCs may precede acute inflammation and formation of lesions [187]. The participation of MCs in the pathogenesis or exacerbation of MS is an attractive hypothesis since MCs associated with vessels adjacent to the meninges are well positioned to promote breach of the blood-brain barrier and entry of inflammatory cells or agents (e.g., proteases, metabolites, and chemokines) [188, 189].

Rodent models of MS yield contradictory conclusions with respect to the function of MCs in experimental autoimmune encephalomyelitis (EAE) [78, 190–192]. Studies using MC-deficient mice (*W/W^v*) with or without adoptive transfer of ex vivo-derived MCs support a role for MCs in exacerbating acute-progressive and relapsing-remitting EAE [193, 194]. However, other studies have failed to replicate these results or found that the influence of MCs in EAE varied with disease-induction method [191, 195]. To further complicate matters, in *Wsh* mice, another c-Kit mutant mouse model devoid of mature MCs, EAE is exacerbated compared to MC-replete controls [196–198]. Finally, using the recently described “Cre-Master” strain, a MC-deficient mouse strain that does not rely on a c-Kit mutation for ablation of mature MC lineage, Feyerabend et al. conclude that MCs do not have a prominent role in the pathophysiology of EAE [191]. Accordingly, it seems that the presence and function of MCs is not a dominant determinant in EAE severity in some mouse strains. Experimental variables such as mouse genetic background [196], the method used to adoptively transfer MCs, specific reagents and methods use for induction of EAE, and perhaps most importantly, the microflora in the vivarium where the experiments are conducted may influence disease severity and are likely responsible for the discrepancies documented in the literature. In addition, some of the discrepancy is semantic, and a summary of the data from all investigators could support the conclusion that the presence of MCs may exacerbate EAE in some mouse strains and under some circumstances but that MCs are not *required* to induce EAE. Keeping in mind that EAE is a rodent *model* of MS, it remains an open question as to whether MCs are important in the initiation, propagation, or dysregulated repair processes in human MS.

6.2 Arthritis

In healthy, non-arthritic human joints, MCs are relatively abundant (~3 % of nucleated cells) in a region within a few cell layers of the synovial lining but not in the synovial lining itself [199]. MC_T is the predominant phenotype of MCs in this layer, especially MCs closest to the synovial lining. However, in healthy joints, only a few MCs show evidence of degranulation (<1 %) [199]. Conversely, in patients suffering from rheumatoid arthritis (RA), osteoarthritis (OA), or spondyloarthritis/psoriatic arthritis (SpA/PsA), MCs are greatly expanded in affected joints and more of them show evidence of degranulation (10–15 %) [199, 200].

The protease/secretory phenotype of MCs in arthritis (MC_{TC} vs. MC_T) is disease type specific and can change over the course of the disease [199, 201]. Mechanistically, degranulation of MCs in joints may promote vascular permeability by release of histamine and serotonin, elaboration of cytokines by release of proteases, or by promoting infiltration of other inflammatory lineages into the joint following secretion of chemoattractants. MCs derived from human arthritic joints have been shown to secrete IL-17, TNF α , and IL-1 β [202–204]. One report finds that 63 % and 26 % of the IL-17-producing cells in synovia tissue explants from SpA and RA joints, respectively, are MCs and represent the main cellular source of IL-17 in these tissues [200].

Mouse models of arthritis have been used extensively to gain functional and mechanistic understanding of the role of MCs in arthritis [205–207]. As for EAE, many of the studies addressing the contribution of MCs in RA models rely on the W/W^Y MC-deficient strain combined with adoptive transfer of mature, ex vivo-derived MCs [205]. These investigations apparently confirmed the requirement for MCs or MC-derived products in arthritic inflammation and seem to corroborate the correlative human clinical findings. However, more recent experiments using the Wsh MC-deficient and “Cre-Master” mouse strains have found that MCs are not required for autoimmune arthritis in mice, and thus, these studies compel a reevaluation of our understanding of MCs in arthritic disease [78, 191, 208].

7 Mast Cells in Tissue Fibrosis and Organ Transplant

7.1 Progressive Kidney Disease

Glomerulonephritic/nephrotic (GN) diseases are a major cause of kidney fibrosis and end-stage renal failure. MCs are rare in healthy kidney but are greatly expanded (~6 to 7-fold) in GN patients regardless of disease etiology [209]. MCs in GN kidney tissue are primarily located in the interstitial tissue rather than the glomerulus, and MC abundance correlates with extent of fibrosis, decline in glomerular filtration rate, rapid disease progression, and poor outcome [209, 210]. Although MC_T cells are more abundant than

MC_{TC} in GN kidney tissue, the MC_{TC} phenotype is more closely associated with severity and fibrosis in rapidly progressive GN [211]. The correlation of fibrosis with MC_{TC} fits with the idea that MC chymases, as angiotensin II (Ang II)-converting enzymes, may promote fibrosis via conversion of Ang II and activation of transforming growth factor beta (TGF β). In addition, MC tryptase acts as a mitogen for smooth muscle cells and fibroblasts [120, 212, 213]. However, it is important to note that fibrosis and disease severity in GN is also associated with infiltration of macrophages and T lymphocytes [210]. Thus, it is not known if the presence of MCs promotes disease progression or is a response to inflammation. In mouse models of autoimmune GN, MCs can attenuate [214] or promote [215] disease so their role in human disease might also be dual purpose.

7.2 Organ Transplant

Abundant MC presence correlates with tissue fibrosis and acute and chronic rejection of transplanted heart, lung, liver, kidney, and intestine (reviewed in ref. 216). The role of MCs in transplantation has been most extensively studied in chronic rejection of kidney. MCs and MC-specific transcripts correlate with scarred areas during chronic rejection. MC numbers (particularly MC_{TC}) in stable renal allografts 3–4 months after transplant are a predictor of chronic allograft nephropathy and interstitial fibrosis [209, 217, 218]. Although it is not known if MCs are the cause or consequence of chronic inflammation in kidney transplant, the participation of MCs in the mechanisms of chronic rejection parallels the processes of tissue fibrosis and is reminiscent of the presence of MCs in GN. Specifically, MC degranulation releases Ang II-converting and TGF β -elaborating proteases that promote activation of fibroblasts and chronic graft failure.

MCs purportedly act as immunomodulators by secretion of cytokines, proteases, and other mediators, presentation of antigens, and modification of immune cell activity via direct cell-cell contacts (reviewed in refs. 180, 181, 189, 219). For example, MCs secrete several cytokines (e.g., IL-10, IL-4, TNF α , and GM-CSF), proteases (e.g., mMCP4, 6 (and the human equivalents)), and other metabolites (e.g., PGE₂) with known anti-inflammatory and tolerogenic-promoting functions [181]. As such, MCs have the potential to influence adaptive immunity by influencing cell trafficking; altering the interaction with (and among) professional antigen presenting cells; and, directly modifying adaptive immune cell effector functions [181]. Indeed, in rodent disease models, MCs promote tolerance by modifying the migration and interaction of DCs and T cells or by encouraging tolerogenic phenotypes [220]. Conversely, MC degranulation near transplanted tissue is associated with a break in immune tolerance and tissue rejection [221]. However, as for the recently contested role for MCs in EAE and arthritis [191], the function of MCs in promoting immune

tolerance in mice may require reexamination since these studies have also relied on the MC-deficient Wsh or W/W^v strains. To our knowledge, there is not yet any direct evidence that MCs promote tolerance in human transplant.

8 Conclusions

MCs have undisputed roles in human health as early responders to pathogens and toxins and, because of their potent activities, have undesirable and potentially lethal consequences in responses to environmental and food allergens. In addition, MCs likely have many more underappreciated roles in human health homeostasis, disease response, and tissue repair. Nevertheless, knowledge and appreciation of MC function have increased in areas such as cardiovascular disease, cancers, autoinflammatory and autoimmune disease, transplant rejection, and tissue fibrosis. The success of clinical treatments targeting MCs (or their products) supports the contribution of MCs in some of these conditions. In most cases MCs appear to be associated with promoting pathological processes; in a few contexts the presence of MCs (with a particular protease expression phenotype) is associated with beneficial signs or better prognosis. Because it is more difficult to distinguish the causal from the consequential in human patients, experimental animal models and *in vitro* studies have allowed us to glean important mechanistic and functional data for MCs in disease. The proliferation of MC-deficient mouse strains that do not rely on *W* locus mutations will allow continued refinement of our understanding of the biological functions of MCs in disease. However, conflicting data arising from animal experimentation emphasizes the limitations of the current methods in addition to the standard cautions that must be applied when translating knowledge from animal disease models to the clinic.

References

1. Hu Z-Q, Zhao W-H, Shimamura T (2007) Regulation of mast cell development by inflammatory factors. *Curr Med Chem* 14: 3044–3050
2. Collington SJ, Williams TJ, Weller CL (2011) Mechanisms underlying the localisation of mast cells in tissues. *Trends Immunol* 32: 478–485
3. Iemura A, Tsai M, Ando A et al (1994) The c-kit ligand, stem cell factor, promotes mast cell survival by suppressing apoptosis. *Am J Pathol* 144:321–328
4. Orinska Z, Föger N, Huber M et al (2010) I787 provides signals for c-Kit receptor internalization and functionality that control mast cell survival and development. *Blood* 116:2665–2675
5. Abraham SN, John ALS (2010) Mast cell-orchestrated immunity to pathogens. *Nat Rev Immunol* 10:440–452
6. Galli SJ, Borregaard N, Wynn TA (2011) Phenotypic and functional plasticity of cells of innate immunity: macrophages, mast cells and neutrophils. *Nat Immunol* 12:1035–1044
7. Moon TC, St Laurent CD, Morris KE et al (2009) Advances in mast cell biology: new understanding of heterogeneity and function. *Mucosal Immunol* 3:111–128

8. Marshall JS (2004) Mast-cell responses to pathogens. *Nat Rev Immunol* 4:787–799
9. Holgate ST, Hardy C, Robinson C et al (1986) The mast cell as a primary effector cell in the pathogenesis of asthma. *J Allergy Clin Immunol* 77:274–282
10. Irani AA, Schechter NM, Craig SS et al (1986) Two types of human mast cells that have distinct neutral protease compositions. *Proc Natl Acad Sci U S A* 83:4464–4468
11. Bax HJ, Keeble AH, Gould HJ (2012) Cytokinergic IgE action in mast cell activation. *Front Immunol* 3:229
12. Iwasaki A, Medzhitov R (2004) Toll-like receptor control of the adaptive immune responses. *Nat Immunol* 5:987–995
13. Williams CMM, Galli SJ (2000) The diverse potential effector and immunoregulatory roles of mast cells in allergic disease. *J Allergy Clin Immunol* 105:847–859
14. Theoharides TC, Aly sandratos K-D, Angelidou A et al (2012) Mast cells and inflammation. *Biochim Biophys Acta* 1822:21–33
15. Valadi H, Ekström K, Bossios A et al (2007) Exosome-mediated transfer of mRNAs and microRNAs is a novel mechanism of genetic exchange between cells. *Nat Cell Biol* 9: 654–659
16. Skokos D, Botros HG, Demeure C et al (2003) Mast cell-derived exosomes induce phenotypic and functional maturation of dendritic cells and elicit specific immune responses in vivo. *J Immunol* 170:3037–3045
17. Pulimood AB, Mathan MM, Mathan VI (1998) Quantitative and ultrastructural analysis of rectal mucosal mast cells in acute infectious diarrhea. *Dig Dis Sci* 43:2111–2116
18. Matsuo T, Ikura Y, Ohsawa M et al (2003) Mast cell chymase expression in Helicobacter pylori-associated gastritis. *Histopathology* 43: 538–549
19. Raqib R, Moly PK, Sarker P et al (2003) Persistence of mucosal mast cells and eosinophils in Shigella-infected children. *Infect Immun* 71:2684–2692
20. Qadri F, Bhuiyan TR, Dutta KK et al (2004) Acute dehydrating disease caused by *Vibrio cholerae* serogroups O1 and O139 induce increases in innate cells and inflammatory mediators at the mucosal surface of the gut. *Gut* 53:62–69
21. Galli SJ, Nakae S, Tsai M (2005) Mast cells in the development of adaptive immune responses. *Nat Immunol* 6:135–142
22. Ha TY, Reed ND, Crowle PK (1983) Delayed expulsion of adult *Trichinella spiralis* by mast cell-deficient W/Wv mice. *Infect Immun* 41: 445–447
23. Alizadeh H, Murrell KD (1984) The intestinal mast cell response to *Trichinella spiralis* infection in mast cell-deficient w/wv mice. *J Parasitol* 70:767
24. Knight PA, Wright SH, Lawrence CE et al (2000) Delayed expulsion of the nematode *Trichinella spiralis* in mice lacking the mucosal mast cell-specific granule chymase, mouse mast cell protease-1. *J Exp Med* 192:1849–1856
25. Lawrence CE, Paterson YYW, Wright SH et al (2004) Mouse mast cell protease-1 is required for the enteropathy induced by gastrointestinal helminth infection in the mouse. *Gastroenterology* 127:155–165
26. Woodbury RG, Miller HRP, Huntley JF et al (1984) Mucosal mast cells are functionally active during spontaneous expulsion of intestinal nematode infections in rat. *Nature* 312: 450–452
27. Urban JF, Katona IM, Paul WE et al (1991) Interleukin 4 is important in protective immunity to a gastrointestinal nematode infection in mice. *Proc Natl Acad Sci U S A* 88: 5513–5517
28. Finkelman FD, Shea-Donohue T, Morris SC et al (2004) Interleukin-4- and interleukin-13-mediated host protection against intestinal nematode parasites. *Immunol Rev* 201:139–155
29. McDermott JR, Bartram RE, Knight PA et al (2003) Mast cells disrupt epithelial barrier function during enteric nematode infection. *Proc Natl Acad Sci U S A* 100:7761–7766
30. Kitamura Y, Go S, Hatanaka K (1978) Decrease of mast cells in W/Wv mice and their increase by bone marrow transplantation. *Blood* 52: 447–452
31. Maurer M, Kostka SL, Siebenhaar F et al (2006) Skin mast cells control T cell-dependent host defense in *Leishmania* major infections. *FASEB J* 20:2460–2467
32. Dudeck A, Suender CA, Kostka SL et al (2011) Mast cells promote Th1 and Th17 responses by modulating dendritic cell maturation and function. *Eur J Immunol* 41:1883–1893
33. Urban BC, Cordery D, Shafi MJ et al (2006) The frequency of BDCA3-positive dendritic cells is increased in the peripheral circulation of Kenyan children with severe malaria. *Infect Immun* 74:6700–6706
34. Schofield L, Grau GE (2005) Immunological processes in malaria pathogenesis. *Nat Rev Immunol* 5:722–735
35. Guermonprez P, Helft J, Claser C et al (2013) Inflammatory Flt3l is essential to mobilize dendritic cells and for T cell responses during *Plasmodium* infection. *Nat Med* 19: 730–738

36. Echtenacher B, Männel DN, Hültner L (1996) Critical protective role of mast cells in a model of acute septic peritonitis. *Nature* 381:75–77
37. Lin T-J, Garduno R, Boudreau RTM et al (2002) *Pseudomonas aeruginosa* activates human mast cells to induce neutrophil transendothelial migration via mast cell-derived IL-1 α and β . *J Immunol* 169:4522–4530
38. Malaviya R, Ikeda T, Ross E et al (1996) Mast cell modulation of neutrophil influx and bacterial clearance at sites of infection through TNF- α . *Nature* 381:77–80
39. Malaviya R, Abraham SN (2000) Role of mast cell leukotrienes in neutrophil recruitment and bacterial clearance in infectious peritonitis. *J Leukoc Biol* 67:841–846
40. Huang C, Friend DS, Qiu W-T et al (1998) Induction of a selective and persistent extravasation of neutrophils into the peritoneal cavity by tryptase mouse mast cell protease 6. *J Immunol* 160:1910–1919
41. Tani K, Ogushi F, Kido H et al (2000) Chymase is a potent chemoattractant for human monocytes and neutrophils. *J Leukoc Biol* 67: 585–589
42. Huang C, Sanctis GTD, O'Brien PJ et al (2001) Evaluation of the substrate specificity of human mast cell tryptase β I and demonstration of its importance in bacterial infections of the lung. *J Biol Chem* 276:26276–26284
43. Nardo AD, Vitiello A, Gallo RL (2003) Cutting edge: mast cell antimicrobial activity is mediated by expression of cathelicidin antimicrobial peptide. *J Immunol* 170:2274–2278
44. Abel J, Goldmann O, Ziegler C et al (2011) *Staphylococcus aureus* evades the extracellular antimicrobial activity of mast cells by promoting its own uptake. *J Innate Immun* 3:495–507
45. Liu F-T, Goodarzi H, Chen H-Y (2011) IgE, mast cells, and eosinophils in atopic dermatitis. *Clin Rev Allergy Immunol* 41:298–310
46. Muñoz S, Rivas-Santiago B, Enciso JA (2009) Mycobacterium tuberculosis entry into mast cells through cholesterol-rich membrane microdomains. *Scand J Immunol* 70:256–263
47. Mañes S, del Real G, Martínez-A C (2003) Pathogens: raft hijackers. *Nat Rev Immunol* 3:557–568
48. Dawicki W, Jawdat DW, Xu N et al (2010) Mast cells, histamine, and IL-6 regulate the selective influx of dendritic cell subsets into an inflamed lymph node. *J Immunol* 184: 2116–2123
49. Gauchat J-F, Henchoz S, Mazzei G et al (1993) Induction of human IgE synthesis in B cells by mast cells and basophils. *Nature* 365: 340–343
50. John ALS, Rathore APS, Yap H et al (2011) Immune surveillance by mast cells during dengue infection promotes natural killer (NK) and NKT-cell recruitment and viral clearance. *Proc Natl Acad Sci U S A* 108: 9190–9195
51. Brown MG, McAlpine SM, Huang YY et al (2012) RNA sensors enable human mast cell anti-viral chemokine production and IFN-mediated protection in response to antibody-enhanced dengue virus infection. *PLoS One* 7:e34055
52. Dietrich N, Rohde M, Geffers R et al (2010) Mast cells elicit proinflammatory but not type I interferon responses upon activation of TLRs by bacteria. *Proc Natl Acad Sci U S A* 107: 8748–8753
53. John ALS, Abraham SN (2013) Innate immunity and its regulation by mast cells. *J Immunol* 190:4458–4463
54. Sundstrom JB, Ellis JE, Hair GA et al (2007) Human tissue mast cells are an inducible reservoir of persistent HIV infection. *Blood* 109: 5293–5300
55. Kasturiratne A, Wickremasinghe AR, de Silva N et al (2008) The global burden of snakebite: a literature analysis and modelling based on regional estimates of envenoming and deaths. *PLoS Med* 5:e218
56. Biló BM, Rueff F, Mosbech H et al (2005) Diagnosis of Hymenoptera venom allergy. *Allergy* 60:1339–1349
57. Rueff F, Dugas-Breit S, Przybilla B (2009) Stinging Hymenoptera and mastocytosis. *Curr Opin Allergy Clin Immunol* 9:338–342
58. Bonadonna P, Zanotti R, Müller U (2010) Mastocytosis and insect venom allergy. *Curr Opin Allergy Clin Immunol* 10:347–353
59. Casewell NR, Wüster W, Vonk FJ et al (2013) Complex cocktails: the evolutionary novelty of venoms. *Trends Ecol Evol* 28:219–229
60. Brown TC, Tankersley MS (2011) The sting of the honeybee: an allergic perspective. *Ann Allergy Asthma Immunol* 107:463–470
61. Metz M, Piliponsky AM, Chen C-C et al (2006) Mast cells can enhance resistance to snake and honeybee venoms. *Science* 313: 526–530
62. Akahoshi M, Song CH, Piliponsky AM et al (2011) Mast cell chymase reduces the toxicity of Gila monster venom, scorpion venom, and vasoactive intestinal polypeptide in mice. *J Clin Invest* 121:4180–4191
63. Maurer M, Wedemeyer J, Metz M et al (2004) Mast cells promote homeostasis by limiting endothelin-1-induced toxicity. *Nature* 432: 512–516

64. Caughey GH (2011) Mast cell proteases as protective and inflammatory mediators. *Adv Exp Med Biol* 716:212–234
65. Siddiqui S, Mistry V, Doe C et al (2008) Airway hyperresponsiveness is dissociated from airway wall structural remodeling. *J Allergy Clin Immunol* 122:335.e3–341.e3
66. Carroll NG, Mutavdzic S, James AL (2002) Distribution and degranulation of airway mast cells in normal and asthmatic subjects. *Eur Respir J* 19:879–885
67. Leckie MJ, ten Brinke A, Khan J et al (2000) Effects of an interleukin-5 blocking monoclonal antibody on eosinophils, airway hyperresponsiveness, and the late asthmatic response. *Lancet* 356:2144–2148
68. Nair P, Pizzichini MMM, Kjarsgaard M et al (2009) Mepolizumab for prednisone-dependent asthma with sputum eosinophilia. *N Engl J Med* 360:985–993
69. Crimi E, Chiaramondia M, Milanese M et al (1991) Increased numbers of mast cells in bronchial mucosa after the late-phase asthmatic response to allergen. *Am Rev Respir Dis* 144:1282–1286
70. Busse W, Corren J, Lanier BQ et al (2001) Omalizumab, anti-IgE recombinant humanized monoclonal antibody, for the treatment of severe allergic asthma. *J Allergy Clin Immunol* 108:184–190
71. Holgate ST, Djukanović R, Casale T et al (2005) Anti-immunoglobulin E treatment with omalizumab in allergic diseases: an update on anti-inflammatory activity and clinical efficacy. *Clin Exp Allergy* 35:408–416
72. Krishna MT, Chauhan A, Little L et al (2001) Inhibition of mast cell tryptase by inhaled APC 366 attenuates allergen-induced late-phase airway obstruction in asthma. *J Allergy Clin Immunol* 107:1039–1045
73. Bischoff SC (2007) Role of mast cells in allergic and non-allergic immune responses: comparison of human and murine data. *Nat Rev Immunol* 7:93–104
74. Rock JR, Randell SH, Hogan BLM (2010) Airway basal stem cells: a perspective on their roles in epithelial homeostasis and remodeling. *Dis Model Mech* 3:545–556
75. Becker M, Reuter S, Friedrich P et al (2011) Genetic variation determines mast cell functions in experimental asthma. *J Immunol* 186: 7225–7231
76. Grimaldeston MA, Chen C-C, Piliponsky AM et al (2005) Mast cell-deficient W-sash c-kit mutant KitW-sh/W-sh mice as a model for investigating mast cell biology in vivo. *Am J Pathol* 167:835–848
77. Nakae S, Ho LH, Yu M et al (2007) Mast cell-derived TNF contributes to airway hyperreactivity, inflammation, and TH2 cytokine production in an asthma model in mice. *J Allergy Clin Immunol* 120:48–55
78. Rodewald H-R, Feyerabend TB (2012) Widespread immunological functions of mast cells: fact or fiction? *Immunity* 37:13–24
79. Baumgart DC, Carding SR (2007) Inflammatory bowel disease: cause and immunobiology. *Lancet* 369:1627–1640
80. Baumgart DC, Sandborn WJ (2007) Inflammatory bowel disease: clinical aspects and established and evolving therapies. *Lancet* 369:1641–1657
81. Farhadi A, Fields J-Z, Keshavarzian A (2007) Mucosal mast cells are pivotal elements in inflammatory bowel disease that connect the dots: stress, intestinal hyperpermeability and inflammation. *World J Gastroenterol* 13: 3027–3030
82. Matricona J, Meleine M, Gelot A et al (2012) Review article: associations between immune activation, intestinal permeability and the irritable bowel syndrome. *Aliment Pharmacol Ther* 36:1009–1031
83. Nolte H, Spjeldnaes N, Kruse A et al (1990) Histamine release from gut mast cells from patients with inflammatory bowel diseases. *Gut* 31:791–794
84. Lilja I, Gustafson-Svärd C, Franzén L et al (2000) Tumor necrosis factor-alpha in ileal mast cells in patients with Crohn's disease. *Digestion* 61:68–76
85. Stoyanova II, Gulubova MV (2002) Mast cells and inflammatory mediators in chronic ulcerative colitis. *Acta Histochem* 104: 185–192
86. Hodges K, Kennedy L, Meng F et al (2012) Mast cells, disease and gastrointestinal cancer: a comprehensive review of recent findings. *Transl Gastrointest Cancer* 1:138–150
87. Odenwald MA, Turner JR (2013) Intestinal permeability defects: is it time to treat? *Clin Gastroenterol Hepatol* 11(9):1075–1083
88. Stead RH, Dixon MF, Bramwell NH et al (1989) Mast cells are closely apposed to nerves in the human gastrointestinal mucosa. *Gastroenterology* 97:575–585
89. Wood JD (2004) Enteric neuroimmunophysiology and pathophysiology. *Gastroenterology* 127:635–657
90. Kurashima Y, Amiya T, Nohchi T et al (2012) Extracellular ATP mediates mast cell-dependent intestinal inflammation through P2X7 purinoreceptors. *Nat Commun* 3:1034
91. Konturek PC, Brzozowski T, Konturek SJ (2011) Stress and the gut: pathophysiology,

clinical consequences, diagnostic approach and treatment options. *J Physiol Pharmacol* 62: 591–599

92. Farhadi A, Keshavarzian A, Van de Kar LD et al (2005) Heightened responses to stressors in patients with inflammatory bowel disease. *Am J Gastroenterol* 100:1796–1804

93. Valatas V, Vakas M, Kolios G (2013) The value of experimental models of colitis in predicting efficacy of biologic therapies for inflammatory bowel diseases. *Am J Physiol Gastrointest Liver Physiol* 305:G763–G785

94. Middel P, Reich K, Polzien F et al (2001) Interleukin 16 expression and phenotype of interleukin 16 producing cells in Crohn's disease. *Gut* 49:795–803

95. Barrett KE, Tashof TL, Metcalfe DD (1985) Inhibition of IgE-mediated mast cell degranulation by sulphasalazine. *Eur J Pharmacol* 107:279–281

96. De Winter BY, van den Wijngaard RM, de Jonge WJ (2012) Intestinal mast cells in gut inflammation and motility disturbances. *Biochim Biophys Acta* 1822:66–73

97. Barbara G, Stanghellini V, De Giorgio R et al (2006) Functional gastrointestinal disorders and mast cells: implications for therapy. *Neurogastroenterol Motil* 18:6–17

98. Stefanini GF, Prati E, Albini MC et al (1992) Oral disodium cromoglycate treatment on irritable bowel syndrome: an open study on 101 subjects with diarrheic type. *Am J Gastroenterol* 87:55–57

99. Matter SE, Bhatia PS, Miner PB Jr (1990) Evaluation of antral mast cells in nonulcer dyspepsia. *Dig Dis Sci* 35:1358–1363

100. Clouse RE, Lustman PJ, Geisman RA et al (1994) Antidepressant therapy in 138 patients with irritable bowel syndrome: a five-year clinical experience. *Aliment Pharmacol Ther* 8:409–416

101. Kaartinen M, Penttilä A, Kovanen PT (1994) Accumulation of activated mast cells in the shoulder region of human coronary atheroma, the predilection site of atheromatous rupture. *Circulation* 90:1669–1678

102. Tsunemi K, Takai S, Nishimoto M et al (2002) Possible roles of angiotensin II-forming enzymes, angiotensin converting enzyme and chymase-like enzyme, in the human aneurysmal aorta. *Hypertens Res* 25:817–822

103. Kovanen PT (2007) Mast cells: multipotent local effector cells in atherothrombosis. *Immunol Rev* 217:105–122

104. Lindstedt KA, Mäyränpää MI, Kovanen PT (2007) Mast cells in vulnerable atherosclerotic plaques—a view to a kill. *J Cell Mol Med* 11:739–758

105. Bot I, Biessen EAL (2011) Mast cells in atherosclerosis. *Thromb Haemost* 106: 820–826

106. Xu J-M, Shi G-P (2012) Emerging role of mast cells and macrophages in cardiovascular and metabolic diseases. *Endocr Rev* 33:71–108

107. Swedenborg J, Mäyränpää MI, Kovanen PT (2011) Mast cells important players in the orchestrated pathogenesis of abdominal aortic aneurysms. *Arterioscler Thromb Vasc Biol* 31:734–740

108. Levick SP, Meléndez GC, Plante E et al (2011) Cardiac mast cells: the centrepiece in adverse myocardial remodelling. *Cardiovasc Res* 89:12–19

109. Bot I, van Berkel TJ, Biessen EA (2008) Mast cells: pivotal players in cardiovascular diseases. *Curr Cardiol Rev* 4:170–178

110. Galkina E, Ley K (2009) Immune and inflammatory mechanisms of atherosclerosis. *Annu Rev Immunol* 27:165–197

111. Cairns A, Constantinides P (1954) Mast cells in human atherosclerosis. *Science* 120:31–32

112. Jeziorska M, McCollum C, Woolley DE (1997) Mast cell distribution, activation, and phenotype in atherosclerotic lesions of human carotid arteries. *J Pathol* 182:115–122

113. Kovanen PT (1996) Mast cells in human fatty streaks and atheromas: implications for intimal lipid accumulation. *Curr Opin Lipidol* 7:281–286

114. Kaartinen M, Penttilä A, Kovanen PT (1996) Mast cells accompany microvessels in human coronary atheromas: implications for intimal neovascularization and hemorrhage. *Atherosclerosis* 123:123–131

115. Willems S, Vink A, Bot I et al (2013) Mast cells in human carotid atherosclerotic plaques are associated with intraplaque microvessel density and the occurrence of future cardiovascular events. *Eur Heart J* 34(48): 3699–3706

116. Lappalainen H, Laine P, Penttilä MO et al (2004) Mast cells in neovascularized human coronary plaques store and secrete basic fibroblast growth factor, a potent angiogenic mediator. *Arterioscler Thromb Vasc Biol* 24:1880–1885

117. Mäyränpää MI, Trosien JA, Fontaine V et al (2009) Mast cells associate with neovessels in the media and adventitia of abdominal aortic aneurysms. *J Vasc Surg* 50:388–395

118. Tsuruda T, Kato J, Hatakeyama K et al (2008) Adventitial mast cells contribute to pathogenesis in the progression of abdominal aortic aneurysm. *Circ Res* 102:1368–1377

119. Anvari MS, Boroumand MA, Mojarrad EA et al (2012) Do adventitial mast cells contribute to

the pathogenesis of ascending thoracic aorta aneurysm? *Int J Surg Pathol* 20:474–479

120. Pejler G, Ronnberg E, Waern I et al (2010) Mast cell proteases: multifaceted regulators of inflammatory disease. *Blood* 115:4981–4990

121. Furubayashi K, Takai S, Jin D et al (2008) Chymase activates promatrix metalloproteinase-9 in human abdominal aortic aneurysm. *Clin Chim Acta* 388:214–216

122. Shi G-P, Sukhova GK, Grubb A et al (1999) Cystatin C deficiency in human atherosclerosis and aortic aneurysms. *J Clin Invest* 104: 1191–1197

123. Lv B-J, Lindholt JS, Wang J et al (2013) Plasma levels of cathepsins L, K, and V and risks of abdominal aortic aneurysms: a randomized population-based study. *Atherosclerosis* 230:100–105

124. Choke E, Thompson MM, Dawson J et al (2006) Abdominal aortic aneurysm rupture is associated with increased medial neovascularization and overexpression of proangiogenic cytokines. *Arterioscler Thromb Vasc Biol* 26:2077–2082

125. Mayraanpaa MI, Heikkila HM, Lindstedt KA et al (2006) Desquamation of human coronary artery endothelium by human mast cell proteases: implications for plaque erosion. *Coron Artery Dis* 17:611–621

126. Patella V, de Crescenzo G, Lamparter-Schummert B et al (1997) Increased cardiac mast cell density and mediator release in patients with dilated cardiomyopathy. *Inflamm Res* 46:31–32

127. Patella V, Marinò I, Arbustini E et al (1998) Stem cell factor in mast cells and increased mast cell density in idiopathic and ischemic cardiomyopathy. *Circulation* 97:971–978

128. Ibrahim M, Terracciano C, Yacoub MH (2012) Can bridge to recovery help to reveal the secrets of the failing heart? *Curr Cardiol Rep* 14:392–396

129. Akgul A, Skrabal CA, Thompson LO et al (2004) Role of mast cells and their mediators in failing myocardium under mechanical ventricular support. *J Heart Lung Transplant* 23:709–715

130. Jahanyar J, Youker KA, Torre-Amione G et al (2008) Increased expression of stem cell factor and its receptor after left ventricular assist device support: a potential novel target for therapeutic interventions in heart failure. *J Heart Lung Transplant* 27:701–709

131. Jahanyar J, Youker KA, Loebe M et al (2007) Mast cell-derived cathepsin G: a possible role in the adverse remodeling of the failing human heart. *J Surg Res* 140:199–203

132. Murray PJ, Wynn TA (2011) Protective and pathogenic functions of macrophage subsets. *Nat Rev Immunol* 11:723–737

133. Qin Y, Shi G-P (2011) Cysteinyl cathepsins and mast cell proteases in the pathogenesis and therapeutics of cardiovascular diseases. *Pharmacol Ther* 131:338–350

134. Krauth MT, Majlesi Y, Sonneck K et al (2006) Effects of various statins on cytokine-dependent growth and IgE-dependent release of histamine in human mast cells. *Allergy* 61:281–288

135. Clejan S, Japa S, Clemetson C et al (2002) Blood histamine is associated with coronary artery disease, cardiac events and severity of inflammation and atherosclerosis. *J Cell Mol Med* 6:583–592

136. Kim J, Ogai A, Nakatani S et al (2006) Impact of blockade of histamine H₂ receptors on chronic heart failure revealed by retrospective and prospective randomized studies. *J Am Coll Cardiol* 48:1378–1384

137. Korkmaz ME, Oto A, Saraclar Y et al (1991) Levels of IgE in the serum of patients with coronary arterial disease. *Int J Cardiol* 31: 199–204

138. Upadhyaya B, Kontos JL, Ardeshirpour F et al (2004) Relation of serum levels of mast cell tryptase of left ventricular systolic function, left ventricular volume or congestive heart failure. *J Card Fail* 10:31–35

139. Deliargyris EN, Upadhyaya B, Sane DC et al (2005) Mast cell tryptase: a new biomarker in patients with stable coronary artery disease. *Atherosclerosis* 178:381–386

140. Xiang M, Sun J, Lin Y et al (2011) Usefulness of serum tryptase level as an independent biomarker for coronary plaque instability in a Chinese population. *Atherosclerosis* 215: 494–499

141. Duda D, Lorenz W, Celik I (2002) Histamine release in mesenteric traction syndrome during abdominal aortic aneurysm surgery: prophylaxis with H1 and H2 antihistamines. *Inflamm Res* 51:495–499

142. Longley BJ, Tyrrell L, Lu S-Z et al (1996) Somatic c-KIT activating mutation in urticaria pigmentosa and aggressive mastocytosis: establishment of clonality in a human mast cell neoplasm. *Nat Genet* 12:312–314

143. Valent P, Horny H-P, Escribano L et al (2001) Diagnostic criteria and classification of mastocytosis: a consensus proposal. *Leuk Res* 25:603–625

144. Nagata H, Worobec AS, Oh CK et al (1995) Identification of a point mutation in the catalytic domain of the protooncogene c-kit in peripheral blood mononuclear cells of patients

who have mastocytosis with an associated hematologic disorder. *Proc Natl Acad Sci U S A* 92:10560–10564

145. Irani AA, Garriga MM, Metcalfe DD et al (1990) Mast cells in cutaneous mastocytosis: accumulation of the MCTC type. *Clin Exp Allergy* 20:53–58

146. Schwartz LB (2006) Diagnostic value of tryptase in anaphylaxis and mastocytosis. *Immunol Allergy Clin North Am* 26: 451–463

147. Compton SJ, Cairns JA, Holgate ST et al (2000) Human mast cell tryptase stimulates the release of an IL-8-dependent neutrophil chemotactic activity from human umbilical vein endothelial cells (HUVEC). *Clin Exp Immunol* 121:31–36

148. He S, Gaça MDA, Walls AF (1998) A role for tryptase in the activation of human mast cells: modulation of histamine release by tryptase and inhibitors of tryptase. *J Pharmacol Exp Ther* 286:289–297

149. Pardanani A (2013) Systemic mastocytosis in adults: 2013 update on diagnosis, risk stratification, and management. *Am J Hematol* 88: 612–624

150. Pardanani A (2013) How I treat patients with indolent and smoldering mastocytosis (rare conditions but difficult to manage). *Blood* 121:3085–3094

151. Horan RF, Sheffer AL, Austen KF (1990) Cromolyn sodium in the management of systemic mastocytosis. *J Allergy Clin Immunol* 85:852–855

152. Edwards AM, Capková S (2011) Oral and topical sodium cromoglicate in the treatment of diffuse cutaneous mastocytosis in an infant. *BMJ Case Rep*: bcr0220113910

153. Siebenhaar F, Förtsch A, Krause K et al (2013) Rupatadine improves quality of life in mastocytosis: a randomized, double-blind, placebo-controlled trial. *Allergy* 68(7):949–952

154. Paraskevopoulos G, Sifnaios E, Christodoulopoulos K et al (2013) Successful treatment of mastocytic anaphylactic episodes with reduction of skin mast cells after anti-IgE therapy. *Eur Ann Allergy Clin Immunol* 45:52–55

155. Gleixner KV, Mayerhofer M, Aichberger KJ et al (2006) PKC412 inhibits in vitro growth of neoplastic human mast cells expressing the D816V-mutated variant of KIT: comparison with AMN107, imatinib, and cladribine (2CdA) and evaluation of cooperative drug effects. *Blood* 107:752–759

156. Gleixner KV, Mayerhofer M, Cerny-Reiterer S et al (2011) KIT-D816V-independent oncogenic signaling in neoplastic cells in systemic mastocytosis: role of Lyn and Btk activation and disruption by dasatinib and bosutinib. *Blood* 118:1885–1898

157. Agarwala MK, George R, Mathews V et al (2013) Role of imatinib in the treatment of pediatric onset indolent systemic mastocytosis: a case report. *J Dermatolog Treat* 24: 481–483

158. Hanahan D, Coussens LM (2012) Accessories to the crime: functions of cells recruited to the tumor microenvironment. *Cancer Cell* 21:309–322

159. Westphal E, Ehrlich P (1891) Über Mastzellen. *Histologie und Klinik des Plutes: gesammelte Mitt (h) eilungen, Ehrlich P.. Farbenanalytische Untersuchungen*. Hirschwald Press, Berlin, pp 17–21

160. Theoharides TC, Conti P (2004) Mast cells: the JEKYLL and HYDE of tumor growth. *Trends Immunol* 25:235–241

161. Zhang W, Stoica G, Tasca SI et al (2000) Modulation of tumor angiogenesis by stem cell factor. *Cancer Res* 60:6757–6762

162. Conti P, Castellani ML, Kempuraj D et al (2007) Role of mast cells in tumor growth. *Ann Clin Lab Sci* 37:315–322

163. Maltby S, Khazaie K, McNagny KM (2009) Mast cells in tumor growth: angiogenesis, tissue remodelling and immune-modulation. *Biochim Biophys Acta* 1796(1):19–26

164. Aaltomaa S, Lipponen P, Papinaho S et al (1993) Mast cells in breast cancer. *Anticancer Res* 13:785–788

165. Dabiri S, Huntsman D, Makretsov N et al (2004) The presence of stromal mast cells identifies a subset of invasive breast cancers with a favorable prognosis. *Mod Pathol* 17: 690–695

166. Ribatti D, Finato N, Crivellato E et al (2007) Angiogenesis and mast cells in human breast cancer sentinel lymph nodes with and without micrometastases. *Histopathology* 51:837–842

167. Ranieri G (2009) Tryptase-positive mast cells correlate with angiogenesis in early breast cancer patients. *Int J Oncol* 35:115–120

168. Rajput AB, Turbin DA, Cheang MC et al (2008) Stromal mast cells in invasive breast cancer are a marker of favourable prognosis: a study of 4,444 cases. *Breast Cancer Res Treat* 107:249–257

169. Amini R-M, Aaltonen K, Nevanlinna H et al (2007) Mast cells and eosinophils in invasive breast carcinoma. *BMC Cancer* 7:165

170. Mangia A, Malfettone A, Rossi R et al (2011) Tissue remodelling in breast cancer: human mast cell tryptase as an initiator of myofibroblast differentiation. *Histopathology* 58: 1096–1106

171. Strouch MJ, Cheon EC, Salabat MR et al (2010) Crosstalk between mast cells and pancreatic cancer cells contributes to pancreatic tumor progression. *Clin Cancer Res* 16: 2257–2265

172. Cai S-W, Yang S-Z, Gao J et al (2011) Prognostic significance of mast cell count following curative resection for pancreatic ductal adenocarcinoma. *Surgery* 149:576–584

173. Chang DZ, Ma Y, Ji B et al (2011) Mast cells in tumor microenvironment promotes the in vivo growth of pancreatic ductal adenocarcinoma. *Clin Cancer Res* 17:7015–7023

174. Esposito I, Menicagli M, Funel N et al (2004) Inflammatory cells contribute to the generation of an angiogenic phenotype in pancreatic ductal adenocarcinoma. *J Clin Pathol* 57: 630–636

175. Nonomura N, Takayama H, Nishimura K et al (2007) Decreased number of mast cells infiltrating into needle biopsy specimens leads to a better prognosis of prostate cancer. *Br J Cancer* 97:952–956

176. Fleischmann A, Schlomm T, Köllermann J et al (2009) Immunological microenvironment in prostate cancer: high mast cell densities are associated with favorable tumor characteristics and good prognosis. *Prostate* 69:976–981

177. Pittoni P, Tripodo C, Piconese S et al (2011) Mast cell targeting hampers prostate adenocarcinoma development but promotes the occurrence of highly malignant neuroendocrine cancers. *Cancer Res* 71:5987–5997

178. Pittoni P, Colombo MP (2012) The dark side of mast cell-targeted therapy in prostate cancer. *Cancer Res* 72:831–835

179. Frenzel L, Hermine O (2013) Mast cells and inflammation. *Joint Bone Spine* 80: 141–145

180. Walker ME, Hatfield JK, Brown MA (2012) New insights into the role of mast cells in autoimmunity: evidence for a common mechanism of action? *Biochim Biophys Acta* 1822:57–65

181. de Vries VC, Noelle RJ (2010) Mast cell mediators in tolerance. *Curr Opin Immunol* 22:643–648

182. Neumann J (1890) Ueber das Vorkommen der sogenannten "Mastzellen" bei pathologischen Veränderungen des Gehirns. *Virchows Arch Pathol Anat Physiol Klin Med* 122:378–380

183. (1963) XVI. Mast cell under pathologic conditions. *Ann N Y Acad Sci* 103:344–354

184. Ibrahim MZM, Reder AT, Lawand R et al (1996) The mast cells of the multiple sclerosis brain. *J Neuroimmunol* 70:131–138

185. Krüger PG (2001) Mast cells and multiple sclerosis: a quantitative analysis. *Neuropathol Appl Neurobiol* 27:275–280

186. Zappulla JP, Arock M, Mars LT et al (2002) Mast cells: new targets for multiple sclerosis therapy? *J Neuroimmunol* 131:5–20

187. Couturier N, Zappulla JP, Lauwers-Cances V et al (2008) Mast cell transcripts are increased within and outside multiple sclerosis lesions. *J Neuroimmunol* 195:176–185

188. Karagkouni A, Alevizos M, Theoharides TC (2013) Effect of stress on brain inflammation and multiple sclerosis. *Autoimmun Rev* 12: 947–953

189. Brown MA, Hatfield JK (2012) Mast cells are important modifiers of autoimmune disease: with so much evidence, why is there controversy? *Front Immunol* 3:147

190. Brown MA, Hatfield JK, Walker ME et al (2012) A game of kit and mouse: the kit is still in the bag. *Immunity* 36:891–892

191. Feyerabend TB, Weiser A, Tietz A et al (2011) Cre-mediated cell ablation contests mast cell contribution in models of antibody- and T cell-mediated autoimmunity. *Immunity* 35: 832–844

192. Rodewald H-R (2012) Response to Brown et al. *Immunity* 36:893–894

193. Sayed BA, Walker ME, Brown MA (2011) Cutting edge: mast cells regulate disease severity in a relapsing-remitting model of multiple sclerosis. *J Immunol* 186:3294–3298

194. Secor VH, Secor WE, Gutekunst C-A et al (2000) Mast cells are essential for early onset and severe disease in a murine model of multiple sclerosis. *J Exp Med* 191:813–822

195. Bennett JL, Blanchet M-R, Zhao L et al (2009) Bone marrow-derived mast cells accumulate in the central nervous system during inflammation but are dispensable for experimental autoimmune encephalomyelitis pathogenesis. *J Immunol* 182:5507–5514

196. Michel A, Schuler A, Friedrich P et al (2013) Mast cell-deficient KitW-sh "Sash" mutant mice display aberrant myelopoiesis leading to the accumulation of splenocytes that act as myeloid-derived suppressor cells. *J Immunol* 190:5534–5544

197. Piconese S, Costanza M, Musio S et al (2011) Exacerbated experimental autoimmune encephalomyelitis in mast-cell-deficient KitW-sh/W-sh mice. *Lab Invest* 91:627–641

198. Li H, Nourbakhsh B, Safavi F et al (2011) Kit (W-sh) mice develop earlier and more severe experimental autoimmune encephalomyelitis due to absence of immune suppression. *J Immunol* 187:274–282

199. Nigrovic PA, Lee DM (2007) Synovial mast cells: role in acute and chronic arthritis. *Immunol Rev* 217:19–37

200. Noordenbos T, Yeremenko N, Gofita I et al (2012) Interleukin-17-positive mast cells contribute to synovial inflammation in spondyloarthritis. *Arthritis Rheum* 64:99–109

201. Eklund KK (2007) Mast cells in the pathogenesis of rheumatic diseases and as potential targets for anti-rheumatic therapy. *Immunol Rev* 217:38–52

202. Kenna TJ, Brown MA (2012) The role of IL-17-secreting mast cells in inflammatory joint disease. *Nat Rev Rheumatol* 9:375–379

203. Sandler C, Lindstedt KA, Joutsniemi S et al (2007) Selective activation of mast cells in rheumatoid synovial tissue results in production of TNF- α , IL-1 β and IL-1Ra. *Inflamm Res* 56:230–239

204. Hueber AJ, Asquith DL, Miller AM et al (2010) Cutting edge: mast cells express IL-17A in rheumatoid arthritis synovium. *J Immunol* 184:3336–3340

205. Lee DM, Friend DS, Gurish MF et al (2002) Mast cells: a cellular link between autoantibodies and inflammatory arthritis. *Science* 297:1689–1692

206. Nigrovic PA, Malbec O, Lu B et al (2010) C5a receptor enables participation of mast cells in immune complex arthritis independently of Fc γ receptor modulation. *Arthritis Rheum* 62:3322–3333

207. Nigrovic PA, Binstadt BA, Monach PA et al (2007) Mast cells contribute to initiation of autoantibody-mediated arthritis via IL-1. *Proc Natl Acad Sci U S A* 104:2325–2330

208. Zhou JS, Xing W, Friend DS et al (2007) Mast cell deficiency in KitW-sh mice does not impair antibody-mediated arthritis. *J Exp Med* 204:2797–2802

209. Holdsworth SR, Summers SA (2008) Role of mast cells in progressive renal diseases. *J Am Soc Nephrol* 19:2254–2261

210. Tóth T, Tóth-Jakabics R, Jimi S et al (1999) Mast cells in rapidly progressive glomerulonephritis. *J Am Soc Nephrol* 10:1498–1505

211. Yamada M, Ueda M, Naruko T et al (2001) Mast cell chymase expression and mast cell phenotypes in human rejected kidneys. *Kidney Int* 59:1374–1381

212. Company C, Piqueras L, Naim Abu Nabah Y et al (2011) Contributions of ACE and mast cell chymase to endogenous angiotensin II generation and leucocyte recruitment in vivo. *Cardiovasc Res* 92:48–56

213. Wasse H, Naqvi N, Husain A (2012) Impact of mast cell chymase on renal disease progression. *Curr Hypertens Rev* 8:15–23

214. Gan P-Y, Summers SA, Ooi JD et al (2012) Mast cells contribute to peripheral tolerance and attenuate autoimmune vasculitis. *J Am Soc Nephrol* 23:1955–1966

215. Scandiuzzi L, Beghdadi W, Daugas E et al (2010) Mouse mast cell protease-4 deteriorates renal function by contributing to inflammation and fibrosis in immune complex-mediated glomerulonephritis. *J Immunol* 185:624–633

216. Jahanyar J, Koerner MM, Loebe M et al (2008) The role of mast cells after solid organ transplantation. *Transplantation* 85:1365–1371

217. Ishida T, Hyodo Y, Ishimura T et al (2005) Mast cell numbers and protease expression patterns in biopsy specimens following renal transplantation from living-related donors predict long-term graft function. *Clin Transplant* 19:817–824

218. Mengel M, Reeve J, Bunnag S et al (2009) Molecular correlates of scarring in kidney transplants: the emergence of mast cell transcripts. *Am J Transplant* 9:169–178

219. Kalesnikoff J, Galli SJ (2008) New developments in mast cell biology. *Nat Immunol* 9:1215–1223

220. de Vries VC, Pino-Lagos K, Nowak EC et al (2011) Mast cells condition dendritic cells to mediate allograft tolerance. *Immunity* 35: 550–561

221. de Vries VC, Wasiuk A, Bennett KA et al (2009) Mast cell degranulation breaks peripheral tolerance. *Am J Transplant* 9: 2270–2280

Chapter 8

The Emerging Prominence of the Cardiac Mast Cell as a Potent Mediator of Adverse Myocardial Remodeling

Joseph S. Janicki, Gregory L. Brower, and Scott P. Levick

Abstract

Cardiac mast cells store and release a variety of biologically active mediators, several of which have been implicated in the activation of matrix metalloproteinases in the volume-overloaded heart, while others are involved in the fibrotic process in pressure-overloaded hearts. Increased numbers of mast cells have been reported in explanted human hearts with dilated cardiomyopathy and in animal models of experimentally induced hypertension, myocardial infarction, and chronic cardiac volume overload. Also, there is evolving evidence implicating the cardiac mast cell as having a major role in the adverse remodeling underlying these cardiovascular disorders. Thus, the cardiac mast cell is the focus of this chapter that begins with a historical background, followed by sections on methods for their isolation and characterization, endogenous secretagogues, phenotype, and ability of estrogen to alter their phenotype so as to provide cardioprotection. Finally the role of mast cells in myocardial remodeling secondary to a sustained cardiac volume overload, hypertension, and ischemic injury and future research directions are discussed.

Key words Mast cell isolation, Mast cell mediators, Myocardial remodeling, Stem cell factor, Estrogen, Hypertension, Cardiac volume overload, Ischemia–reperfusion, Myocardial infarction, Mast cell secretagogues

1 Introduction

To compensate for a sustained abnormal myocardial stress secondary to injury, disease, or chronic ventricular volume or pressure overload, a progressive, structural remodeling process of the muscular, vascular, and extracellular matrix components of the myocardium is initiated. However, the ability to normalize the elevated stress is limited, and as a result, the ventricle dilates with an inappropriate wall thickness, and eventually the clinical signs and symptoms of heart failure become apparent [1, 2]. Because fibrillar collagen provides a supportive framework which interconnects cardiomyocytes and blood vessels and thereby maintains ventricular size and shape [3, 4], such architectural alterations have to be preceded by a disruption of the collagen network. Co-localized with the

interstitial myocardial collagen matrix is a largely latent, matrix metalloproteinase (MMP) system [5], which when activated will cause rapid collagen degradation alterations in the extracellular matrix. Recently cardiac mast cells, which are known to store and release a variety of biologically active mediators including tumor necrosis factor- α (TNF- α) and proteases such as tryptase, chymase, and stromelysin [6–10], have been implicated in the activation of MMPs in the volume-overloaded heart [11]. Mast cells are derived from precursor cells in the bone marrow and locally mature under the influence of the c-Kit ligand, stem cell factor (SCF), with their final phenotype being dependent on the microenvironment in which they reside. Increased numbers of mast cells have been reported in explanted human hearts with dilated cardiomyopathy [12, 13] and in animal models of experimentally induced hypertension [14–16], myocardial infarction [17], and chronic volume overload secondary to aortocaval fistula [11] and mitral regurgitation [18, 19]. Furthermore, there is evolving evidence implicating the cardiac mast cell as having a major role in the adverse remodeling underlying these cardiovascular disorders. Thus, the cardiac mast cell will be the focus of this chapter, which will begin with a historical background, followed by sections on methods for mast cell isolation and characterization, its endogenous secretagogues, its phenotype and the ability of estrogen to alter it, and its role in myocardial remodeling secondary to a sustained cardiac volume overload, hypertension, and ischemic injury.

2 Historical Background

In 1863, Friedrich Daniel von Recklinghausen identified granular cells in the mesentery of the frog [20], which in 1878 Paul Ehrlich named *MASTZELLEN* or the “well-fed cell” because the cytoplasm of this relatively large cell was stuffed with prominent granules [21]. Surprisingly, articles addressing cardiac mast cells did not appear until 1968. These and several subsequent studies, however, were focused primarily on observations of increased numbers of cardiac mast cells associated with: (1) endomyocardial fibrosis and eosinophilic myocarditis [22, 23], (2) the right ventricle following pulmonary artery banding in rats [16], (3) the subepicardial layer of the infarcted region following experimental myocardial infarction in rats [17], (4) the first week after creation of an infrarenal aortocaval fistula in rats [11], (5) dog hearts 4 months after the onset of experimental mitral regurgitation [18], and (6) explanted hearts from patients with dilated cardiomyopathy [12].

In addition, several articles have been published which addressed the functional role of mast cells in cardiac diseases. In 1986, clear evidence of cardiac mast cell degranulation was correlated with significant interstitial edema in endomyocardial biopsies

from two cardiac patients by Ann M. Dvorak [24]. In 1992, Li and his coworkers analyzed serial endomyocardial biopsies from transplanted human hearts and concluded that cardiac mast cells are associated with interstitial and perimyocytic fibrosis [25]. In 1995, Petri T. Kovanen reviewed the accumulating evidence regarding a “cause and effect” role of increased mast cells in atherosclerotic plaque formation and the erosion or rupture of coronary atheromas [26]. In 2002, our laboratory reported a marked, rapid increase in cardiac mast cell density during the first 5 days after creation of an infrarenal aortocaval fistula in rats, which was responsible for MMP activation and subsequent fibrillar collagen degradation [11].

More recently, genetically modified rodent models further demonstrated the adverse functional role of mast cells. For example, in 2002, Hara et al. [27] reported that, in contrast to their wild-type counterpart, heart and lung weights were markedly attenuated, ventricular dilatation was prevented, and fractional shortening was preserved in hypertensive mast cell-deficient mice. Other studies have utilized mast cell-deficient mice to determine the role of mast cells in ischemia–reperfusion injury and myocardial infarction (MI) [28–30]. However, as will be seen below, the data accumulated thus far is somewhat contradictory regarding the role of mast cells in ischemia–reperfusion and MI. In 2007, the mast cell’s role in the formation of atherosclerotic plaques was clearly verified using low-density lipoprotein receptor-deficient ($Ldlr(-/-)$) mast cell-deficient ($Kit(W-sh)/(W-sh)$) mice [31]. In 2008, we utilized mast cell-deficient rats to demonstrate causality between mast cells and adverse myocardial remodeling. In comparison to the wild-type rat following volume overload, left ventricular dilatation was markedly reduced, MMP-2 activity was not increased, and, thus, collagen degradation was prevented at 5 days and 8 weeks post fistula [32].

From this brief historic overview, it is clear that cardiac mast cell density becomes significantly elevated when subjected to the increased myocardial stress of ischemic injury, cardiomyopathy, and sustained cardiac pressure or volume overload and that an understanding of their role as mediators of ventricular remodeling is beginning to emerge.

3 Cardiac Mast Cell Phenotype, Isolation Techniques, and Endogenous Secretagogues

Two distinct mast cell phenotypes have been identified in the mucosa, skin, and lungs that are classified according to their neutral protease content [8, 33]: the MC_T is typically found in mucosal tissue having granules which contain only tryptase, while the MC_{TC} found predominantly in connective tissue contain chymase, cathepsin G, and carboxypeptidase, in addition to tryptase. There are at least three studies that characterize cardiac mast cells as being

consistent with the MC_{TC} subtype [34–36]. Mature cardiac mast cells are relatively large and are easily visualized using light microscopy after staining tissue sections with toluidine blue. Cardiac mast cells have also been shown to contain preformed tumor necrosis factor-alpha (TNF- α) [9]. Its role and the roles of other mast cell products including histamine, transforming growth factor-beta (TGF- β), tryptase, and chymase in mast cell-mediated remodeling will be discussed subsequently.

The density of cardiac mast cells in normal hearts is remarkably low across species ranging from 1.4 cells/mm² in Wistar Kyoto rats [37] to 5.3 cells/mm² in humans [12]. In chronically stressed or diseased hearts, the cardiac mast cell density has been reported to increase in the range of 1.7- [11] to 6-fold [22]. While cardiac mast cells can be isolated enzymatically, we have shown that enzymatic dispersion methods trigger the spontaneous release of histamine throughout the isolation process without producing harsh perturbations to the plasma membrane sufficient to cause mast cell disruption [36]. As a result, collagenase digestion yields mast cells that are minimally responsive to exogenous secretagogues such as compound 48/80 and calcium ionophore A23187 [38]. This is in contrast to peritoneal or pleural cavity mast cells that remain fully functional when isolated nonenzymatically using injected buffers and mechanical dispersion.

These observations led our group to develop a novel technique for isolating viable epicardial mast cells [39]. In addition to the Morgan et al. article [39], we recently published a detailed video and accompanying text of this procedure [40]. The following is a brief description of this technique using rat hearts. A ventral midline incision is made in the abdomen and extended to the level of the xiphoid cartilage allowing for the dissection of the diaphragm to gain access to the pericardium. The left ventral thoracic wall is then retracted medially to expose the heart still encapsulated by the pericardium. Next, a Teflon® catheter attached to a syringe is inserted into the pericardium at a point in the middle of the sternopericardial ligament (preferably more cranial than caudal). Room temperature Hank's buffer [HBSS composed of (1) Hank's calcium and magnesium free salt solution, (2) HEPES (13 mM), (3) 607 units/ml of deoxyribonuclease, and (4) an antibiotic–antimycotic mixture of penicillin G sodium, streptomycin sulfate, and amphotericin B] is then gradually introduced into the pericardial sac, filling it with approximately 3–3.5 ml. At this stage in the isolation, the beating of the heart provides gentle mechanical dispersion. After a short period of time, the HBSS cell solution is gently aspirated from the pericardial sac and stored on ice. This process of buffer injection and aspiration is repeated two to three times. The extracted buffer is then subjected to centrifugation for 10 min at 200 $\times g$ (4 °C). After centrifugation the cell pellet is reconstituted in 1 mL of HyClone buffer [HBSS containing magnesium sulfate

(1.1 mM), calcium chloride (1.3 mM), and phenol red]. We have characterized the resulting isolate and demonstrated a mixed population of lymphocytes (~70 %) and macrophages (~12 %) in addition to mast cells (~12 %) [41].

By avoiding the enzymatic dispersion of tissue, this technique minimizes spontaneous histamine release attributable to cellular degradation and produces a twofold greater recovery of mast cells from rat hearts (i.e., approximately 110,000 cells) compared to previous observations using enzymatic mast cell isolation [36, 39]. Also, the functional responsiveness of epicardial mast cells is not altered as evidenced by a significant histamine release triggered by concentrations of compound 48/80 as low as 0.3 µg/ml [39]. These findings are in stark contrast to our results obtained using cardiac mast cells isolated by enzymatic methods, in which 10 µg/ml of compound 48/80 elicited the release of less than 2 % of the histamine from cells [36]. Other studies using enzymatically isolated cardiac mast cells have also reported a negligible response to compound 48/80 (i.e., <2 % histamine release), even after incubating the cells overnight to allow for recovery [35, 38]. Also, in contrast to the existing literature indicating that cardiac mast cells do not respond to substance P [34, 35], a significant release of histamine from these epicardial cells was obtained in response to substance P as well as the calcium ionophore A23187 [39, 42]. Accordingly, the heterogeneity of cardiac mast cells from that of non-cardiac mast cells alluded to in the literature is an artifact of the enzymatic methodology. Nevertheless, the supposition of heterogeneity of connective tissue mast cells is reinforced by our recent study using this new technique which established that cardiac mast cells do not degranulate in response to atrial natriuretic peptide [43] unlike peritoneal mast cells which we and others have shown to be activated by atrial natriuretic peptide [43–45]. While the utility of epicardial mast cell isolates to characterize its response to secretagogues via histamine release is readily apparent, the fact that the extract is a mixed cell population should always be considered when investigating the release of other substances such as TNF- α .

In addition to the neuropeptide, substance P, neurotensin has been shown to be an endogenous cardiac mast cell secretagogue. Neurotensin is found in nerve fibers associated with the coronary vasculature, myocytes, and intracardiac ganglia [46]. While there are only two articles reporting the effect of neurotensin on cardiac mast cells, the findings are rather convincing. One of the studies by Rioux et al. [47] demonstrated that infusion of neurotensin to isolated hearts resulted in a rapid release of histamine, and the other by Pang et al. [48] reported that immobilization stress-induced cardiac mast cell degranulation was prevented by neurotensin receptor blockade.

Recently, endothelin 1 (ET-1) has also been shown to be capable of activating cardiac mast cells. Murray et al. [49] demonstrated

that administration of a 20 pg/ml bolus of ET-1 to blood-perfused, isolated rat hearts resulted in cardiac mast cell degranulation, MMP-2 activation, collagen degradation, and moderate ventricular dilatation which was prevented by the mast cell membrane stabilizing compound nedocromil. Nedocromil and cromolyn sodium have been used extensively to study mast cell function. However, they have low oral bioavailability and therefore are typically administered experimentally via an osmotic mini-pump or time release pellets implanted subcutaneously. Another mast cell stabilizing drug that has been used experimentally, ketotifen, can be administered orally.

Evidence is accumulating to indicate that reactive oxygen species can also act as a cardiac mast cell secretagogue. We have found that incubation of isolated rat epicardial mast cells with Na_2SO_3 induced a concentration-dependent histamine release [50] which could be either prevented or attenuated by the antioxidant compounds ebselen and diphenyleneiodonium, respectively. Further evidence was provided by Masini and colleagues [51]. They reported that the superoxide dismutase mimetic M40403 was able to prevent the occurrence of mast cell degranulation following reperfusion of the ischemic rat heart.

While there are many other known non-cardiac mast cell secretagogues, those discussed above are the few that are known to serve as cardiac mast cell secretagogues. However, this list will undoubtedly expand with future research. For example, IL-33 which is a member of the IL-1 family of cytokines and a functional ligand of the ST2 receptor has been shown to regulate mast cell function in arthritis [52]. Extending this to the heart, we have performed preliminary studies which indicate that IL-33 also activates isolated rat-derived epicardial mast cells (unpublished observations).

4 Source of Cardiac Mast Cells

Mast cells are derived from blood-borne, multipotent hematopoietic progenitor cells that, once located in tissue, differentiate to a final phenotype under the influence of the local microenvironment [53]. As mentioned above, even though the density of cardiac mast cells is normally low, it has been reported to be increased severalfold in the chronically stressed or diseased heart. In the case of chronic volume overload, the increase occurs as early as 12 h after initiating the overload condition [11] and has been shown to be primarily due to a rapid maturation of immature resident mast cells with no evidence of proliferation [54]. Here immature and mature cells were identified according to their granules staining predominantly blue with the alcian blue–safranin reaction or having mostly safranin-positive granules. That is, the alcian blue–safranin reaction distinguishes between weakly sulfated (immature cells) and strongly sulfated mucopolysaccharides (mature cells) by a shift from alcian

blue to safranin staining. The stimulus for this maturation process appears to be primarily fibroblast-derived stem cell factor (SCF), which we have recently shown to be transiently increased as early as 6 h after initiating the volume overload condition and to remain elevated by a factor of two through the second day of overload; at day three the level was back to normal. Corresponding to this SCF response was a 58–67 % increase in cardiac mast cell density at days 1 and 3 of volume overload with the peak value occurring on the first day. Furthermore, incubation of left ventricular tissue slices (250 μ m thick) with SCF for 16 h resulted in a doubling of mast cell density which occurred concomitantly with a significant decrease in the number of immature mast cells [55]. Thus, the rapid increase in mast cell density in the cardiac volume overload model appears to be related primarily to a SCF-driven maturation of resident immature mast cells as opposed to cell proliferation or migration.

In the cardiac volume overload model, there is a definite relation between mast cell activation and an increase in mast cell density which in all likelihood is related to mast cell-derived chymase stimulating the synthesis and release of SCF from fibroblasts in a positive feedback fashion [56, 57]. Accordingly, when activation of mast cells was prevented using either cromolyn [11] or the NK-1 receptor antagonist L732138 [42], the volume overload-induced increase in mast cell density was prevented. Recently, we obtained direct evidence of this relation via the incubation of left ventricular tissue slices with the chemical secretagogue, compound 48/80, for 16 h. As a result of this chemical activation, SCF levels in both the left ventricular slices and media together with mast cell density were increased [55].

As stated earlier, mast cell density is also increased in the hypertensive heart, and, here too, it would appear that SCF is responsible [14]. However, unlike the volume overload condition, the hypertension-related increase does not appear to be the result of mast cell activation. In the spontaneous hypertensive rat (SHR) treated with nedocromil, mast cell density was found to increase [37]. Mast cell density also has been reported to be significantly increased in sympathectomized SHR [41]. Here it is assumed that, as a result of sympathectomy, substance P was depleted thereby preventing mast cell activation. While SCF was not measured in these two studies, the results of Shiota et al. [14] would indicate that it would remain elevated despite the prevention of mast cell degranulation and hence result in an increase in mast cell density.

Mast cell density is also increased in the failing heart regardless of etiology [12–14, 17]. While little is known regarding their source, it seems reasonable to assume that elevated levels of SCF represent the stimulus for both migration into the myocardium and maturation. Shiota's findings of elevated mRNA for soluble SCF and its receptor, c-Kit, as well as a marked increase in mast cell density in elderly SHR who were in congestive heart failure support

this assumption [14]. Further support is gleaned from the study of Jahanyar et al. [58]. They found that left ventricular assist device support of patients with congestive heart failure resulted in an increase of SCF and c-Kit gene expression that coincided with a marked increase in the number of mast cells after ventricular unloading.

5 Myocardial Infarction and Ischemia–Reperfusion Injury

The data accumulated thus far in experimental animal studies seem to convincingly suggest an important role for mast cells in ischemia–reperfusion injury. However, due to the conflicting nature of the results between mouse studies, it is far less clear as to the role of mast cells following myocardial infarction without reperfusion. Frangogiannis et al. [59] have shown an increase in mast cell numbers during the healing phase in a canine model of ischemia–reperfusion, with maximum accumulation in areas of collagen deposition. Furthermore, increased numbers of degranulating mast cells were found to co-localize with newly recruited macrophages and neutrophils and were closely associated with vascular structures after 7 days of reperfusion following ischemia in a canine model of MI [60]. Jaggi et al. [61] demonstrated the involvement of mast cells in ischemia–reperfusion injury by subjecting isolated rat hearts treated with ketotifen to 30 min of global ischemia followed by 120 min of reperfusion. They found mast cell degranulation and myocardial injury to be decreased in the treated hearts. In an alternative approach they degranulated mast cells with compound 48/80 effectively removing mast cell mediators from the heart prior to inducing ischemia–reperfusion. This too resulted in attenuation of injury. Recent studies have begun to utilize mast cell (c-Kit)-deficient mice to attempt to determine the role of mast cells in ischemia–reperfusion injury and MI. Using a protocol of 30 min ischemia followed by 6 h of reperfusion in the W/W^v strain of mast cell-deficient mice, Bhattacharya et al. [28] found that the amount of viable myocardium was significantly greater in the reperfused mast cell-deficient mice.

The role of cardiac mast cells is less clear in myocardial infarction without reperfusion. Using female W/W^v mast cell-deficient mice, Cimini et al. [29] reported that these mice have a greater infarct area, ventricular dilatation, and reduced infarct thickness at 14 days post MI. However, they discounted the importance of mast cells to myocardial remodeling due to their small number and concluded that diminished recruitment of myofibroblasts accounted for the impaired healing of the scar. Interestingly, mast cells are known to have a prominent role in regulating myofibroblast function [62]. Ayach et al. [30] examined long-term remodeling and cardiac function in male W/W^v mice as well as W/W^v mice reconstituted with bone marrow cells at 35 days post MI. Their results indicated

that *W/W^v* mice developed larger hearts with more collagen deposition, albeit with an increased stroke volume, even though they had reduced rates of contraction and relaxation. However, there was virtually no difference in survival rate between the wild-type and *W/W^v* mice 35 days post MI. Improvements were observed in all parameters measured post MI in mast cell-deficient mice reconstituted with bone marrow-derived mast cells. We have also sought to determine the role of mast cells to post-MI myocardial remodeling using *W/W^v* mice. In contrast to the previously mentioned studies, our preliminary results, conducted at 7 days post MI, indicate that chamber dilatation was significantly greater in the wild-type hearts compared to *W/W^v* hearts (126 % vs. 73 % increase in end diastolic volume, respectively). Also, the wild-type mice had thinner walls and increased collagen deposition in the viable myocardium. Based on these discrepancies, it would appear that additional research is needed regarding the role of mast cells in myocardial infarction-induced remodeling. Furthermore, given that post-infarction healing is a progressive process which may include mast cell-induced extracellular matrix degradation followed by mast cell-induced fibrosis, temporal studies are warranted. It should be noted that while mast cell-deficient mice are a powerful tool for studying mast cell biology, they are not without confounding variables. The *W/W^v* and *Sl/Sl^d* mice suffer from anemia, sterility, and a lack of hair pigmentation, as well as decreased numbers of bone marrow granulocytes and megakaryocytes. Other problems include the spontaneous development of lymphocytic leukemia, severe ulcerative dermatitis, stomach papillomas, and chronic ulcers of the gastric antrum [63]. Alternatively, the Kit(*W^{sh}/W^{sh}*) mouse is deficient in mast cells, but does not display anemia or sterility [64]. These mice also did not show a high incidence of idiopathic dermatitis, ulcers, or squamous papillomas of the stomach, but do still lack interstitial cells of Cajal in the gut.

6 Hypertension

A link between increased pressure overload and mast cells in the heart has been established by Olivetti et al. [16] who observed increases in cardiac mast cell density in the right ventricle following pulmonary artery banding in rats. Following that, Panizo and coworkers [15] similarly observed increases in mast cell density in the left ventricle of SHR. This increase in mast cell density strongly correlated with myocardial collagen concentration. In keeping with these findings, Shiota et al. [14] reported cardiac mast cell density to be increased dramatically above control levels at birth and throughout the lifespan of the SHR. Isolated heart studies have also shown that cardiac mast cells can be a significant source of NF- κ B and IL-6 expression in the left ventricle of

compensated 12-month-old SHR. However, all of these studies while making interesting observations failed to establish a causal relationship between cardiac mast cells and adverse remodeling in the hypertensive heart. To this end, Hara et al. [27] used the aortic banding model of experimentally induced pressure overload in mast cell-deficient mice to focus on the role of mast cells in the progression to heart failure. They found that, in contrast to their wild-type counterpart, heart and lung weights were markedly attenuated, ventricular dilatation was prevented, and fractional shortening was preserved. Alternatively, we have focused our investigation on the role of mast cells in fibrosis in the hypertensive heart. We treated SHR with nedocromil and found that fibrosis was completely prevented [37]. Mast cell stabilization was also able to prevent macrophage recruitment and normalized myocardial tryptase, IL-4, and IFN- γ levels. Interestingly, mast cell stabilization also prevented the decrease in the anti-inflammatory cytokine IL-10 that was observed in untreated SHR.

7 Volume Overload and Heart Failure

Cardiac mast cell density increases in the left ventricle under conditions of volume overload such as that which occurs with mitral regurgitation [19]. Using the aortocaval (AV) fistula model of volume overload, we have been able to demonstrate that mast cell stabilization prevented the increase in myocardial MMP-2 activity and the accompanying reduction in collagen volume fraction that occurs in the first 5 days following induction of volume overload [11, 32]. Treatment of rats with nedocromil for a period of 8 weeks post fistula [65] attenuated left ventricular hypertrophy and pulmonary edema, prevented ventricular dilatation and the increase in compliance, and prevented the decrease in intrinsic contractile function. Most important, there was a significant decrease in mortality. Further studies in mast cell-deficient rats with cardiac volume overload support these findings in that they did not have: (1) elevated MMP activity, (2) collagen degradation, or (3) dilatation of the left ventricle [32]. Further, Chancey et al. [66] administered a bolus of compound 48/80 to normal hearts, using a blood-perfused isolated heart preparation, and found that the subsequent mast cell degranulation produced an increase of 126 % in MMP activity and a nearly 50 % decrease in myocardial collagen volume fraction within 30 min. A tendency for the left ventricle to dilate was also evident despite a significant histamine-induced myocardial edema. The fact that mast cell density is also increased in the left ventricle of dogs with experimentally induced mitral regurgitation [19] demonstrates that mast cell-mediated myocardial remodeling in response to volume overload is not species or model specific.

8 Mast Cell Mediators and Myocardial Remodeling

From the previous section of this chapter, it should be clear that mast cells play dual roles to induce remodeling in the heart. They can either stimulate collagen synthesis leading to fibrosis (e.g., in hypertension and ischemia–reperfusion) or induce MMP activation resulting in collagen degradation and ultimately ventricular dilatation. Understanding how mast cells in the heart are regulated to produce these seemingly disparate effects represents the next important phase of cardiac mast cell biology research. The function of mast cells in various cardiac pathologies likely is regulated by signaling pathways emanating from an interaction between myocytes, interstitial cells, and mast cells as well as from a neurohormonal influence which result in the production and release of different mast cell mediators. Below is a brief discussion of several such mast cell mediators which are known to influence remodeling. The role of these mediators in mast cell-induced collagen synthesis and degradation is summarized in Figs. 1 and 2.

8.1 TNF- α

Several studies have indicated that mast cells are an important source of TNF- α in the heart. Frangogiannis et al. [9] used labeling techniques and found that almost all TNF- α in the canine heart was localized to cardiac mast cells. When assessed again following 1 h of ischemia and 3 h of reperfusion, cardiac mast cells were still

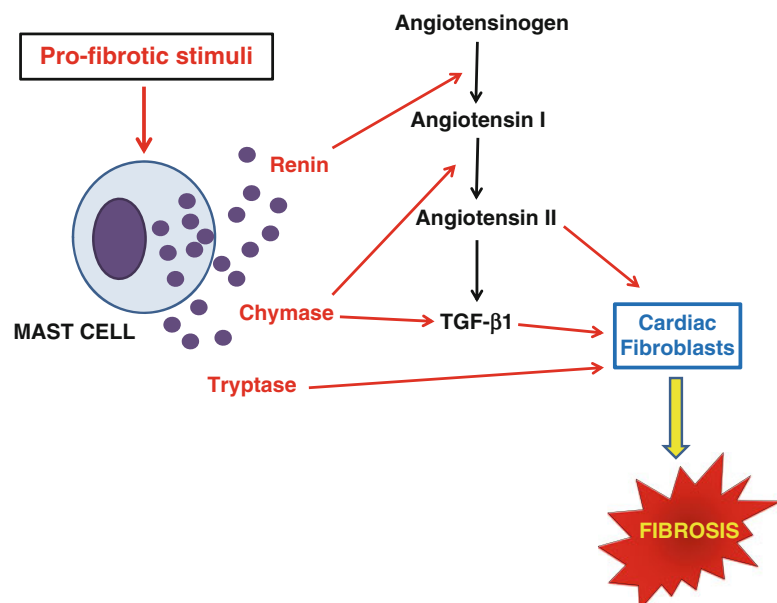


Fig. 1 Depicts the interactions of mast cell products currently thought to be involved in mast cell-induced fibrosis in the heart. The various mediators are discussed in detail in the text

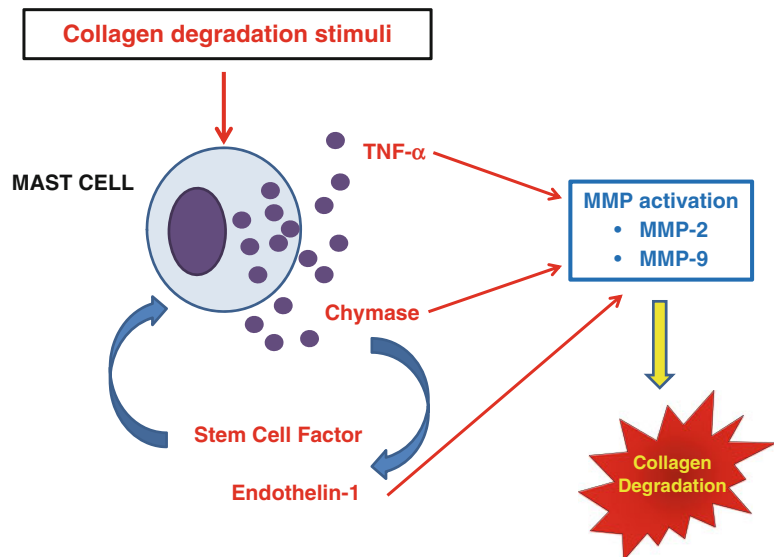


Fig. 2 Depicts the interactions of mast cell products currently thought to be involved in mast cell-induced degradation of collagen in the heart. The various mediators are discussed in detail in the text

the predominant source of TNF- α , and mast cells in the infarct area (but not the remote region) could be seen releasing TNF- α . Gilles et al. [67] also suggested that this was the case, based on the observation that ketotifen and cromolyn sodium prevented the increase in myocardial TNF- α levels following reperfusion. In further agreement with these findings, we found that TNF- α was almost undetectable in the hearts of mast cell-deficient rats following 5 days of volume overload; conversely, wild-type rats had dramatically increased myocardial TNF- α levels in response to cardiac volume overload [32]. TNF- α can activate MMPs [68], and the infusion of TNF- α in rats has been shown to induce collagen degradation and dysfunction in the heart [69]. In cardiac volume overload, inhibition of TNF- α prevented collagen degradation [70]. However, TNF- α may also be pro-fibrotic in hypertension since it can increase angiotensin II-stimulated production of collagen by increasing angiotensin II type 1 receptors [71]. Furthermore, fibrosis and hypertrophy are attenuated in TNF- α knockout mice following transverse aortic constriction [72].

8.2 Histamine

Frangogiannis et al. [9] observed degranulating cardiac mast cells and an ~twofold increase in histamine levels in cardiac lymph following ischemia–reperfusion in the canine heart. Histamine receptor antagonist in a canine model of ischemia–reperfusion revealed that blockade of the histamine type 2 (H₂), but not H₁, receptors decreased infarct size regardless of whether the H₂

antagonist was administered during ischemia or reperfusion [73]. Interestingly, this did not lead to functional improvements. However, in retrospective and prospective clinical studies, the H₂ receptor antagonist famotidine was found to reduce plasma brain natriuretic peptide (BNP) levels (a marker of left ventricular hypertrophy) as well as left ventricular diameter in diastole and systole while improving New York Heart Association (NYHA) functional class [74]. The ultimate effect of histamine on regulation of the extracellular matrix remains unclear. Upregulation of connective tissue growth factor mRNA has been reported in lung fibroblasts [75], while synovial fibroblasts isolated from rheumatoid synovial tissue release MMP-1 and MMP-3 as well as PGE₂ in response to histamine [76]. Cardiac fibroblasts release PGE₂ as well as the stable metabolite of the cardioprotective PGI₂, 6-keto-PGF1 α , in response to histamine [77].

8.3 Chymase/Renin/ Angiotensin II

Chymase activity has been found to be increased in both the remote and infarcted areas of the myocardium following 1 h of ischemia and 3 h of reperfusion in pigs [78]. Chymase inhibition resulted in a reduction of necrosis in the risk area. The effects of mast cells on the myocardium may ultimately involve the production of angiotensin II. Mast cells contain chymase, which is capable of cleaving inactive angiotensin I to the active angiotensin II [79]. In support of this, an AT₁ receptor antagonist had an efficacious effect on mortality post MI in hamsters, while an ACE inhibitor did not [80]. Further, ACE-independent angiotensin II formation was important for the release of norepinephrine from sympathetic nerves following an ischemic event in the human heart [81]. Also significant amounts of angiotensin II were mast cell-derived following ischemia–reperfusion in the guinea pig heart [82] with mast cell-derived angiotensin II being responsible for increased norepinephrine levels and norepinephrine-induced arrhythmias. It is unclear whether chymase can push the balance toward collagen synthesis or collagen degradation in vivo. Neonatal cardiac fibroblasts proliferate and produce collagen in response to chymase by inducing TGF- β production and activation of Smad pathways [83]. More recently, Roberto Levi's group identified cardiac mast cells as a source for renin in the heart [82, 84]. Mast cell production of renin would obviously aid in the production of angiotensin II in concert with chymase to produce a pro-fibrotic outcome. However, chymase can activate MMP-2 and MMP-9 [85], and chymase activity is also elevated in dogs with mitral regurgitation where collagen degradation predominates [19]. In fact, inhibition of chymase in pigs undergoing ischemia–reperfusion resulted in a decrease in MMP-9 activity [78]. Also, chymase is capable of activating SCF [55], converting Big ET-1 to ET-1 [86], and cleaving latent TGF- β to the active form [87, 88].

8.4 Tryptase

Studies linking peritoneal and skin mast cells to tissue remodeling have shown that mast cell tryptase can activate interstitial collagenase (MMP-1) and stromelysin (MMP-3) under in vitro conditions [6, 10]. However, Gruber et al. [89] demonstrated that tryptase was unable to directly activate MMP-1. Instead, tryptase first cleaves proMMP-3, with active MMP-3 then activating MMP-1. In contrast, we have clearly demonstrated that tryptase is profibrotic in the heart. We initially observed that tryptase was increased in the SHR heart [37] and upon further investigation were able to demonstrate that tryptase causes isolated adult rat cardiac fibroblasts to proliferate, convert to a myofibroblast phenotype, and produce collagen [37, 90]. These effects occurred via tryptase activation of protease-activated receptor-2 (PAR-2), which induced ERK1/2 phosphorylation, but not p38 or JNK activation. Cardiac fibroblasts isolated from SHR hearts had this same pattern of selective activation, and blockade of PAR-2 in SHR was able to prevent fibrosis from occurring, suggesting that our in vitro findings were indicative of what was occurring in vivo.

8.5 TGF- β

Mast cell chymase is capable of cleaving latent TGF- β to the active form. The pro-fibrotic effects of TGF- β in the heart have been well documented. As mentioned above, TGF- β and subsequent activation of Smad pathways may mediate the proliferative and collagen-producing effects of chymase on neonatal cardiac fibroblasts [83]. More recently, Zhang et al. [91] co-incubated mast cells with cardiac fibroblasts and found that α -smooth muscle actin expression, proliferation, and collagen messenger RNA expression were all increased in cardiac fibroblasts isolated from mice overexpressing TNF- α when compared to fibroblasts from wild-type controls. However, it is important to consider that this study used MC/9 mast cells, which are derived from murine fetal livers. In view of the fact that the differentiation of mast cells is dependent on their microenvironment, the relevance of MC/9 and other mast cell lines to cardiac mast cells is questionable.

9 Modulation of Cardiac Mast Cell Phenotype by Estrogen

Although there are clear gender differences in the prevalence and severity of cardiovascular disease in humans [92], our understanding of the underlying mechanisms responsible for the lower incidence of cardiac disease in premenopausal females is poor. In this regard, we had made the observation that degranulation of mast cells with compound 48/80 in isolated hearts from ovariectomized female rats caused an increase in MMP-2 activation, which led to collagen degradation and ventricular dilatation when compared to hearts from normal females [93]. Restoration of estrogen to ovariectomized female rats was able to prevent the increase in MMP-2

activation, collagen degradation, and ventricular dilatation. These observations have led us to hypothesize that estrogen may confer cardioprotection in part by modulating cardiac mast cell phenotype. That is, estrogen may downregulate synthesis of or prevent the release of mast cell proteases [94] or other products such as TNF- α [95] as has been shown in non-cardiac mast cells. In support of this, we recently reported that, in contrast to male rat hearts, cardiac mast cell density does not increase in response to volume overload in female rat hearts [96]; as a result, collagen degradation did not occur. However, when female rats were ovariectomized, cardiac mast cell density did increase following 3 days of volume overload leading to collagen degradation at 5 days, which is identical to the response seen in male rats. Further, myocardial TNF- α levels were not increased in intact female rats following volume overload but were increased in ovariectomized female rats following volume overload. The increase in TNF- α in ovariectomized hearts was regulated by mast cells since nedocromil normalized TNF- α values. In keeping with the changes in mast cell density following volume overload, stem cell factor (SCF) increased by almost 50 % in ovariectomized female rats as compared to ~10 % in female rats that had not been ovariectomized.

10 Summary

Mast cells are known to store and release a variety of biologically active mediators which are known to be involved in myocardial remodeling including histamine, cytokines such as TNF- α , proteases such as tryptase and chymase, and growth factors such as TGF- β . Early observations regarding cardiac mast cells were limited to reports of increases in mast cell density in hearts subjected to sustained elevations in myocardial stress or injury; subsequently elevations in stem cell factor and its receptor have been implicated as being the underlying stimuli for this increase via maturation of resident mast cells and possibly enhanced migration of precursor cells. There has been no evidence to indicate the occurrence of mast cell proliferation in the heart. Continuing research has identified the cardiac mast cell as playing a central role in the myocardial remodeling that occurs as a result of pathologic myocardial stress or ischemic damage. Cardiac mast cells cannot be isolated via enzymatic dispersion techniques because spontaneous degranulation has been shown to occur throughout the process. Consequently, the isolated cells are minimally responsive to secretagogues. This problem has been circumvented using a technique whereby epicardial cells are obtained via a pericardial washing. While a mixture of cell types is obtained, the harvested mast cells release significant amounts of histamine in response to activating compounds. However, because of the relatively low density of mast cells in the

heart, this technique yields approximately 100,000 mast cells from an adult rat heart, which is usually insufficient for further studies thus requiring the pooling of cells from several hearts or using larger animals. Also, further insight into the functional role of cardiac mast cells can continue to be obtained using mast cell membrane stabilizing drugs and mast cell-deficient rodents. To this end there are numerous questions which remain to be answered. These include: (1) while we know that mast cell secretory products can activate matrix metalloproteinases, it is not known how they mediate pro-fibrotic processes; (2) while there is evidence in other tissue that mast cells interact with other inflammatory cells, it is not known whether such an interaction occurs in the heart; (3) other than ET-1 and substance P, other exogenous secretagogues for cardiac mast cells, if any, remain to be identified; and (4) given that estrogen infers cardioprotection via its effect on mast cells, the influence of male and female hormones on cardiac mast cell phenotype as well as their regulatory pathways need to be investigated in detail.

Acknowledgment

This work was supported in part by grants from NHLBI (to J.S.J.—#s RO1-HL-59981, R01-HL-62228, R21-HL-089483 and to S.P.L. R00-HL-093215).

References

1. Pfeffer JM et al (1991) Progressive ventricular remodeling in rat with myocardial infarction. *Am J Physiol* 260:H1406–H1414
2. Grossman W et al (1975) Wall stress and patterns of hypertrophy in the human left ventricle. *J Clin Invest* 56:56–64
3. Borg TK, Caulfield JB (1981) The collagen matrix of the heart. *Fed Proc* 40:2037–2041
4. Robinson TF et al (1988) Structure and function of connective tissue in cardiac muscle: collagen types I and III in endomysial struts and pericellular fibers. *Scanning Microsc* 2:1005–1015
5. Montfort I, Perez-Tamayo R (1975) The distribution of collagenase in normal rat tissues. *J Histochem Cytochem* 23:910–920
6. Lees M et al (1994) Mast cell proteinases activate precursor forms of collagenase and stromelysin, but not of gelatinases A and B. *Eur J Biochem* 223:171–177
7. Marone G et al (1999) Immunological modulation of human cardiac mast cells. *Neurochem Res* 24:1195–1202
8. Metcalfe DD (1997) Mast cells. *Physiol Rev* 77:1033–1079
9. Frangogiannis NG et al (1998) Resident cardiac mast cells degranulate and release pre-formed TNF- α , initiating the cytokine cascade in experimental canine myocardial ischemia/reperfusion. *Circulation* 98:699–710
10. Suzuki K et al (1995) Activation of precursors for matrix metalloproteinases 1 (interstitial collagenase) and 3 (stromelysin) by rat mast-cell proteinases I and II. *Biochem J* 305(Pt 1): 301–306
11. Brower GL et al (2002) Cause and effect relationship between myocardial mast cell number and matrix metalloproteinase activity. *Am J Physiol* 283:H518–H525
12. Patella V et al (1997) Increased cardiac mast cell density and mediator release in patients with dilated cardiomyopathy. *Inflamm Res* 46:S31–S32
13. Patella V et al (1998) Stem cell factor in mast cells and increased mast cell density in idiopathic and ischemic cardiomyopathy. *Circulation* 97: 971–978
14. Shiota N et al (2003) A role for cardiac mast cells in the pathogenesis of hypertensive heart disease. *J Hypertens* 21:1823–1825
15. Panizo A et al (1995) Are mast cells involved in hypertensive heart disease? *J Hypertens* 13:1201–1208
16. Olivetti G et al (1989) Long-term pressure-induced cardiac hypertrophy: capillary and

mast cell proliferation. *Am J Physiol Heart Circ Physiol* 257:H1766–H1772

- 17. Engels W et al (1995) Transmural changes in mast cell density in rat heart after infarct induction in vivo. *J Pathol* 177:423–429
- 18. Dell’Italia LJ et al (1997) Volume-overload cardiac hypertrophy is unaffected by ACE inhibitor treatment in dogs. *Am J Physiol Heart Circ Physiol* 273:H961–H970
- 19. Stewart JA et al (2003) Cardiac mast cell- and chymase-mediated matrix metalloproteinase activity and left ventricular remodeling in mitral regurgitation in the dog. *J Mol Cell Cardiol* 35:311–319
- 20. von Recklinghausen FD (1863) Über eiter- und bindegewebskörperchen. *Virchows Arch Pathol Anat Physiol Klin Med* 28:157–197
- 21. Crivellato E et al (2003) Paul Ehrlich’s doctoral thesis: a milestone in the study of mast cells. *Br J Haematol* 123:19–21
- 22. Estensen RD (1984) Eosinophilic myocarditis: a role for mast cells? *Arch Pathol Lab Med* 108:358–359
- 23. Fernex M (1968) In: The mast-cell system: its relationship to atherosclerosis, fibrosis and eosinophils. The Williams & Wilkins Company, Baltimore, pp 93–95
- 24. Dvorak AM (1986) Mast-cell degranulation in human hearts. *N Engl J Med* 315:969–970
- 25. Li QY et al (1992) The relationship of mast cells and their secreted products to the volume of fibrosis in posttransplant hearts. *Transplantation* 53:1047–1051
- 26. Kovanan PT (1995) Role of mast cells in atherosclerosis. *Chem Immunol* 62:132–170
- 27. Hara M et al (2002) Evidence for a role of mast cells in the evolution to congestive heart failure. *J Exp Med* 195:375–381
- 28. Bhattacharya K et al (2007) Mast cell deficient W/Wv mice have lower serum IL-6 and less cardiac tissue necrosis than their normal littermates following myocardial ischemia-reperfusion. *Int J Immunopathol Pharmacol* 20:69–74
- 29. Cimini M et al (2007) c-Kit dysfunction impairs myocardial healing after infarction. *Circulation* 116:I-77
- 30. Ayach BB et al (2006) Stem cell factor receptor induces progenitor and natural killer cell-mediated cardiac survival and repair after myocardial infarction. *Proc Natl Acad Sci U S A* 103:2304–2309
- 31. Sun J et al (2007) Mast cells promote atherosclerosis by releasing proinflammatory cytokines. *Nat Med* 13:719–724
- 32. Levick SP et al (2008) Protection from adverse myocardial remodeling secondary to chronic volume overload in mast cell deficient rats. *J Mol Cell Cardiol* 45:56–61
- 33. Galli SJ (1997) The Paul Kallos memorial lecture. The mast cell: a versatile effector cell for a challenging world. *Int Arch Allergy Immunol* 113:14–22
- 34. Patella V et al (1995) Human heart mast cells: a definitive case of mast cell heterogeneity. *Int Arch Allergy Immunol* 106:386–393
- 35. Patella V et al (1995) Human heart mast cells. Isolation, purification, ultrastructure, and immunologic characterization. *J Immunol* 154:2855–2865
- 36. Forman MF et al (2004) Spontaneous histamine secretion during isolation of rat cardiac mast cells. *Inflamm Res* 53:453–457
- 37. Levick SP et al (2009) Cardiac mast cells mediate left ventricular fibrosis in the hypertensive rat heart. *Hypertension* 53:1041–1047
- 38. Ali H, Pearce FL (1985) Isolation and properties of cardiac and other mast cells from the rat and guinea-pig. *Agents Actions* 16:138–140
- 39. Morgan LG et al (2008) A novel technique for isolating functional mast cells from the heart. *Inflamm Res* 57:1–6
- 40. McLarty JL et al (2011) Isolation of functional cardiac immune cells. *J Vis Exp* 58:pii: 3020. doi:[10.3791/3020](https://doi.org/10.3791/3020)
- 41. Levick SP et al (2010) Sympathetic nervous system modulation of inflammation and remodeling in the hypertensive heart. *Hypertension* 55:270–276
- 42. Melendez GC et al (2011) Substance P induces adverse myocardial remodeling via a mechanism involving cardiac mast cells. *Cardiovasc Res* 92:420–429
- 43. Murray DB et al (2007) Response of cardiac mast cells to atrial natriuretic peptide. *Am J Physiol Heart Circ Physiol* 293:H1216–H1222
- 44. Opgenorth TJ et al (1990) Atrial peptides induce mast cell histamine release. *Peptides* 11:1003–1007
- 45. Yoshida H et al (1996) Histamine release induced by human natriuretic peptide from rat peritoneal mast cells. *Regul Pept* 61:45–49
- 46. Reinecke M et al (1982) Localization of neuropeptid Y immunoreactive nerve fibers in the guinea-pig heart: evidence derived by immunohistochemistry, radioimmunoassay and chromatography. *Neuroscience* 7:1785–1795
- 47. Rioux F et al (1985) Characterization of the histamine releasing effect of neuropeptid Y in the rat heart. *Peptides* 6:121–125
- 48. Pang X et al (1998) A neuropeptid Y receptor antagonist inhibits acute immobilization stress-induced cardiac mast cell degranulation,

a corticotropin-releasing hormone-dependent process. *J Pharmacol Exp Ther* 287:307–314

49. Murray DB et al (2008) Effects of nonselective endothelin-1 receptor antagonism on cardiac mast cell-mediated ventricular remodeling in rats. *Am J Physiol Heart Circ Physiol* 294:H1251–H1257

50. Melendez GC et al (2010) Oxidative stress mediated cardiac mast cell degranulation. *Toxicol Environ Chem* 92:1293–1301

51. Masini E et al (2002) Protective effects of M40403, a selective superoxide dismutase mimetic, in myocardial ischaemia and reperfusion injury in vivo. *Br J Pharmacol* 136:905–917

52. Xu D et al (2008) IL-33 exacerbates antigen-induced arthritis by activating mast cells. *Proc Natl Acad Sci U S A* 105:10913–10918

53. Crivellato E et al (2011) The history of the controversial relationship between mast cells and basophils. *Immunol Lett* 141(1):10–17

54. Forman MF et al (2006) Rat cardiac mast cell maturation and differentiation following acute ventricular volume overload. *Inflamm Res* 55:408–415

55. Li J et al (2012) Stem cell factor is responsible for the rapid response in mature mast cell density in the acutely stressed heart. *J Mol Cell Cardiol* 53:469–474

56. Tomimori Y et al (2002) Mast cell chymase regulates dermal mast cell number in mice. *Biochem Biophys Res Commun* 290:1478–1482

57. Longley BJ et al (1997) Chymase cleavage of stem cell factor yields a bioactive, soluble product. *Proc Natl Acad Sci U S A* 94:9017–9021

58. Jahanyar J et al (2008) Increased expression of stem cell factor and its receptor after left ventricular assist device support: a potential novel target for therapeutic interventions in heart failure. *J Heart Lung Transplant* 27:701–709

59. Frangogiannis NG et al (1998) Stem cell factor induction is associated with mast cell accumulation after canine myocardial ischemia and reperfusion. *Circulation* 98:687–698

60. Somasundaram P et al (2005) Mast cell tryptase may modulate endothelial cell phenotype in healing myocardial infarcts. *J Pathol* 205:102–111

61. Jaggi AS et al (2007) Cardioprotective effects of mast cell modulators in ischemia-reperfusion-induced injury in rats. *Methods Find Exp Clin Pharmacol* 29:593–600

62. Gailit J et al (2001) The differentiation and function of myofibroblasts is regulated by mast cell mediators. *J Invest Dermatol* 117:1113–1119

63. Galli SJ, Kitamura Y (1987) Genetically mast-cell-deficient W/W^y and Sl/Sld mice. Their value for the analysis of the roles of mast cells in biologic responses in vivo. *Am J Pathol* 127:191–198

64. Grimaldeston MA et al (2005) Mast cell-deficient W-sash c-kit Mutant KitW-sh/W-sh mice as a model for investigating mast cell biology in vivo. *Am J Pathol* 167:835–848

65. Brower GL, Janicki JS (2005) Pharmacologic inhibition of mast cell degranulation prevents left ventricular remodeling induced by chronic volume overload in rats. *J Card Fail* 11: 548–556

66. Chancey AL et al (2002) Cardiac mast cell-mediated activation of gelatinase and alteration of ventricular diastolic function. *Am J Physiol* 282:H2152–H2158

67. Gilles S et al (2003) Release of TNF- α during myocardial reperfusion depends on oxidative stress and is prevented by mast cell stabilizers. *Cardiovasc Res* 60:608–616

68. Seguin CA et al (2008) TNF-alpha induces MMP2 gelatinase activity and MT1-MMP expression in an in vitro model of nucleus pulposus tissue degeneration. *Spine* 33:356–365

69. Bozkurt B et al (1998) Pathophysiologically relevant concentrations of tumor necrosis factor- α promote progressive left ventricular dysfunction and remodeling in rats. *Circulation* 97:1382–1391

70. Jobe LJ et al (2009) TNF- α inhibition attenuates adverse myocardial remodeling in a rat model of volume overload. *Am J Physiol Heart Circ Physiol* 297:H1462–H1468

71. Gurantz D et al (2005) IL-1 β and TNF- α upregulate angiotensin II type 1 (AT1) receptors on cardiac fibroblasts and are associated with increased AT1 density in the post-MI heart. *J Mol Cell Cardiol* 38:505–515

72. Sun M et al (2007) Tumor necrosis factor- α mediates cardiac remodeling and ventricular dysfunction after pressure overload state. *Circulation* 115:1398–1407

73. Asanuma H et al (2006) Blockade of histamine H2 receptors protects the heart against ischemia and reperfusion injury in dogs. *J Mol Cell Cardiol* 40:666–674

74. Kim J et al (2006) Impact of blockade of histamine H2 receptors on chronic heart failure revealed by retrospective and prospective randomized studies. *J Am Coll Cardiol* 48: 1378–1384

75. Kunzmann S et al (2007) Connective tissue growth factor expression is regulated by histamine in lung fibroblasts: potential role of histamine in airway remodeling. *J Allergy Clin Immunol* 119:1398–1407

76. Tetlow LC, Woolley DE (2004) Effect of histamine on the production of matrix

metalloproteinases-1, -3, -8 and -13, and TNFalpha and PGE(2) by human articular chondrocytes and synovial fibroblasts in vitro: a comparative study. *Virchows Arch* 445:485–490

77. Linssen MC et al (1993) Production of arachidonic acid metabolites in adult rat cardiac myocytes, endothelial cells, and fibroblast-like cells. *Am J Physiol Heart Circ Physiol* 264:H973–H982

78. Oyamada S et al (2011) Chymase inhibition reduces infarction and matrix metalloproteinase-9 activation and attenuates inflammation and fibrosis after acute myocardial ischemia/reperfusion. *J Pharmacol Exp Ther* 339:143–151

79. Caughey GH et al (2000) Angiotensin II generation by mast cell α - and β -chymases. *Biochim Biophys Acta* 1480:245–257

80. Jin D et al (2001) Possible roles of cardiac chymase after myocardial infarction in hamster hearts. *Jpn J Pharmacol* 86:203–214

81. Maruyama R et al (2000) Angiotensin-converting enzyme-independent angiotensin formation in a human model of myocardial ischemia: modulation of norepinephrine release by angiotensin type 1 and angiotensin type 2 receptors. *J Pharmacol Exp Ther* 294:248–254

82. Mackins CJ et al (2006) Cardiac mast cell-derived renin promotes local angiotensin formation, norepinephrine release, and arrhythmias in ischemia/reperfusion. *J Clin Invest* 116:1063–1070

83. Zhao XY et al (2008) Chymase induces profibrotic response via transforming growth factor-beta 1/Smad activation in rat cardiac fibroblasts. *Mol Cell Biochem* 310:159–166

84. Silver RB et al (2004) Mast cells: a unique source of renin. *Proc Natl Acad Sci U S A* 101:13607–13612

85. Tchougounova E et al (2005) A key role for mast cell chymase in the activation of pro-matrix metalloproteinase-9 and pro-matrix metalloproteinase-2. *J Biol Chem* 280:9291–9296

86. Wypij DM et al (1992) Role of mast cell chymase in the extracellular processing of big-endothelin-1 to endothelin-1 in the perfused rat lung. *Biochem Pharmacol* 43:845–853

87. Taipale J et al (1995) Human mast cell chymase and leukocyte elastase release latent transforming growth factor-beta 1 from the extracellular matrix of cultured human epithelial and endothelial cells. *J Biol Chem* 270:4689–4696

88. Lindstedt KA et al (2001) Activation of paracrine TGF-beta1 signaling upon stimulation and degranulation of rat serosal mast cells: a novel function for chymase. *FASEB J* 15:1377–1388

89. Gruber BL et al (1989) Synovial procollagenase activation by human mast cell tryptase dependence upon matrix metalloproteinase 3 activation. *J Clin Invest* 84:1657–1662

90. McLarty JL et al (2011) Tryptase/protease-activated receptor 2 interactions induce selective mitogen-activated protein kinase signaling and collagen synthesis by cardiac fibroblasts. *Hypertension* 58:264–270

91. Zhang W et al (2011) The development of myocardial fibrosis in transgenic mice with targeted overexpression of tumor necrosis factor requires mast cell-fibroblast interactions. *Circulation* 124:2106–2116

92. Hayward CS et al (2000) The roles of gender, the menopause and hormone replacement on cardiovascular function. *Cardiovasc Res* 46:28–49

93. Chancey AL et al (2005) Modulation of cardiac mast cell-mediated extracellular matrix degradation by estrogen. *Am J Physiol Heart Circ Physiol* 289:H316–H321

94. Harnish DC et al (2004) Beneficial effects of estrogen treatment in the HLA-B27 transgenic rat model of inflammatory bowel disease. *Am J Physiol Gastrointest Liver Physiol* 286:G118–G125

95. Kim MS et al (2001) Estrogen regulates cytokine release in human mast cells. *Immunopharmacol Immunotoxicol* 23:495–504

96. Lu H et al (2011) Prevention of adverse cardiac remodeling to volume overload in female rats is the result of an estrogen-altered mast cell phenotype. *Am J Physiol Heart Circ Physiol* 302:H811–H817

Chapter 9

The Parasympathetic Nervous System as a Regulator of Mast Cell Function

Paul Forsythe

Abstract

Often considered as the archetype of neuroimmune communication, much of our understanding of the bidirectional relationship between the nervous and immune systems has come from the study of mast cell-nerve interaction. Mast cells play a role in resistance to infection and are extensively involved in inflammation and subsequent tissue repair. Thus, the relationship between mast cells and neurons enables the involvement of peripheral and central nervous systems in the regulation of host defense mechanisms and inflammation.

Recently, with the identification of the cholinergic anti-inflammatory pathway, there has been increased interest in the role of the parasympathetic nervous system in regulating immune responses. Classical neurotransmitters and neuropeptides released from cholinergic and inhibitory NANC neurons can modulate mast cell activity, and there is good evidence for the existence of parasympathetic nerve—mast cell functional units in the skin, lung, and intestine that have the potential to regulate a range of physiological processes.

Key words Neuroimmune communication, Inflammatory axon reflex, Vagus nerve, Nitric oxide, Vasoactive intestinal peptide, Cholinergic anti-inflammatory pathway, Mast cell, Parasympathetic nervous system

1 Introduction

The body maintains homeostasis and protects against external threats through the coordinated action of the nervous and immune systems [1–3]. It is clear that mast cells play an important role in communication between the immune system and nerves and can exhibit variably functional aspects of both systems [4]. Much of our understanding of the bidirectional relationship between the nervous and immune systems has come from the study of mast cell-nerve interaction that is often considered as the archetype of neuroimmune communication. Mast cells can be activated by a range of neurotransmitters, and reciprocally a variety of molecules, including histamine and serotonin, synthesized and released by mast cells can influence neuronal activity [5, 6] while mast cell-derived

cytokines, including tumor necrosis factor (TNF), and growth factors, such as NGF (nerve growth factor), lower the threshold for activation of local neurons and promote nerve fiber growth [7–10]. Much of the work on mast cell interaction with nerves has focused largely on the relationship between mast cells, sensory neurons, and associated neuropeptides, interactions that underlie the classical inflammatory axon reflex. However, more recently, there has been renewed interest in the role of the parasympathetic nervous system in regulating immune responses, and here we will discuss the evidence for parasympathetic regulation of the mast cell and furthermore that bidirectional communication between parasympathetic nervous system and mast cells may lead to the development of neuroimmune functional units that have the potential to regulate a range of physiological processes.

2 The Parasympathetic Nervous System

The parasympathetic nervous system is a division of the autonomic nervous system. The functions of parasympathetic nerves include slowing the heart rate, contracting the bronchioles, inducing the secretion of insulin bile and digestive juices, and dilating peripheral blood vessels.

The primary parasympathetic neurotransmitter is acetylcholine (Ach), which binds to two general receptor subtypes, nicotinic and muscarinic cholinergic receptors, each of which consists of many different subunits that heterodimerize and provide cell and tissue specificity for cholinergic effects [11, 12]. Both of these receptors are found on immune cells including mast cells [13–16]. In addition to Ach, vasoactive intestinal peptide (VIP) and nitric oxide are prominent parasympathetic neurotransmitters that can be found both in cholinergic neurons where they act as co-transmitters and independently from Ach in inhibitory nonadrenergic-noncholinergic (NANC) nerves [17].

In modulating the immune response, the parasympathetic nervous system can act through both the efferent and afferent fibers of the vagus nerve. For example, the afferent fibers of the vagus nerve can signal the presence of peripheral inflammation to the brain, through IL-1 receptors expressed by paraganglia cells located in the parasympathetic ganglia. Therefore, IL-1 released by activated innate immune cells during inflammation binds to paraganglia cells, activates afferent fibers of the vagus nerve, and induces rapid activation of the parasympathetic brainstem regions [18, 19]. This is the initial step in what has been termed the “inflammatory reflex,” which leads to the release of acetylcholine from efferent vagus nerve fibers and resultant negative feedback control of inflammation [20]. Consequently cutting the vagus nerve prevents immune signaling to the brain with the associated activation of

cholinergic brainstem regions and removes vagal control of inflammation and toxic shock [18–20].

3 The Relationship Between Mast Cells and the Vagus Nerve

The structural relationship of vagal afferents and mast cells in the intestine was first examined by Stead and colleagues using injection of the carbocyanine dye, DiI, into the nodose ganglia and immunolabeling sections of these tissues for rat mast cell protease II (RMCP II) [21]. In this study processes of vagal nerves were seen projecting throughout the jejunal mucosa, often contacting the RMCP II-immunoreactive intestinal mucosal mast cells. It was determined that 10–15 % of intestinal mucosal mast cells contacted vagal afferent terminals; however, the authors indicated that these were likely underestimates given the inefficient nature of the DiI injections and the fact that the nodose ganglia were injected unilaterally [21].

That the vagus may have some influence over mast cell function was supported by findings that vagotomized rats had approximately 25 % fewer mast cells in the jejunal mucosa than sham-operated controls and that this reduction was not related to changes in the volume of mucosa or a general cellular depletion [22].

To address the potential functional connectivity between vagal nerves and intestinal mast cells Gottwald et al. applied bilateral peripheral electrical stimulation to the cervical vagi, after crushing and ligating them centrally [23]. Examination of the jejunum using Alcian blue staining of intestinal mucosal mast cells revealed no change in the mast cell density or granularity. Consistent with this, tissue levels of RMCP II were not significantly different between groups. However, the amount of histamine present in the jejunal wall was markedly elevated, particularly in those animals receiving 1.0 mA stimulation. Subsequent immunohistochemistry for histamine confirmed that this was mast cell associated and predominantly in mucosal mast cells [23]. Furthermore, both the numbers of mast cells that contained detectable histamine immunoreactivity and the intensity of histamine staining increased following vagal stimulation. Electrical stimulation of vagotomized animals revealed that histamine immunoreactivity was similar to control, unstimulated animals, whereas sham-operated animals that had their vagi stimulated had significantly increased histamine staining in mast cells. The increased histamine immunoreactivity of intestinal mucosal mast cells following vagal stimulation suggested either increased synthesis or decreased release [23, 24].

4 The Cholinergic Anti-inflammatory Pathway

The most recent advances in understanding the immunoregulatory role of the parasympathetic nervous system have focused on the cholinergic anti-inflammatory pathway. The anti-inflammatory function of the vagus nerve was first highlighted in studies conducted by Tracey and colleagues who demonstrated electrical stimulation of the peripheral vagus nerve *in vivo* during lethal endotoxemia in rats. This protective effect of vagal stimulation was mediated through inhibition of TNF synthesis by macrophages [25]. The macrophage has been suggested to be the main target of the anti-inflammatory function of the vagus nerve in a murine model of inflammatory bowel disease [26]. The downregulation of immune responses by the vagus is mediated largely by the action of acetylcholine (Ach) on nicotinic receptors. Correspondingly, nicotine is as efficient as Ach in inhibiting pro-inflammatory cytokine release from human macrophages *in vitro* [27] while the increased disease severity observed in animal models of IBD following vagotomy can be counteracted by nicotine [26].

Nicotinic acetylcholine receptors (nAChR) are pentameric ligand-gated ion channels that can be made up of a number of different subunits (identified neuronal subtypes include $\alpha 2-\alpha 10$ and $\beta 2-\beta 4$). While it has been reported that the homo pentameric $\alpha 7$ subtype of nAChR may be essential in mediating the anti-inflammatory effect of acetylcholine [27–29], it is clear that additional nAChR can be involved in the immunomodulatory actions of the vagus [15, 30].

Given the potential importance of the vagus nerve-mediated anti-inflammatory response in a number of inflammatory conditions including food allergy, there is limited knowledge regarding the potential targeting of mast cells by the cholinergic anti-inflammatory pathway. As described previously, there is anatomical evidence for vagal nerves in contact with intestinal mucosal mast cells, and while vagal stimulation has also been demonstrated to increase histamine content of intestinal mucosal mast cells, it is not known whether this is due to increased synthesis of histamine or stabilization of the cell and decreased mediator release [23].

There is indirect evidence that just such a pathway may be operating in a model of postoperative ileus, a mast cell-mediated process. It has been demonstrated that the cholinergic anti-inflammatory pathway can be activated by the administration of lipid-rich nutrition and subsequent activation of cholecystokinin (CCK) receptors [31, 32]. Interestingly, administration of lipid-rich nutrition reduced release of rat mast cell protease II (RMCP II) following induction of postoperative ileus, suggesting an inhibition of manipulation-induced degranulation.

While there is currently no direct evidence that the vagus acts to inhibit mast cell activation, studies have demonstrated that

nicotinic receptor agonist does attenuate certain responses of the cell, and this may explain reported therapeutic effects of nicotine on models of food allergy [13]. Mouse BMMC express mRNA encoding α 3, α 7, and β 2 nAChR. Agonists of nicotinic receptors, including the α 7 specific agonist GTS-21, inhibited antigen-induced degranulation of these cells in a dose-dependent manner, an effect prevented by an α 7 antagonist. More recently a study utilizing the rat mast/basophil cell line RBL-2H3 demonstrated that these cells express nicotinic acetylcholine receptors (nAChRs) α 7, α 9, and α 10 [15]. Exposure to nanomolar levels of nicotine suppressed the late-phase leukotriene/cytokine production but did not inhibit degranulation. The suppressive effect of nicotine on the late-phase response was blocked by the α 7/ α 9-nAChR antagonists methyllycaconitine and α -bungarotoxin, as well as by small interfering RNA knockdown of α 7-, α 9-, or α 10-nAChRs [15]. This data suggests that at least three nAChRs interact functionally to mediate the effects of nicotine on the late-phase response of mast cells. From these studies it is also clear that mast cells in different tissue sites may have distinct responses to vagal input based on AchR receptor expression. Furthermore, receptor expression may change in allergic disease. A study of human skin mast cells found that mast cells from atopic dermatitis lesions but not in healthy skin showed α 3 and α 5 subunit immunoreactivity [33].

5 Cholinergic Activation of Mast Cells

It is interesting to note that the earliest description of potential cholinergic regulation of mast cells was not through an inhibitory action at nicotinic receptors but activation and induction of degranulation by acetylcholine acting at muscarinic receptors [14, 34, 35]. Mannaioni and colleagues reported that histamine secretion from rat mast cells occurs in the presence of nanomolar concentrations of acetylcholine, an effect that was competitively blocked by atropine [34, 35]. However, other studies failed to show any effect of acetylcholine on rat mast cell degranulation [36, 37]. Masini et al. [14] went on to identify heterogeneity in response to acetylcholine with the virtual lack of sensitivity or by the full reaction to nanomolar concentrations of acetylcholine, observed in samples of serosal mast cells isolated from rats. The incubation of isolated rat mast cells with IgE induced a homogenous “responder” population, with acetylcholine-induced histamine release proportional to the IgE concentration. Again this suggests that parasympathetic regulation of mast cells may vary significantly depending on the local tissue environment and allergic status.

Masini and colleagues also demonstrated that stimulation of parasympathetic nerve endings, either preganglionic, through the vagus nerve, or postganglionic through selective field stimulation

of the nerve terminals, led to an increase of acetylcholine release accompanied by release of histamine [38]. While it cannot be certain that mast cells are the source of histamine released from tissue following stimulation, the fact that atropine competitively inhibited the physiological response and the release of histamine after parasympathetic activation while serine potentiated the physiological effects of stimulation and extended the duration of histamine release suggests a postsynaptic muscarinic modulation of histamine output. Furthermore, there was a decrease in mast cell granule metachromasia after vagal stimulation both in isolated guinea-pig auricles and in the isolated rat ileum suggesting that vagal stimulation did indeed induce mast cell degranulation and histamine release [38].

How then can this potential activation of mast cells following vagal stimulation be reconciled with a potential cholinergic, nicotinic receptor-induced inhibition of mast cell activity? These contrasting findings suggest that, perhaps unsurprisingly, there may be a complex parasympathetic regulation of mast cells with the functional outcome of vagal input depending on the acetylcholine receptor subtype expressed by the cells. Furthermore, different frequencies of stimulation may have different profiles of co-transmitter secretion from parasympathetic nerves. It is generally accepted that “conventional” neurotransmitters, such as ACh, are released in greater quantities at lower firing frequencies while neuropeptide release is increased at higher frequencies [39]. For example, in the airways of guinea pigs, Moffat et al. demonstrated that preganglionic stimulation of the vagus nerve induced NANC relaxation of the trachealis muscle only at frequencies above 4 Hz [40]. It is therefore worth discussing the potential effects of the major inhibitory NANC neurotransmitters on mast cells.

6 Vasoactive Intestinal Peptide

Vasoactive intestinal peptide (VIP) is a 28-amino acid peptide that exerts its action on cells through two G-protein-coupled receptors, VPAC1 and VPAC2 [41]. VIPergic signaling is involved in regulating intestinal motility and cardiac vasodilation and, centrally, plays an essential role in maintenance of circadian rhythm [42]. VIP is expressed widely in the nervous system, the endocrine system, and the immune system and can be considered a true neuroimmunoendocrine mediator.

The interactions between VIP and mast cells appear complex, and our understanding of their functional significance is limited. Mast cells can produce VIP [43, 44], express VIP receptors [45, 46], and degranulate in response to the peptide [47, 48]. However, there is also evidence that VIP can stabilize mast cells *in vivo* [49, 50]. Furthermore, mast cell-derived proteases degrade

VIP [51–53] and have been demonstrated to limit toxicity associated with high concentrations of VIP [51].

Systemically administered VIP can attenuate the motor response changes, neuronal cell death, and myelin sheet loss characteristic of a rat model of Parkinson's disease 6-OHDA administration into the corpus striatum [54]. Evidence suggests that the protective effect of VIP in this model could at least in part be mediated by brain mast cells. Electron microscopic studies of mast cells in the corpus stratum demonstrated that VIP treatment changes the ultrastructural morphology of mast cells in a manner characteristic of piecemeal degranulation [54].

Pretreatment of mast cells with VIP increases the chemoattractant effect of FKN fractalkine (FKN, CX3CL1) on mast cells [55]. Interestingly FKN is [55] secreted by human airway smooth muscle cells, and in asthmatic patients, there is an increase in both FKN and VIP expression in airway smooth muscle [56, 57] and a positive correlation between VIP staining and mast cell infiltration of the smooth muscle layer [55]. It has therefore been suggested that VIP and airway smooth-derived FKN may act together to promote mast cell recruitment in asthma.

7 Nitric Oxide

Nitric oxide is a major gaseous neurotransmitter that can be released from inhibitory NANC nerves and also co-stored and released with acetylcholine. While the direct role of neural derived NO on mast cells is uncertain, it is clear that NO is a potent regulator of mast cell function [58]. A number of studies have been conducted on the relationship between NO and mast cell mediator release. NO donors such as sodium nitroprusside (SNP) inhibited the release of histamine evoked by compound 48/80 or calcium ionophore A23187 from isolated rat peritoneal mast cells [59–61]. SNP also dramatically decreased Fc ϵ RI-mediated β -hexosaminidase and TNF release from mouse bone marrow-derived mast cells [62]. There is also increasing evidence that NO regulates cytokine and chemokine production by mast cells. Coleman and colleagues [63] showed that pretreatment with an NO donor blocked the induction of IL-4, IL-6, and TNF mRNA in mast cells following IgE-mediated stimulation. The effect of NO on mast cell function is not limited to mediator secretion. Studies in the human mast cell line HMC-1 indicated that NO could potently downregulate adhesion of these cells to the extracellular matrix component, fibronectin [64]. The NO-induced downregulation of adhesion can be attributed in part to inhibition of the cysteine protease, calpain, an enzyme associated with control of integrin activation [64]. A physiological role for NO interaction with mast cells in the gastrointestinal tract is suggested by studies identifying that inhibition

of nitric oxide synthesis increases intestinal permeability in the rat associated with increased release of rat MC protease II [65], and conversely, a nitric oxide donor could protect against cholera toxin A-mediated ileal chloride secretion and permeability through inhibition of intestinal mast cells [66]. However, while vagal stimulation has been demonstrated to protect against injury-associated increases in intestinal permeability [67, 68], to date, the involvement of nitrergic parasympathetic nerves and mast cells has not been determined.

8 Mast Cell and Parasympathetic Nerves: A Functional Unit in the Airways

The parasympathetic nervous system is the dominant neuronal pathway for airway smooth muscle tone. In several species, including humans, lower airway parasympathetic postganglionic neurons that project axons to airway smooth muscle are either cholinergic or NANC, the latter synthesizing vasoactive intestinal peptide and nitric oxide, but not Ach. Stimulation of cholinergic nerves causes bronchoconstriction mucus secretion and bronchial vasodilation. Mast cells are located throughout the airways, including the trachea, bronchus, and sparsely in the parenchyma [17, 69, 70], and the role for the mast cell interaction with the autonomic nervous system in the lung is supported by the fact that mast cells have been shown to be closely associated with airway nerves [71, 72].

As described previously inhibitory, parasympathetic, NANC nerves contain VIP and nitric oxide, both potent relaxants of the airway that counteract bronchoconstriction. Although dysfunction of inhibitory NANC nerves has also been proposed in asthma, no difference in inhibitory NANC responses has been found between asthmatics and healthy subjects. The tachykinins and calcitonin gene-related peptide (CGRP) are the major excitatory neuropeptides in the airways. For example, it has been reported that substance P-containing nerves in the rat trachea interact with mast cells to cause Ag-specific, and dependent, changes in lung solute clearance and epithelial chloride ion secretion [71, 73, 74]. Furthermore, substance P and neurokinin A (NKA) induce histamine release from human airway mast cells [75]. However, ablation of sensory C-fibers with capsaicin in either adults or neonatal mice fails to alter airway function after antigen challenge in passively sensitized mice [76], indicating that capsaicin-sensitive C-fibers do not play a primary role in allergic airway constriction.

Indeed, antigen-induced contraction of mouse trachea requires both acetylcholine release from parasympathetic neurons and serotonin release from airway mast cells [16, 76]. There have been a number of mechanisms proposed to explain how this functional

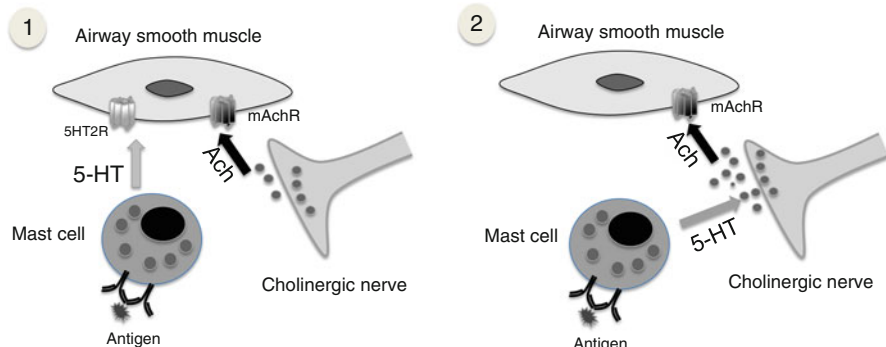


Fig. 1 Mast cell and parasympathetic nerve interactions mediate antigen-induced bronchoconstriction. Proposed models: (1) mast cell-derived serotonin enhances the release of acetylcholine from nerve terminals that, in turn, activates airway smooth muscle cells and (2) mast cell-derived serotonin directly activates airway smooth muscle cell contraction only when there is concurrent activation of muscarinic receptors by acetylcholine released constitutively from parasympathetic fibers. 5-HT (serotonin), Ach (acetylcholine), 5HT2R (type 2 5HT receptor), mAChR (muscarinic acetylcholine receptor). Based on the work of Weigand et al. [16] and Cyphert et al. [76]

unit of cholinergic nerves and mast cells acts to bring about antigen-induced bronchoconstriction (Fig. 1). In one model, activation of serotonin receptors on airway smooth muscle leads to smooth muscle contraction only when acetylcholine, which is released at low levels constitutively by the parasympathetic fibers, occupies muscarinic M3 receptors present on airway smooth muscle. This concept is supported by findings that only a receptor antagonist of 5-HT2A, a receptor localized to airway smooth muscle and not cholinergic fibers, can attenuate antigen-induced bronchoconstriction [76]. In another proposed mechanism, direct activation of 5-HT2 receptors on pre- or postganglionic terminals of parasympathetic cholinergic neurons leads to enhanced acetylcholine release that in turn stimulates smooth muscle contraction via activation of muscarinic receptors. This is supported by the location of mast cells in the mouse trachea, situated in the smooth muscle portion of the tissue well beneath the epithelium and adjacent to postganglionic parasympathetic nerves [77, 78], and by ex vivo studies that have measured an increase in acetylcholine levels after stimulation with antigen in both mouse and canine tracheal rings [16, 79, 80]. It is proposed that a model requiring the action of both acetylcholine and serotonin on airway smooth muscle may provide a safeguard, separating the pro-inflammatory and bronchoconstrictor roles of the mast cell-nerve interactions, limiting the activity of smooth muscle modulators stored by mast cells, while at the same time allowing mast cells to protect the airway against infectious agents through rapid release of inflammatory mediators.

9 Conclusion

The relationship between mast cells and neurons enables the involvement of peripheral and central nervous systems in the regulation of defense mechanisms, inflammation, and response to infection.

As described above there is good evidence for anatomical and functional interactions between the parasympathetic nervous system and mast cells. However, the extent to which these interactions influence health and disease is still obscure, and there is much we have yet to understand about the mechanisms underlying the relationship between mast cells and the PNS.

The level of individual neurotransmitters release can influence immune responses in ways that do not follow a classical dose response. A clear example of this has been described in a mouse model of diabetes where low subnormal local levels of substance P are pathogenic leading to increased autoreactive T cells and inflammation which does not occur at either normal levels or the complete absence of the neuropeptide [81]. It is likely that such nonclassical dose-dependent effects exist for other neurotransmitters including those of the PNS. Indeed, there is evidence that while high concentrations of VIP induce degranulation of mast cells [47, 48], lower concentrations can stabilize the cell *in vivo* [54].

While the majority of published studies focus on the impact of individual neurotransmitters on the mast cell, neural regulation of immune responses involves synergistic and antagonistic interactions, not only between different branches of the nervous system but also between neurotransmitters within the same neuron. Thus a greater understanding of how the balance of PNS co-transmitter release is differentially regulated in states of health and disease is required. This will include knowledge of how the brain regulates efferent parasympathetic tone and mediator secretion in response to afferent signals indicating changes in the microenvironment of peripheral tissue.

Given the inherent heterogeneity and plasticity of mast cells [82–85], the cell subtype and local tissue microenvironment likely determine the expression of specific neurotransmitter receptors and thus the response to PNS signaling. An example of this is the demonstration that the pattern of nicotinic receptor expression is different in skin mast cells from dermatitis patients compared to healthy controls [33]. Thus the identification of receptor targets for therapeutic intervention needs to be context specific; receptors determined to regulate cell activity *in vitro* or in healthy subjects may not be key in disease situations. Similarly, evidence is emerging that certain cytokines may play an important role in tailoring a microenvironment-specific mast cell response to neuronal signals. Theoharides et al. demonstrated that substance P induces vascular endothelial growth factor (VEGF) production and secretion from

human mast cells and that this response is significantly enhanced by coadministration of the pro-inflammatory cytokine IL-33 [86].

Further study of the parasympathetic regulation of mast cells will provide us with deeper understanding of how nerves participate in a range of processes including host defense, wound repair, inflammation, and associated pain responses and will consequently lead to the development of novel therapeutic strategies for a range of pathologic conditions.

References

1. Sternberg EM (2006) Neural regulation of innate immunity: a coordinated nonspecific host response to pathogens. *Nat Rev Immunol* 6:318–328
2. Kin NW, Sanders VM (2006) It takes nerve to tell T and B cells what to do. *J Leukoc Biol* 79:1093–1104
3. Wrona D (2006) Neural-immune interactions: an integrative view of the bidirectional relationship between the brain and immune systems. *J Neuroimmunol* 172:38–58
4. Theoharides TC (1996) The mast cell: a neuroimmunoendocrine master player. *Int J Tissue React* 18:1–21
5. Frieling T, Cooke HJ, Wood JD (1991) Serotonin receptors on submucous neurons in guinea pig colon. *Am J Physiol* 261:G1017–G1023
6. Frieling T, Cooke HJ, Wood JD (1993) Histamine receptors on submucous neurons in guinea pig colon. *Am J Physiol* 264:G74–G80
7. van Houwelingen AH, Kool M, de Jager SCA et al (2002) Mast cell-derived TNF- α primes sensory nerve endings in a pulmonary hypersensitivity reaction. *J Immunol* 168:5297–5302
8. Leon A, Buriani A, Dal Toso R et al (1994) Mast cells synthesize, store, and release nerve growth factor. *Proc Natl Acad Sci U S A* 91:3739–3743
9. Kakurai M, Monteforte R, Suto H, Tsai M, Nakae S, Galli SJ (2006) Mast cell-derived tumor necrosis factor can promote nerve fiber elongation in the skin during contact hypersensitivity in mice. *Am J Pathol* 169:1713–1721
10. Arnett HA, Wang Y, Matsushima GK, Suzuki K, Ting JP (2003) Functional genomic analysis of remyelination reveals importance of inflammation in oligodendrocyte regeneration. *J Neurosci* 23:9824–9832
11. Brann MR, Ellis J, Jorgensen H, Hill-Eubanks D, Jones SV (1993) Muscarinic acetylcholine receptor subtypes: localization and structure/function. *Prog Brain Res* 98:121–127
12. Wu J, Lukas RJ (2011) Naturally-expressed nicotinic acetylcholine receptor subtypes. *Biochem Pharmacol* 82:800–807
13. Kageyama-Yahara N, Suehiro Y, Yamamoto T, Kadowaki M (2008) IgE-induced degranulation of mucosal mast cells is negatively regulated via nicotinic acetylcholine receptors. *Biochem Biophys Res Commun* 377:321–325
14. Masini E, Fantozzi R, Conti A, Blandina P, Brunelleschi S, Mannaioni PF (1985) Mast cell heterogeneity in response to cholinergic stimulation. *Int Arch Allergy Appl Immunol* 77:184–185
15. Mishra NC, Rir-sima-ah J, Boyd RT et al (2010) Nicotine inhibits Fc epsilon RI-induced cysteinyl leukotrienes and cytokine production without affecting mast cell degranulation through alpha 7/alpha 9/alpha 10-nicotinic receptors. *J Immunol* 185:588–596
16. Weigand LA, Myers AC, Meeker S, Undem BJ (2009) Mast cell-cholinergic nerve interaction in mouse airways. *J Physiol* 587:3355–3362
17. Barnes PJ (1986) Non-adrenergic non-cholinergic neural control of human airways. *Arch Int Pharmacodyn Ther* 280:208–228
18. Maier SF, Goehler LE, Fleshner M, Watkins LR (1998) The role of the vagus nerve in cytokine-to-brain communication. *Ann N Y Acad Sci* 840:289–300
19. Watkins LR, Goehler LE, Relton JK et al (1995) Blockade of interleukin-1 induced hyperthermia by subdiaphragmatic vagotomy: evidence for vagal mediation of immune-brain communication. *Neurosci Lett* 183:27–31
20. Tracey KJ (2002) The inflammatory reflex. *Nature* 420:853–859
21. Williams RM, Berthoud HR, Stead RH (1997) Vagal afferent nerve fibres contact mast cells in rat small intestinal mucosa. *Neuroimmuno modulation* 4:266–270
22. Gottwald T, Lhotak S, Stead RH (1997) Effect of truncal vagotomy and capsaicin on mast cells and IgA-positive plasma cells in rat jejunal mucosa. *Neurogastroenterol Motil* 9:25–32

23. Gottwald TP, Hewlett BR, Lhotak S, Stead RH (1995) Electrical stimulation of the vagus nerve modulates the histamine content of mast cells in the rat jejunal mucosa. *Neuroreport* 7:313–317
24. Stead RH, Colley EC, Wang B et al (2006) Vagal influences over mast cells. *Auton Neurosci* 125:53–61
25. Borovikova LV, Ivanova S, Zhang M et al (2000) Vagus nerve stimulation attenuates the systemic inflammatory response to endotoxin. *Nature* 405:458–462
26. Ghia JE, Blennerhassett P, Kumar-Ondiveeran H, Verdu EF, Collins SM (2006) The vagus nerve: a tonic inhibitory influence associated with inflammatory bowel disease in a murine model. *Gastroenterology* 131:1122–1130
27. Wang H, Yu M, Ochani M et al (2003) Nicotinic acetylcholine receptor alpha7 subunit is an essential regulator of inflammation. *Nature* 421:384–388
28. van Westerloo DJ, Giebeln IA, Florquin S et al (2006) The vagus nerve and nicotinic receptors modulate experimental pancreatitis severity in mice. *Gastroenterology* 130:1822–1830
29. Pavlov VA, Ochani M, Yang LH et al (2007) Selective alpha7-nicotinic acetylcholine receptor agonist GTS-21 improves survival in murine endotoxemia and severe sepsis. *Crit Care Med* 35:1139–1144
30. Karimi K, Bienenstock J, Wang L, Forsythe P (2010) The vagus nerve modulates CD4+ T cell activity. *Brain Behav Immun* 24:316–323
31. Luyer MD, Greve JW, Hadfoune M, Jacobs JA, Dejong CH, Buurman WA (2005) Nutritional stimulation of cholecystokinin receptors inhibits inflammation via the vagus nerve. *J Exp Med* 202:1023–1029
32. Tracey KJ (2005) Fat meets the cholinergic antiinflammatory pathway. *J Exp Med* 202: 1017–1021
33. Kindt F, Wiegand S, Niemeier V et al (2008) Reduced expression of nicotinic alpha subunits 3, 7, 9 and 10 in lesional and nonlesional atopic dermatitis skin but enhanced expression of alpha subunits 3 and 5 in mast cells. *Br J Dermatol* 159:847–857
34. Blandina P, Fantozzi R, Mannaioni PF, Masini E (1980) Characteristics of histamine release evoked by acetylcholine in isolated rat mast cells. *J Physiol* 301:281–293
35. Fantozzi R, Masini E, Blandina P, Mannaioni PF, Bani-Sacchi T (1978) Release of histamine from rat mast cells by acetylcholine. *Nature* 273:473–474
36. Leung KB, Pearce FL (1984) A comparison of histamine secretion from peritoneal mast cells of the rat and hamster. *Br J Pharmacol* 81: 693–701
37. Kazimierczak W, Adamas B, Maslinski C (1980) Failure of acetylcholine to release histamine from rat mast cells. *Agents Actions* 10:1–3
38. Bani-Sacchi T, Barattini M, Bianchi S et al (1986) The release of histamine by parasympathetic stimulation in guinea-pig auricle and rat ileum. *J Physiol* 371:29–43
39. Vilim FS, Cropper EC, Price DA, Kupfermann I, Weiss KR (1996) Release of peptide cotransmitters in Aplysia: regulation and functional implications. *J Neurosci* 16:8105–8114
40. Moffatt JD, Dumsday B, McLean JR (1999) Characterization of non-adrenergic, non-cholinergic inhibitory responses of the isolated guinea-pig trachea: differences between pre- and post-ganglionic nerve stimulation. *Br J Pharmacol* 128:458–464
41. Abad C, Gomariz RP, Waschek JA (2006) Neuropeptide mimetics and antagonists in the treatment of inflammatory disease: focus on VIP and PACAP. *Curr Top Med Chem* 6:151–163
42. Sherwood NM, Krueckl SL, McRory JE (2000) The origin and function of the pituitary adenylate cyclase-activating polypeptide (PACAP)/glucagon superfamily. *Endocr Rev* 21:619–670
43. Goetzel EJ, Sreedharan SP, Turck CW (1988) Structurally distinctive vasoactive intestinal peptides from rat basophilic leukemia cells. *J Biol Chem* 263:9083–9086
44. Wershil BK, Turck CW, Sreedharan SP et al (1993) Variants of vasoactive intestinal peptide in mouse mast cells and rat basophilic leukemia cells. *Cell Immunol* 151:369–378
45. Goetzel EJ, Pankhaniya RR, Gaufo GO, Mu Y, Xia M, Sreedharan SP (1998) Selectivity of effects of vasoactive intestinal peptide on macrophages and lymphocytes in compartmental immune responses. *Ann N Y Acad Sci* 840:540–550
46. Waschek JA, Bravo DT, Richards ML (1995) High levels of vasoactive intestinal peptide/pituitary adenylate cyclase-activating peptide receptor mRNA expression in primary and tumor lymphoid cells. *Regul Pept* 60:149–157
47. Kulka M, Sheen CH, Tancowny BP, Grammer LC, Schleimer RP (2008) Neuropeptides activate human mast cell degranulation and chemokine production. *Immunology* 123: 398–410
48. Lowman MA, Benyon RC, Church MK (1988) Characterization of neuropeptide-induced histamine release from human dispersed skin mast cells. *Br J Pharmacol* 95: 121–130

49. Undem BJ, Dick EC, Buckner CK (1983) Inhibition by vasoactive intestinal peptide of antigen-induced histamine release from guinea-pig minced lung. *Eur J Pharmacol* 88:247–250

50. Tuncel N, Tore F, Sahinturk V, Ak D, Tuncel M (2000) Vasoactive intestinal peptide inhibits degranulation and changes granular content of mast cells: a potential therapeutic strategy in controlling septic shock. *Peptides* 21:81–89

51. Akahoshi M, Song CH, Piliponsky AM et al (2011) Mast cell chymase reduces the toxicity of Gila monster venom, scorpion venom, and vasoactive intestinal polypeptide in mice. *J Clin Invest* 121:4180–4191

52. Caughey GH, Leidig F, Viro NF, Nadel JA (1988) Substance P and vasoactive intestinal peptide degradation by mast cell tryptase and chymase. *J Pharmacol Exp Ther* 244:133–137

53. Tam EK, Caughey GH (1990) Degradation of airway neuropeptides by human lung tryptase. *Am J Respir Cell Mol Biol* 3:27–32

54. Tuncel N, Sener E, Cerit C et al (2005) Brain mast cells and therapeutic potential of vasoactive intestinal peptide in a Parkinson's disease model in rats: brain microdialysis, behavior, and microscopy. *Peptides* 26:827–836

55. El-Shazly A, Berger P, Girodet PO et al (2006) Fractalkine produced by airway smooth muscle cells contributes to mast cell recruitment in asthma. *J Immunol* 176:1860–1868

56. Rimaniol AC, Till SJ, Garcia G et al (2003) The CX3C chemokine fractalkine in allergic asthma and rhinitis. *J Allergy Clin Immunol* 112:1139–1146

57. Groneberg DA, Springer J, Fischer A (2001) Vasoactive intestinal polypeptide as mediator of asthma. *Pulm Pharmacol Ther* 14:391–401

58. Forsythe P, Gilchrist M, Kulka M, Befus AD (2001) Mast cells and nitric oxide: control of production, mechanisms of response. *Int Immunopharmacol* 1:1525–1541

59. Iikura M, Takaishi T, Hirai K et al (1998) Exogenous nitric oxide regulates the degranulation of human basophils and rat peritoneal mast cells. *Int Arch Allergy Immunol* 115:129–136

60. Peh KH, Moulson A, Wan BY, Assem EK, Pearce FL (2001) Role of nitric oxide in histamine release from human basophils and rat peritoneal mast cells. *Eur J Pharmacol* 425:229–238

61. Eastmond NC, Banks EM, Coleman JW (1997) Nitric oxide inhibits IgE-mediated degranulation of mast cells and is the principal intermediate in IFN-gamma-induced suppression of exocytosis. *J Immunol* 159:1444–1450

62. Bidri M, Becherel PA, Le Goff L et al (1995) Involvement of cyclic nucleotides in the immunomodulatory effects of nitric oxide on murine mast cells. *Biochem Biophys Res Commun* 210:507–517

63. Davis BJ, Flanagan BF, Gilfillan AM, Metcalfe DD, Coleman JW (2004) Nitric oxide inhibits IgE-dependent cytokine production and Fos and Jun activation in mast cells. *J Immunol* 173:6914–6920

64. Forsythe P, Befus AD (2003) Inhibition of calpain is a component of nitric oxide-induced down-regulation of human mast cell adhesion. *J Immunol* 170:287–293

65. Kanwar S, Wallace JL, Befus D, Kubes P (1994) Nitric oxide synthesis inhibition increases epithelial permeability via mast cells. *Am J Physiol* 266:G222–G229

66. Qiu B, Pothoulakis C, Castagliuolo I, Nikulasson Z, LaMont JT (1996) Nitric oxide inhibits rat intestinal secretion by *Clostridium difficile* toxin A but not *Vibrio cholerae* enterotoxin. *Gastroenterology* 111:409–418

67. Costantini TW, Bansal V, Krzyzaniak M et al (2010) Vagal nerve stimulation protects against burn-induced intestinal injury through activation of enteric glia cells. *Am J Physiol Gastrointest Liver Physiol* 299:G1308–G1318

68. Krzyzaniak M, Peterson C, Loomis W et al (2011) Postinjury vagal nerve stimulation protects against intestinal epithelial barrier breakdown. *J Trauma* 70:1168–1175, discussion 1175–6

69. Carr MJ, Undem BJ (2003) Bronchopulmonary afferent nerves. *Respirology* 8:291–301

70. Andersson RG, Grundstrom N (1987) Innervation of airway smooth muscle. Efferent mechanisms. *Pharmacol Ther* 32:107–130

71. Kowalski ML, Didier A, Lundgren JD, Igarashi Y, Kaliner MA (1997) Role of sensory innervation and mast cells in neurogenic plasma protein exudation into the airway lumen. *Respirology* 2:267–274

72. Undem BJ, Riccio MM, Weinreich D, Ellis JL, Myers AC (1995) Neurophysiology of mast cell-nerve interactions in the airways. *Int Arch Allergy Immunol* 107:199–201

73. Akiyama H, Amano H, Bienenstock J (2005) Rat tracheal epithelial responses to water avoidance stress. *J Allergy Clin Immunol* 116:318–324

74. Sestini P, Bienenstock J, Crowe SE et al (1990) Ion transport in rat tracheal epithelium in vitro. Role of capsaicin-sensitive nerves in allergic reactions. *Am Rev Respir Dis* 141:393–397

75. Forsythe P, McGarvey LP, Heaney LG, MacMahon J, Ennis M (2000) Sensory

neuropeptides induce histamine release from bronchoalveolar lavage cells in both nonasthmatic coughers and cough variant asthmatics. *Clin Exp Allergy* 30:225–232

76. Cyphert JM, Kovarova M, Allen IC et al (2009) Cooperation between mast cells and neurons is essential for antigen-mediated bronchoconstriction. *J Immunol* 182:7430–7439
77. Myers AC, Undem BJ, Weinreich D (1991) Influence of antigen on membrane properties of guinea pig bronchial ganglion neurons. *J Appl Physiol* 71:970–976
78. Kajekar R, Undem BJ, Myers AC (2003) Role of cyclooxygenase activation and prostaglandins in antigen-induced excitability changes of bronchial parasympathetic ganglia neurons. *Am J Physiol Lung Cell Mol Physiol* 284:L581–L587
79. Mitchell RW, Ndukuw IM, Ikeda K, Arbetter K, Leff AR (1993) Effect of immune sensitization on stimulated ACh release from trachealis muscle in vitro. *Am J Physiol* 265:L13–L18
80. Larsen GL, Fame TM, Renz H et al (1994) Increased acetylcholine release in tracheas from allergen-exposed IgE-immune mice. *Am J Physiol* 266:L263–L270
81. Razavi R, Chan Y, Afifiyan FN et al (2006) TRPV1+ sensory neurons control beta cell stress and islet inflammation in autoimmune diabetes. *Cell* 127:1123–1135
82. Forsythe P, Ennis M (2000) Clinical consequences of mast cell heterogeneity. *Inflamm Res* 49:147–154
83. Moon TC, St Laurent CD, Morris KE et al (2010) Advances in mast cell biology: new understanding of heterogeneity and function. *Mucosal Immunol* 3:111–128
84. Shanahan F, Denburg JA, Fox J, Bienenstock J, Befus D (1985) Mast cell heterogeneity: effects of neuroenteric peptides on histamine release. *J Immunol* 135:1331–1337
85. Kitamura Y, Kanakura Y, Sonoda S, Asai H, Nakano T (1987) Mutual phenotypic changes between connective tissue type and mucosal mast cells. *Int Arch Allergy Appl Immunol* 82:244–248
86. Theoharides TC, Zhang B, Kempuraj D et al (2010) IL-33 augments substance P-induced VEGF secretion from human mast cells and is increased in psoriatic skin. *Proc Natl Acad Sci U S A* 107:4448–4453

Chapter 10

Growth of Human Mast Cells from Bone Marrow and Peripheral Blood-Derived CD34⁺ Pluripotent Hematopoietic Cells

Geethani Bandara, Dean D. Metcalfe, and Arnold S. Kirshenbaum

Abstract

Human mast cells (HuMCs) are derived from CD34⁺ pluripotent hematopoietic cells which are KIT (CD117)⁺ and Fc ϵ RI⁻, and lack lineage-specific surface markers. Bone marrow and peripheral blood are the two readily available sources for obtaining CD34⁺ cells from which HuMCs can be cultured. CD34⁺ cells are isolated and enriched by magnetic separation columns and stored under specific conditions until ready for use. Alternatively, enriched CD34⁺ cells may be immediately cultured in serum-free culture media containing recombinant human (rh) stem cell factor (SCF), rhIL-6, and rhIL-3 (added only during the first week). Weekly hemidepletions and removal of adherent cells and/or debris enables the investigator to obtain HuMC cultures, identified by Wright-Giemsa and acidic toluidine blue stains, by 8–10 weeks.

Key words Human mast cells, CD34⁺ cells, Pluripotent hematopoietic cells, Bone marrow, Peripheral blood

1 Introduction

HuMCs are derived from CD34⁺ pluripotent hematopoietic cells which are KIT (CD117)⁺ and Fc ϵ RI⁻ and lack T-cell (CD2), B-cell (CD19, CD20), macrophage (CD14), and eosinophil lineage surface markers [1]. In addition to peripheral blood and bone marrow, HuMCs have been derived from CD34⁺ cells from cord blood [2–4] and from fetal liver [5, 6]. In vitro studies have documented that the mature HuMC progeny will differ, depending on the tissue of origin. Furthermore, in the presence of rhSCF and rhIL-6, HuMCs require at least 8–10 weeks in culture to fully mature. Monocytes and other lineages that appear in vitro are depleted with each weekly passage. This may prevent competition for growth factors and release of inhibitory growth factors such as IFN γ [1] that may inhibit HuMC proliferation and maturation.

The use of peripheral blood leukapheresis to collect mononuclear cells, followed by immunomagnetic or affinity column

enrichment of CD34⁺ cells, provides large numbers of CD34⁺ cells and significantly increases the HuMC yield. Laboratory methods detailing the isolation CD34⁺ cells from bone marrow or peripheral blood and the growth of HuMCs from these progenitors are described.

2 Materials

1. MACS LS Separation Columns and MACS Separator (Miltenyi Biotec, San Diego, CA).
2. Anti-FITC (fluorescein isothiocyanate) MicroBeads (Miltenyi Biotec, San Diego, CA).
3. StemPro-34 serum-free medium (SFM) with nutrient supplement (Invitrogen, Carlsbad, CA).
4. 100× L-glutamine stock: 200 mM L-glutamine in sterile water.
5. 100× penicillin-streptomycin stock: 10,000 I.U./mL penicillin, 10 mg/mL streptomycin (Mediatech, Herndon, VA).
6. Ammonium chloride solution: 0.8 % NH₄Cl, 0.1 mM EDTA in ddH₂O (StemCell Technologies, Vancouver, Canada).
7. Recombinant human (rh) IL-3, rhIL-6, and rhSCF (PeproTech, Rocky Hill, NJ).
8. 75 cm² tissue culture flasks (Fisher Scientific, Pittsburgh, PA).
9. 5 mL polystyrene and 15 mL and 50 mL polypropylene tubes (Becton-Dickinson Labware, Franklin Lakes, NJ).
10. Blocking buffer: 1× phosphate buffered saline (PBS) (pH 7.2), 0.5 % bovine serum albumin (BSA), 2 mM ethylenediaminetetraacetic acid (EDTA). Prepare sterile or filter sterilize (0.22 µm).
11. FITC-conjugated antihuman CD34 (anti-HPCA2, Becton-Dickinson, San Jose, CA).
12. Toluidine blue (acidic): Add 0.5 g of toluidine blue to 30 mL of absolute ethanol. Bring the volume to 100 mL with distilled deionized water. Adjust to a pH<1.0 with 1N HCl. Store at room temperature (RT).
13. Mota's fixative: Prepare in a 100 mL bottle with a magnetic stirrer by adding 4 g lead acetate (basic) to 50 mL of distilled deionized water. Stir at slow speed and add 2–4 mL of glacial acetic acid to dissolve the lead acetate and make the solution clear. Add 50 mL of absolute ethanol. Keep tightly closed and store at RT. Prepare fresh every 1–2 months.
14. Hema-Tek-2000 Wright-Giemsa slide stainer (Bayer Corporation, Elkhart, IN).

15. Cytospin 3 (Shandon, Pittsburgh, PA).
16. M199 media: 1× with Earle's salts, L-glutamine, sodium bicarbonate, HEPES buffer (Invitrogen, Carlsbad, CA).
17. Preservative-free heparin sodium (1,000 Units/mL) (American Pharmaceutical Partners, Schaumburg, IL).
18. Lymphocyte separation media (ICN Biomedicals, Aurora, OH).
19. 30 µm nylon net filter (Millipore, Bedford, MA).
20. Nalgene Cryo 1°C freezing container (Daigger, Vernon Hills, IL).
21. Nunc 1.8 mL SI (377267) cryotubes (Fisher Scientific, Pittsburgh, PA).
22. Cryopreservation solutions:
 - (a) Solution A: Mix M199 media with dimethyl sulfoxide (DMSO) in a 4:1 v/v ratio. Aliquot in 15 mL tubes, and keep frozen at -20 °C until use.
 - (b) Solution B: Add 3,000 U/mL preservative-free heparin to fetal bovine serum (FBS), aliquot in 15 mL tubes, and keep frozen at -20 °C until use.

3 Methods

3.1 Preparation of Bone Marrow or Peripheral Blood for CD34⁺ Selection

Collect CD34⁺ cells from either normal or patient donor bone marrow or peripheral blood. On average, bone marrow contains approximately 1 % CD34⁺ cells, and peripheral blood contains 0.01–0.07 % CD34⁺ cells [7], so yields will differ significantly by source:

1. Preload 10 or 50 mL syringes with 0.5 or 1 mL of preservative-free heparin sodium, respectively. Collect aspirated bone marrow in 10 mL syringes. Collect venipuncture-derived peripheral blood into 50 mL syringes. Mix cells and heparin by rotating the syringes for 1 min.
2. Prepare complete media containing StemPro-SFM media, nutrient supplement, 2 mM L-glutamine, 100 I.U./mL penicillin, and 100 µg/mL streptomycin. Complete media should be stored at 4 °C and be remade fresh every 1–2 months.
3. Place a maximum of 10 mL of either heparinized bone marrow or peripheral blood into a 50 mL tube. Add 25 mL of complete media and resuspend the cells by gentle pipetting.
4. Place 14 mL of lymphocyte separation media into another 50 mL tube, and carefully overlay the cell suspension on top of the lymphocyte separation media. Centrifuge tubes at 675 $\times g$

for 20 min at RT. The red cells will collect below the separation media at the bottom of the tube. Identify the mononuclear cells in the interface layer, and pipette off the complete media just above the interface.

5. Using a 2 mL pipette, gently skim off and collect the mononuclear cells and transfer to a 50 mL tube (*see Note 1*). Discard the remaining red cell pellet and separation media. Add 25 mL of complete media and centrifuge the mononuclear cells at $300 \times g$ for 10 min to remove debris. Remove the supernatant, and resuspend the pelleted mononuclear cells in 25 mL of media. Repeat twice.
6. Resuspend mononuclear cells in 5 mL of blocking buffer solution. Remove clumps, aggregates, or particles by passing the cell suspension through a sterile 30 μ m nylon net filter into a 15 mL tube (*see Note 2*). Count cells.

3.2 CD34⁺ Cell Selection and Enrichment (See Note 3)

CD34⁺ purity is important for eliminating unwanted cells from cultures. Magnetic separation columns initially yield a CD34⁺ cell purity between 65 and 75 %. A second CD34⁺ enrichment using a new column may be necessary to obtain purities of 90–95 % CD34⁺ cells:

1. Resuspend 10^7 mononuclear cells in 100 μ L of blocking buffer in a 5 mL tube. Add 10 μ L of FITC-conjugated antihuman CD34 and incubate for 30 min at 37 °C.
2. Add 2 mL of blocking buffer and centrifuge at $210 \times g$ for 5 min. Remove the supernatant completely, and resuspend the cell pellet in 80 μ L of blocking buffer. Add 20 μ L of MACS anti-FITC microbeads/ 10^7 cells, and incubate the cells for 15 min at 4–8 °C.
3. Add 2 mL of blocking buffer and centrifuge at $210 \times g$ for 5 min. Remove the supernatant completely, and resuspend the cells at a concentration up to 10^8 cells/500 μ L of blocking buffer.
4. Place the MACS LS column in the magnetic field, and run 3 mL of blocking buffer through the column. Pipette the cell suspension onto the column, and collect the effluent in a 15 mL tube as the negative fraction. Rinse the column with 3 mL of sterile blocking buffer three times. Remove the column from the magnetic cell separator, and place on a new 15 mL collection tube. Apply 5 mL of buffer onto the column, and flush out CD34⁺ cells by applying the plunger supplied with the column. Count the cells.

3.3 Cryopreservation of CD34⁺ Cells

A minimum of 5×10^6 CD34⁺ cells/mL of cryopreservative mixture is recommended for preservation and recovery (*see Note 4*). The cryopreservative mixture consists of two solutions:

1. To cryopreserve $5-10 \times 10^6$ cells, prepare one tube containing 0.5 mL of cold (4 °C) solution A and 1 tube containing 0.5 mL of cold (4 °C) solution B.
2. Add $2.5-5.0 \times 10^6$ cells into each tube, and keep on ice for several minutes.
3. Combine the 2 tubes into a total of 1 mL, and transfer into 1.8 mL cryotubes. Allow cells to equilibrate at 4 °C for 30 min.
4. Transfer cells to a Nalgene Cryo 1 °C freezing container, and place in a -70 °C freezer overnight. After 24 h, transfer cryotubes to liquid nitrogen.

3.4 CD34⁺ and HuMC Cultures

Under ideal conditions, 5×10^6 CD34⁺ cells placed in culture for 7–10 weeks may give rise to $10-20 \times 10^6$ HuMCs with less than 5 % contamination with other cell types, as determined by Wright-Giemsa and acidic toluidine blue staining:

1. Quick-thaw a vial of CD34⁺ cells at 37 °C, resuspend in 10 mL of complete media, and centrifuge at $450 \times g$ for 5 min. Remove supernatant completely to prevent any DMSO carryover. Resuspend cells in 5–10 mL of complete media containing 100 ng/mL rhSCF, 100 ng/mL rhIL-6, and 30 ng/mL rhIL-3. Transfer into a 175 mL flask and bring the final volume up to 30 mL. IL-3 is only used during the first week of culture. During subsequent weeks, complete media is supplemented with only 100 ng/mL rhSCF and 100 ng/mL rhIL-6. Incubate the flask for 1 week at 37 °C, 5 % CO₂ (see Note 5).
2. After 1 week, add 30 mL of complete media containing 100 ng/mL rhSCF and 100 ng/mL rhIL-6 and transfer 30 mL of the diluted culture to another flask, thus dividing the culture into two flasks. Repeat the same procedure after 1 more week in culture.
3. At the third week, pipette and transfer culture medium from each flask into a 50 mL tube and centrifuge at $450 \times g$ for 5 min at RT. Remove 15 mL of the supernatant and resuspend the cells in the remaining medium. Transfer to a new 175 mL flask, and bring the final volume up to 30 mL with new complete medium containing 100 ng/mL rhSCF and 100 ng/mL rhIL-6. Repeat this procedure weekly. Check flasks weekly for adherent cells or debris. Monocytes and other cells will proliferate initially and compete for growth factors in suspension, resulting in adherent cells or debris from cell death. This extraneous material may have a deleterious effect on HuMC yields and must be removed weekly. If adherent cells are present, gently transfer nonadherent HuMCs and growth media to a new flask. In the event of cell debris, pipette nonadherent HuMCs and growth media into a 50 mL tube, and centrifuge at slow speed ($150 \times g$) for 5 min. Resuspend the cell pellet in 30 mL

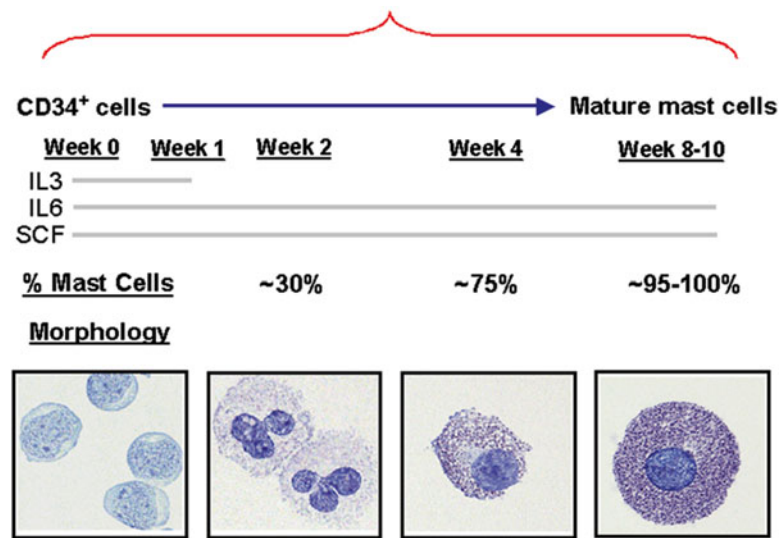


Fig. 1 Human mast cells derived from CD34+ peripheral blood leukocytes. Originally published in [8] Copyright © 2004 Karger Publishers, Basel, Switzerland

of fresh complete media with 100 ng/mL rhSCF and 100 ng/mL rhIL-6, and culture in new flasks (see Note 6).

4. Continue to culture for 7–10 weeks, at which point mature mast cells are present. Check total and HuMC counts weekly by staining with Wright-Giemsa and acidic toluidine blue (Fig. 1) [8].

3.5 HuMC Histochemical Stains

HuMC numbers are calculated by determining the percentage of acidic toluidine blue-positive cells out of total Wright-Giemsa positive cells. Acidic toluidine blue positive HuMC numbers can be confirmed by tryptase staining.

Wright-Giemsa

1. Count cells directly out of flasks, and concentrate at $210 \times g$ for 5 min to at least 2×10^5 cells/mL, for optimal cytopsins.

2. Add 100 μ l of cell suspension to cytospin sample chambers and clean slides. Spin slides at $14 \times g$ for 5 min. Let slides air-dry, and place on an automated Hema-Tek-2000 for Wright-Giemsa stain. Add 1–2 drops of Permount and mount with a coverslip.

Acidic Toluidine Blue

1. Fix cytopsins by adding several drops of Mota's fixative to cover the cells for 10 min. Mota's fixative evaporates quickly, so replenish drops once or twice to prevent crystal formation.

2. Slowly run water down the slides, not directly on cells, to remove fixative and blot any droplets. Do not disturb the cells.

3. Add 2–3 drops of acidic toluidine blue to the slide and let stain for 20 min. Run water down the slide to remove the excess stain, and blot dry. Add 1–2 drops of Permount and mount with a coverslip.

4 Notes

1. Prior to skimming off of mononuclear cells, if clots are noted in the interface or below, suction clots with a 10 or 25 mL pipette placed directly on the clot. The interface is minimally disturbed and clots are avoided in the mononuclear cell suspension.
2. Red blood cells normally contaminate most preparations and will not affect HuMC yields if left in culture. For significant red cell contamination, lyse red blood cells by adding ammonium chloride to cells in a 4:1 ratio, incubate cells on ice for 10 min, and centrifuge at $300 \times g$ for 5 min at 22 °C. Resuspend the mononuclear cell pellet in complete media with growth factors.
3. MACS LS magnetic separation columns have a maximum capacity of 2×10^9 total cells and 10^8 magnetically labeled cells. Degas buffer by applying a vacuum to the buffer at RT. Excessive gas in the buffer will form bubbles and decrease the CD34⁺ cell yields. Use the column immediately after filling to avoid formation of air bubbles. Use a maximum cell concentration of 10^8 cells/500 μ l of buffer.
4. CD34⁺ cells generally survive cryopreservation well, with some variation between procedures. Cell loss due to crystallization can occur and affect the overall yield of cells. Viability as measured by trypan blue dye exclusion may yield viabilities ranging between 75 and 90 %. Remove cell debris from thawed CD34⁺ cells by centrifuging at $150 \times g$ for at least 5 min. Resuspend CD34⁺ cells in complete media with growth factors.
5. CD34⁺ cells may initially proliferate 100 times or more the starting number of cells if rhSCF is combined with rhIL-3 and rhIL-6, so do not culture greater than 5×10^4 cells/mL. Conspicuous growth is seen over the first 2–3 weeks, though debris will begin to accumulate due to non-HuMC lineage cell apoptosis and necrosis. Adherent macrophages also may start to proliferate by 2 weeks. Check cultures weekly and separate nonadherent HuMC committed progenitors from adherent cells and debris. Gently pipette and remove nonadherent cells to a new flask, or centrifuge nonadherent cells and culture media at $150 \times g$ for 5 min, resuspend cells in complete

media with growth factors, and culture in a new flask. The 4 week time point appears to be a critical juncture, and cultures not properly cared may undergo significant HuMC loss. To counteract this, remove and replenish 95 % of the media at 4 weeks.

6. SCF alone will give rise over 7–10 weeks to pure HuMC cultures; however, HuMC numbers are less, and less cell debris is seen at all weeks in culture. IL-3 increases all cell lineages and is a basophil growth factor, but will not give rise to significant numbers of basophils if used only for the first week in the presence of rhSCF and rhIL-6. IL-6 helps supports HuMC growth and maturation and prevents apoptosis.

Acknowledgments

The authors thank Dr. Alasdair Gilfillan for reviewing this manuscript. This research is supported by the Intramural Research Program of the NIH, NIAID.

References

1. Metcalfe DD (2008) Mast cells and mastocytosis. *Blood* 112:946–956
2. Lee E, Min HK, Oskeritzian CA, Kambe N, Schwartz LB, Chang HW (2003) Recombinant human (rh) stem cell factor and rhIL-4 stimulate differentiation and proliferation of CD3⁺ cells from umbilical cord blood and CD3⁺ cells enhance Fc ϵ R1 expression on fetal liver-derived mast cells in the presence of rhIL-4. *Cell Immunol* 226:30–36
3. Matsuzawa S, Sakashita K, Kinoshita T, Ito S, Yamashita T, Koike K (2003) IL-9 enhances the growth of human mast cell progenitors under stimulation with stem cell factor. *J Immunol* 170:3461–3467
4. Piliponsky AM, Gleich GJ, Nagler A, Bar I, Levi-Schaffer F (2003) Non-IgE-dependent activation of human lung- and cord blood-derived mast cells is induced by eosinophil major basic protein and modulated by the membrane form of stem cell factor. *Blood* 101:1898–1904
5. Kambe N, Kambe M, Chang HW, Matsui A, Min HK, Hussein M, Oskeritzian CA, Kochan J, Irani AA, Schwartz LB (2000) An improved procedure for the development of human mast cells from dispersed fetal liver cells in serum-free culture medium. *J Immunol Methods* 240: 101–110
6. Kambe M, Kambe N, Oskeritzian CA, Schechter N, Schwartz LB (2001) IL-6 attenuates apoptosis, while neither IL-6 nor IL-10 affect the numbers or protease phenotype of fetal liver-derived human mast cells. *Clin Exp Allergy* 31: 1077–1085
7. Anderson HB, Holm M, Hetland TE, Dahl C, Junker S, Schoitz PO, Hoffman HJ (2008) Comparison of short term in vitro cultured human mast cells from different progenitors—peripheral blood-derived progenitors generate highly mature and functional mast cells. *J Immunol Methods* 336:166–174
8. Tkaczyk C, Okayama Y, Metcalfe DD, Gilfillan AM (2004) Fc receptors on mast cells: activatory and inhibitory regulation of mediator release. *Int Arch Allergy Immunol* 133: 305–315

Chapter 11

Isolation and Characterization of Human Intestinal Mast Cells

Axel Lorentz, Gernot Sellge, and Stephan C. Bischoff

Abstract

Mast cells are granulated immune cells typically located at barrier sites of the body, such as the skin and the mucosa of the respiratory, urogenital, and gastrointestinal tract. They are well known for their capacity to participate in the orchestration of inflammatory and immune responses by releasing a broad array of mediators as a consequence of IgE-dependent and IgE-independent activation. Mast cells derive from myeloid progenitors, but in contrast to other myeloid cells, they leave the bone marrow in an immature state; therefore, mast cells are not visible in the blood under normal conditions. For full maturation, the tissue environment is necessary. Thus, mature mast cells can be only isolated from tissue such as skin or mucosal sites, which makes mast cell isolation complicated. This chapter describes methods to isolate, purify, and culture mast cells from the human intestinal mucosa. Human mucosal mast cells can be used to characterize their mediators and to study the mechanisms of human mast cell activation, signal transduction, and exocytosis in response to specific stimuli.

Key words Mast cells, Human, Intestinal, Gut, Bowel, Cell isolation, Cell culture, Cell activation, Mediator release assay

1 Introduction

Mast cells are heavily granulated immune cells that are dispersed throughout the body. They originate from immature, bone marrow-derived CD34⁺ hematopoietic stem cells circulating in the peripheral blood as committed progenitors before homing [1–3]. Unlike other immune cells, mature mast cells are only found in tissues, not in the blood. They are located at sites of the host–environment interface, such as the skin and the mucosa of the respiratory, urogenital, and gastrointestinal tract [1–4]. The normal human gastrointestinal tract contains numerous mast cells. The largest number is found in the *lamina propria*, where 2–3 % of the cells are mast cells [4]. According to their protease content, human mast cells have been divided into two subtypes, namely, cells containing both tryptase and chymase (MC_{TC}, similar to the so-called

connective tissue-type mast cells in rodents) and mast cells containing only tryptase (MC_T , similar to the so-called mucosal-type mast cells in rodents). Most of mast cells found in the *lamina propria* belong to the tryptase-positive, chymase-negative subtype (MC_T).

Mature mast cells are involved in physiological processes such as host defense against bacteria and tissue remodeling [1–5]. Apart from these functions, mast cells are known to be of particular importance in the pathophysiology of immediate-type allergic reactions and of other chronic inflammatory diseases. They exert their biological functions by releasing a broad array of mediators as a consequence of IgE-dependent and IgE-independent activation. These mediators are either preformed such as histamine, chymase, and tryptase and released from cytoplasmic granules or de novo synthesized such as various lipid compounds (leukotrienes and prostaglandins) with pleiotropic inflammatory and chemotactic functions as well as a number of cytokines, chemokines, and growth factors [1–3]. Cross-linking of the high-affinity IgE receptor (Fc ϵ RI) by receptor-bound IgE and antigen is the major trigger for mast cell activation [6]. In addition, particular cytokines such as the mast cell growth factor/stem cell factor (SCF) and IL-4 have been identified as important regulators of human mast cell function [7–13]. In the gut, mast cells interact with nerves and epithelial cells to regulate various physiological processes such as intestinal motility, intestinal permeability, or ion and fluid secretion. Furthermore, intestinal mast cells are involved in intestinal inflammation, e.g., in the course of allergic enteritis or IBD [4, 14, 15].

Most studies aimed to analyze mechanisms regulating mast cell-driven diseases or the physiological importance of mast cells have been performed in rodent mast cells. However, to understand how these responses pertain to human physiology or disease, human mast cell models are of particular interest. Because of the restricted Fc ϵ RI expression and the very low levels of proteases, human mast cell lines such as HMC-1 and LAD2 can serve as surrogates of tissue mast cells to a very limited degree only [16]. Thus, a number of systems have been developed to obtain sufficient quantities of primary human mast cells. The newly developed method for obtaining mast cells from human embryonic stem cells is not allowed in all countries [17]. Mast cells generated from immature precursors derived from peripheral blood or cord blood release the appropriate suite of inflammatory mediators in response to mast cell activators including antigen and are frequently used [18]. However, mast cells undergo their final phase of differentiation in the tissues and display functional diversity depending on the tissue in which they differentiate. We have established methods to isolate and purify human intestinal mast cells, providing a unique source of tissue-derived mature human mast cells. Similar methods have been used for the isolation of human mast cells from other organs such as the lung or the skin [19–21].

The following protocols describe the isolation of cells from the human intestinal mucosa by a combination of mechanical fragmentation and enzymatic digestion, the purification of mast cells by magnetic cell separation, and the culture of mast cells. Furthermore, we describe methods for the characterization of effector functions of human intestinal mast cells with the focus on mediator release, cytokine production, and activation of signaling molecules.

2 Materials

2.1 Cell Isolation

1. Shaking water bath (37 °C).
2. Tyrode's buffer: 137 mM NaCl, 2.7 mM KCl, 0.36 mM Na₂HPO₄, 5.55 mM glucose; adjust to pH 7.4 and store at 4 °C.
3. Tissue storage buffer: Tyrode's buffer, ampicillin 0.5 mg/mL, gentamicin 0.2 mg/mL, and metronidazole 0.2 mg/mL. Store at 4 °C.
4. TE buffer: Tyrode's buffer containing 2 mM ethylenediaminetetraacetic acid (EDTA); store at 4 °C.
5. TGMD buffer: Tyrode's buffer supplemented with gelatin (1 mg/mL) and 1.23 mM MgCl₂. Make fresh as required.
6. Enzyme solution PCh: 25 mL of TE buffer, 75 mg of pronase (*Roche Diagnostics*), and 13 mg of chymopapain (*Sigma-Aldrich*); make fresh as required.
7. Enzyme solution Co: 50 mL of TGMD buffer, 75 mg of collagenase NB 4G (*Serva*), 15 µg/mL DNase (*Roche Diagnostics*); make fresh as required.
8. GIBCO® Media RPMI 1640 with phenol red, GlutaMAX, and 25 mM HEPES (*Life Technologies*).
9. Culture medium: GIBCO® Media RPMI 1640 supplemented with 10 % (v/v) heat inactivated fetal calf serum (FCS), 100 µg/mL streptomycin, 100 µg/mL gentamicin, 100 U/mL penicillin, and 2.5 µg/mL amphotericin B.
10. Trypan blue.
11. May-Grünwald/Giemsa stain.
12. Giemsa (Azure Eosin Methylene Blue).
13. Tweezers and scissors, kept in sterile beaker with 70 % ethanol.
14. Bottle-top filter.
15. Nylon mesh, pore size 250 and 100 µm.
16. 50 mL conical tubes.
17. *N*-Acetyl-L-cysteine.

2.2 Purification of Intestinal Mast Cells

1. 80 cm² or 175 cm² cell culture flask.
2. Auto MACS Rinsing Solution (*Miltenyi Biotec*).
3. Bovine serum albumin (BSA).
4. Dead Cell Removal Kit (*Miltenyi Biotec*).
5. CD117 human MicroBead Kit directed against human *c-Kit* (*Miltenyi Biotec*).
6. MACS LS Columns (*Miltenyi Biotec*).
7. MidiMACS Separation Unit (*Miltenyi Biotec*).
8. MACS Multi Stand (*Miltenyi Biotec*).
9. Nylon mesh, pore size 30 µm.
10. Trypan blue, May–Grünwald/Giemsa stain, bottle-top filter, 50 mL conical tubes, culture medium (see Subheading 2.1).

2.3 Culture of Intestinal Mast Cells

1. CO₂ incubator.
2. Human recombinant SCF (rhSCF).
3. Human recombinant IL-4 (rhIL-4).
4. 6-, 12-, 24-, 48-, or 96-well flat-bottom plates.
5. Trypan blue, May–Grünwald/Giemsa stain, culture medium (see Subheading 2.1).

2.4 Stimulation of Intestinal Mast Cells and Measurement of Mediators and Signaling Molecules

1. Human myeloma IgE, antihuman IgE antibodies (provided by Dr. U. Blank, INSERM Unite 699, Paris, France) or antihuman Fc ϵ RI alpha antibodies or Ionomycin and PMA.
2. Stimulation buffer with 135 mM NaCl, 5 mM KCl, 5.6 mM glucose, 10 mM HEPES (pH 7.3), 1.8 mM CaCl₂, 1 mM MgCl₂, and 0.5 mg/mL BSA.
3. Citrate buffer: 0.05 M trisodium citrate-dihydrate dissolved in 50 mL bi-distilled water; adjust to pH 4.5.
4. 4-Nitrophenyl-N-acetyl- β -D-glucosaminide (pNAG) solution: 1.3 mg/mL pNAG in 0.05 M citrate buffer. Store at -20 °C.
5. Glycine buffer: 0.2 M glycine solution; adjust to pH 10.7 and store at 4 °C.
6. Extraction buffer: 25 mM Tris–HCl (pH 7.5), 0.5 mM EDTA, 0.5 mM EGTA, 0.05 % Triton X-100, 10 mM β -mercaptoethanol, supplemented with the protease inhibitor cocktail Complete™ Mini (*Roche Diagnostics*); make fresh as required.
7. RNeasy Mini Kit (*Qiagen*).
8. Histamine enzyme-linked immunosorbent assay (ELISA).
9. Cysteinyl leukotriene ELISA.
10. Cytokine ELISA.

11. Cytokine assays.
12. Proteome Profiler Array (*R&D Systems*).

2.5 Inhibition of Intracellular Proteins

1. Water bath.
2. Crushed ice.
3. Calcium-free Hanks' balanced salt solution (HBSS) with 30 mM HEPES; adjust to pH 7.0.
4. Streptolysin O.
5. Neutralizing antibodies.
6. RPMI containing 2 mM CaCl₂ and 10 % FCS.

3 Methods

3.1 Isolation of Cells from the Intestinal Mucosa

For the isolation of cells from the human intestinal mucosa, we use the modified four-step enzymatic tissue dispersion method originally described by Schulman et al. [19]. Other investigators have succeeded in isolating intestinal cells using simpler methods [22, 23]. In our hands, the method described here is superior in terms of cell yield, mast cell percentage, and cell integrity.

1. Obtain intestinal tissue from surgical specimens of patients who underwent bowel resection (*see Note 1*).
2. Wash specimen with water and remove adherent mesentery and fat from tissue using tweezers and scissors. Place specimen immediately in tissue storage buffer (*see Note 2*).
3. Separate mucosa from the submucosa/muscular layer using tweezers and scissors. Discard submucosa/muscularis.
4. Transfer mucosa to a 50 mL conical tube containing 30–40 mL of TE buffer + 1 mg/mL *N*-acetyl-L-cysteine. Incubate for 10 min in a shaking water bath at 37 °C. After incubation, agitate tube gently to remove mucus. Repeat **step 4** if mucus is not adequately removed.
5. Transfer mucosa in a 50 mL conical tube containing 30–40 mL of Tyrode's buffer + 5 mM EDTA. Incubate for 20 min in a shaking water bath at 37 °C. After incubation, agitate tube gently to remove epithelial cells and residual mucus.
6. Place tissue in a plastic Petri dish containing 15 mL TE buffer and cut with scissors into 1 mm³ pieces.
7. Place tissue suspension on a bottle-top filter containing nylon mesh with a pore size of 250 µm. Wash with 50 mL of TE buffer (*see Note 3*). Discard filtrate. Close the bottle-top filter with the stopper.
8. Suspend tissue in 25 mL of enzyme solution PCh and transfer suspension in a 50 mL conical tube. Incubate 30 min in a shaking

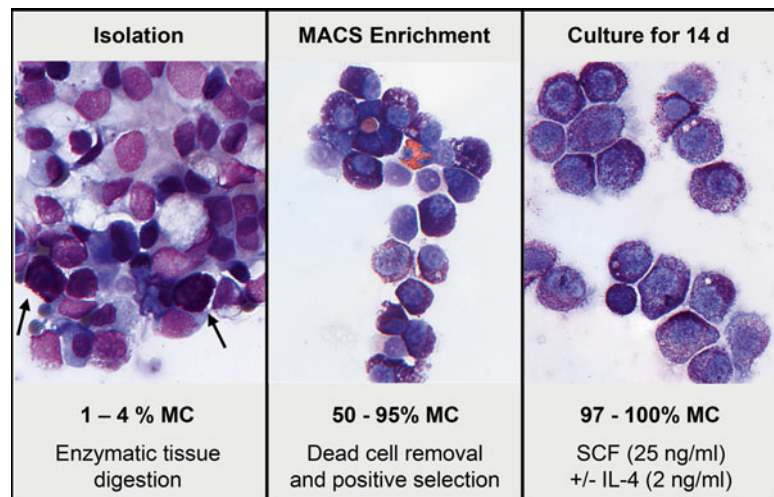


Fig. 1 May-Grünwald/Giemsa stain of cell fractions obtained after cell isolation (arrows, mast cells), MACS enrichment, and culture for 14 days (d) in the presence of SCF (25 ng/mL)

water bath at 37 °C. Filter as in **step 7** and wash with 50 mL of TGMD buffer. Discard filtrate.

9. Suspend tissue in 25 mL of enzyme solution Co and transfer suspension in a 50 mL conical tube. Incubate 30 min in a shaking water bath at 37 °C. Filter as in **step 7** and wash with 25 mL of TGMD buffer. Centrifuge filtrate ($300 \times g$, 10 min), remove supernatant, resuspend cells in 1–2 mL of cell culture medium, and place at 4 °C.
10. Repeat **step 9**.
11. Pool cells collected in **steps 9** and **10**, resuspend in 20 mL of RPMI, and filtrate through a bottle-top filter containing nylon mesh with a pore size of 100 µm. Wash with 30 mL of RPMI. Centrifuge ($300 \times g$, 10 min) and resuspend in 10 mL of culture medium.
12. Count the cells after staining with trypan blue. Prepare cytocentrifuge smears and stain with May-Grünwald/Giemsa to perform a differential count (see **Note 4**, Fig. 1).

3.2 Enrichment of Intestinal Mast Cells by Dead Cell Removal and Positive Selection Using Magnetic Cell Separation

Enrichment of human intestinal mast cells can be performed by using magnetic cell sorting (MACS). In general, mast cells are 50–75 % pure after positive sorting by immunomagnetic labeling of c-Kit. In some cell preparations, the purity can be greater than 90 %. Further purification, as much as 100 %, is possible by culture of the cells (see Subheading 3.3). Purification of mast cells can be achieved also by long-term culture of non-enriched cell fractions [24]. This approach has the advantage of higher cell numbers and a better culture sufficiency, but the purity is often poor and the

required culture period quite long. Thus, MACS is the method of choice for the purification of mast cells.

1. Culture freshly isolated intestinal cells at 4×10^6 /mL in culture medium for 1–2 h or overnight in 75 cm² (up to 1.2×10^8 cells) or 150 cm² (up to 2.5×10^8 cells) tissue culture flasks (see Note 5).
2. Harvest cells by gently shaking (see Note 6). Count after staining with trypan blue (see Note 7).
3. To remove clumps, pass cells through a 30 µm filter. Centrifuge cells ($300 \times g$, 10 min, 4 °C) and remove supernatant.
4. Resuspend cells in *Dead Cell Removal MicroBeads* solution (100 µL per 1×10^7 cells) and incubate for 15 min at room temperature (RT).
5. Place a positive selection column-type LS in the magnetic field of an appropriate MACS separator. Wash the column with 5 mL of 1× *Binding Buffer* according to the manufacturer's instructions. Discard eluate.
6. Give 1–10 mL of 1× *Binding Buffer* onto the cell suspension, mix gently, and apply the mixture onto the column.
7. Let the negative cells pass through and wash the column four times with 500 µL 1× *Binding Buffer*. Collect effluent as live cell fraction.
8. Count the cells after staining with trypan blue. Prepare cytocentrifuge smears and stain with May–Grünwald/Giemsa to perform a differential count.
9. Centrifuge cells, remove supernatant, and resuspend cells in *Auto MACS Rinsing Solution* (300 µL/10⁸ cells) and add 100 µL *FcR Blocking Reagent* (human IgG) and 100 µL of CD117 MicroBeads. Mix well, and incubate for 15 min in a refrigerator at 4 °C.
10. Wash cells with 10–20 mL of *Auto MACS Rinsing Solution* containing 5 mg/mL BSA, centrifuge, remove supernatant, and resuspend in *Auto MACS Rinsing Solution* containing 5 mg/mL BSA (1–2 mL) again.
11. Place a positive selection column-type LS in the magnetic field of an appropriate MACS separator. Wash with 5 mL *Auto MACS Rinsing Solution* containing 5 mg/mL BSA according to the manufacturer's instructions. Discard eluate.
12. Transfer cell suspension as many as 10^8 cells to the top of the MACS column (see Note 8). Once the cell suspension has completely entered, start washing the column with at least 10 mL *Auto MACS Rinsing Solution* containing 5 mg/mL BSA. Collect the effluent in a 50 mL conical tube (mast cell-depleted fraction).

13. Remove MACS column from the separator. Fill column with *Auto MACS Rinsing Solution* containing 5 mg/mL BSA (as much as 7 mL), firmly flush out the positive fraction using the supplied plunger, and collect cells in an appropriate tube.
14. Centrifuge cells and resuspend in culture medium. Count the cells after staining with trypan blue. Prepare cyt centrifuge smears and stain with May–Grünwald/Giemsa to perform a differential count (see Note 9, Fig. 1).

3.3 Culture of Intestinal Mast Cells

In the absence of growth factors, MACS-enriched mast cells die completely within 3–7 days. Long-term culture of human intestinal mast cells can be achieved in the presence of recombinant SCF preventing mast cell apoptosis and inducing proliferation [24, 25]. Additional factors such as IL-3 and IL-4 enhance mast cell growth in the presence of SCF by decreasing apoptosis (IL-3) or increasing proliferation (IL-4). In the absence of SCF, IL-4 has no effect and IL-3 has only a minimal effect on mast cell survival. The addition of IL-3, IL-4, or IL-3 + IL-4 to the culture medium in combination with SCF can enhance mast cell numbers after 2–3 weeks of culture approximately two-, three-, or fourfold, respectively, in comparison with mast cells cultured with SCF alone [8, 26].

The purity of mast cells largely increases during culture. If the mast cells are enriched by MACS before culture, purity is generally 85–95 % after 1 week and 95–100 % after 2 weeks of culture (Fig. 1).

Cultured mast cells release much higher amounts of mediators in response to Fc ϵ receptor I (Fc ϵ RI) cross-linking than freshly isolated mast cells, which is most likely related to the fact that the isolation and purification procedure causes a reversible damage of the cells that reduces their functional capacities. During culture, mast cells regain the full capacity to respond to Fc ϵ RI cross-linking. This suggests that cultured mast cells reflect more accurately the phenotype of mast cells *in vivo* than freshly isolated mast cells [8, 24, 25].

1. Culture mast cells in culture medium. Adjust the cell concentration to $1\text{--}2 \times 10^5$ mast cells/mL for MACS-enriched cells or to 2×10^6 of total cells/mL for unpurified cells. Culture of intestinal mast cells can be performed in 96-, 48-, 24-, 12-, or 6-well flat-bottomed plates in 0.2, 0.5, 1, 2, or 5 mL of cell culture medium, respectively (see Note 10).
2. Add SCF at a concentration of 25 ng/mL. If required, add other cytokines (see Note 11).
3. Maintain cells in a humidified atmosphere containing 5 % CO₂ at 37 °C.
4. Change 50 % of the culture medium twice during the first week and then once a week thereafter. Add new growth factors each time.
5. Subculture cells if required (see Note 12).

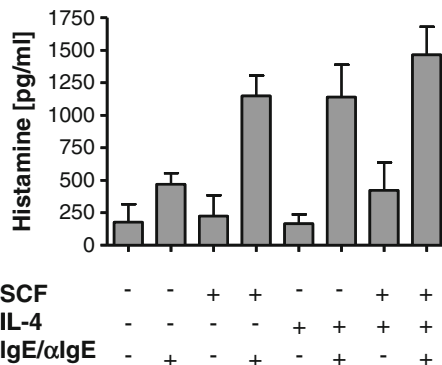


Fig. 2 Combined activation by Fc ϵ RI cross-linking, SCF stimulation, or IL-4 priming induces potentiated release of histamine in human intestinal mast cells. Mast cells were cultured with SCF alone or with IL-4 (+) in addition to SCF for 10 days (d). SCF was withdrawn overnight and cells were treated with myeloma IgE for 90 min and stimulated with antihuman IgE (IgE/αIgE) (+), SCF (+) or a combination of both

6. After an appropriate culture period (see text above), harvest mast cells by gently mixing with a pipette. Count the cells after staining with trypan blue. Prepare cytocentrifuge smears and stain with May-Grünwald/Giemsa to perform a differential count.

3.4 Mediator Release and Cytokine Production in Human Intestinal Mast Cells

The procedure of isolation, purification, and culture of mast are powerful methods to obtain pure tissue-derived mature human mast cells. These cells can be used to identify mast cell mediators and to study both the mechanisms of mast cell activation and signal transduction as well as the molecular process of exocytosis during mediator release in response to specific stimuli. For the study of mast cell mediator release and cytokine production in response to cell activation, we have been using protocols optimized to use as small cell numbers as possible. Figure 2 shows that combined activation by Fc ϵ RI cross-linking, SCF stimulation, or IL-4 priming induce potentiated release of inflammatory mediators such as histamine in human intestinal mast cells [13].

Stimulation Assay for the Study of Expression and Release of Mediators and Activation of Signaling Molecules

1. Wash mast cells twice in PBS (see Note 13).
2. Resuspend mast cells in stimulation buffer (50–1,000 μ L per condition as required), and transfer them into appropriate tubes (see Note 14).
3. Prepare cell lysates for the detection of total β -hexosaminidase or histamine (see Subheading “Preparation of Mast Cell Lysates”).
4. Incubate tubes at 37 °C for 10 min without agonists.
5. Add trigger/agonist of interest (e.g., for Fc ϵ RI cross-linking add IgE (1 μ g/mL)) and incubate at 37 °C for 90 min. Leave control untreated or add appropriate isotype control.

6. Wash cell suspension two times with PBS (discard supernatant) and resuspend cells in stimulation buffer.
7. Add anti-IgE and incubate at 37 °C for 10 min to determine phosphorylation status of signaling molecules, for 90 min to analyze the mRNA expression of cytokines/chemokines, or for 6 h to examine the release of cytokines/chemokines (see Note 15).
8. Harvest cells after time of interest and transfer them to an RNase free 1.5 mL microfuge tube. Centrifuge cells (300 $\times g$, 10 min, 4 °C) and collect supernatants. Store aliquots at -80 °C. Resuspend pellet immediately in RLT buffer provided by the RNeasy Mini Kit to isolate total RNA and to determine mRNA expression by real-time reverse transcription polymerase chain reaction. Resuspend pellet immediately in extraction buffer to analyze protein expression or activation by SDS-PAGE and Western blot (see Note 16).
9. Measure mediators of interest in the supernatants by β -hexosaminidase release assay (see Subheading “ β -Hexosaminidase Release Assay”), appropriate ELISA, or multiplex bead immunoassay according to the manufacturer’s instructions and using an appropriate *cytokine assay*. Dilution of samples might be required (in particular for histamine). Calculate degranulation as: (β -hexosaminidase activity in the supernatant fraction/total β -hexosaminidase activity in the cellular and supernatant fraction) \times 100. Assay mRNA levels by real-time reverse transcription polymerase chain reaction. Analyze cell protein extracts by SDS-PAGE and Western blot or *Proteome Profiler Arrays*.

Preparation of Mast Cell Lysates

1. Place 100 μ L of the cell suspension in an appropriate tube and add 100 μ L of water.
2. Freeze cell suspension at -80 °C.
3. Before determination of mediators, thaw suspension and sonicate for 3–5 min.
4. Centrifuge cell debris down and use supernatant for analysis.

β -Hexosaminidase Release Assay

1. Place 50 μ L of pNAG solution in a well of a 96-well plate.
2. Add 20 μ L of supernatant or cell lysates of 1×10^6 stimulated cells/mL to the well and incubate for 90 min at 37 °C.
3. After incubation stop reaction by adding 150 μ L of glycine buffer.
4. Determine optical density with a photometer at $\lambda=405$ nm.

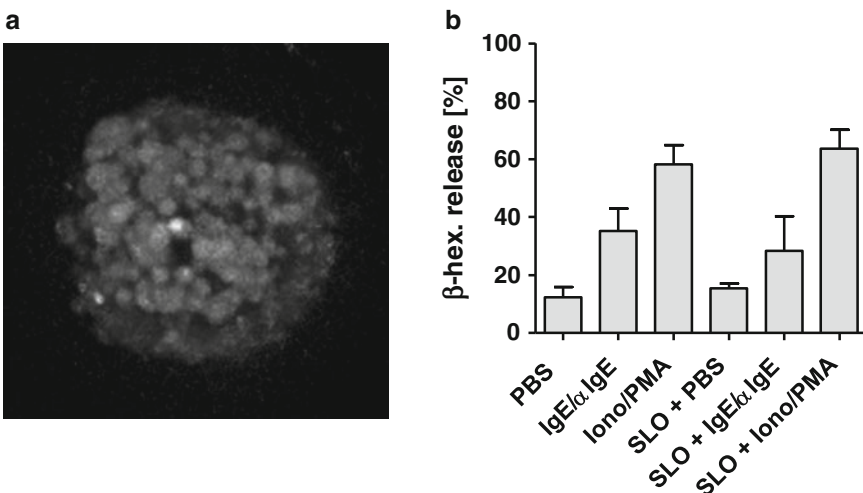


Fig. 3 Staining of intracellular vesicle-associated membrane protein (VAMP)-3 after SLO treatment (a) and β -hexosaminidase (β -hex) release in response to Fc ϵ RI cross-linking (IgE/αIgE) or to Ionomycin (Iono)/PMA (each 1 μ M) following SLO treatment (b)

Inhibition of Intracellular Proteins Prior to Cell Activation

Inhibition of proteins is required to show their functional impact. We used an alternative approach to gene silencing (see Note 17) by administration of specific neutralizing antibodies to analyze the role of soluble *N*-ethylmaleimide-sensitive factor attachment protein receptors (SNAREs) in mast cell mediator release [27, 28]. Antibodies directed against different SNARE isoforms recognize cytoplasmic NH₂-terminal region required for SNARE binding. The bacterial-derived toxin streptolysin O (SLO) allows a temporary permeabilization of vital cells in a dose-dependent manner to deliver antibodies [29]. Figure 3 shows that SLO treatment allows intracellular vesicle staining (a) but does not affect responsiveness of the cells after activation by Fc ϵ RI cross-linking or administration of Ionomycin and PMA (b).

1. Wash cells with calcium-free HBSS and transfer into appropriate tubes.
2. Add SLO at concentrations yielding approximately 60–80 % trypan blue staining of the cells (20–40 μ g/mL) and the neutralizing antibodies at 20 μ g/mL.
3. Incubate at 37 °C for 15 min in a water bath.
4. Stop the reaction and seal the pores by addition of at least threefold ice cold RPMI medium containing 2 mM CaCl₂ and 10 % FBS (3:1) and incubate on ice for 60 min.
5. Centrifuge the cell suspension, discard the supernatant, and resuspend the cells in appropriate buffer.
6. Go on performing the stimulation assay.

4 Notes

1. Tissue can be obtained from all parts of the bowel. Most specimens we have obtained have come from patients who underwent resection because of large bowel cancer.
2. Tissue can be stored at 4 °C overnight, although immediate processing is preferential. In our hands, numbers and viability of isolated mast cell are only slightly impaired after overnight storage of the tissue specimen.
3. Tissue suspension needs to be stirred using tweezers or with other appropriate instruments to avoid obstruction of the filter. If residual mucus completely clogs the mesh, transfer tissue suspension to a new bottle-top filter.
4. Approximately $1\text{--}2.5 \times 10^7$ cells can be obtained from 1 g of mucosal tissue. As much as 10 g can be used in one preparation. If more tissue is available, perform two (or more) preparations in parallel. Normally isolated cells contain 1–4 % mast cells, but the percentage can be higher in selected patients. Cell preparations contain 10–40 % erythrocytes, which has to be taken in account by calculating mast cell numbers.
5. Do not add SCF to the culture medium because it downregulates *c-Kit* in mast cells and, therefore, diminishes the enrichment efficiency and recovery.
6. Mast cells are semi-adherent. Cells can be harvested by resuspending the cells with the pipet only.
7. Normally, 20–50 % of the cells are trypan positive after overnight culture (mast cell survival is generally higher). If more than 60 % of the cells are trypan positive, we do not recommend performing a positive selection by MACS because the enrichment efficiency and mast cell recovery will be very low.
8. Although it is passed through a 30 µm filter, the cell suspension might obstruct the MACS column, which is related to the high amount of cell clumps and residual mucus. We recommend applying cells in small fractions of 1–2 mL. In the case of obstruction, remove the rest of the cell suspension on the top of the column and replace it with 2 mL of MACS buffer. The obstruction can be overcome by pulling up and down the buffer with a pipet. Continue with this column as recommended in the protocol. For the remaining cells, use a new column.
9. Metachromatic staining of mast cells after MACS is sometimes poor, and exact quantification is difficult. Generally, between 0.5 and 3×10^6 mast cells can be obtained from 5 to 10 g of mucosa.
10. More than the half of the MACS-enriched cell preparation dies completely within the first days of culture. This may be related to the damage of the cells acquired during the cell separation.

11. To obtain high amounts of pure mast cells, we recommend adding IL-4 at a concentration of 2 ng/mL (in combination with SCF) to the culture. Keep in mind that IL-4 changes the mast cell phenotype [8, 9, 13] (Fig. 2). IL-4 can be added at the beginning of the culture or later. The *IL-4 phenotype* will be obtained after 1–2 weeks.
12. In some cultures mast cells proliferate strongly in particular if IL-4 is added to the culture medium. Proliferation will stop if mast cell numbers exceed $0.5\text{--}1 \times 10^6/\text{mL}$. Then, split cells in a new culture plate.
13. Washing of cultured mast cells is very important because culture supernatants contain high amounts of histamine.
14. For the measurement of β -hexosaminidase, histamine, or LTC₄ after Fc ϵ RI cross-linking, cell concentrations $0.5\text{--}1 \times 10^6$ cells/mL are used. We perform experiments in 50–100 μL in tubes. For the measurement of cytokines after Fc ϵ RI cross-linking, cell concentrations 1×10^6 cells/mL are used. We perform experiments in 100–300 μL in tubes or in a 96 or 48 or 24-well plate. For mRNA studies, we use at least 8×10^4 mast cells/condition (preferable is 1×10^5).
15. For the analysis of mRNA induction for most cytokines upon Fc ϵ RI cross-linking, the optimal time point is 90 min. Upregulation of mRNA is still detectable after 6 h. To measure cytokines in the supernatants, we recommend incubation periods of 6 h or longer. If you wish to analyze only degranulation and eicosanoid production, stimulation for 30–60 min is enough. We usually stop the reaction after 30 min in a standard assay for the investigation of degranulation and eicosanoid production in response to Fc ϵ RI cross-linking. For histamine, approximately 3–5 min and for leukotrienes approximately 10–15 min are required for maximal release [7]. Degranulation and eicosanoid release can also be studied after longer stimulation time such as 6 h. Because of longer incubation time, spontaneous histamine release is higher and eicosanoids might be partly degraded.
16. For the analysis of protein expression or activation, at least 2×10^5 cells/condition are lysed in 50 μL extraction buffer. Cell debris should be pelleted ($14,000 \times g$ for 5 min at 4 °C) and supernatants stored at –80 °C until used for analysis.
17. We undertook extensive efforts to transfet primary human mast cells with siRNA. In contrast to SLO permeabilization, the cells must be viable for at least 48–72 h if not longer after transfection to block the transcription of the corresponding proteins. We tested a number of different transfection systems either without seeing efficient transfection or the transfection was accompanied by a loss of responsiveness to cell activation.

Acknowledgments

The authors thank all former and current colleagues and in particular C. A. Dahinden, K. Wordelmann, S. Schwengberg, C. T. Mierke, G. Weier, T. Gebhardt, L. E. Sander, S. P. Frank, A. Mrasori, K. Feuser, and Y. Soltow who were involved in establishing the methods described here.

References

1. Bischoff SC (2007) Role of mast cells in allergic and non-allergic immune responses: comparison of human and murine data. *Nat Rev Immunol* 7:93–104
2. Kalesnikoff J, Galli SJ (2008) New developments in mast cell biology. *Nat Immunol* 9:1215–1223
3. Galli SJ, Grimaldston M, Tsai M (2008) Immunomodulatory mast cells: negative, as well as positive, regulators of innate and acquired immunity. *Nat Rev Immunol* 8: 478–486
4. Bischoff SC (2009) Physiological and pathophysiological functions of intestinal mast cells. *Semin Immunopathol* 31:185–205
5. Marshall JS (2004) Mast cell responses to pathogens. *Nat Rev Immunol* 4:787–799
6. Rivera J, Gilfillan AM (2006) Molecular regulation of mast cell activation. *J Allergy Clin Immunol* 117:1214–1225
7. Bischoff SC, Dahinden CA (1992) c-Kit ligand: a unique potentiator of mediator release by human lung mast cells. *J Exp Med* 175:237–244
8. Bischoff SC, Sellge G, Lorentz A, Sebald W, Raab R, Manns MP (1999) IL-4 enhances proliferation and mediator release in mature human mast cells. *Proc Natl Acad Sci U S A* 96:8080–8085
9. Lorentz A, Schwengberg S, Sellge G, Manns MP, Bischoff SC (2000) Human intestinal mast cells are capable of producing different cytokine profiles: role of IgE receptor cross-linking and IL-4. *J Immunol* 164:43–48
10. Babina M, Guhl S, Starke A, Kirchhof L, Zuberbier T, Henz BM (2004) Comparative cytokine profile of human skin mast cells from two compartments strong resemblance with monocytes at baseline but induction of IL-5 by IL-4 priming. *J Leukoc Biol* 75:244–252
11. Hundley TR, Gilfillan AM, Tkaczyk C, Andrade MV, Metcalfe DD, Beaven MA (2004) Kit and Fc ϵ RI mediate unique and convergent signals for release of inflammatory mediators from human mast cells. *Blood* 104:2410–2417
12. Lorentz A, Wilke M, Sellge G, Worthmann H, Klempnauer J, Manns MP, Bischoff SC (2005) IL-4 induced priming of human intestinal mast cells for enhanced survival and Th2 cytokine generation is reversible and associated with an increased activity of ERK1/2 and c-Fos. *J Immunol* 174:6751–6756
13. Feuser K, Feilhauer K, Staib L, Bischoff SC, Lorentz A (2011) Akt crosslinks IL-4 priming, stem cell factor signaling, and IgE dependent activation in mature human mast cells. *Mol Immunol* 48:546–552
14. Lorentz A, Schwengberg S, Mierke C, Manns MP, Bischoff SC (1999) Human intestinal mast cells produce IL-5 in vitro upon IgE receptor cross-linking and in vivo in the course of intestinal inflammatory disease. *Eur J Immunol* 29:1496–1503
15. He SH (2004) Key role of mast cells and their major secretory products in inflammatory bowel disease. *World J Gastroenterol* 10: 309–318
16. Guhl S, Babina M, Neou A, Zuberbier T, Artuc M (2010) Mast cell lines HMC-1 and LAD2 in comparison with mature human skin mast cells—drastically reduced levels of tryptase and chymase in mast cell lines. *Exp Dermatol* 19:845–847
17. Kovarova M, Latour AM, Chason KD, Tilley SL, Koller BH (2010) Human embryonic stem cells: a source of mast cells for the study of allergic and inflammatory diseases. *Blood* 115:3695–3703
18. Rådinger M, Jensen BM, Kuehn HS, Kirshenbaum A, Gilfillan AM (2010) Generation, isolation, and maintenance of human mast cells and mast cell lines derived from peripheral blood or cord blood. *Curr Protoc Immunol Chapter 7:Unit 7.37*

19. Schulman ES, Macglashan DW, Peters SP, Schleimer RP, Newball HH, Lichtenstein LM (1982) Human lung mast cells: purification and characterization. *J Immunol* 129: 2662–2667
20. Gibbs BF, Wierecky J, Welker P, Henz BM, Wolff HH, Grabbe J (2001) Human skin mast cells rapidly release preformed and newly generated TNF-alpha and IL-8 following stimulation with anti-IgE and other secretagogues. *Exp Dermatol* 10:312–320
21. Kulka M, Metcalfe DD (2010) Isolation of tissue mast cells. *Curr Protoc Immunol Chapter 7:Unit 7.25*
22. Befus AD, Dyck N, Goodacre R, Bienenstock J (1987) Mast-cells from the human intestinal lamina propria—isolation, histochemical subtypes, and functional-characterization. *J Immunol* 138:2604–2610
23. Lowman MA, Rees PH, Benyon RC, Church MK (1988) Human mast cell heterogeneity: histamine release from mast cells dispersed from skin, lung, adenoids, tonsils, and colon in response to IgE-dependent and nonimmunologic stimuli. *J Allergy Clin Immunol* 81:590–597
24. Bischoff SC, Schwengberg S, Raab R, Manns MP (1997) Functional properties of human intestinal mast cells cultured in a new culture system: enhancement of IgE receptor-dependent mediator release and response to stem cell factor. *J Immunol* 159:5560–5567
25. Bischoff SC, Sellge G, Schwengberg S, Lorentz A, Manns MP (1999) Stem cell factor-dependent survival, proliferation and enhanced releasability of purified mature mast cells isolated from human intestinal tissue. *Int Arch Allergy Immunol* 118:104–107
26. Gebhardt T, Sellge G, Lorentz A, Raab R, Manns MP, Bischoff SC (2002) Cultured human intestinal mast cells express functional IL-3 receptors and respond to IL-3 by enhancing growth and IgE receptor-dependent mediator release. *Eur J Immunol* 32:2308–2316
27. Sander LE, Frank SP, Bolat S, Blank U, Galli T, Bigalke H, Bischoff SC, Lorentz A (2008) Vesicle associated membrane protein (VAMP)-7 and VAMP-8, but not VAMP-2 or VAMP-3, are required for activation-induced degranulation of mature human mast cells. *Eur J Immunol* 38:855–863
28. Frank SP, Thon KP, Bischoff SC, Lorentz A (2011) SNAP-23 and syntaxin-3 are required for chemokine release by mature human mast cells. *Mol Immunol* 49(1–2):353–358
29. Walev I, Bhakdi SC, Hofmann F, Djondor N, Valeva A, Aktories K, Bhakdi S (2001) Delivery of proteins into living cells by reversible membrane permeabilization with streptolysin-O. *Proc Natl Acad Sci U S A* 98:3185–3190

Chapter 12

Human Mast Cell Activation with Viruses and Pathogen Products

Ian D. Haidl and Jean S. Marshall

Abstract

Mast cells have been demonstrated to have critical roles in host defense against a number of types of pathogens. In order to better understand how mast cells participate in effective immune responses, it is important to evaluate their ability to respond directly to pathogens and their products. In the current chapter we provide a methodology to evaluate human mast cell responses to a number of bacterial and fungal pathogen products and to mammalian reovirus as a model of acute viral infection. These methods should provide key information necessary to aid in the effective design of experiments to evaluate human mast cell responses to a number of other organisms. However, it is important to carefully consider the biology of the mast cell subsets and pathogens involved and the optimal experimental conditions necessary to evaluate mediators of interest.

Key words Mast cell, Cytokine, Leukotriene, Inflammation, Innate immunity, Pattern recognition receptor

1 Introduction

Mast cells are often located at sites that act as an interface with our environment such as the skin, airways, and intestine. Traditionally, mast cells have been primarily studied as effector cells in allergic disease. However, their wide range of products and ability to produce both preformed and lipid mediators within minutes of activation makes them excellent sentinel cells, contributing to the very earliest stages of innate host defense (reviewed in refs. 1, 2). Mast cell-derived chemokines [3–6] and lipid mediators, together with proteases [7–9] and histamine [10, 11], are thought to be important for the selective recruitment of appropriate effector cells to combat several types of infection. Mast cell-derived TNF has also been shown to be critical for host defense through multiple mechanisms [12–15]. Other mast cell-derived cytokines, such as IL-6, may have a key role in both innate immune function and the generation of acquired immune responses [16–22], particularly

through interactions with dendritic cells and modulation of lymph node hypertrophy [23]. As infection or injury resolves, mast cells also participate in tissue remodeling events. Determining the nature of human mast cell responses in vitro to bacteria, viruses, and their products has provided important clues to the in vivo role of mast cells in mobilizing early host defense and in establishing optimal long-term effective immunity. In the current chapter, we will discuss current effective methods and models for examining human mast cell responses to pathogens and pathogen products.

In order to most effectively apply the methods we will describe for assessment of mast cell activity, it is important to have an appreciation of the complexity of the current state of knowledge of human mast cell responses. Overwhelming evidence has accumulated in recent years describing a critical role for mast cells in host defense against infection. Early reports of such activity were confined to host defense against parasites, such as nematodes [24, 25], and these activities have been confirmed in more recent elegant studies that demonstrate mast cells can reduce the burden of both primary and secondary nematode infections [26, 27]. In this context, mast cell's release of preformed mediators, such as granule-associated proteases, has been shown to be of particular importance [27–32]. During the 1990s we became aware of the ability of mast cells to respond to bacterial products such as LPS [19, 33–36] and the critical role of mast cells, through TNF and other mediator production, to participate in host defense against a number of bacterial infections in vivo [14, 15, 37]. These studies demonstrated that the presence of mast cells was essential for survival following certain bacterial challenges in mice. More recent studies have identified that mast cells can be activated by bacteria and fungi through numerous pattern recognition receptors including Toll-like receptors (TLR) and NOD-like receptors (NLR) as well as numerous other receptors such as lectin-like receptors [38] and complement receptors [39–43]. Of these receptor pathways, the TLRs have been most extensively studied with evidence that human mast cells can express TLR1, TLR2, TLR3, TLR4, TLR5, TLR6, TLR7, TLR8, and TLR9 [19, 33–35, 44–46]. However, the full profile of TLRs may not be expressed in all mast cell types, and the levels of TLR protein expression are often very low. For example, some types of primary cultured human mast cells require the addition of IL-4 to the culture medium to express significant levels of TLR4 [33], and there is some controversy as to the functional levels of TLR3 and TLR9 expressed by primary human mast cells and mast cell lines. NLRs including Nod1, Nod2, and NLRP3 are expressed in mast cells. Activation of NLR can result in direct cytokine production and/or potentiation of TLR-induced cytokine production [16, 47–49]. Furthermore, dysregulated or mutant NLR expression in mast cells plays a role in diseases such as Crohn's disease and histamine-independent urticaria [48, 49]. It is likely

that the expression of each of these types of receptors is modulated in vivo by the tissue microenvironment, including the presence of inflammatory mediators.

As might be expected from their wide range of mediator production and multiple pathogen product and immunoglobulin receptors, mast cells have several distinct roles in host defense. Direct antibacterial effects of mast cells are thought to include the generation of reactive oxygen species [50–55] and, more controversially, the generation of reactive nitrogen species [56–59]. Mast cells are very effective in the phagocytosis of yeast and bacteria [60–63]. In some mast cell-rich sites, such as the skin and urogenital tract, this mechanism might be of in vivo importance. Direct responses to virus infection include the production of type 1 interferons [45, 64], which can enhance the antiviral state of neighboring cells as well as strengthen other aspects of early immunity. While such direct mechanisms may be important in the mast cell response to selected pathogens, a potentially more important response to a wider range of pathogens is the mast cell-dependent, selective recruitment of appropriate effector cells. Early studies of mast cell-dependent antibacterial responses revealed the critical importance of mast cell-derived TNF in neutrophil recruitment in bacterial infections. This is most likely due to enhanced adhesion molecule expression and function of vascular endothelium following local mast cell activation by bacterial products. More recently, LTB₄ has been shown to be important for the recruitment of certain T cell subsets [65] in addition to its ability to induce the migration of neutrophils. In the context of viral infection, mast cells have also been shown to produce mediators capable of activating vascular endothelial cells such as IL-1 and TNF [66]. In addition, mast cell-dependent NK cell and CD56-positive T cell recruitment responses have been noted in vitro using human mast cells [6], while in animal models of viral infection, mast cell-dependent CD8-positive T cell, NK cell, and NKT cell recruitment has been observed [6, 67, 68]. In the case of NK cells, the mast cell-mediated recruitment of human NK cells appears to be highly dependent upon virus-induced CXCL8 [6] while CD56-positive T cell responses are dependent upon other chemokine receptors. However, we are probably only just beginning to understand the impact of mast cells on effector cell recruitment, since mast cells produce specific profiles of chemokines in response to different organisms. For example, while most viral infections of human mast cells lead to the increased production of CCL5, only certain viruses have been shown to induce substantial CXCL8 responses.

In addition to the impacts of mast cells on innate immune function, mast cells also influence the development and activity of the acquired immune response. These effects occur at several levels. Mast cells have been shown to be important in the initial lymph node response to infection and can enhance the process whereby T cells

and B cells accumulate in nodes draining inflamed or infected sites [23, 69–73]. Mast cells can also contribute to the mobilization of dendritic cell subsets, such as Langerhans cells and plasmacytoid dendritic cells, from both the tissue and the blood stream following a challenge with bacterial products [23]. A number of more direct effects of mast cells on T cell function and development have also been reported. Mast cells have been reported to influence the development of contact hypersensitivity responses [74–78], graft rejection [79–81], and the outcome of immunization [82, 83]. It remains to be seen how much these and other interactions between mast cells and T cells impact the outcome of human infections. However, work from animal models suggests that such mechanisms might be particularly important in the skin and in modifying responses to antigens provided at mucosal sites. Understanding such interactions, which may either enhance or inhibit T cell-mediated activity *in vivo* (reviewed in ref. 84), will be extremely important in helping to define the ability of mast cells to modify T cell-mediated responses in response to infection or in inflammatory disease.

Several cellular models have been used to examine human mast cell responses to pathogens. Ideally, mast cells obtained directly from human tissues should be used for such studies. However, since mast cells are not found in the blood, there is limited availability of tissues for such procedures. Relatively low numbers of cells can be obtained at high purity from some tissues, and there is substantial heterogeneity in response between mast cells from different tissue sites. Harsh enzymatic treatments are required to obtain mast cells from most relevant tissue, which means that cells often have to be cultured for a period of time after purification in order to regain their full functional capacity. Such culture may further modify their responses to pathogens and their products. For these reasons, many laboratories have chosen to use primary cultured human mast cells to evaluate mast cell responses to infection and pathogen products. These can be derived using published methods from bone marrow [85, 86], from umbilical cord blood [87, 88], or from isolated CD34-positive (CD34⁺) stem cells obtained from peripheral blood [89–92]. These mast cells are well granulated, express a wide range of mast cell surface markers such as Fc ϵ RI and c-Kit, and have a range of protease content including tryptase alone (MC_T) and both tryptase and chymase (MC_{TC}).

As an alternative for certain types of experiments, where very large numbers of mast cell are required or when even very low numbers of contaminating cells could interfere with interpretation, various mast cell lines have been widely used. HMC-1 is an immature mast cell line that is easy to grow in culture but is poorly granulated and in most laboratories does not express relevant amounts of Fc ϵ RI [93–95]. KU812 cells were originally described as an immature basophil cell line and express Fc ϵ RI [96, 97].

These cells can be differentiated in culture [98] to express a wider range of mast cell characteristics including tryptase-containing granules. The more recently described LAD2 cells have proven to be a better mast cell line for many studies [99]. These cells require SCF supplementation, which can be costly, and grow relatively slowly in culture. However, they share more of the characteristics of primary human tissue-derived mast cells than either HMC-1 or differentiated KU812 cells. In general, however, it is good practice to confirm the key results obtained with any of the mast cell lines with either primary cultured human mast cells or with tissue-derived human mast cells.

In the sections below, the methodology for evaluating human mast cell responses to a number of specific pathogens and pathogen products are described. Many of these methods can be easily adapted for alternate organisms and potential mast cell activators. However, each pathogen or product might require consideration of specific pathogen growth requirements or co-receptors (e.g., CD14) that might be essential *in vitro* in order to best mimic the potential interactions observed in the context of host defense *in vivo*.

2 Materials

All cells, materials, and viruses should be handled and stored according to local biosafety regulations. The use of primary cells from human subjects should receive approval from the appropriate local ethical committee(s).

2.1 Cells and Cell Lines

1. Human cord blood-derived mast cells (CBMC) are differentiated from the mononuclear cells obtained from umbilical cord blood as described below.
2. The HMC-1 cell line is an immature mast cell line that produces chemokines/cytokines in response to pathogen products but is poorly granulated. Some subclones have been reported to express low levels of Fc ϵ RI [93, 95].
3. KU812 (ATCC® CRL-2099™) is a human immature mast cell/basophil line that also produces cytokines in response to pathogen products or infection [4, 100]. KU812 cells can also be differentiated to achieve a more mature, granulated phenotype [98].

2.2 Cell Culture

High-quality reagents from commercial suppliers should be used for mast cell culture medium, and care should be taken to avoid endotoxin contamination of any materials.

1. HMC-1 cell culture medium: IMDM, 10 % fetal bovine serum (FBS), 10 mM HEPES.
2. HMC-1 activation medium: IMDM, 1 % FBS, 10 mM HEPES.

3. KU812 cell culture medium: RPMI 1640, 10 % FBS, 10 mM HEPES.
4. KU812 activation medium: RPMI 1640, 1 % FBS, 10 mM HEPES.
5. CBMC differentiation medium [88]: RPMI 1640 supplemented with 20 % supernatant from CCL-204 cells (source of IL-6), PGE₂ (3.4×10^{-7} M), 20 % FBS, human stem cell factor (SCF) (75 ng/mL), 10 mM HEPES, penicillin/streptomycin. Recombinant human (rh) IL-6 (10 ng/mL) may be used in place of CCL-204 supernatant.
6. CBMC resting medium: RPMI 1640, 20 % FBS, 10 ng/mL SCF, 20 % CCL-204 conditioned medium (or 10 ng/mL rhIL-6), 10 mM HEPES, pen/strep. Do not add PGE₂.
7. CBMC activation medium: RPMI 1640, 1 % FBS, 10 mM HEPES, 10 ng/mL SCF.

2.3 Pathogen Products

Components of bacterial, viral, and fungal pathogens that activate mast cells can be purified from the respective organisms or purchased from commercial sources. Brief sonication of pathogen products may be necessary to disperse aggregates formed by their lipophilic and/or multimolecular structures (*see Note 1*).

1. Lipopeptides: For our studies of TLR2-mediated mast cell activation, we have used synthetic versions of di- and triacyl lipopeptides (FSL-1 and Pam₃CSK₄, respectively).
 - (a) Resuspend FSL-1 to 1 mg/mL in endotoxin-free water. Sonicate for 1 min on ice and aliquot into sterile endotoxin-free tubes. Store at -80 °C.
 - (b) Resuspend Pam₃CSK₄ to 5 mg/mL in endotoxin-free water. Sonicate for 1 min on ice and aliquot into sterile endotoxin-free tubes. Store at -80 °C.
2. Peptidoglycan (PGN): PGN can be purchased commercially, although it is important to assess the potential endotoxin contamination in each batch (*see Note 2*).
 - (a) Resuspend the PGN to 5 mg/mL in endotoxin-free water. Sonicate for 1 min on ice and aliquot into sterile endotoxin-free tubes. Store at -80 °C.
3. dsRNA: To address mechanisms of mast cell activation by viruses, we have used the dsRNA analog, polyinosinic/poly-cytidylic acid (poly (I:C)), which can activate TLR3 and cytosolic pattern recognition receptors such as RIG-I [45, 101]. It is important to select the appropriate size of poly(I:C) for the activation pathway you are interested in. In some cases, the poly(I:C) may need to be transfected into cells for maximal effectiveness (*see Note 3*).

- (a) Resuspend the poly(I:C) to 5 mg/mL in endotoxin-free water and aliquot into sterile endotoxin-free tubes. Store at -80 °C.
- 4. Ca²⁺ ionophore: As a positive control for mast cell activation, the calcium ionophore A23187 can be used. Prepare a 1×10^{-2} M stock solution in DMSO and store in aliquots at -20 °C. A final concentration of 5×10^{-7} M is used for activation in cytokine/chemokine production, degranulation, and leukotriene production.

2.4 Viruses

- 1. *Reovirus*: Reovirus is a non-enveloped dsRNA virus that is typically associated with subclinical enteric infection. Reovirus is able to infect and replicate in a wide range of cells making it a useful virus for comparing responses in a variety of cells, including mast cells. We have used the reovirus serotype 3 Dearing to infect CBMC and determine which chemokines/cytokines are produced [6]. High titer stocks ($1-5 \times 10^{10}$ (plaque-forming units) PFU/mL) can be prepared and stored at 4 °C [102].
 - (a) HMC-1 wash medium: IMDM with 10 mM HEPES.
 - (b) KU812 and CBMC wash medium: RPMI 1640 with 10 mM HEPES.
- 2. *Other viruses*. Other virus models with more direct clinically relevant insights into the response of mast cells to virus infection can also be investigated. For example, dengue virus type 2 (strain 16681), respiratory syncytial virus (RSV), and HIV have been employed in human systems, and Newcastle disease virus has been used in mice. Dengue virus is an enveloped single-stranded RNA (positive) virus that causes dengue hemorrhagic fever and dengue shock syndrome. RSV is an enveloped single-stranded RNA (negative) virus that is a major cause of respiratory tract infections in infants and young children. Care must always be taken to use appropriate biocontainment and related safety procedures for the specific pathogen being studied.

2.5 Mediator Assays

Chemokine Arrays

Initially, a broad screening tool should be used to identify the chemokines/cytokines produced by mast cells in response to pathogen products or virus infection. There are a variety of commercially available systems including bead-based immunoassays, microchip protein arrays, and membrane-based protein arrays. We have used membrane-based microarrays from RayBiotech for the initial screening of supernatants from human and mouse mast cell activations [6, 103]. We have also employed mRNA array analysis following pathogen or pathogen product activation of mast cells, which also allows for the evaluation of changes in the mRNA expression of signaling molecules and pathogen sensors.

Table 1
Examples of reagents/conditions used to detect chemokines/cytokines by ELISA

Chemokine/ cytokine	Source	Coating Ab (μg/mL)	Detection Ab (ng/mL)	Standard range (ng/mL)
CCL4	R&D	1	50	15.6–1,000
CCL5	PeproTech	1	100	4.1–3,000
CXCL8	R&D	1	20	5.5–4,000
CXCL10	PeproTech	2	100	5.5–4,000
IL-1 β	R&D	1	150	3.9–250
IL-6	PeproTech	1	100	5.5–4,000
GM-CSF	PeproTech	1	100	5.5–4,000
TNF	R&D	4	350	15.6–1,000

ELISA

Once the number of chemokines/cytokines has been narrowed down, ELISA can be used to sensitively quantify individual mast cell products. Antibody pairs for the majority of cytokines/chemokines are commercially available. Table 1 lists some of the chemokine/cytokine ELISAs that we most commonly perform and the antibody pairs we use. Store the antibody aliquots at –20 °C or –80 °C and aliquots of the standards at –80 °C. We also use the Invitrogen ELISA Amplification System to increase the sensitivity of most ELISA assays.

In addition to the commercially supplied antibodies, standards, and solutions, purchase or prepare the following:

1. Flat-bottom 96-well immunoassay plates (e.g., Nunc MaxiSorp).
2. Coating buffer: 0.1 M NaHCO₃, 0.5 M NaCl, pH 8.5 in water.
3. Wash buffers: 0.05 % Tween-20 in PBS and TBS.
4. Blocking buffer: 2 % BSA in PBS.
5. Assay buffer: 0.2 % BSA, 0.05% Tween-20 in PBS.
6. Stop solution: 0.3 M H₂SO₄ in water.

Degranulation

The degree of mast cell degranulation from pure mast cell populations can be measured by quantifying the amount of the granule-associated enzyme, β -hexosaminidase, that is released into the supernatant after activation. The following reagents are required:

1. Flat-bottom 96-well immunoassay plates (e.g., Nunc MaxiSorp).
2. 0.1 M citrate buffer pH 4.5: 0.053 M citric acid, 0.047 M sodium citrate.
3. 1 mM p-nitrophenyl-n-acetyl- β -D-glucosaminide (pNAG) in 0.1 M citrate buffer.

4. 0.1 M carbonate buffer, pH 10.5: 0.08 M Na_2CO_3 , 0.02 M NaHCO_3 .
5. HEPES Tyrode's Buffer (HTB), pH 7.35: 0.14 M NaCl, 5.6 mM glucose, 0.1 % BSA, 10 mM HEPES, 1.4 mM KCl, 1.0 mM $\text{CaCl}_2 \cdot 2\text{H}_2\text{O}$, 0.35 mM $\text{NaH}_2\text{PO}_4 \cdot \text{H}_2\text{O}$. Initially add water to 80 % of the final volume, adjust the pH to 7.35, and measure the osmolality. To achieve a final osmolality of 300 mOsm, add 1.24 mL water per 1 mOsm over 300 mOsm.

Leukotriene Production

1. IMDM, 0.1 % BSA.
2. Leukotriene (LTC_4 and LTB_4) detection kits (Cayman Chemical Company) (*see Note 4*).

3 Methods

3.1 Mast Cell Culture

We utilize CBMC as our primary cell culture model of mast cells. Others have described methods to derive mast cells from peripheral blood or bone marrow CD34^+ progenitors [86, 104, 105]. To test responses to pathogen products and viral infection of mast cell lines, we have also utilized the HMC-1 and KU812 cell lines that are readily grown in cell culture as indicated.

CBMC Derivation and Culture

A more detailed description of CBMC culture can be found in Radinger et al. [89]. Our culture method is similar to that of Saito et al. [106].

1. Dilute heparinized cord blood 1:1 with PBS, layer onto Ficoll-Paque and then centrifuge at $400 \times g$ for 20 min at 20 °C.
2. Harvest the cells at the interface and then wash twice with 50 mL PBS (centrifuge at $300 \times g$ for 5 min at 4 °C).
3. Culture cells in CBMC differentiation medium in a humidified 5 % CO_2 incubator (37 °C) at a density of $0.5\text{--}1.0 \times 10^6$ cells/mL for 6–12 weeks. Change CBMC differentiation medium once per week.
4. Use cells for experiments when greater than 95 % of culture stains positive with Toluidine blue.

HMC-1 Culture

1. Rapidly thaw a frozen vial of HMC-1 at 37 °C. Add 10 mL HMC-1 medium and then pellet cells in a centrifuge ($300 \times g$, 5 min, room temperature (RT)).
2. Resuspend the pellet in 10 mL HMC-1 medium and count the cells. Adjust density to 1×10^5 cells/mL with HMC-1 medium. Add the cells to an appropriately sized flask and culture in a humidified 5 % CO_2 incubator at 37 °C. Do not allow the cell density to exceed 2×10^6 cells/mL.

- Passage the cells every 3–4 days. Pipette up and down to remove the semi-adherent cells prior to counting. Dilute the cells in fresh medium to 1×10^5 cells/mL.

KU812 Cells

- Rapidly thaw a frozen vial of KU812 cells at 37 °C and add 10 mL KU812 medium. Pellet cells in a centrifuge (300×*g*, 5 min, RT).
- Resuspend the pellet in 10 mL KU812 medium, count, and adjust the cells to 1×10^5 cells/mL. Add the cells to an appropriately sized flask and culture in a humidified 5 % CO₂ incubator at 37 °C. Do not allow the cell density to exceed 2×10^6 cells/mL.
- Passage the cells every 3–4 days. Dilute the cells in a fresh medium to 1×10^5 cells/mL.

3.2 Activation of Mast Cells with Pathogen Products

Chemokine/Cytokine Production

- Cultured HMC-1 and KU812 do not normally require serum or factor deprivation prior to simulation with pathogen products.
- For CBMC cells, culture overnight (~16 h) in CBMC resting medium containing a lower concentration of SCF (10 ng/mL) and without PGE₂ prior to activation experiments.

- Wash the cells twice with 25 mL of the appropriate activation medium (see Note 5). Centrifuge CBMC at 200×*g*, 10 min, 4 °C and HMC-1 or KU812 at 300×*g*, 5 min, 4 °C.
- Resuspend CBMC to 2×10^6 /mL or HMC-1 and KU812 cells to 1×10^6 /mL in the appropriate activation medium (see Note 6).
- Prepare dilutions of the pathogen products at 2× of the final concentration in the respective activation medium (e.g., for Pam₃CSK₄ prepare 20 µg/mL for activation at 10 µg/mL).
- Combine an equal volume of cells and pathogen product in an appropriately sized multi-well plate. Culture in a humidified 5 % CO₂ incubator at 37 °C for 6 h to detect early chemokines/cytokines such as TNF or 24 h for most other chemokines and cytokines.
- Harvest the supernatants by pelleting the cells. Centrifuge CBMC at 200×*g*, 10 min, 4 °C and HMC-1 or KU812 at 300×*g*, 5 min, 4 °C. Aliquot the supernatants into convenient volumes and store at -20 °C or -80 °C for protein arrays or ELISA analyses (see Note 7).

Degranulation

Since HMC-1 and KU812 are poorly granulated, mast cell degranulation in response to pathogen products is better assayed with CBMC. More granulated cell lines such as LAD2 have also been reported to give strong degranulation responses [107, 108].

- Wash the CBMC twice with 25 mL ice-cold HTB. Centrifuge the cells at 200×*g*, 10 min, 4 °C.
- Resuspend CBMC to 2×10^6 /mL in ice-cold HTB.

3. Prepare dilutions of the pathogen products at 2 \times of the final concentration in HTB (e.g., for Pam₃CSK₄ prepare 20 μ g/mL for activation at 10 μ g/mL).
4. Pre-warm the cells and pathogen products to 37 °C. Combine an equal volume of cells and pathogen product in a 1.5 mL microfuge tube. Incubate at 37 °C for 20 min.
5. Harvest the supernatants by pelleting CBMC at 200 \times g, 5 min, 4 °C. Resuspend the pellet in an equal volume of fresh HTB. Vortex to resuspend the pellet and snap-freeze at -80 °C or with liquid nitrogen. Thaw the frozen cells and repeat the freeze/thaw cycle twice more. Analyze immediately for β -hexosaminidase activity or store the supernatants and lysates at -20 °C or -80 °C.

Leukotriene Production

Since HMC-1 and KU812 produce very low amounts of leukotrienes, the production of leukotrienes by mast cells in response to pathogen products is best assayed with CBMC.

1. Wash the CBMC twice with 25 mL IMDM, 0.1%BSA. Pellet the cells at 200 \times g, 10 min, 4 °C.
2. Resuspend CBMC to 2 \times 10⁶/mL in IMDM containing 0.1 % BSA.
3. Prepare dilutions of the pathogen products at 2 \times of the final concentration in IMDM, 0.1 % BSA (e.g., for Pam₃CSK₄ prepare 20 μ g/mL for activation at 10 μ g/mL).
4. Pre-warm the cells and pathogen products to 37 °C. Combine an equal volume of cells and pathogen product in a U-bottom 96-well plate or 1.5 mL microfuge tube. Incubate at 37 °C for 20 min.
5. Harvest the supernatants by centrifuging CBMC at 200 \times g, 5 min, 4 °C. Analyze immediately for leukotrienes (e.g., LTC₄ or LTB₄) or store the supernatants at -80 °C (see Note 8).

3.3 Virus Infection of Mast Cells

Cultured HMC-1, KU812, and CBMC (overnight in resting medium) are ready for virus infection. Similar to the variations described above for pathogen products, the virus infection protocols vary depending on the type of response being assayed (chemokine/cytokine production, degranulation, or leukotriene production). Although a detailed protocol for the culture and preparation of viral stocks is beyond the scope of this chapter which focused on mast cells, we have provided an example protocol for reovirus infection of mast cells (see Note 9).

Chemokine/Cytokine Production

1. Wash the cells twice with 25 mL of the appropriate wash medium. Centrifuge CBMC at 200 \times g, 10 min, 4 °C and HMC-1 or KU812 at 300 \times g, 5 min, 4 °C.
2. Resuspend the cells to 5 \times 10⁶/mL in wash medium. Add 20 ng/mL SCF to CBMC.
3. Prepare ultraviolet radiation (UV)-inactivated reovirus by exposing the virus to 6 \times 10⁶ μ J/cm² UV light on ice in a Stratalinker.

To achieve a multiplicity of infection (MOI) of 20 (viral particles per cell), dilute live and UV-inactivated reovirus to 1×10^8 PFU/mL in wash medium.

4. Combine washed cells with an equal volume of medium only (mock), UV-inactivated reovirus, or live reovirus in a 15 mL centrifuge tube. Incubate at 37 °C for 60 min with shaking every 10 min.
5. Wash the cells twice with 15 mL of the appropriate wash medium. Centrifuge CBMC at $200 \times g$, 10 min, 4 °C and HMC-1 or KU812 at $300 \times g$, 5 min, 4 °C.
6. Resuspend CBMC to 1×10^6 /mL or HMC-1 and KU812 cells to 0.5×10^6 /mL in the same wash medium supplemented with 1 % FBS (and 10 ng/mL SCF for CBMC). Transfer the cells to an appropriately sized tissue culture plate.
7. Culture in a humidified 5 % CO₂ incubator at 37 °C for 6 h to detect early chemokines/cytokines such as TNF or 24 h for most chemokines/cytokines.
8. Harvest the supernatants by pelleting CBMC at $200 \times g$, 10 min, 4 °C and HMC-1 or KU812 at $300 \times g$, 5 min, 4 °C. UV-inactivate the supernatants immediately by exposing to 6×10^6 µJ/cm² UV light on ice in a Stratalinker. Aliquot the supernatants into convenient volumes and store at -20 °C or -80 °C for protein arrays or ELISA analyses.

Degranulation

Since HMC-1 and KU812 are poorly granulated, mast cell degranulation in response to viruses is best assayed with CBMC. More granulated cell lines such as LAD2 have also been reported to give strong degranulation responses [107, 109, 110].

1. Wash the CBMC twice with 25 mL HTB. Centrifuge the cells at $200 \times g$, 10 min, 4 °C.
2. Resuspend CBMC to 2×10^6 /mL in HTB.
3. Prepare UV-inactivated reovirus by exposing the virus to 6×10^6 µJ/cm² UV light in a Stratalinker. To achieve a multiplicity of infection (MOI) of 20, dilute live and UV-inactivated reovirus to 1×10^8 PFU/mL in HTB.
4. Pre-warm the cells and virus to 37 °C. Combine cells with an equal volume of HTB (mock) or HTB containing UV-inactivated reovirus or live reovirus in a 1.5 mL microfuge tube. Incubate at 37 °C for 60 min with gentle shaking every 10 min.
5. Harvest the supernatants by centrifuging CBMC at $200 \times g$, 5 min, 4 °C. Resuspend the pellet in a volume of fresh HTB equal to the activation volume. UV-inactivate the supernatants and pellets immediately by exposing the virus to 6×10^6 µJ/cm² UV light on ice in a Stratalinker. To lyse the cells in the pellets,

vortex to resuspend the cells and snap-freeze at -80°C or with liquid nitrogen. Thaw the frozen cells and repeat the freeze/thaw cycle twice more. Analyze immediately for β -hexosaminidase activity or store the supernatants and pellets at -20°C or -80°C .

Leukotriene Production

Since HMC-1 and KU812 produce very low amounts of leukotrienes, the production of leukotrienes by mast cells in response to viruses is best assayed with CBMC.

1. Wash the CBMC twice with 25 mL IMDM, 0.1 % BSA. Centrifuge the cells at $200 \times g$, 10 min, 4°C .
2. Resuspend CBMC to $2 \times 10^6/\text{mL}$ in IMDM, 0.1 % BSA, 20 ng/mL SCF.
3. Prepare UV-inactivated reovirus by exposing the virus to $6 \times 10^6 \mu\text{J}/\text{cm}^2$ UV light in a Stratalinker. To achieve a multiplicity of infection (MOI) of 20, dilute live and UV-inactivated reovirus to $1 \times 10^8 \text{ PFU}/\text{mL}$ in IMDM, 0.1 % BSA.
4. Pre-warm the cells and virus to 37°C . Combine an equal volume of cells and IMDM, 0.1 % BSA (mock), UV-inactivated reovirus, or live reovirus in a U-bottom 96-well plate or 1.5 mL microfuge tube. Incubate at 37°C for a series of time points between 15 and 60 min with gentle shaking every 10 min.
5. Harvest the supernatants by centrifuging CBMC at $200 \times g$, 5 min, 4°C . Since leukotrienes are sensitive to UV light, the samples must be analyzed without UV inactivation. *Therefore, all wash solutions in the assay should be treated as infectious waste.* Analyze immediately for leukotrienes (e.g., LTC₄ or LTB₄) or store the supernatants at -80°C .

3.4 Mediator Assays

Protein Arrays

1. Thaw the mast cell activation supernatants to be tested, including the test sample and control supernatants (e.g., reovirus, mock, and UV-inactivated virus) (*see Note 10*).
2. Incubate the blocked membranes with 1 mL of supernatants overnight at 4°C on a rocker.
3. Following the wash steps, add the biotinylated anti-chemokine/cytokine antibodies to the membrane and incubate again overnight at 4°C on a rocker.
4. Wash the membranes and incubate with SA-HRP for 2 h at RT on a rocker.
5. Wash membranes and then apply substrate for chemiluminescence-based detection. Acquire a range of exposures to ensure that the detected signals are not saturated.
6. Analyze using commercial image analysis software.

ELISA

Table 1 lists some details about chemokine/cytokine ELISAs that we most commonly perform. We typically perform duplicates of the standards and samples.

1. Prepare the diluted capture Ab at the correct concentration in freshly made coating buffer and add 50 μ L/well in a 96-well ELISA plate.
2. Seal the plate with parafilm and incubate overnight at 4 °C.
3. Prepare the blocking buffer.
4. Wash plates by quickly inverting and flicking the plate to remove the coating Ab. Tap the inverted plate forcefully onto a stack of paper towels to remove any remaining fluid. Fill the wells with wash buffer (200 μ L or more per well) and repeat the inverting/flicking/tapping sequence to thoroughly wash the wells.
5. Add 200 μ L of blocking buffer to each well. Incubate for at least 2 h at RT.
6. Prepare dilutions of the samples and standards in activation medium (e.g., RPMI with 1 % FBS and 10 mM HEPES) (*see Note 11*).
7. After blocking, wash 2 \times with wash buffer as described in **step 4**.
8. Add 50 μ L of the samples and standards to the wells, seal the plate with parafilm, and incubate overnight at 4 °C.
9. Prepare the biotinylated detection antibody at the appropriate concentration in assay buffer.
10. Wash the plate three times with wash buffer as described in **step 4**.
11. Add 50 μ L of the diluted detection antibody to each well and incubate for 2 h at RT.
12. Prepare a 1/2,000 dilution of the streptavidin-conjugated alkaline phosphatase (SA-AP) (Invitrogen ELISA Amplification System) in assay buffer.
13. Wash the plate three times with wash buffer as described in **step 4**.
14. Add 50 μ L of the diluted SA-AP to each well.
15. Incubate for 30 min at RT.
16. Prepare the substrate and amplifier components (Invitrogen ELISA Amplification System).
17. Wash the plate three times with TBS with 0.05 % Tween-20 as described in **step 4**.
18. Add 50 μ L of the substrate solution per well and incubate for 30 min at RT. Add 50 μ L of amplifier solution and incubate

until the standard curve shows the detection of low concentrations without overdeveloping the higher concentrations (typically 5–30 min).

19. Add 50 μ L of the stop solution to each well and read the plate at 490 nm.
20. Plot the results to attain the standard curve and calculate the cytokine/chemokine concentration in the samples.

Degranulation

1. Thaw the supernatant and lysate samples. Vortex and then pellet samples at $12,000 \times g$ (approximately 1 min at RT) to remove any debris.
2. Transfer 50 μ L samples of supernatant and lysate in duplicate to a flat-bottomed 96-well ELISA plate. Use HTB as a blank.
3. Add 50 μ L of 1 mM pNAG to each well and incubate for 1 h at 37 °C.
4. Add 200 μ L of 0.1 M carbonate buffer to each well and read the plate at 405 nm.
5. Calculate the extent of degranulation: $(A_{405\text{ supernatant}} - A_{405\text{ blank}}) / ((A_{405\text{ supernatant}} - A_{405\text{ blank}}) + (A_{405\text{ lysate}} - A_{405\text{ blank}}))$

Leukotriene Detection

1. Add 50 μ L of standards or samples in duplicate to the appropriate wells. Add 50 μ L of the acetylcholinesterase-labeled leukotriene and 50 μ L of the antileukotriene Ab (see **Note 12**).
2. Seal the plate and incubate overnight at 4 °C.
3. Wash the plate 5 times and prepare one vial of the Ellman's reagent provided (Ellman's reagent contains the acetylcholinesterase substrate).
4. Add 200 μ L Ellman's reagent to each well and develop for 90–120 min with shaking in the dark.
5. Read the plate between 405 and 420 nm (optimum $\lambda = 412$ nm).
6. Plot the results to attain the standard curve and calculate the leukotriene levels in the samples.

The methods provided above provide an outline of the protocols necessary to evaluate the responses of human mast cells to pathogens and pathogen products. Similar techniques can be used in many cases on mast cells derived from other species. However, care needs to be taken in all these studies to consider the variability of mast cell subsets derived from different sources and the nature of the infection. Consideration of the clinical features and course of infection as well as animal data from infections in mast cell-containing and mast cell-deficient mice can provide important insights into the potential role of mast cells and the most appropriate experimental design strategy.

4 Notes

1. Sonication is required to maximize the effectiveness and improve the reproducibility of responses to many pathogen products that are provided in particulate form or which are lipophilic (e.g., Pam_3CSK_4). Use of a probe sonicator is recommended, but the probe should be treated with 5N NaOH and rinsed with endotoxin-free water to remove endotoxin. Care must be taken to prevent overheating the sample during sonication, for example, by use of an ice bath. Appropriate ear protection should always be used when sonicating.
2. Endotoxin contamination is a particular problem when using pathogen products and recombinant materials for mast cell activation. It can easily be introduced into reagents if sufficient care is not taken to avoid the use of washed glass containers and pipettes and to avoid contact with contaminated materials and equipment. The endotoxin content of all reagents should be assessed using commercial endotoxin assays. In some cases, treatment of reagents with polymyxin B beads can help reduce endotoxin content sufficiently.
3. Poly (I:C) responses are highly dependent upon the length and 5' phosphorylation of the poly (I:C) preparations employed [111]. Care should be taken to select a poly (I:C) product that is known to activate the RNA sensor or TLR pathways of interest. For most poly (I:C) activations transfection of the double-stranded RNA analog using standard techniques (such as Lipofectamine) will give a stronger response than extracellular poly (I:C) treatment. However, the appropriate method of poly (I:C) exposure and the best type to use is dependent upon the questions being addressed by the experiment. For transfection-based treatments, control transfections are essential for effective interpretations of the results obtained.
4. Mast cells can produce leukotriene(s) within 5 min after activation. We utilize leukotriene assays from Cayman Chemical Company for the detection of LTC₄ (Cat#520211) and LTB₄ (Cat#520111). We have also used the anti-LTC4 mAb 6E7 in a modified ELISA protocol [112] to quantitate LTC₄ production.
5. It is important to carefully consider the FBS concentration used for activation. A number of cytokine responses (e.g., IL-6) are serum dependent, and serum factors can be important to provide cofactors for pathogen product signaling (e.g., LPS binding protein and soluble CD14). However, too high a concentration of serum can lead to high “background” levels of production of some chemokines (e.g., CXCL8). If supernatants are to be used directly in bioassays, such as chemotaxis

assays, high serum concentrations may also be inappropriate. The choice of FCS concentration may range from 10 % for some types of experiments to <1 % for others and needs to be carefully considered when designing experiments.

6. In general, for cytokine analyses we will set up CBMC at a concentration of 1 million cells per mL. However, if more rapidly dividing cells such as HMC-1 or KU812 cells are used for these experiments, they are usually used at a lower concentration, such as 0.5 million per mL, so that they do not become too crowded by the end of a 24 h incubation period.
7. The protocol for activations does not vary substantially between different pathogen products, except for the concentrations used. Care needs to be taken in considering the need for potential cofactors for certain activators (e.g., soluble CD14) and the stability of products in serum-containing media. However, the protocols do vary depending on the type of response being assayed (chemokine/cytokine production, degranulation, or leukotriene production). For functional assays, such as cell chemotaxis, further adjustments to activation protocols may be required.
8. Some leukotrienes, such as LTC₄, are extremely labile. Samples should be either assayed immediately following harvest or stored, in the dark, at -80 °C and carefully thawed for analysis. Snap freezing of samples following activation is recommended if they are going to be stored. Peptidases, present in serum, can enhance the degradation process for cysteinyl leukotrienes so serum should be omitted, or at least kept to a minimum, for analysis of lipid mediator production.
9. In addition to reovirus, other viruses can be used to infect mast cells. For example, we have used dengue virus and respiratory syncytial virus (RSV) to infect mast cells [4, 100]. Dengue virus and RSVs are more labile than reovirus, are more difficult to propagate, and have lower rates of infection but are more clinically relevant viruses. Each virus will require an optimization of infection conditions, MOI, and kinetics of infection. For example, dengue virus infection of CD209-negative mast cells requires anti-dengue virus antibody-enhanced conditions [4, 100, 113] unless extremely high doses of virus are employed that would not likely be observed *in vivo*.
10. The antibody arrays from RayBiotech contain all the reagents necessary to perform the cytokine/chemokine detection. The detection can be performed according to the manufacturer's instructions and is therefore not described in detail here. When performing RayBiotech and similar arrays, although they contain internal controls, our experience is that the control and test (activated/infected) samples need to be both run and

developed in parallel for effective comparison. There can be considerable day-to-day and batch-to-batch variation in control and background readings between membranes developed at different times, even if very similar conditions are employed.

11. We typically do two dilutions for each sample that are tenfold different (e.g., 1/3 and 1/30). This assists in the interpretation of a wider range of cytokine/chemokine responses; however, where possible, responses should be compared at the same dilution.
12. We typically do two dilutions for each sample that are tenfold different (e.g., 1/2 and 1/20) in IMDM + 0.1 % BSA. As mentioned above, we are currently using commercially available assays from Cayman Chemical Company to determine the levels of LTC₄ and LTB₄ produced by CBMC. These are competition-based assays in which the LTC₄ or LTB₄ in the samples inhibits the binding of acetylcholinesterase-labeled LTC₄ or LTB₄. Therefore, the amount of acetylcholinesterase retained in each well is inversely proportional to the amount of LTC₄ or LTB₄ present in each sample.

References

1. Galli SJ, Tsai M (2010) Mast cells in allergy and infection: versatile effector and regulatory cells in innate and adaptive immunity. *Eur J Immunol* 40:1843–1851
2. Marshall JS (2004) Mast-cell responses to pathogens. *Nat Rev Immunol* 4:787–799
3. Lin TJ, Maher LH, Gomi K, McCurdy JD, Garduno R, Marshall JS (2003) Selective early production of CCL20, or macrophage inflammatory protein 3alpha, by human mast cells in response to *Pseudomonas aeruginosa*. *Infect Immun* 71:365–373
4. King CA, Anderson R, Marshall JS (2002) Dengue virus selectively induces human mast cell chemokine production. *J Virol* 76: 8408–8419
5. Specht S, Frank JK, Alferink J, Dubben B, Layland LE, Denece G, Bain O, Forster I, Kirschning CJ, Martin C, Hoerauf A (2011) CCL17 controls mast cells for the defense against filarial larval entry. *J Immunol* 186: 4845–4852
6. Burke SM, Issekutz TB, Mohan K, Lee PW, Shmulevitz M, Marshall JS (2008) Human mast cell activation with virus-associated stimuli leads to the selective chemotaxis of natural killer cells by a CXCL8-dependent mechanism. *Blood* 111:5467–5476
7. Huang C, De Sanctis GT, O'Brien PJ, Mizgerd JP, Friend DS, Drazen JM, Brass LF, Stevens RL (2001) Evaluation of the substrate specificity of human mast cell tryptase beta I and demonstration of its importance in bacterial infections of the lung. *J Biol Chem* 276:26276–26284
8. Thakurdas SM, Melicoff E, Sansores-Garcia L, Moreira DC, Petrova Y, Stevens RL, Adachi R (2007) The mast cell-restricted tryptase mMCP-6 has a critical immunoprotective role in bacterial infections. *J Biol Chem* 282:20809–20815
9. Caughey GH (2011) Mast cell proteases as protective and inflammatory mediators. *Adv Exp Med Biol* 716:212–234
10. Arizmendi-Puga NG, Enciso JA, Ortega-Pierres G, Zhao Z, Duszyk M, Ulanova M, Befus AD, Yepez-Mulia L (2006) *Trichinella spiralis*: histamine secretion induced by TSL-1 antigens from unsensitized mast cells. *Exp Parasitol* 114:67–76
11. Hosoda M, Yamaya M, Suzuki T, Yamada N, Kamanaka M, Sekizawa K, Butterfield JH, Watanabe T, Nishimura H, Sasaki H (2002) Effects of rhinovirus infection on histamine and cytokine production by cell lines from human mast cells and basophils. *J Immunol* 169:1482–1491
12. Piliponsky AM, Chen CC, Grimaldeston MA, Burns-Guydish SM, Hardy J, Kalesnikoff J, Contag CH, Tsai M, Galli SJ (2010) Mast cell-derived TNF can exacerbate mortality during severe bacterial infections in C57BL/

6-KitW-sh/W-sh mice. *Am J Pathol* 176: 926–938

13. Furuta T, Kikuchi T, Iwakura Y, Watanabe N (2006) Protective roles of mast cells and mast cell-derived TNF in murine malaria. *J Immunol* 177:3294–3302
14. Malaviya R, Ikeda T, Ross E, Abraham SN (1996) Mast cell modulation of neutrophil influx and bacterial clearance at sites of infection through TNF-alpha. *Nature* 381:77–80
15. Maurer M, Echtenacher B, Hultner L, Kollrias G, Mannel DN, Langley KE, Galli SJ (1998) The c-kit ligand, stem cell factor, can enhance innate immunity through effects on mast cells. *J Exp Med* 188:2343–2348
16. Haidl ID, McAlpine SM, Marshall JS (2011) Enhancement of mast cell IL-6 production by combined toll-like and nucleotide-binding oligomerization domain-like receptor activation. *Int Arch Allergy Immunol* 154:227–235
17. Sutherland RE, Olsen JS, McKinstry A, Villalta SA, Wolters PJ (2008) Mast cell IL-6 improves survival from Klebsiella pneumonia and sepsis by enhancing neutrophil killing. *J Immunol* 181:5598–5605
18. Mrabet-Dahbi S, Metz M, Dudeck A, Zuberbier T, Maurer M (2009) Murine mast cells secrete a unique profile of cytokines and prostaglandins in response to distinct TLR2 ligands. *Exp Dermatol* 18:437–444
19. McCurdy JD, Olynich TJ, Maher LH, Marshall JS (2003) Cutting edge: distinct Toll-like receptor 2 activators selectively induce different classes of mediator production from human mast cells. *J Immunol* 170: 1625–1629
20. Chung SW, Wong PM, Shen-Ong G, Ruscetti S, Ishizaka T, Eaves CJ (1986) Production of granulocyte-macrophage colony-stimulating factor by Abelson virus-induced tumorigenic mast cell lines. *Blood* 68:1074–1081
21. Chiba N, Masuda A, Yoshikai Y, Matsuguchi T (2007) Ceramide inhibits LPS-induced production of IL-5, IL-10, and IL-13 from mast cells. *J Cell Physiol* 213:126–136
22. Helmby H, Gencis RK (2003) Contrasting roles for IL-10 in protective immunity to different life cycle stages of intestinal nematode parasites. *Eur J Immunol* 33:2382–2390
23. Dawicki W, Jawdat DW, Xu N, Marshall JS (2010) Mast cells, histamine, and IL-6 regulate the selective influx of dendritic cell subsets into an inflamed lymph node. *J Immunol* 184:2116–2123
24. Moqbel R, Wakelin D, MacDonald AJ, King SJ, Gencis RK, Kay AB (1987) Release of leukotrienes during rapid expulsion of *Trichinella spiralis* from immune rats. *Immunology* 60:425–430
25. Woodbury RG, Miller HR, Huntley JF, Newlands GF, Palliser AC, Wakelin D (1984) Mucosal mast cells are functionally active during spontaneous expulsion of intestinal nematode infections in rat. *Nature* 312:450–452
26. Pennock JL, Gencis RK (2006) The mast cell and gut nematodes: damage and defence. *Chem Immunol Allergy* 90:128–140
27. McDermott JR, Bartram RE, Knight PA, Miller HR, Garrod DR, Gencis RK (2003) Mast cells disrupt epithelial barrier function during enteric nematode infection. *Proc Natl Acad Sci U S A* 100:7761–7766
28. Hashimoto K, Uchikawa R, Tegoshi T, Takeda K, Yamada M, Arizono N (2010) Immunity-mediated regulation of fecundity in the nematode *Heligmosomoides polygyrus*—the potential role of mast cells. *Parasitology* 137:881–887
29. Knight PA, Brown JK, Wright SH, Thornton EM, Pate JA, Miller HR (2007) Aberrant mucosal mast cell protease expression in the enteric epithelium of nematode-infected mice lacking the integrin alphavbeta6, a transforming growth factor-beta1 activator. *Am J Pathol* 171:1237–1248
30. Onah DN, Uchiyama F, Nagakui Y, Ono M, Takai T, Nawa Y (2000) Mucosal defense against gastrointestinal nematodes: responses of mucosal mast cells and mouse mast cell protease 1 during primary *Strongyloides venezuelensis* infection in FcRgamma-knockout mice. *Infect Immun* 68:4968–4971
31. Donaldson LE, Schmitt E, Huntley JF, Newlands GF, Gencis RK (1996) A critical role for stem cell factor and c-kit in host protective immunity to an intestinal helminth. *Int Immunol* 8:559–567
32. Miller HR, Woodbury RG, Huntley JF, Newlands G (1983) Systemic release of mucosal mast-cell protease in primed rats challenged with *Nippostrongylus brasiliensis*. *Immunology* 49:471–479
33. Varadarajalou S, Feger F, Thieblemont N, Hamouda NB, Pleau JM, Dy M, Arock M (2003) Toll-like receptor 2 (TLR2) and TLR4 differentially activate human mast cells. *Eur J Immunol* 33:899–906
34. Supajatura V, Ushio H, Nakao A, Okumura K, Ra C, Ogawa H (2001) Protective roles of mast cells against enterobacterial infection are mediated by Toll-like receptor 4. *J Immunol* 167:2250–2256
35. McCurdy JD, Lin TJ, Marshall JS (2001) Toll-like receptor 4-mediated activation of murine mast cells. *J Leukoc Biol* 70: 977–984
36. Leal-Berumen I, Conlon P, Marshall JS (1994) IL-6 production by rat peritoneal mast

cells is not necessarily preceded by histamine release and can be induced by bacterial lipopolysaccharide. *J Immunol* 152:5468–5476

37. Echtenacher B, Mannel DN, Hultner L (1996) Critical protective role of mast cells in a model of acute septic peritonitis. *Nature* 381:75–77
38. Olynch TJ, Jakeman DL, Marshall JS (2006) Fungal zymosan induces leukotriene production by human mast cells through a dectin-1-dependent mechanism. *J Allergy Clin Immunol* 118:837–843
39. Wojta J, Kaun C, Zorn G, Ghannadan M, Hauswirth AW, Sperr WR, Fritsch G, Printz D, Binder BR, Schatzl G, Zwirner J, Maurer G, Huber K, Valent P (2002) C5a stimulates production of plasminogen activator inhibitor-1 in human mast cells and basophils. *Blood* 100: 517–523
40. Werfel T, Oppermann M, Begemann G, Gotze O, Zwirner J (1997) C5a receptors are detectable on mast cells in normal human skin and in psoriatic plaques but not in weal and flare reactions or in urticaria pigmentosa by immunohistochemistry. *Arch Dermatol Res* 289:83–86
41. Werfel T, Oppermann M, Butterfield JH, Begemann G, Elsner J, Gotze O, Zwirner J (1996) The human mast cell line HMC-1 expresses C5a receptors and responds to C5a but not to C5a(desArg). *Scand J Immunol* 44:30–36
42. Legler DF, Loetscher M, Jones SA, Dahinden CA, Arock M, Moser B (1996) Expression of high- and low-affinity receptors for C3a on the human mast cell line, HMC-1. *Eur J Immunol* 26:753–758
43. Ghebrehiwet B, Kew RR, Gruber BL, Marchese MJ, Peerschke EI, Reid KB (1995) Murine mast cells express two types of C1q receptors that are involved in the induction of chemotaxis and chemokinesis. *J Immunol* 155:2614–2619
44. Hayashi T, Cottam HB, Chan M, Jin G, Tawatao RI, Crain B, Ronacher L, Messer K, Carson DA, Corr M (2008) Mast cell-dependent anorexia and hypothermia induced by mucosal activation of Toll-like receptor 7. *Am J Physiol Regul Integr Comp Physiol* 295:R123–R132
45. Kulkarni M, Alexopoulou L, Flavell RA, Metcalfe DD (2004) Activation of mast cells by double-stranded RNA: evidence for activation through Toll-like receptor 3. *J Allergy Clin Immunol* 114:174–182
46. Marshall JS, McCurdy JD, Olynch T (2003) Toll-like receptor-mediated activation of mast cells: implications for allergic disease? *Int Arch Allergy Immunol* 132:87–97
47. Enoksson M, Ejendal KF, McAlpine S, Nilsson G, Lunderius-Andersson C (2011) Human cord blood-derived mast cells are activated by the Nod1 agonist M-TriDAP to release pro-inflammatory cytokines and chemokines. *J Innate Immun* 3:142–149
48. Okumura S, Yuki K, Kobayashi R, Okumura S, Ohmori K, Saito H, Ra C, Okayama Y (2009) Hyperexpression of NOD2 in intestinal mast cells of Crohn's disease patients: preferential expression of inflammatory cell-recruiting molecules via NOD2 in mast cells. *Clin Immunol* 130:175–185
49. Nakamura Y, Kambe N, Saito M, Nishikomori R, Kim YG, Murakami M, Nunez G, Matsue H (2009) Mast cells mediate neutrophil recruitment and vascular leakage through the NLRP3 inflammasome in histamine-independent urticaria. *J Exp Med* 206:1037–1046
50. Swindle EJ, Metcalfe DD (2007) The role of reactive oxygen species and nitric oxide in mast cell-dependent inflammatory processes. *Immunol Rev* 217:186–205
51. Swindle EJ, Metcalfe DD, Coleman JW (2004) Rodent and human mast cells produce functionally significant intracellular reactive oxygen species but not nitric oxide. *J Biol Chem* 279:48751–48759
52. Swindle EJ, Hunt JA, Coleman JW (2002) A comparison of reactive oxygen species generation by rat peritoneal macrophages and mast cells using the highly sensitive real-time chemiluminescent probe pholasin: inhibition of antigen-induced mast cell degranulation by macrophage-derived hydrogen peroxide. *J Immunol* 169:5866–5873
53. Brooks AC, Whelan CJ, Purcell WM (1999) Reactive oxygen species generation and histamine release by activated mast cells: modulation by nitric oxide synthase inhibition. *Br J Pharmacol* 128:585–590
54. Frederiks WM, Bosch KS, Vreeling-Sindelarova HA (1997) In situ detection of constitutive superoxide anion production in granules of mast cells. *Histochem J* 29:287–291
55. Wolfreys K, Oliveira DB (1997) Alterations in intracellular reactive oxygen species generation and redox potential modulate mast cell function. *Eur J Immunol* 27:297–306
56. Sekar Y, Moon TC, Munoz S, Befus AD (2005) Role of nitric oxide in mast cells: controversies, current knowledge, and future applications. *Immunol Res* 33:223–239
57. McCauley SD, Gilchrist M, Befus AD (2005) Nitric oxide: a major determinant of mast cell phenotype and function. *Mem Inst Oswaldo Cruz* 100 Suppl 1:11–14
58. Gilchrist M, Hesslinger C, Befus AD (2003) Tetrahydrobiopterin, a critical factor in the production and role of nitric oxide in mast cells. *J Biol Chem* 278:50607–50614
59. Forsythe P, Gilchrist M, Kulkarni M, Befus AD (2001) Mast cells and nitric oxide: control of

production, mechanisms of response. *Int Immunopharmacol* 1:1525–1541

60. Padawer J, Fruhman GJ (1968) Phagocytosis of zymosan particles by mast cells. *Experientia* 24:471–472

61. Padawer J (1971) Phagocytosis of particulate substances by mast cells. *Lab Invest* 25: 320–330

62. Otani I, Conrad DH, Carlo JR, Segal DM, Ruddy S (1982) Phagocytosis by rat peritoneal mast cells: independence of IgG Fc-mediated and C3-mediated signals. *J Immunol* 129:2109–2112

63. Malaviya R, Ross EA, MacGregor JI, Ikeda T, Little JR, Jakschik BA, Abraham SN (1994) Mast cell phagocytosis of FimH-expressing enterobacteria. *J Immunol* 152:1907–1914

64. Dietrich N, Rohde M, Geffers R, Kroger A, Hauser H, Weiss S, Gekara NO (2010) Mast cells elicit proinflammatory but not type I interferon responses upon activation of TLRs by bacteria. *Proc Natl Acad Sci U S A* 107: 8748–8753

65. Ott VL, Cambier JC, Kappler J, Marrack P, Swanson BJ (2003) Mast cell-dependent migration of effector CD8+ T cells through production of leukotriene B4. *Nat Immunol* 4:974–981

66. Brown MG, Hermann LL, Issekutz AC, Marshall JS, Rowter D, Al-Aff A, Anderson R (2011) Dengue virus infection of mast cells triggers endothelial cell activation. *J Virol* 85:1145–1150

67. St John AL, Rathore AP, Yap H, Ng ML, Metcalfe DD, Vasudevan SG, Abraham SN (2011) Immune surveillance by mast cells during dengue infection promotes natural killer (NK) and NKT-cell recruitment and viral clearance. *Proc Natl Acad Sci U S A* 108:9190–9195

68. Orinska Z, Bulanova E, Budagian V, Metz M, Maurer M, Bulfone-Paus S (2005) TLR3-induced activation of mast cells modulates CD8+ T-cell recruitment. *Blood* 106: 978–987

69. Jawdat DM, Rowden G, Marshall JS (2006) Mast cells have a pivotal role in TNF-independent lymph node hypertrophy and the mobilization of Langerhans cells in response to bacterial peptidoglycan. *J Immunol* 177:1755–1762

70. Demeure CE, Brahim K, Hacini F, Marchand F, Peronet R, Huerre M, St-Mezard P, Nicolas JF, Brey P, Delespesse G, Mecheri S (2005) Anopheles mosquito bites activate cutaneous mast cells leading to a local inflammatory response and lymph node hyperplasia. *J Immunol* 174:3932–3940

71. Jawdat DM, Albert EJ, Rowden G, Haidl ID, Marshall JS (2004) IgE-mediated mast cell activation induces Langerhans cell migration in vivo. *J Immunol* 173:5275–5282

72. Shelburne CP, Nakano H, St John AL, Chan C, McLachlan JB, Gunn MD, Staats HF, Abraham SN (2009) Mast cells augment adaptive immunity by orchestrating dendritic cell trafficking through infected tissues. *Cell Host Microbe* 6:331–342

73. McLachlan JB, Hart JP, Pizzo SV, Shelburne CP, Staats HF, Gunn MD, Abraham SN (2003) Mast cell-derived tumor necrosis factor induces hypertrophy of draining lymph nodes during infection. *Nat Immunol* 4:1199–1205

74. Norman MU, Hwang J, Hulliger S, Bonder CS, Yamanouchi J, Santamaria P, Kubes P (2008) Mast cells regulate the magnitude and the cytokine microenvironment of the contact hypersensitivity response. *Am J Pathol* 172: 1638–1649

75. Hart PH, Grimaldeston MA, Swift GJ, Jaksic A, Noonan FP, Finlay-Jones JJ (1998) Dermal mast cells determine susceptibility to ultraviolet B-induced systemic suppression of contact hypersensitivity responses in mice. *J Exp Med* 187:2045–2053

76. Geba GP, Ptak W, Anderson GM, Paliwal V, Ratzlaff RE, Levin J, Askenase PW (1996) Delayed-type hypersensitivity in mast cell-deficient mice: dependence on platelets for expression of contact sensitivity. *J Immunol* 157:557–565

77. Kerdel FA, Belsito DV, Scotto-Chinnici R, Soter NA (1987) Mast cell participation during the elicitation of murine allergic contact hypersensitivity. *J Invest Dermatol* 88: 686–690

78. Grimaldeston MA, Nakae S, Kalesnikoff J, Tsai M, Galli SJ (2007) Mast cell-derived interleukin 10 limits skin pathology in contact dermatitis and chronic irradiation with ultraviolet B. *Nat Immunol* 8:1095–1104

79. de Vries VC, Elgueta R, Lee DM, Noelle RJ (2010) Mast cell protease 6 is required for allograft tolerance. *Transplant Proc* 42: 2759–2762

80. de Vries VC, Wasiuk A, Bennett KA, Benson MJ, Elgueta R, Waldschmidt TJ, Noelle RJ (2009) Mast cell degranulation breaks peripheral tolerance. *Am J Transplant* 9:2270–2280

81. Lu LF, Lind EF, Gondek DC, Bennett KA, Gleeson MW, Pino-Lagos K, Scott ZA, Coyle AJ, Reed JL, Van Snick J, Strom TB, Zheng XX, Noelle RJ (2006) Mast cells are essential intermediaries in regulatory T-cell tolerance. *Nature* 442:997–1002

82. Meng S, Liu Z, Xu L, Li L, Mei S, Bao L, Deng W, Lei R, Xie L, Qin C, Zhang L (2011) Intranasal immunization with recombinant HA and mast cell activator C48/80

elicits protective immunity against 2009 pandemic H1N1 influenza in mice. *PLoS One* 6:e19863

83. McGowen AL, Hale LP, Shelburne CP, Abraham SN, Staats HF (2009) The mast cell activator compound 48/80 is safe and effective when used as an adjuvant for intradermal immunization with *Bacillus anthracis* protective antigen. *Vaccine* 27:3544–3552

84. Galli SJ, Grimaldaston M, Tsai M (2008) Immunomodulatory mast cells: negative, as well as positive, regulators of immunity. *Nat Rev Immunol* 8:478–486

85. Brightling CE, Kaur D, Berger P, Morgan AJ, Wardlaw AJ, Bradding P (2005) Differential expression of CCR3 and CXCR3 by human lung and bone marrow-derived mast cells: implications for tissue mast cell migration. *J Leukoc Biol* 77:759–766

86. Shimizu Y, Sakai K, Miura T, Narita T, Tsukagoshi H, Satoh Y, Ishikawa S, Morishita Y, Takai S, Miyazaki M, Mori M, Saito H, Xia H, Schwartz LB (2002) Characterization of 'adult-type' mast cells derived from human bone marrow CD34(+) cells cultured in the presence of stem cell factor and interleukin-6. Interleukin-4 is not required for constitutive expression of CD54, Fc epsilon RI alpha and chymase, and CD13 expression is reduced during differentiation. *Clin Exp Allergy* 32: 872–880

87. Nilsson G, Blom T, Harvima I, Kusche-Gullberg M, Nilsson K, Hellman L (1996) Stem cell factor-dependent human cord blood derived mast cells express alpha- and beta-tryptase, heparin and chondroitin sulphate. *Immunology* 88:308–314

88. Saito H, Ebisawa M, Sakaguchi N, Onda T, Iikura Y, Yanagida M, Uzumaki H, Nakahata T (1995) Characterization of cord-blood-derived human mast cells cultured in the presence of Steel factor and interleukin-6. *Int Arch Allergy Immunol* 107:63–65

89. Radinger M, Jensen BM, Kuehn HS, Kirshenbaum A, Gilfillan AM (2010) Generation, isolation, and maintenance of human mast cells and mast cell lines derived from peripheral blood or cord blood. *Curr Protoc Immunol Chapter 7:Unit 7.37*

90. Andersen HB, Holm M, Hetland TE, Dahl C, Junker S, Schiøtz PO, Hoffmann HJ (2008) Comparison of short term in vitro cultured human mast cells from different progenitors—peripheral blood-derived progenitors generate highly mature and functional mast cells. *J Immunol Methods* 336:166–174

91. Kirshenbaum AS, Metcalfe DD (2006) Growth of human mast cells from bone marrow and peripheral blood-derived CD34+ pluripotent progenitor cells. *Methods Mol Biol* 315:105–112

92. Rottem M, Okada T, Goff JP, Metcalfe DD (1994) Mast cells cultured from the peripheral blood of normal donors and patients with mastocytosis originate from a CD34+/Fc epsilon RI- cell population. *Blood* 84:2489–2496

93. Nilsson G, Blom T, Kusche-Gullberg M, Kjellen L, Butterfield JH, Sundstrom C, Nilsson K, Hellman L (1994) Phenotypic characterization of the human mast-cell line HMC-1. *Scand J Immunol* 39:489–498

94. Butterfield JH, Weiler D, Dewald G, Gleich GJ (1988) Establishment of an immature mast cell line from a patient with mast cell leukemia. *Leuk Res* 12:345–355

95. Weber S, Babina M, Kruger-Krasagakes S, Grutzkau A, Henz BM (1996) A subclone (5C6) of the human mast cell line HMC-1 represents a more differentiated phenotype than the original cell line. *Arch Dermatol Res* 288:778–782

96. Valent P, Besemer J, Kishi K, Kaltenbrunner R, Kuhn B, Maurer D, Lechner K, Bettelheim P (1990) IL-3 promotes basophilic differentiation of KU812 cells through high affinity binding sites. *J Immunol* 145:1885–1889

97. Kishi K, Takahashi M, Aoki S, Nagai K, Hiroswa H, Koike T, Sakai C, Aoyagi Y, Sanada M, Moriyama Y et al (1984) A new Ph1 positive cell line (KU812) from a patient with blastic crisis of chronic myelogenous leukemia. *Nihon Ketsueki Gakkai Zasshi* 47:709–718

98. Saito H, Miura K, Takahashi G, Ebisawa M, Matsumoto K, Shichijo M, Onda T, Iikura Y, Yanagihara Y, Ra C (1995) Development of tryptase-positive KU812 cells cultured in the presence of Steel factor. *Int Arch Allergy Immunol* 107:330–332

99. Kirshenbaum AS, Akin C, Wu Y, Rottem M, Goff JP, Beaven MA, Rao VK, Metcalfe DD (2003) Characterization of novel stem cell factor responsive human mast cell lines LAD 1 and 2 established from a patient with mast cell sarcoma/leukemia; activation following aggregation of FcepsilonRI or FcgammaRI. *Leuk Res* 27:677–682

100. King CA, Marshall JS, Alshurafa H, Anderson R (2000) Release of vasoactive cytokines by antibody-enhanced dengue virus infection of a human mast cell/basophil line. *J Virol* 74:7146–7150

101. Yoneyama M, Kikuchi M, Natsukawa T, Shinobu N, Imaizumi T, Miyagishi M, Taira K, Akira S, Fujita T (2004) The RNA helicase RIG-I has an essential function in double-stranded RNA-induced innate antiviral responses. *Nat Immunol* 5:730–737

102. Marcato P, Shmulevitz M, Pan D, Stoltz D, Lee PW (2007) Ras transformation mediates reovirus oncolysis by enhancing virus uncoating, particle infectivity, and apoptosis-dependent release. *Mol Ther* 15:1522–1530

103. Oldford SA, Haidl ID, Howatt MA, Leiva CA, Johnston B, Marshall JS (2010) A critical role for mast cells and mast cell-derived IL-6 in TLR2-mediated inhibition of tumor growth. *J Immunol* 185:7067–7076

104. Holm M, Andersen HB, Hetland TE, Dahl C, Hoffmann HJ, Junker S, Schiøtz PO (2008) Seven week culture of functional human mast cells from buffy coat preparations. *J Immunol Methods* 336:213–221

105. Shimizu Y, Matsumoto K, Okayama Y, Sakai K, Maeno T, Suga T, Miura T, Takai S, Kurabayashi M, Saito H (2008) Interleukin-3 does not affect the differentiation of mast cells derived from human bone marrow progenitors. *Immunol Invest* 37:1–17

106. Saito H, Ebisawa M, Tachimoto H, Shichijo M, Fukagawa K, Matsumoto K, Iikura Y, Awaji T, Tsujimoto G, Yanagida M, Uzumaki H, Takahashi G, Tsuji K, Nakahata T (1996) Selective growth of human mast cells induced by Steel factor, IL-6, and prostaglandin E2 from cord blood mononuclear cells. *J Immunol* 157:343–350

107. Zhang B, Alysandratos KD, Angelidou A, Asadi S, Sismanopoulos N, Delivanis DA, Weng Z, Miniati A, Vasiadi M, Katsarou-Katsari A, Miao B, Leeman SE, Kalogeromitros D, Theoharides TC (2011) Human mast cell degranulation and preformed TNF secretion require mitochondrial translocation to exocyto- sis sites: relevance to atopic dermatitis. *J Allergy Clin Immunol* 127(1522–1531):e1528

108. Kulka M, Sheen CH, Tancowny BP, Grammer LC, Schleimer RP (2008) Neuropeptides activate human mast cell degranulation and chemokine production. *Immunology* 123: 398–410

109. Guo Q, Subramanian H, Gupta K, Ali H (2011) Regulation of C3a receptor signaling in human mast cells by G protein coupled receptor kinases. *PLoS One* 6:e22559

110. Kashem SW, Subramanian H, Collington SJ, Magotti P, Lambris JD, Ali H (2011) G protein coupled receptor specificity for C3a and compound 48/80-induced degranulation in human mast cells: roles of Mas-related genes MrgX1 and MrgX2. *Eur J Pharmacol* 668: 299–304

111. Jiang M, Osterlund P, Sarin LP, Poranen MM, Bamford DH, Guo D, Julkunen I (2011) Innate immune responses in human monocyte-derived dendritic cells are highly dependent on the size and the 5' phosphorylation of RNA molecules. *J Immunol* 187: 1713–1721

112. Volland H, Vulliez Le Normand B, Mamas S, Grassi J, Creminon C, Ezan E, Pradelles P (1994) Enzyme immunoassay for leukotriene C4. *J Immunol Methods* 175: 97–105

113. Brown MG, King CA, Sherren C, Marshall JS, Anderson R (2006) A dominant role for Fc γ RII in antibody-enhanced dengue virus infection of human mast cells and associated CCL5 release. *J Leukoc Biol* 80: 1242–1250

Part III

Molecular Mechanisms of Mast Cell Function

Chapter 13

Basic Techniques to Study Fc ϵ RI Signaling in Mast Cells

Yuko Kawakami and Toshiaki Kawakami

Abstract

Mast cells are the crucial effector cells for allergic reactions. They are activated through the aggregation of the high-affinity IgE receptor (Fc ϵ RI) with allergen and allergen-specific IgE. Tyrosine phosphorylation of Fc ϵ RI subunits and various signaling proteins is an initial triggering event, leading to the activation of several signaling pathways in mast cells. Much has been learned from analysis of mast cells derived from gene-targeted mice. Therefore, in this chapter we will first describe how to generate mast cells from mouse bone marrow cells and how to correct the genetic defect by retroviral transduction. Then we will describe how to assess early activation events by measuring several protein-tyrosine kinases (PTKs) and serine/threonine kinases (PS/TKs) such as Akt (protein kinase B), protein kinase C (PKC), and JNK. As signal transduction is highly dependent on protein-protein interactions, we will describe experimental details of co-immunoprecipitation methods that are used to confirm such interactions.

Key words Mast cell, Fc ϵ RI, Lyn, Fyn, Src, Syk, Btk, JNK, PKC, Akt, Co-immunoprecipitation, Retroviral transduction, In vitro kinase assay

1 Introduction

In spite of a recent flurry of papers indicating roles of mast cells in innate immunity, autoimmune disease models, angiogenesis, chronic cardiac failure, etc., immediate hypersensitivity and allergic diseases remain the most important focus in mast cell research [1]. As allergic reactions in these diseases are largely dependent on allergen and allergen-specific IgE, the study of the effector cells that are activated by these allergy-triggering agents is central to our understanding of allergy. Mast cells (and basophils) are considered to be the major effector cell type. IgE is bound to the high-affinity IgE receptor, Fc ϵ RI, on the surface of mast cells, and IgE-bound Fc ϵ RI molecules are aggregated with multivalent allergen. The Fc ϵ RI expressed on mast cells consists of IgE-binding α subunit, a signal-amplifying β subunit, and two disulfide-bonded γ subunits with a signal-initiating capability [2]. Upon receptor aggregation, receptor-bound Src family PTKs, such as Lyn [3], Fyn [4], Hck [5], and Fgr [6] are activated. Activated Src PTKs phosphorylate

tyrosine residues in the immunoreceptor tyrosine-based activation motifs (ITAMs) in the β and γ subunits. Phosphorylation of ITAMs in the β and γ subunits creates the binding sites for Lyn and Syk (another PTK with two tandem SH2 domains upstream of its catalytic domain), respectively. These PTKs are activated and phosphorylate a variety of substrates, including adaptor proteins, enzymes (kinases, phosphatases, phospholipases, etc.), transcription factors, and cytoskeletal proteins. These phosphorylations eventually lead to the activation of several signaling pathways such as phospholipase C/ Ca^{2+} , Ras/MAP kinase, NF- κ B, AP-1, and NFAT. Finally, coordinate activation of these pathways results in degranulation, synthesis and release of lipid mediators, and synthesis and secretion of cytokines and chemokines [7, 8].

Much of signaling networks has been figured out by analysis of mast cells derived from gene-targeted mice. Therefore, this chapter will begin with a description of how to generate mast cells from bone marrow cells [9]. Biological and biochemical phenotypes found in mast cells derived from gene-targeted mice can most definitively be ascribed to the lack of the gene by reconstituting the mutant cells with wild-type gene or cDNA. The current standard method of gene transduction in mast cells is retroviral transduction [10], although a recent study used lentiviral transduction in human mast cells [11]. Therefore, we will describe our standard procedures for retroviral transduction. Although the research in Fc ϵ RI signaling deals with many classes of molecules, our description here will be focused on early activation events, i.e., activation of PTKs of the Src, Syk, and Tec families and several serine/threonine kinases (PS/TKs). Because signal transduction often depends on protein-protein interactions, experimental details in co-immunoprecipitation will be depicted as well.

2 Materials

2.1 Reagents for BMMC Generation

1. Bone marrow-derived mast cell (BMMC) medium: 10 % *not* heat-inactivated fetal calf serum (FCS), 2 mM L-glutamine, 0.1 mM non-essential amino acids (NEAA), 50 μ g/mL gentamicin sulfate, 50 μ M 2-mercaptoethanol (2-ME) in RPMI 1640 supplement with ~7 % D11 (IL-3)-conditioned media (or 10 ng/mL recombinant mIL-3).
2. To make 600 mL BMMC media: To 500 mL RPMI 1640, add 60 mL FCS, 40 mL D11 (see Note 1), 6 mL L-glutamine (200 mM stock), 6 mL NEAA (10 mM stock), 0.6 mL gentamicin sulfate (50 μ g/mL stock), and 0.6 mL 2-ME (50 μ M stock).

2.2 Reagents for Retroviral Transduction

1. SCF-derived bone marrow-derived mast cell (sBMMC) medium: 15 % FCS, 2 mM L-glutamine, 0.1 mM NEAA, 50 μ g/mL gentamicin sulfate, 50 μ M 2-ME in RPMI 1640

supplemented with 10 % D11 (IL-3)-conditioned media (or 10 ng/mL recombinant mIL-3), and 50 ng/mL recombinant mouse stem cell factor (rmSCF).

2. To make 600 mL sBMMC media: To 438 mL RPMI 1640, add 90 mL FCS, 60 mL D11 (*see Note 1*), 6 mL L-glutamine (200 mM stock), 6 mL NEAA (10 mM stock), 0.6 mL gentamicin sulfate (50 μ g/mL stock), and 0.6 mL 2-ME (50 μ M stock). Supplement with 50 ng/mL rmSCF.
3. Plat-E medium: 10 % *heat-inactivated* FCS (HI-FCS), 2 mM L-glutamine, 0.1 mM NEAA, 50 μ M 2-ME in Dulbecco's Modified Eagle's Medium (DMEM).
4. To make 500 mL Plat-E medium: To 439.5 mL DMEM, add 50 mL heat-inactivated FCS, 5 mL L-glutamine (200 mM stock), 5 mL NEAA (10 mM stock), and 0.5 mL 2-ME (50 mM stock).
5. TransIT-LT1 transfection reagent (Mirus, Madison, WI).
6. Polybrene stock: 8 mg/mL.

2.3 Reagents for Fc ϵ RI Stimulation

1. Tyrode's buffer: 112 mM NaCl, 2.7 mM KCl, 0.4 mM NaH₂PO₄, 1.6 mM CaCl₂, 1 mM MgCl₂, 10 mM HEPES pH 7.94, 0.05 % gelatin, 0.1 % glucose.
2. Anti-DNP IgE [12].
3. DNP₂₃-HSA (Biosearch Technologies, Inc.)

2.4 Reagents for Kinase Assays

1. Lysis buffer: 1 % NP40 or 1 % Igepal CA-630 (*see Note 2*), 20 mM Tris-HCl (pH 7.5), 0.15 M NaCl, 0.1 % Na₃N.
2. Add protease and phosphatase inhibitors to lysis buffer right before use: 1 mM Na₃VO₄, 1 mM PMSF, 1 mg/mL aprotinin, 1 μ g/mL leupeptin, 1 μ M pepstatin, 25 μ M *p*-nitrophenyl *p*'-guanidinobenzoate, 2 mM NaF.
3. 5 \times SDS/DTT sample buffer: 0.5 M DTT, 10 % SDS, 0.4 M Tris-HCl (pH 6.8), 50 % glycerol.
4. PTK (protein-tyrosine kinase) assay buffer (without ATP): 20 mM HEPES (pH 7.5), 10 mM MgCl₂ 10 mM MnCl₂.
5. Autophosphorylation PTK assay buffer: 20 mM HEPES (pH 7.5), 10 mM MgCl₂ 10 mM MnCl₂ with 0.1 mM "cold" ATP with 10 μ Ci [γ -³²P] ATP per reaction.
6. Substrate PTK assay buffer: 20 mM HEPES (pH 7.5), 10 mM MgCl₂ 10 mM MnCl₂ with 0.1 mM "cold" ATP with 10 μ Ci [γ -³²P] ATP and 2 μ g enolase per reaction.
7. Preparation of acid-denatured enolase.
 - (a) Thaw a 100 μ L aliquot of frozen enolase (2 mg/mL in water kept at -20 °C).
 - (b) Add 100 μ L of 50 mM acetic acid.

- (c) Incubate at room temperature (RT) for 5 min.
- (d) Add 50 μ L of 1 M HEPES (pH 7.0).
- (e) Keep at RT until used in assay.

2.5 Reagents for Immunoprecipitation

1. Antibodies (clone name): Anti-Lyn (44), anti-Btk (M138), anti-PKC α (C-20), anti-PKC β I (C-16), anti-PKC β II (C-18). All antibodies are from Santa Cruz Biotechnology.
2. Protein G PLUS-agarose (Santa Cruz).
3. High salt wash buffer for co-immunoprecipitation: 1 M NaCl, 1 % Triton X-100, 10 mM Tris-HCl (pH 7.2).

2.6 Equipment

1. Culture flasks and tubes.
2. Dissection kit: Forceps, scissors.
3. 10 cc syringes and 26 G needles.
4. SDS-PAGE apparatus.
5. Gel transfer apparatus.

3 Methods

The methods described below will outline (Subheadings 3.1–3.2) the generation and activation of mouse bone marrow-derived mast cells (hereafter abbreviated as BMMC), (Subheading 3.3) the genetic manipulation of BMMC by retroviral transduction, (Subheading 3.4) the measurement of PTKs and PS/TKs, and (Subheading 3.5) a detailed procedure to detect protein-protein interactions by co-immunoprecipitation.

3.1 Generation of BMMC

The following are the description of our standard procedures for BMMC generation that usually take 5–6 weeks. After this period, mast cells constitute more than 95 % of live cells, as assessed by flow cytometry for positive expression of Fc ϵ RI and c-Kit. With this high percentage, the cells are ready for biological (e.g., assays for degranulation, leukotriene, and cytokine secretion), biochemical (e.g., kinase assays, phosphatase assays, GTPase measurement, etc.), genetic (e.g., cDNA transfection, siRNA, etc.), and pharmacological (e.g., inhibitors and activators) experimentations.

Day 1

1. Euthanize a mouse by CO₂ asphyxiation followed by cervical dislocation (or other approved humane method of euthanasia).
2. Drench the mouse in 70 % alcohol to sterilize it.
3. Strip off the skin from one leg.
4. Holding the femur with the forceps, cut away as much of the quadriceps muscle as possible. Then cut the muscles behind the knee joint.

5. Bend the knee joint in the “unnatural” or “incorrect” direction to dislocate it. Cut off the lower leg at the broken knee joint.
6. Snip off a small amount of bone from each end to expose the bone marrow.
7. While holding the femur above the open small flasks (25 cm²), load a syringe with 10 mL BMMC media, install a 26 G needle, and insert the tip of the needle into the exposed bone marrow.
8. Push the full 10 mL of media through the femur slowly and into the flask to wash out the cells and collect the drops in the flask.
9. Repeat steps 3–7 with the other leg.
10. Store the flasks in a 37 °C, 5 % CO₂ incubator for 2 days.

Day 3

11. Transfer each 10 mL culture from the small flask to a medium flask (75 cm²) containing 40 mL of BMMC media.

Day 8

12. Transfer the cultures to 50 mL tubes.
13. Centrifuge the cells at 300 \times g for 5 min and aspirate supernatant.
14. Resuspend the cells in an optimum volume of BMMC medium and transfer to a new flask (see Note 3).
15. Return the cultures to the incubator and maintain for 1 week.

Day 15

16. Change the media and flasks again.
17. Maintain the cultures in the incubator for 1 week.

Day 22 and 29

18. Change the media and flasks again as on Day 15.
19. Maintain the cultures in the incubator for 1 week.

Day 35

20. Change the media and flasks again.
21. The cells are now ready to use. At this point, BMMC cells can be maintained in culture with weekly changes to the media for about 1–2 more weeks (see Note 4).

3.2 Fc ϵ RI Stimulation of BMMC

Sensitization

1. Enumerate mast cells in culture manually using a hemocytometer.
2. Transfer BMMCs to 200 or 50 mL conical centrifuge tubes.

3. Spin down the cells in at $300 \times g$ for 5 min.
4. Resuspend the cells in BMMC medium to a density of 2×10^6 cells/mL.
5. Add IgE to a final concentration of 0.5 μ g/mL.
6. Incubate overnight (37°C , 5 % CO_2).

Stimulation

7. Spin down the cells in a 50 mL tube for 5 min at $300 \times g$.
8. Wash once in Tyrode's buffer.
9. Resuspend the cells in Tyrode's buffer to 2×10^7 cells/mL.
10. Make 1 mL aliquots.
11. Add antigen (DNP₂₃-HSA) to a final concentration of 1–1,000 ng/mL.
12. Incubate at 37°C for predetermined periods (depending on the purpose of the experiment).
13. Spin down the cells and aspirate supernatant. In some experiments (e.g., degranulation assay or isolation of exosomes), one may wish to keep the supernatants for analysis.
14. If you continue the experiment, add an appropriate buffer to the pellet. Otherwise, freeze down the cells in dry ice and keep frozen at -80°C until use.

3.3 Retroviral Transduction of BMMC

This section can be divided into Subheadings “the Construction of Retroviral Vector, the Generation of Recombinant Retrovirus, and the Infection of Mast Cells and Selection of Transgene-Expressing Cells.”

Construction of Retroviral Vector

A Moloney murine leukemia virus-based vector, pMX-puro [13, 14], has been extensively used for transfection of mouse BMMC. As almost all gene-targeted mice have a “neo” gene cassette in their genome, the retroviral vector must have a different drug-resistance gene such as the puromycin resistance gene or another way of selection (e.g., a green fluorescent protein (GFP) gene in the bicistronic gene expression allele). The expression of the latter can be detected by flow cytometry or fluorescent microscopy. The most popular vector pMX-puro can accommodate a gene or cDNA in the region between the *Bam HI* (nucleotide 1884) and *Not I* (nucleotide 3161) sites. Standard molecular biological techniques are used to construct recombinant vectors.

Generation of Recombinant Retrovirus

Recombinant retroviral vectors can be transfected into a packaging cell line to generate infectious virus particles. There are several packaging cell lines available for this purpose: e.g., BOSC23 [15], Phoenix [16], and Plat-E [17]. Our experience indicates that all of these packaging cell lines yield titers of viruses high enough to

Infection of Mast Cells and Selection of Transgene-Expressing Cells

produce transfected BMMC in a scale of $5\text{--}20 \times 10^7$ cells after puromycin selection. These numbers of transfectants allow for most of biological and some biochemical analyses. In this section, we will describe our standard protocol using Plat-E cells.

Retroviral genomes can integrate into a host genome only when host cells are replicating. While IL-3 is usually used as a growth factor to generate BMMC, IL-3 alone is not strong enough to induce vigorous cell cycling for efficient retroviral transduction in BMMC. For this purpose, we and others feed bone marrow cells in IL-3 and stem cell factor (SCF) to generate BMMC that are ready for retroviral infection (hereafter abbreviated as sBMMC) (see Notes 5 and 6).

Ten days prior to transfection

1. Reconstitute a vial of frozen Plat-E cells in Plat-E medium.
2. After the cells become confluent, passage every 3 or 4 days by three- to fivefold dilution.
3. Aspirate medium very carefully with Pasteur pipette and wash once with 5 mL PBS.
4. Add 1 mL of trypsin-EDTA and incubate at RT for 1–2 min.
5. Add 3 mL of DMEM and pipette well to separate individual cells. It is very important to disperse cell clumps.
6. Centrifuge the cells for 5 min at $300 \times g$.
7. Suspend in 8 mL of Plat-E medium per 10 cm dish.
8. Plate Plat-E cells homogenously. Pipette the cells well in order to prevent them from making clumps.

One day prior to transfection

9. Plate 5×10^6 Plat-E (I) cells in 10 mL Plat-E medium in 10 cm dish for Day 1 transfection.
10. Plate 4×10^6 Plat-E (II) cells for Day 2 transfection.

Day 1: Transfect Plat-E (I) cells

11. Add 45 μ L TransIT-LT1 to 1.5 mL DMEM containing 20 mM HEPES (pH 7.4) (without FCS), vortex briefly, let it sit at room temperature (RT) for 5 min.
12. Add 10–15 μ g plasmid, vortex briefly, and then incubate at RT for 15 min.
13. Add the above plasmid mixture dropwise to Plat-E (I) cells.
14. Put the Plat-E cells back into the incubator (37°C , 5 % CO_2).

Day 2: Change Plat-E (I) medium and transfect Plat-E (II) cells

15. Change medium of Plat-E (I). Aspirate old medium, add 10 mL of Plat-E medium.

16. Transfect Plat-E (II) cells with plasmid as described on Day 1, **steps 1–4**.
17. Harvest BMMC as described in Subheading 3.1. Resuspend the cells to 1×10^6 cells/mL in sBMMC medium. Seed 5 mL of BMMC in a 6-well tissue culture plate.

Day 3: Infect BMMC culture

18. Harvest virus supernatant from Plat-E (I), centrifuge at $50 \times g$ for 5 min at RT.
19. Make 10 mL of virus cocktail (sufficient for 2 BMMC transfection wells (**step 21**):
 - (a) 8 mL Plat-E culture supernatant.
 - (b) 1 mL D11-conditioned media (IL-3).
 - (c) 1 mL FCS.
 - (d) 5 μ L SCF (100 μ g/mL stock).
 - (e) 7 μ L Polybrene (8 mg/mL stock).
20. Remove 2.5 mL sBMMC medium from each well of the 6-well plate.
21. Add 5 mL virus cocktail to each well of sBMMC.
22. Centrifuge the whole 6-well plate at $800 \times g$ for 1 h at 32 °C.
23. Incubate the cells in the incubator set at 32 °C with 5 % CO₂ for 4 h (*see Note 7*).
24. Transfer the cells to 37 °C incubator with 5 % CO₂.

Day 4: Infect BMMC culture

25. Make 10 mL of virus cocktail from Plat-E (II) cell supernatant as in **step 19** of Day 3.
26. Remove 3 mL of medium from each well of the sBMMC.
27. Repeat **steps 21–23** of Day 3.

Day 5: Change sBMMC medium

28. Change medium containing virus to sBMMC medium.
29. Incubate the cells at 37 °C with 5 % CO₂.

Day 8 (48 h after the second infection): Begin drug selection

30. Add selection reagent (such as puromycin) or sort the cells.
31. Maintain the cultures with sBMMC medium as described in the Subheading 3.2.

Experimentation with infected sBMMCs

32. Two days prior to experimentation, wash the cells twice with sBMMC medium to remove the selection reagent.
33. Resuspend the cells in sBMMC medium and maintain in culture for 48 h.

34. Wash the cells twice with BMMC medium to remove SCF from medium.
35. Incubate the cells in BMMC medium with or without 0.5 μ g/mL of IgE for 6–8 h (see Note 8).
36. Stimulate the cells with antigen as described in Subheading 3.2, steps 7–14.

3.4 *In Vitro Kinase Assay*

Although anti-phospho-specific antibodies are widely used for the evaluation of activities of many kinases, *in vitro* kinase assay is still the most reliable, direct assay to measure the activity of kinases. A representative method will be described here for Btk, in which reaction products are analyzed by SDS-PAGE and followed by blotting. The method can be adapted for other PTKs or protein serine/threonine kinases P(S/T)Ks using proper substrates and kinase reaction conditions. These methods are also easy to be adapted when different sources of enzyme, e.g., purified or recombinant kinases, are used in place of cell lysates (see Notes 9 and 10).

Cell lysis

1. Add 200 μ L of lysis buffer (+inhibitors) to the tube containing 2×10^7 cells (see Note 11).
2. Incubate on ice with occasional vortexing for 10 min.
3. Spin down the cells at 4 °C for 12 min at $13,000 \times g$ and save supernatant.

Measurement of protein concentration

4. Measure the protein concentration of cleared cell lysate using a Bio-Rad (detergent compatible (DC)) Protein Assay Kit following the manufacturer's protocol.
5. Calculate the protein concentration.
6. Make 0.5–1 mg (depends on the protein you want to IP) aliquots at 200–500 μ L (make up with lysis buffer as needed).

Immunoprecipitation for Btk kinase assay

7. To 1 mg of the lysate, add 4 μ g of anti-Btk (M138) antibody.
8. Let it sit on ice for 1.5 h.
9. Add 20 μ L of Protein G PLUS beads to each tube and vortex at 4 °C for 30 min.
10. Wash Protein G PLUS beads 4× with 1 mL lysis buffer.
11. Wash beads 1× with 1 mL PTK assay buffer (–ATP).
12. Remove all supernatant using a 1 cc syringe with 30 G needle.

Kinase assay reaction

13. Add 20 μ L of PTK assay buffer (–ATP) to the Protein G PLUS-agarose, carefully mix by swirling the tube using plastic pipette tip (200 μ L) (see Note 12).

14. Let it sit on ice.
15. Add 20 μ L of PTK assay buffer (+ATP) and mix well by tapping.
16. Incubate at 30 °C for 10 min.
17. Stop reaction by adding 10 μ L of 5× SDS/DTT sample buffer.

SDS-PAGE and blotting

18. Boil the samples and load onto 8 % SDS-polyacrylamide gel.
19. Run the gel overnight at ~40 V.
20. Transfer the proteins to PVDF membrane (Millipore) and then dry the membrane.
21. Detect the kinase activity by autoradiography.

3.5 Co-immunoprecipitation (co-IP)

Protein-protein interactions can be studied by a variety of methods: the yeast two-hybrid experiment has been used to identify a novel binding partner for many years. With the advent of proteomics techniques, a more recently invented method termed tandem affinity purification (TAP) [18] is more often used. Structural requirements for interactions between a given protein and its partner have been studied using “pull-down” methods with a precipitable affinity ligand incubated with cell lysates that express the binding partner or a purified or recombinant binding protein. There is a wide selection of affinity ligands such as GST (glutathione S-transferase), hexahistidine, maltose-binding protein, etc. However, interactions between endogenous cellular proteins are usually confirmed by co-IP of interacting proteins: a protein will be immunoprecipitated by a specific antibody, and immune complexes are analyzed by SDS-PAGE and followed by immunoblotting with an antibody to the interacting partner (see Note 13).

Co-IP of Btk and PKC β I

1. The cells are sensitized and stimulated as shown in Subheading 3.3.
2. Add 500 μ L of 1 % NP40 lysis buffer containing inhibitors to 4–5 $\times 10^7$ cells. Incubate on ice with occasional vortexing for 10 min, centrifuge at 13,000 $\times g$ for 12 min, and save the supernatant.
3. Measure the protein concentration using Bio-Rad detergent-compatible (DC) Protein Assay Kit following the manufacturer's protocol.
4. Preclear the lysate with Protein G PLUS-agarose. Add 30 μ L of Protein G PLUS-agarose per 1 mg of lysate, incubate at 4 °C for 30 min on the shaker.
5. Spin down at 13,000 $\times g$ for 5 min and save the supernatant.
6. Add 5 μ g of anti-Btk (raised in rabbit against mouse Btk carboxyl terminal peptide) or 5 μ g of normal rabbit IgG to 2 mg of the precleared lysate, let it sit on ice for 1.5 h.

7. Use 5 μ g of anti-PKC β I (C-16) for the PKC IP.
8. Add 25 μ L of Protein G PLUS-agarose and shake at 4 °C for 30 min.
9. Wash once with 1 % NP40 lysis buffer, once with high salt wash buffer, then twice with 1 % NP40 lysis buffer.
10. Remove the washing buffer using a 1 cc syringe with 30 G needle, then add 40 μ L of SDS/DTT sample buffer.
11. Boil at 95 °C for 3 min and load onto 8 % Tris-SDS acrylamide gel.
12. Transfer the protein onto PVDF membrane and blot against anti-PKC β I (C-16) or anti-Btk (C-20).

4 Notes

1. D11 is a culture supernatant of IL-3 gene-transfected cells S15 72 F-D11 [19].
2. NP40 is not commercially available. Igepal CA-630 is recommended as the substitute for NP40 by Sigma, and we have been using this agent without any problem.
3. The optimum cell concentration is about $3\text{--}5 \times 10^5$ cells/mL.
4. The number of BMMC obtained by our protocol widely varies from 5×10^7 to 4×10^8 cells per mouse, mainly due to mouse strain: BALB/c mice tend to give lower numbers of BMMC while C57BL/6 mice give larger numbers. Knockout of some genes might also affect mast cell generation. Although we use mouse IL-3 gene-transfected fibroblasts (D11) as a source of IL-3 because of economy, one can use recombinant IL-3 instead. Some laboratories use WEHI-3 culture supernatants as a source of IL-3. Prior optimization for IL-3 sources is required by culturing bone marrow cells as described above. Similarly, lots of fetal bovine serum should be tested using bone marrow cells.
5. Heterogeneity of mast cells generated in vitro as well as those in tissues has been well known [20]. BMMC generated in our standard protocol are “immature” mast cells with similarities to mucosal mast cells. When bone marrow cells or BMMC that have been generated in IL-3 are exposed to SCF for some time, the resultant mast cells become more “mature” with similarities to connective-tissue mast cells [21]. Therefore, it will not be so surprising to see differences in phenotypes between BMMC and sBMMC. One should carefully assess whether an observed difference is due to an effect of differentiation or genetic difference or simply due to c-Kit (SCF receptor) signaling.

6. Retroviral transduction of a transgene results in its integration into the host (sBMMC) genome. Although the integration event is thought to be a sequence-nonspecific phenomenon, the randomness of integration may not be absolute. Regardless of the extent of randomness, the positional effect associated with transgene insertion is an inherent problem with retroviral transduction (be reminded of the recent leukemia complications in patients who received a gene therapy [22]). One way to avoid this problem is to use other vectors that do not involve transgene integration. Unfortunately, no systematic application of such vectors has been attempted with mast cells. However, a practical solution is to study mass populations of retrovirally transduced cells. Even using such populations of mast cells, one has to keep it in mind that the resultant cells might be skewed to have a growth advantage in SCF-containing media. We usually perform three or more transduction experiments before we draw a conclusion on the effect of gene knockout on a mast cell phenotype.
7. The optimum temperature for virus replication is generally lower than that for cells. Keep the plates at 32 °C for the first 4 h to obtain the best efficiency of retrovirus infection.
8. This sensitization protocol is different from the one described in Subheading 3.3. Because sBMMC start to die from apoptosis 10–24 h after SCF depletion, one needs to shorten the sensitization time.
9. Most PTKs have an autophosphorylating capacity. Autophosphorylating activity is usually more robust in in vitro kinase assays than the activity to phosphorylate an exogenous substrate. It is generally assumed that autophosphorylating activity is correlated with endogenous substrate-phosphorylating activity. Traditionally, acid-denatured enolase has been used as an exogenous substrate for Src family PTKs. Enolase is also a substrate for Btk. Although several other substrates such as poly-(Glu-Tyr) and band III have been used for the same purpose, it is not known whether phosphorylation of these substrates in vitro faithfully reflects the activity of the tested kinase in situ. This question can be addressed by immunoblotting cell lysates by a phospho-specific antibody that detects an activated kinase (or an antibody that detects an inactivated kinase) and by confocal microscopic analysis of cells stained by a phospho-specific antibody.
10. Synthetic peptides have been extensively used as a substrate for a variety of kinases, particularly PS/TKs. Phosphorylation of synthetic peptides can be quantified by SDS-PAGE and autoradiography or by counting the radioactivity of filter papers that are spotted with reaction mixtures. Unlike the latter

method, SDS-PAGE analysis gives a higher level of confidence for results because the detected radioactive band can make sure of the identity of the substrate. However, short peptides (<10 residues) cannot be analyzed by the former method. Another potential problem is that some peptides contain more than one phosphorylatable residue. This could be particularly problematic when an enzyme source comes from a complex mixture of proteins such as cell lysates. Fortuitous co-precipitation of an unintended kinase might phosphorylate the peptide at an unintended residue.

11. 2×10^7 cells makes ~1 mg of lysate when lysed in 1 % NP40 lysis buffer.
12. Do not vortex or tap hard. The agarose beads will jump up and stick on the wall.
13. To perform a proper negative control precipitation is critical, given that nonspecific bands are usually seen by immunoblotting total cell lysates even with preimmune sera. Our experience also indicates that antibody-precipitating media, such as Pansorbin, protein A agarose, and protein G agarose, precipitate from cell lysates of numerous proteins that can be detected by staining SDS-PAGE gels. Therefore, it is imperative to show negative control data. We believe such data are essential even when time course studies are carried out. Remember that some proteins such as PKC are very sticky. How can you reduce the chance of fortuitous precipitations of your protein? Because of its unpredictable nature, there is no fixed way to solve this problem. Once you are faced with it, you can try several tricks: (1) change of precipitating media, (2) coating precipitating media with BSA or gelatin, (3) change of lysis buffer from a mild detergent to a harsher detergent, (4) wash the precipitate with high salt buffer, and (5) a combination of these changes. These changes were all tried before we could generate the clean co-IP data on Btk-PKC interactions [23].

References

1. Galli SJ, Lantz CS (1999) Fundamental immunology, 4th edn. Lippincott-Raven Publishers, Philadelphia, PA
2. Kinet JP (1999) The high-affinity IgE receptor (Fc epsilon RI): from physiology to pathology. *Annu Rev Immunol* 17:931–972
3. Eiseman E, Bolen JB (1992) Engagement of the high-affinity IgE receptor activates src protein-related tyrosine kinases. *Nature* 355:78–80
4. Parravicini V, Gadina M, Kovarova M, Odom S, Gonzalez-Espinosa C, Furumoto Y, Saitoh S, Samelson LE, O’Shea JJ, Rivera J (2002) Fyn kinase initiates complementary signals required for IgE-dependent mast cell degranulation. *Nat Immunol* 3:741–748
5. Hong H, Kitaura J, Xiao W, Horejsi V, Ra C, Lowell CA, Kawakami Y, Kawakami T (2007) The Src family kinase Hck regulates mast cell activation by suppressing an inhibitory Src family kinase Lyn. *Blood* 110:2511–2519
6. Lee JH, Kim JW, Kim do K, Kim HS, Park HJ, Park DK, Kim AR, Kim B, Beaven MA, Park KL,

Kim YM, Choi WS (2011) The Src family kinase Fgr is critical for activation of mast cells and IgE-mediated anaphylaxis in mice. *J Immunol* 187:1807–1815

7. Turner H, Kinet JP (1999) Signalling through the high-affinity IgE receptor Fc epsilonRI. *Nature* 402:B24–B30
8. Kawakami T, Galli SJ (2002) Regulation of mast-cell and basophil function and survival by IgE. *Nat Rev Immunol* 2:773–786
9. Kawakami T, Inagaki N, Takei M, Fukamachi H, Coggeshall KM, Ishizaka K, Ishizaka T (1992) Tyrosine phosphorylation is required for mast cell activation by Fc epsilon RI cross-linking. *J Immunol* 148:3513–3519
10. Hata D, Kawakami Y, Inagaki N, Lantz CS, Kitamura T, Khan WN, Maeda-Yamamoto M, Miura T, Han W, Hartman SE, Yao L, Nagai H, Goldfeld AE, Alt FW, Galli SJ, Witte ON, Kawakami T (1998) Involvement of Bruton's tyrosine kinase in Fc epsilon RI-dependent mast cell degranulation and cytokine production. *J Exp Med* 187:1235–1247
11. Furumoto Y, Brooks S, Olivera A, Takagi Y, Miyagishi M, Taira K, Casellas R, Beaven MA, Gilfillan AM, Rivera J (2006) Cutting Edge: lentiviral short hairpin RNA silencing of PTEN in human mast cells reveals constitutive signals that promote cytokine secretion and cell survival. *J Immunol* 176:5167–5171
12. Liu FT, Bohn JW, Ferry EL, Yamamoto H, Molinaro CA, Sherman LA, Klinman NR, Katz DH (1980) Monoclonal dinitrophenyl-specific murine IgE antibody: preparation, isolation, and characterization. *J Immunol* 124:2728–2737
13. Onishi M, Kinoshita S, Morikawa Y, Shibuya A, Phillips J, Lanier LL, Gorman DM, Nolan GP, Miyajima A, Kitamura T (1996) Applications of retrovirus-mediated expression cloning. *Exp Hematol* 24:324–329
14. Kawakami Y, Miura T, Bissonnette R, Hata D, Khan WN, Kitamura T, Maeda-Yamamoto M, Hartman SE, Yao L, Alt FW, Kawakami T (1997) Bruton's tyrosine kinase regulates apoptosis and JNK/SAPK kinase activity. *Proc Natl Acad Sci U S A* 94:3938–3942
15. Pear WS, Nolan GP, Scott ML, Baltimore D (1993) Production of high-titer helper-free retroviruses by transient transfection. *Proc Natl Acad Sci U S A* 90:8392–8396
16. Grignani F, Kinsella T, Mencarelli A, Valtieri M, Riganelli D, Lanfrancone L, Peschle C, Nolan GP, Pelicci PG (1998) High-efficiency gene transfer and selection of human hematopoietic progenitor cells with a hybrid EBV/retroviral vector expressing the green fluorescence protein. *Cancer Res* 58:14–19
17. Morita S, Kojima T, Kitamura T (2000) Plat-E: an efficient and stable system for transient packaging of retroviruses. *Gene Ther* 7: 1063–1066
18. Rigaut G, Shevchenko A, Rutz B, Wilm M, Mann M, Seraphin B (1999) A generic protein purification method for protein complex characterization and proteome exploration. *Nat Biotechnol* 17:1030–1032
19. Yokota T, Lee F, Arai N, Rennick D, Zlotnick A, Mosmann T, Miyajima A, Takebe Y, Kastlein R, Zurawski G, Arai K (1986) Strategies for cloning mouse and human lymphokine genes using mammalian cDNA expression vector. *Lymphokines* 13:1–19
20. Wong GW, Friend DS, Stevens RL (1998) Mouse and rat models of mast cell development. In: Razin E, Rivera J (eds) Signal transduction in mast cells and basophils. Springer, New York, pp 39–53
21. Galli SJ, Tsai M, Lantz CS (1999) The regulation of mast cell and basophil development by the Kit ligand, SCF, and IL-3. In: Razin E, Rivera J (eds) Signal transduction in mast cells and basophils. Springer, New York, pp 11–30
22. Staal FJ, Pike-Overzet K, Ng YY, van Dongen JJ (2008) Sola dosis facit venenum. Leukemia in gene therapy trials: a question of vectors, inserts and dosage? *Leukemia* 22:1849–1852
23. Yao L, Kawakami Y, Kawakami T (1994) The pleckstrin homology domain of Bruton tyrosine kinase interacts with protein kinase C. *Proc Natl Acad Sci U S A* 91:9175–9179

Chapter 14

Membrane-Cytoskeleton Dynamics in the Course of Mast Cell Activation

Pavel Dráber and Petr Dráber

Abstract

Aggregation of the high-affinity IgE receptor (Fc ϵ RI) on the plasma membrane of mast cells and basophils initiates signaling events leading to a rapid release of preformed inflammatory mediators from secretory granules, and overall changes in cell morphology. Mast cell activation also causes reorganization of cytoskeletal components associated with membrane ruffling, spreading, and migration. Here we describe methods used for visualization of mast cell cytoskeleton, focusing on its two major components, microfilaments and microtubules, and their changes after cell triggering.

Key words Mast cells, Plasma membrane, Actin, Tubulin, Microfilaments, Microtubules

1 Introduction

Engagement of immunoreceptors, such as the B cell receptor (BCR), T cell receptor (TCR), and Fc receptors including the high-affinity IgE receptor (Fc ϵ RI) on mast cells and basophils, leads to dynamic remodeling of the plasma membrane, facilitating initiation and propagation of intracellular signaling. These early signaling events are followed by other signaling steps resulting in changes in cell morphology, migration, adhesion to various substrates, and, in case of mast cells and basophils, degranulation. Many of these events are dependent on the activity of cytoskeletal components [1–3].

1.1 The Role of Cytoskeletal Components in Mast Cell Physiology

The first indication that cytoskeleton is involved in mast cell signaling was obtained in studies on rat basophilic leukemia (RBL)-2H3 cell line [4]. It was shown that binding of multivalent antigen to IgE-Fc ϵ RI complexes induced formation of membrane ridges (lamellipodia). These ridges were observed 30 s after cell triggering, reaching the peak at 5 min, and their formation required continuous presence of antigen. Removal of the antigen resulted in complete reversion of the surface transformation within 5 min.

The extent of lamellipodia formation in IgE-sensitized cells depended on antigen concentration. The lowest dose of antigen was 1 ng/ml and the maximum response was observed at 5 µg/ml. These changes were accompanied by a rapid increase in the amount of filamentous (F)-actin. Enhanced formation of F-actin after cell triggering was reported in several other studies using RBL-2H3 cells [5–7], rat peritoneal mast cells [8], and mouse bone marrow-derived mast cells (BMMCs) [9]. A role of cytoskeleton was also implicated in the formation of signalosomes containing the Fc ϵ RI and some key enzymes (kinases and phosphatases) and several adaptor proteins [10–13]. Research has mostly focused on two cytoskeletal systems, namely microfilaments composed of actin, and microtubules formed by $\alpha\beta$ -tubulin dimers.

1.2 Microfilaments

Microfilaments, also called actin filaments, are polar and flexible polymers of actin subunits. Actin filaments of about 6 nm in diameter are the thinnest fibers of the cytoskeleton. The two ends of an actin filament polymerize at different rates. The fast-growing end is called the plus (barbed) end, whereas the slow-growing end is called the minus (pointed) end. Although actin filaments are dispersed throughout the cell, they are mostly concentrated in the cortex, beneath the plasma membrane. Cortical actin cytoskeleton is connected to the plasma membrane through an array of closely related cytoplasmic proteins of the ERM (Ezrin, Radixin, Moesin) family. The C-terminal domains of the ERM proteins bind directly to actin filaments, whereas the N-terminal domains bind to transmembrane glycoproteins. Actin filaments are involved in cell movement, changes in cell shape, and organization of cytoplasmic components. They are assembled in two types of structure, bundles and networks.

Most of the studies analyzing the role of microfilaments in mast cell activation have used pharmacological inhibitors, cytochalasin D or latrunculin B. These drugs inhibit actin polymerization by different mechanisms: cytochalasin D by capping the barbed ends of actin filaments and thus preventing their elongation [14], whereas latrunculin B by sequestering the monomeric actin [15]. Previous studies showed that pretreatment of RBL-2H3 cells with inhibitors of actin polymerization enhanced Ca²⁺ mobilization and degranulation [5, 6]. Interestingly, latrunculin B alone initiated some activation pathways, suggesting that actin polymerization is critical for setting the threshold for mast cell triggering [7]. It should be noted, however, that long (1 h) exposure to high concentrations of latrunculin B (40 µg/ml) inhibited degranulation in compound 48/80-activated rat peritoneal mast cells [8]. These data indicate a positive role of F-actin in mast cell degranulation. Pretreatment with latrunculin B completely inhibited the antigen-induced migration [16] or spreading of mast cells on fibronectin ([9] and our unpublished results).

1.3 Microtubules

Microtubules are highly dynamic cytoskeletal polymers that are similarly as microfilaments inherently polar, and contain two structurally distinct ends: minus ends are stably anchored in centrosomes, whereas the plus ends are highly dynamic and switch between phases of growth and shrinkage [17]. Growing microtubules are characterized by accumulation of specialized microtubule-associated proteins, such as the end-binding (EB) family proteins [18]. Tagged versions of these proteins facilitate tracing the growing microtubules in living cells. It is well established that microtubules are involved in mast cell degranulation, since the movement of secretory granules depends on intact microtubules [19, 20]. This is supported by demonstration that agents inhibiting tubulin polymerization (e.g., nocodazole) also suppress degranulation [21, 22]. Importantly, Fc ϵ RI aggregation triggers the reorganization of microtubules at cell periphery [20, 22, 23]. It is of interest that several signal transduction molecules of RBL-2H3 cells and BMMCs form complexes with γ -tubulin, a minor component of the tubulin family, that is essential for microtubule nucleation [23, 24].

2 Materials

2.1 Cells

Several cell types have been used in studies on mast cell cytoskeleton: freshly isolated mast cells, cultured primary mast cells, and cell lines. RBL-2H3 cells and BMMCs predominate.

RBL-2H3 Cells

RBL-2H3 cells [25] grow as adherent to tissue culture-treated plastic or glass surfaces. The cells can be cultured in medium consisting of 1:1 mixture of RPMI-1640 and minimal essential medium (MEM) supplemented with nonessential amino acids, 3 mM L-glutamine, 1 mM sodium pyruvate, antibiotics [penicillin (100 units/ml) and streptomycin (100 μ g/ml)], extra D-glucose (2.5 mg/ml), and 10 % (v/v) heat-inactivated fetal calf serum (FCS). The cultures are maintained at 37 °C in humidified atmosphere of 5 % CO₂ in air. The cell monolayers are dissociated with 0.2 % EDTA in phosphate-buffered saline (PBS), pH 7.4, and subcultured twice a week. RBL-2H3 cells express large amount of Fc ϵ RI and therefore are useful for studies of this receptor. The disadvantage is that they are tumor-derived cells and some of their signaling pathways are therefore changed. They carry a mutation in c-kit [26] and, in contrast to BMMCs, do not thus require stem cell factor (SCF) for continuous growth in culture.

Bone Marrow-Derived Mast Cells

Bone marrow contains mast cell precursors that can be isolated from the femurs and tibias of 6–10-week-old mice. The cells are cultured in RPMI-1640 supplemented with FCS, antibiotics, recombinant interleukin (IL)-3 (PeproTech EC) at concentration 20 ng/ml, and recombinant stem cell factor (SCF) (PeproTech EC)

at a concentration 40 ng/ml for 5–7 weeks. In such cultures almost all cells (>95 %) express the Fc ϵ RI and cKIT. Before activation, BMMCs are cultured for 16–20 h in culture medium without SCF, followed by incubation for 3–4 h in SCF- and IL-3-free medium, supplemented with trinitrophenyl (TNP)- or dinitrophenyl (DNP)-specific IgE. The IgE-sensitized cells are then washed in buffered saline solution (BSS; 20 mM HEPES, pH 7.4, 135 mM NaCl, 5 mM KCl, 1.8 mM CaCl₂, 5.6 mM glucose, 1 mM MgCl₂) supplemented with 0.1 % bovine serum albumin (BSA) and challenged with various concentrations of TNP- or DNP-conjugated BSA. Alternatively, cells are cultured for 16 h in culture medium without SCF, followed by incubation in medium deprived for 3–4 h of SCF and IL-3 and activated for various time intervals with H₂O₂, perva-nadate (a mixture of H₂O₂ and Na₃VO₄), thapsigargin, or other activators.

Cells of the mouse BMMC line denoted BMMCL [22] have been cultured in medium RPMI-1640, supplemented with 20 mM HEPES, pH 7.5, antibiotics, 100 μ M MEM nonessential amino acids, 1 mM sodium pyruvate, 10 % FCS, and 10 % WEHI-3 cell supernatant as a source of IL-3.

2.2 Antibodies, Chemicals, and Kits

1. Primary and secondary antibodies used are summarized in Table 1.
2. Cell-Tak, Cell and tissue adhesive (BD Biosciences, San Jose, CA, USA).

Table 1
Specificity of antibodies and applications

Antigen	Species/clone/supplier, or reference	Conjugation
DNP	Mouse mAb, SPE-7, Sigma	None
TNP	Mouse mAb, IGEL b4 1, [36]	None
Fc ϵ RI β subunit	Mouse mAb, JRK, [37]	None
oxPTP	Mouse mAb, 335636, R&D Systems	None
Lyn	Mouse mAb, Lyn-01/Pr [38]	None
Syk	Mouse mAb, Syk-01/Pr [39]	None
α -Tubulin	Rabbit Ab, GeneTex	None
γ -Tubulin	Mouse mAb, TU-30, [40]	None
β -Tubulin	Mouse mAb, TUB 2.1, Sigma	Cy3
Mouse IgG	Goat Ab, Jackson ImmunoResearch Labs	Cy3
Rabbit IgG	Goat Ab, Invitrogen	Alexa Fluor 488
Mouse IgG	Goat Ab, Jackson ImmunoResearch Labs	12 nm gold particles

oxPTP oxidized protein tyrosine (PTP), Cy3 indocarbocyanate

3. DNP conjugated with BSA (Invitrogen, Molecular Probes; OR, USA).
4. Fibronectin from bovine plasma for cell culture (Sigma-Aldrich; Cat. No. F1141).
5. Fluorescein isothiocyanate (FITC)-labeled phalloidin (Sigma-Aldrich).
6. Alexa Fluor 488- or Alexa Fluor 555-labeled phalloidin (Invitrogen, Molecular Probes).
7. Mouse macrophage kit for nucleofection (Lonza Cologne AG, Köln, Germany).
8. MOWIOL 4-88 Reagent (Merck, Darmstadt, Germany).
9. Streptavidin conjugated with 5 nm colloidal gold particles (BBInternational; Cardiff, UK).
10. Poly-L-lysine hydrobromide (PLL; Sigma-Aldrich).

2.3 Buffers and Media

1. Buffered saline solution (BSS): 20 mM HEPES, pH 7.4, 135 mM NaCl, 5 mM KCl, 1.8 mM CaCl₂, 5.6 mM glucose, 1 mM MgCl₂.
2. BSS-BSA: 0.1 % BSA (w/v) in BSS.
3. Glutamate/EGTA buffer (GBE): 137 mM K-glutamate, 2 mM MgCl₂, 3 mM EGTA, and 20 mM PIPES, adjusted to pH 6.8 with KOH.
4. HEPES buffer: 25 mM HEPES, adjusted pH to 7.0 with NaOH, 25 mM KCl, 2.5 mM magnesium acetate.
5. Microtubule-stabilizing buffer (MSB): 100 mM MES, adjusted to pH 6.9 with KOH, 2 mM MgCl₂, 2 mM EGTA, 4 % (w/v) polyethylene glycol 6000.
6. RPMI medium for live-cell imaging: RPMI-1640 without phenol red, riboflavin, folic acid, pyridoxal, Fe(NO₃)₃, supplemented with 20 mM HEPES.
7. Osmium tetroxide in cacodylate buffer: 1 ml of 4 % (w/v) osmium tetroxide is mixed with 2.0 ml of 0.2 M sodium cacodylate buffer (pH 7.4) and 1 ml H₂O (*see Note 1*).
8. 1 % aqueous tannic acid: 0.5 g tannic acid is dissolved in 50 ml H₂O. Solution is filtered through 0.2 µm filter disc.
9. 1 % aqueous uranyl acetate: 2 % uranyl acetate (saturated solution) is prepared. Immediately before use, the required amount of the solution is filtered through 0.2 µm filter and mixed with equal volume of H₂O (*see Note 2*).

2.4 Other Materials and Equipment

1. Round glass cover slips, 12 mm in diameter (*see Note 3*).
2. Round glass cover slips, 10 mm in diameter, No. 1.
3. 35 mm glass-bottom culture dishes (MatTek Corp., Ashland, MA, USA).

4. Perfusion insert for 35 mm culture dish (Warner Instruments, Hamden, CT, USA; model RC-37F).
5. 8-Well multitest slides (MP Biomedicals, Irvine, CA, USA).
6. Electron microscopy nickel grids, Athene New 300, 3.05 mm (Ted Pella, Inc., Redding, CA, USA).
7. Thermo-conductive platform (BioCision, Mill Valley, CA, USA).
8. Amaxa Nucleofector II (Lonza Cologne AG, Cologne, Germany).
9. Olympus AX70 Provis microscope equipped with 60 \times water-immersion and 100 \times oil-immersion objectives and SensiCam cooled CCD camera (PCO IMAGING, Kelheim, Germany) for recording images.
10. Confocal laser scanning microscope Leica TCS SP5 equipped with 63 \times /1.4 NA oil-immersion objective.
11. Leica AM TIRF MC (Leica Microsystems): time-lapse sequences are acquired in TIRF mode using HCX PL APO 100 \times /1.46 NA oil-immersion TIRF objective.
12. Electron microscope Morgagni 268 operating at 80 kV (FEI Czech Republic, Brno, The Czech Republic).
13. Milli-Q water purification system (Millipore S.A., Molsheim, France).

2.5 Software

1. Image J software, version 1.38 (National Institutes of Health, Bethesda, MD, USA) or Olympus Scan^R analysis software (Olympus).
2. Huygens Deconvolution Software (Scientific Volume Imaging, Hilversum, The Netherlands).
3. Ellipse software, version 2.07 (ViDiTo, Systems, Košice, Slovakia).

3 Methods

3.1 Visualization of Microfilaments and Their Interactions with the Plasma Membrane

Immunofluorescence Microscopy

To study the distribution of actin filaments and their changes in the course of mast cell activation, phalloidin labeled with FITC or other fluorescent dyes are used. BMMCs and other nonadherent cells are immobilized to fibronectin-coated surfaces using Cell-Tak and processed as indicated below.

1. To each well of 6 mm multitest slide add 13 μ l of the solution containing 50 mM NaHCO₃, 50 μ g/ml fibronectin, and Cell-Tak (8 μ g/ml) and incubate for 12–16 h at 4 °C in a humidified chamber (*see Note 4*).
2. Wash fibronectin/Cell-Tak-coated wells once with BSS-BSA.
3. Add into each well 1.5 \times 10⁴ IgE-sensitized cells in 30 μ l of BSS-BSA.

4. Incubate the cells at 37 °C to allow their attachment.
5. After 1 h wash the cells with BSS-BSA.
6. Activate the cells by adding various concentrations of antigen (1–1,000 ng/ml).
7. After selected time intervals, fix the cells for 20 min at RT (RT) with 3 % paraformaldehyde in GBE buffer supplemented with 4 % polyethylene glycol (MW 3200).
8. For F-actin staining, wash the cells with 50 mM glycine in GBE and then add phalloidin conjugated with FITC, Alexa Fluor 488 or Alexa Fluor 555 diluted in GBE buffer supplemented with mild detergent, L- α -lysophosphatidylcholine (120 μ g/ml).
9. After 30 min, wash the cells four times with GBE and mount cover slips using Mowiol 4-88 containing 2 μ g/ml 4',6-diamidino-2-phenylindole (DAPI) and 6.25 % propyl gallate (w/v).
10. Take confocal images (e.g., on Leica TCS SP microscope).
11. Using Image J 1.38 software or Olympus Scan^R analysis software determine the mean cell area (*see Note 5*).
12. For each condition, evaluate at least 200 cells.

A typical distribution of actin filaments in nonactivated and activated cells stained by the procedure described above is shown in Fig. 1

Electron Microscopy

To analyze the topography of individual plasma membrane-bound components, plasma membrane sheets are isolated and then analyzed by two-step procedures using antibodies for target structures (antigens) as the first-step reagents and gold nanoparticle-labeled anti-antibodies as the second-step reagents. Alternatively, biotin-labeled antibodies or other ligands such as phalloidin can be used for detection of the target structures and visualized with gold-labeled streptavidin. Both adherent (RBL) and nonadherent (BMMC) cells can be analyzed. Data documenting the applicability of this procedure for analyzing cell signaling events in RBL cells and BMCCs have been presented [10–13, 27–32]. Below is described a protocol for studies using cultured BMCCs which are nonadherent to tissue culture-treated plastic or glass surfaces and require IL-3 and SCF for optimal growth.

1. To sensitize the cells, transfer BMCCs into fresh complete culture medium supplemented with IL-3- and DNP-specific IgE, but without SCF (*see Note 6*).
2. After 16–24 h, wash the cells in BSS-BSA, count them, and adjust concentration to 1×10^7 /ml in 1:4 mix of PBS and complete culture medium with FCS, but without SCF, IL-3, and IgE (activation medium).

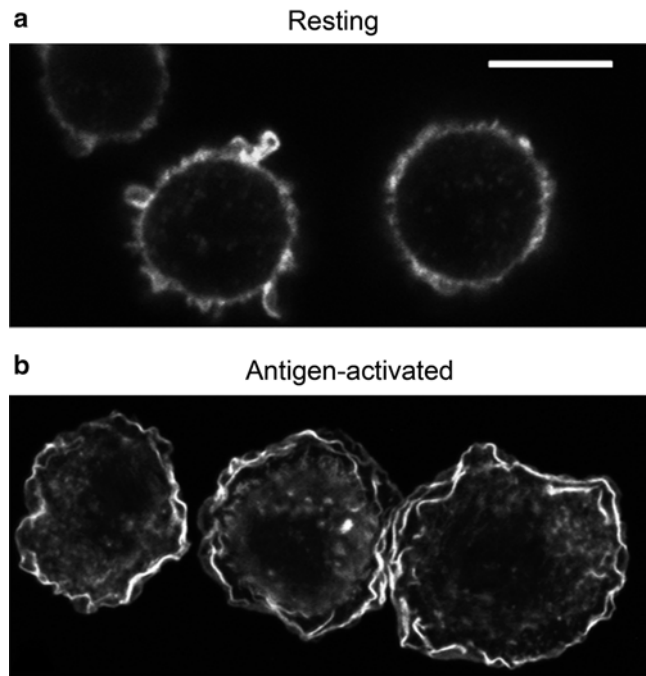


Fig. 1 Topography of actin filaments in nonactivated and activated mast cells visualized by light microscopy. IgE-sensitized BMMCs were attached to fibronectin-coated glass surface and then exposed to BSS alone (a; *resting*) or BSS supplemented with antigen (b; *antigen activated*). After 20 min at 37 °C, the cells were fixed and stained for F-actin using Alexa Fluor 488-labeled phalloidin. The images are confocal micrographs taken at equatorial planes. Scale bar, 10 μm. Reproduced by permission from ref. 9. Copyright 2011; John Wiley and Sons

3. Transfer 200 μl aliquots of the cell suspension into each well of 24-well plate containing ultraclean fibronectin-coated cover slips (*see Note 7*).
4. After 1 h, add 1 μg/ml of antigen (DNP-BSA conjugate) to activate the cells (*see Note 8*).
5. During activation, prepare a beaker with ice containing a thermal tray. Then transfer wet nitrocellulose on the thermal tray followed by poly-L-lysine hydrobromide (PLL)-covered electron microscopy grids put on the wet nitrocellulose (*see Note 9*).
6. Stop antigen-mediated activation of the cells by immersing the cover slips in ice-cold HEPES buffer.
7. Press cover slips with face-down oriented cells for 10 s onto PLL-covered EM grids placed on wet nitrocellulose filter on ice-cold thermal tray using rubber stopper. This creates a sandwich containing cells bound to both cover slip (via fibronectin) and EM grid (via PLL) (Fig. 2a). Then side-lift the cover slip, exposing the cells to shearing force leading to cell disruption (Fig. 2b).

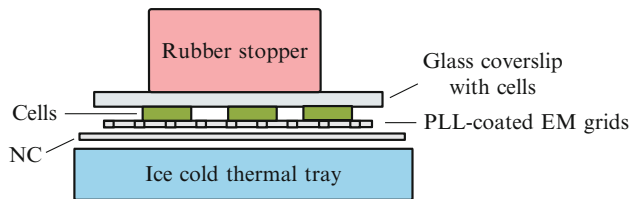
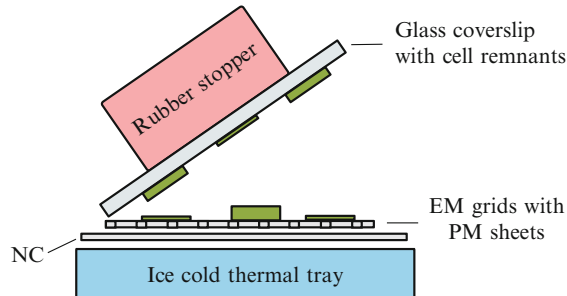
a A sandwich formed by cells bound to EM grid and glass**b** Isolation of EM grids-bound PM sheets

Fig. 2 Schematic outline of the method used for isolation of plasma membrane (PM) sheets bound to electron microscopy grids. **(a)** A sandwich is formed by consecutively adding on thermal tray placed in a beaker with ice (1) NC paper wetted with HEPES buffer, (2) EM grids with the PLL sides up, (3) cover slip with bound/spread cells facing the EM grids, and (4) rubber stopper to facilitate firm pressing of the cells on cover slips towards EM grids. **(b)** Plasma membrane sheets are then isolated by rapid side-lifting of the cover slip exposing the cells to shearing forces and resulting in tearing off the plasma membranes bound to PLL layer on EM grids and glass cover slip

In this way, dorsal plasma membrane is bound to PLL on EM grid and cytoplasmic side is amenable for analysis.

8. Immediately, transfer EM grids with teared PM sheets facing down onto surface of ice-cold HEPES buffer in a beaker.
9. After 5–10 s, transfer floating EM grids into another beaker with ice-cold 2 % paraformaldehyde in HEPES buffer.
10. Fix the cells for 10 min, then transfer sequentially the floating grids into three beakers with PBS, and incubate for 10–20 min in each beaker to remove the fixative.
11. Transfer the grids into another beaker with PBS-0.1 % BSA and incubate for 15 min at 20–25 °C to block the protein-reactive sites.
12. To label the intracellular leaflet proteins, incubate the grids for 30 min on drops of PBS-0.1 % BSA supplemented with selected first-layer antibodies/reagents, followed by four 5-min washes with PBS.

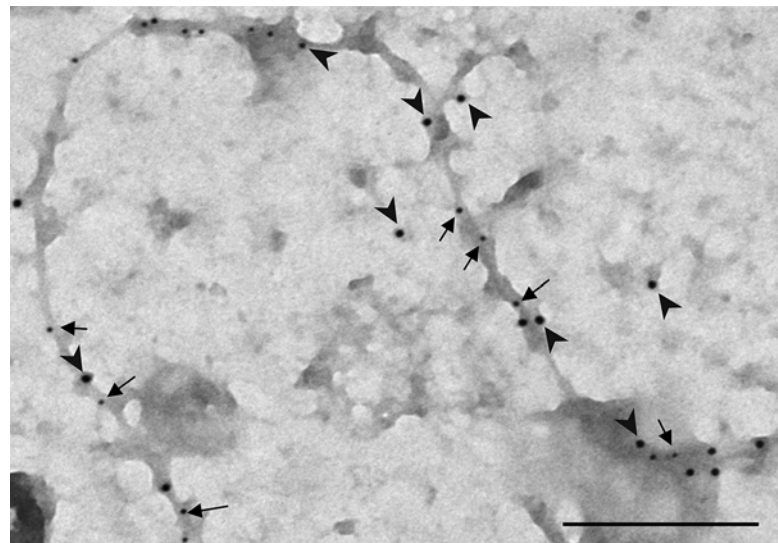


Fig. 3 Topography of actin filaments and oxidized phosphatases visualized by electron microscopy on isolated plasma membrane sheets. Plasma membrane sheets were isolated from BMMCs activated with 0.2 mM perva-nanate for 5 min. The sheets were labeled from the cytoplasmic side for oxidized PTPs with oxPTP mAb followed by goat antibody anti-mouse IgG conjugated to 12 nm gold particles (arrowheads), and for F-actin with biotin-labeled phalloidin, followed by streptavidin conjugated with 5 nm gold particles (arrows). Scale bar, 200 nm. Reproduced from ref. 32. Copyright 2010; the American Society for Biochemistry and Molecular Biology

13. Then incubate the grids with gold-labeled second-layer antibodies and again wash with PBS as above.
14. Postfix the specimens with 2.5 % glutaraldehyde in PBS for 10 min and again wash with PBS for 30 min.
15. Stain the samples with 1 % OsO₄ in cacodylate buffer for 10 min, followed by three 5-min washes in water.
16. Incubate the specimens with 1 % aqueous tannic acid and again wash three times with water.
17. Stain the membranes with 1 % aqueous uranyl acetate and wash again with water.
18. Air-dry the samples and observe them in an electron microscope such as FEI Morgagni 268 operating at 80 kV.
19. Analyze the distribution of gold nanoparticles using proper software (*see Note 10*).

Figure 3 shows the distribution of actin filaments and oxidized phosphatases on cytoplasmic side of the plasma membrane in BMMCs as detected by electron microscopy on isolated plasma sheets from BMMCs prepared by a method as described in this section.

3.2 Visualization of Microtubules and Their Dynamic Changes

Immunofluorescence Microscopy

To study the distribution of microtubules and their changes in the course of mast cell activation, direct or indirect immunofluorescence microscopy with antibodies to tubulin is usually applied. Microtubules are labile structures and therefore proper fixation/extraction conditions have to be selected for their detection with antibodies [33]. When BMMCs are used, they are immobilized on fibronectin-coated surfaces and processed as indicated below.

1. Lay down cover slips (10 mm in diameter) on 30 μ l droplets of fibronectin solution (50 μ g/ml in 50 mM NaHCO₃) on Parafilm and incubate for 12–16 h at 4 °C in a humidified chamber. Rinse, thereafter, cover slips in PBS. Coating of cover slips with fibronectin can be speeded up by incubation at 37 °C for 60 min in a humidified chamber.
2. Transfer cover slips to Petri dishes (diameter 3.5 cm, fibronectin side up) and overlay them with suspension of control or IgE-sensitized cells at a concentration 1.5–2.0 \times 10⁶ cells/ml (see Note 11).
3. Incubate cells for 1 h at 37 °C to allow their attachment.
4. Wash cells, then activate at 37 °C by adding various concentrations of antigen (10–1,000 ng/ml), and incubate for selected time intervals (1–10 min). Alternatively, activate cells by peroxanate or thapsigargin [22].
5. Fix samples for 20 min at 37 °C with 3 % (w/v) paraformaldehyde in MSB, wash three times with MSB at 37 °C (5 min each wash), extract for 4 min at 37 °C with 0.5 % (v/v) Triton X-100 in MSB, and finally wash again three times with MSB at 37 °C (5 min each wash) (see Note 12).
6. Label the cells for 60 min at RT with anti-tubulin antibody. Dilute monoclonal antibody to β -tubulin TUB 2.1 conjugated with Cy3 1:600 in 2 % (w/v) BSA in PBS (see Note 13).
7. Wash the cells three times with PBS at RT (5 min each wash).
8. Mount cover slips in MOWIOL 4-88 reagent containing 1 μ g/ml 4',6-diamidino-2-phenylindole (DAPI).
9. Observe samples in laser scanning confocal microscope such as Leica TCS SP microscope equipped with 63 \times /1.4 NA oil-immersion objective. For Cy3 visualization use excitation and emission wavelengths 561 nm and 566–633 nm, respectively (diode-pumped solid-state laser). Acquire optical sections in 125 nm steps, and make z series from 70 sections. Perform deconvolution and rotation using Huygens Deconvolution Software.
10. Perform three independent immunofluorescence experiments to estimate the number of cells that respond to activation events by generation of protrusions containing microtubules [22]. In each experiment examine approximately 500 cells.

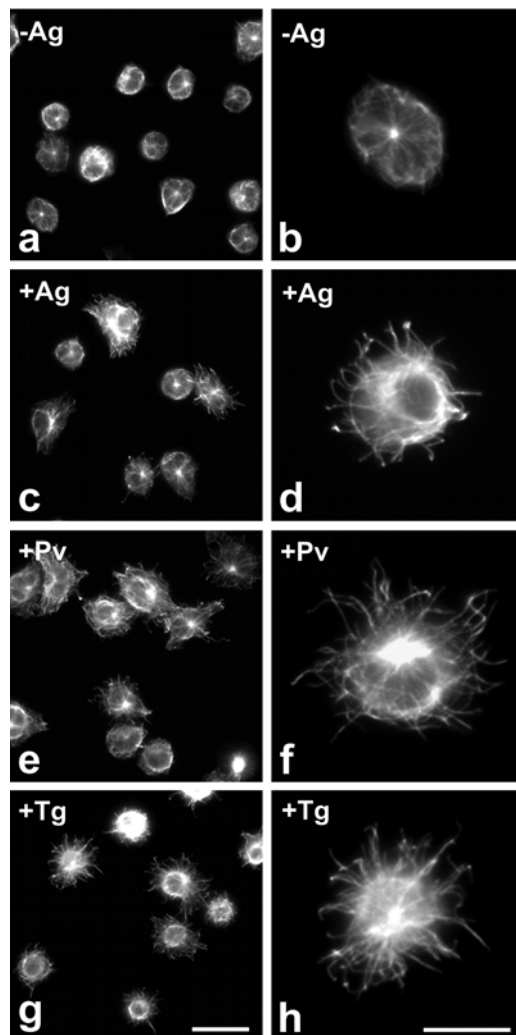


Fig. 4 Organization of microtubules in resting and activated mast cells. Resting BMMCs (**a, b**; $-Ag$), cells activated by Fc ϵ RI aggregation (**c, d**; $+Ag$), pervanadate (**e, f**; $+Pv$), or thapsigargin (**g, h**; $+Tg$) were fixed in formaldehyde and extracted in Triton X-100. Staining for β -tubulin. Scale bars, 20 μ m (**g**) and 10 μ m (**h**). Comparable magnifications are in **a, c, e, g** and in **b, d, f, h**. Reproduced by permission from ref. 22. Copyright 2011; The American Association of Immunologists, Inc.

A typical distribution of microtubules in non-activated and activated BMMCs stained by the procedure described above is shown in Fig. 4. Deconvoluted 3-D images from laser scanning confocal microscopy, shown in Fig. 5, demonstrate that microtubule protrusions in BMMCs do not reflect merely the spreading of cells during activation events, since they are also found on the dorsal side. A typical location of γ -tubulin in resting RBL-2H3 cells is demonstrated in Fig. 6. γ -Tubulin concentrates on centrosomes of interphase and mitotic cells from which microtubules are nucleated.

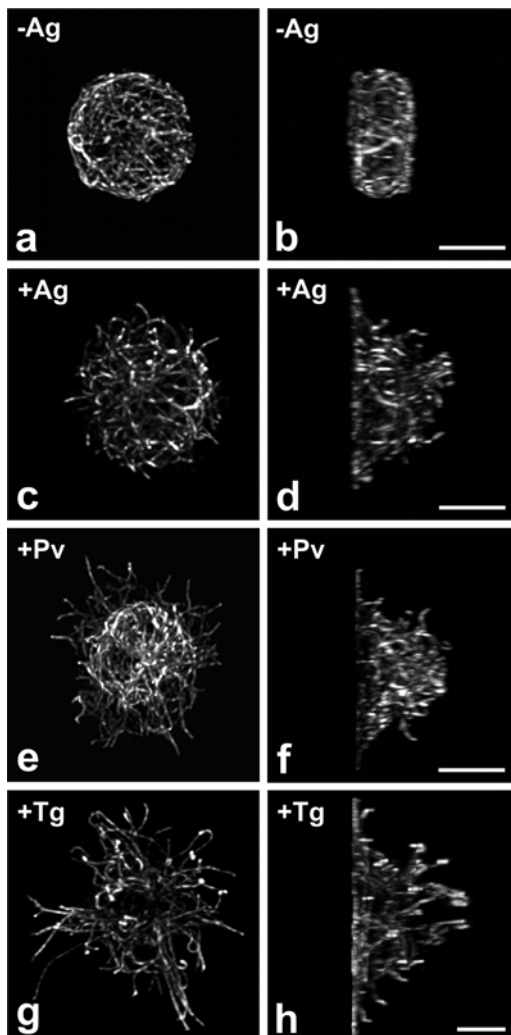


Fig. 5 Laser scanning confocal microscopy of microtubules in resting and activated BMMCs. Resting cells (**a**, **b**; $-Ag$), cells activated by Fc ϵ RI aggregation (**c**, **d**; $+Ag$), pervanadate (**e**, **f**; $+Pv$), or thapsigargin (**g**, **h**; $+Tg$) were fixed in formaldehyde and extracted in Triton X-100. Staining for β -tubulin. The stacks of confocal sections were deconvoluted and subjected to three-dimensional reconstruction. Resulting 3-D images viewed from top of the cells (**a**, **c**, **e**, **g**) and from the plane perpendicular to the plane of cell adhesion (**b**, **d**, **f**, **h**). Each pair, **a/b**, **c/d**, **e/f**, and **g/h** represents the same cells. Scale bars, 5 μ m. Reproduced by permission from ref. 22. Copyright 2011; The American Association of Immunologists, Inc.

Time-Lapse Imaging by Total Internal Reflection Fluorescence Microscopy (TIRFM)

To study the dynamics of microtubules on their plus ends in the course of mast cell activation, TIRFM on living cells, expressing tagged EB1 protein, is performed. Expression plasmid coding mouse EB1 fused with GFP (pEB1-GFP) was used in the following protocol [34].

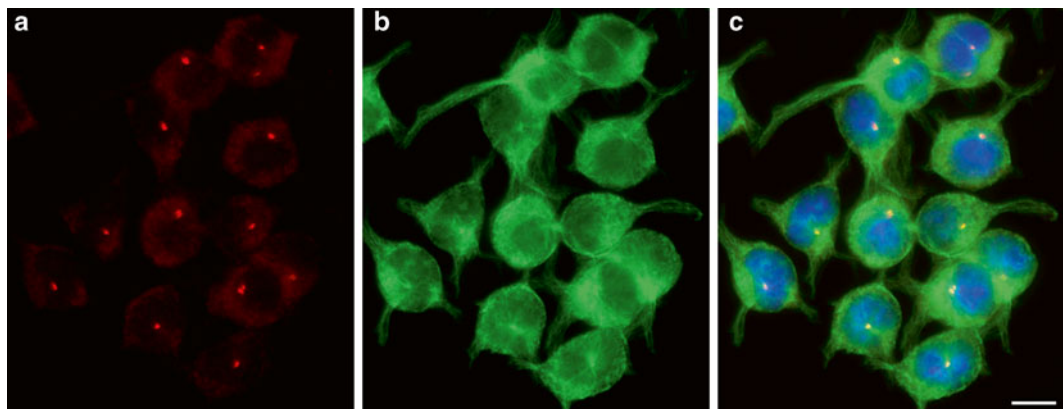


Fig. 6 Distribution of microtubules formed by $\alpha\beta$ -tubulin dimers and γ -tubulin in resting RBL-2H3 cells. Cells were fixed with cold methanol before staining with mouse monoclonal antibody TU-30 to γ -tubulin (**a**, red) and rabbit antibody to α -tubulin dimer (**b**, green). DNA was stained with DAPI (*blue*). Superposition of $\alpha\beta$ -tubulin and γ -tubulin is shown in **C**. Scale bar, 10 μ m. Photography E. Dráberová (Institute of Molecular Genetics AS CR, Prague)

1. Transfect cells with pEB1-GFP by nucleofection using Mouse Macrophage Kit and program Y-001 on Amaxa Nucleofector II according to the manufacturer's instructions. After nucleofection, transfer cells into culture media supplemented with IL-3 and culture for 24 h before analysis.
2. Overlay a 35 mm glass-bottom culture dish (MatTek) precoated with fibronectin, as in Subheading "Immunofluorescence Microscopy," **step 1**, with 100 μ l sample of cell suspension at a concentration 1.5×10^6 cells/ml. Allow cells to attach for 1 h at 37 °C.
3. Insert perfusion insert for 35 mm culture dish, wash cells, and subsequently incubate in RPMI-1640 medium for live-cell imaging.
4. Observe cells in TIRF microscope such as Leica AM TIRF MC at 37 °C. Acquire time-lapse sequences of EB1-GFP in TIRF mode (GFP cube, laser line 488 nm, Ex: 470/40, Em: 525/50, penetration depth 150 nm) using HCX PL APO 100 \times /1.46 NA oil-immersion TIRF objective. Take images for 3 min at 1-s intervals with 30-40 % laser power and exposure times ranging from 500 to 800 ms. Scan cells before, during, and after adding the activation agents (*see Note 14*).
5. Adjust time-lapse sequences and analyze by particle-tracking program. Detect regions of pixels with distance less than 3 μ m from cell boundary. Calculate the speed of particles as the ratio of particle trajectory length and trajectory duration. Calculate the histogram of the particle speed from the trajectory speed weighted by the trajectory duration (*see Note 15*).

6. Compute statistical data from a total of 15 to 21 different cells tracked in three independent experiments.

Activation of mast cells raises the number of growing microtubules in cell periphery as documented in Fig. 7.

4 Notes

1. Osmium tetroxide is extremely toxic heavy metal and, therefore, all work with it should be done carefully. Sodium cacodylate is also highly toxic by ingestion, inhalation, or skin contact. Work with osmium and sodium cacodylate should be done in fume hood.
2. Uranyl acetate is extremely toxic heavy metal and slightly radioactive (0.37–0.51 $\mu\text{Ci/g}$). Therefore, all work with it should be done carefully and in fume hood.
3. Glass cover slips should be thoroughly cleaned with synthetic detergent. After cleaning, the cover slips must be washed several times with ultraclean water (deionized water further purified to resistivity of $\geq 18 \text{ M}\Omega\cdot\text{cm}$ using a Milli-Q water purification system) to remove all traces of detergent, followed by a brief wash with 96 % ethanol, drying and transferring individually into a beaker with 35 % HCl. After 20–24 h the cover slips are washed several times with ultraclean water to remove all HCl. Finally, they are washed with ethanol and stored in ethanol until use.
4. To enhance the adhesiveness of BMMCs on fibronectin-coated glass, the cell adhesive BD Cell-Tak (8 $\mu\text{l/ml}$) is combined with fibronectin; importantly, cell spreading on Cell-Tak alone is not apparent.
5. The areas of activated cells can be normalized to the mean area of appropriate resting cells. The proportion of spread cells is calculated from the total number (100 %) of rounded, spread, and “ambiguous” cells.
6. RBL and some other mast cell lines can be cultured in simplified culture medium lacking IL-3 and SCF.
7. Cover slips are covered with fibronectin by incubation at 4 °C for 18–24 h with fibronectin (50 $\mu\text{g/ml}$ in 0.43 M NaHCO₃), followed by washing with distilled H₂O.
8. The cells can be activated with various concentrations of antigen or with other activators, such as 0.2 mM pervanadate [32].
9. EM grids covered with pioloform and coated with carbon are glow-discharged for 45–60 s by 300 V, incubated for 30 min with 1 mg/ml PLL in H₂O, washed for 5 s in H₂O, and dried. Immediately before isolation of PM sheets, EM grids are placed

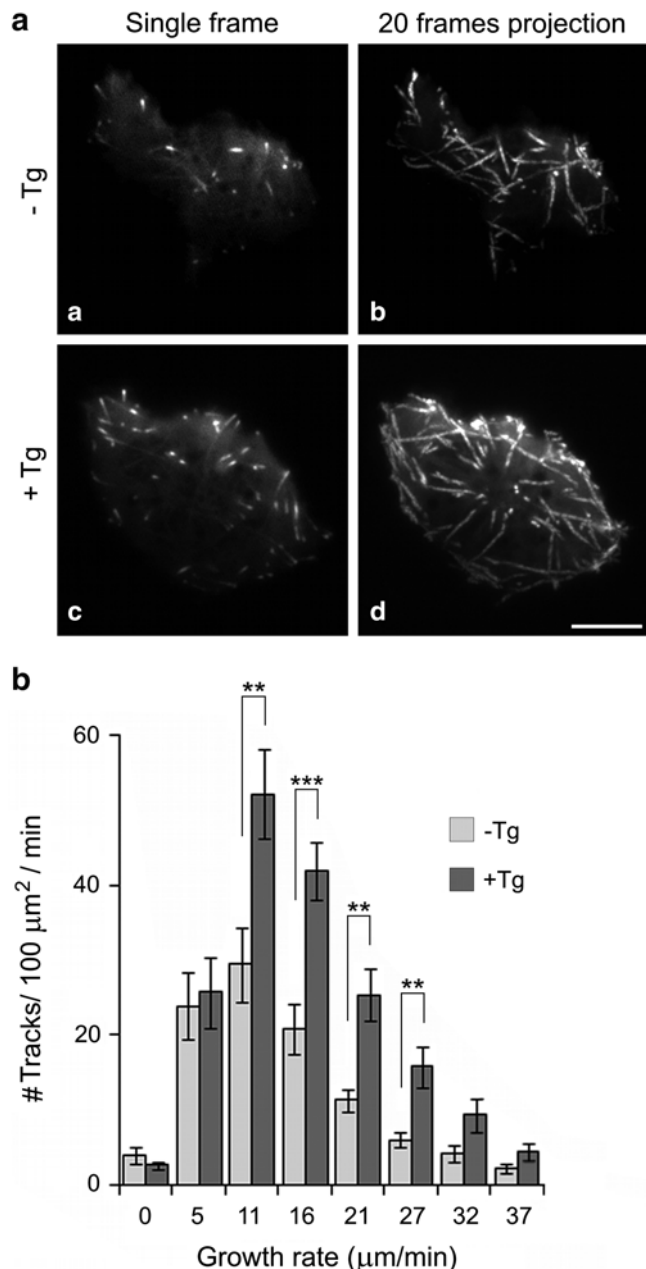


Fig. 7 Changes in the number of growing microtubules in cell periphery during mast cell activation as determined by TIRFM time-lapse imaging in living cells. **(A)** Time-lapse imaging of resting (*a*, *b*) and thapsigargin-activated (*c*, *d*) BMMCs expressing EB1-GFP. Still images of EB1 (*a*, *c*) and tracks of EB1 comets over 20 s created by maximum intensity projection of the 20 consecutive frames (*b*, *d*). Scale bar, 5 μm . **(B)** Histogram of microtubule growth rates in cell periphery of resting (-Tg) and thapsigargin-activated (+Tg) cells. A total of 15 different cells were tracked in five independent experiments. Values indicate mean \pm SE, $n=15$ (** $p < 0.01$; *** $p < 0.001$). Reproduced by permission from ref. 22. Copyright 2011; The American Association of Immunologists, Inc.

with the PLL side up onto a HEPES buffer-soaked nitrocellulose membrane filter (Millipore, 0.45 μ m pores) kept on ice-cold thermo-conductive platform.

10. Typically, three independent experiments are performed for each condition and 10–20 micrographs covering 22–44 μ m² of the plasma membrane are obtained from each grid. The coordinates of gold particles are determined using ImageJ software. Statistical evaluation of particle clustering is based on program Gold [35] using the pair correlation function (PCF), which expresses the ratio of the density of gold particles at a given distance from typical particle to the average density of such particles.
11. When cells are activated by pervanadate or thapsigargin, the sensitization step is skipped.
12. Fixation with formaldehyde followed by extraction in Triton X-100 is preferable for direct immunofluorescence staining of microtubules with Cy3-TUB 2.1 conjugate. When γ -tubulin is detected, cold methanol fixation is used. In this case, samples are incubated for 20 min in methanol precooled to –20 °C.
13. In double-label experiments intended to detect both microtubules and γ -tubulin, the methanol-fixed cells are washed with PBS at RT (three times, 5 min each wash) and incubated simultaneously with primary antibodies for 60 min at RT. Rabbit antibody to α -tubulin is diluted 1:200 and mouse monoclonal antibody to γ -tubulin (TU-30; spent hybridoma culture medium) to 1:5 in 2 % (w/v) BSA in PBS. After washing with PBS at RT (three times, 5 min each wash), the cover slips are incubated simultaneously for 45 min at RT, with conjugated secondary antibodies. Alexa Fluor 488-conjugated anti-rabbit antibody is diluted 1:200 and Cy3-conjugated anti-mouse antibody 1:1,000.
14. To follow the depolymerization of microtubules by TIRFM, nocodazole can be added at a concentration of 10 μ M.
15. For analysis of time-lapse sequences we have been using in-house-written particle-tracking plug-in that is implemented into Ellipse software version 2.07 [22].

Acknowledgements

We thank Dr. M. Hibbs (Ludwig Institute for Cancer Research, Melbourne, Australia) for the gift of BMMCs cell line and Dr. Y. Mimori-Kiyosue (KAN Research Institute, Kyoto, Japan) for EB1-GFP construct. Work on mast cells in the laboratories of authors has been funded, over the years, by several grants including 204/09/1777, P302/14/09807S, P305/14/00703S, and

P302/12/G101 from the Czech Science Foundation; Grants LC545, LD12073, LD 13015, and 1M6837805001 from the Ministry of Education, Youth and Sports of the Czech Republic; Project KAN200520701 and M200520901 from Academy of Sciences of the Czech Republic; and the Institutional Research Support (RVO 68378050).

References

1. Batista FD, Treanor B, Harwood NE (2010) Visualizing a role for the actin cytoskeleton in the regulation of B-cell activation. *Immunol Rev* 237:191–204
2. Smith-Garvin JE, Koretzky GA, Jordan MS (2009) T cell activation. *Annu Rev Immunol* 27:591–619
3. Bugajev V, Bambousková M, Dráberová L, Dráber P (2010) What precedes the initial tyrosine phosphorylation of the high affinity IgE receptor in antigen-activated mast cell? *FEBS Lett* 584:4949–4955
4. Pfeiffer JR, Seagrave JC, Davis BH, Deanin GG, Oliver JM (1985) Membrane and cytoskeletal changes associated with IgE-mediated serotonin release from rat basophilic leukemia cells. *J Cell Biol* 101:2145–2155
5. Frigeri L, Apgar JR (1999) The role of actin microfilaments in the down-regulation of the degranulation response in RBL-2H3 cells. *J Immunol* 162:2243–2250
6. Holowka D, Sheets ED, Baird B (2000) Interactions between Fc ϵ RI and lipid raft components are regulated by the actin cytoskeleton. *J Cell Sci* 113:1009–1019
7. Tolarová H, Dráberová L, Heneberg P, Dráber P (2004) Involvement of filamentous actin in setting the threshold for degranulation in mast cells. *Eur J Immunol* 34:1627–1636
8. Pendleton A, Koffer A (2001) Effects of latrunculin reveal requirements for the actin cytoskeleton during secretion from mast cells. *Cell Motil Cytoskeleton* 48:37–51
9. Tůmová M, Koffer A, Šimíček M, Dráberová L, Dráber P (2010) The transmembrane adaptor protein NTAL signals to mast cell cytoskeleton via the small GTPase Rho. *Eur J Immunol* 40:3235–3245
10. Wilson BS, Pfeiffer JR, Oliver JM (2000) Observing Fc ϵ RI signaling from the inside of the mast cell membrane. *J Cell Biol* 149:1131–1142
11. Wilson BS, Pfeiffer JR, Surviladze Z, Gaudet EA, Oliver JM (2001) High resolution mapping of mast cell membranes reveals primary and secondary domains of Fc ϵ RI and LAT. *J Cell Biol* 154:645–658
12. Volná P, Lebduška P, Dráberová L, Šimová S, Heneberg P, Boubelík M, Bugajev V, Malissen B, Wilson BS, Hořejší V, Malissen M, Dráber P (2004) Negative regulation of mast cell signaling and function by the adaptor LAB/NTAL. *J Exp Med* 200:1001–1013
13. Heneberg P, Lebduška P, Dráberová L, Korb J, Dráber P (2006) Topography of plasma membrane microdomains and its consequences for mast cell signaling. *Eur J Immunol* 36: 2795–2806
14. Cooper JA (1987) Effects of cytochalasin and phalloidin on actin. *J Cell Biol* 105:1473–1478
15. Coue M, Brenner SL, Spector I, Korn ED (1987) Inhibition of actin polymerization by latrunculin A. *FEBS Lett* 213:316–318
16. Kitaura J, Eto K, Kinoshita T, Kawakami Y, Leitges M, Lowell CA, Kawakami T (2005) Regulation of highly cytokinergic IgE-induced mast cell adhesion by Src, Syk, Tec, and protein kinase C family kinases. *J Immunol* 174: 4495–4504
17. Nogales E, Wang HW (2006) Structural mechanisms underlying nucleotide-dependent self-assembly of tubulin and its relatives. *Curr Opin Struct Biol* 16:221–229
18. Akhmanova A, Steinmetz MO (2008) Tracking the ends: a dynamic protein network controls the fate of microtubule tips. *Nat Rev Mol Cell Biol* 9:309–322
19. Smith AJ, Pfeiffer JR, Zhang J, Martinez AM, Griffiths GM, Wilson BS (2003) Microtubule-dependent transport of secretory vesicles in RBL-2H3 cells. *Traffic* 4:302–312
20. Nishida K, Yamasaki S, Ito Y, Kabu K, Hattori K, Tezuka T, Nishizumi H, Kitamura D, Goitsuka R, Geha RS, Yamamoto T, Yagi T, Hirano T (2005) Fc ϵ RI-mediated mast cell degranulation requires calcium-independent microtubule-dependent translocation of granules to the plasma membrane. *J Cell Biol* 170: 115–126

21. Martin-Verdeaux S, Pombo I, Iannascoli B, Roa M, Varin-Blank N, Rivera J, Blank U (2003) Evidence of a role for Munc18-2 and microtubules in mast cell granule exocytosis. *J Cell Sci* 116:325–334
22. Hájková Z, Bugajev V, Dráberová E, Vinopal S, Dráberová L, Janáček J, Dráber P, Dráber P (2011) STIM1-directed reorganization of microtubules in activated mast cells. *J Immunol* 186:913–923
23. Sulimenko V, Dráberová E, Sulimenko T, Macurek L, Richterová V, Dráber P, Dráber P (2006) Regulation of microtubule formation in activated mast cells by complexes of gamma-tubulin with Fyn and Syk kinases. *J Immunol* 176:7243–7253
24. Dráberová L, Dráberová E, Surviladze Z, Dráber P, Dráber P (1999) Protein tyrosine kinase p53/p56(lyn) forms complexes with gamma-tubulin in rat basophilic leukemia cells. *Int Immunol* 11:1829–1839
25. Barsumian EL, Isersky C, Petrino MG, Siraganian RP (1981) IgE-induced histamine release from rat basophilic leukemia cell lines: isolation of releasing and nonreleasing clones. *Eur J Immunol* 11:317–323
26. Tsujimura T, Furitsu T, Morimoto M, Kanayama Y, Nomura S, Matsuzawa Y, Kitamura Y, Kanakura Y (1995) Substitution of an aspartic acid results in constitutive activation of c-kit receptor tyrosine kinase in a rat tumor mast cell line RBL-2H3. *Int Arch Allergy Immunol* 106:377–385
27. Dráberová L, Lebduška P, Hálová I, Tolar P, Štokrová J, Tolarová H, Korb J, Dráber P (2004) Signaling assemblies formed in mast cells activated via Fce receptor I dimers. *Eur J Immunol* 34:2209–2219
28. Lebduška P, Korb J, Tůmová M, Heneberg P, Dráber P (2007) Topography of signaling molecules as detected by electron microscopy on plasma membrane sheets isolated from non-adherent mast cells. *J Immunol Methods* 328: 139–151
29. Wilson BS, Pfeiffer JR, Raymond-Stintz MA, Lidke D, Andrews N, Zhang J, Yin W, Steinberg S, Oliver JM (2007) Exploring membrane domains using native membrane sheets and transmission electron microscopy. *Methods Mol Biol* 398:245–261
30. Dráberová L, Shaik GM, Volná P, Heneberg P, Tůmová M, Lebduška P, Korb J, Dráber P (2007) Regulation of Ca^{2+} signaling in mast cells by tyrosine-phosphorylated and unphosphorylated non-T cell activation linker. *J Immunol* 179:5169–5180
31. Smrž D, Lebduška P, Dráberová L, Korb J, Dráber P (2008) Engagement of phospholipid scramblase 1 in activated cells: implication for phosphatidylserine externalization and exocytosis. *J Biol Chem* 283:10904–10918
32. Heneberg P, Dráberová L, Bambousková M, Pomach P, Dráber P (2010) Down-regulation of protein tyrosine phosphatases activates an immune receptor in the absence of its translocation into lipid rafts. *J Biol Chem* 285: 12787–12802
33. Dráber P, Dráberová E, Linhartová I, Viklický V (1989) Differences in the exposure of C- and N-terminal tubulin domains in cytoplasmic microtubules detected with domain-specific monoclonal antibodies. *J Cell Sci* 92: 519–528
34. Mimori-Kiyosue Y, Shiina N, Tsukita S (2000) The dynamic behavior of the APC-binding protein EB1 on the distal ends of microtubules. *Curr Biol* 10:865–868
35. Philimonenko AA, Janáček J, Hozák P (2000) Statistical evaluation of colocalization patterns in immunogold labeling experiments. *J Struct Biol* 132:201–210
36. Rudolph AK, Burrows PD, Wabl MR (1981) Thirteen hybridomas secreting hapten-specific immunoglobulin E from mice with Ig^a or Ig^b heavy chain haplotype. *Eur J Immunol* 11: 527–529
37. Rivera J, Kinet J-P, Kim J, Pucillo C, Metzger H (1988) Studies with a monoclonal antibody to the β subunit of the receptor with high affinity for immunoglobulin E. *Mol Immunol* 25:647–661
38. Dráberová L, Amoui M, Dráber P (1996) Thy-1-mediated activation of rat mast cells: the role of Thy-1 membrane microdomains. *Immunology* 87:141–148
39. Tolar P, Dráberová L, Dráber P (1997) Protein tyrosine kinase Syk is involved in Thy-1 signaling in rat basophilic leukemia cells. *Eur J Immunol* 27:3389–3397
40. Nováková M, Dráberová E, Schurmann W, Czihak G, Viklický V, Dráber P (1996) Gamma-tubulin redistribution in taxol-treated mitotic cells probed by monoclonal antibodies. *Cell Motil Cytoskeleton* 33:38–51

Chapter 15

Fc ϵ RI Expression and Dynamics on Mast Cells

Eon J. Rios and Janet Kalesnikoff

Abstract

Mast cells are key effector and immunoregulatory cells in IgE-associated immune responses, including allergic disorders. IgE antibodies bind to the high-affinity IgE receptor, Fc ϵ RI, expressed on the surface of mast cells; antigen-induced cross-linking of Fc ϵ RI-bound IgE molecules activates the mast cell to release an array of proinflammatory and immunomodulatory mediators. Because mast cells often respond to very low levels of antigen in vivo, the level of Fc ϵ RI expressed on the surface of these cells is an important factor in determining the responsiveness of these cells to antigen. Fc ϵ RI surface expression is regulated by a number of processes, including Fc ϵ RI stabilization, Fc ϵ RI recycling, and antigen-induced internalization. Although members of the Rab family of small GTPases and the ubiquitin ligase, Cbl, have recently emerged as major regulators of many of the membrane trafficking events that govern Fc ϵ RI expression levels, the mechanisms and intracellular pathways that regulate Fc ϵ RI trafficking remain poorly defined. This chapter outlines a number of flow cytometry-based assays that can be used to investigate cell surface Fc ϵ RI expression and dynamics (stabilization, recycling, and internalization) on bone marrow-derived mast cells (BMCMCs), the most commonly used model system for studying mast cells in vitro. Given the importance of Fc ϵ RI levels to mast cell responsiveness and function, the characterization of Fc ϵ RI expression and dynamics on different mast cell populations is critical when trying to compare IgE-dependent processes between different mast cell populations.

Key words Mast cells, BMMCs, BMCMCs, Allergy, IgE, Fc ϵ RI, Receptor internalization, Ubiquitin, Membrane trafficking, Receptor recycling, Receptor stabilization

1 Introduction

Although mast cells have important effector and immunoregulatory roles in a variety of innate and adaptive immune responses that are thought to be independent of immunoglobulin E (IgE), these cells are best known for the critical roles they play in IgE-associated immediate hypersensitivity reactions and other allergic disorders. IgE primes mast cells to undergo antigen-dependent activation by binding to the high-affinity IgE receptor, Fc ϵ RI. In both humans and rodents, Fc ϵ RI is expressed on the surface of mast cells as a heterotetrameric complex composed of an IgE-binding α subunit, a four-transmembrane spanning β subunit (which serves as an

important amplifier of IgE plus antigen-induced signaling events), and two identical disulfide-linked γ subunits (which are important for initiating signaling events downstream of this receptor because they each contain one immunoreceptor tyrosine-based activation motif [ITAM]) [1, 2]. IgE binds to Fc ϵ RI at a very high affinity and this interaction has a slow rate of dissociation [1]; thus, Fc ϵ RI binds IgE and retains it for long periods setting the stage for an immediate allergic or inflammatory response upon exposure to environmental antigen. Aggregation of two or more Fc ϵ RI-bound IgE molecules by bivalent or multivalent antigens triggers the rapid release of mediators stored as preformed in mast cell granules (degranulation), the de novo synthesis of lipid mediators, and the synthesis and release of cytokines, chemokines, and growth factors, as well as mast cell adhesion and migration [2–5].

The expression of Fc ϵ RI on the surface of mast cells and the processes that regulate its expression (including receptor stabilization, recycling, and ligand-induced internalization) are critical for mast cells to mount optimal responses to antigens. Receptor regulation is particularly important in responding to low concentration of ligands, as mast cells are able to do. The membrane trafficking events that regulate Fc ϵ RI expression levels remain poorly defined; however, members of the Rab family of small GTPases [6–8] and the ubiquitin ligase, Cbl [9], have recently emerged as major regulators of many of Fc ϵ RI membrane trafficking events.

The stability of Fc ϵ RI on the mast cell surface is a chief determinant of Fc ϵ RI expression levels. Fc ϵ RI stability can be influenced by both intracellular molecules, such as RabGEF1 [10] and Rabaptin-5 [11], and external factors, such as IgE binding [2, 12, 13]. Unoccupied Fc ϵ RI complexes are not very stable on the surface of mast cells; unoccupied Fc ϵ RI is lost from the cell surface via endocytosis (not receptor shedding, as reported for the low affinity IgE receptor, Fc ϵ RII/CD23 [14]) and partially recycled back to the cell surface [11, 15, 16]. Recycling of unoccupied Fc ϵ RI back to the surface increases the chances of capturing circulating IgE molecules, which have the lowest serum concentration of all immunoglobulins. IgE binding stabilizes the Fc ϵ RI complex on the surface of mast cells [2, 12, 13]; there is a tight correlation between serum IgE levels and the density of Fc ϵ RI on the surface of mast cells *in vivo* [2, 13, 17–20]. IgE-mediated stabilization of Fc ϵ RI may have important implications in allergic individuals with elevated IgE levels; for example, mast cells with higher Fc ϵ RI expression levels on their surface will mount stronger responses to a given amount of antigen and will respond to lower levels of antigen [2, 11, 18, 20].

Cross-linking of Fc ϵ RI-bound IgE molecules induces the activation of Lyn, which phosphorylates Fc ϵ RI ITAMs, and other kinases and signaling molecules (both positive and negative signaling molecules) downstream of this receptor [5, 21]. Aggregation

of this receptor also triggers the ligand-induced internalization (or endocytosis) of Fc ϵ RI to remove activated receptors from the cell surface (and turn downstream signaling events “off”). While many studies suggest that rapid and efficient antigen-dependent Fc ϵ RI internalization occurs via clathrin-mediated endocytosis [22–24], the accumulation of engaged Fc ϵ RI subunits into lipid rafts (specialized regions of the plasma membrane enriched in cholesterol and glycosphingolipid) has recently been shown to be required for full activation and ubiquitination of Fc ϵ RI [25–27]. Ubiquitination is a posttranslational modification required for efficient receptor internalization and endosomal sorting [28]; thus, lipids raft appear to play an important role in antigen-dependent Fc ϵ RI internalization. Early endosomes receive cargo destined to be recycled back to the plasma membrane or to be sorted along the endocytic machinery and delivered to a lysosomal compartment for degradation. The fate of the internalized receptor (recycling versus degradation) depends, at least in part, on signals presented by the internalized receptor; for example, ubiquitination of Fc ϵ RI is required for efficient receptor internalization, sorting, and degradation by lysosomes [26, 27].

Given the importance of Fc ϵ RI levels to mast cell responsiveness and functional activation, it is very important to assess baseline levels of Fc ϵ RI expression on the surface of any mast cell populations you want to study (e.g., mast cells generated from knockout mice lacking a particular gene of interest, mast cells treated with shRNA to knockdown a particular gene of interest, etc.) and compare these levels to those observed on appropriate control (wild-type) mast cells. Moreover, if the gene or protein you are studying is involved in endocytosis or membrane trafficking events, ubiquitination pathways, or other signaling pathways downstream of the Fc ϵ RI, it may be important to look at Fc ϵ RI stability, recycling, and antigen-induced internalization in addition to baseline expression levels. This chapter describes a number of flow cytometry-based assays to investigate cell surface Fc ϵ RI expression and dynamics in bone marrow-derived cultured mast cells (BMCMCs), the most commonly used model system for studying mast cells *in vitro*. For detailed protocols on how to generate and culture BMCMCs and assess maturity, please *see* Kalesnikoff and Galli 2011 [29]. Although we developed these protocols using BMCMCs, they could easily be adapted and used to studying Fc ϵ RI dynamics on other mast cell types or other cells that express Fc ϵ RI.

The protocols described herein can be used as a starting point to examine the effect of intracellular receptor trafficking inhibitors, genetic deficiencies (knockout or knockdown studies), or other receptor perturbations on Fc ϵ RI receptor dynamics. These dynamics are extremely important when trying to compare IgE-dependent processes between two mast cell populations (e.g., mast cells lacking a particular gene of interest generated from knockout mice

(or via shRNA knockdown studies) versus wild-type mast cells), which require Fc ϵ RI expression and receptor dynamics to be similar between populations. If preliminary experiments reveal that two mast cell populations have different baseline Fc ϵ RI expression levels, the protocols described herein serve as a foundation to explore the underlying biologic processes responsible for this difference in Fc ϵ RI expression. We outline an assay to examine surface half-life of Fc ϵ RI (or other receptors of interest) by examining the decay of surface Fc ϵ RI after blocking protein synthesis (using cycloheximide) or blocking exit from the endoplasmic reticulum (using brefeldin A). Recycling of Fc ϵ RI may also contribute to altered surface expression; thus, we describe a method to examine both the extent and kinetics of Fc ϵ RI recycling using fragment antigen-binding (Fab) fragments that selectively label Fc ϵ RI without inducing receptor aggregation. Conversely, if preliminary experiments reveal that two mast cell populations have similar Fc ϵ RI expression levels, but there is concern that stimulation-induced internalization may be perturbed (e.g., due to alterations in Rab- or ubiquitination-dependent pathways), we outline steps to determine the kinetics of stimulation-induced Fc ϵ RI internalization. Because differences in this very proximal event can have a profound influence on the extent of mast cell activation [10], stimulation-induced internalization experiments are also important to perform on mast cell populations with different baseline Fc ϵ RI expression levels.

We focus herein on flow cytometry-based assays to study Fc ϵ RI dynamics for a number of reasons. First, this system allows for quick and user-friendly experiments with equipment that is ubiquitous in most research settings. One only needs a few antibodies, standard reagents used in many assays, and a flow cytometer (a machine that is becoming more available to individual labs and becoming increasingly easier to operate). Second, flow cytometry permits the scientist to perform analyses on small quantities of cells (an important advantage when working with rare cell populations or freshly isolated cells, such as peritoneal mast cells). Moreover, flow cytometry allows the scientist to look at individual cells (a property intrinsic to flow cytometry) in a population of cells and then pool the single-cell data to generate average (mean) values for a population of cells being studied (this is the standard in other techniques that have been used in examining protein trafficking events, including subcellular fractionation to assess receptor localization in different compartments, surface radiolabeling, or surface biotinylation experiments). By examining the distribution of the protein of interest in a population (and not just the population average), the investigator may gain additional insight about the kinetics of a phenomenon or be better suited to choose the correct method by which to analyze the data (comparing means, medians, or sub-grouping cell populations). Third, flow cytometry has the

advantage of allowing the scientist to exclude dead or dying cells (which have drastically different receptor dynamics) from analyses with the use of vital dyes such as propidium iodide (PI). Finally, with more sophisticated experiments than those described herein, one can compare a number of different cell populations in one experiment or even in the same tube. This is important when studying freshly isolated cells *ex vivo* because one can use surface protein expression to identify cell populations of interest and exclude potentially confounding cell populations. Further, for transgene experiments, cells transfected or transduced with bi-cis-tronic vectors expressing fluorophores that can be analyzed with the flow cytometer's filter set (e.g., GFP, CFP, mTomato, or mCherry) allow for the simultaneous comparison of initially homogenous populations in the same staining sample or experimental group, and these populations can be separated later for analysis.

2 Materials

A flow cytometer with a 488 nm fixed argon laser and three-color detection capability (i.e., FL1, FL2, and FL3) is essential for the methods described below. Using APC or Alexa Fluor[®] 647-conjugated antibodies, the flow cytometry will require a flow cytometer with argon and red diode laser (635 nm) with four-color detection capability. For the materials and methods described below, we used a FACSCalibur[®] flow cytometer (BD Biosciences).

2.1 Assessing Baseline Fc ϵ RI Expression in BMCMCs

1. Flow cytometry (FACS) buffer: phosphate buffered saline (PBS) supplemented with 2 % fetal bovine serum (FBS) (*see Note 1*).
2. 5 mL polystyrene round bottom tubes (FACS tubes) or other tubes compatible with the flow cytometer instrument (*see Note 2*).
3. Purified anti-mouse CD16/32, clone 93 (*see Note 3*).
4. APC (allophycocyanin)-conjugated anti-mouse Fc ϵ RI α , clone MAR-1 (*see Note 4*).
5. APC-conjugated isotype control antibody (if desired).
6. Propidium iodide (PI): prepare a 1 mg/mL stock in PBS.

2.2 Stimulation-Induced Internalization of Fc ϵ RI-Bound IgE

1. Dulbecco's Modified Eagle's Medium (DMEM) supplemented with 0.1 % bovine serum albumin (BSA) (*see Note 5*).
2. DMEM supplemented with 10 % FBS.
3. Purified IgE (*see Note 6*).
4. 15–50 mL conical polystyrene tubes.
5. 1.5 mL capped microcentrifuge (Eppendorf) tubes for stimulation.

6. FACS buffer (*see Subheading 2.1 and Note 1*).
7. 5 mL FACS tubes (*see Note 2*).
8. APC-conjugated streptavidin (*see Note 4*).
9. Biotin rat anti-mouse IgE (clone R35-72).
10. Propidium iodide (PI) stock: 1 mg/mL solution in PBS.

2.3 Fc ϵ RI Stability Assay

1. DMEM supplemented with 0.1 % BSA.
2. DMEM supplemented with 10 % FBS.
3. FACS buffer (*see Subheading 2.1 and Note 1*).
4. 5 mL FACS tubes (*see Note 2*).
5. Cycloheximide (CHX) stock solution: 100 mg/mL in dimethyl sulfoxide (DMSO).
6. Brefeldin A (BFA) stock solution: 10 mg/mL in DMSO.
7. Purified anti-mouse CD16/32, clone 93 (*see Note 3*).
8. APC-conjugated anti-mouse Fc ϵ RI α , clone MAR-1 (*see Note 4*).
9. PI stock solution: 1 mg/mL in PBS.

2.4 Fc ϵ RI Recycling Assay

1. DMEM supplemented with 0.1 % BSA.
2. DMEM supplemented with 10 % FBS.
3. FACS buffer (*see Subheading 2.1 and Note 1*).
4. 5 mL FACS tubes (*see Note 2*).
5. Purified anti-mouse CD16/32, clone 93 (*see Note 3*).
6. Alexa Fluor[®] 647 (AF647)-conjugated monovalent streptavidin (SA) and unlabeled monovalent SA, generated from pET21a-Streptavidin-Dead (Addgene plasmid number 20859; *see Note 7*).
7. Biotinylated anti-mouse Fc ϵ RI α , clone MAR-1 antigen-binding (Fab) fragments: prepare 0.1–1 mg/mL stock solution in PBS (*see Note 8*).
8. PI stock solution: prepare 1 mg/mL in PBS.

3 Methods

3.1 Assessing Baseline Fc ϵ RI Expression in BMCMCs

1. Approximately 5×10^4 – 5×10^5 cells are required for each condition (there will be two or three conditions for each population of BMCMCs being studied, as described in **step 3**, Subheading 3.1). Wash cells with 3 mL 4 °C FACS buffer (*see Note 1*) in a 5 mL FACS tube (*see Note 2*). Centrifuge at $500 \times g$, 5 min, 4 °C. Aspirate the supernatant down to the pellet.
2. Prepare Fc γ R blocking solution: dilute anti-mouse CD16/CD32, clone 93 (*see Note 3*), 1/200 in FACS buffer (2 µg/mL final

concentration of α -CD16/ α -CD32). Add 10 μ L Fc γ R blocking solution to each pellet (resuspend pellet or flick tube to agitate). This step blocks nonspecific binding of antibodies. Incubate for 5 min on ice.

3. Prepare anti-mouse Fc ϵ RI α staining solution: dilute APC-conjugated anti-mouse Fc ϵ RI α (see Note 4) 1/200 in FACS buffer. Add 20 μ L anti-mouse Fc ϵ RI α staining solution to the desired tubes from step 2. For each BMCMC population, it is best to have one tube of cells that receives the APC-conjugated anti-mouse Fc ϵ RI α staining solution (“stained”) and one tube of cells that does not receive staining solution (“unstained”) or a tube that receives an APC-conjugated isotype control antibody (see Note 9). Incubate for 15–30 min on ice protected from light. If working with peritoneal mast cells, see Note 10. *Important:* From this step forward, protect samples from direct light (use lid on ice bucket).
4. Wash cells with 3 mL 4 °C FACS buffer. Centrifuge at 500 $\times g$, 5 min, 4 °C. Aspirate the supernatant.
5. Prepare propidium iodide (PI) staining solution: dilute PI stock 1/1,000 in FACS buffer (final PI concentration 1 μ g/mL). Resuspend pellet in 200 μ L PI staining solution.
6. Acquire cell-associated APC and PI fluorescence on a flow cytometer (no compensation is usually necessary for these two fluorophores).
7. Analyze results using data analysis software. We use FlowJo software (Tree Star, Ashland, OR), but other software, such as software that comes with the flow cytometer, can be used.

3.2 Stimulation-Induced Internalization of Fc ϵ RI-Bound IgE

1. Approximately 1×10^5 cells are required for each condition or time point (see Note 11). Remove the desired number of BMCMCs and wash with 10 mL of pre-warmed (37 °C) DMEM + 10 % FCS. Centrifuge at 500 $\times g$, 5 min, 20–25 °C (room temperature (RT)). Aspirate the supernatant.
2. Prepare IgE solution: dilute monoclonal mouse IgE (see Note 6) to a concentration of 1–2 μ g/mL in DMEM + 10 % FCS. Resuspend cell pellet in appropriate volume of IgE solution to achieve the desired concentration of 1×10^6 cells/mL. Transfer cells to the appropriate size tissue culture dish (e.g., 24-well plate). Incubate for 16–18 h at 37 °C in a tissue culture incubator. This step “preloads” the mast cells with IgE.
3. Transfer cells from culture dish or wells to a 15 mL tube. Wash cells with 5–10 mL of 20–25 °C (room temperature) DMEM + 0.1 % BSA to remove excess/unbound IgE. Centrifuge at 500 $\times g$, 5 min, 4 °C. Aspirate the supernatant.
4. Repeat wash step with 5–10 mL 4 °C DMEM + 0.1 % BSA. Centrifuge at 500 $\times g$, 5 min, 4 °C. Aspirate the supernatant.

5. Resuspend pellet to achieve 2×10^6 cells/mL concentration in 4 °C DMEM + 0.1 % BSA. Remove an aliquot (1×10^5 cells; 50 μ L) for unstained control; add cells to a 5 mL FACS tube (*see Note 2*) containing 3 mL of 4 °C FACS buffer and keep on ice (until all time points have been collected in **step 10**, and then proceed to **step 11**, Subheading 3.2).
6. To the remaining cells, add biotin rat anti-mouse IgE antibody to a final concentration of 1 μ g/mL (stock is 500 μ g/mL : 1/500 dilution). Incubate for 1 h on ice. The antibodies will cross-link IgE-bound Fc ϵ RI α receptors.
7. Wash cells with 5–10 mL 4 °C DMEM + 0.1 % BSA. Centrifuge at $500 \times g$, 5 min, 4 °C. Aspirate the supernatant. Repeat **step 7**, once more.
8. Resuspend at 1×10^6 cells/mL in pre-warmed (37 °C) DMEM + 0.1 % BSA. Immediately remove an aliquot (1×10^5 cells; 100 μ L) for 0 min time point; add cells to a FACS tube containing 3 mL of 4 °C FACS buffer and keep on ice (until all time points have been collected in **step 10**; then proceed to **step 11**, Subheading 3.2).
9. Transfer the remaining cells to a 1.5 mL microcentrifuge (Eppendorf) tube and place tube in a 37 °C water bath. Remove aliquots (1×10^5 cells each; 100 μ L each) at 5, 15, 30, 60, and 90 min; add cells to a 5 mL FACS tube containing 3 mL of 4 °C FACS buffer and keep on ice (until all time points have been collected).
10. Centrifuge all samples at $500 \times g$, 5 min, 4 °C. Aspirate the supernatant.
11. Prepare streptavidin staining solution: dilute APC-conjugated streptavidin (*see Note 4*) 1/200 in FACS buffer. Add 20 μ L streptavidin staining solution to all samples. Incubate for 20 min on ice protected from light. *Important:* From this step forward, protect samples from direct light (use lid on ice bucket).
12. Wash cells with 3 mL 4 °C FACS buffer. Centrifuge at $500 \times g$, 5 min, 4 °C. Aspirate the supernatant.
13. Prepare propidium iodide (PI) staining solution: dilute PI stock 1/1,000 in FACS buffer (final PI concentration 1 μ g/mL). Resuspend pellet in 200 μ L PI staining solution.
14. Acquire cell-associated APC and PI fluorescence on a flow cytometer (no compensation is usually necessary for these two fluorochromes).
15. Analyze results using data analysis software. To calculate percent Fc ϵ RI internalization, we use the flow cytometry data analysis software to calculate mean fluorescence intensity (MFI) of the APC channel for each time point (after gating out

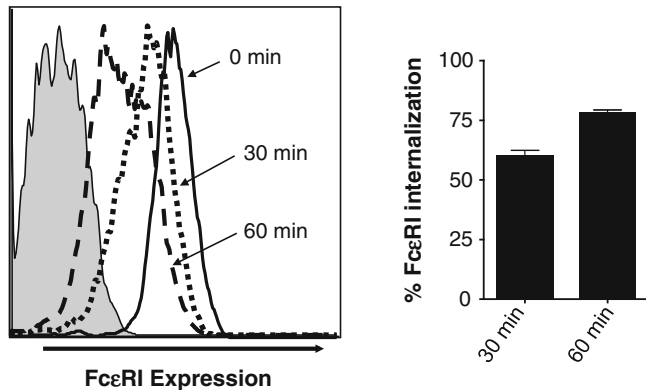


Fig. 1 Fc ϵ RI internalization assay. BMCMCs were sensitized with 1–2 μ g/mL IgE, and then stimulated with 1 μ g/mL biotinylated anti-mouse IgE antibodies (α -IgE) for the indicated times, as described in Subheading 3.2. Surface α -IgE was assessed by streptavidin (SA)-APC fluorescence and analyzed by flow cytometry, as described in Subheading 3.2. The histogram (*left panel*) shows representative results obtained from a single batch of BMCMCs; gray represents SA-APC staining only. The *bar graph* (*right panel*) shows the mean + SEM of percentage Fc ϵ RI internalization determinations from three separate batches of BMCMCs

PI-positive/dead cells). Using the MFI for each time point, calculate percent internalization using the following equation: $[\text{MFI}(\text{time } X) - \text{MFI}(\text{time } 0')]/\text{MFI}(\text{time } 0')$. An abbreviated time course histogram and compiled results are depicted in Fig. 1.

3.3 Fc ϵ RI Stability Assay

1. Approximately 2×10^5 BMCMCs are required for each condition or time point (*see Note 12*). Remove the desired number of BMCMCs and wash with 10 mL of warm (37 °C) DMEM + 10 % FCS. Centrifuge at $500 \times g$, 5 min, 20–25 °C (RT). Aspirate the supernatant.
2. Resuspend at 1×10^6 cells/mL in 37 °C DMEM + 10 % FCS. Immediately remove two aliquots (1×10^5 cells each; 100 μ L each) for unstained control and 0 min time point; add cells to a 5 mL FACS tube containing 3 mL of 4 °C FACS buffer and centrifuge at $500 \times g$, 5 min, 4 °C. Aspirate the pellet, and then proceed to **step 2** of the protocol listed in Subheading 3.1 to assess Fc ϵ RI expression (do not add APC-conjugated anti-mouse Fc ϵ RI α (*see Note 4*) antibodies to unstained control in **step 3**, Subheading 3.1).
3. Split the remaining volume of cells into three equal portions (for treatment with vehicle (DMSO), cycloheximide, or brefeldin A); transfer cells to the appropriate size tissue culture dish (e.g., 48-well plate). To the vehicle (DMSO)-treated cells, add a volume of DMSO to generate a final concentration of DMSO equal to that of the highest concentration of DMSO

being used with cycloheximide or brefeldin A treatment (we typically use 1 % DMSO). To the cycloheximide-treated cells, add cycloheximide to a final concentration of 1.5 μ g/mL (see Note 13). To the brefeldin A-treated cells, add brefeldin A to a final concentration of 50–100 μ g/mL (see Note 13). Transfer cells to 37 °C tissue culture incubator.

4. Remove aliquots (1×10^5 cells each; 100 μ L each) from all treatment groups (vehicle [DMSO], cycloheximide, and brefeldin A) at 2, 4, 6, and 12 h (or other predetermined time points); add cells to a 5 mL FACS tube containing 3 mL of 4 °C FACS buffer, and centrifuge at $500 \times g$, 5 min, 4 °C. Aspirate the supernatant, and then proceed to step 2 of the protocol listed in Subheading 3.1 to assess Fc ϵ RI expression. Given the long intervals between time points, stain each sample as it becomes available.
5. Analyze results using data analysis software. Calculate MFI of the APC channel (see Note 4) for each time point (after gating out PI-positive/dead cells). To generate decay curves, first, calculate percent Fc ϵ RI expression relative to baseline using the following equation: (MFI time X/MFI time 0) $\times 100$. Pool data from three or more experiments to generate decay curves using data analysis software (we use Prism (GraphPad, La Jolla, CA), but other software can be used). Compare decay curves between experimental groups at each time point to look for differences in experimental groups. An example of a typical Fc ϵ RI stability time course after exposure to brefeldin A or cycloheximide is depicted in Fig. 2.

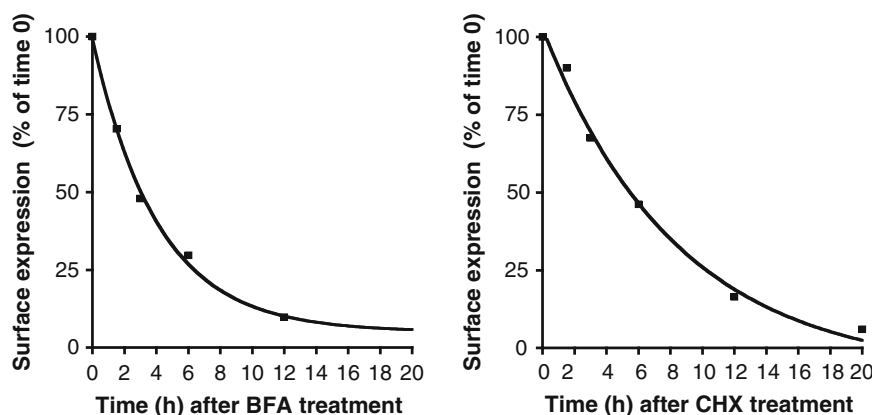


Fig. 2 Fc ϵ RI α half-life assay. Fc ϵ RI α half-life was measured in BMCMCs by exposing cells to 100 μ g/mL brefeldin A (BFA; *left panel*) or 1.5 μ g/mL cycloheximide (CHX; *right panel*) for the indicated times, and surface Fc ϵ RI was assessed by flow cytometry as described in Subheading 3.3. Expression relative to time 0 was calculated for the indicated time points. Data from three experiments were pooled, averaged, and fit to exponential decay curves

3.4 Fc ϵ RI Recycling Assay

1. Approximately 1×10^5 BMCMCs are required for each condition or time point (see Note 14). Remove the desired number of BMCMCs and wash with 10 mL of DMEM + 10 % FCS (at 20–25 °C). Centrifuge at $500 \times g$, 5 min, RT. Aspirate the supernatant.
2. Resuspend at 1×10^6 cells/mL in 20–25 °C DMEM + 10 % FCS. Remove an aliquot (1×10^5 cells; 100 μ L) for unstained control; use a 5 mL FACS tube containing 3 mL of 4 °C FACS buffer and keep on ice (until all time points have been collected in step 11; then proceed to step 12, Subheading 3.4).
3. Transfer the remaining cells to the appropriate size tissue culture dish (e.g., 48-well plate). Add biotinylated anti-mouse Fc ϵ RI α Fab fragments to a final concentration of 0.5 μ g/mL. Incubate for 3 h at 37 °C in a tissue culture incubator (see Note 15).
4. Transfer cells to a 15 mL tube. Wash cells with 10 mL of DMEM + 0.1 % BSA (at 20–25 °C). Centrifuge at $500 \times g$, 5 min, 4 °C. Aspirate the supernatant.
5. Repeat wash step with 4 °C DMEM + 0.1 % BSA. Centrifuge at $500 \times g$, 5 min, 4 °C. Aspirate the supernatant.
6. Resuspend at 1×10^6 cells/mL in 4 °C DMEM + 0.1 % BSA. Remove an aliquot (1×10^5 cells; 100 μ L) to assess baseline surface Fc ϵ RI expression; add cells to a 5 mL FACS tube containing 3 mL of 4 °C FACS buffer, and then centrifuge at $500 \times g$, 5 min, 4 °C. Aspirate the pellet and stain this aliquot with AF647-conjugated monovalent streptavidin as outlined in step 9 (Subheading 3.4), and then wash cells with 3 mL of 4 °C FACS buffer and proceed to step 12, Subheading 3.4.
7. To the remaining cells, add unlabeled monovalent streptavidin to a final concentration of 100 μ g/mL. Incubate for 30 min on ice; the unlabeled monovalent streptavidin will bind to the biotinylated Fab fragments (see Note 16).
8. Wash cells with 4 mL 4 °C DMEM + 0.1 % BSA. Centrifuge at $500 \times g$, 5 min, 4 °C. Aspirate the supernatant.
9. Resuspend at 1×10^6 cells/mL in 4 °C DMEM + 0.1 % BSA. Add AF647-conjugated monovalent streptavidin to a final concentration of 25 μ g/mL. Incubate for 30 min on ice. *Important:* From this step forward, protect samples from direct light (use lid on ice bucket and aluminum foil for tubes in water bath)
10. Remove an aliquot (1×10^5 cells; 100 μ L) for 0 min time point (see Note 17); add cells to a 5 mL FACS tube containing 3 mL of 4 °C FACS buffer and keep on ice (until all time points have been collected).
11. Transfer the remaining cells to a 1.5 mL microcentrifuge (Eppendorf) tube and place tube in a 37 °C water bath.

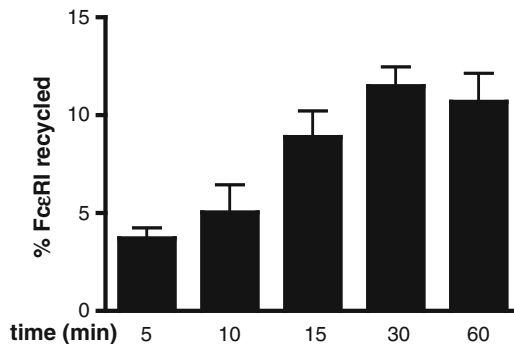


Fig. 3 Fc ϵ RI recycling assay. Fc ϵ RI recycling was assessed in BMCMCs using biotinylated α -Fc ϵ RI α Fab fragments, as described in Subheading 3.4. The bar graph represents mean + SEM of percentage Fc ϵ RI recycled determinations from three separate batches of BMCMCs

Remove aliquots (1×10^5 cells each; 100 μ L each) at 5, 15, 30, and 60 min; add cells to a 5 mL FACS tube containing 3 mL of 4 $^{\circ}$ C FACS buffer and keep on ice (until all time points have been collected).

12. Centrifuge tubes at $500 \times g$, 5 min, 4 $^{\circ}$ C. Aspirate the supernatant.
13. Prepare propidium iodide (PI) staining solution: dilute PI stock 1/1,000 in FACS buffer (final PI concentration 1 μ g/mL). Resuspend the pellet in 200 μ L PI staining solution.
14. Acquire cell-associated AF647 and PI fluorescence on a flow cytometer (no compensation is usually necessary for these two fluorophores).
15. Analyze results using data analysis software (we use FlowJo software [Tree Star, Ashland, OR], but other software, such as software that comes with the flow cytometer, can be used). Calculate MFI of the AF647 channel (*see Note 4*) for each time point (after gating out PI-positive/dead cells). Using the MFI for each time point, calculate percent recycled Fc ϵ RI using the following equation: [MFI (time X) – MFI (time 0)]/baseline MFI. An example of the typical results produced is shown in Fig. 3.

4 Notes

1. It is acceptable to use PBS + 2 % FBS, PBS + 0.5 % FBS, PBS + 0.1 % BSA, or PBS as FACS buffer for flow cytometry staining. Prepare FACS buffer fresh (on the day of experiment) or add 0.1 % sodium azide (NaN_3) to FACS buffer and store at 4 $^{\circ}$ C.

2. If you have a limited number of cells (e.g., less than 5×10^4), you can use a microcentrifuge (Eppendorf) tube so that the pellet can be visualized (if compatible with the flow cytometer being used). Wash volumes will need to be adjusted accordingly (depending on tube capacity).
3. Anti-mouse CD16/CD32 clone 93 or clone 2.4G2 antibodies can be used to block mast cell expressed Fc binding to antibodies used for flow cytometry.
4. Anti-mouse Fc ϵ RI α (MAR-1) antibodies or streptavidin can be coupled to other convenient fluorophores. We chose APC (or similar excitation/emission spectra fluorophores such as Alexa Fluor[®] 633 or Alexa Fluor[®] 647)-conjugated antibodies or streptavidin for our experiments to minimize compensation-induced changes from green- and red-emitting fluorophores that may effect the mean fluorescence intensities (MFI) that we compute and compare between populations.
5. It is acceptable to culture or stimulate BMCMCs in Iscove's Modified Dulbecco's Medium (IMDM) for all protocols that refer to DMEM.
6. A growing field of data shows that different mouse monoclonal IgE molecules vary in their ability to induce signaling events (and survival) in mouse mast cells in the absence of known antigen. Of the IgE antibodies studied so far, the mouse monoclonal anti-DNP IgE, clone SPE-7 (Sigma), displays the strongest signaling potential in mast cells [30, 31] and has been called highly cytokinetic [32], whereas other IgE clones (e.g., H1 ϵ -206 and H1 ϵ -26) that minimally activate mast cells [33, 34] have been called poorly cytokinetic [32]. When studying Fc ϵ RI dynamics, it is important to know whether you are using a poorly or highly cytokinetic IgE, since different mouse monoclonal IgE molecules may cause differences in Fc ϵ RI surface expression, internalization, and receptor cycling (e.g., SPE-7 can stimulate receptor internalization in the absence of known antigen). We used poorly cytokinetic IgE (i.e., H1 ϵ -26) for our studies, but it may be useful and interesting to examine the effects of highly cytokinetic IgE molecules in certain model systems.
7. Monovalent streptavidin is necessary in the Fc ϵ RI α flow cytometric recycling assay to label biotinylated anti-Fc ϵ RI α Fab fragments without cross-linking the Fc ϵ RI receptors. Cross-linking the Fc ϵ RI receptors would likely induce signaling-mediated internalization of the receptor and interfere with the study of Fc ϵ RI α dynamics. Normal or wild-type streptavidin cannot be used because it can bind up to four biotin moieties. The Ting Lab [35] has generated and made available a modified streptavidin molecule that only has one biotin

binding site, thus eliminating the possibility of streptavidin-induced cross-linking of biotinylated Fc ϵ RI α Fabs. Using the protocol listed in the nature protocol exchange site <http://www.nature.com/protocolexchange/protocols/413> and the Addgene vector (plasmid number 20859), one can generate and purify these extremely useful molecules. We labeled our monovalent streptavidin with AF647 using the Alexa Fluor[®] 647 protein labeling kit (Invitrogen; catalog #A20173), but monovalent streptavidin can be coupled to other convenient fluorophores, such as AF633 or APC (*see Note 4*).

8. To generate anti-mouse Fc ϵ RI α monovalent Fab fragments, we used the Pierce Fab Micro Preparation Kit (catalog #44685), as per manufacturer's instructions. Briefly, 100 μ g of whole anti-mouse Fc ϵ RI α , clone MAR-1, antibody was digested with immobilized papain for 16 h in digestion buffer. Undigested antibodies and Fc fragments were removed by Protein A spin columns. The flow-through fraction, containing the Fab fragments, was purified with desalting spin columns (to remove cysteine and EDTA) and analyzed by reducing and nonreducing polyacrylamide gel electrophoresis (PAGE) to confirm the absence of contaminating F(ab') 2 fragments. The purified Fab fragments were conjugated to NHS-biotin using the Pierce EZ-Link Sulfo-NHS-Biotinylation Kit (catalog #21925), as per manufacturer's instructions. The concentration of the biotinylated anti-mouse Fc ϵ RI α Fab fragments was determined by measuring UV absorbance at 280 nm. Dilute biotinylated anti-mouse Fc ϵ RI α Fab fragments in PBS to prepare a 0.1–1 mg/mL stock solution.
9. To prepare APC-conjugated isotype control antibody staining solution, dilute APC-conjugated isotype control antibody 1/200 in FACS buffer. Add 20 μ L staining solution to desired tubes (as described in Subheading 3.1). If anti-mouse Fc ϵ RI α antibodies are conjugated to a fluorophore other than APC (*see Note 4*), be sure to use an isotype control antibody conjugated to the same fluorophore.
10. If using purified peritoneal mast cells (or BMCMCs that have been incubated with IgE), the best way to accurately assess total Fc ϵ RI levels is to stain the cells with anti-mouse Fc ϵ RI α antibodies (as described in Subheading 3.1) plus anti-IgE antibodies coupled to the same fluorophore as the anti-mouse Fc ϵ RI α antibodies. It appears that when IgE is bound to its receptor, Fc ϵ RI α is no longer recognized or is recognized at much lower efficiency by anti-mouse Fc ϵ RI α , clone MAR-1, antibodies (perhaps IgE binding causes a conformational change in the Fc ϵ RI α chain or steric effects that occlude antibody binding). Alternatively, one can use this information to assess the IgE-bound versus free pools of Fc ϵ RI α on the

surface of mast cells by staining with anti-mouse Fc ϵ RI α antibodies and anti-IgE antibodies coupled to different fluorophores.

11. For each population of cells being studied, a typical experiment requires an unstained control and cells that have been activated with anti-IgE for 0, 5, 15, 30, 60, and 90 min at 37 °C. Thus, we typically used 7×10^5 cells/experiment when studying stimulation-induced internalization of IgE-bound Fc ϵ RI α ($\sim 1 \times 10^5$ cells for each condition or time point).
12. For each population of cells being studied, a typical experiment requires an unstained control and cells that have been at 37 °C for 0, 2, 4, 6, and 12 h. For the 2-, 4-, 6-, and 12-h time points, cells were treated with vehicle (DMSO), cycloheximide, or brefeldin A in separate wells. Thus, we typically used 3×10^6 cells/experiment when studying Fc ϵ RI (2×10^5 cells for each condition or time point).
13. When initiating studies with cycloheximide and brefeldin A, it is worthwhile to test a range of concentrations to determine the lowest concentration that will exhibit effects, given that both of these compounds are documented to be toxic to cells.
14. For each population of cells being studied, a typical experiment requires an unstained control and cells that have been at 37 °C for 0, 5, 15, 30, and 60 min. Thus, we typically used 6×10^5 cells/experiment when studying Fc ϵ RI recycling (1×10^5 cells for each condition or time point).
15. Biotinylated anti-mouse Fc ϵ RI α Fab fragments will bind to Fc ϵ RI receptors expressed on the surface of BMCMCs. The extended incubation time at this step allows a number of rounds of Fc ϵ RI recycling to occur; Fc ϵ RI α -bound Fab fragments will be internalized during the normal turnover of the Fc ϵ RI complex. Thus, at the end of this step, the Fc ϵ RI complexes undergoing intracellular recycling and those expressed on the surface of BMCMCs will be labeled with biotinylated anti-mouse Fc ϵ RI α Fab fragments.
16. This step will effectively saturate or block the biotin moieties on the Fab fragments bound to Fc ϵ RI complexes on the surface of the BMCMCs; thus, only Fab fragments bound to intracellular Fc ϵ RI complexes will be free to bind the AF647-conjugated monovalent streptavidin added in subsequent steps.
17. AF647-conjugated monovalent streptavidin will bind to biotinylated anti-mouse Fc ϵ RI α Fab fragments on the surface of the BMCMCs that were not blocked with unlabeled monovalent streptavidin. Typically, the fluorescence observed at the 0 min time point is similar to that observed in the unstained control; however, fluorescence can be higher at the 0 min time point. As intracellular Fc ϵ RI α -bound Fab fragments reach the surface of the cell (as observed when the cells are incubated at 37 °C

in subsequent steps), the AF647-conjugated monovalent streptavidin will bind to the biotinylated anti-mouse Fc ϵ RI α Fab fragments and increase cell-associated AF647 fluorescence. An important control experiment is to incubate cells that have not been exposed to Fab fragments with AF647-conjugated monovalent streptavidin to ensure that the pinocytosis does not contribute substantially to cell-associated AF647 fluorescence during the time frame of your experiment.

Acknowledgment

We thank Stephen J. Galli for critical review of this manuscript.

References

1. Kinet JP (1999) The high-affinity IgE receptor (Fc epsilon RI): from physiology to pathology. *Annu Rev Immunol* 17:931–972
2. Galli SJ, Kalesnikoff J, Grimaldston MA et al (2005) Mast cells as “tunable” effector and immunoregulatory cells: recent advances. *Annu Rev Immunol* 23:749–786
3. Turner H, Kinet JP (1999) Signalling through the high-affinity IgE receptor Fc epsilon RI. *Nature* 402:B24–B30
4. Abramson J, Pecht I (2007) Regulation of the mast cell response to the type 1 Fc epsilon receptor. *Immunol Rev* 217:231–254
5. Rivera J, Fierro NA, Olivera A et al (2008) New insights on mast cell activation via the high affinity receptor for IgE. *Adv Immunol* 98:85–120
6. Pfeffer SR (2001) Rab GTPases: specifying and deciphering organelle identity and function. *Trends Cell Biol* 11:487–491
7. Seabra MC, Mules EH, Hume AN (2002) Rab GTPases, intracellular traffic and disease. *Trends Mol Med* 8:23–30
8. Zerial M, McBride H (2001) Rab proteins as membrane organizers. *Nat Rev Mol Cell Biol* 2:107–117
9. Gasparrini F, Molfetta R, Santoni A et al (2011) Cbl family proteins: balancing Fc epsilonRI-mediated mast cell and basophil activation. *Int Arch Allergy Immunol* 156:16–26
10. Kalesnikoff J, Rios EJ, Chen CC et al (2007) Roles of RabGEF1/Rabex-5 domains in regulating Fc epsilon RI surface expression and Fc epsilon RI-dependent responses in mast cells. *Blood* 109:5308–5317
11. Rios EJ, Piliponsky AM, Ra C et al (2008) Rabaptin-5 regulates receptor expression and functional activation in mast cells. *Blood* 112:4148–4157
12. Mekori YA, Metcalfe DD (2000) Mast cells in innate immunity. *Immunol Rev* 173:131–140
13. Saini SS, MacGlashan D (2002) How IgE upregulates the allergic response. *Curr Opin Immunol* 14:694–697
14. Marolewski AE, Buckle DR, Christie G et al (1998) CD23 (FcepsilonRII) release from cell membranes is mediated by a membrane-bound metalloprotease. *Biochem J* 333(Pt 3):573–579
15. Holowka D, Gosse JA, Hammond AT et al (2005) Lipid segregation and IgE receptor signaling: a decade of progress. *Biochim Biophys Acta* 1746:252–259
16. MacGlashan DW Jr (2007) Endocytosis, recycling, and degradation of unoccupied FcepsilonRI in human basophils. *J Leukoc Biol* 82:1003–1010
17. MacGlashan DW Jr, Bochner BS, Adelman DC et al (1997) Serum IgE level drives basophil and mast cell IgE receptor display. *Int Arch Allergy Immunol* 113:45–47
18. Conroy MC, Adkinson NF Jr, lichtenstein LM (1977) Measurement of IgE on human basophils: relation to serum IgE and anti-IgE-induced histamine release. *J Immunol* 118:1317–1321
19. Shaikh N, Rivera J, Hewlett BR et al (1997) Mast cell Fc epsilonRI expression in the rat intestinal mucosa and tongue is enhanced during *Nippostrongylus brasiliensis* infection and can be up-regulated by in vivo administration of IgE. *J Immunol* 158:3805–3812
20. Yamaguchi M, Lantz CS, Oettgen HC et al (1997) IgE enhances mouse mast cell Fc(epsilon)RI expression in vitro and in vivo: evidence for a novel amplification mechanism

in IgE-dependent reactions. *J Exp Med* 185:663–672

21. Kalesnikoff J, Galli SJ (2008) New developments in mast cell biology. *Nat Immunol* 9:1215–1223

22. Molfetta R, Belleudi F, Peruzzi G et al (2005) CIN85 regulates the ligand-dependent endocytosis of the IgE receptor: a new molecular mechanism to dampen mast cell function. *J Immunol* 175:4208–4216

23. Oliver JM, Pfeiffer JR, Surviladze Z et al (2004) Membrane receptor mapping: the membrane topography of Fc(epsilon)RI signaling. *Subcell Biochem* 37:3–34

24. Wilson BS, Pfeiffer JR, Oliver JM (2000) Observing Fc epsilon RI signaling from the inside of the mast cell membrane. *J Cell Biol* 149:1131–1142

25. Fattakhova GV, Masilamani M, Narayanan S et al (2009) Endosomal trafficking of the ligated Fc epsilon RI receptor. *Mol Immunol* 46:793–802

26. Molfetta R, Gasparrini F, Peruzzi G et al (2009) Lipid raft-dependent Fc epsilon RI ubiquitination regulates receptor endocytosis through the action of ubiquitin binding adaptors. *PLoS One* 4:e5604

27. Molfetta R, Gasparrini F, Santoni A et al (2010) Ubiquitination and endocytosis of the high affinity receptor for IgE. *Mol Immunol* 47:2427–2434

28. Hicke L, Dunn R (2003) Regulation of membrane protein transport by ubiquitin and ubiquitin-binding proteins. *Annu Rev Cell Dev Biol* 19:141–172

29. Kalesnikoff J, Galli SJ (2011) Antiinflammatory and immunosuppressive functions of mast cells. *Methods Mol Biol* 677:207–220

30. Kitaura J, Eto K, Kinoshita T et al (2005) Regulation of highly cytokinergic IgE-induced mast cell adhesion by Src, Syk, Tec, and protein kinase C family kinases. *J Immunol* 174:4495–4504

31. Kalesnikoff J, Huber M, Lam V et al (2001) Monomeric IgE stimulates signaling pathways in mast cells that lead to cytokine production and cell survival. *Immunity* 14:801–811

32. Kawakami T, Galli SJ (2002) Regulation of mast-cell and basophil function and survival by IgE. *Nat Rev Immunol* 2:773–786

33. Asai K, Kitaura J, Kawakami Y et al (2001) Regulation of mast cell survival by IgE. *Immunity* 14:791–800

34. Kawakami T, Kitaura J, Xiao W et al (2005) IgE regulation of mast cell survival and function. *Novartis Found Symp* 271:100–107, discussion 108–114, 145–151

35. Howarth M et al (2006) A monovalent streptavidin with a single femtomolar biotin binding site. *Nat Methods* 3(4):267–273. doi:[10.1038/NMETHXXX](https://doi.org/10.1038/NMETHXXX)

Chapter 16

Regulation of Mast Cell Survival and Apoptosis

Christine Möller Westerberg, Maria Ekoff, and Gunnar Nilsson

Abstract

One key characteristic of certain mast cell populations is their longevity. Mast cell survival can also be promoted by Fc-receptor activation. Regulation of cell survival and apoptosis is regulated by the Bcl-2 family that consists of pro- and anti-apoptotic proteins. Depending on their relative cellular expression levels, the cells are either rescued or destined for apoptosis. To determine the regulation of mast cell survival and apoptosis, the expression of different Bcl-2 protein family members can be measured by western blot. The amount of viable versus apoptotic cells is decided by AnnexinV/propidium iodide staining, and cell lysates are prepared for western blot analysis from the appropriated time points.

Key words Bcl-2 family, Apoptosis, Western blot, Flow cytometry, IgE, Mast cells

1 Introduction

Exceptional for mast cells is their long lifespan within tissues. For their existence, mast cells are dependent on stem cell factor (SCF) and undergo apoptosis upon its depletion. SCF is the major growth and survival factor for human mast cells and is a prerequisite for their development [1, 2]. In vivo, lack of functional SCF receptor KIT or the membrane-bound form of SCF results in depletion of mast cells in mice [3, 4]. Furthermore, suppression of SCF production in vivo causes considerable reduction of mast cell numbers within the tissues [5], whereas infusion of SCF increases the number of tissue mast cells [6]. On the other hand, mouse mast cells are merely dependent on interleukin-3 (IL-3) for their in vitro development and survival. Upon IL-3 withdrawal these in vitro-developed mouse mast cells undergo apoptosis but are rescued by the addition of SCF [7, 8].

Apoptosis is regulated by two coexisting pathways, the extrinsic and the intrinsic pathways. Both pathways depend on caspase activation and result in degradation of targeted cellular structures and formation of apoptotic bodies [9]. The extrinsic pathway is triggered by external, extracellular, signals transmitted through

death receptors on the cell surface [10]. The Bcl-2 family of proteins plays a central role in the intrinsic pathway of apoptosis which is triggered by intracellular stress factors such as growth factor deprivation and DNA damage [11]. Since the primary site of the Bcl-2 family action is at the mitochondrial membrane, the intrinsic pathway is often called the mitochondrial pathway [12].

Major regulators of cell survival are the Bcl-2 family of proteins that includes members that promote cell death, as well as proteins that maintain cell survival. The pro-survival family members (Bcl-2, A1/Bfl-1, Mcl-1, Bcl-XL, and Bcl-w) protect the cells from death-inducing factors. Two other Bcl-2 subfamilies instead contribute to apoptosis. The BH3-only proteins (Bik, Bad, Bid, Bim, Bmf, Hrk, Noxa, and Puma) are sensitizers of apoptotic signals and initiate apoptosis either directly by activating Bax and Bak or indirectly by neutralizing pro-survival Bcl-2 proteins [11]. The Bax-like apoptotic factors (Bax and Bak) are the actual activators of the downstream cell death cascade, as absence of Bax and Bak abolishes most apoptotic responses sensed by BH3-only proteins [13]. Given that pro- and anti-apoptotic Bcl-2 family proteins can interact and bind to each other suggests that their relative concentrations are crucial for cell fate. Therefore it is of high interest to measure the different Bcl-2 protein family members by western blot, to obtain information on their relative expression levels, and to acquire knowledge of the regulation of mast cell survival and apoptosis.

Mast cells can undergo an activation-induced cell survival process upon cross-linking of the high-affinity IgE receptor Fc ϵ RI (IgER-CL) or IgG receptor, Fc γ RI [14–18]. IgER-CL activates a signaling cascade leading to an upregulation of the pro-survival Bcl-2 family gene A1/Bfl-1 [14, 17], Bcl-XL, and to some degree Bcl-2 [19, 20], which promotes mast cell survival. Mast cells deficient in A1 degranulate upon Fc ϵ RI activation but cannot revive, probably due to the lack of the pro-survival effect of A1 [14]. In human mast cells, the expression of the A1 homologue Bfl-1 is enhanced together with Mcl-1 upon IgE receptor aggregation [17, 21].

Cell apoptosis is characterized by biochemical and morphological changes including loss of plasma membrane integrity, DNA cleavage and nuclear condensation, and formation of apoptotic bodies [22]. Loss of plasma membrane integrity is an early feature which is easily detected by propidium iodide (PI) and AnnexinV staining [23]. In apoptotic cells the membrane phospholipid phosphatidylserine (PS) moves from the inner to the outer side of the plasma membrane. AnnexinV is a phospholipid-binding protein with high affinity for PS [24]. Conjugated to a fluorochrome, AnnexinV/PI serves as a sensitive marker for exposed PS on early apoptotic cells. Viable cells with intact membrane exclude PI, while the membranes of dead or damaged cells are permeable to PI.

Cells stained positive for AnnexinV-FITC and negative for PI are undergoing apoptosis, while double-positive cells are in the final stages of apoptosis or already dead. Non-stained cells are healthy and not undergoing measurable apoptosis [23, 24].

In this chapter, techniques are described on how to measure mast cell survival and apoptosis in resting and activated cells. Mast cell viability is determined by PI/AnnexinV staining and expression of Bcl-2 family proteins, involved in the intrinsic pathway of apoptosis, by western blot analysis.

2 Materials

2.1 Cell Culture Mediums

Human Mast Cell Medium

RPMI 1620 medium supplemented with 10 % FCS, 10 mM HEPES, 0.1 mM MEM nonessential amino acids, 50 μ M 2-mercaptoethanol, 2 mM L-glutamine, 100 IU/mL penicillin G, 100 μ g/mL streptomycin, 100 ng/mL recombinant (human) SCF, and 10 ng/mL (human) IL-6.

Murine Mast Cell Medium

RPMI 1640 medium supplemented with 10 % FCS, 10 mM HEPES, 1 mM sodium pyruvate, 0.1 mM MEM nonessential amino acids, 50 μ M 2-mercaptoethanol, 4 mM L-glutamine, 100 UI/mL penicillin G, 100 μ g/mL streptomycin, and 10 ng/mL (mouse) IL-3.

2.2 IgE for Mast Cell Fc ϵ RI Cross-Linking

1. Trinitrophenol (TNP)-BSA (Biosearch Technologies, Inc.).
2. IGEL-b4 supernatant (ATCC® TIB141™).
3. Human IgE AG30P (Millipore).
4. Monoclonal mouse anti-IgE (Sigma).

2.3 AnnexinV/PI Kit

1. AnnexinV-FITC apoptosis detection kit (BD Pharmingen). The kit includes AnnexinV-FITC, propidium iodide, and 10 \times AnnexinV binding buffer. *Important:* Dilute the 10 \times AnnexinV binding buffer to 1 \times with water.

2.4 Western Blot

Equipment

1. XCell SureLock Mini-Cell.
2. XCell II Blot Module.
3. NuPAGE Bis-Tris mini gel.

Western Blot Reagents

1. 2 \times SDS lysis buffer: 62.5 mM Tris-HCl (pH 6.8), 2 % w/v SDS, 10 % glycerol, 50 mM DTT, 0.01 % w/v bromophenol blue.
2. 500 mL running buffer: 20 \times MOPS (1 M) or 20 \times MES (1 M): 1 M TrisBase, 69.3 mM SDS, 20.5 mM EDTA. Add water up to 500 mL.

Table 1
Antibodies used to detect proteins involved in mast cell survival and apoptosis

Antibody	Source	Specificity	Size (kDa)	Dilution for Western blot	Company
A1	Rat	Mouse	17	1 µg/mL	R&D Systems
Bim EL, L, S	Rabbit	Human, mouse, rat	23, 16, 13	0.05 µg/mL	Affinity Bioreagents
Bax	Mouse	Human, mouse, rat	21	1 µg/mL	Trevigen
Bcl-XL, S	Mouse	Human, mouse	29, 21	0.2 µg/mL	Chemicon Inc.
Mcl-1	Rabbit	Mouse	35.2	1.6 µg/mL	Rockland
Mcl-1	Rabbit	Human, dog, guinea pig, monkey, pig, rabbit	42/43	0.2 µg/mL	Assay Designs
Puma	Rabbit	Human, mouse	23	2 µg/mL	ProSci
Caspase-3	Rabbit	Human, mouse, rat	35, 19, 17	1:1,000 (N/A µg/mL)	Cell Signaling

3. SeeBlue® Plus2 Pre-Stained Standard.
4. Transfer buffer: Take 25 mL 20× NuPage transfer buffer and 50 mL ethanol/gel to be transferred and fill up to a total volume of 500 mL with water. Add 500 µL antioxidant.
5. Nitrocellulose membranes.
6. 10× Tris-buffered saline (TBS) stock. To make 1 L: Add 24.2 g Tris base and 80 g NaCl to 950 mL ddH₂O. Adjust pH to 7.6 with HCl and add water to 1 L.
7. 1× TBS-T: Add 1 mL Tween-20 when preparing 1 L of 1× Tris-buffered saline from the 10× TBS stock.
8. 5 % milk blocking solution, 26 mL: 1.3 g nonfat dry milk powder in 26 mL 1× TBS-T.
9. 5 % BSA/Tween-20 blocking and primary antibody solution: 2.5 g bovine serum albumin in 1× TBS-T.
10. Primary antibodies used to detect proteins involved in mast cell survival and apoptosis (e.g., *see* Table 1).
11. Developing solutions: Enhanced chemiluminescence (ECL) system (LumiGLO, New England Biolabs).
12. Hybond ECL film.
13. ReBlot Solution Mild (Millipore).

3 Methods

3.1 Induction of Mast Cell Apoptosis by Cytokine Deprivation

1. Wash mast cells twice in 50 mL PBS. Pellet at $300 \times g$ for 10 min.
2. Resuspend cells at 1×10^6 cells/mL in RPMI cell culture medium deprived of cytokines but still supplemented with 10 % FCS (*see Note 1*).
3. Incubate cells in a humidified incubator at 37 °C, 5 % CO₂ for the desired time periods (*see Note 2*).

3.2 Activation-Induced Mast Cell Survival by IgE-R-CL

1. Wash mast cells twice in 50 mL PBS. Pellet at $300 \times g$ for 10 min.
2. Mouse mast cells are resuspended at 1×10^6 cells/mL in RPMI medium deprived of cytokines but still supplemented with 10 % FCS (*see Note 1*). Human mast cells are resuspended in full medium (containing both cytokines and FCS).
3. Mouse mast cells are sensitized using monoclonal murine IgE anti-TNP antibody (IGE1-b4) (used as 15 % hybridoma supernatant) for 90 min in 5 % CO₂ at 37 °C (*see Note 2*). Human mast cells are sensitized with 1 µg/mL IgE AG30P overnight, 5 % CO₂ at 37 °C.
4. Wash mast cells twice in 50 mL PBS. Pellet at $300 \times g$ for 10 min.
5. Human and mouse mast cells are resuspended at 1×10^6 cells/mL in RPMI deprived of cytokines but still supplemented with 10 % FCS.
6. Mouse mast cells are challenged with 100 ng/mL TNP-BSA and human mast cells with 20 µg/mL anti-IgE for the desired time periods.

3.3 Annexin V/Propidium Iodide Staining

1. Transfer 100 µL cell suspension to 5 mL tube (*see Note 3*).
2. Wash mast cells twice in 50 mL PBS. Pellet at $300 \times g$ for 10 min.
3. Discard the supernatant (*see Note 4*).
4. Resuspend the cells in 100 µL 1× Annexin V binding buffer.
5. Add 0.3 µg/mL of AnnexinV-FITC and 2 µg/mL PI.
6. Mix by gently shaking the tubes.
7. Incubate for 15 min at RT in the dark.
8. Add 200 µL PBS and analyze by flow cytometry within an hour.

3.4 Preparation of Western Blot Lysates

1. Starve your cells for the desired time (*see Note 3*).
2. At different time points, count your cells and take out $1-2 \times 10^6$ cells/point.

3. Terminate the incubation by pelleting cells at $300 \times g$ for 10 min in cold (*see Note 5*).
4. Pour off the supernatant by inverting your tubes (*see Note 6*) and transfer the cell pellet, using the small medium volume left, into 1.5 mL microfuge tubes (*see Note 4*). Keep on ice!
5. Lyse cells in 100 μ L 2 \times SDS lysis buffer (*see Note 7*).
6. Sonicate on ice for 7 s (repeat sonication once more) (*see Note 8*).
7. Freeze your samples at -20°C or keep them on ice until loading on to the Bis–Tris mini gel.

3.5 Western Blot

1. Make 700 mL 1 \times running buffer (MOPS or MES) by diluting the 20 \times stock to 1 \times in water (*see Note 9*).
2. Pour 200 mL of the 700 mL 1 \times running buffer into a new vial and add 500 μ L antioxidant.
3. Choose a 10- or 12-well Bis–Tris mini gel.
4. Remove the tape from the gel!
5. Put together the gel aggregate as described by the manufacturer.
6. Add the 200 mL 1 \times running buffer into the inner chamber and the 500 mL 1 \times running buffer to the outer chamber.
7. Remove the comb and rinse the wells with running buffer (*see Note 10*).
8. Prior to loading your samples, heat them at 95°C for 5 min and then chill on ice.
9. Spin down your samples at 4°C for 5 min at $12,000 \times g$.
10. Keep your samples on ice!
11. Load 3.5 μ L ladder and 10–20 μ L sample/well.
12. Run the gel at 200 V for 50–60 min until the blue dye front has reached the end of the gel.
13. Make 500 mL 1 \times transfer buffer, take 25 mL 20 \times transfer buffer and 50 mL methanol/gel (*see Note 11*), and fill up to 500 mL with water. Add 500 μ L antioxidant.
14. Soak the pads in the transfer buffer (*see Note 12*).
15. Disassemble the gel aggregate.
16. Crack the plastic surrounding the gel and cut off unnecessary gel.
17. Transfer the gel onto a transfer buffer-soaked filter paper (e.g., Whatman[®] blotting papers or its equivalent).
18. Place two air bubble free pads into the transfer cassette.
19. Place the gel with the filter paper closest to the pads.
20. Place a transfer buffer-soaked nitrocellulose membrane on top of the gel.

21. Place another transfer buffer-soaked filter paper on top of the membrane.
22. Place one pad on top before adding the other filter paper–gel–membrane–filter paper “sandwich” by repeating **steps 17 and 19–21**.
23. Fill up the transfer cassette with pads to the edge and then add one extra that will exceed the edge.
24. Put on the lid on the transfer cassette and put it into the gel aggregate.
25. Add transfer buffer into the cassette just covering the pads.
26. Fill the outer chamber with water for cooling.
27. Run transfer for 1 h at 30 V.
28. Take out your membrane and start blocking (*see Note 13*).

Blocking Membrane and Primary Antibody Incubation

29. Place the membrane into the 5 % milk blocking solution with gentle agitation for 1 h at RT (*see Note 14*).
30. Place the membrane into a plastic pocket and add the primary antibody, usually diluted in 5 % BSA/TBS-T (*see Note 15*).
31. Remove all big air bubbles before sealing the pocket (*see Note 16*).
32. Put the pocket in between two glass plates (*see Note 17*).
33. Incubate the membrane at 4 °C with gentle agitation overnight (*see Note 18*).

Secondary Antibody Incubation

34. Remove the membrane from the plastic pocket.
35. Put the membrane into a plastic tray and add 15 mL 1× TBS-T.
36. Put on gentle agitation for 5 min before exchanging the buffer for another 15 mL buffer.
37. Repeat the washing (**step 36**) four more times (*see Note 19*).
38. Mix 10 mL blocking solution (*see Note 20*).
39. Use 10 mL of blocking solution to dilute the secondary antibody.
40. Provide gentle agitation at RT for 1 h.
41. Repeat the washing steps as in **steps 35–37** above.

Development

42. Add 4.5 mL water into a 15 mL tube.
43. Bring plastic pockets, developing solutions, tweezers, timer, cassette, and membrane into the dark room.

44. Add 250 μ L of each of the two developing solutions (A and B) into the tube containing 4.5 mL water.
45. Pour the solution over the membrane and incubate for 1 min (*see Note 21*).
46. Pour off the solution and gently press the edge of the membrane against a paper towel to remove excess solution.
47. Place the membrane into a plastic pocket.
48. Put a film onto the membrane.
49. Develop the film for the desired time.
50. Repeat until you get the right exposure/strength of the protein bands onto the film.

Stripping the Membrane

51. Add 1 mL of the 10 \times re-blot solution to 9 mL water.
52. Place the membrane in a plastic tray and add the solution.
53. Incubate for 15 min at RT with gentle agitation.
54. Re-block the membrane and then it is ready to use for another antibody.

4 Notes

1. Approximately 1–2 \times 10 6 living cells are needed per time point when the cell lysates are made for the western blots. If a high rate of apoptosis is expected, this must be taken into consideration when setting up the experiment, and an excess of cells should be used, to ensure that enough final cells for the experiment will be present if both western blot and PI/AnnexinV are to be measured.
2. The IGEL-b4 hybridoma supernatant is produced from TIB-141TM (ATCC) cells. The cells are expanded and then kept in the same culture medium for 10 days when approximately 50 % of the cells have died. The supernatant, containing the IgE, is collected and sterile filtered. Upon IgE sensitization, 15 % of the IGEL-b4 hybridoma supernatant is added to the cell culture.
3. Apoptosis is measured by PI/AnnexinV staining at 0, 24, 48, 72, and 96 h past cytokine deprivation. The time for stimulation or starvation of the cells for protein analysis differs between the proteins of interest.
4. When the cells are spun down, 100 μ L medium will still remain in the tubes after the supernatant has been discarded by inverting the tubes.

5. For short stimulations examining phosphorylated proteins, stop experiment by adding ice cold PBS and keep the tubes on ice! Spin down the cells in a precooled centrifuge 4 °C, 400×*g* for 5 min.
6. Press the edge of the tube against a paper towel to remove as much excess medium as possible.
7. Prepare the 2× SDS buffer without DTT and store at room temperature. Add DTT freshly before each cell lysis. Add 100 µL 2× SDS buffer with DTT to the tubes containing 100 µL cell suspension, resulting in 1× SDS buffer. When adding the buffer to the tubes, do not pipette up and down since it becomes sticky!
8. Sonicate the samples to shear DNA and reduce sample viscosity. Sometimes it is preferable to sonicate four times for 5 s each instead of twice for 7 s in order to more gently and efficiently prepare the samples.
9. Buffer selection depends on the size of the band of interest. MOPS and MES separate the protein bands differently (which is also dependent on the type of Bis–Tris gel).
10. The wells need to be rinsed from excess gel debris in order to get nice straight bands.
11. Proteins can be transferred from two gels at the same time. To get the optimal protein transfers from the gel to the membrane, add 50 mL methanol for each membrane transfer.
12. Remove any air bubbles in the pads before assembling the western blot sandwich, since air bubbles will impair the transfer of proteins from the gel to the membrane.
13. The pre-stained standard ladder usually fades during the washing steps so use a dull tweezers to mark each standard line. Be careful not to punch through the membrane.
14. The choice of blocking solution depends on the antibody of interest. Milk contains a phosphoprotein, casein, that sometimes can interfere and give high background/nonspecific binding when using phospho-specific antibodies. A BSA blocking reagent can then be used instead for these applications.
15. In case of background binding, use the 5 % milk blocking solution instead.
16. In order to get an even distribution of the antibody solution all over the membrane, remove as many bubbles as possible.
17. To facilitate even antibody distribution, put the plastic-wrapped membrane under light pressure between two glass plates. These plates also facilitate even cooling during incubation.
18. Membranes are preferably incubated with primary antibody at 4 °C to reduce nonspecific binding, contamination, and

destruction of proteins (especially phospho groups). Agitation during incubation with antibody enables even covering of the membrane and prevents uneven binding.

19. Excess unbound antibody is washed away to minimize background staining.
20. Polyclonal rabbit antibodies give the highest signal/background in 5 % BSA blocking solution, while monoclonal antibodies are best used in 5 % milk blocking solution.
21. The membrane should be placed in a tray without any buffers prior to adding the developing solution.

References

1. Irani AM, Nilsson G, Miettinen U, Craig SS, Ashman LK, Ishizaka T, Zsebo KM, Schwartz LB (1992) Recombinant human stem cell factor stimulates differentiation of mast cells from dispersed human fetal liver cells. *Blood* 80: 3009–3021
2. Valent P, Spanbloch E, Sperr WR, Sillaber C, Zsebo KM, Agis H, Strobl H, Geissler K, Bettelheim P, Lechner K (1992) Induction of differentiation of human mast cells from bone marrow and peripheral blood mononuclear cells by recombinant human stem cell factor/kit-ligand in long-term culture. *Blood* 80: 2237–2245
3. Kitamura Y, Go S, Hatanaka K (1978) Decrease of mast cells in W/Wv mice and their increase by bone marrow transplantation. *Blood* 52: 447–452
4. Kitamura Y, Go S (1979) Decreased production of mast cells in S1/S1d anemic mice. *Blood* 53:492–497
5. Finotto S, Mekori YA, Metcalfe DD (1997) Glucocorticoids decrease tissue mast cell number by reducing the production of the c-kit ligand, stem cell factor, by resident cells: in vitro and in vivo evidence in murine systems. *J Clin Invest* 99:1721–1728
6. Galli SJ, Iemura A, Garlick DS, Gamba-Vitalo C, Zsebo KM, Andrews RG (1993) Reversible expansion of primate mast cell populations in vivo by stem cell factor. *J Clin Invest* 91: 148–152
7. Mekori YA, Oh CK, Metcalfe DD (1993) IL-3-dependent murine mast cells undergo apoptosis on removal of IL-3. Prevention of apoptosis by c-kit ligand. *J Immunol* 151: 3775–3784
8. Iemura A, Tsai M, Ando A, Wershil BK, Galli SJ (1994) The c-kit ligand, stem cell factor, promotes mast cell survival by suppressing apoptosis. *Am J Pathol* 144:321–328
9. Hotchkiss RS, Strasser A, McDunn JE, Swanson PE (2009) Cell death. *N Engl J Med* 361:1570–1583
10. Strasser A, Jost PJ, Nagata S (2009) The many roles of FAS receptor signaling in the immune system. *Immunity* 30:180–192
11. Youle RJ, Strasser A (2008) The BCL-2 protein family: opposing activities that mediate cell death. *Nat Rev Mol Cell Biol* 9:47–59
12. Green DR, Reed JC (1998) Mitochondria and apoptosis. *Science* 281:1309–1312
13. Cheng EH, Wei MC, Weiler S, Flavell RA, Mak TW, Lindsten T, Korsmeyer SJ (2001) BCL-2, BCL-X(L) sequester BH3 domain-only molecules preventing BAX- and BAK-mediated mitochondrial apoptosis. *Mol Cell* 8: 705–711
14. Xiang Z, Ahmed AA, Moller C, Nakayama K, Hatakeyama S, Nilsson G (2001) Essential role of the prosurvival bcl-2 homologue A1 in mast cell survival after allergic activation. *J Exp Med* 194:1561–1569
15. Yoshikawa H, Nakajima Y, Tasaka K (1999) Glucocorticoid suppresses autocrine survival of mast cells by inhibiting IL-4 production and ICAM-1 expression. *J Immunol* 162: 6162–6170
16. Kitaura J, Xiao W, Maeda-Yamamoto M, Kawakami Y, Lowell CA, Kawakami T (2004) Early divergence of Fc epsilon receptor I signals for receptor up-regulation and internalization from degranulation, cytokine production, and survival. *J Immunol* 173:4317–4323
17. Xiang Z, Moller C, Nilsson G (2006) IgE-receptor activation induces survival and Bfl-1 expression in human mast cells but not basophils. *Allergy* 61:1040–1046

18. Karlberg M, Xiang Z, Nilsson G (2008) Fc gamma RI-mediated activation of human mast cells promotes survival and induction of the pro-survival gene Bfl-1. *J Clin Immunol* 28: 250–255
19. Alfredsson J, Puthalakath H, Martin H, Strasser A, Nilsson G (2005) Proapoptotic Bcl-2 family member Bim is involved in the control of mast cell survival and is induced together with Bcl-XL upon IgE-receptor activation. *Cell Death Differ* 12:136–144
20. Moller C, Xiang Z, Nilsson G (2003) Activation of mast cells by immunoglobulin E-receptor cross-linkage, but not through adenosine receptors, induces A1 expression and promotes survival. *Clin Exp Allergy* 33:1135–1140
21. Berent-Maoz B, Salemi S, Mankuta D, Simon HU, Levi-Schaffer F (2008) TRAIL mediated signaling in human mast cells: the influence of IgE-dependent activation. *Allergy* 63: 333–340
22. Kerr JF, Wyllie AH, Currie AR (1972) Apoptosis: a basic biological phenomenon with wide-ranging implications in tissue kinetics. *Br J Cancer* 26:239–257
23. Vermes I, Haanen C, Steffens-Nakken H, Reutelingsperger C (1995) A novel assay for apoptosis. Flow cytometric detection of phosphatidylserine expression on early apoptotic cells using fluorescein labelled Annexin V. *J Immunol Methods* 184:39–51
24. Martin SJ, Reutelingsperger CP, McGahon AJ, Rader JA, van Schie RC, LaFace DM, Green DR (1995) Early redistribution of plasma membrane phosphatidylserine is a general feature of apoptosis regardless of the initiating stimulus: inhibition by overexpression of Bcl-2 and Abl. *J Exp Med* 182:1545–1556

Chapter 17

Protein Tyrosine Phosphatases in Mast Cell Signaling

Alexander Geldman and Catherine J. Pallen

Abstract

For a time, mast cells were viewed as simple granulocytic effector cells that mediate allergic symptoms. More recent discoveries show that mast cells can also function as potent pro- and anti-inflammatory immune regulators in a plethora of human diseases. Much of the current knowledge about mast cell functions comes from studies on rodent models. The membrane receptors for antigen/IgE and growth factors are the core initiators of signaling cascades that trigger various mast cell responses. Yet, the regulation and multifunctionality of key receptor-proximal protein tyrosine phosphorylation events are still not well understood. The roles of the members of the protein tyrosine phosphatase superfamily of enzymes in regulating mast cell development, survival, and immune activation will be reviewed in this chapter.

Key words Mast cells, PTPs, Fc ϵ RI, c-Kit, SFKs, Anaphylaxis, Degranulation, Phosphotyrosine

1 Tyrosine Phosphorylation in Mast Cell Signaling

Mature mast cells are characterized by the expression of the stem cell factor (SCF) receptor tyrosine kinase c-Kit and the high-affinity IgE receptor Fc ϵ RI. These transmembrane receptors initiate many of the crucial signaling pathways that determine the development, migration, and immune activation of mast cells. The earliest event in c-Kit and Fc ϵ RI-mediated signaling is the tyrosine phosphorylation of several sites on the receptors themselves. Indeed, regulated protein tyrosine phosphorylation and dephosphorylation is a key mechanism controlling signaling downstream of these receptors. This chapter focuses on known and emerging actions of specific protein tyrosine phosphatases (PTPs) in mast cell signaling to promote or limit cell movement and activation, outcomes that are key to physiological and pathological mast cell roles.

Detailed descriptions of Fc ϵ RI and c-Kit mast cell signaling events can be found in several comprehensive reviews [1–3]. Briefly, the binding of antigen to IgE/Fc ϵ RI complexes, or of SCF to c-Kit, induces the formation of phosphotyrosyl receptor or receptor-linked tyrosine kinase complexes. Aggregated Fc ϵ RI, phosphorylated on

ITAMs (immunoreceptor tyrosine-based activation motifs) in its β - and γ -chains by Lyn, is associated with the Src family tyrosine kinases (SFKs) Lyn and Fyn and with the non-SFK tyrosine kinase Syk. These kinases phosphorylate diverse scaffolding/adaptor proteins (such as the Syk and Lyn substrates LAT1 and LAT2) and enzymes to coordinate the formation of activated signaling complexes that promote Ca^{2+} influx and degranulation as well as gene transcription and secretion. An overlapping cast of molecular players is mobilized by SCF binding to c-Kit. In this case, receptor dimerization activates the intrinsic tyrosine kinase activity of c-Kit and its trans-autophosphorylation. Phosphotyrosyl-c-Kit serves as a platform to recruit signaling molecules, including the kinases Lyn and Fyn and other enzymes such as PI3K and PLC γ that are also involved in Fc ϵ RI signaling. SCF/c-Kit signaling regulates mast cell migration, proliferation, survival, differentiation, and maturation.

2 The Protein Tyrosine Phosphatase Superfamily

The human PTP superfamily contains 107 phosphatases that are grouped into four families based on evolutionary relationships and structure, and use of a cysteine- or aspartate-based catalytic mechanism [4–6]. The Class I family is by far the largest, comprising a subfamily of 38 classical tyrosine-specific PTPs (transmembrane and intracellular) and another large subfamily of 61 dual-specific (for phosphotyrosine and phosphoserine/threonine) PTPs. The sole member of the Class II family is the tyrosine-specific low molecular weight (LMW) PTP, while the Class III family contains the three dual-specific CDC25 enzymes. Class I, II, and III PTP catalysis is mediated by an invariant active site cysteine residue. In contrast, the 4 Eya (eyes absent) members of Class IV employ an aspartic acid-based mechanism of tyrosine dephosphorylation [7–9] and also catalyze threonine dephosphorylation through a distinct domain [10].

3 PTP Expression in Mast Cells

Much of the knowledge of the mast cell roles of PTPs, all of which belong to the Class I family (Fig. 1), has come from studies of PTP-deficient mice and bone marrow-derived mast cells (BMMCs) as described in more detail below (Table 1). Over sixty different PTPs are expressed in mast cells, all of which are also expressed in seven other immune cell lineages: T cells, NKT cells, NK cells, B cells, immature DCs, macrophages, and neutrophils [11]. Interestingly, up to eleven other PTPs show mast cell-restricted expression among these types of immune cells. These PTPs comprise a receptor-like (*Ptpgr*) and three non-receptor tyrosine-specific

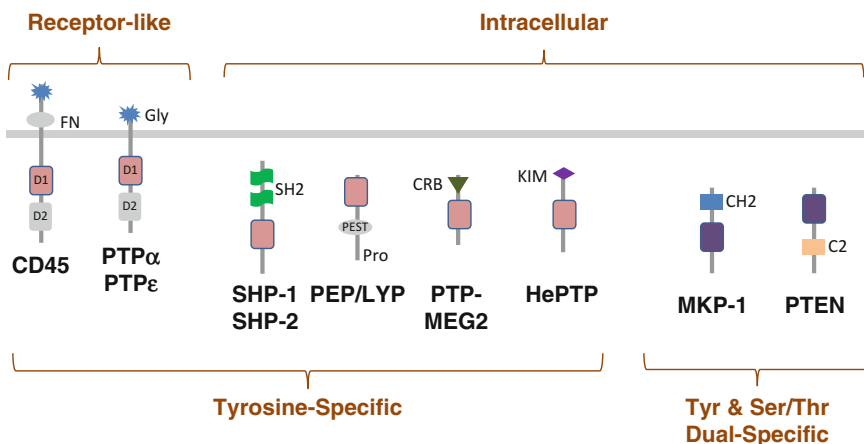


Fig. 1 Schematic representations of key protein tyrosine phosphatases affecting mast cell biology. Domain structures are abbreviated: *Gly* highly glycosylated; *D1* and *D2* membrane-proximal and membrane-distal receptor PTP domains; *FN* fibronectin-like; *SH2* Src homology domain 2; *PEST* rich in proline, glutamic acid, serine, and threonine; *Pro* proline-rich; *CRB* cellular retinaldehyde-binding protein-like; *KIM* kinase interaction motif; *CH2* Cdc25 homology domain 2; *C2* protein kinase C conserved region 2

Class I members (*Ptpn13*, *Ptpn20*, *Ptpn21*), six representatives of several types of dual-specific Class I enzymes (*Dusp3*, *Dusp9*, *Dusp23*, *Dusp26*, *Epm2a*, *Ssh3*), and a single Class IV PTP (*EyA4*) [11]. Their unique mast cell expression in this particular immune cell lineage panel suggests that at least some of these PTPs may function in specialized granulocytic processes in the mast cell context, although this remains to be determined.

4 Receptor-Like PTPs in Mast Cells

4.1 CD45

The leukocyte-specific receptor-like PTP CD45 (*Ptprc*) is generally recognized as a positive regulator of Fc ϵ RI signaling and mast cell secretory responses [12–14]. Alternatively spliced exons encoding the extracellular domain allow the expression of several variants of CD45 in leukocytes [15], although murine BMMCs lack the larger B220, RA, RB, and RC isoforms [14]. The CD45 cytoplasmic region contains two tandem catalytic domains, and as is the case with most other receptor-like PTPs, the membrane-proximal D1 domain is responsible for catalytic activity while the membrane-distal D2 domain is inactive. Extensive investigation of the role of CD45 in T and B cells has identified members of the Src family of tyrosine kinases as key CD45 substrates, with CD45 regulating Lck in T cell receptor-mediated T cell activation and Lyn in B cell receptor-mediated B cell activation [16, 17]. CD45 activates these kinases by dephosphorylating an inhibitory tyrosine residue in the C-terminal tail region. CD45 can also repress SFK activity by dephosphorylating an activation-associated tyrosine residue in the kinase domain.

Table 1
PTP-deficient mast cell phenotypes

PTP deficiency	Signalling effects	Altered responses	Reference
CD45 ^{-/-} BMMCs	<ul style="list-style-type: none"> Hyper-phosphorylation of Tyr-507 on Lyn Enhanced IL-3-induced tyrosine phosphorylation of Jak2 	<ul style="list-style-type: none"> Decreased Ag-induced degranulation and release of IL-6 Enhanced cell proliferation in response to cytokines IL-3 and SCF Increased cell death upon withdrawal of cytokines Enhanced IL-3-mediated cell proliferation 	[14, 19]
PTP α ^{-/-} BMMCs and mice	<ul style="list-style-type: none"> Decreased Ag-induced activation of Lyn and Fyn kinases Reduced SCF-induced activation Fyn kinase 	<ul style="list-style-type: none"> Enhanced Ag-induced degranulation and release of IL-2, IL-6, TNFα, and leukotrienes Enhanced Ag-induced anaphylaxis in mice Altered tissue distribution of mast cells Reduced spreading, polarization, and chemotaxis of SCF-treated BMMCs 	[20, 28]
PTP ϵ ^{-/-} BMMCs and mice	<ul style="list-style-type: none"> Enhanced Ag-induced activation of Syk 	<ul style="list-style-type: none"> Enhanced Ag-induced degranulation and release of IL-6 and TNFα Enhanced Ag-induced anaphylaxis 	[21]
PTP γ ^{-/-} (me) BMMCs and mice	<ul style="list-style-type: none"> Increased tyrosine phosphorylation of adaptor protein Shc after stimulation with SCF Enhanced Ag-induced phosphorylation of LAT and SLP-76 Reduced PLCγ1/2 activation, association with SLP-76 	<ul style="list-style-type: none"> Severe spontaneous lung inflammation and lethality of <i>me</i> mice Increased mast cell numbers in c-Kit-deficient mice Enhanced SCF-induced survival of BMMCs Enhanced IgE-mediated release of IL-6 and TNFα Reduced mast cell degranulation 	[37, 43]
PTP γ mutant (me) mice and BMMCs	<ul style="list-style-type: none"> Antigen stimulation induces SHP-1 to bind to NTAL, and without SHP-1 activity NTAL tyrosine phosphorylation is increased Increased antigen-induced phosphorylation of Tyr-396 on Lyn and Tyr-1020 on SHIP 	<ul style="list-style-type: none"> <i>me</i> mice have more mast cell progenitors in the bone marrow <i>me</i> BMMCs are more resistant to apoptosis, but proliferate more slowly than WT cells <i>me</i> BMMCs have enhanced spontaneous degranulation and in response to antigen Enhanced release of cytokines with various stimuli Reduced IgE-mediated release of IL-6 and TNFα cytokines 	[35, 39]

SHP-1-deficient (<i>me</i>) and (<i>mer</i>) BMMCs	<ul style="list-style-type: none"> Increased IL-3-induced phosphorylation of Erk kinases Enhanced proliferation with low IL-3 doses and greater apoptosis with high IL-3 doses Greater survival upon IL-3 cytokine starvation Reduced proliferation of BMMCs with high IL-3 doses 	[30]
BMMCs depleted of ~75 % of SHP-2	<ul style="list-style-type: none"> Increased inhibitory phosphorylation of Tyr-531 on Fyn kinase upon Ag stimulation Reduced association of SHP-2 with adaptor Gab2 and SCF-induced Rac/βNK activation Reduced secretion of TNFα, but not degranulation Reduced SCF-induced proliferation of BMMCs 	[50, 55]
PEP-/- BMMCs and mice	<ul style="list-style-type: none"> Reduced Ag-induced phosphorylation of PLCγ1 and calcium mobilization Increased activation of JNK MAP kinases Reduced IgE-mediated degranulation of mast cell and systemic anaphylaxis in mice Reduced anti-anaphylactic effects of glucocorticoids 	[56]
MKP-1 $^{-/-}$ BMMCs and mice	<ul style="list-style-type: none"> Enhanced Ag-induced activation of p38 Enhanced IgE-mediated degranulation and anaphylaxis in mice 	[62]
PTEN $^{-/-}$ BMMCs and mice	<ul style="list-style-type: none"> Increased activating phosphorylation on STAT5 and Akt proteins Enhanced proliferation and survival of tissue mast cells and IgE-mediated anaphylaxis Secretory hypersensitivity to antigen and SCF 	[67]

CD45-deficient BMMCs exhibit almost no degranulation upon stimulation by Ag cross-linking, indicating an essential role for CD45 in this response [12, 14]. IL-6 secretion is similarly impaired [14] and CD45-deficient mice are resistant to IgE-mediated systemic anaphylaxis [12]. Consistent with SFKs being the major substrates of CD45 and with the interaction of CD45 and Lyn in BMMCs, the enhanced inhibitory phosphorylation of Lyn at Tyr-507 (and possibly of Hck at Tyr-519) is the most upstream defect detected in CD45^{-/-} BMMCs [14]. This is accompanied by a consequent reduction in tyrosine phosphorylation of the Lyn substrate Cbp/PAG and its reduced ability to recruit Csk. Other defects include reduced Akt, Erk1/2, p38, and SHIP-1 phosphorylation. Ag-induced calcium mobilization is also compromised. Parallel studies of BMMCs from mice expressing an activated mutant CD45 (E613R) that cannot form inhibitory dimers reveal a potential ability of CD45 to mediate activation of the Fyn-PI3K-Akt pathway [14].

The above findings provide evidence of essential positive roles for CD45 in mast cell activation. An additional complexity of CD45 action is indicated by findings in alternate experimental systems. For example, while CD45 inhibitors suppress Ag-induced degranulation by BMMCs and murine peritoneal mast cells and inhibit systemic anaphylaxis, treatment of BMMCs with a 30–200-fold lower concentration of inhibitor enhances activation responses [14, 18]. Rat basophilic leukemia (RBL) cell lines have been often used to model Fc ϵ RI-mediated mast cell events, and RBL-2H3 variant lines stably expressing a low level of CD45 exhibit reduced or delayed Fc ϵ RI-dependent responses at low doses of antigen but normal responses at high antigen dose, relative to cells stably expressing a high level of CD45 [13]. Taken in the contexts of the known ability of CD45 to repress and activate SFK activity in other immune cells, and of the positive and negative regulatory actions of the CD45 substrate Lyn in mast cell activation, it is probable that a spectrum of CD45-mediated Lyn-dependent and CD45-mediated Lyn-independent effects can be titrated by factors such as antigen dose and the population of responsive CD45.

CD45^{-/-} BMMCs develop normally in vitro, indicating that this PTP is not required for mast cell differentiation [12, 14, 19]. Proliferation of CD45-deficient BMMCs in response to IL-3 and/or SCF (murine SF) is increased [14, 19] or not affected [12], with differing observations perhaps due to differences in the amounts or nature (recombinant vs. conditioned medium) of the cytokine/growth factors used. Increased proliferation is accompanied by increased apoptosis upon IL-3 withdrawal [14]. The basis for the enhanced cytokine-stimulated proliferation of CD45^{-/-} BMMCs lies with the discovery of a non-SFK substrate of CD45. In IL-3 stimulated BMMCs, CD45 plays a negative regulatory role, dephosphorylating Jak2 to limit STAT3 and STAT5 tyrosine phosphorylation and repress cyclin D1 expression [19].

4.2 PTP α and PTP ϵ

PTP α (*Ptpra*) and PTP ϵ (*Ptpre*) are closely related receptor-like PTPs that feature short, glycosylated extracellular domains and tandem cytoplasmic catalytic domains. In response to antigen, BMMCs from mice lacking PTP α or PTP ϵ hyperdegranulate and have augmented cytokine production [20, 21]. The PTP α -null, but not the PTP ϵ -null, BMMC response also includes the elevated release of cysteinyl leukotrienes. Mice lacking either PTP α or PTP ϵ exhibit enhanced anaphylactic reactions. Thus, these two transmembrane PTPs negatively regulate IgE-/Fc ϵ RI-dependent mast cell activation.

PTP α characteristically functions as a Src family kinase (SFK) phosphatase in numerous cell types and tissues, dephosphorylating and activating various SFKs [22]. PTP α fulfills this role in antigen-stimulated BMMCs, activating Lyn and Fyn. PTP α also suppresses the activity of the SFK Hck, possibly through Lyn-mediated regulation of Hck [20]. The reduced Lyn activation in PTP α ^{-/-} BMMCs is likely responsible for reduced phosphorylation of Fc ϵ RI and the inhibitory inositol phosphatase SHIP, as both are substrates of Lyn. At low-intensity stimulation, Lyn positively regulates signaling events in BMMC activation [23]; however the hyperactive phenotype of Lyn^{-/-} BMMCs revealed the key role of this kinase in negatively regulating BMMC activation [23–26]. Overall, the role of PTP α in limiting mast cell activation and anaphylactic allergic reactions appears to be due to the action of PTP α in mediating this Lyn-dependent negative regulatory signaling [20]. PTP ϵ can also act as an activator of SFKs [27], but difficulty in detecting significant antigen-induced Lyn activation in wild-type BMMCs has precluded the determination of whether Lyn activation is affected in PTP ϵ -null BMMCs [21].

Antigen-induced activation of the tyrosine kinase Syk is enhanced in BMMCs lacking either PTP α or PTP ϵ , despite the reduced association of Syk with the hypophosphorylated Fc ϵ RI in PTP α ^{-/-} BMMCs [20, 21]. In the latter cells, Syk phosphorylation is increased at tyrosine residues associated with kinase activation and reduced at a site linked to kinase inhibition, reinforcing the notion that PTP α mediates negative regulatory signals to limit mast cell activation. Elevated phosphorylation of the Syk substrates Gab2, LAT, and SLP-76 correlates with Syk hyperactivation in the absence of PTP α or PTP ϵ , as do enhanced calcium mobilization and activation of downstream signaling molecules such as the MAPKs [20, 21]. These observations point to similar actions and regulatory roles of PTP α and PTP ϵ in signaling to control mast cell activation. Nevertheless, the defective IgE-/Fc ϵ RI-dependent phenotype of either the PTP α ^{-/-} or PTP ϵ ^{-/-} mice and BMMCs indicates that these PTPs are not, at least at physiological expression levels, redundant.

Altered numbers of resident mast cells were noted in certain tissues of PTP α -null mice but not in PTP ϵ -null mice [21, 28]. The PTP α -null phenotype could be due to defective signaling by

the SCF receptor c-Kit that regulates mast cell migration, since BMMCs lacking PTP α display reduced spreading, polarization, and chemotaxis towards SCF [28]. In SCF/c-Kit signaling, PTP α promotes the activation of receptor-proximal Fyn and c-Kit tyrosine phosphorylation. In the absence of PTP α , these upstream signaling events are impaired, with further defects in Gab2, SHP-2, and Vav1 phosphorylation and activation of Rac, Cdc42, PAK, and MAPKs [28].

5 SH2 Domain-Containing Intracellular PTPs in Mast Cells

5.1 SHP-1 and the Motheaten Phenotypes

The Src homology region 2 domain-containing phosphatase 1 (SHP-1, PTP1C) has been extensively studied as a crucial regulator of mast cell development, survival, and immune responses [29, 30]. SHP-1 is an intracellular, Class I tyrosine-specific PTP that is expressed mainly in hematopoietic cells [31] and contains two tandem SH2 domains that target it to specific phosphotyrosine protein sites [32]. Spontaneous loss-of-function mutation of its coding gene (*Ptpn6*) is responsible for the severe physiological aberrations in motheaten (*me*) mice, first described nearly four decades ago [33]. Young homozygous recessive *me* mice have stunted growth and patchy dermatitis and die by three weeks of age. Tissue analyses show spontaneous, vast accumulation of mast cells and other leukocytes in various organs, high levels of serum auto-antibodies with immune complex depositions, and a progressive development of hemorrhagic pneumonitis in the absence of any pathogens [34, 35].

A different mutation that causes the loss of phosphatase activity of SHP-1 protein produces a milder phenotype in motheaten viable (*mev*) mice and extends their life relative to SHP-1-null mice [36]. While the bone marrow of *mev* mice contains many more mast cell progenitors than in wild-type (WT) mice, SHP-1-deficient BMMCs actually proliferate more slowly when supplemented with the growth factor for mouse mast cells, IL-3 [35]. The increased numbers of mast cells in both motheaten phenotypes are believed to result from enhanced anti-apoptotic signaling in SHP-1-deficient BMMCs, prolonging their survival under various types of cell stress. Upon withdrawal of IL-3, SHP-1-null BMMCs are more resistant to apoptosis than WT cells, due to higher intrinsic activation of the Erk kinases and expression of the anti-apoptotic protein BCL-X_L [30]. Additionally, a high concentration of IL-3 induces apoptosis in *me* BMMCs, whereas a much lower dose of IL-3 enhances their proliferation relative to normal mast cells. This suggests that the strength of IL-3 receptor stimulation may alter the SHP-1-dependent temporal induction of Erk protein signaling and its influence on the mast cell survival and activation. It is plausible that SHP-1 directly dephosphorylates the β -subunit of the IL-3 receptor or its associated adaptor protein Shc, since either of

these events has been shown to reduce the activation of the Ras/MAPK pathway in other cell types [30].

Mast cells are indeed essential for the development of the severe motheaten phenotype. The loss of mast cells due to mutations in the growth factor receptor c-Kit greatly reduces the lethal autoimmunity in SHP-1-deficient mice [35, 37]. Interestingly, the loss of SHP-1 function also partially restores the reduced mast cell populations in c-Kit^{-/-} mice as well as increases the numbers of tissue-resident mast cells in c-Kit^{+/+} mice [37]. In accordance with previous reports [37], mast cell-deficient (Kit^{W-Sh}) *mev* mice are protected from the development of spontaneous lung inflammation caused by the lack of SHP-1 phosphatase activity [35]. This reciprocal alleviation of the SHP-1 and c-Kit-deficient phenotypes suggests that the WT SHP-1 protein may be inhibiting signaling downstream of the c-Kit receptor to limit the *in vivo* expansion of mast cells. As described in the following sections, regulatory phosphotyrosine sites on membrane receptors such as c-Kit and FcεRI, their associated tyrosine kinases (Lyn, Syk), and adaptor proteins may serve as targets of SHP-1 phosphatase activity in various cell models. However, whether SHP-1 directly dephosphorylates these proteins to regulate mast cell activation pathways requires further validation.

5.2 SHP-1 in FcεRI Signaling and Responses

Similarly to growth factor starvation, sustained antigen stimulation of mast cells can also promote cell death that is in part mediated by SHP-1 signaling. BMMCs from *me* mice are more resistant to antigen-induced externalization of phosphatidylserine and fragmentation of DNA [38] that signal the induction of apoptosis. Loss of SHP-1 in these cells reduces the activity of the store-operated Ca²⁺ channel (SOC) and reduces pro-apoptotic mitochondrial permeability with cytochrome C release. SHP-1 also negatively regulates the pro-survival MAPK and BCL-X_L pathways [38], most likely via dephosphorylation of tyrosine residues on upstream adaptor/scaffolding proteins for the Ras/MAPK cascades such as LAT, as observed in other immune signaling pathways. SHP-1 may target proteins that control mitochondrial integrity and/or calcium channels, though such actions in Ag-stimulated mast cells have not yet been described. Taken together, these results show that enhanced cell survival is largely responsible for the abnormal increase in the numbers of tissue-resident mast cells that contributes to the spontaneous systemic inflammation in SHP-1-deficient mice [35, 38].

SHP-1 phosphatase activity-deficient *mev* mice have more mast cells in the lungs that store and spontaneously release higher levels of histamine than in WT mice. BMMCs from *mev* mice overall exhibit secretory hyperresponsiveness to LPS, oxidative stress, PMA, antigen, and/or SCF [35]. The heterozygous *me*/⁺ mice are also susceptible to allergic and Th2-type immune activation, including ovalbumin-induced lung inflammation and

airway hyperresponsiveness to methacholine challenge [29]. Mast cells from *me/me* mice spontaneously produce more IL-6 and IL-13 when treated with antigen, and T cells from these mice secrete much higher amounts of IL-4, IL-13, and IL-5 than wild-type cells upon T cell receptor stimulation and contribute to the moth-eaten-type phenotype [29].

The receptor-associated Lyn and SHP-1 proteins can reciprocally modulate each other's activation via their respective tyrosine kinase and phosphatase activities. Stimulation with low antigen concentrations (1 ng/ml) does not promote the recruitment of Lyn to Fc ϵ RI β -subunit and does not induce Lyn-mediated overall phosphorylation of tyrosine residues on SHP-1 [23]. Hypophosphorylation of SHP-1 is believed to reduce its inhibitory phosphatase activity in proximity to the Fc ϵ RI receptor, resulting in increased phosphorylation of Fc ϵ RI β -subunit ITAMs and Syk kinase-mediated induction of mast cell secretory responses. A high concentration of antigen (100 ng/ml) promotes Lyn-mediated recruitment and phosphorylation of SHP-1 and of the inhibitory inositol 5'-phosphatase SHIP-1, which together serve to downregulate mast cell activation [23].

However, the activity of the SHP-1 protein may also positively regulate mast cell activation and secretion of inflammatory cytokines. Stimulation of Fc ϵ RI receptor enhances SHP-1-mediated dephosphorylation of Tyr-396 on Lyn and Tyr-1020 on SHIP-1 to reduce their inhibitory effects on Fc ϵ RI signaling [39]. This interaction between SHP-1 and Lyn is mediated by the adaptor functions of the phospholipase family protein PLC β -3. Furthermore, in hematopoietic and mast cell progenitor cells, Lyn can phosphorylate Tyr-564 of SHP-1 to activate its phosphatase activity and suppress the activation of the transcription factor STAT5 to control the proliferation of myeloid cells. The activating phosphorylation of Tyr-536 on SHP-1 can be catalyzed by several kinases [40]. Interestingly, evidence from RBL-2H3 cells suggests that SHP-1 can auto-dephosphorylate Tyr-536, thus self-limiting the negative regulation of Fc ϵ RI signaling [41].

Evidence from several Fc ϵ RI-expressing cell systems suggests that SHP-1 differentially regulates the signaling pathways for mast cell degranulation and cytokine secretion [39]. In the RBL-2H3 cell line, exogenously expressed SHP-1 decreases the tyrosine phosphorylation of Fc ϵ RI subunits and Syk, promotes the Jnk-mediated secretion of TNF α , and has no effect on downstream antigen-induced release of histamine [42]. In another study, antigen-stimulated SHP-1-deficient BMMCs were found to have higher levels of MAP kinase activation downstream of Fc ϵ RI, resulting in enhanced release of IL-6 and TNF α cytokines. Nevertheless, PLC γ -mediated calcium mobilization and degranulation are reduced in these cells [43]. Aggregation of Fc ϵ RI can also induce the phosphorylation of Tyr-564 on SHP-1 and facilitate its association with the adaptor protein

3BP2, which positively regulates the production of TNF α but not degranulation in RBL-2H3 cells [44]. The phosphorylation of Tyr-564 on SHP-1 may serve to recruit Syk, Lyn, LAT, and/or PLC γ -2 proteins, via 3BP2, allowing SHP-1 to regulate cytokine secretion via direct tyrosine dephosphorylation of these Fc ϵ RI pathway-associated signaling mediators.

Overall data suggest that Fc ϵ RI and Syk may be the key *in vivo* targets of SHP-1 phosphatase activity in antigen-stimulated mast cells that allow SHP-1 to inhibit downstream signaling activation. The ability of SHP-1 to transiently form various receptor-proximal protein complexes may also account for some of the positive regulatory effects of SHP-1 in mast cell activation. As described earlier, the intensity of stimulation of receptors for antigen and/or cytokines can further alter the regulatory roles of individual signaling proteins, such as Lyn and SHP-1. Additionally, the dissimilar origin of rat basophilic leukemia (RBL-2H3) cells from bone marrow-derived mast cells, the abnormal expression levels of SHP-1, and possibly other tyrosine phosphatases/kinases in this cell line could alter the effect of individual PTPs on Ag-induced mediator release. Thus, it remains to be proven whether any of the proteins that are direct targets of SHP-1 in leukocytes also play key roles in the regulation of Fc ϵ RI signaling in mast cells.

5.3 SHP-2 and SHP-1: Similarities and Differences

Both Src homology region 2 domain-containing phosphatases 1 and 2 feature tandem SH2 domains near the N-terminal tails and a protein tyrosine phosphatase domain near the C-terminus. Yet, these cytoplasmic PTPs share only 55 % overall amino acid sequence and play generally opposing roles in the activation of cell signaling [45]. Unlike the mainly inhibitory functions of SHP-1 in hematopoietic cells, SHP-2 (*Ptpn11*) is ubiquitously expressed and typically facilitates the signaling of growth factor receptors [46]. Dissimilarities in the SH2 and PTP domains allow SHP-1 and SHP-2 to associate with and dephosphorylate different regulatory tyrosine residues [32]. Interestingly, both SH2-containing PTPs are co-expressed in mast cells and other leukocytes, where they regulate the PI3K, Akt, Jak2/STAT, MAPK, and NF- κ B signaling cascades [47]. SHP-2 also facilitates the hematopoietic differentiation of murine stem cells that can give rise to mast cells [48].

Both SHP-1 and SHP-2 work in close proximity to regulate mast cell activation through c-Kit, Fc ϵ RI, and immune receptors with tyrosine-based inhibitory motifs (ITIMs). The binding of SHP-1 at Tyr-569 and SHP-2 at Tyr-567 of the tyrosine kinase receptor c-Kit inhibits SCF-induced signaling and proliferation of Ba/F3 Pro-B cells [49]. However, the association of SHP-2 with the adaptor protein Gab2 at c-Kit Tyr-567 also activates the Rac/Jnk pathway and proliferation of mouse mast cells [50]. Despite the ability of SHP-1 and SHP-2 to bind and/or dephosphorylate multiple tyrosine kinases and adaptor proteins *in vitro*, their direct

protein targets that allow both positive and negative regulation of c-Kit downstream signaling in mast cells have not been fully elucidated. Evidence from other cell types suggests that reciprocal regulation of tyrosine phosphorylation stimulus by Src family kinases and SHPs plays an important role in several mast cell activation pathways [40, 42].

The β -subunit of Fc ϵ RI constitutively associates with SHP-1, whereas SHP-2 is recruited upon aggregation of Fc ϵ RI. Receptor stimulation is followed by activating tyrosine phosphorylation of both PTPs, most likely by receptor-associated SFKs. Fc ϵ RI ITAMs can also be directly dephosphorylated by SHP-1 and SHP-2 in vitro [51]. Antigen stimulation of mouse BMMCs induces phosphorylation of Tyr-58 and Tyr-47 on Fc ϵ RI- γ . Tyr-58 is more important for the recruitment of Syk kinase and calcium signaling and is preferentially dephosphorylated by SHP-1 and SHP-2 over Tyr-47 [52]. The loss of SHP-2 from mast cells also reduces the activation of Fyn and Erk and the secretion of TNF α . SHP-1 and SHP-2 can inhibit the influx of calcium during mast cell activation through their recruitment to ITIMs in the immunoglobulin superfamily receptor gp49B1 [53], which functions to inhibit anaphylactic reactions in mice [54]. However, similarly to SHP-1, the loss of SHP-2 protein alone may not affect the overall antigen-induced degranulation of mast cells [55].

Given the complexity of the involvement of both SHP-1 and SHP-2 in multiple signaling pathways that control the differentiation, survival, and inflammatory activation of mast cells, it is unsurprising that both PTPs appear to have mixed effects on mast cell-mediated pathologies. Further research will elucidate the key direct binding partners and phosphatase substrates that allow SHP-1 and SHP-2 to exert both positive and negative regulation of important processes in mast cells.

6 Other Intracellular Mast Cell PTPs

6.1 Tyrosine-Specific PTPs: PEP, HePTP, and PTP-MEG2

The PEST domain-enriched tyrosine phosphatase (PEP, *Ptpn22*) in mouse mast cells (known as LYP in humans) promotes antigen-induced activation of PLC γ 1, calcium mobilization, degranulation, and IgE-mediated systemic anaphylaxis in mice [56]. Anti-inflammatory glucocorticoids can also upregulate the expression of PEP in BMMCs. Upregulated PEP acts to reduce the anti-anaphylactic effects of glucocorticoids, since direct chemical inhibition of PEP activity enhances the anti-anaphylactic effects of glucocorticoids, making it a potential drug target [56]. Mice lacking the expression of PEP phosphatase have a decreased capacity for anaphylactic reactions, but they do not gain additional protection from glucocorticoids. On the other hand, in T cell receptor signaling, PEP can physically associate with the inhibitory tyrosine kinase Csk to downregulate cell activation [57].

In general, Csk kinase antagonizes the activating dephosphorylations of SFKs by leukocyte PTPs.

In resting RBL-3H2 mast cells, the hematopoietic tyrosine phosphatase (HePTP, *Ptpn7*) is evenly distributed throughout the cytosol. Fc ϵ RI signaling induces HePTP to aggregate in many small, globular compartments in the cytoplasm and become tyrosine phosphorylated following the intracellular influx of calcium [58]. In other cell types HePTP can directly dephosphorylate Erk2 and possibly other MAP kinases to downregulate growth factor receptor signaling pathways [59]. However, it is not yet known whether HePTP protein itself significantly affects mast cell responses.

Expression of the megakaryocyte protein tyrosine phosphatase 2 (PTP-MEG2, *PTPN9*) in RBL-3H2 mast cells causes fusion and enlargement of vesicles near the *trans*-Golgi network. In Jurkat T leukemia cells, PTP-MEG2 tyrosine phosphatase activity can also inhibit the induced secretion of IL-2 [60]. Therefore, PTP-MEG2 may similarly regulate the formation or exocytosis of secretory vesicles in mast cells.

6.2 Dual-Specific PTPs: MKP-1 and PTEN

Dual-specific phosphatases are capable of catalyzing the removal of phosphates from tyrosine, serine, and threonine protein residues [61]. The MAP kinase phosphatase 1 (MKP-1) is a dual-specific phosphatase that regulates the phosphorylation and activation of MAPKs crucial for the activation of mast cells and other leukocytes [62]. In rodent mast cells, anti-inflammatory corticosteroid drugs increase the protein levels of MKP-1 (*Dusp1*) and other dual-specific PTPs by upregulating their gene transcription and inhibiting the proteosomal degradation of MKP-1 proteins [63]. MKP-1 then reduces the antigen-induced mast cell degranulation and cytokine production by dephosphorylating the activating tyrosine and threonine residues on Erk and p38 MAP kinases. MKP-1 also protects mice from IgE-mediated systemic anaphylaxis. However, MKP-1 can be dispensable for other anti-inflammatory functions of glucocorticoids in the mouse [62, 63]. In rat peritoneal mast cells, MKP-1 also reduces the SCF-induced phosphorylation of p38 to inhibit mast cell migration and release of cytokines [64, 65].

Perhaps the most unusual mast cell PTP is PTEN (phosphatase and tensin homolog deleted on chromosome ten), which was originally identified as a tumor suppressor gene mutated in many types of human cancers [66]. The PTEN protein contains domains homologous to protein tyrosine phosphatases and to the actin-binding protein tensin. PTEN was initially classified as a dual-specific phosphatase, due to its ability to dephosphorylate tyrosine, as well as serine and threonine, protein residues in vitro. However, the main *in vivo* function of PTEN is to antagonize cell-activating PI3K signaling by dephosphorylating the 3' position of the lipid second messenger PIP₃. Recently, mice lacking PTEN (*Pten*) were shown to have hyperproliferation of tissue-resident mast cells [67].

PTEN-deficient BMMCs are also more resistant to apoptosis due to elevated expression of pro-survival factors. PTEN^{-/-} BMMCs exhibit enhanced intrinsic and growth factor (SCF, IL-3)-induced activation of the transcription factor STAT5 for cell growth as well as PI3K-mediated activation of the kinase Akt. Loss of mast cell PTEN also contributes to secretory hyperresponsiveness to antigen and SCF and enhanced anaphylaxis in the mouse [67]. Though it is unknown whether the lack of tyrosine phosphatase activity of PTEN contributes to these phenotypes, its lipid phosphatase-dependent ability to downregulate PI3K signaling is crucial for controlling proliferation and immune activation of mast cells.

7 Oxidative Regulation of Mast Cell PTPs

The production of small reactive oxygen and nitrogen molecules is strongly associated with the inflammatory activation of mast cells and other leukocytes [68]. The amount of oxidative stress within mast cells may also influence their secretory responses [69]. Additionally, general inhibition of PTPs by peroxide and/or vanadate (pervanadate) ions induces the phosphorylation of tyrosine residues on the β - and γ -subunits of Fc ϵ RI, calcium influx, and degranulation of mast cells. However, treatment with pervanadate does not promote the movement of Fc ϵ RI complexes to lipid rafts, in contrast to the localization to rafts that occurs during aggregation of the Fc ϵ RI receptors by antigen [70, 71]. As with oxidizing reagents, antigen signaling leads to the reversible oxidation of active site cysteine residues of several PTPs (SHP-1, SHP-2, HePTP, PTP-MEG2) associated with the regulation of mast cell secretory responses. Furthermore, oxidation of mast cell PTPs can differentially alter their catalytic activities and induce their co-localization with the plasma membrane actin cytoskeleton [71]. In most cell systems, reversible oxidation generally reduces the catalytic activity of cysteine-based PTPs [72] and can promote the inhibitory dimerization of the receptor-like PTPs CD45, PTP α , and PTP ϵ [21, 73, 74]. Overall, this suggests that small oxidizing molecules produced by activated mast cells and/or nearby leukocytes may modulate Fc ϵ RI signaling and mast cell responsiveness by altering the catalytic activity and protein interactions of PTPs, thus affecting the tyrosine phosphorylation status of key signaling proteins.

8 Future Perspectives

In recent years, mast cells have been implicated in the pathogenesis of various forms of autoimmunity, cancer, and other severe chronic conditions [75, 76]. In addition to their pro-inflammatory effector

functions in allergies and infections, mast cells are also capable of downregulating several immune responses. In peripheral allografts, mast cells cooperate with regulatory T cells to suppress other leukocytes and promote allograft tolerance [77]. Additionally, mast cells can secrete the anti-inflammatory cytokine interleukin-10 during skin exposure to toxins and UV-B irradiation, reducing the extent of hypersensitivity dermatitis [78]. The abilities of mast cells to modulate immune environments, promote angiogenesis, and remodel the extracellular matrix is exploited by tumors to promote metastasis [79]. Colorectal tumors can recruit mast cells to systemically influence regulatory T cells to begin secretion of pro-inflammatory mediators that may promote cancer progression [80]. Additionally, in a mouse model of pancreatic tumor initiation, the release of angiogenic factors by recruited mast cells is an essential step for the growth of these tumors [81].

For such reasons, targeted regulation of mast cell responses may lessen the severity of human allergies, cancers, and autoimmune disorders. Knowledge gained from rodent mast cell models demonstrates that several PTPs are probably also crucial for the normal and aberrant functions of human mast cells.

References

1. Gilfillan AM, Tkaczyk C (2006) Integrated signalling pathways for mast-cell activation. *Nat Rev Immunol* 6:218–230
2. Gilfillan AM, Rivera J (2009) The tyrosine kinase network regulating mast cell activation. *Immunol Rev* 228:149–169
3. Alvarez-Errico D, Lessmann E, Rivera J (2009) Adapters in the organization of mast cell signaling. *Immunol Rev* 232:195–217
4. Alonso A, Sasin J, Bottini N, Friedberg I, Friedberg I, Osterman A, Godzik A, Hunter T, Dixon J, Mustelin T (2004) Protein tyrosine phosphatases in the human genome. *Cell* 117:699–711
5. Andersen JN, Mortensen OH, Peters GH, Drake PG, Iversen LF, Olsen OH, Jansen PG, Andersen HS, Tonks NK, Moller NP (2001) Structural and evolutionary relationships among protein tyrosine phosphatase domains. *Mol Cell Biol* 21:7117–7136
6. Tonks NK (2006) Protein tyrosine phosphatases: from genes, to function, to disease. *Nat Rev Mol Cell Biol* 7:833–846
7. Rayapureddi JP, Kattamuri C, Steinmetz BD, Frankfort BJ, Ostrin EJ, Mardon G, Hegde RS (2003) Eyes absent represents a class of protein tyrosine phosphatases. *Nature* 426:295–298
8. Tootle TL, Silver SJ, Davies EL, Newman V, Latek RR, Mills IA, Selengut JD, Parlikar BE, Rebay I (2003) The transcription factor eyes absent is a protein tyrosine phosphatase. *Nature* 426:299–302
9. Li X, Oghi KA, Zhang J, Krones A, Bush KT, Glass CK, Nigam SK, Aggarwal AK, Maas R, Rose DW, Rosenfeld MG (2003) Eya protein phosphatase activity regulates Six1-dach-eya transcriptional effects in mammalian organogenesis. *Nature* 426:247–254
10. Okabe Y, Sano T, Nagata S (2009) Regulation of the innate immune response by threonine-phosphatase of eyes absent. *Nature* 460:520–524
11. Arimura Y, Yagi J (2010) Comprehensive expression profiles of genes for protein tyrosine phosphatases in immune cells. *Sci Signal* 3:rs1
12. Berger SA, Mak TW, Paige CJ (1994) Leukocyte common antigen (CD45) is required for immunoglobulin E-mediated degranulation of mast cells. *J Exp Med* 180:471–476
13. Murakami K, Sato S, Nagasawa S, Yamashita T (2000) Regulation of mast cell signaling through high-affinity IgE receptor by CD45 protein tyrosine phosphatase. *Int Immunol* 12:169–176
14. Grochowly G, Hermiston ML, Kuhny M, Weiss A, Huber M (2009) Requirement for CD45 in fine-tuning mast cell responses mediated by different ligand-receptor systems. *Cell Signal* 21:1277–1286

15. Zikherman J, Weiss A (2008) Alternative splicing of CD45: the tip of the iceberg. *Immunity* 29: 839–841
16. Saunders AE, Johnson P (2010) Modulation of immune cell signalling by the leukocyte common tyrosine phosphatase, CD45. *Cell Signal* 22:339–348
17. Hermiston ML, Xu Z, Weiss A (2003) CD45: a critical regulator of signaling thresholds in immune cells. *Annu Rev Immunol* 21: 107–137
18. Hamaguchi T, Takahashi A, Manaka A, Sato M, Osada H (2001) TU-572, a potent and selective CD45 inhibitor, suppresses IgE-mediated anaphylaxis and murine contact hypersensitivity reactions. *Int Arch Allergy Immunol* 126:318–324
19. Irie-Sasaki J, Sasaki T, Matsumoto W, Opavsky A, Cheng M, Welstead G, Griffiths E, Krawczyk C, Richardson CD, Aitken K, Iscove N, Koretzky G, Johnson P, Liu P, Rothstein DM, Penninger JM (2001) CD45 is a JAK phosphatase and negatively regulates cytokine receptor signalling. *Nature* 409:349–354
20. Samayawardhena LA, Pallen CJ (2010) PTPalpha activates lyn and fyn and suppresses hck to negatively regulate Fc ϵ RI-dependent mast cell activation and allergic responses. *J Immunol* 185: 5993–6002
21. Akimoto M, Mishra K, Lim KT, Tani N, Hisanaga SI, Katagiri T, Elson A, Mizuno K, Yakura H (2009) Protein tyrosine phosphatase epsilon is a negative regulator of Fc ϵ RI-mediated mast cell responses. *Scand J Immunol* 69:401–411
22. Pallen CJ (2003) Protein tyrosine phosphatase alpha (PTPalpha): a src family kinase activator and mediator of multiple biological effects. *Curr Top Med Chem* 3:821–835
23. Xiao W, Nishimoto H, Hong H, Kitaura J, Nunomura S, Maeda-Yamamoto M, Kawakami Y, Lowell CA, Ra C, Kawakami T (2005) Positive and negative regulation of mast cell activation by lyn via the Fc ϵ RI. *J Immunol* 175:6885–6892
24. Parravicini V, Gadina M, Kovarova M, Odom S, Gonzalez-Espinosa C, Furumoto Y, Saitoh S, Samelson LE, O'Shea JJ, Rivera J (2002) Fyn kinase initiates complementary signals required for IgE-dependent mast cell degranulation. *Nat Immunol* 3:741–748
25. Odom S, Gomez G, Kovarova M, Furumoto Y, Ryan JJ, Wright HV, Gonzalez-Espinosa C, Hibbs ML, Harder KW, Rivera J (2004) Negative regulation of immunoglobulin E-dependent allergic responses by lyn kinase. *J Exp Med* 199: 1491–1502
26. Hernandez-Hansen V, Smith AJ, Surviladze Z, Chigaev A, Mazel T, Kalesnikoff J, Lowell CA, Krystal G, Sklar LA, Wilson BS, Oliver JM (2004) Dysregulated Fc ϵ RI signaling and altered fyn and SHIP activities in lynch-deficient mast cells. *J Immunol* 173:100–112
27. Gil-Henn H, Elson A (2003) Tyrosine phosphatase-epsilon activates src and supports the transformed phenotype of neu-induced mammary tumor cells. *J Biol Chem* 278: 15579–15586
28. Samayawardhena LA, Pallen CJ (2008) Protein-tyrosine phosphatase alpha regulates stem cell factor-dependent c-kit activation and migration of mast cells. *J Biol Chem* 283: 29175–29185
29. Kamata T, Yamashita M, Kimura M, Murata K, Inami M, Shimizu C, Sugaya K, Wang CR, Taniguchi M, Nakayama T (2003) Src homology 2 domain-containing tyrosine phosphatase SHP-1 controls the development of allergic airway inflammation. *J Clin Invest* 111: 109–119
30. Nakata K, Suzuki Y, Inoue T, Ra C, Yakura H, Mizuno K (2011) Deficiency of SHP1 leads to sustained and increased ERK activation in mast cells, thereby inhibiting IL-3-dependent proliferation and cell death. *Mol Immunol* 48: 472–480
31. Zhang J, Somani AK, Siminovitch KA (2000) Roles of the SHP-1 tyrosine phosphatase in the negative regulation of cell signalling. *Semin Immunol* 12:361–378
32. Songyang Z, Shoelson SE, Chaudhuri M, Gish G, Pawson T, Haser WG, King F, Roberts T, Ratnofsky S, Lechleider RJ (1993) SH2 domains recognize specific phosphopeptide sequences. *Cell* 72:767–778
33. Green MC, Shultz LD (1975) Motheaten, an immunodeficient mutant of the mouse. I. Genetics and pathology. *J Hered* 66:250–258
34. Bignon JS, Siminovitch KA (1994) Identification of PTP1C mutation as the genetic defect in motheaten and viable motheaten mice: a step toward defining the roles of protein tyrosine phosphatases in the regulation of hemopoietic cell differentiation and function. *Clin Immunol Immunopathol* 73: 168–179
35. Zhang L, Oh SY, Wu X, Oh MH, Wu F, Schroeder JT, Takemoto CM, Zheng T, Zhu Z (2010) SHP-1 deficient mast cells are hyperresponsive to stimulation and critical in initiating allergic inflammation in the lung. *J Immunol* 184:1180–1190
36. Shultz LD, Coman DR, Bailey CL, Beamer WG, Sidman CL (1984) "Viable motheaten," a new allele at the motheaten locus. I. Pathology. *Am J Pathol* 116:179–192
37. Paulson RF, Vesely S, Siminovitch KA, Bernstein A (1996) Signalling by the W/Kit

receptor tyrosine kinase is negatively regulated in vivo by the protein tyrosine phosphatase Shp1. *Nat Genet* 13:309–315

- 38. Inoue T, Suzuki Y, Mizuno K, Nakata K, Yoshimaru T, Ra C (2009) SHP-1 exhibits a pro-apoptotic function in antigen-stimulated mast cells: positive regulation of mitochondrial death pathways and negative regulation of survival signaling pathways. *Mol Immunol* 47: 222–232
- 39. Xiao W, Kashiwakura J, Hong H, Yasuda H, Ando T, Maeda-Yamamoto M, Wu D, Kawakami Y, Kawakami T (2011) Phospholipase C-beta3 regulates Fcvar epsilon RI-mediated mast cell activation by recruiting the protein phosphatase SHP-1. *Immunity* 34:893–904
- 40. Xiao W, Ando T, Wang HY, Kawakami Y, Kawakami T (2010) Lyn- and PLC-beta3-dependent regulation of SHP-1 phosphorylation controls Stat5 activity and myelomonocytic leukemia-like disease. *Blood* 116:6003–6013
- 41. Ozawa T, Nakata K, Mizuno K, Yakura H (2007) Negative autoregulation of src homology region 2-domain-containing phosphatase-1 in rat basophilic leukemia-2H3 cells. *Int Immunol* 19:1049–1061
- 42. Xie ZH, Zhang J, Siraganian RP (2000) Positive regulation of c-jun N-terminal kinase and TNF-alpha production but not histamine release by SHP-1 in RBL-2H3 mast cells. *J Immunol* 164:1521–1528
- 43. Nakata K, Yoshimaru T, Suzuki Y, Inoue T, Ra C, Yakura H, Mizuno K (2008) Positive and negative regulation of high affinity IgE receptor signaling by src homology region 2 domain-containing phosphatase 1. *J Immunol* 181: 5414–5424
- 44. Chihara K, Nakashima K, Takeuchi K, Sada K (2011) Association of 3BP2 with SHP-1 regulates SHP-1-mediated production of TNF-alpha in RBL-2H3 cells. *Genes Cells* 16: 1133–1145
- 45. Neel BG (1993) Structure and function of SH2-domain containing tyrosine phosphatases. *Semin Cell Biol* 4:419–432
- 46. Soulsby M, Bennett AM (2009) Physiological signaling specificity by protein tyrosine phosphatases. *Physiology* 24:281–289
- 47. Chong ZZ, Maiese K (2007) The src homology 2 domain tyrosine phosphatases SHP-1 and SHP-2: diversified control of cell growth, inflammation, and injury. *Histol Histopathol* 22:1251–1267
- 48. Zou GM, Chan RJ, Shelley WC, Yoder MC (2006) Reduction of shp-2 expression by small interfering RNA reduces murine embryonic stem cell-derived in vitro hematopoietic differentiation. *Stem Cells* 24:587–594
- 49. Kozlowski M, Larose L, Lee F, Le DM, Rottapel R, Siminovitch KA (1998) SHP-1 binds and negatively modulates the c-kit receptor by interaction with tyrosine 569 in the c-kit juxtamembrane domain. *Mol Cell Biol* 18: 2089–2099
- 50. Yu M, Luo J, Yang W, Wang Y, Mizuki M, Kanakura Y, Besmer P, Neel BG, Gu H (2006) The scaffolding adapter Gab2, via shp-2, regulates kit-evoked mast cell proliferation by activating the Rac/JNK pathway. *J Biol Chem* 281:28615–28626
- 51. Kimura T, Zhang J, Sagawa K, Sakaguchi K, Appella E, Siraganian RP (1997) Syk-independent tyrosine phosphorylation and association of the protein tyrosine phosphatases SHP-1 and SHP-2 with the high affinity IgE receptor. *J Immunol* 159:4426–4434
- 52. Yamashita T, Suzuki R, Backlund PS, Yamashita Y, Yerger AL, Rivera J (2008) Differential dephosphorylation of the FcRgamma immunoreceptor tyrosine-based activation motif tyrosines with dissimilar potential for activating syk. *J Biol Chem* 283:28584–28594
- 53. Lu-Kuo JM, Joyal DM, Austen KF, Katz HR (1999) gp49B1 inhibits IgE-initiated mast cell activation through both immunoreceptor tyrosine-based inhibitory motifs, recruitment of src homology 2 domain-containing phosphatase-1, and suppression of early and late calcium mobilization. *J Biol Chem* 274:5791–5796
- 54. Daheshia M, Friend DS, Grusby MJ, Austen KF, Katz HR (2001) Increased severity of local and systemic anaphylactic reactions in gp49B1-deficient mice. *J Exp Med* 194:227–234
- 55. McPherson VA, Sharma N, Everingham S, Smith J, Zhu HH, Feng GS, Craig AW (2009) SH2 domain-containing phosphatase-2 protein-tyrosine phosphatase promotes Fc epsilon RI-induced activation of fyn and erk pathways leading to TNF alpha release from bone marrow-derived mast cells. *J Immunol* 183:4940–4947
- 56. Obiri DD, Flink N, Maier JV, Neeb A, Maddalo D, Thiele W, Menon A, Stassen M, Kulkarni RA, Garabedian MJ, Barrios AM, Cato AC (2012) PEST-domain-enriched tyrosine phosphatase and glucocorticoids as regulators of anaphylaxis in mice. *Allergy* 67:175–182
- 57. Gjorloff-Wingren A, Saxena M, Williams S, Hammi D, Mustelin T (1999) Characterization of TCR-induced receptor-proximal signaling events negatively regulated by the protein tyrosine phosphatase PEP. *Eur J Immunol* 29: 3845–3854
- 58. Swieter M, Berenstein EH, Swaim WD, Siraganian RP (1995) Aggregation of IgE receptors in rat basophilic leukemia 2H3 cells induces tyrosine phosphorylation of the cytosolic

protein-tyrosine phosphatase HePTP. *J Biol Chem* 270:21902–21906

59. Pettiford SM, Herbst R (2000) The MAP-kinase ERK2 is a specific substrate of the protein tyrosine phosphatase HePTP. *Oncogene* 19:858–869

60. Wang X, Huynh H, Gjorloff-Wingren A, Monosov E, Stridsberg M, Fukuda M, Mustelin T (2002) Enlargement of secretory vesicles by protein tyrosine phosphatase PTP-MEG2 in rat basophilic leukemia mast cells and jurkat T cells. *J Immunol* 168:4612–4619

61. Patterson KI, Brummer T, O'Brien PM, Daly RJ (2009) Dual-specificity phosphatases: critical regulators with diverse cellular targets. *Biochem J* 418:475–489

62. Maier JV, Brema S, Tuckermann J, Herzer U, Klein M, Stassen M, Moorthy A, Cato AC (2007) Dual specificity phosphatase 1 knockout mice show enhanced susceptibility to anaphylaxis but are sensitive to glucocorticoids. *Mol Endocrinol* 21:2663–2671

63. Kassel O, Sancono A, Kratzschmar J, Kreft B, Stassen M, Cato AC (2001) Glucocorticoids inhibit MAP kinase via increased expression and decreased degradation of MKP-1. *EMBO J* 20:7108–7116

64. Craig AW, Greer PA (2002) Fer kinase is required for sustained p38 kinase activation and maximal chemotaxis of activated mast cells. *Mol Cell Biol* 22:6363–6374

65. Jeong HJ, Na HJ, Hong SH, Kim HM (2003) Inhibition of the stem cell factor-induced migration of mast cells by dexamethasone. *Endocrinology* 144:4080–4086

66. Li J, Yen C, Liaw D, Podsypanina K, Bose S, Wang SI, Puc J, Miliarexis C, Rodgers L, McCombie R, Bigner SH, Giovanello BC, Ittmann M, Tycko B, Hibshoosh H, Wigler MH, Parsons R (1997) PTEN, a putative protein tyrosine phosphatase gene mutated in human brain, breast, and prostate cancer. *Science* 275: 1943–1947

67. Furumoto Y, Charles N, Olivera A, Leung WH, Dillahunt S, Sargent JL, Tinsley K, Odom S, Scott E, Wilson TM, Ghoreshi K, Kneilling M, Chen M, Lee DM, Bolland S, Rivera J (2011) PTEN deficiency in mast cells causes a mastocytosis-like proliferative disease that heightens allergic responses and vascular permeability. *Blood* 118:5466–5475

68. Swindle EJ, Metcalfe DD (2007) The role of reactive oxygen species and nitric oxide in mast cell-dependent inflammatory processes. *Immunol Rev* 217:186–205

69. Wolfreys K, Oliveira DB (1997) Alterations in intracellular reactive oxygen species generation and redox potential modulate mast cell function. *Eur J Immunol* 27:297–306

70. Teshima R, Ikebuchi H, Nakanishi M, Sawada J (1994) Stimulatory effect of pervanadate on calcium signals and histamine secretion of RBL-2H3 cells. *Biochem J* 302(Pt 3): 867–874

71. Heneberg P, Draberova L, Bambouskova M, Pomach P, Draber P (2010) Down-regulation of protein-tyrosine phosphatases activates an immune receptor in the absence of its translocation into lipid rafts. *J Biol Chem* 285: 12787–12802

72. Heneberg P, Draber P (2005) Regulation of cys-based protein tyrosine phosphatases via reactive oxygen and nitrogen species in mast cells and basophils. *Curr Med Chem* 12: 1859–1871

73. Tertoolen LG, Blanchetot C, Jiang G, Overvoorde J, Gadella TW Jr, Hunter T, den Hertog J (2001) Dimerization of receptor protein-tyrosine phosphatase alpha in living cells. *BMC Cell Biol* 2:8

74. Groen A, Overvoorde J, van der Wijk T, den Hertog J (2008) Redox regulation of dimerization of the receptor protein-tyrosine phosphatases RPTPalpha, LAR, RPTPmu and CD45. *FEBS J* 275:2597–2604

75. Gilfillan AM, Austin SJ, Metcalfe DD (2011) Mast cell biology: Introduction and overview. *Adv Exp Med Biol* 716:2–12

76. Kalesnikoff J, Galli SJ (2008) New developments in mast cell biology. *Nat Immunol* 9:1215–1223

77. Lu LF, Lind EF, Gondek DC, Bennett KA, Gleeson MW, Pino-Lagos K, Scott ZA, Coyle AJ, Reed JL, Van Snick J, Strom TB, Zheng XX, Noelle RJ (2006) Mast cells are essential intermediaries in regulatory T-cell tolerance. *Nature* 442:997–1002

78. Grimaldeston MA, Nakae S, Kalesnikoff J, Tsai M, Galli SJ (2007) Mast cell-derived interleukin 10 limits skin pathology in contact dermatitis and chronic irradiation with ultraviolet B. *Nat Immunol* 8:1095–1104

79. Maltby S, Khazaie K, McNagny KM (2009) Mast cells in tumor growth: angiogenesis, tissue remodelling and immune-modulation. *Biochim Biophys Acta* 1796:19–26

80. Blatner NR, Bonertz A, Beckhove P, Cheon EC, Krantz SB, Strouch M, Weitz J, Koch M, Halverson AL, Bentrem DJ, Khazaie K (2010) In colorectal cancer mast cells contribute to systemic regulatory T-cell dysfunction. *Proc Natl Acad Sci U S A* 107: 6430–6435

81. Soucek L, Lawlor ER, Soto D, Shchors K, Swigart LB, Evan GI (2007) Mast cells are required for angiogenesis and macroscopic expansion of myc-induced pancreatic islet tumors. *Nat Med* 13:1211–1218

Chapter 18

MicroRNA Function in Mast Cell Biology: Protocols to Characterize and Modulate MicroRNA Expression

Steven Maltby, Maximilian Plank, Catherine Ptaschinski, Joerg Mattes, and Paul S. Foster

Abstract

MicroRNAs (miRNAs) are small noncoding RNA molecules that can modulate mRNA levels through RNA-induced silencing complex (RISC)-mediated degradation. Recognition of target mRNAs occurs through imperfect base pairing between an miRNA and its target, meaning that each miRNA can target a number of different mRNAs to modulate gene expression. miRNAs have been proposed as novel therapeutic targets and many studies are aimed at characterizing miRNA expression patterns and functions within a range of cell types. To date, limited research has focused on the function of miRNAs specifically in mast cells; however, this is an emerging field. In this chapter, we will briefly overview miRNA synthesis and function and the current understanding of miRNAs in hematopoietic development and immune function, emphasizing studies related to mast cell biology. The chapter will conclude with fundamental techniques used in miRNA studies, including RNA isolation, real-time PCR and microarray approaches for quantification of miRNA expression levels, and antagomir design to interfere with miRNA function.

Key words MicroRNA, RNA isolation, Microarray, Real-time PCR, Antagomir

1 Introduction

1.1 MicroRNA Biogenesis and Structure

More than 1,000 miRNAs have been identified in humans, and miRNAs predate early invertebrates, identifying a key role for miRNA function in biological processes [1, 2]. In fact, miRNAs may regulate the expression of >60 % of all genes in humans [3]. miRNAs are commonly encoded either within the introns of protein-coding genes or as independent genes and are generally transcribed by RNA polymerase II [4, 5]. Some miRNAs are grouped in clusters, which are transcribed as single transcripts and processed to generate multiple functional miRNAs [5].

After transcription, the primary transcript (pri-miRNA) is processed by the nuclear RNase III enzyme Drosha and DGCR8 (DiGeorge syndrome critical region gene 8), excising the pre-miRNA stem-loop structure [6]. The double-stranded RNA hairpin

pre-miRNA is exported from the nucleus by exportin 5 and further spliced by the cytoplasmic RNase III enzyme Dicer and TAR RNA-binding protein 2 (TRBP) into an miRNA-miRNA* duplex approximately 22 nucleotides (nt) in length [7, 8]. The miRNA duplex is finally unwound and one miRNA is incorporated into the RISC complex, which also contains proteins from the Argonaute family of RNA-binding RNA endonucleases and other proteins [9]. The RISC complex is finally directed to mRNA strands with sequence complementary to the mature miRNA and functions to reduce target mRNA expression [9, 10].

1.2 *MicroRNA Function*

miRNAs modulate target mRNA levels by binding to the 3' untranslated region (UTR) of mRNA transcripts [11]. Target recognition occurs through complementary binding of the highly specific, ~7 nt-spanning seed sequence at the 5' end of a miRNA to a target mRNA [12]. While seed sequence recognition is highly specific, sequence complementarity throughout the rest of the miRNA is often quite low, allowing individual miRNAs to target multiple mRNA targets and making it difficult to predict miRNA targets based on sequence information alone [12–15].

How miRNAs modulate mRNA translation is still not fully understood; however, three general mechanisms have been proposed. Initial studies suggested that miRNAs function through (1) direct suppression of mRNA translation: these studies demonstrate that miRNA expression decreases levels of the target mRNA-encoded proteins without affecting the levels or stability of the target mRNA itself [16]. miRNAs accomplish this by blocking the initiation of translation or by blocking access of the ribosome to the target mRNA, causing the ribosome to fall off the target mRNA during elongation [17–19]. More recent studies have also demonstrated (2) miRNA-mediated modulation of mRNA stability. Expression of certain miRNAs can result in decreased levels of target mRNAs through direct miRNA-mediated mRNA degradation [20]. This process occurs through de-adenylation of the target mRNA transcript, followed by removal of the mRNA 5' cap, resulting in degradation of the transcript in the cytoplasm [21, 22]. Additionally, miRNA recognition of target mRNAs can result in (3) sequestration of target mRNA transcripts into processing (P) bodies. P bodies are structures within the cytoplasm involved in mRNA storage and degradation. Some of the Argonaute family members (present within the RISC complex) localize to P bodies, and certain miRNAs move to P bodies after binding to target mRNAs [23]. Within the P bodies, mRNA target degradation can occur, or alternatively, sequestration within the P bodies alone can result in decreased mRNA translation, as P bodies are largely devoid of ribosomes. Each of these mechanisms likely occurs for different subsets of miRNAs and/or mRNA targets resulting in the observed fine-tuning of protein expression.

1.3 MicroRNA in Hematopoietic Cells

miRNA studies generally fall into two broad categories: (1) studies profiling miRNA expression across multiple cell types aimed at characterizing broad expression patterns and (2) functional studies of small numbers of miRNAs aimed at characterizing individual miRNA functions. To date, several studies profiling broad miRNA expression patterns in the hematopoietic lineage have included mast cells, and a growing number of studies have focused on the effects of specific miRNAs in mast cell development and function.

1.4 MicroRNA Functions in Hematopoietic Development and Differentiation

A number of studies have focused on roles for miRNAs in hematopoietic stem cell differentiation and self-renewal. Conditional loss of Dicer results in reduced hematopoietic contribution in a competitive bone marrow reconstitution model [24], while loss of Ars2 (a molecule required for miRNA-mediated repression) results in impaired cell proliferation and bone marrow failure in adult mice [25]. As Dicer and Ars2 are broadly required for miRNA processing and function, these findings suggest that one or more miRNAs are critical for long-term bone marrow maintenance. Several studies have identified mir-125a (along with other members of the cluster, mir-99b and let-7e) as preferentially expressed in long-term repopulating hematopoietic stem cells (LT-HSCs) [24, 26], and mir-125a plays a role in HSC expansion via targeting of Bak1 [24]. Overexpression of mir-125a results in reduced progenitor apoptosis and increased HSC numbers [24]. Mir-125a expression levels also correlate with HSC numbers across inbred mouse strains [24]. Further, forced overexpression of mir-125a confers an advantage in competitive reconstitution models, ultimately resulting in the development of myeloproliferative neoplasms [26]. The miR-125a homologue (miR-125b) is also upregulated in HSCs, and overexpression confers a similar advantage in competitive reconstitution assays, along with a dose-dependent progression to lethal myeloid leukemia [27]. MiR-155 expression is increased in human CD34⁺ hematopoietic stem-progenitor cells (HSPCs), and overexpression results in reduced myeloid and erythroid differentiation, suggesting that miR-155 helps maintain progenitor status and blocks maturation and/or differentiation [28]. Finally, miR-221 and miR-222 are highly expressed in CD34⁺ cord blood progenitor cells and dampen kit expression, a key molecule in the maintenance of stem cells [29]. Enforced overexpression of miR-221 and miR-222 results in impaired stem cell engraftment in transplant models, and downregulation is required for appropriate differentiation along the erythroid lineage [29].

miRNAs also play key roles in the regulation of more mature, multipotent progenitor populations. MiR-150 is preferentially expressed in megakaryocyte-erythrocyte progenitors (MEPs) and promotes megakaryocyte lineage commitment, at the expense of erythroid development, by targeting the transcription factor MYB [30]. In granulocyte progenitors, miR-223 negatively regulates

progenitor proliferation and differentiation by targeting the transcription factor Mef2c [31]. MiR-223 also affects mature granulocytes by dampening activation, and loss of miR-223 expression in mature cells results in increased sensitivity to activating stimuli and increased fungicidal activity [31].

In the lymphoid lineage, conditional deletion of Dicer results in impaired survival of immature $\alpha\beta$ T cells, with no effects on either $\gamma\delta$ T cells or CD4/CD8 lineage commitment [32]. MiR-181a expression is increased during T cell maturation, downregulating a number of phosphatases and resulting in increased T cell receptor sensitivity [33]. Conversely, inhibition of miR-181a results in reduced receptor sensitivity and impaired positive and negative selection during T cell maturation [33]. In B cell development, conditional loss of Dicer expression results in a differentiation block at the pro- to pre-B cell transition, likely through a miR-17-92-mediated mechanism targeting the proapoptotic molecule Bim [34]. In addition, loss of Argonaute 2 (Ago2) results in reduced miRNA levels and impaired B cell and erythroid development [35]. MiR-150 also plays a key role in the regulation of the transcription factor c-MyB in developing B cells, and premature expression blocks B cell maturation [36, 37]. Similarly, constitutive expression of miR-34a blocks B cell development, resulting in reduced B cell numbers by targeting the transcription factor Foxp1 [38].

In myeloid populations, miR-17-5p, miR-20a, and miR-106a are downregulated during monocyte differentiation, resulting in increased levels of the transcription factor acute myeloid leukemia-1 (AML1) [39]. Enforced expression of these miRNAs results in increased blast proliferation and inhibition of monocyte differentiation and maturation [39]. Further, miR-223 exhibits “myeloid gene” characteristics and is upregulated by the myeloid transcription factor PU.1 and the C/EBP transcription factors [40]. In human granulocyte precursors, miR-223 expression is regulated by competition between the transcription factors NFI-A and C/EBP α , and expression promotes granulocyte differentiation [41].

While miRNAs clearly have functional roles in normal hematopoietic differentiation, they are better understood for their role in malignancy, when expression patterns are altered. Some examples include miR-155, miR-29a, miR-15a, and miR-16-1. Levels of miR-155 accumulate in certain B cell lymphomas, and forced overexpression of miR-155 results in a preleukemic B cell proliferation in the spleen, followed by progression to B cell malignancy [42]. Similarly, miR-155 promotes normal myeloid differentiation but is overexpressed in patients with acute myeloid leukemia (AML) and contributes to malignancy following forced overexpression [43]. Ectopic expression of miR-29a in progenitor populations results in aberrant progenitor self-renewal capacity, myeloid differentiation, and ultimately progression to AML [44]. Finally, miR-15a and miR-16-1 deletion can lead to accelerated B cell proliferation by

modulation of cell cycle genes, and both miR-15a and miR-16-1 are often deleted in B cell chronic lymphocytic leukemias (B-CLL) [45, 46].

1.5 MicroRNA Functions in Innate and Adaptive Immunity

In addition to roles in cell differentiation and development, miRNAs play key roles in regulating immune cell function. In innate immune function, miRNA modulation of Toll-like receptor (TLR)-mediated signaling has been extensively studied. TLRs recognize pathogen-associated molecular patterns (PAMPs) and are key molecules required for initiation of the innate immune response to pathogens. TLR4 surface expression is regulated by let-7 [47]. MiR-9 is upregulated by TLR stimulation (as well as by TNF- α or IL-1 β) in both monocytes and neutrophils and dampens NFKB1 expression to control inflammation [48]. TLR stimulation (or activation with IFN- β) of macrophages also stimulates increased miR-155 expression [49] and activates miR-147, which dampens inflammatory cytokine release [50]. Similarly, LPS stimulation of human peripheral blood mononuclear cells (PBMCs) increases miR-21 expression, which reduces levels of its target PDCD4, a molecule required for induced NF κ B activity in proinflammatory responses [51]. In human monocytes, miR-146a is induced in response to LPS treatment, in an NF κ B-dependent manner [52]. MiR-146a in turn targets TNF receptor-associated factor 6 (TRAF6) and IL-1 receptor-associated kinase 1 (IRAK), two molecules downstream of TLR signaling [52].

miRNAs also play roles in adaptive immune cell function. MiR-155 deficiency results in impaired B, T, and dendritic cell function, and miR-155 normally modulates a wide range of cytokines, chemokines, and transcription factors [53]. Further, miR-155 is critical for T cell-dependent antibody responses in germinal centers [54]. MiR-326 and MiR-181a both play key roles in modulating T cell function, with miR-326 expression promoting Th17 differentiation by targeting Ets-1 [55] and miR-181a modulating T cell signaling sensitivity [33].

Of particular interest for the mast cell field, two miRNAs have been identified that regulate allergic inflammation and airway disease. In a mouse model of house dust mite (HDM)-induced allergic disease, we identified a key role for miR-126 [56]. Following disease induction, miR-126 expression is upregulated in the lung, via a TLR4- and MyD88-dependent pathway [56]. Blocking miR-126 activity resulted in decreased disease pathology, including decreased eosinophil recruitment, reduced mucus production, suppressed cytokine levels, and abolished airway hyperresponsiveness [56]. In both ovalbumin (OVA) and aspergillus models of experimental allergic asthma, miR-21 expression is also increased, primarily in lung macrophages and dendritic cells [57]. MiR-21 targets IL-12p35, decreasing IL-12 production and increasing Th2 responses, eosinophilia and allergic airway inflammation [57].

MiR-21 is also upregulated in a bleomycin-induced lung fibrosis model and in patients with idiopathic pulmonary fibrosis, inducing TGF- β 1 from primary fibroblasts [58]. Mast cells have classically had a prominent role in these diseases, and while current studies have not addressed miRNA function in mast cells in these models, this will likely be a key area of future research.

1.6 MicroRNA in Mast Cell Biology

Numerous roles are emerging for miRNAs in hematopoietic immune cell function. However, to date, relatively little attention has been focused on roles in mast cell biology. Mast cells have only been included in a few of the broad miRNA profiling studies. In the first study, Monticelli et al. [59] assessed 181 miRNAs across a range of hematopoietic cell types, including cultured BMMCs (bone marrow-derived mast cells). BMMCs express high levels of miR-26a, miR-24, and miR-27a and low levels of miR-223 compared to other hematopoietic lineages. Interestingly, BMMC expression patterns are most similar to mature T cell subsets, which the authors attributed to the similar terminal maturation states of these cell lineages. In a more recent study, Kuchen et al. [60] profiled 600 miRNAs and identified a novel miRNA transcript “1073496_chr3” within the CPA3 gene, which was highly expressed in the mast cell and basophil lineages. These profiling studies provide a starting point for studying miRNA function in mast cells and a first step toward characterizing miRNA expression in mast cells.

In addition to profiling studies, a number of recent studies have explored functional roles for mast cell-expressed miRNAs. Several miRNAs have been implicated in the regulation of mast cell cycle, proliferation, and maturation. miR-221 and miR-222 are increased in bone marrow-derived mast cells (BMMCs) after activation, and overexpression dampens cell proliferation, with no effect on differentiation or cell survival [61]. During homeostasis, miR-381 and miR-539 targets microphthalmia-associated transcript factor (MITF) expression, maintaining appropriate mast cell proliferation [62]. In patients with mastocytosis, an activating kit receptor mutation results in decreased levels of miR-381 and miR-539, resulting in increased MITF expression and increased mast cell proliferation [62]. During mast cell maturation, miR-126 downregulation results in increased levels of its target Spred1 (Sprouty-related Ena/VASP homology-1 domain-containing protein), regulating mast cell numbers and cytokine production [63]. Conversely, conditional knockout of Spred1 results in increased mast cell numbers and increased cytokine production following activation [63].

Several miRNAs have also been implicated in the modulation of mast cell activation, degranulation, and migration. In addition to its role modulating cell cycle, miR-221 also modulates mast cell adhesion and migration. miR-221-overexpression results in

increased degranulation and cytokine production, decreased cell migration, and increased cell adhesion through a number of proposed target genes [64]. miR-132 levels in BMMCs increase following activation via IgE cross-linking, and miR-132 dampens heparin-binding EGF-like growth factor (HB-EGF) activation in a proposed negative feedback mechanism on mast cell activation [65].

1.7 Future Perspectives

miRNAs fine-tune expression of a large number of mRNA targets and clearly play key roles in immune cell development and function. Current data, although limited, indicates that miRNAs modulate many aspects of mast cell behavior, and this remains an emerging field of research. In the remaining portion of this chapter, we outline key techniques necessary to identify, quantify, and characterize miRNA expression for future studies of the role of miRNAs in mast cell biology. These techniques include microarray for broad surveys of miRNA expression, real-time PCR for miRNA validation and quantification, and antagomir development to target miRNAs *in vitro* and *in vivo*. These methods, and novel methods that continue to be developed, will underpin studies into understanding the role that miRNAs play in mast cell development and function.

2 Materials

2.1 Preparation of Samples

1. Cells of interest.
2. Microtubes, 1.5 mL or appropriate centrifuge tubes.
3. Phosphate-buffered saline (PBS).
4. TRI Reagent (TRIzol) at 4 °C. (NB: TRI Reagent is toxic and should only be used in a fume hood.)

2.2 Total RNA Isolation

1. Microtubes, 1.5 mL.
2. Chloroform—molecular grade (NB: Chloroform is harmful and should only be used in a fume hood).
3. Optional: Glycogen—working stock (5 µg/µL), store at -20 °C.
4. Isopropanol—molecular grade. (NB: Isopropanol is an irritant and is also highly flammable.)
5. Autoclaved Kimwipes.
6. 80 % ethanol: Add 80 mL of 100 % molecular-grade ethanol to 20 mL of nuclease-free water. (NB: Ethanol is highly flammable.)
7. Nuclease-free water.
8. Absorbance reader (e.g., NanoDrop).
9. Biological sample analyzer to determine RNA integrity (e.g., Agilent Bioanalyzer).

2.3 Reverse Transcription of miRNAs

1. Microtubes or microplates.
2. Nuclease-free water.
3. TaqMan miRNA reverse transcription kit (includes dNTPs (100 mM), MultiScribe Reverse Transcriptase (50 U/μL), RT buffer (10×), and RNase inhibitor (20 U/μL); Life Technologies), store at -20 °C.
4. TaqMan RT primers, specific for individual miRNAs, from TaqMan miRNA Assays (Life Technologies), store at -20 °C.
5. Thermocycler.

2.4 Real-Time PCR Detection of miRNAs

1. Microtubes.
2. Nuclease-free water.
3. TaqMan Universal PCR Master Mix (2×; Life Technologies), store at 4 °C.
4. TaqMan miRNA Assays (containing TaqMan probe and PCR primer set, 20×) for each specific miRNA to be analyzed (Life Technologies), store at -20 °C.
5. Optical microplates (96-well or 384-well).
6. Optical adhesive film.
7. Real-time PCR instrument.

2.5 TaqMan Low Density miRNA Arrays for miRNA Profiling

1. Microtubes.
2. Nuclease-free water.
3. Megaplex RT primers (10×, includes MgCl₂ (25 mM); Life Technologies), store at -20 °C.
4. TaqMan miRNA reverse transcription kit (includes dNTPs (100 mM), MultiScribe Reverse Transcriptase (50 U/μL), RT buffer (10×), and RNase inhibitor (20 U/μL); Life Technologies), store at -20 °C.
5. TaqMan Universal Master Mix II, No AmpErase UNG (Life Technologies), store at 4 °C.
6. TaqMan miRNA Array Cards (Life Technologies), light sensitive, store at 4 °C.
7. Real-time PCR instrument capable of holding TaqMan miRNA Array Cards (e.g., Applied Biosystems 7900HT, ViiA7, or QuantStudio 12K Flex machines).

2.6 Targeting miRNA Function with Antagomirs

1. Cells of interest (e.g., primary mast cells, BMMCs, or mast cell line).
2. Appropriate culture medium (dependent on cells of interest).
3. Nuclease-free water.
4. Antagomir stocks.

3 Methods

3.1 Preparation of Samples

The initial step in all experiments aimed at quantifying or assessing miRNA levels will be isolation of total RNA samples from your cells of interest.

1. Pellet cells of interest by centrifugation at $1,000 \times g$ for 5 min.
2. Discard supernatant and wash cell pellet with 1 mL PBS.
3. Centrifuge at $1,000 \times g$ for 5 min.
4. Repeat steps 2 and 3 to wash cells.
5. Discard supernatant, resuspend cell pellet in 1 mL TRI Reagent, and homogenize by repeated pipetting.
6. Store lysate at -80°C until required.

3.2 Total RNA Isolation

In our experience, TRI Reagent gives a very good yield of total RNA at consistently high purity. This is crucial for downstream applications such as reverse transcription.

1. Allow samples to defrost completely before starting isolation (see Note 1).
2. Add 200 μL chloroform (per 1 mL of TRI Reagent), mix vigorously by hand for 15 s, let stand at RT for 5 min, and centrifuge at no more than $12,000 \times g$ for 10 min at 4°C .
3. While samples are spinning prepare and label fresh tubes.
4. Optional: Add 2 μL of 5 $\mu\text{g}/\mu\text{L}$ glycogen to fresh tubes, for samples with low levels of RNA (see Note 2).
5. Carefully transfer the colorless, upper aqueous phase to the freshly prepared tubes. Use a 200 μL pipette tip to carefully remove this phase. Avoid disturbing the interphase (see Note 3).
6. Optional: When using glycogen, lightly vortex samples to ensure resuspension.
7. Add 500 μL isopropanol, mix thoroughly by inversion, let it stand at RT for 10 min, and centrifuge at no more than $12,000 \times g$ for 10 min at 4°C (see Note 4).
8. Pour off supernatant and tap off remaining supernatant on a clean Kimwipe. Wash with 1 mL 80 % ethanol. Centrifuge at no more than $7,500 \times g$ for 5 min at 4°C .
9. Very carefully remove the supernatant by using pipette tips of progressively smaller volume to avoid disturbing the pellet (the pellet is often loose). Wash with another 1 mL of 80 % ethanol. Centrifuge at no more than $7,500 \times g$ for 5 min at 4°C .
10. Very carefully remove all the supernatant.
11. Air-dry pellets at RT for 5–10 min until all residual ethanol has evaporated (see Note 5).

12. Label a final set of fresh tubes. Carefully resuspend RNA pellet in required volume of pre-warmed 50 °C nuclease-free water (e.g., 10–15 µL for small quantities of RNA from ~100,000 initial cells) (*see Note 6*).
13. Once resuspended, transfer volume to a fresh tube. Quantify final RNA concentration and assess for impurities by measuring absorbance (e.g., NanoDrop) (*see Note 7*).
14. Optional: Analyze samples on a biological analyzer to confirm good RNA integrity (*see Note 8*).
15. Store at –80 °C.

3.3 Reverse Transcription of miRNAs

There are various approaches to assay miRNA expression levels via quantitative real-time PCR. We focus on the most commonly used approach in this protocol, the TaqMan miRNA Assay (Life Technologies). Reverse transcription (RT) is performed with miRNA-specific RT primers that contain a stem-loop structure, which enables the selective detection of mature miRNAs. In our experience, the use of TaqMan probes grants high specificity and sensitivity.

1. Dilute the isolated total RNA (as described in Subheading 3.2) to 0.2 to 2 ng/µL with nuclease-free water (5 µL volume required per miRNA to be assayed).
2. Prepare one RT master mix per miRNA as follows (volume for one sample, allow for pipetting error) (*see Notes 9–11*):

Nuclease-free water	4.16 µL
Reverse transcription (RT) buffer (10×)	1.50 µL
dNTPs (100 mM)	0.15 µL
RNase inhibitor (20 U/µL)	0.19 µL
MultiScribe Reverse Transcriptase (50 U/µL)	1.00 µL
TaqMan miRNA-specific RT primer (5×)	3.00 µL
Total	10.00 µL

3. Mix RT master mix by pipetting and add 10 µL per PCR well. Use multiple tubes/wells, if multiple miRNAs are to be reverse transcribed from the same sample.
4. Add 5 µL of diluted RNA from **step 1** per well. Seal wells with strips.
5. Gently vortex and lightly centrifuge samples to bring volume to the bottom of wells.
6. Place samples in thermocycler and run the following cycle:

(a)	16 °C for 30 min
(b)	42 °C for 30 min
(c)	85 °C for 5 min

7. Store miRNA cDNA at -20 °C until required.

3.4 Real-Time PCR Detection of miRNAs

Real-time PCR allows for detection of specific miRNAs within a starting sample as well as relative or absolute quantification of miRNA levels. Quantification is based on comparison to endogenous controls and other experimental samples (relative) or comparison to known standards (absolute).

1. Prepare PCR master mix as follows (volume per well, allow for pipetting error) (*see Note 12*):

TaqMan Universal PCR Master Mix (2×)	10.00 µL
Nuclease-free water	7.67 µL
TaqMan miRNA Assay (20×)	1.00 µL
Total	18.67 µL

2. Mix PCR master mix by pipetting and add 18.67 µL per well in optical microplates compatible with your real-time PCR machine. Use separate wells if multiple miRNAs are to be amplified from the same sample (i.e., multiple cDNAs per sample). Run each miRNA in triplicates. Also include controls lacking template (*see Note 13*).
3. Transfer 1.33 µL of the RT product generated in Subheading 3.3 above to each well.
4. Seal the plate with an optical adhesive cover.
5. Briefly centrifuge microplate to bring solution to bottom of wells.
6. Run plate at the following cycle parameters on a real-time PCR instrument:

(a)	95 °C for 10 min
(b)	95 °C for 15 s
(c)	60 °C for 60 s
(d)	Run 40 cycles of steps (b) and (c)

7. Analyze real-time PCR relative quantification data, comparing cycle number to endogenous control genes or different treatment groups, depending on the experimental setup.

3.5 *TaqMan Low Density miRNA Arrays for miRNA Profiling*

miRNA array profiling allows the assessment of a broad number of miRNAs within a single isolated sample. Individual miRNA expression levels should be confirmed and validated by subsequent real-time PCR experiments.

1. Dilute RNA (if necessary) to a concentration of 350–1,000 ng of total RNA in 3 μ L RNA per reaction. Keep the total amount of RNA consistent for all samples within one experiment (*see Note 14*).
2. Prepare Megaplex RT master mix as follows (volume per sample):

Nuclease-free water	0.2 μ L
RT buffer (10 \times)	0.8 μ L
dNTPs (100 mM)	0.2 μ L
Megaplex RT primers (10 \times)	0.8 μ L
MgCl ₂ (25 mM)	0.9 μ L
RNase inhibitor (20 U/ μ L)	0.1 μ L
MultiScribe Reverse Transcriptase (50 U/ μ L)	1.5 μ L
Total	4.5 μ L

3. Mix gently and centrifuge to bring solution to the bottom of tube.
4. For each sample add 3 μ L of RNA per 4.5 μ L Megaplex RT master mix.
5. Run sample on thermocycler at the following parameters (*see Notes 15 and 16*):

(a) 16 °C for 2 min
(b) 42 °C for 1 min
(c) 50 °C for 1 s
(d) Repeat steps (a)–(c) for 40 cycles
(e) 85 °C for 5 min

6. Allow TaqMan miRNA Array Card to warm to room temperature (*see Note 17*).
7. Prepare PCR reaction mix as follows (volume for one array):

TaqMan Universal PCR Master Mix	450 μ L
Megaplex RT product	6 μ L
Nuclease-free water	444 μ L
Total	900 μ L

8. Manually shake tube to mix reagents well.
9. Dispense 100 μ L of PCR reaction mix into each of the eight ports on the TaqMan miRNA Array Card.
10. Centrifuge TaqMan miRNA Array Cards at $300 \times g$ for two consecutive 1 min spins (see Note 18).
11. Seal TaqMan miRNA Array Cards using the array card stacker (see Note 19).
12. Load and run TaqMan miRNA Array Cards at the following cycling parameters in standard mode:

(a) 50 °C for 2 min
(b) 95 °C for 10 min
(c) 95 °C for 15 s
(d) 60 °C for 1 min
(e) Repeat steps (c) and (d) for 40 cycles

13. Analyze quantification data.

3.6 Targeting miRNA Function with Antagomirs

Antagomirs are chemically engineered nucleotides designed with complete sequence complementarity to specific miRNAs. The use of antagomirs *in vitro* or *in vivo* results in specific blockade of miRNA function, allowing for assessment of miRNA function in an assay of interest.

Antagomir Design

1. Obtain the mature miRNA sequences for the miRNAs of interest from miRBase: the microRNA database, Faculty of Life Sciences, University of Manchester, United Kingdom (<http://www.mirbase.org/>).
2. Generate the complementary RNA sequence for the miRNAs of interest. Annotate in 5'- to 3' orientation.
3. Add the following sequence modifications:
 - 2'-O-methyl-modified phosphoramidites for all nucleotides (annotated as m, before each nucleotide).
 - Phosphorothioate linkages for the first 2 and the last 4 nucleotides (annotated as *, after appropriate nucleotides).
 - Hydroxyprolinol-linked cholesterol at the 3'-end (annotated as -Chol).
 - Optional: Addition of a fluorescent modification at the 5'-end (e.g., fluorescein) allows for the visualization and tracking of antagomir-treated cells.
4. Order the antagomir from a custom oligo synthesis service provider (see Note 20). An example of a design for a specific antagomir targeting mmu-miR-21-5p:

Step	Description	Sequence
1	Mature mmu-miR-21-5p	5'UAGCUUAUCAGACUGAUGUUGA-3'
2	Complementary sequence to mmu-miR-21-5p	5'UCAACAUCAUCAGUCUGAUAGCUA-3'
3	Antagomir for mmu-miR-21-5p	5'mU.*.mC.*.mA.mA.mC.mA.mU.mC.mA.mG.mU.mC.mU.mG.mA.mU.mA.mA.mG.*.mC.*.mU.*.mA.*.3'-Chol

Antagomir Application

5. Select cells of interest and culture under appropriate conditions.
6. Resuspend lyophilized antagomirs in nuclease-free water at a concentration of 100 μ M.
7. Add specific antagomir or control (scrambled antagomir) at varying concentrations. Start with concentrations in the range of 0.5–5 μ M.
8. Assay effect of the antagomir treatment by monitoring cell numbers, morphology, or performing your functional assays of interest (see Note 21).
9. Assess effectiveness of miRNA knockdown via real-time PCR (see Note 22).

4 Notes

1. Wear lab coat, safety goggles, and blue nitrile gloves over a pair of latex gloves during all extraction procedures. Work in the fume hood. Work with sterile technique and filtered pipette tips to avoid contamination. Use RNase-free solutions kept aside for RNA work only.
2. If using samples with low levels of RNA, glycogen addition can help increase the precipitation of RNA for better yields.
3. Following centrifugation, the mixture will separate into a lower red, phenol chloroform phase (containing protein), and a colorless upper aqueous phase (containing RNA) separated by an interphase (containing DNA). Care should be taken when pipetting the aqueous phase to avoid transfer of contaminating DNA from the interphase section. We recommend leaving some of the upper aqueous phase to minimize carry-over of DNA contamination.
4. Volumes are based on an expected aqueous phase volume of 500 μ L, from the previous step. If the actual amount differs, adjust the volume of isopropanol added to make a 1:1 ratio. If using samples with low levels of RNA, samples can be incubated overnight at –20 °C at this step to maximize RNA precipitation. When loading tubes into the centrifuge, it helps

to have all tubes in the same orientation. This ensures RNA pellets are in the same position in each tube, making it easier to identify the pellets. The pellet is slightly white in color and should be visible at this stage. It is easier to identify against a dark background, e.g., blue gloves.

5. Do not allow pellet to air-dry completely, as this will decrease its solubility. Once pellet begins to change from a white to transparent color, add RNase-free water to resuspend.
6. Do not vortex or mix vigorously. Pipette sample up and down thoroughly to avoid leaving residues on the side of the tube.
7. RNA purity is assessed by determining the ratio of absorbance at 260 versus 230 and 280 nm. A ratio of approximately 2.0 indicates good quality RNA sample. A lower ratio may indicate the presence of protein, phenol, salt, or other contaminants, potentially carried over from the isolation procedure.
8. Determining the purity of RNA is important for downstream applications. However, it does not give any indication on the integrity of the purified RNA. One approach to determine RNA integrity is using an Agilent Bioanalyzer. This will also allow for the identification of DNA contamination. In the case of DNA contamination, we strongly recommend DNase treatment of RNA samples prior to further processing.
9. There are a number of different manufacturer's products and approaches for miRNA reverse transcription and real-time PCR experiments. For the protocols in this chapter, we will present approaches using Applied Biosystems TaqMan kits (Life Technologies).
10. When preparing the RT master mix, multiply each reagent by the number of samples to be analyzed. Make one RT master mix for each miRNA to be analyzed. Always include ~10 % excess to allow for pipetting error.
11. Before opening a tube of TaqMan RT primer, centrifuge to bring solution to the bottom of the tube to prevent loss of liquid trapped in the lid.
12. When preparing the PCR master mix, multiply reagents by the number of samples to be analyzed. Make one PCR master mix for each miRNA to be analyzed. Always include ~10 % reagent excess to allow for pipetting error. Allow for triplicate wells for each sample and each miRNA.
13. Always perform endogenous control assays for each sample used on the plate to maintain experiment-to-experiment reproducibility. "No template" controls should also be performed for each different miRNA assay on the assay plate to confirm reaction specificity.
14. We suggest adding the PCR master mix to the wells first, followed by addition of the RT product.

15. If using a PCR master mix containing AmpErase UNG, add a 50 °C for 2 min step before step (a) in the PCR protocol to induce activity of AmpErase UNG.
16. Samples with a total RNA concentration of 115 ng/µL or above can be reverse transcribed into cDNA for direct use in Taqman Low Density MicroRNA Arrays. For samples with a lower concentration it is recommended to perform a pre-amplification before performing Taqman Low Density MicroRNA Arrays.
17. Array cards A and B are available for both human and mouse samples. Each panel A and B must be used in separate RT reactions using Megaplex primer pools A or B. We recommend performing the reaction for each panel for all samples at the same time.
18. Visually confirm that the PCR master mix is loaded on the array card. The level for all eight loading ports should be equal; individual cells should all contain PCR master mix and no bubbles should be present within the cells.
19. Take care that the stacker and TaqMan miRNA Array Card are in the correct orientation before sealing the card, as sealing in the wrong orientation will damage the backing foil and destroy the array.
20. Prior to ordering antagonists, confirm the proper annotations with each synthesis provider and their capability to integrate each of the required modifications to ensure desired products are produced.
21. If using fluorescently labeled antagonist, cells can be assessed under the fluorescent microscope or via flow cytometry to assess antagonist uptake.
22. Knockdown of mature miRNA levels is often observed at these suggested antagonist concentrations, but the detection, confirmation, and degree of knockdown may vary by cell type, experimental setup, and initial miRNA expression levels in the cells.

References

1. Lewis BP, Burge CB, Bartel DP (2005) Conserved seed pairing, often flanked by adenines, indicates that thousands of human genes are microRNA targets. *Cell* 120(1):15–20
2. Berezikov E (2011) Evolution of microRNA diversity and regulation in animals. *Nat Rev Genet* 12(12):846–860
3. Friedman RC et al (2009) Most mammalian mRNAs are conserved targets of microRNAs. *Genome Res* 19(1):92–105
4. Lee Y et al (2004) MicroRNA genes are transcribed by RNA polymerase II. *EMBO J* 23(20):4051–4060
5. Lee Y et al (2002) MicroRNA maturation: stepwise processing and subcellular localization. *EMBO J* 21(17):4663–4670
6. Denli AM et al (2004) Processing of primary microRNAs by the Microprocessor complex. *Nature* 432(7014):231–235
7. Hutvagner G et al (2001) A cellular function for the RNA-interference enzyme Dicer in the maturation of the let-7 small temporal RNA. *Science* 293(5531):834–838
8. Ketting RF et al (2001) Dicer functions in RNA interference and in synthesis of small RNA involved in developmental timing in *C. elegans*. *Genes Dev* 15(20):2654–2659

9. Bartel DP (2004) MicroRNAs: genomics, biogenesis, mechanism, and function. *Cell* 116(2):281–297
10. Weinmann L et al (2009) Importin 8 is a gene silencing factor that targets argonaute proteins to distinct mRNAs. *Cell* 136(3):496–507
11. Hammond SM et al (2001) Argonaute2, a link between genetic and biochemical analyses of RNAi. *Science* 293(5532):1146–1150
12. Mallory AC et al (2004) MicroRNA control of PHABULOSA in leaf development: importance of pairing to the microRNA 5' region. *EMBO J* 23(16):3356–3364
13. Liu J (2008) Control of protein synthesis and mRNA degradation by microRNAs. *Curr Opin Cell Biol* 20(2):214–221
14. Lewis BP et al (2003) Prediction of mammalian microRNA targets. *Cell* 115(7):787–798
15. Lim LP et al (2005) Microarray analysis shows that some microRNAs downregulate large numbers of target mRNAs. *Nature* 433(7027):769–773
16. Wightman B, Ha I, Ruvkun G (1993) Posttranscriptional regulation of the heterochronic gene lin-14 by lin-4 mediates temporal pattern formation in *C. elegans*. *Cell* 75(5):855–862
17. Pillai RS et al (2005) Inhibition of translational initiation by Let-7 MicroRNA in human cells. *Science* 309(5740):1573–1576
18. Nottrott S, Simard MJ, Richter JD (2006) Human let-7a miRNA blocks protein production on actively translating polyribosomes. *Nat Struct Mol Biol* 13(12):1108–1114
19. Petersen CP et al (2006) Short RNAs repress translation after initiation in mammalian cells. *Mol Cell* 21(4):533–542
20. Bagga S et al (2005) Regulation by let-7 and lin-4 miRNAs results in target mRNA degradation. *Cell* 122(4):553–563
21. Giraldez AJ et al (2006) Zebrafish MiR-430 promotes deadenylation and clearance of maternal mRNAs. *Science* 312(5770):75–79
22. Wu L, Fan J, Belasco JG (2006) MicroRNAs direct rapid deadenylation of mRNA. *Proc Natl Acad Sci U S A* 103(11):4034–4039
23. Liu J et al (2005) MicroRNA-dependent localization of targeted mRNAs to mammalian P-bodies. *Nat Cell Biol* 7(7):719–723
24. Guo S et al (2010) MicroRNA miR-125a controls hematopoietic stem cell number. *Proc Natl Acad Sci U S A* 107(32):14229–14234
25. Gruber JJ et al (2009) Ars2 links the nuclear cap-binding complex to RNA interference and cell proliferation. *Cell* 138(2):328–339
26. Gerrits A et al (2012) Genetic screen identifies microRNA cluster 99b/let-7e/125a as a regulator of primitive hematopoietic cells. *Blood* 119(2):377–387
27. O'Connell RM et al (2010) MicroRNAs enriched in hematopoietic stem cells differentially regulate long-term hematopoietic output. *Proc Natl Acad Sci U S A* 107(32):14235–14240
28. Georgantas RW 3rd et al (2007) CD34+ hematopoietic stem-progenitor cell microRNA expression and function: a circuit diagram of differentiation control. *Proc Natl Acad Sci U S A* 104(8):2750–2755
29. Felli N et al (2005) MicroRNAs 221 and 222 inhibit normal erythropoiesis and erythroleukemic cell growth via kit receptor down-modulation. *Proc Natl Acad Sci U S A* 102(50):18081–18086
30. Lu J et al (2008) MicroRNA-mediated control of cell fate in megakaryocyte-erythrocyte progenitors. *Dev Cell* 14(6):843–853
31. Johnnidis JB et al (2008) Regulation of progenitor cell proliferation and granulocyte function by microRNA-223. *Nature* 451(7182):1125–1129
32. Cobb BS et al (2005) T cell lineage choice and differentiation in the absence of the RNase III enzyme Dicer. *J Exp Med* 201(9):1367–1373
33. Li QJ et al (2007) miR-181a is an intrinsic modulator of T cell sensitivity and selection. *Cell* 129(1):147–161
34. Koralov SB et al (2008) Dicer ablation affects antibody diversity and cell survival in the B lymphocyte lineage. *Cell* 132(5):860–874
35. O'Carroll D et al (2007) A Slicer-independent role for Argonaute 2 in hematopoiesis and the microRNA pathway. *Genes Dev* 21(16):1999–2004
36. Xiao C et al (2007) MiR-150 controls B cell differentiation by targeting the transcription factor c-Myb. *Cell* 131(1):146–159
37. Zhou B et al (2007) miR-150, a microRNA expressed in mature B and T cells, blocks early B cell development when expressed prematurely. *Proc Natl Acad Sci U S A* 104(17):7080–7085
38. Rao DS et al (2010) MicroRNA-34a perturbs B lymphocyte development by repressing the forkhead box transcription factor Foxp1. *Immunity* 33(1):48–59
39. Fontana L et al (2007) MicroRNAs 17-5p-20a-106a control monocytogenesis through AML1 targeting and M-CSF receptor upregulation. *Nat Cell Biol* 9(7):775–787
40. Fukao T et al (2007) An evolutionarily conserved mechanism for microRNA-223 expression revealed by microRNA gene profiling. *Cell* 129(3):617–631

41. Fazi F et al (2005) A minicircuity comprised of microRNA-223 and transcription factors NFI-A and C/EBPalpha regulates human granulopoiesis. *Cell* 123(5):819–831
42. Costinean S et al (2006) Pre-B cell proliferation and lymphoblastic leukemia/high-grade lymphoma in E(mu)-miR155 transgenic mice. *Proc Natl Acad Sci U S A* 103(18):7024–7029
43. O'Connell RM et al (2008) Sustained expression of microRNA-155 in hematopoietic stem cells causes a myeloproliferative disorder. *J Exp Med* 205(3):585–594
44. Han YC et al (2010) microRNA-29a induces aberrant self-renewal capacity in hematopoietic progenitors, biased myeloid development, and acute myeloid leukemia. *J Exp Med* 207(3):475–489
45. Calin GA et al (2002) Frequent deletions and down-regulation of micro-RNA genes miR15 and miR16 at 13q14 in chronic lymphocytic leukemia. *Proc Natl Acad Sci U S A* 99(24):15524–15529
46. Klein U et al (2010) The DLEU2/miR-15a/16-1 cluster controls B cell proliferation and its deletion leads to chronic lymphocytic leukemia. *Cancer Cell* 17(1):28–40
47. Chen XM et al (2007) A cellular micro-RNA, let-7i, regulates Toll-like receptor 4 expression and contributes to cholangiocyte immune responses against Cryptosporidium parvum infection. *J Biol Chem* 282(39):28929–28938
48. Bazzoni F et al (2009) Induction and regulatory function of miR-9 in human monocytes and neutrophils exposed to proinflammatory signals. *Proc Natl Acad Sci U S A* 106(13):5282–5287
49. O'Connell RM et al (2007) MicroRNA-155 is induced during the macrophage inflammatory response. *Proc Natl Acad Sci U S A* 104(5):1604–1609
50. Liu G et al (2009) miR-147, a microRNA that is induced upon Toll-like receptor stimulation, regulates murine macrophage inflammatory responses. *Proc Natl Acad Sci U S A* 106(37):15819–15824
51. Sheedy FJ et al (2010) Negative regulation of TLR4 via targeting of the proinflammatory tumor suppressor PDCD4 by the microRNA miR-21. *Nat Immunol* 11(2):141–147
52. Taganov KD et al (2006) NF-kappaB-dependent induction of microRNA miR-146, an inhibitor targeted to signaling proteins of innate immune responses. *Proc Natl Acad Sci U S A* 103(33):12481–12486
53. Rodriguez A et al (2007) Requirement of bic/microRNA-155 for normal immune function. *Science* 316(5824):608–611
54. Thai TH et al (2007) Regulation of the germinal center response by microRNA-155. *Science* 316(5824):604–608
55. Du C et al (2009) MicroRNA miR-326 regulates TH-17 differentiation and is associated with the pathogenesis of multiple sclerosis. *Nat Immunol* 10(12):1252–1259
56. Mattes J et al (2009) Antagonism of microRNA-126 suppresses the effector function of TH2 cells and the development of allergic airways disease. *Proc Natl Acad Sci U S A* 106(44):18704–18709
57. Lu TX, Munitz A, Rothenberg ME (2009) MicroRNA-21 is up-regulated in allergic airway inflammation and regulates IL-12p35 expression. *J Immunol* 182(8):4994–5002
58. Liu G et al (2010) miR-21 mediates fibrogenic activation of pulmonary fibroblasts and lung fibrosis. *J Exp Med* 207(8):1589–1597
59. Monticelli S et al (2005) MicroRNA profiling of the murine hematopoietic system. *Genome Biol* 6(8):R71
60. Kuchen S et al (2010) Regulation of microRNA expression and abundance during lymphopoiesis. *Immunity* 32(6):828–839
61. Mayoral RJ et al (2009) MicroRNA-221-222 regulate the cell cycle in mast cells. *J Immunol* 182(1):433–445
62. Lee YN et al (2011) KIT signaling regulates MITF expression through miRNAs in normal and malignant mast cell proliferation. *Blood* 117(13):3629–3640
63. Ishizaki T et al (2011) miR126 positively regulates mast cell proliferation and cytokine production through suppressing Spred1. *Genes Cells* 16(7):803–814
64. Mayoral RJ et al (2011) MiR-221 influences effector functions and actin cytoskeleton in mast cells. *PLoS One* 6(10):e26133
65. Molnar V et al (2012) MicroRNA-132 targets HB-EGF upon IgE-mediated activation in murine and human mast cells. *Cell Mol Life Sci* 69(5):793–808

Part IV

Mast Cell Products and Mediators

Chapter 19

Assay of Mast Cell Mediators

Madeleine Rådinger, Bettina M. Jensen, Emily Swindle, and Alasdair M. Gilfillan

Abstract

Mediator release from activated mast cells is a major initiator of the symptomology associated with allergic disorders such as anaphylaxis and asthma. Thus, methods to monitor the generation and release of such mediators have widespread applicability in studies designed to understand the processes regulating mast cell activation and for the identification of therapeutic approaches to block mast cell-driven disease. In this chapter, we discuss approaches used for the determination of mast cell degranulation, lipid-derived inflammatory mediator production, and cytokine/chemokine gene expression as well as cytokine release.

Key words Mast cell, IgE sensitization, Degranulation, PGD₂, LTC₄, Cytokines, Cytometric bead array, RT-PCR, Chemokines, ELISA

Abbreviations

BMMC	Bone marrow-derived mast cells
Fc ϵ RI	High-affinity IgE receptor
HuMC	Human mast cell
IL	Interleukin
LT	Leukotriene
PG	Prostaglandin
TNF- α	Tumor necrosis factor-alpha

1 Introduction

The inappropriate or exaggerated release of proinflammatory mediators from activated mast cells represents a central event in the initiation and perpetuation of allergic reactions associated with asthma, allergic rhinitis, anaphylaxis, and certain allergic dermatological and ocular disorders [1, 2]. Such events are generally a consequence of binding of antigen (Ag)-specific IgE molecules to high-affinity receptors for IgE (Fc ϵ RI) expressed on the mast cell

surface, and subsequent aggregation of these receptors as a result of Ag-mediated cross-linking of the Fc ϵ RI-bound IgE [3]. However, under specific circumstances, other stimuli can also contribute to mast cell activation [4]. The ability to measure the release of mast cell mediators is thus fundamental to the understanding of how mast cells can be activated in health and disease and for the identification of potential therapeutic approaches for the treatment of allergic disorders.

Although mast cells release a wide array of mediators in this manner, these mediators can generally be considered to belong to three major categories based on their mode of production, storage, and/or release: (1) pre-synthesized mediators which are stored in cytoplasmic granules, the contents of which are released by the process of exocytosis; (2) lipid-derived mediators such as the eicosanoids prostaglandin (PG)D₂ and leukotriene (LT)C₄, which are synthesized de novo then immediately released; and (3) cytokines, chemokines, and growth factors which are generated following induction of gene expression then subsequently released [2–4]. Histamine is certainly the most important pre-synthesized mast cell granule component in terms of disease, and extremely sensitive competition-based assays are available which can effectively measure histamine release from very few cells. Nevertheless, the relative cost of these assays precludes their use for wide-scale studies and for high-throughput screening aimed at identifying inhibitors of mast cell degranulation. For this reason, most laboratories monitor degranulation through determination of the release of the granule component β -hexosaminidase which can be readily assayed by a simple colorimetric determination of its enzymatic activity. Although not as sensitive as the currently available assays for histamine, it is sufficiently sensitive to allow determination of degranulation in relatively small numbers of mast cells and is amenable to a 96-well format. Due to the differences in granularity, however, this is highly dependent on the source of the mast cells; human mast cells (HuMCS), including the LAD2 human mast cell line, requiring approximately 1×10^4 cells per well; mouse bone marrow-derived mast cells (BMMCs), 3×10^4 to 5×10^4 cells per well; and the rat RBL 2H3 mast cell line, approximately 4×10^4 cells per well.

The traditional means of assay of eicosanoid generation and release through preloading of cells with the radiolabeled precursor, arachidonic acid, has now largely been circumvented by the widespread use of sensitive ELISA-based assays for the quantitation of released LTC₄ and PGD₂. These assays have a high degree of sensitivity, requiring only 1×10^4 cells per well for both assays. Besides the increased sensitivity, a distinct advantage of this assay format is that it avoids the use of radioactivity. Nevertheless, the ELISA kits are fairly expensive so studies must be conducted on a more selective basis than for degranulation.

There is much more flexibility in the approaches that can be used to monitor cytokine/chemokine production and hence release than those utilized for measuring either degranulation or eicosanoid generation. Both mRNA and protein determination have been utilized to assess cytokine generation based on the assumed correlation between mRNA levels and the amount of protein generated and released from the mast cells. It must be remembered, however, that mRNA levels do not always predict protein production. Several platforms are available that can simultaneously quantitate mRNA or protein levels of multiple cytokines/chemokines. The production or release of individual cytokines can subsequently be respectively assessed by quantitative real-time PCR and ELISA. These assays however require more cells (1×10^6 and 0.5×10^6 , respectively) than for the determination of degranulation and eicosanoid production.

In this chapter, we describe protocols that will allow researchers to readily monitor mast cell degranulation, eicosanoid release, and cytokine generation and release. These methods are highly reproducible and can be adapted to monitoring mediator release in mast cells from multiple sources. We, however, will primarily focus our discussions on mediator release from mouse bone marrow-derived mast cells (BMMCs) and from human mast cells (HuMCs) derived from CD34⁺ peripheral blood progenitors.

2 Materials

2.1 IgE Sensitization and Stimulation

1. Mouse anti-DNP IgE, clone SPE-7 (Sigma-Aldrich, St Louis, MO, USA).
2. Human myeloma IgE (Calbiochem, Millipore, Billerica, MA, USA) biotinylated as described [5] or by using an appropriate commercially available biotinylation kit.
3. Streptavidin (Sigma-Aldrich).
4. Goat anti-human IgE (KPL, Gaithersburg, MD, USA).
5. DNP (dinitrophenol)-HSA (Sigma-Aldrich).
6. Anti-Fc ϵ RI α antibody (eBioscience, San Diego, CA, USA).

2.2 β -Hexosaminidase Release Assay (Degranulation)

1. HEPES degranulation buffer (pH 7.4): 10 mM HEPES, 137 mM NaCl, 2.7 mM KCl, 0.4 mM sodium phosphate (dibasic), 5.6 mM glucose, 1.8 mM calcium chloride, 1.3 mM magnesium sulfate. To make 1 L, add 2.38 g HEPES, 8.00 g NaCl, 0.2 g KCl, 0.103 g Na₂HPO₄·7H₂O, 1.008 g glucose to 800 mL distilled H₂O (dH₂O). Adjust pH to 7.4 with NaOH (5 M) and add 0.265 g CaCl₂·2H₂O (1.8 mM), 0.32 g MgSO₄·7H₂O (1.3 mM). Adjust volume to 1 L with dH₂O, sterilize by filtration, and store at 4 °C.

2. Citrate buffer (pH 4.5): 40 mM citric acid, 20 mM sodium phosphate dibasic. To make 200 mL, add 1.681 g citric acid and 1.072 g $\text{Na}_2\text{HPO}_4 \cdot 7\text{H}_2\text{O}$ (20 mM) to 180 mL dH₂O. Adjust pH to 4.5 with NaOH (5 M), add dH₂O to 200 mL, sterilize by filtration, and store at 4 °C.
3. Glycine (400 mM, pH 10.7): Add 15.1 g glycine to 480 mL dH₂O, and adjust pH to 10.7 with NaOH (5 M). Adjust volume to 500 mL and sterilize by filtration and store at RT.
4. HEPES buffer (pH 7.4) with 0.04 % BSA: Add 0.04 g BSA (bovine serum albumin) to 100 mL HEPES buffer degranulation buffer (pH 7.4).
5. *p*-Nitro-*N*-acetyl- β -D-glucosaminide (pNAG) solution: 3.5 mg/mL pNAG (Sigma-Aldrich) solution is made up in citrate buffer and needs to be sonicated to dissolve.
6. 0.1 % (v/v) Triton X-100: Add 100 μL of Triton X-100 to 100 mL dH₂O. Cut the end of the pipette tip prior to pipetting Triton X-100.
7. 96-well cell culture plate (Nunc, Rochester, NY, USA).

2.3 Cytokine/ Chemokine Expression by qPCR

1. RNeasy Mini Kit (Qiagen).
2. RNase-free water (UltraPure grade).
3. QIAshredders (Qiagen).
4. QuantiTect reverse transcription kit containing genomic DNA elimination reagent (Qiagen).
5. SYBR green primer-probe sets including TNF- α , IL-8, etc. (Qiagen).
6. QuantiTect SYBR green PCR mastermix (containing HotStarTaq DNA polymerase) (Qiagen).

2.4 Multiplex Cytokine Bead Array (Flow Cytometry)

1. BD Cytometric Bead Array Mouse Th1/Th2/Th17 Cytokine Kit (BD Biosciences, San Jose, CA) or appropriate array kit for human samples.
2. 24- or 48-well cell culture plate (Costar).
3. BMMC medium without IL-3 [6].
4. Human mast cell culture medium [7].
5. A flow cytometer capable of detecting and distinguishing fluorescence emission at 576 and 670 nm and BD CellQuest™ or BD CellQuest Pro software.
6. 15 mL conical polypropylene tubes.
7. BD Falcon™ 12 \times 75 mm sample acquisition tubes or equivalent.
8. BD Calibrite™ 3 beads.
9. BD Calibrite APC beads.
10. FCAP Array software.

2.5 Cytokine Secretion Assay by ELISA

1. Cytokine assay kit (e.g., R&D Systems).
2. 24- or 48-well cell culture plate (Costar).
3. BMMC medium without IL-3 [6].
4. Human mast cell culture medium [7].

2.6 Eicosanoid Generation Assay

1. HEPES buffer + 0.04 % BSA (same as for β -hexosaminidase assay).
2. LTC₄ enzyme immunoassay (Cayman Chemicals).
3. PGD₂ MOX enzyme immunoassay (Cayman Chemicals).

3 Methods

3.1 IgE Sensitization

Mast cell stimulation can be Fc ϵ RI dependent and Fc ϵ RI independent. Fc ϵ RI-dependent stimulation might require IgE sensitization prior to stimulation as follows:

1. Prepare mature human or rodent mast cells (see Note 1). Propagate a sufficient number of mast cells (HuMCs or mouse BMMCs) needed for the specific analysis (see Note 2) and resuspend in cell culture medium at a concentration between 2×10^5 and 1×10^6 cells/mL (see Note 3).
2. Add human or mouse IgE (see Note 4) to a final concentration of 100 ng/mL.
3. Sensitize cells with IgE for a minimum of 1 h up to 18 h as desired.
4. Remove the cell culture medium by centrifugation ($300 \times g$, 10 min, RT).
5. Wash cells to remove free IgE by resuspending in culture medium or appropriate buffer, and centrifuge $300 \times g$ for 10 min and repeat once more.
6. The cells are now ready for Fc ϵ RI-mediated stimulation—resuspend at the desired concentration in the appropriate buffer or medium (see following sections) where different approaches can be used: anti-IgE antibodies; IgE-specific Ag; or in the case of biotinylated IgE, streptavidin). Mast cells can also be stimulated directly through Fc ϵ RI using an anti-Fc ϵ RI α antibody. See Note 5 for examples of non-Fc ϵ RI-mediated stimulation.

3.2 Monitoring Degranulation by Measuring β -Hexosaminidase Release (See Note 6)

All procedures are conducted at room temperature (RT) unless otherwise specified.

1. Use human mast cells at a concentration of 0.5 to 1×10^4 cells per well in a 96-well reaction plate (U-bottom). BMMCs are used at a concentration of 3 to 5×10^4 cells per well. For IgE sensitization and cytokine starvation, see Subheading 3.1 and Notes 2 and 3.

2. Pre-warm freshly prepared HEPES degranulation buffer with 0.04 % BSA to 37 °C.
3. To remove excess IgE, wash sensitized cells three times by adding HEPES degranulation buffer with 0.04 % BSA (up to 10×10^6 cells in 10 mL buffer), then centrifuge at $300 \times g$ for 10 min, and repeat twice, as described in Subheading 3.1.
4. Resuspend cells so that 90 μ L contains the final cell number needed for each well (total final volume is 100 μ L). Aliquot cells into a U-bottomed 96-well plate (reaction plate). Place the plate at 37 °C (non-gassed hot air oven or equivalent) for 10 min.
5. Prepare stimulants in HEPES + 0.04 % BSA: Make dilutions at $10 \times$ final concentration. Add 10 μ L buffer (vehicle control) or stimulant and incubate for 30 min at 37 °C.
6. Meanwhile, prepare 3.5 mg pNAG/mL citrate buffer solution. Remember to make sufficient pNAG solution for both supernatants and cell lysates. Aliquot 100 μ L per well in a flat bottom 96-well plate. Make one plate for supernatant and one for lysate.
7. After incubation, spin plate for 5 min, $300 \times g$ at 4 °C, to terminate the reaction and sediment the cells.
8. Remove 50 μ L supernatant and add to supernatant-pNAG plate (“supernatant”) and incubate for 90 min at 37 °C.
9. Lyse the remaining cells in the reaction plate by adding 150 μ L 0.1 % Triton X-100—use a multichannel pipette and pipette up and down 5 times, and change tips for each row. Leave plate at 37 °C for 10 min and transfer 50 μ L of lysis solution to lysate-pNAG plate (“lysate”) and incubate for 90 min at 37 °C.
10. Stop reaction in both the supernatant and lysate plates by adding 100 μ L of a 400 mM glycine solution (a yellow color indicates presence of β -hexosaminidase) and read absorbance using a plate reader at $\lambda = 405$ nm with reference filter $\lambda = 620$ nm.
11. To calculate β -hexosaminidase release (degranulation), determine the relative amount of β -hexosaminidase in the supernatant as a percentage of the total β -hexosaminidase in the cells prior to stimulation as follows:

$$\beta\text{-Hexosaminidase release (\%)} = [\beta\text{-hexosaminidase released}] / [\text{total } \beta\text{-hexosaminidase present in supernatant and cell contents}] = 2 \times (\Delta\text{supernatant}_{(A405 \text{ nm})}) / (\Delta\text{supernatant}_{(A405 \text{ nm})} + (4 \times \Delta\text{cell lysate}_{(A405 \text{ nm})})) \times 100 \text{ \%}.$$

See Note 7 for equation explanation.

Typical examples of degranulation values and kinetics of release are shown in Fig. 1.

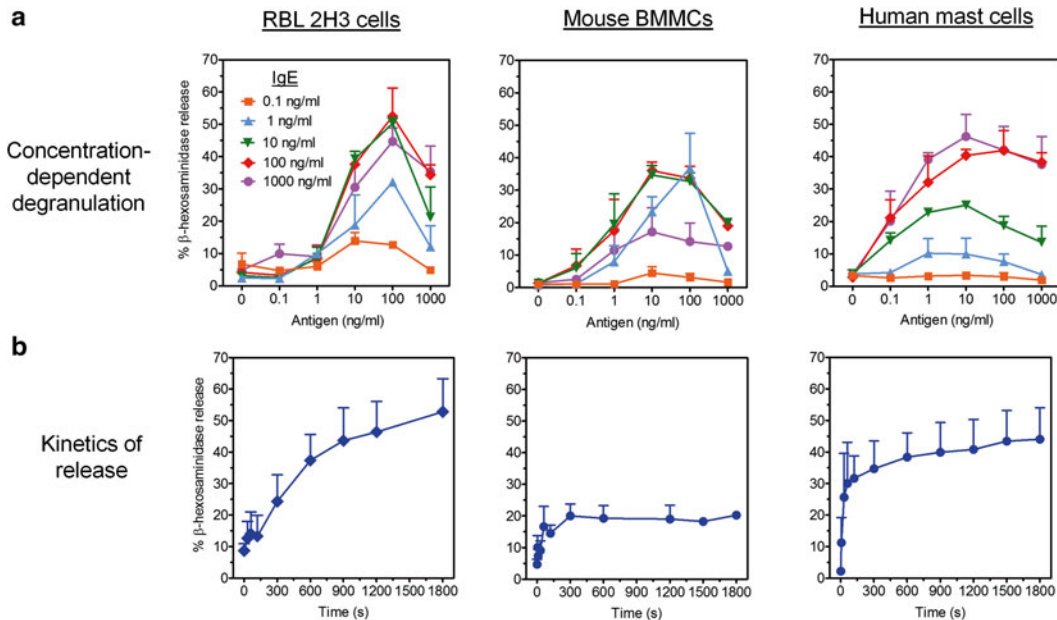


Fig. 1 Typical titration curves and degranulation kinetic of mast cells stimulated with IgE plus antigen. (a) Titration curves obtained for IgE and antigen in RBL 2H3 cells, mouse BMMCs, and HuMCs. Cells were sensitized overnight in the indicated concentrations of IgE and then challenged for 30 min with the indicated concentrations of antigen. (b) Kinetics of degranulation of IgE (100 ng/mL)-sensitized RBL 2H3 cells, mouse BMMCs, and HuMCs in response to an optimal concentration of antigen (100 ng/mL). Results are means \pm SE of 2–4 experiments

3.3 Measuring Cytokine and Chemokine Gene Expression by Quantitative PCR

Isolation of Total RNA from Mast Cells Using RNeasy Mini Kit

Typically, mast cells are stimulated for 2–24 h prior to processing of samples for gene expression analysis.

The use of the commercially available RNeasy Mini Kit (Qiagen) for isolating RNA from mast cells typically yields 8–16 μ g per 10^6 cells for HuMCs and 8–14 μ g per 10^6 cells for BMMCs and produces RNA of excellent quality for quantitative PCR (qPCR) and SuperArrays (see Note 8). A brief description of the protocol is described below (refer to manufacturer's instructions for more detail).

1. After the desired stimulation, transfer mast cells to conical tubes (15 mL) and centrifuge at $300 \times g$ for 10 min. Remove supernatant, resuspend cell pellet by flicking the tube, and then lyse cells by adding RLT lysis buffer (350 μ L).
2. Further lyse cells by pipetting up and down 5 times prior to transferring directly onto a QIAshredder spin column in a 2 mL collection tube. Centrifuge at $8,000 \times g$ for 2 min.

3. Add 70 % ethanol (350 μ L) to the cell homogenate. Mix well by pipetting prior to transferring to an RNeasy spin column placed in a 2 mL collection tube. Centrifuge at $8,000 \times g$ for 30 s. Ethanol is added to the cell homogenate to allow optimum binding of RNA to the silica membrane within the spin column.
4. Remove the supernatant and wash the silica membrane by adding RW1 buffer (700 μ L) to the spin column and centrifuge at $8,000 \times g$ for 30 s.
5. Remove the supernatant and add RPE buffer (500 μ L) to the spin column and centrifuge at $8,000 \times g$ for 2 min.
6. Transfer the spin column to a 1.5 mL microtube and add 40 μ L of RNase- and DNase-free water and centrifuge at $8,000 \times g$ for 2 min.
7. Remove the spin column and retain the supernatant containing the eluted RNA in water. This can be stored at -80°C until required or used immediately for cDNA preparation.
8. Assess RNA yield ($[\text{RNA}] = \text{absorbance at } \lambda = 260 \text{ nm} (\text{OD}_{260\text{nm}}) \times 40 \text{ } \mu\text{g/mL}$ (1 $\text{OD}_{260\text{nm}}$ unit)) and purity ($\text{OD}_{260\text{nm}} / \text{OD}_{280\text{nm}}$ ratio) using a nanodrop spectrophotometer. A typical yield of RNA from 1 million BMMC or HuMC is 300 μ g/mL with an $\text{OD}_{260\text{nm}} / \text{OD}_{280\text{nm}}$ ratio of 1.8–2.0.

Preparation of cDNA for Quantitative PCR

1. Transfer 1 μ g of total cellular RNA from mast cells to a thin-walled microtube (0.2 mL) containing 2 μ L of genomic wipe-out buffer (7 \times) and make up to a volume of 14 μ L with RNase-free water.
2. Vortex the samples to ensure proper mixing of the reagents, centrifuge briefly to collect the liquid at the bottom of the microtube, and then heat samples at 42°C for 2 min using a thermocycler machine.
3. While samples are heating, prepare a stock of reverse transcription mastermix (1 \times) in a thin-walled microtube (200 μ L) by aliquoting reverse transcriptase (RT) enzyme (1 μ L/sample, contains Omniscript and Sensiscript RT with RNase inhibitor), RT buffer (4 μ L/sample, containing dNTPs), and RT primer mix (1 μ L/sample, containing oligo-dTs). Make enough RT mastermix stock to obtain 6 μ L per genomic DNA (gDNA)-free RNA sample.
4. Take the gDNA-free RNA sample (14 μ L), add 6 μ L of reverse transcription mastermix, vortex, and then centrifuge briefly to collect the liquid at the bottom of the microtube. Total volume of reaction is 20 μ L.
5. Transfer to a thermocycler and incubate at 42°C for 15 min and 95°C for 3 min, followed by 4°C for 10 min. The cDNA is now ready to be used in qPCR or can be stored at -20°C until required.

*Measuring
Gene Expression
by Quantitative PCR*

Gene expression by mast cells can be quantified using reagents from various companies. We routinely use Qiagen SYBR green real-time PCR reagents for individual primer/probe sets and SuperArray for determining numerous cytokine genes expressed at once.

1. Prepare individual PCR reaction mix stock solutions for each primer/probe set of interest by adding QuantiTect SYBR green PCR mastermix (12.5 μ L, containing the HotStarTaq DNA polymerase enzyme, SYBR green buffer, and SYBR I and ROX reference dyes) with the appropriate QuantiTect primer/probe sets of genes of interest (2.5 μ L) or housekeeping gene (12.5 μ L), and aliquot 15 μ L per well in triplicate to thin-walled PCR microtubes (200 μ L).
2. Dilute mast cell cDNA (1 μ g in 20 μ L) 1 in 10 with RNase-free water (180 μ L) to give a total volume of 200 μ L and final concentration of 50 ng/10 μ L.
3. Take 10 μ L aliquots (100 ng per reaction) of cDNA and add to PCR microtubes containing the PCR reaction mix to give a total volume of 25 μ L. Unused cDNA can be stored at -20 °C.
4. As a control, each RNA sample, which had not been reverse transcribed to cDNA, is used in a PCR reaction to determine whether nonspecific amplification of contaminating DNA in RNA samples is present.
5. Seal the microtubes and transfer to a real-time PCR cycler machine (ABI PRISM 7700, Applied Biosystems) and perform the following reaction:
95 °C for 15 min (PCR activation step), followed by 40 cycles of:
 - (a) 95 °C for 15 s (denaturation step).
 - (b) 5 °C for 30 s (annealing step).
 - (c) 72 °C for 34 s (extension, data collection period).
6. After each PCR reaction, perform a dissociation curve on each sample to determine that each PCR product has a single peak relating to the SYBR green fluorescence. Products that have a double peak should be discounted.

Gene expression is analyzed using the RT-PCR cycler ABI PRISM 7700. The relative fold expression of genes of interest is calculated as follows: for each sample, the threshold cycle (C_t) is determined and normalized to the housekeeping gene (β -actin or GAPDH) (ΔC_t). For differences in gene expression between samples, the ΔC_t of treated cells is subtracted from untreated control cells ($\Delta \Delta C_t$), and the relative fold expression is calculated using the formula $2^{\Delta \Delta C_t}$. Complementary DNA stocks are taken from three different batches of BMMC or HuMC to determine relative quantities across multiple runs.

3.4 Measuring Cytokine Generation by Multiplex

One advantage of using multiplex cytometric bead arrays to measure cytokine release is the use of fewer samples as compared to the conventional ELISA method. In addition, multiple cytokine proteins in one research sample can be detected simultaneously. From **step 6**, this protocol is according to the manufacturer's instructions for measuring mouse cytokines (BD Cytometric Bead Array Cytokine Kit) with some minor adjustments. All procedures are conducted at room temperature, and the incubations are performed in a humidified 37 °C, 5 % CO₂ incubator.

1. Sensitize BMMCs in cytokine-free medium with mouse anti-DNP IgE as described in Subheading 3.1. If HuMCs are used, sensitize overnight with 100 ng/mL human biotinylated IgE in complete HuMC medium (*see Note 9*).
2. The next day, wash the cells three times with 5–10 mL pre-warmed (37 °C) BMMC or HuMC medium, respectively, to remove excess of IgE as described in Subheading 3.1.
3. Resuspend BMMCs in cytokine-free medium at a concentration of 0.5 to 1 × 10⁶ cells/mL. Place the plate at 37 °C for 10 min. HuMCs are resuspended in complete medium, and aliquot cells into 24- or 48-well plates (culture plate) at a concentration of 1 × 10⁶ cells/mL (in a volume of 450 µL for 48-well plates and 900 µL for 24-well plates).
4. Prepare stimulant in cytokine-free BMMC medium or HuMC medium: Make stock solutions of stimulants at 10× final concentration. Add 50 µL (for 48-well plate) or 100 µL (for 24-well plate) buffer or stimulant and incubate for 4–8 h at 37 °C (*see Note 10*).
5. After incubation, transfer the cells into 1.5 mL microcentrifuge tubes and centrifuge for 5 min at 1,000 ×*g*, 4 °C. Collect the cell-free supernatants. Samples can either be used directly or stored at –80 °C until assayed.
6. BD Cytometric Bead Array is used to measure multiple cytokines. Prepare cytokine standards (20–5,000 pg/mL) according to the manufacturer's instructions.
7. Mix the cytokine-capture beads according to the manufacturer's instructions, and add 10 µL of each bead suspension, for each tube to be analyzed, into a 15 mL Falcon tube marked "mixed capture beads." Vortex the mixture beads carefully.
8. Thaw and dilute your samples if necessary by using the appropriate volume of assay diluent and mix carefully.
9. Add 50 µL mixed capture beads to all assay tubes.
10. Add 50 µL of the cytokine standard dilutions to the tubes marked "standard" according to the manufacturer's instructions.
11. Add 50 µL of your unknown sample to the labeled "sample" tubes.

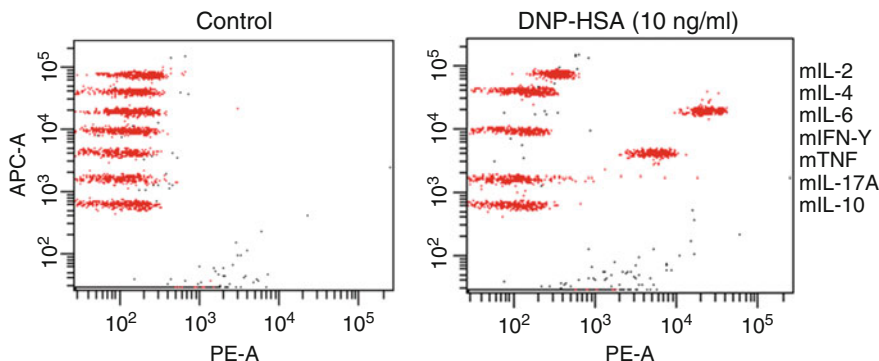


Fig. 2 Typical sample data from BMMCs obtained by BD Cytometric Bead Array Cytokine Kit for mouse Th1/Th2 cytokine profile. Cells were sensitized overnight with IgE-DNP (100 ng/mL) and then stimulated for DNP-HSA (10 ng/mL) for 6 h (control is unstimulated BMMCs). Samples were acquired using BD CellQuest software

12. Add 50 μ L of the detection reagent to all assay tubes, and incubate for 2 h at room temperature, in the dark. In the meantime, perform cytometer setup as described in the manufacturer's instructions for the cytometric bead array.
13. After 2 h incubation, add 1 mL of wash buffer to each assay tube and centrifuge at $200 \times g$ for 5 min.
14. Discard the supernatant from each assay tube and add 300 μ L wash buffer.
15. Acquire your samples on the flow cytometer according to manufacturer's instruction.

Data are acquired using BD CellQuest software on a BD FACSaria™ II cytometer. FCAP Array software is used to analyze the cytokine data. Typical sample data from BMMCs obtained by BD Cytometric Bead Array Cytokine Kit for mouse Th1/Th2 cytokine profile are seen in Fig. 2.

3.5 Measuring Cytokine Release by ELISA

All procedures are performed at room temperature and the incubations are performed in a humidified 37 °C, 5 % CO₂ incubator.

1. Prepare sufficient HuMCs or BMMCs to perform cytokine measurements at least in duplicate. HuMCs or BMMCs are sensitized overnight in appropriate medium as described in Subheading 3.1.
2. The next day, wash the cells three times with 5–10 mL pre-warmed (37 °C) HuMC medium or BMMC medium, respectively, to remove excess of IgE as described in the sensitization protocol (Subheading 3.1).
3. Resuspend HuMCs at the desired concentration for the appropriate assay in complete medium, and aliquot the cells into 24- or 48-well plates (culture plate) at a concentration of

1×10^6 cells/mL (in a volume of 450 μ L for 48-well plates and 900 μ L for 24-well plates). Resuspend BMMCs in cytokine-free medium at a concentration of 0.5 to 1×10^6 cells/mL. Place the plate at 37 °C for 10 min.

4. Prepare stimulant in HuMC medium or in cytokine-free BMMC medium. Make dilutions 10 \times final concentration. Add 50 μ L (for 48-well plates) or 100 μ L (for 24-well plates) buffer or stimulant, and incubate for 4–8 h at 37 °C (see Note 10).
5. After incubation, pipette the supernatant(s) into 1.5 mL microcentrifuge tubes, and centrifuge for 5 min at 1,000 \times g, 4 °C; then collect the cell-free supernatants. Store the supernatants at –80 °C until assayed.
6. Measure the cytokine or chemokine content using an appropriate kit according to the manufacturer's instructions (see Note 11).

3.6 Measuring Eicosanoid Generation

The protocol below describes the measurement of the release of prostaglandin D2 (PGD₂) and leukotriene C4 (LTC₄) from Ag-stimulated mast cells of human and mouse origin using commercially available kits (Cayman Chemicals). Generally, PGD₂ release is lower than LTC₄ release following Ag stimulation, and BMMCs release greater amounts of LTC₄ than do HuMCs. Therefore, cell numbers have to be adjusted accordingly. Since the assay is based on a competitive enzyme immunoassay, it is critical to determine the optimum cell number and activation period. Since there are further dilutions of supernatants after stimulation, it is feasible to use the same cell samples for analysis of both eicosanoids.

Preparing Sample Supernatants for Eicosanoid Measurement

Human or mouse mast cells are sensitized overnight in appropriate medium as described in Subheading 3.1.

1. Warm freshly prepared HEPES + 0.04 % BSA (assay buffer) to 37 °C.
2. Wash cells in pre-warmed HEPES + 0.04 % BSA (10 mL) by centrifugation at 300 \times g for 10 min. Remove supernatant carefully, resuspend cells in HEPES + 0.04 % BSA, and centrifuge again.
3. Repeat wash one more time (step 2).
4. Resuspend cells for PGD₂ and LTC₄ assays as follows. Prepare HuMCs or the LAD2 human mast cell line to a density of 2×10^3 cells per 80 μ L or BMMCs to a density of 1×10^5 cells per 80 μ L.
5. Aliquot cells (80 μ L per well) into a U-bottomed 96-well plate (reaction plate) and place at 37 °C for 10 min.

6. While cells are equilibrating to 37 °C, prepare stimulants in HEPES + 0.04 % BSA: Make working concentrations of stimulants at 5× final concentrations. Add 20 µL assay buffer or stimulant and incubate for 20 min at 37 °C.
7. After 20 min incubation, spin plate at 4 °C for 5 min, 300×*g*.
8. For PGD₂ assay, take supernatants (25 µL) and transfer to thin-walled tubes (200 µL) containing freshly prepared methoximating (MOX) reagent (25 µL), and derivatize samples at 60 °C for 30 min using a thermocycler machine (as per manufacturer's instructions). Also add freshly prepared MOX reagent to an aliquot of PGD₂ stock (25 µL, 40 ng/mL) to produce a PGD₂-MOX stock of 20 ng/mL. These MOX samples can either be used directly in the EIA or stored for up to 6 weeks at 4 °C.
9. For LTC₄ assay, take supernatants (30 µL) and place into 200 µL microcentrifuge tubes. These samples can either be used directly in the EIA or stored at -80 °C.

Measuring PGD₂ in Cell-Free Supernatants

This protocol is a brief summary of the manufacturer's instructions (Cayman Chemicals) with some minor adjustments for cell density relevant to mast cell activation. The reader is advised to refer to the manufacturer's instructions for a complete and detailed protocol.

1. For HuMC or LAD2 samples, add 10 µL of MOX-cell-free supernatants to EIA plate (pre-coated with mouse anti-rabbit IgG) containing 40 µL HEPES + 0.04 % BSA buffer. For BMMC samples, dilute MOX-cell-free supernatants 1 in 10 prior to adding 10 µL of cell-free supernatants to EIA plate containing 40 µL HEPES + 0.04 % BSA buffer.
2. Prepare PGD₂ standards (7.8–1,000 pg/mL) from the PGD₂-MOX stock of 20 ng/mL and add 50 µL per well in duplicate to EIA plate.
3. Add 50 µL per well of PGD₂-MOX AChE tracer.
4. Add 50 µL per well of PGD₂-MOX antiserum, seal plate with an adhesive plastic film, and incubate for 18 h at 4 °C.
5. The following day, wash the microplate 5× with EIA wash buffer (200 µL/well).
6. Add 200 µL of freshly prepared Ellman's reagent to each well, seal plate with adhesive plastic film, and incubate on orbital shaker in the dark at room temp for 60 min.
7. Read plate at a wavelength of 405–420 nm when absorbance of B₀ well is in the range 0.3–0.8 AU (after blank subtracted).

The amount of PGD₂ in each sample is then calculated from the standard curve.

Typical examples of PGD₂ release are shown in Fig. 3.

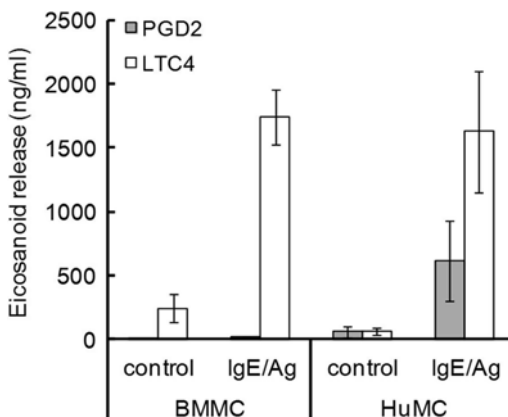


Fig. 3 Eicosanoid release by mouse and human mast cells following Fc ϵ RI-dependent activation. Mouse BMMCs or HuMCs were sensitized overnight with IgE-DNP (100 ng/mL) or biotinylated IgE (100 ng/mL), respectively, and then challenged for 20 min respectively with DNP-HSA (30 ng/mL) or streptavidin (100 ng/mL). Results are means \pm SE of 4 independent experiments performed in duplicate

Measuring LTC₄ in Cell-Free Supernatants

This protocol is a brief summary of the manufacturer's instructions (Cayman Chemicals) with some minor adjustments for cell density relevant to mast cell activation. The reader is advised to refer to the manufacturer's instructions for a complete and detailed protocol.

1. For HuMC or LAD2 samples, add 25 μ L of cell-free supernatants to EIA plate (pre-coated with mouse anti-rabbit IgG) containing 25 μ L HEPES + 0.04 % BSA buffer. For BMMC samples, dilute 1 in 100 (two serial dilutions of 1 in 10) prior to adding 50 μ L of cell-free supernatants to EIA plate.
2. Prepare LTC₄ standards (7.8–1,000 pg/mL) from the LTC₄ stock of 20 ng/mL and add 50 μ L per well in duplicate to EIA plate.
3. Add 50 μ L per well of LTC₄-AChE tracer.
4. Add 50 μ L per well of LTC₄ antiserum, seal plate with an adhesive plastic film, and incubate for 18 h at RT.
5. The next day, remove liquid from wells and wash 5 \times with EIA wash buffer (200 μ L/well).
6. Add 200 μ L of freshly prepared Ellman's reagent to each well, seal plate with plastic film, and incubate on orbital shaker in the dark at room temperature for 60 min.
7. Read plate at 405–420 nm when absorbance of B₀ well is in the range 0.3–0.8 AU (blank subtracted).

The amount of LTC₄ in each sample is then calculated from the standard curve. Typical examples of LTC₄ release are shown in Fig. 3.

4 Notes

1. For the examples provided in this chapter, we prepared primary HuMCs from CD34⁺ peripheral blood progenitors [7] isolated from healthy volunteers after informed consent under a protocol (NCT00001756) approved by the NIH Institutional Review Board. BMMCs were prepared from mouse bone marrow [6] under a protocol approved by the NIAID Animal Care and Use Committee.
2. Recommended cell concentrations (Table 1) and stimulation times (Table 2) for different mast cell assays.
3. For some experiments, cytokines normally present in the mast cell maintenance/growth culture medium should be omitted (e.g., SCF/IL-3, if the effect of SCF/IL-3 stimulation is investigated). Cytokine starvation should not exceed 24 h.
4. When thawing an aliquot of IgE, the suspension should be centrifuged at high speed (>16,000 $\times g$) for 60 min in order to

Table 1
Recommended cell concentrations for specific mast cell assays

Cell concentrations necessary for specific assays		
	Human (cell/sample)	Mouse (cell/sample)
Degranulation	5,000–10,000	30,000–50,000
Cytokine release	500,000	500,000
Eicosanoids: LTC ₄	1,000	10,000
PGD ₂	2,000	100,000
mRNA	1,000,000 50–100 ng/reaction	1,000,000 50–100 ng/reaction

Table 2
Stimulation time for specific mast cell assays

Stimulation time for specific assays (see also Note 10)		
	Human	Mouse
Degranulation	30–60 min	30–60 min
Cytokine release	4–24 h	4–24 h
Eicosanoids	20 min	20 min
mRNA	2–24 h	2–24 h

remove aggregated IgE. Aggregated IgE may activate the cell during sensitization.

5. The following are some examples of traditional stimulants and working concentrations used for mast cell stimulation: compound 48/80 (0.05–5 mg/mL), substance P (1–10 μ M), complement 5a (0.1–1 μ g/mL), and LPS (100 ng/mL). Stimulation time depends on which mediators are being examined.
6. Besides β -hexosaminidase release, degranulation can also be monitored by histamine (fluorometric assay from RefLab ApS or EIA from Immunotech) and tryptase release (Phadia).
7. Equation explanation for β -hexosaminidase release: Δ supernatant (OD_{405nm}): absorbance reading of supernatant (OD_{405nm})—absorbance reading of buffer only (i.e., blank (OD_{405nm})). Δ cell lysate (OD_{405nm}): absorbance reading of cell lysate (includes product from $\frac{1}{2}$ of supernatant)—absorbance reading of buffer only (i.e., blank (OD_{405nm})). Value “2” in the nominator: correction factor applied since only $\frac{1}{2}$ of the supernatant volume is sampled (with the other $\frac{1}{2}$ remaining with the cell lysate). Value of “4” in the denominator: correction factor since only $\frac{1}{4}$ of cell lysate is sampled. This cell lysate contains the intracellular contents plus $\frac{1}{2}$ of the supernatant. Note that only 1 \times (Δ supernatant) appears in the denominator since the “ Δ cell lysate” value includes the equivalent of 1 \times (Δ supernatant).
8. RNA extraction from mast cells can be performed by the TRIzol® method or use of an appropriate lysis buffer. For real-time PCR, we found the use of the Qiagen RNeasy kits provided the best quality RNA (OD_{260nm}/OD_{280nm} ratios of 1.95–2.07) with Ct values for housekeeping genes lower than with TRIzol extraction.
9. In HuMCs, antigen or SCF alone fails to generate sufficient cytokine release. Thus, in order to generate sufficient cytokine release, it is recommended to stimulate HuMCs with both antigen and SCF.
10. The stimulation time for cytokine secretion (and also mRNA synthesis or stability) is dependent on the specific cytokines investigated.
11. The amount of cytokine or chemokine release can vary depending on cell condition; thus, if the samples absorbance (OD) is above the standard range, the sample needs to be diluted.

Acknowledgments

Financial support for work in the authors' laboratories was provided by the Division of Intramural Research of NIAID within the National Institutes of Health (AMG), VBG-GROUP Centre for Asthma and Allergy Research, Herman Krefting Foundation Against Asthma and Allergy (MR), Wellcome Trust Value in People Award, and Faculty of Medicine, University of Southampton (EJS).

References

1. Metcalf DD (2008) Mast cells and mastocytosis. *Blood* 112(4):946–956
2. Metcalf DD, Baram D, Mekori YA (1997) Mast cells. *Physiol Rev* 77(4):1033–1079
3. Kraft S, Kinet JP (2007) New developments in Fc ϵ RI regulation, function and inhibition. *Nat Rev Immunol* 7(5):365–378
4. Gilfillan AM, Tkaczyk C (2006) Integrated signalling pathways for mast-cell activation. *Nat Rev Immunol* 6(3):218–230
5. Kuehn HS, Radinger M, Gilfillan AM (2010) Measuring mast cell mediator release. *Curr Protoc Immunol* Chapter 7:Unit 7 38
6. Jensen BM, Swindle EJ, Iwaki S, Gilfillan AM (2006) Generation, isolation, and maintenance of rodent mast cells and mast cell lines. *Curr Protoc Immunol* Chapter 3: Unit 3 23
7. Radinger M, Jensen BM, Kuehn HS, Kirshenbaum A, Gilfillan AM (2010) Generation, isolation, and maintenance of human mast cells and mast cell lines derived from peripheral blood or cord blood. *Curr Protoc Immunol* Chapter 7: Unit 7 37

Chapter 20

Induction of Mast Cell Apoptosis by a Novel Secretory Granule-Mediated Pathway

Fabio R. Melo, Sara Wernersson, and Gunnar Pejler

Abstract

Mast cells (MCs) have detrimental functions in the context of numerous pathologies, and regimens aimed at neutralizing MCs or individual MC products can thus be of therapeutic value. One way to target MCs in disease is to selectively induce MC apoptosis, but there is so far no agent available that selectively induces apoptosis in MCs. Mast cells are heavily loaded with secretory granules containing large amounts of fully active proteases bound to serglycin proteoglycan. Damage to the secretory granules will thus lead to the release of serglycin-protease complexes into the cytosol. A potential consequence of this would be that the unleashed granular proteases cause apoptosis by proteolytic activation of proapoptotic compounds located in the cytosol. Indeed, we have recently found that MCs are highly sensitive to apoptosis induced by permeabilization of the secretory granules. In this chapter, we describe the methods used to study MC apoptosis induced by this novel, secretory granule-mediated pathway.

Key words Mast cells, Apoptosis, Proteases, Granules, Caspases

Abbreviations

AO	Acridine orange
CHAPS	3-[(3-Cholamidopropyl)dimethylammonio]-1-propanesulfonate hydrate
DMSO	Dimethyl sulfoxide
DTT	Dithiothreitol
EDTA	Ethylenediaminetetraacetic acid
EGTA	Ethylene glycol tetraacetic acid
FITC	Fluorescein isothiocyanate
HEPES	4-(2-Hydroxyethyl)-1-piperazineethanesulfonic acid
LDH	Lactate dehydrogenase
LLME	H-Leu-Leu-OMe·HBr
NAO	Acridine orange 10-nonyl bromide
PI	Propidium iodide
PIPES	Piperazine- <i>N,N'</i> -bis(2-ethanesulfonic acid)

R110	Rhodamine 110
SDS-PAGE	Sodium dodecyl sulfate polyacrylamide gel electrophoresis
Z-DEVD-FMK	Z-Asp(O-Me)-Glu(O-Me)-Val-Asp(O-Me) fluoromethyl ketone
Z-VAD-FMK	<i>N</i> -Benzylloxycarbonyl-Val-Ala-Asp(O-Me) fluoromethyl ketone

1 Introduction

Mast cells (MCs) are highly versatile cells, having a number of both harmful and beneficial functions in connection with pathological settings. For example, MCs are recognized as central players in the pathology of allergic disease including atopic asthma, and MCs also have crucial detrimental functions in the context of arthritis, diabetes, atherosclerosis, and aneurysm formation [1, 2]. On the other hand, MCs are also known to be beneficial, being essential in the body's defense toward a range of microbes [3].

Considering the harmful effect of MCs in connection with diseases, an attractive goal for therapy in many diseases would be to block functions mediated by MCs. One way to accomplish this is to use various MC stabilizers, i.e., agents that block MC degranulation, in this way preventing the release of the preformed mediators that are stored within the MC secretory granules [4, 5]. Another way to block MC-mediated pathology is to prevent the action of individual MC-secreted products, i.e., by using specific inhibitors.

A third way to counteract harmful effects of MCs is to eliminate MC altogether, by inducing MC apoptosis. Previous attempts to accomplish this have led to the identification of several agents that cause MC apoptosis [6]. Clearly, the use of such compounds may have the potential to dampen MC-mediated pathologies. However, it should be realized that none of the so far identified MC apoptosis-inducing agents are highly selective for MCs, and it can thus not be excluded that unwanted side effects due to toxicity in other cell types may be encountered.

A unique feature of MCs is their high content of secretory granules, packed with fully active neutral proteases (tryptases, chymases, carboxypeptidase A) bound to serglycin proteoglycan [7, 8]. Damage to the secretory granules, for example, by agents that cause permeabilization of the granule membrane, will thus lead to the leakage of active proteases into the cytosol. A potential consequence of this is that the granule proteases cause proteolytic activation of proapoptotic compounds that are located in the cytosol, i.e., leading to apoptosis (Fig. 1). We therefore hypothesized that MCs are prone to apoptosis induced by this regimen. Indeed, we have recently shown that MCs are highly sensitive to apoptosis induced by permeabilization of the secretory granules [9], and we showed that serglycin and serglycin-bound proteases contribute profoundly to this secretory granule-mediated pathway of apoptosis. In this chapter, we describe the methods that we use for induc-

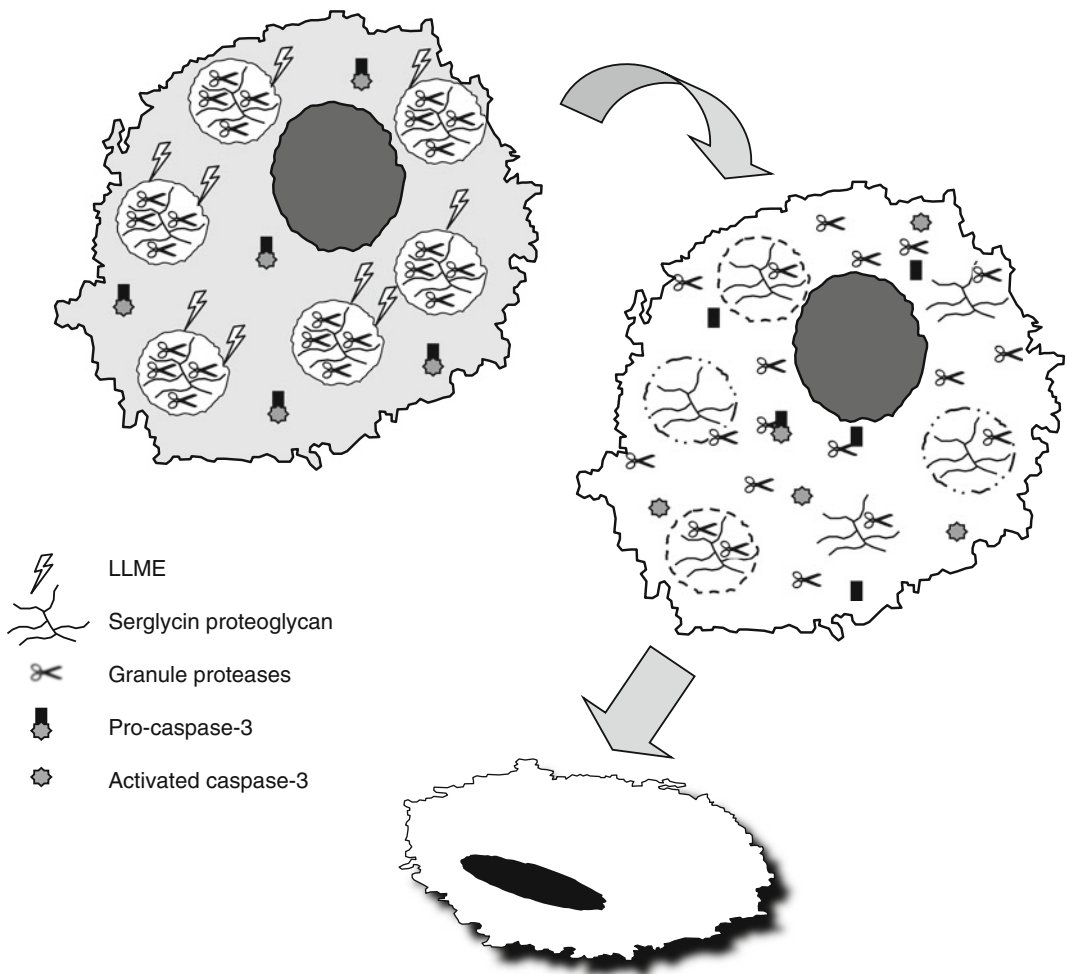


Fig. 1 Cartoon showing the presence of serglycin and serglycin-bound proteases in MC secretory granules. The figures depict how the release of proteases from the granules into the cytosol can induce apoptosis by activating cytosolic proapoptotic compounds, leading to caspase-3 activation and eventually to apoptosis

ing granule-mediated apoptosis in MCs and the methods that we use for monitoring apoptosis and granule damage.

2 Materials

2.1 Induction of Secretory Granule Permeabilization

1. LLME: H-Leu-Leu-OMe·HBr (l-leucyl-l-leucine methyl ester) (Bachem, Bubendorf, Switzerland).
2. Phosphate-buffered saline (PBS).
3. Dilute LLME in PBS to desired concentration (e.g., 0.1, 0.05, and 0.02 M) and keep stocks frozen until use.
4. Cultured mast cells (e.g., bone marrow-derived mast cells) prepared and cultured as described [10].

2.2 Measurement of Cell Viability

1. CellTiter-Blue® cell viability assay kit (Promega, Madison, WI).

2.3 Measurement of Apoptosis

1. FITC Annexin V Apoptosis Detection Kit (BD Pharmingen™, San Diego, CA).
 - (a) Binding buffer: 10 mM HEPES (pH 7.4), 0.14 M NaCl, 2.5 mM CaCl₂. Adjust pH to 7.4 with NaOH.
 - (b) Annexin V-FITC conjugate: 50 µg/mL Annexin V-FITC in 50 mM Tris-HCl (pH 7.4), 0.1 M NaCl.
 - (c) Propidium iodide (PI): 100 µg/mL in 10 mM PBS (pH 7.4).

2.4 Acridine Orange and Nonyl-Acridine Orange Staining

1. AO: Acridine orange hemi (zinc chloride) salt (Sigma-Aldrich, Steinheim, Germany) dissolved in distilled water (1 mg/mL).
2. NAO: Acridine orange 10-nonyl bromide (Sigma-Aldrich, Steinheim, Germany) dissolved in distilled water (1 mg/mL).
3. Prepare AO and NAO fresh and store in the dark at 4–8 °C until use.

2.5 Preparation of Cytosolic Extracts

1. Digitonin (Sigma-Aldrich, Steinheim, Germany).
2. Extraction buffer: 20 mM HEPES (pH 7.5), 250 mM sucrose, 10 mM KCl, 1.5 mM MgCl₂, 1 mM EDTA, 1 mM EGTA.
3. Bradford protein concentration assay (Bio-Rad, Hertfordshire, UK).

2.6 Measurement of Protease Activities in Cytosolic Extracts

Lactate Dehydrogenase (LDH) Activity

1. LDH reaction buffer: 10 mM Tris-HCl (pH 7.3), 10 mM sodium pyruvate, 0.5 mM β-NADH (β-nicotinamide adenine dinucleotide, reduced dipotassium salt).

Cysteine Cathepsin Activity

2. Cysteine cathepsin substrate: Z-Phe-Arg-AMC (Bachem, Bubendorf, Switzerland). Prepare 10 mM Z-Phe-Arg-AMC in DMSO (store at -20 °C).
3. Cathepsin reaction buffer: PBS (pH 6.0), 1 mM EDTA, 1 mM dithiothreitol (DTT).

2.7 Measurement of Caspase-3 Activation

1. EnzChek® caspase-3 assay kit #2 (Molecular probes, Eugene, OR).
2. Z-DEVD-R110 substrate.
3. Cell lysis buffer: 10 mM Tris-HCl (pH 7.5), 0.1 M NaCl, 1 mM EDTA, 0.01 % Triton X-100.
4. Reaction buffer: 10 mM PIPES (pH 7.4), 2 mM EDTA, 0.1 % CHAPS.
5. Dithiothreitol (DTT).
6. Ac-DEVD-CHO inhibitor.

7. Rhodamine 110 (R110) reference standard.

2.8 Western Blot Analysis of Proapoptotic Compounds

1. ClearPage™ SDS-PAGE gels (VWR International, West Chester, PA).
2. ClearPage SDS-PAGE running buffer (VWR International).
3. PageRuler™ Plus Prestained Protein Ladder (Fermentas International Inc, Ontario, Canada).
4. 5× SDS-PAGE sample buffer: 250 µL 20 % SDS, 600 µL glycerol, 100 µL 2-mercaptoethanol, 50 µL bromophenol blue.
5. Mini Trans-Blot Cell cassettes transfer system (Bio-Rad, Hertfordshire, UK).
6. Methanol.
7. Odyssey blocking buffer (LI-COR Biosciences, Lincoln, NE).
8. TWEEN®-20 (Merck, Darmstadt, Germany).
9. Primary antibody to protein of interest.
10. Blotting paper (VWR International).
11. Fluorescence optimized polyvinylidifluoride membrane (e.g., Immobilon PVDF-FL membranes (Millipore, Bedford, MA)).
12. Black Western incubation box (LI-COR).
13. Odyssey Infrared Imager (LI-COR).

2.9 Effect of Protease Inhibitors on Apoptosis

Protease Inhibitors

1. Caspase-3, caspase-6, caspase-7, caspase-8 and caspase-10 inhibitors: Z-DEVD-FMK (Z-Asp(O-Me)-Glu(O-Me)-Val-Asp (O-Me) fluoromethyl ketone. Prepare 5 mM stock solutions in DMSO. Store frozen at -20 °C.
2. Caspase-1 and caspase-3 inhibitors: Z-VAD-FMK (N-Benzyl-oxy carbonyl-Val-Ala-Asp(O-Me) fluoromethyl ketone). Prepare 5 mM stock solutions in DMSO. Store frozen at -20 °C.
3. Cysteine cathepsin inhibitor: E-64d. Prepare 5 mM stock solution in DMSO. Store frozen at -20 °C.
4. Serine protease inhibitor: Pefabloc® SC. Prepare a 20 mM stock solution in dH₂O. Store frozen at -20 °C.
5. Aspartic acid protease inhibitor: Pepstatin A. Prepare a 10 mM stock solution in dH₂O. Store frozen at -20 °C.
6. All of the above inhibitors can be purchased from Sigma-Aldrich or other commercial suppliers.

3 Methods

3.1 Induction of Secretory Granule Permeabilization

H-Leu-Leu-OMe·HBr (LLME) is a detergent used to permeabilize lysosomes and other acidic compartments (see Note 1). LLME is taken up through receptor-mediated endocytosis and becomes protonated

within acidic compartments where it accumulates and polymerizes, increasing the pH and causing membrane permeabilization [11].

1. Resuspend mast cells to 0.5×10^6 cells/mL in appropriate cell culture medium (containing 10 % FCS) and transfer 1 mL/well (triplicates) to a 24-well plate.
2. Add 5 μ L/well of each LLME stock (0.02, 0.05, and 0.1 M) to achieve final LLME concentrations of 100, 250, and 500 μ M, respectively (see Note 2).
3. Mix each individual sample by pipetting up and down three times.
4. Incubate at 37 °C in 5 % CO₂ for 24 h.
5. A negative control should be prepared by incubating cells in the absence of apoptosis-inducing agents.

3.2 Measurement of Cell Viability

The CellTiter-Blue® cell viability assay (Promega) is a fluorometric method based on the metabolic capacity of cells. Viable cells retain the ability to reduce resazurin into resorufin, which is highly fluorescent. Nonviable cells rapidly lose their metabolic capacity, do not reduce the indicator dye, and thus do not generate a fluorescent signal.

1. Transfer 100 μ L/well of mast cell suspensions in appropriate cell culture medium (triplicates) (concentration $\geq 5 \times 10^5$ cells/mL) to a 96-well plate.
2. Add 20 μ L/well CellTiter-Blue® reagent.
3. Shake for 10 s.
4. Incubate at 37 °C in 5 % CO₂ for 1–4 h (see Note 3).
5. Shake plate for 10 s and record fluorescence (excitation (Ex) $\lambda = 560$ nm, emission (Em) $\lambda = 590$ nm) using a fluorescence microplate reader (e.g., Infinite M200—TECAN, Männedorf, Switzerland).
6. Recommended controls:
 - (a) Control without cells. Set up triplicate wells using only medium as a negative control to determine background fluorescence.
 - (b) Untreated cells.

3.3 Measurement of Apoptosis

Annexin V is a Ca²⁺-dependent phospholipid-binding protein that has a high affinity for phosphatidylserine (PS), a membrane phospholipid translocated from the inner to the outer leaflet of the plasma membrane during apoptosis. Annexin V conjugated with the fluorochrome FITC retains its high affinity for PS and thus serves as a sensitive probe useful for flow cytometric analysis. Propidium iodide (PI) is a fluorescent molecule that binds to DNA. Viable cells with intact membranes exclude PI, but when the cell membrane has been damaged and thereby permeabilized, PI will enter the cell and the nucleus and will bind to DNA. Therefore, viable cells are Annexin V and PI negative; cells in early apoptosis are Annexin V positive and PI negative; and cells that are in

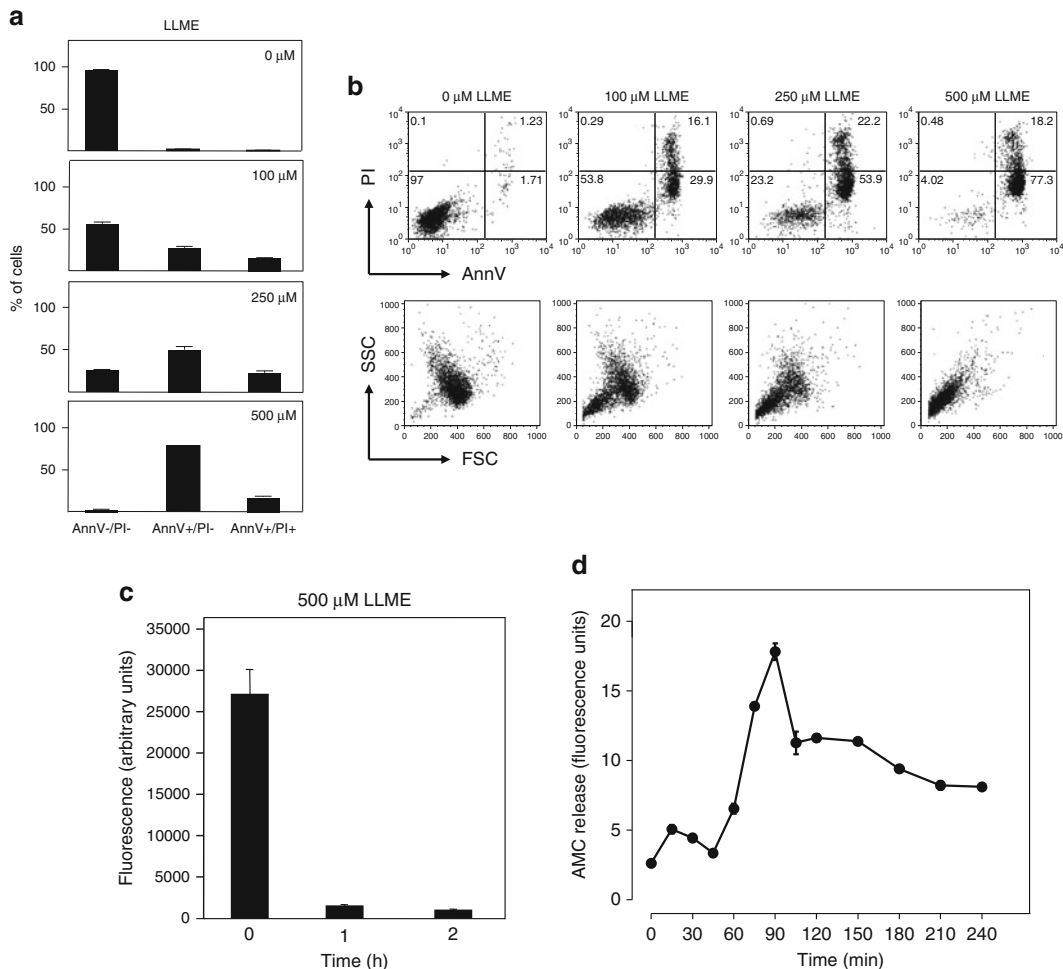


Fig. 2 (a) Gradual decrease in viable cells (AnnV⁻/PI⁻) after exposure of MCs to increasing concentrations of LLME, accompanied by the appearance of apoptotic (AnnV⁺/PI⁻) and late stage apoptotic/necrotic (AnnV⁺/PI⁺) cells. *AnnV* Annexin V, *PI* propidium iodide. (b) Dot plots showing the gates used for identification of apoptotic and late stage apoptotic/necrotic MCs (*upper panels*). The *lower panels* depict the reduction in size as judged by forward scatter (FSC) of MCs after exposure to LLME, characteristic of apoptotic cell death. (c) Dramatic decrease in acridine orange staining of MCs after treatment with LLME. The reduction in acridine orange staining indicates lysosomal/secretory granule damage. (d) Cysteine cathepsin activity present in cytosolic extracts at various time points after addition of LLME. Note the rapid appearance of activity at early time points after LLME addition. The data displayed in this figure were originally published in *The Journal of Biological Chemistry*. Melo et al. A role for serglycin proteoglycan in mast cell apoptosis induced by a secretory granule-mediated pathway. *J Biol Chem*. 2011; 286: 5423–5433. © the American Society for Biochemistry and Molecular Biology

late stage apoptosis or necrotic are Annexin V and PI double positive (*see Fig. 2a, b*).

1. Transfer 500 μ L of cells (5×10^5 MCs/mL) to a 5 mL FACS tube.
2. Wash the cells twice with cold PBS (centrifugation at $300 \times g$, 8 min), and resuspend cells in 500 μ L of Annexin V binding buffer.

3. Add 2.5 μ L of Annexin V-FITC staining solution and 5.0 μ L of PI solution per tube.
4. Vortex cells and incubate for 10 min at room temperature (RT) (22–25 °C) in the dark (see Note 4).
5. Analyze by flow cytometry within 1 h (FACScan®, Becton Dickinson, San Jose, CA).

3.4 Acridine Orange and Nonyl-Acridine Orange Staining

Acridine orange (AO) is a dye frequently used to label acidic compartments such as secretory granules and lysosomes. AO has a distinct red fluorescence, and secretory granules should therefore appear red. On the other hand, nonyl-acridine orange (NAO) is a metachromatic dye useful as a mitochondrial probe in living cells. NAO binds to cardiolipin, which is a phospholipid present specifically on the mitochondrial membrane [12]. Damage to lysosomes will lead to decreased AO staining (see Fig. 2c), and damage to the mitochondria will result in decreased NAO staining.

1. Add 5 μ L of AO or NAO stock solution to 1 mL mast cell suspension (5×10^5 cells/mL) in appropriate cell culture medium (triplicates) to a 24-well plate.
2. Mix each individual sample by pipetting up and down three times.
3. Incubate at 37 °C in 5 % CO₂ for 30 min.
4. Wash the cells three times with PBS (centrifuge at 300 $\times g$, 8 min) and resuspend cells in 1 mL of PBS (see Note 5).
5. Transfer 100 μ L/well samples to a 96-well plate.
6. Record fluorescence: AO (Ex λ 488 nm/Em λ 650 nm) and NAO (Ex λ 485 nm/Em λ 538 nm).
7. A negative control should be prepared by incubating cells in the absence of apoptosis-inducing agent.

3.5 Preparation of Cytosolic Extracts

Optimizing the Concentration of Digitonin

Digitonin extraction is the easiest method to measure the release of secretory granule proteases into the cytosol during apoptosis induced by secretory granule permeabilization (see Fig. 2d). Digitonin is a glycoside, which effectively solubilizes lipids, and can serve as an efficient detergent for permeabilization of cell membranes. By titrating the digitonin concentration carefully, cell membrane permeabilization can be achieved without compromising the integrity of lysosomes/granules.

There is usually a narrow window of digitonin concentration that causes cell membrane permeabilization without significantly affecting the integrity of the lysosomes. Therefore, perform serial dilutions of digitonin as recommended below to identify the lowest digitonin concentration that causes cell membrane permeabilization (as measured by LDH release).

1. Culture mast cells in appropriate medium and use 10^6 cells (in 1 mL) for each digitonin concentration.
2. Prepare serial dilutions of digitonin (1–200 $\mu\text{g}/\text{mL}$) in digitonin extraction buffer. Centrifuge cells ($300 \times g$, 8 min) in 1.5 mL microfuge tubes, remove supernatant, and add 300 μL of ice-cold digitonin dilutions to the cell pellets (on ice).
3. Vortex tubes for 5 s and then keep them on ice for 10 min with continuous shaking.
4. Centrifuge tubes ($9,300 \times g$ in microfuge, 4 °C, 3 min) and remove the supernatant quickly.
5. Measure LDH activity, cathepsin activity (see Subheading 3.6), and protein concentration using Bradford or a similar assay.

3.6 Measurement of Protease Activities in Cytosolic Extracts

The presence of LDH activity in the digitonin extracts is used as a marker of cell membrane permeability, whereas cysteine cathepsin activity is used as a marker of lysosomal leakage. The appropriate digitonin concentration to be used for preparation of cytosolic extracts is the lowest digitonin concentration where LDH activity shows an increase, where the cysteine cathepsin activity remains low, and where the protein extraction (Bradford) is nearly complete.

LDH Activity

1. Add 100 μL /well of LDH reaction buffer to a 96-well plate (triplicates). Add 50 μL /well μL supernatant collected from Subheading 3.5, step 5.
2. NADH oxidation is measured for 20 min at 37 °C using a microplate reader (Sunrise—TECAN); NADH oxidation leads to decreased absorbance at 340 nm.

Cysteine Cathepsin Activity

1. Prior to use thaw an aliquot and dilute the 10 mM Z-Phe-Arg-AMC substrate solution (prepared in DMSO) to 400 μM (1:25, v/v) and then serially dilute to 200 μM (1:1, v/v) with reaction buffer to achieve working substrate solution.
2. Transfer samples (corresponding to 50–100 μg of protein) from the cytosolic extracts to individual wells of a 96-well plate and add dH₂O to bring final volume per well to 40 μL .
3. Add 50 μL of reaction buffer and incubate for 15 min at 37 °C.
4. Add 10 μL of the working substrate solution to achieve 20 μM final concentration.
5. Measure AMC-release (Ex λ 380 nm/Em λ 460 nm) at 37 °C using a fluorescence microplate reader (Infinite M200—TECAN).

3.7 Measurement of Caspase-3 Activation

The EnzChek® caspase-3 assay kit #2 can be used to continuously monitor the activity of caspase-3 and closely related proteases (e.g., caspase-7) in cell extracts and purified enzyme preparations using a fluorescence microplate reader (Infinite M200—TECAN).

1. Prepare stock solutions according to the specifications from the manufacturer.
2. Induce apoptosis in cells using the desired method. Use 10^6 cells per sample.
3. Harvest the cells by centrifugation ($300 \times g$, 8 min). Cell pellets can be stored frozen at -80°C for analyses at a later time.
4. Resuspend each cell sample in 50 μL of cell lysis buffer.
5. Vortex quickly and incubate on ice for 30 min.
6. Centrifuge the lysed cells ($2,300 \times g$, 5 min, 4°C).
7. Transfer 30 μL of the supernatant from each sample to individual wells of a 96-well plate, and add cell lysis buffer to 50 μL . Use 50 μL of cell lysis buffer as a negative control. As a control (extra plate) for specificity of the assay, add 1 μL of caspase inhibitor (1 mM Ac-DEVD-CHO) to selected samples. Cover and incubate at RT for 10 min.
8. An extra negative control should be prepared by incubating cells in the absence of apoptosis-inducing agent.
9. Add 50 μL of the 2 \times substrate working solution to each sample and control.
10. The assay is continuous and fluorescence measurements ($\text{Ex}\lambda 496 \text{ nm}/\text{Em}\lambda 520 \text{ nm}$) can be made at multiple time points.

3.8 Western Blot Analysis of Proapoptotic Compounds

1. Induce apoptosis in cells using the desired method. Use 1.5×10^6 cells per sample (see Note 6).
2. Harvest the cells by centrifugation ($300 \times g$, 8 min) and wash once in PBS. Cell pellets can be stored frozen at -80°C for analyses at a later time.
3. Add 10 μL 5 \times SDS-PAGE sample buffer and 40 μL dH₂O to each cell pellet. Boil for 5 min in a heating block (100°C).
4. Sonicate samples for 10 min to decrease viscosity (see Note 7).
5. Set up a ClearPageTM SDS-PAGE gel (percentage depending on the size of the protein to be detected), and fill the electrophoresis tank with ClearPage SDS-PAGE running buffer. Load the samples and protein ladder.
6. Run the gel as follows:
 - (a) Run at 90 V until the sample has migrated through the stacking gel.
 - (b) Increase to 110 V and run until the blue line is at the bottom of the gel.
7. Wet transfer of gel to membrane.
 - (a) Use PVDF-FL membranes. Wet the dry membrane in methanol before transfer. Note, the membranes are sensitive to scratches and bending, marks will be visible in the scanning.

- (b) Presoak the filter papers and “sponges” in transfer buffer.
- (c) Place in the following order: sponge, two filter papers, membrane, gel, two filter papers, and sponge.
- (d) Place the holder in the following order: (–) cathode, gel, membrane, and anode (+), and place the ice block inside the transfer box.
- (e) Cover with transfer buffer to the top of the cassettes (transfer buffer can be reused). Transfer conditions: 200 mA (approximately 1 h).

8. Prepare blocking buffer by diluting the Odyssey blocking buffer 1:1 in TBS or PBS (*see Note 8*).
9. Block for approximately 1 h at RT on a rocking table.
10. Incubate the membranes with primary antibody. Dilute primary antibody (1:100–2,000) in blocking buffer (reuse the blocking buffer from the blocking step). Place membranes in plastic bags, and add 5 mL diluted primary antibody for each membrane and seal the bags. Incubate on a rocking table at 4 °C overnight (or for 2 h at RT).
11. Remove the primary antibody solution. Wash membranes three time with TBS, 0.1 % Tween-20 (10 min each wash) followed by a final 5 min wash with TBS (no Tween-20).
12. Incubate the membranes with secondary antibody. Dilute near-infrared (NIR) fluorescent-labeled anti-rabbit Ig antibody (or anti-rat or anti-mouse Ig, depending on the primary antibody) 1:1,000 in Odyssey blocking buffer. Use approximately 5–10 mL per membrane.
13. Incubate membranes in the dark (use black boxes) on a rocking table for approximately 1–2 h (*see Note 9*).
14. Remove the secondary antibody solution. Wash the membrane twice in TBS, 0.1 % Tween-20, followed by a final 10 min wash in TBS. Keep membranes in the dark at all times until reading IR fluorescence on imager.
15. Scan membranes using an Odyssey Infrared Imager.

3.9 Effect of Protease Inhibitors on Apoptosis

Mast cell secretory granules contain a wide array of proteases, including cysteine cathepsins, aspartic acid, and also serine proteases. Many of these have been implicated in apoptosis [13, 14]. In order to evaluate the role of specific proteases in apoptosis, inhibitory assays should be performed (*see Note 10*).

1. Resuspend mast cells to 5×10^5 cells/mL in appropriate cell culture medium [10] and transfer 1 mL/well (triplicates) to a 24-well plate.
2. Add 4 μ L/well of Z-DEVD-FMK, Z-VAD-FMK or E-64d and 5 μ L/well of Pefabloc® SC or Pepstatin A to achieve final concentrations of 20, 20, 100, and 50 μ M, respectively.

3. Mix each individual sample by pipetting up and down three times.
4. Incubate at 37 °C in 5 % CO₂ for 30 min.
5. Induce apoptosis in cells using the desired method and proceed as described in Subheading 3.3.

4 Notes

1. LLME effectiveness may vary between different mast cell types. To find the best settings, a dose response experiment should be performed. Also, the kinetics of apoptosis induction should be initially monitored.
2. Primary mast cells are highly sensitive to LLME, whereas other cell types may require LLME concentrations above 500 µM (up to 2–4 mM) to undergo cell death.
3. When a high number of cells are incubated with CellTiter-Blue® (viability test) for extended periods of time, a secondary reduction reaction may occur in which the fluorescent resorufin is further reduced to the colorless, non-fluorescent hydroresorufin. To stop and stabilize the reaction, add 3 % SDS (1:2, v/v).
4. Annexin V-FITC and PI are light sensitive and only provide fluorescence during a short time period (~1 h). In order to extend the staining time, keep samples on ice and in the dark.
5. In order to decrease the background and to improve the resolution of AO or NAO staining, extra PBS washing steps can be introduced.
6. Proapoptotic mediators such as Bid and cytochrome c are usually present in very low concentrations in cells. In order to detect such proteins, highly concentrated cell samples are required.
7. To avoid viscous samples for Western blot analyses, instead of using sonication (as recommended), samples can be treated with Benzonase® Nuclease (Novagen) prior to addition of SDS-PAGE sample buffer. The recombinant endonuclease will completely degrade DNA and RNA and is free from proteolytic activity.
8. Do not use Tween-20 in the blocking buffer because it may increase background fluorescence during detection of near infrared-coupled fluorochromes by LI-COR. The risk of increased background from Tween-20 is reduced after blocking.
9. Do not keep the fluorescently labeled antibodies in the light! Use black Western incubation boxes for incubations.
10. When assessing the role of cysteine cathepsins in regulating apoptosis, make sure to use the membrane-permeable form of the inhibitor (E-64d) rather than the non-permeable form (E-64).

Acknowledgments

The authors of this article receive support from The Swedish Research Council, Formas, King Gustaf V 80-year Anniversary Fund, Torsten and Ragnar Söderberg Foundation, The Vårdal Foundation, The Swedish Society of Medicine, Åke Wiberg Foundation, Konsul Th C Bergh Foundation, and The Swedish Cancer Foundation.

References

1. Kalesnikoff J, Galli SJ (2008) New developments in mast cell biology. *Nat Immunol* 9: 1215–1223
2. Bischoff SC (2007) Role of mast cells in allergic and non-allergic immune responses: comparison of human and murine data. *Nat Rev Immunol* 7:93–104
3. Dawicki W, Marshall JS (2007) New and emerging roles for mast cells in host defence. *Curr Opin Immunol* 19:31–38
4. Peachell P (2006) Regulation of mast cells by beta-agonists. *Clin Rev Allergy Immunol* 31: 131–142
5. Lundequist A, Pejler G (2011) Biological implications of preformed mast cell mediators. *Cell Mol Life Sci* 68:965–975
6. Karra L, Berent-Maoz B, Ben-Zimra M, Levi-Schaffer F (2009) Are we ready to downregulate mast cells? *Curr Opin Immunol* 21: 708–714
7. Pejler G, Abrink M, Wernersson S (2009) Serglycin proteoglycan: regulating the storage and activities of hematopoietic proteases. *Biofactors* 35:61–68
8. Pejler G, Åbrink M, Ringvall M, Wernersson S (2007) Mast cell proteases. *Adv Immunol* 95: 167–255
9. Melo FR, Waern I, Ronnberg E, Abrink M, Lee DM, Schlenner SM, Feyerabend TB, Rodewald HR, Turk B, Wernersson S, Pejler G (2011) A role for serglycin proteoglycan in mast cell apoptosis induced by a secretory granule-mediated pathway. *J Biol Chem* 286:5423–5433
10. Rönnberg E, Pejler G (2012) Serglycin- the master of the mast cell. *Methods Mol Biol* 836:201–217
11. Ivanova S, Repnik U, Bojic L, Petelin A, Turk V, Turk B (2008) Lysosomes in apoptosis. *Meth Enzymol* 442:183–199
12. Lutsenko GV (2010) Flow-cytometry assay for apoptosis using fluorophore 10-nonyl acridine orange. *Biol Membrany* 27:430–439
13. Boya P, Kroemer G (2008) Lysosomal membrane permeabilization in cell death. *Oncogene* 27:6434–6451
14. Turk B, Turk V (2009) Lysosomes as “suicide bags” in cell death: myth or reality? *J Biol Chem* 284:21783–21787

Chapter 21

Measurement of Nitric Oxide in Mast Cells with the Fluorescent Indicator DAF-FM Diacetate

Chris D. St. Laurent, Tae Chul Moon, and A. Dean Befus

Abstract

The production of nitric oxide in mast cells has been difficult to measure due to the low amounts made by mast cells, as well as limitations in the specificity and sensitivity of the assays available. We present here a sensitive and specific 96-well plate-based method to directly measure NO using the cell-permeable fluorescent compound DAF-FM diacetate.

Key words Mast cell, Nitric oxide, DAF-FM diacetate, Nitric oxide synthase, Griess reaction

1 Introduction

Nitric oxide (NO) is an important signaling molecule and mediator of mast cell (MC) function. NO is synthesized by the conversion of L-arginine to L-citrulline by the enzyme nitric oxide synthase (NOS). NO has a half-life of only a few seconds and hence has been historically difficult to measure. To this end, NOS activity and more stable by-products of NO reactions such as nitrite and nitrate (NO_2^- and NO_3^-) have been used as surrogates for the measurement of NO in MC, by measuring the production of tritiated citrulline from tritiated arginine, and the Griess reaction, respectively [1, 2]. Unfortunately, these assays are indirect measures of NO and the sensitivity is low. To address many of the problems associated with the measurement of NO, diaminofluorescein (DAF) was developed by Kojima et al. [3, 4], and DAF-FM (4-amino-5-methylamino-2,7-difluorescein) and the cell-permeable DAF-FM diacetate (DAF-FM-DA) have been used to detect NO in many different cell types and settings, including flow cytometry [5], live cell imaging [6], and live animal imaging [7].

There has been some confusion and debate in the literature as to whether MCs make NO. MCs arise from their progenitors that originate in bone marrow and migrate into the blood stream and

then to tissues where they differentiate and mature into various phenotypes driven by local factors. There is an expanding literature on the heterogeneity of MC *in situ* [8, 9], and we have begun to understand the complex phenotypic differences of MC not only *in situ*, but in culture as well. NO production in MC is influenced by this heterogeneity, and species differences and changing culture conditions play a dramatic role in the ability of MC to express NOS and produce NO. For example, culturing mouse bone marrow-derived MC in the presence of IL-3 alone generates a phenotype that is nonpermissive for the production of NO, while culturing with IL-4 and stem cell factor results in MC that can be stimulated with interferon gamma and lipopolysaccharide to produce NO in most cases (a small percentage of cultures studied fail to produce NO) [10]. Interestingly, in nasal tissue from normal human subjects, 40 % of MCs express at least one of the three NOS isoforms, whereas in nasal polyp tissue over 65 % of MCs express NOS2 [11]. Clearly, MCs have the ability to synthesize NO; however, it is not fully understood how this is regulated in different MC phenotypes, and there is variability in NOS expression and NO production even in our current “best” culture conditions.

Although MCs produce NO, they do so at relatively low levels compared to other cell types such as macrophages. This adds to the difficulty of detecting NO and methods such as the Griess assay are not ideal for the detection of NO in MC because of low sensitivity (detection limit of $\sim 1 \mu\text{M}$). Thus, we have worked with the fluorescent compound DAF-FM-DA, which has a detection limit of $\sim 5 \text{ nM}$, to establish a method of detecting NO in MC. We present in this chapter an assay that we have developed to directly quantitate intracellular NO using DAF-FM-DA and a 96-well plate-based fluorescent reader. This assay can be used to screen MC for NO production. However, we stress that the variability and limits of our current MC culture methodology and isolation techniques and our limited understanding of MC phenotypic heterogeneity may influence the results of this assay. A comprehensive set of tools to study NO in MC may also include assaying the expression of NOS by PCR and Western blot.

2 Materials

2.1 Experimental Design

When designing an experiment in which this assay will be used, there are several important controls that must be included. We rigorously optimized the assay with a series of NO donors and scavengers to ensure that the fluorescent signal detected is due to NO, and not other reactive species. The NO donor NOR-3 ((\pm)-(E)-ethyl-2-[(E)-hydroxymino]-5-nitro-3-hexeneamide, FK 409) and the NO scavenger PTIO (2-phenyl-4,4,5,5-tetramethylimidazoline-1-oxyl-3-oxide) should be included as controls to

Table 1
Summary of controls used in the DAF-FM-DA assay

Condition	DAF-FM-DA	PTIO	NOR-3	Rationale
A. Background				Subtract this from all other values
B. DAF-FM-DA control	✓		✓	To ensure DAF is working
C. Scavenger control	✓	✓	✓	To ensure scavenger is working
D. Test	✓			The cells you are actually testing
E. Test control	✓	✓		To ensure the signal is NO mediated

All conditions (A–E) include the cells you are testing and a combination of DAF-FM-DA, the nitric oxide scavenger PTIO, and the nitric oxide donor NOR-3. A. The background values obtained are from your mast cells alone and are to be subtracted from all other values obtained in the assay. B. The DAF-FM-DA control should detect a large amount of exogenous nitric oxide, regardless of the amount your cells produce. C. The increase in fluorescence seen in B can be scavenged by the scavenger PTIO to ensure that PTIO is working properly. D. This condition is the actual cells you wish to test using this assay. E. The fluorescence generated from your cells by DAF-FM-DA should be scavenged to ensure the signal you are receiving is due to nitric oxide

ensure that the assay is working each time it is run. In addition, the assay should be further controlled by ensuring that the fluorescent signal can be scavenged from test samples. A summary of these controls is presented in Table 1.

An important factor to keep in mind when designing the experiment is that the assay is dependent on adherence of MC to the bottom of a 96-well plate, using fibronectin (detailed in Note 5). Additionally, the availability of color-free growth medium for your MC is crucial, or the use of HEPES-Tyrode's buffer (HTB) will be necessary, and MC viability in HTB will need to be assessed prior to starting this assay (detailed in Note 1).

Due to the variable nature of NO expression in MC and the technically challenging methodology of this assay, it is recommended to first test this assay on a cell population such as macrophages. Macrophages can synthesize about tenfold more NO than MC, and you can familiarize yourself with the difficult aspects of this assay on a cell population that produces an abundance of NO before applying it to a MC population.

2.2 Types of Mast Cells

There are several types of MCs commonly used as experimental tools including: primary mouse bone marrow-derived MC, primary rat peritoneal MC, primary human cord blood or peripheral blood-derived MC, LAD2 cell line, and HMC-1 cell line. To begin to use this assay, you should have collected the MC you will use with your desired protocol.

2.3 DAF-FM Diacetate Assay

1. A fluorescent reader capable of reading 96-well plates, at excitation wavelength 495 nm and emission wavelength 515 nm. The reader must also be able to read the fluorescence from the bottom of the plate.
2. Black walled, clear-bottom 96-well plates.
3. 10 μ g/mL plasma fibronectin from human, rat, or mouse. Use fibronectin appropriate for MC species in assay.
4. HEPES-Tyrode's buffer (HTB): 4 g NaCl, 0.5 g glucose, 0.1 g KCl, 73.5 mg CaCl₂·2H₂O, 0.5 g bovine serum albumin (BSA), 1.43 g HEPES, 31.2 mg NaH₂PO₄·1H₂O. Add to 500 mL water and adjust the pH to 7.4.
5. Phenol red-free media specific for growing mast cells of interest (*see Note 1*).
6. 20 mM NOR-3 stock solution (NO donor): 1 mg NOR-3 in 232 μ L DMSO (*see Note 2*).
7. 40 mM PTIO stock solution (NO scavenger): 10 mg PTIO in 1.08 mL water (*see Note 3*).
8. 1 mM DAF-FM diacetate stock solution: 50 μ g DAF-FM-DA in 50 μ L DMSO (*see Note 4*).

3 Methods

1. Pre-coat the wells of a 96-well black plate with fibronectin (*see Note 5*). Add 100 μ L of a 10 μ g/mL fibronectin solution to each well, and incubate overnight at 4 °C or 2 h at 37 °C.
2. Stimulate the MC to produce NO in the desired manner and/or treat with the desired compounds (*see Note 6*).
3. Wash the fibronectin-coated wells from **step 1** two times with HTB. Aspirate the liquid from the well and add 300 μ L HTB with a pipette.
4. Count the MCs and resuspend them at 5×10^5 per mL in phenol red-free media (*see Note 1*).
5. Add 1×10^5 MCs (200 μ L) to each well of the 96-well black plate. Do this in triplicate for each condition and controls. For a detailed explanation of controls, *see Note 7*.
6. Add 1 μ L of the 40 mM NOR3 stock to the positive control wells to a final concentration of 100 μ M. Gently mix with a pipette (*see Note 8*).
7. Add 5 μ L of the 40 mM PTIO stock to the appropriate control wells to a final concentration of 1 mM. Gently mix with a pipette.

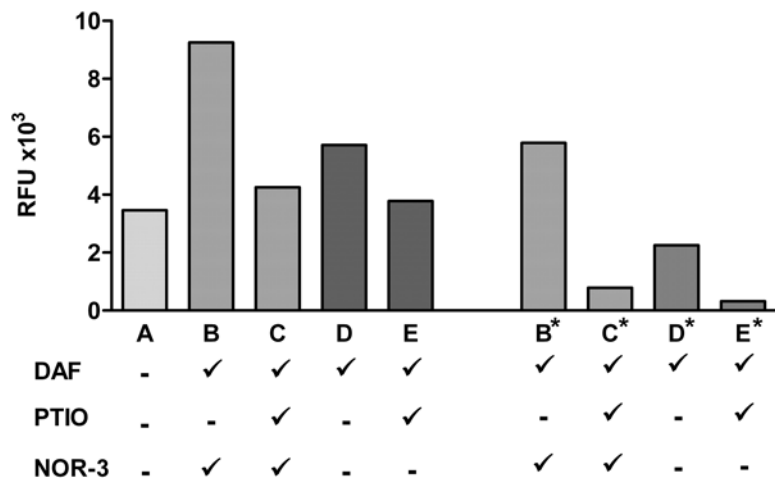


Fig. 1 Graphical representation of results from the DAF-FM-DA assay. Mast cells were isolated from the peritoneal cavity of 12-week-old male Sprague Dawley rats. Prior to the assay cells in Bars A, D, and E were treated for 18 h with 200 U of IFN α and β to induce nitric oxide expression. Bar A is the background value obtained from the assay, which is shown here for informative purposes only, and can be subtracted from each of the other bars. Bar B is the DAF-FM-DA positive control. Bar C is the positive control scavenged with PTIO. Bar D is the value obtained from the cells you actually wish to test nitric oxide expression from. Bar E is the scavenged value from D. Bars B*-E* represent the values from each condition minus the background fluorescence from bar A. Values obtained from the assay are expressed as relative fluorescent units (RFU)

8. Add 1 μ L of the 1 mM DAF-FM-DA stock to each well of the assay to a final concentration of 10 μ M. Gently mix with a pipette.
9. Incubate the plate at 37 °C for 1 h in a tissue culture incubator (5 % CO₂).
10. Gently aspirate the media out of the well with a pipette and wash each well two times with HTB (*see Note 8*). Add 200 μ L fresh phenol red-free media to each well. If you do not have phenol red-free media, you can now add 200 μ L of HTB to each well instead (*see Note 1*).
11. Incubate the plate for 30 min at 37 °C in a tissue culture incubator (5 % CO₂).
12. Read the plate on a fluorescent plate reader at excitation wavelength 495 nm and emission wavelength 515 nm (*see Note 9*).
13. Subtract the background obtained from the wells containing cells alone from each measured value to obtain the corrected reading for each well. Average the three readings for each condition to obtain a final value for each condition. A sample data set is illustrated in Fig. 1.

4 Notes

1. Phenol red contained in most cell culture media can interfere with the fluorescent signal from DAF-FM-DA. If possible, phenol red-free versions of the cell culture media should be used in this assay. If there are no phenol red-free versions available of the media needed to maintain survival of your MC, use phenol red-containing media during the first half of this protocol, and then switch the cells to HTB during **step 10**, before reading the fluorescence. We have tested this assay with several different types of MC in HTB and have experienced no cell death or changes in NO production during the short time the cells are in HTB (30 min) versus using phenol red-free growth media. Before using this method, however, you must test this to ensure that your MC populations will not be affected by the lack of their specific growth media.
2. Further dilutions of NOR-3 should be made in cell culture media or directly into the 96-well plate containing the MC, in order to dilute the DMSO concentration so that it does not stimulate or otherwise alter your cells. We have tested the final concentration of DMSO used in this assay and it has no effect on the measurement of NO production. NOR-3 is stable for 1 month stored at -80 °C once dissolved in DMSO.
3. PTIO is stable for 1 year at -20 °C once dissolved in water.
4. Further dilutions of DAF-FM-DA should be made in cell culture media or directly into the 96-well plate, as in **Note 2**. DAF-FM-DA is stable for 6 months stored at -80 °C once dissolved in DMSO.
5. We have found fibronectin to be effective in anchoring the MC to the bottom of the 96-well plate and have tested this with HMC-1 and LAD2 human MC cultures, as well as primary rat peritoneal MC. This assay includes several washing and mixing steps, which in our experience tends to result in a loss of cells at each step in plates not coated with fibronectin.
6. Depending on the species and phenotype of your MC, you will likely need to stimulate them to induce NO production and/or treat them with drugs or other compounds that you may be testing. For example, IL-4/SCF mouse bone marrow-derived MC cultures require stimulation with 100 ng/mL LPS and 50 nM IFN γ for 18 h to induce NO production, and rat peritoneal MCs require stimulation with 200 U/mL IFN γ or 200 U/mL each of an IFN α /β mixture for 18 h.
7. In addition to the MC you wish to assay for NO production, it is essential to run several controls to ensure the assay is working properly. We include wells containing the NO donor NOR-3 to ensure that we can successfully induce DAF-FM-DA

fluorescence as a positive assay control and also include the NO scavenger PTIO to reduce this fluorescence to ensure we are specifically detecting only NO. We also include wells with cells alone, to control for background fluorescence. An example of the different controls we include is illustrated in Table 1.

8. Although we have added fibronectin to each well to anchor the MC in place and greatly reduce cell loss, care must be taken in all washing and mixing steps to not wash or pipette too vigorously or loss of cells will still occur. To remove media or buffer, we recommend aspirating with a 200 μ L pipette, and avoid touching the bottom of the well. When adding back media or buffer, place the pipette on the sidewall of the well, and slowly pipette in the desired amount, without touching the bottom of the well. When mixing, use a 20 μ L pipette and slowly draw the liquid up and down four to five times.
9. The reading should be taken from the bottom of the well, and not the top of the well, as the cells should all be anchored to the bottom of the well by the fibronectin. The fluorescence may not be detected if read from the top. Most current fluorescent readers have the option to read from both the bottom and the top of the wells.

References

1. Mannaioni PF et al (1997) Interaction between histamine and nitric oxide in rat mast cells and in isolated guinea pig hearts. *Int Arch Allergy Immunol* 113:297–299
2. Stone WL, Yang H, Qui M (2006) Assays for nitric oxide expression. *Methods Mol Biol* 315: 245–256
3. Kojima H et al (1998) Detection and imaging of nitric oxide with novel fluorescent indicators: diaminofluoresceins. *Anal Chem* 70:2446–2453
4. Kojima H et al (1998) Development of a fluorescent indicator for nitric oxide based on the fluorescein chromophore. *Chem Pharm Bull (Tokyo)* 46:373–375
5. Paul DM, Vilas SP, Kumar JM (2011) A flow-cytometry assisted segregation of responding and non-responding population of endothelial cells for enhanced detection of intracellular nitric oxide production. *Nitric Oxide* 25: 31–40
6. Gilchrist M, Hesslinger C, Befus AD (2003) Tetrahydrobiopterin, a critical factor in the production and role of nitric oxide in mast cells. *J Biol Chem* 278:50607–50614
7. Lepiller S et al (2007) Imaging of nitric oxide in a living vertebrate using a diamino-fluorescein probe. *Free Radic Biol Med* 43: 619–627
8. Moon TC et al (2009) Advances in mast cell biology: new understanding of heterogeneity and function. *Mucosal Immunol* 3:111–128
9. Valent P et al (2010) Phenotypic heterogeneity, novel diagnostic markers, and target expression profiles in normal and neoplastic human mast cells. *Best Pract Res Clin Haematol* 23: 369–378
10. Moon TC et al (2011) Microenvironmental regulation of inducible nitric oxide synthase expression and nitric oxide production in mouse bone marrow-derived mast cells. *J Leukoc Biol* 91:581–590
11. Yoshimura T et al (2011) Expression of nitric oxide synthases in leukocytes in nasal polyps. *Ann Allergy Asthma Immunol* 108:172–177

Chapter 22

Real-Time Imaging of Ca^{2+} Mobilization and Degranulation in Mast Cells

Roy Cohen, David A. Holowka, and Barbara A. Baird

Abstract

Mast cells play a key role in allergy and inflammation processes as part of the immune response. The activation of mast cells via antigen binding and cross-linking of IgE receptors initiates the onset of dramatic calcium (Ca^{2+}) mobilization dynamics that promote the release of mediators of inflammation and allergy. Ca^{2+} signaling in mast cells has been studied extensively using a variety of research tools and techniques. In these studies, a large number of proteins have been identified to participate in various stages of these processes.

Here we describe single-cell imaging as an important approach for examining Ca^{2+} signaling and exocytosis in mast cells. Single-cell imaging tools have advanced significantly over the last 10 years, in part due to improvements in microscope technology and in part due to the development of a new generation of Ca^{2+} indicators and genetically encoded Ca^{2+} sensors. The single-cell imaging techniques described here provide the spatial and temporal resolution required to decipher the signaling events that are critical for mast cell functions.

Key words Live-cell imaging, Calcium (Ca^{2+}) signaling, Calcium dynamics, Mast cell degranulation

1 Introduction

1.1 Regulation of Ca^{2+} Signaling and Ca^{2+} Influx in Mast Cell Function

Mast cell signaling is tightly regulated by cytosolic Ca^{2+} dynamics, which are mediated by stimulated Ca^{2+} release from intracellular stores and Ca^{2+} entry via several channels at the plasma membrane [1]. Elevation in cytosolic Ca^{2+} activates a cascade of downstream events that trigger exocytosis of secretory granules. This process, also known as degranulation, is responsible for the release of mediators of allergy and inflammation due to antigen binding to IgE that is associated with its high-affinity receptor, Fc ϵ RI. For recent reviews on mast cell Ca^{2+} signaling, see [1, 2]. Investigating the spatial and temporal aspects of Ca^{2+} dynamics and identifying the channels involved in these signaling events are crucial to our understanding of mast cell regulation and function. Cytosolic Ca^{2+} in resting mast cells is maintained in the ~100 nM range, whereas activation of these cells results in a rapid rise to μM concentrations.

Under physiological conditions, Fc ϵ RI-mediated activation of mast cells induces this rapid elevation via activation of phospholipase C γ (PLC γ) to produce inositol 1,4,5-trisphosphate (IP₃), which binds to IP₃ receptors at the endoplasmic reticulum (ER) membrane to release a concentrated store of Ca²⁺. Release of Ca²⁺ from intracellular stores then stimulates store-operated Ca²⁺ entry (SOCE), giving rise to a sustained phase of Ca²⁺ elevation. During the past two decades, live-cell microscopy has significantly advanced, making single-cell imaging possible for a wide variety of applications. In parallel to advances in microscopy, probes to monitor changes in Ca²⁺ concentrations have improved significantly, with fluorescent dyes and genetically encoded proteins providing a panel of specific and versatile tools for the visualization and quantification of Ca²⁺ dynamics. We previously showed that spatial regulation of the initial Ca²⁺ rise in RBL mast cells depends on TRPC1-mediated influx of extracellular Ca²⁺ [3]. These events were identified as Ca²⁺ waves that propagate release of Ca²⁺ from the ER and move directionally through the cytoplasm. Ca²⁺ waves in mast cells are followed by SOCE, which mediates oscillatory changes in cytosolic Ca²⁺ concentration. The oscillations most likely encode temporal information required for the regulation of various cell functions.

Under conditions of weak stimulation by low but physiologically relevant doses of antigen (Ag), we observe spatially restricted Ca²⁺ elevations, termed Ca²⁺ puffs. The nature and function of these puffs in mast cells is not completely understood, but they frequently appear in cellular protrusions, and in many cells they precede full waves and activation of downstream events.

1.2 Ca²⁺ Mobilization and Entry in Mast Cells

Real-Time Imaging

Ca²⁺ Sensors and Indicator Dyes

In contrast to single-cell imaging, Ca²⁺ measurements can be made on large populations, using either a fluorimeter with suspended cells or a plate reader with adherent cells. A major benefit of single-cell imaging experiments is the opportunity for spatial resolution, and this approach should be applied when morphology, motility, or expression pattern of associated proteins are relevant to the scientific question. On the other hand, when information about spatial regulation is not imperative, population experiments provide superior statistical significance with considerably less effort by the researcher.

Fura2 was the one of the first indicators used to monitor cytosolic changes in Ca²⁺ levels. Since its development by Tsien and colleagues [4], the availability of Ca²⁺ indicators to suit different experimental criteria has expanded widely. In parallel to the development of synthetic Ca²⁺ dyes, the technology for genetically encoding Ca²⁺ sensors within cellular proteins has improved significantly over the last decade.

The growing list of synthetic Ca²⁺ dyes provides an excellent toolkit for investigating a range of Ca²⁺-related phenomena, not only those occurring in the cytosol but also in particular cellular

organelles as well as near the plasma membrane (PM). Researchers who employ Ca^{2+} imaging as an integral part of their experimental investigation should consider the benefits and drawbacks of the two different families of Ca^{2+} indicators: synthetic or genetic.

Synthetic dyes provide superior brightness and ease of delivery (mainly by AM loading, *see* below), and a panel of dyes with various spectra and affinities for range of Ca^{2+} concentrations have become available. Additionally, some of these dyes provide the possibility of ratiometric measurements of actual Ca^{2+} concentrations (i.e., fura-2 and indo-1 [4]).

Possible limitations associated with synthetic dyes include phototoxicity, leakage from the cells, and concentration in subcellular organelles. Another significant concern stems from relatively fast loading of these dyes into cells and fast diffusion kinetics, which facilitate Ca^{2+} buffering and its unwanted (or unknown) effects on cell physiology. We found this to be a problem in mast cells, and, for example, we previously showed significant differences in Ca^{2+} mobilization dynamics when using fluo4 and fluo5 in comparison to genetically encoded GCaMP2 [3].

Genetically encoded Ca^{2+} indicators (GECI) provide an alternative that is often preferable to synthetic dyes for live-cell Ca^{2+} imaging. These fluorescent recombinant proteins have improved dramatically over the last decade in terms of their expression levels as well as their sensitivity and rate of response to changes in Ca^{2+} concentrations. The previous generation of FRET-based sensors (i.e., “ameleon” [5]) has been replaced with permuted GFP constructs that are bright and stable and display fast kinetics. The new generation of GECI, including GCaMP3 and 5 [6] as well as the multicolor sensor GECO proteins [7], now offers a considerably enhanced toolkit for Ca^{2+} imaging.

Although using these GECIs involves transfection of cells, they benefit from several advantages over synthetic dyes including gradual expression that maintains the cell’s Ca^{2+} homeostasis, as well as very low or no leakage from the cells or into organelles. In addition, GECI can be targeted to specific organelles by means of fusion with targeting peptide sequences for subcellular and local Ca^{2+} measurements. For more information on GECI, *see* McCombs and Palmer [8].

1.3 Pharmacological Tools for Isolation of Specific Ca^{2+} Pathways in Mast Cells

Several channel and transporter families play a role in mast cell Ca^{2+} regulation. The major players include transient receptor potential channels (TRPC), calcium-release-activated calcium channels (CRAC), inositol trisphosphate receptors (IP3R) and ion transporters (plasma membrane Ca^{2+} ATPase (PMCA), and sarco/endoplasmic reticulum Ca^{2+} -ATPase (SERCA). Numerous pharmacological agents target these various Ca^{2+} channels with variable specificity. Some of the common pharmacological agents include:

SERCA inhibitors (thapsigargin and cyclopiazonic acid), IP3R inhibitors (adenophostin A, xestospongin C, and possibly 2-aminoethoxydiphenyl borate (2-APB)), and SOCE inhibitors (lanthanides, nickel, 2-APB, and other nonspecific Ca^{2+} channel blockers).

In some experiments it is useful to eliminate Ca^{2+} influx from the processes being observed. For this purpose, a Ca^{2+} -free buffer (with or without the addition of Ca^{2+} chelators) can be used. Although Ca^{2+} -free buffer involves less nonspecific effects, various pharmacology agents offer the means to isolate selected channel pathways. However, one must always take into account and control for potential nonspecific effects of any reagent used.

1.4 Ca^{2+} Signaling Dynamics in Mast Cells: Puffs, Waves, and Oscillations

Mast cell Ca^{2+} dynamics involve a complex ensemble of spatially and temporally restricted changes in Ca^{2+} concentrations. Antigen-stimulated signaling mediated by IgE receptors causes local and global changes in Ca^{2+} levels with regulated amplitudes and durations. We recently described Ca^{2+} puffs, waves, and oscillations, which exhibited dynamics that depend on the stimulus and experimental conditions [3]. Ca^{2+} oscillations were reported in mast cells more than a decade ago [9]. Additional characterization of Ca^{2+} waves and puffs provides a more complete view of regulation of Ca^{2+} signaling in mast cells. We observed a compelling association between mast cell morphology and Ca^{2+} signaling dynamics [3] in which elongated protrusions are sites for initiating spatially restricted changes in Ca^{2+} concentration following IgE cross-linking by Ag. Elongated protrusions are common to mast cells *in vivo* [10–12], and these are also manifested in cells grown in culture (see Fig. 1). Puffs and waves both demonstrate directional propagation in Ca^{2+} elevation, initiating mostly from the tips of protrusions. However, Ca^{2+} puffs are spatially confined and localized responses, whereas waves propagate through the entire cell. As in the case of waves, Ca^{2+} oscillations radiate throughout the cell and do not display lateral propagation.

Several features of Ca^{2+} waves in mast cells can be quantified using simple analysis. These include the region of origin, wave velocity, and overall Ca^{2+} elevation (see section 3.4). Other parameters of interest include rise time and decay that can be calculated from wave curve fitting and correlated with Ca^{2+} -induced calcium release (CICR) and Ca^{2+} clearance mechanisms. Features of Ca^{2+} oscillations that are of interest include amplitude and frequency (peak-to-peak time), as well as oscillation rise and decay times. Here we provide some basic tools for analyzing Ca^{2+} signaling in mast cells. Examination and quantification of other features, not covered here, may also be useful for addressing specific questions about these dynamic responses.

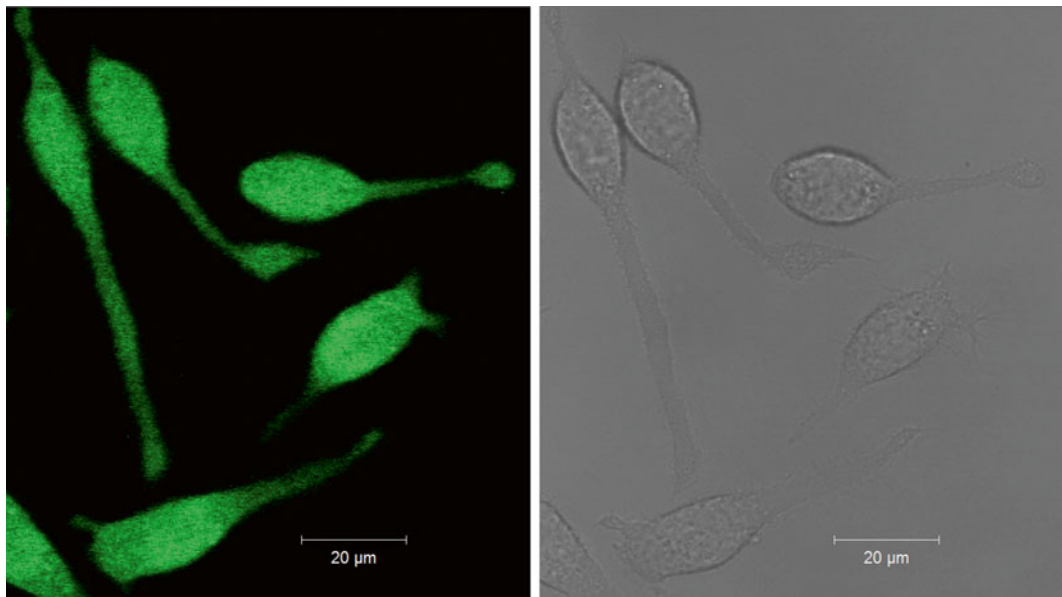


Fig. 1 Elongated morphology of mast cells. Image of RBL-2H3 mast cells in culture demonstrates their elongated morphology. Typically, cells will have one or two protrusions extending to various lengths away from the cell body. Morphological features of mast cells (length, angle, volume, etc.) can be quantified using various overlay tools in ImageJ or other image processing software. Fluorescent label is fluo4

1.5 Imaging Mast Cell Degranulation

Regulation of Mast Cell Exocytosis

Mast Cell Degranulation

As in excitable cells, exocytosis of granules in mast cells depends on Ca^{2+} mobilization. As for other membrane fusion processes, degranulation has been shown to involve specific sets of SNARE proteins (soluble NSF attachment protein receptor proteins) and associated regulators including synaptotagmins (for a recent review, *see* [13]). Synaptotagmins trigger membrane-membrane fusion in a process that depends on C2 domain binding to a Ca^{2+} /phosphatidylinositol 4,5-bisphosphate complex [14].

Various methods for measuring granule exocytosis in mast cells have been utilized, including measurement of β -hexosaminidase release [15], amperometry [9], and immunodetection of plasma membrane-associated granule proteins [16]. In addition, a number of methods have been developed to visualize individual granule exocytotic events in mast cells [17]. Early studies utilized acridine orange, a fluorescent weak base that accumulates in acidified vesicles [18, 19]. However, a recent study demonstrated that photo-sensitization of this dye during imaging limits its utility [20]. Other strategies have utilized granule-localized serotonin fluorescence imaged using multiphoton microscopy, together with complementary membrane and lysosome-labeling probes [21]. Although these methods allow detection of individual stimulated granule exocytotic events in mast cells, they are technically demanding and therefore limited in their usage.

**Real-Time Monitoring
of Mast
Cell Exocytosis**

The method we describe here utilizes preloading of fluorescein isothiocyanate-conjugated dextran (FITC-dextran) into mast cell granules via fluid-phase endocytosis, taking advantage of the pH sensitivity of FITC fluorescence. Visualization of granule exocytosis in real time is possible by detection of pH-dependent FITC dequenching that takes place once the granule fuses with the PM and its pH is equilibrated with the extracellular medium (Fig. 4). As will be described later, this FITC-dextran method provides a robust and sensitive method for visualizing individual granule exocytosis events, which can be related to other cellular activities.

The high sensitivity of FITC to pH, together with the robust loading of the dextran into secretory granules, makes this method highly suitable for measurements of degranulation in mast cells with excellent temporal and spatial resolution (Fig. 5). In addition, FITC-dextran loading can be used as a tool to measure degranulation in a population of cells (suspended or adherent) using a fluorimeter (as described in section 3.5) or a plate reader. This approach provides a means for screening and high-throughput assays.

**Simultaneous Imaging
of Degranulation and Ca^{2+}
Mobilization**

To allow real time, direct monitoring of the relationship between Ca^{2+} mobilization and granule exocytosis in mast cells, we devised a combined imaging strategy that uses a Ca^{2+} indicator together with FITC-dextran. This strategy provides excellent spatial and temporal resolution of both Ca^{2+} and degranulation dynamics to evaluate how Ca^{2+} waves, puffs, and oscillations relate to exocytosis of secretory granules in mast cells. To combine FITC-dextran-based degranulation and Ca^{2+} imaging, one can use a Ca^{2+} indicator dye with red emission (Ca^{2+} Red Asanate or Fura Red; *see* Fig. 6) or, alternatively, a red-shifted GECI (R-GECO; [7]) in combination with FITC-dextran.

2 Materials

**2.1 Genetically
Encoded Calcium
Indicators (GECI) cDNA
Expression Plasmids**

1. GECI plasmid: 5–8 μ g of purified plasmid (e.g., GCaMP2 and GCaMP3) per reaction (5×10^6 mast cells) (*see Note 1*).

**2.2 Chemicals
and Reagents**

1. Synthetic Ca^{2+} indicators: A large number of Ca^{2+} -sensitive fluorescent dyes are currently available, and describing all the possibilities is beyond the scope of this chapter. We find that for measurements of Ca^{2+} dynamics in mast cells, the relatively newly developed fluo4 family, including fluo4-AM, fluo5F-AM, and fluo5N-AM (Invitrogen), is most appropriate. These dyes have a range of affinities for Ca^{2+} , and they are bright, stable,

and available as acetoxymethyl esters (AM) for simple and fast loading into cells.

2. Reagents: We use multivalent antigen (DNP-BSA), thapsigargin, Ca^{2+} ionophore (A23187), sulfinpyrazone, hydroxytryptamine (5HT), and FITC-dextran (150 kDa) in our studies.

2.3 Tissue Culture

1. Mast cells (RBL-2H3 mast cells or bone marrow-derived mast cells) (*see Note 2*).
2. Complete medium: Minimal essential medium (MEM) containing 20 % fetal bovine serum (FBS) and 10 $\mu\text{g}/\text{mL}$ gentamicin sulfate.

2.4 Imaging Equipment

1. Glass bottom dishes (*see Note 3*).
2. Picospritzer (*see Note 4*).
3. Temperature-controlled microscope/objective (*see Note 5* and Subheading 2.6).

2.5 Solutions and Buffers

1. Balanced salt solution (BSS): 135 mM NaCl, 5 mM KCl, 1.8 mM CaCl_2 , 1 mM MgCl_2 , 1 mg/mL glucose, 20 mM HEPES (pH 7.2–7.4).
2. BSS + BSA: BSS with 1 mg/mL bovine serum albumin (BSA).
3. Electroporation buffer: 137 mM NaCl, 2.7 mM KCl, 1 mM MgCl_2 , 1 mg/mL glucose, 20 mM HEPES (pH 7.4).
4. Stimulating solution: BSS + BSA with antigen (DNP-BSA at 1 ng to 1 $\mu\text{g}/\text{mL}$ final concentration).

2.6 Microscope and Data Analysis Software

1. Confocal or wide-field microscopy can be used to monitor Ca^{2+} flux and degranulation. The image acquisition rate and detector sensitivity are most important for successful Ca^{2+} imaging. If using an objective heater, an oil immersion objective should be considered for better thermal conductance. To obtain adequate spatial resolution, 40 \times through 100 \times objectives with high numerical apertures should be considered.
2. Data acquisition software is usually an integral part of the microscope system being used, and different microscope brands provide different acquisition software with varying control over imaging parameters.
3. Data analysis software. Several commercial and open source options are available. ImageJ (NIH) and Fiji are two open source platforms that enable simple modifications and programming to support specific analysis needs. In addition, ImageJ has numerous readily available plug-ins that are especially useful for live-cell imaging and analysis. Some of the most useful plug-ins are discussed in Note 9.

3 Methods

3.1 Cell Preparation

1. Maintain RBL-2H3 mast cells [22] in monolayer culture in MEM with 20 % FBS and 10 μ g/mL gentamicin sulfate.
2. Transfect cells with GECI plasmid as follows:
 - (a) Resuspend 5×10^6 cells in 0.5 mL of cold electroporation buffer containing 5–8 μ g of plasmid DNA.
 - (b) Electroporate at 280 V and 950 μ F (Gene Pulser X (Bio-Rad)).
3. Plate cells directly onto MatTek dishes ($\sim 5 \times 10^5$ cells/plate).
4. Sensitize transfected cells with 0.5 μ g/mL anti-DNP IgE during overnight cell culture [23].
5. Under these conditions, the cell transfection efficiency with GCaMP2 is typically 20–30 % (*see Note 6*).
6. Load cells with synthetic Ca^{2+} indicators (fluo4-AM family of dyes is recommended). When Ca^{2+} dyes are to be used, harvest cells 3–5 days after passage, and plate overnight (16–24 h) in MatTek coverslip dishes in 2 mL of complete medium (5×10^5 cells/dish).
7. The next day, incubate cells for 30 min at 37 °C in BSS containing 0.5 μ M of the Ca^{2+} indicator and 2.5 mM sulfipyrazone.
8. Wash cells into BSS + BSA buffer.
9. Cells can be incubated in BSS + BSA buffer at 37 °C for up to 1 h before imaging.

3.2 Microscope Setup

1. Before preparing cell samples, ensure that microscope is operating and ready for image acquisition (e.g., excitation light source and filters should be ready).
2. Set temperature of objective or chamber to maintain at 37 °C.
3. If using the picospritzer, prepare capillary by loading with stimulating solution.
 - (a) Adjust micromanipulator and attach pipette.
 - (b) Calibrate picospritzer (required for initial experiments) using fluorescently labeled solution (e.g., FITC-dextran) to monitor stimulating puff intensity and spreading.
 - (c) Fabricate glass capillaries using a puller device so that the tip has a final diameter of $\sim 5 \mu\text{m}$.
4. If a picospritzer or an equivalent instrument is not available, add stimulant-containing solution to the dish by pipetting. Remember to adjust the concentration of stimulant according to the desired final concentration and dilution factor.

3.3 Imaging

1. 24 h after GECI transfection (or after loading cells with Ca^{2+} indicator dye), wash cells with pre-warmed (37 °C) BSS + BSA, and mount on the microscope.
2. Select appropriate illumination wavelength and filter lines. For GCaMP2, fluo4, or fluo5F use 488-nm excitation and view with a 505–530 nm band-pass filter.
3. Locate cells in the dish that express GECI (or are loaded with fluo dyes).
4. Zoom in as much as possible for best resolution (*see* Fig. 1 for common morphology of RBL-2H3 cells in culture).
5. If using the picospritzer, approach cells with a ~5-μm-diameter pulled-glass capillary, until positioned within ~100 μm distance from the cell.
6. Image cells at approximately 10–30 Hz. Ca^{2+} dynamics in mast cells should be easily detectable when recorded at 5–20 Hz (*see* Note 7).
7. Care should be taken to optimize conditions for Ca^{2+} imaging. These include dye loading, temperature, and cell density (*see* Note 8).

3.4 Image Processing and Analysis

Here we describe some simple and basic tools for image analysis that we use for evaluating fundamental Ca^{2+} dynamics in RBL mast cells. Researchers are encouraged to try these and various other analysis approaches and tools. More information about image processing, analysis, and quantification methods is available. *See* ImageJ documentation (<http://rsbweb.nih.gov/ij/docs/index.html>) or reference [24], for examples. In addition, ImageJ has numerous readily available plug-ins that are especially useful for live-cell imaging and analysis. Some of the most useful plug-ins are described in Note 9.

3.5 Fluorimetry-Based Ca^{2+} Measurements

1. Ca^{2+} waves (*see* Figs. 2 and 3):
 - (a) Spatial origin of the waves can be determined visually, based on the site of the initial Ca^{2+} elevation.
 - (b) Wave velocity can be calculated from the number of frames required for a wave to propagate along the cell.
2. Ca^{2+} puffs (*see* Fig. 2c, d): Spatial and temporal dynamics of puffs can be determined as described for waves.
3. Ca^{2+} oscillations (*see* Fig. 3): Features of the oscillations can be calculated from a plot of fluorescence intensity over time and integrating the fluorescence signal over a specified region of interest (ROI) (e.g., over the cell body).
1. Harvest cells 3–5 days after passage.
2. Resuspend 10^6 cells in 1 mL BSS supplemented with 2.5 mM sulfinpyrazone (to reduce dye leakage).

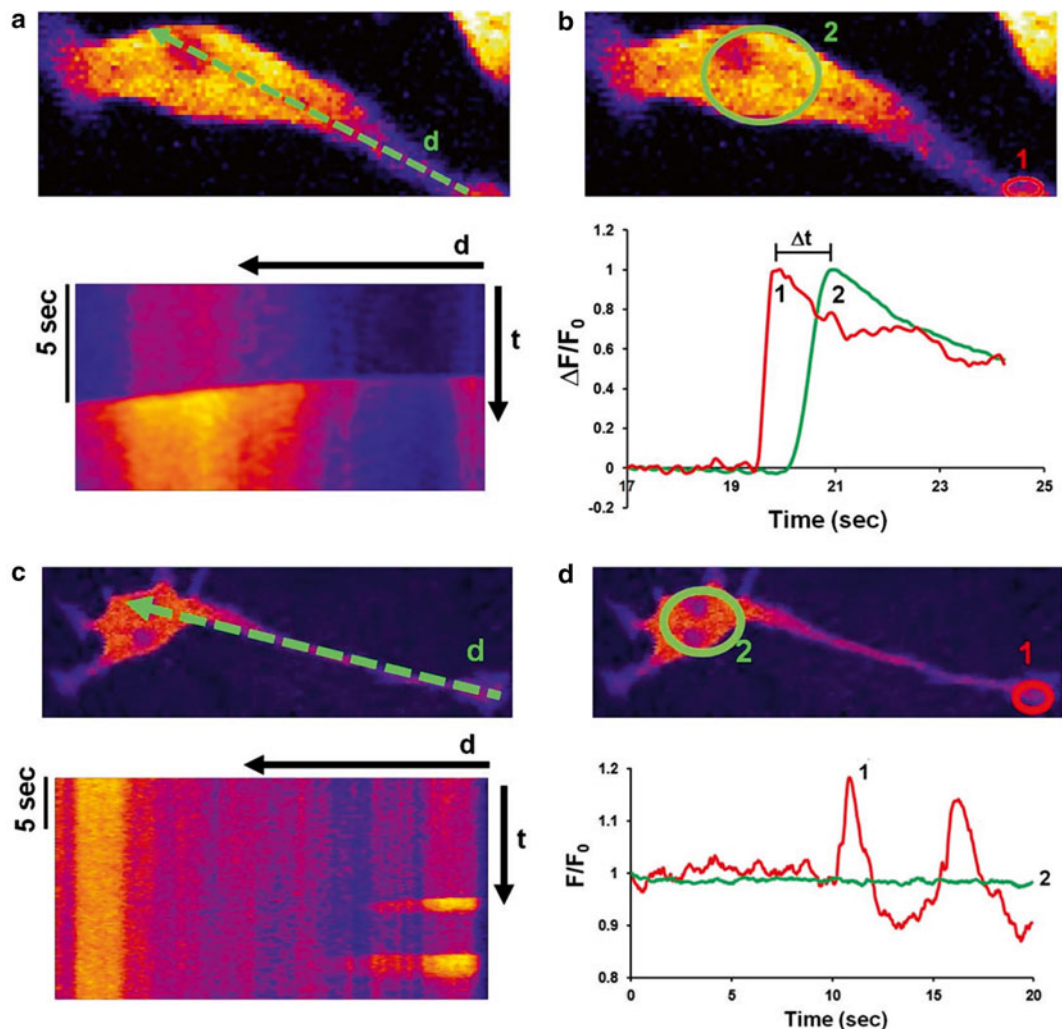


Fig. 2 Imaging and quantifying Ca^{2+} waves and puffs. In these examples, RBL-2H3 cells expressing the Ca^{2+} sensor GCaMP2 were monitored for fluorescence intensity as a function of time before and after stimulation by antigen, and changes in Ca^{2+} concentration are presented in pseudo colors (warmer colors represent higher Ca^{2+} levels). **(a)** *Upper*, image of cell, with direction of Ca^{2+} wave indicated; *lower*, timeline analysis (“virtual linescan” plug-in for ImageJ) provides both spatial and temporal information about changes in Ca^{2+} concentration. This analysis measures the changes in fluorescence over time along a designated line across the cell. Here the line width is 2 pixels. This visualization can be used to determine the point of origin of the wave. **(b)** Wave propagation can be visualized and quantified by plotting the fluorescence signal from two regions of interest (ROI; 1—protrusion, 2—cell body) over time and measuring the time difference between them (Δt) as a function of distance (in μm ; “Z Profiler” plug-in for ImageJ). The ROI quantification can be used to determine wave velocity. **(c)** As described for waves in **a**, timeline analysis can be used to detect and visualize the spatial attributes of Ca^{2+} puffs. In this example, the puffs are localized and confined to the cell’s protrusion. **(d)** Temporal dynamics of Ca^{2+} puffs can be quantified from fluorescence (F) vs. time plots, as in the case of waves. Here we integrated the fluorescence intensity over the cell body (2) or protrusion (1) to show the transient Ca^{2+} elevation during puffs

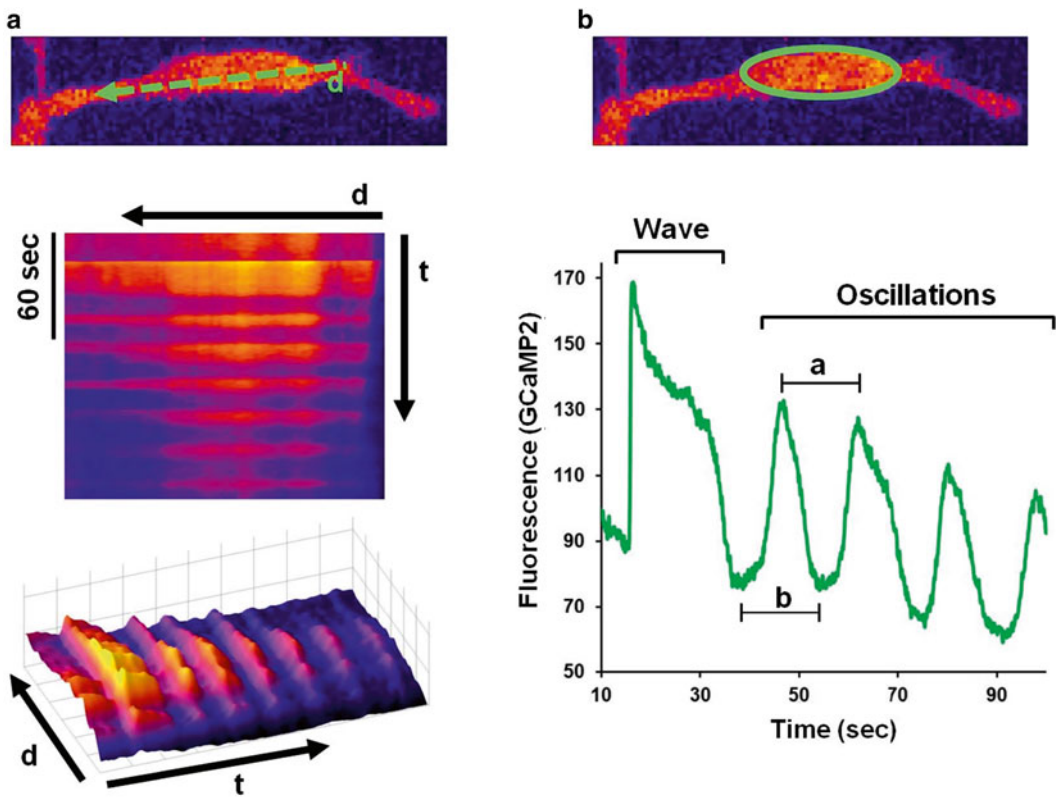


Fig. 3 Visualizing and quantifying Ca^{2+} oscillations. RBL-2H3 cell expressing GCaMP2 was stimulated with Ag and imaged for ~ 100 s. (a) Timeline analysis along the cell body (upper panel) reveals repetitive Ca^{2+} oscillations (middle panel; warmer colors represent higher Ca^{2+}). Lower panel illustrates a “3D” representation of the kymograph (“Interactive 3D Surface Plot” plug-in for ImageJ), for enhanced visualization of spatial and temporal dynamics of the oscillations. (b) Integration of the fluorescence signal over the cell body plotted against time can be used to quantify the oscillation’s dynamics. With this approach, one can measure the oscillation peak-to-peak interval (a, frequency) and peak width (b). Additional parameters can be extracted including oscillation rise phase (representing Ca^{2+} influx), down phase (representing Ca^{2+} clearance), and the integrated Ca^{2+} elevation during various time points

3. Add 0.5 μM fluo4-AM (or other fluorescent indicating dyes; set emission and excitation filters accordingly) and immediately mix. Incubate at 37 °C for 1 min.
4. Add 9 mL of BSS + BSA, and incubate cells in 37 °C for 30 min; during this incubation sensitize cells with IgE (2 $\mu\text{g}/\text{mL}$).
5. Wash the cells into fresh BSS + BSA, and verify appropriate dye loading by microscopy. It is important to make sure that the dye is loaded into the cytosol and not into organelles.
6. Use steady-state fluorimeter to measure changes in Ca^{2+} concentration upon addition of various stimulants to stirred cells at 37 °C.
7. Add Triton X-100 (0.1 %) at the end of the experiment to determine maximal indicator response to 2 mM Ca^{2+} , followed by excess EGTA (10 mM) to assess background signal when no Ca^{2+} is bound.

3.6 Monitoring Degranulation with Fluorescence

1. Harvest cells 3–5 days after passage and plate in MatTek dishes.
2. Culture 1×10^6 cells in 2 mL of full medium in the presence of 2 mg/mL FITC-dextran and anti-DNP IgE (0.5 μ g/mL) (if desired) for 24 h at 37 °C.
3. Optional: Add 5-hydroxytryptamine (HT) (0.2 mM final concentration) to induce increased granule diameter for better visualization with microscopy [25].
4. After 24 h incubation (37 °C) with FITC-dextran (\pm IgE), wash cells once with PBS, and resuspend in fresh buffer (BSS+BSA) at 1×10^6 cells/mL.
5. Incubate washed cells for 1 h at 37 °C.
6. Add 0.5 mL of the resuspended cells (approx. 2.5×10^5 cells) to 1.5 mL BSS in a stirred acrylic cuvette.
7. Monitor FITC fluorescence (excitation ($\lambda=490$ nm), emission ($\lambda=520$ nm)) at 37 °C using an SLM 8100C steady-state fluorimeter (SLM Instruments, Urbana, IL)—or similar instrument—in a time-based acquisition mode.
8. Add 0.1 % Triton X-100 to lyse cells at the end of each experiment to record unquenched FITC fluorescence to normalize the time course.
9. Degranulation analysis: For basic analysis, *see* Figs. 4, 5 and 6.
10. Optional co-imaging of degranulation and Ca^{2+} changes.
 - (a) If using dye for Ca^{2+} imaging, load dye following the wash step as indicated in Ca^{2+} imaging section (i.e. Fura Red; *see* Fig. 6).
 - (b) Image acquisition: As described in the Ca^{2+} imaging section.
11. Care should be taken to optimize conditions for imaging degranulation. These include temperature and dye and dextran loading (*see* Note 10).

4 Notes

1. Several families of GECI are currently available, and newer versions are being developed. Of special interest are the GCaMP indicators, constructed of permuted GFP fused together with calmodulin (CaM) and the M13 peptide. The GCaMP indicators have improved significantly in recent years, and a panel with diverse sensitivity and fluorescent spectra is currently available (e.g., GCaMP2 and GCaMP3, 5 R-GECO, G-GECO, B-GECO, organelle targeted, PM-targeted, etc. Our experience has been mainly with GCaMP2 and GCaMP3, but other GECI could be used with similar procedures).

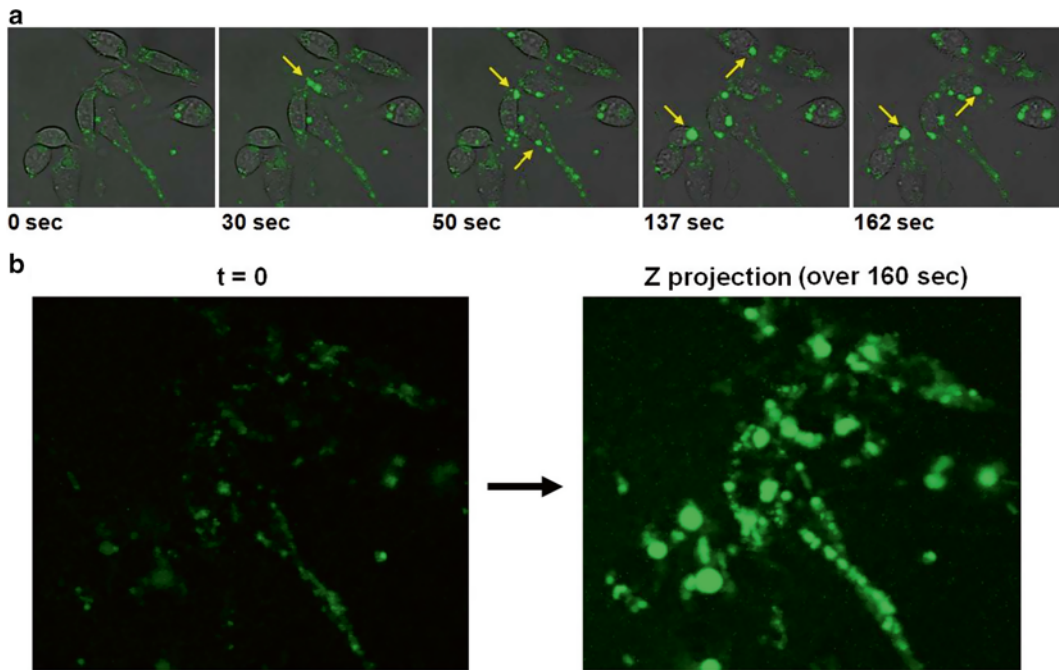


Fig. 4 Imaging of single-cell degranulation events using FITC-dextran. (a) Individual frames taken from ~3 min of imaging RBL-2H3 cells loaded with FITC-dextran and stimulated with Ag. Arrows point to some of the degranulation events taking place in each frame. (b) For initial evaluation of the total degranulation magnitude from cells, a Z projection (integrating 160 s) can be used which shows the sum of all or a range of frames

2. Mast cells: Our experimental system is based on RBL-2H3 mast cells [22]. These mast cells are typically sensitized with monoclonal IgE specific for anti-2, 4-dinitrophenyl (DNP) [23].
3. We typically use coverslip dishes from MatTek Corp. These dishes combine the convenience of disposable plastic petri dishes with the optical quality of glass. Several other brands are available. The dish diameter and glass bottom thickness should be selected based on the dimensions of the microscope in use.
4. This device supplies repeatable pressure pulses for local delivery of a stimulating solution. The system we use requires preparation of pulled capillaries (Parker Hannifin Corp.).
5. There are many thermal/environmental regulation and control systems available for microscopy. For our purposes we found that a simple objective heater (e.g., from BioOptics Inc) provides sufficient control over temperature.
6. Several methods of transfection are available, and Ca^{2+} phosphate is probably the simplest and commonly used. However, for the experiments with GCaMP2 as the Ca^{2+} indicator, we typically use electroporation because of its relatively high efficiency with RBL-2H3 cells.

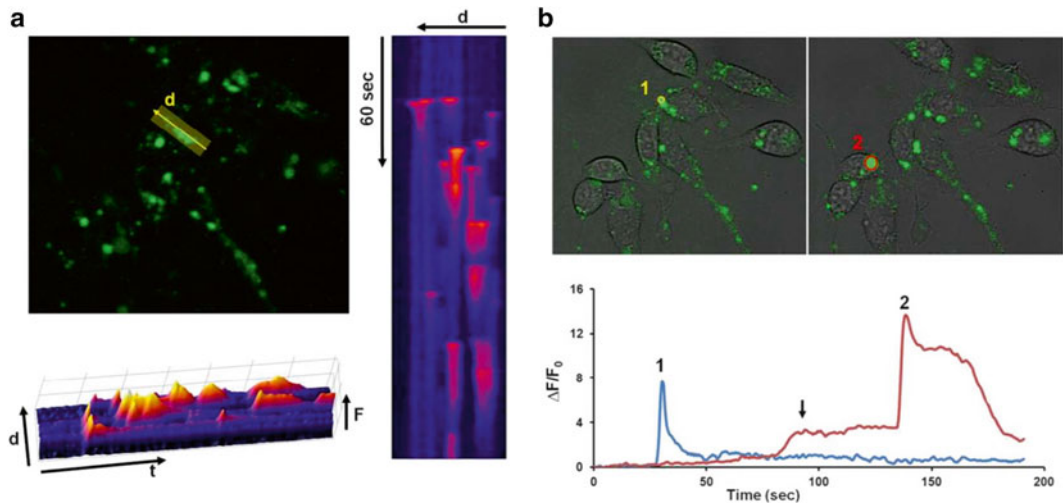


Fig. 5 Quantification of single-cell degranulation events using FITC-dextran. As for Ca^{2+} waves and oscillations, integration of fluorescence intensity over ROI or timeline analysis can be used for quantification of degranulation visualized with FITC-dextran. (a) Timeline analysis (middle panel) over cell of interest (upper left panel, broader yellow line) reveals the spatial and temporal dynamics of degranulation events as they occur along the cell in a single kymograph. Further enhancement of visualization can be achieved by a 3D representation (lower panel). This analysis can be used, for example, to evaluate the spatial distribution of degranulation events across the cell. (b) Integration of fluorescence intensity over individual degranulation events provides a simple tool for quantifying the exocytosis dynamics. Here we show a fast exocytosis event (left panel, 1) and a biphasic degranulation event where the granule undergoes two-step fusion and release of contents (right panel, 2). This method enables detection and distinction between “kiss and run,” “full,” and “compound” types of exocytosis common to mast cells [26]

7. Slower imaging rate might impair the temporal resolution of these events. Faster imaging could provide better resolution, but at the cost of increased photobleaching. Pharmacological reagents can be added to the dish just before initiating data collection or earlier as required. It is not recommended to add any solution during acquisition as it may move the dish and impair imaging.
8. Troubleshooting Ca^{2+} imaging.
 - (a) Ca^{2+} dynamics and temperature: Suboptimal temperature can dramatically reduce the antigen-induced Ca^{2+} response in mast cells and significantly slow its kinetics. To avoid these issues, it is recommended that cells are kept in 37 °C at all times and that temperature of the dish is monitored regularly. Buffers and media to be added should be warmed (37 °C) in advance.
 - (b) Optimization of cell density in single-cell imaging: For single-cell imaging only a few hundred cells per dish are sufficient. We previously showed that protrusions play key functions in mast cell activation [3], and these need sufficient cell-free area to develop and be visualized. In addition,

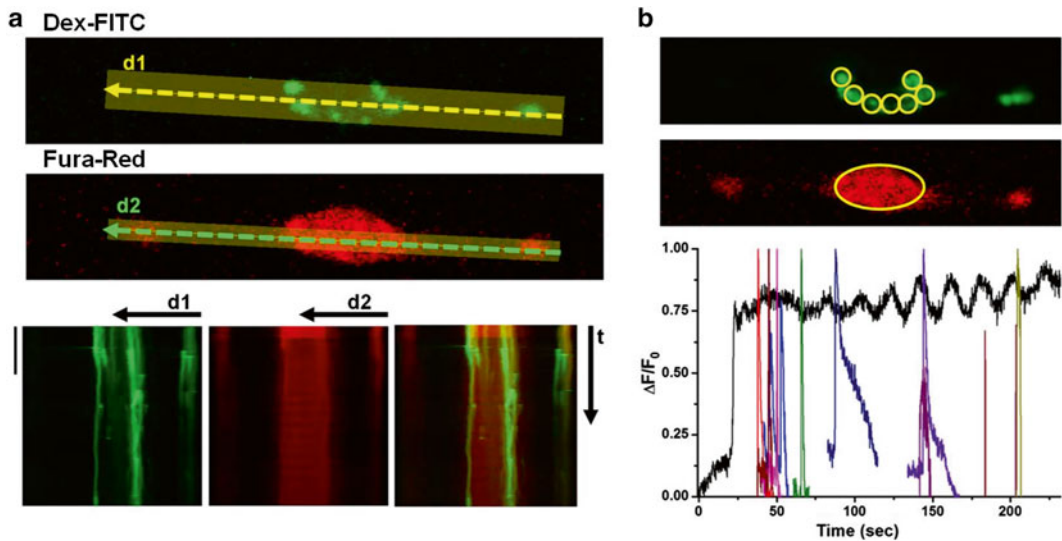


Fig. 6 Simultaneous imaging of Ca^{2+} mobilization and degranulation in cells using Fura Red and FITC-dextran. In these experiments a fluorescent Ca^{2+} indicator (synthetic or GECI) is used in combination with FITC-dextran loaded into to cells. In this case we used Fura Red to measure Ca^{2+} changes. (a) Timeline analysis of Ca^{2+} concentration changes (red) or degranulation (green) channels is shown separately (left and middle lower panels) and combined to create an overlay kymograph (right panel). The overlay kymograph provides temporal and spatial view of the Ca^{2+} changes and degranulation throughout the cell. (b) Integration of fluorescence over ROI in red or green channels provides high temporal resolution of correlated Ca^{2+} mobilization and degranulation events over particular regions of the cell (e.g., protrusions or cell body), as can be seen in the plot of $\Delta F/F_0$ vs. time (lower panel). Black trace shows Ca^{2+} response, and individual colors show different exocytotic events

cell-cell interactions might interfere with Ca^{2+} mobilization. Thus, we recommend plating low numbers of cells when preparing for microscopy experiments, as described.

(c) Optimization of Ca^{2+} dye loading: For reasons described in the first section, we recommend using genetically encoded indicators for mast cell Ca^{2+} imaging. However, using synthetic Ca^{2+} indicator dyes can also provide useful information. For these experiments dye-loading conditions must be optimized including: dye concentration, concentration of leakage inhibitor, sulfinpyrazone, duration, and temperature of incubation. In our hands, using low-affinity Ca^{2+} indicators (such as fluo5F) improves Ca^{2+} responses in the cells and yet provides sufficient resolution and sensitivity.

9. ImageJ functions and plug-ins for analysis and quantification of Ca^{2+} imaging.

(a) Timeline analysis (“virtual linescan” plug-in)—this plug-in is used for generation of kymographs (see Fig. 2a).

(b) Z profiler plug-in—this plug-in can be used for plotting F (intensity) over time (see Fig. 2b).

(c) Interactive 3D Surface Plot—a useful plug-in for generating a more vivid visual representation of fluorescence as a function of time (F/t ; see Fig. 3a lower panel).

(d) All plug-ins can be downloaded directly from ImageJ website (<http://rsbweb.nih.gov/ij/>).

10. Troubleshooting FITC-dextran degranulation imaging.

(a) As for Ca^{2+} imaging, degranulation is highly temperature sensitive, and special care should be taken to make sure cells are maintained at 37 °C at all times.

(b) Sulfinpyrazone used for loading of Ca^{2+} indicator dyes should be avoided in degranulation experiments as it can inhibit of this cellular response.

(c) Increasing FITC-dextran concentration during loading period could improve signal-to-noise ratio under conditions where low degranulation may occur. Up to 4 mg/mL dextran-FITC can be used.

(d) Combining FITC-dextran with a non-pH-sensitive fluorophore conjugated to the dextran (such as Texas Red-dextran) can confirm proper loading into granules. This can also be useful in focusing on the cells (and finding the right field of cells), zooming, or focusing for FITC-dextran imaging. In addition, this combination enables the researcher to follow granule movement in the cells prior to exocytosis.

References

1. Ma HT, Beaven MA (2009) Regulation of Ca^{2+} signaling with particular focus on mast cells. *Crit Rev Immunol* 29(2):155–186
2. Holowka D, Calloway N, Cohen R, Gadi D, Lee J, Smith NL, Baird B (2012) Roles for Ca^{2+} mobilization and its regulation in mast cell functions. *Front Immunol* 3:104. doi: [10.3389/fimmu.2012.00104](https://doi.org/10.3389/fimmu.2012.00104)
3. Cohen R, Torres A, Ma HT, Holowka D, Baird B (2009) Ca^{2+} waves initiate antigen-stimulated Ca^{2+} responses in mast cells. *J Immunol* 183(10): 6478–6488. doi: [10.4049/jimmunol.0901615](https://doi.org/10.4049/jimmunol.0901615)
4. Grynkiewicz G, Poenie M, Tsien RY (1985) A new generation of Ca^{2+} indicators with greatly improved fluorescence properties. *J Biol Chem* 260(6):3440–3450
5. Miyawaki A, Llopis J, Heim R, McCaffery JM, Adams JA, Ikura M, Tsien RY (1997) Fluorescent indicators for Ca^{2+} based on green fluorescent proteins and calmodulin. *Nature* 388(6645):882–887. doi: [10.1038/42264](https://doi.org/10.1038/42264)
6. Tian L, Hires SA, Mao T, Huber D, Chiappe ME, Chalasani SH, Petreanu L, Akerboom J, McKinney SA, Schreiter ER, Bargmann CI, Jayaraman V, Svoboda K, Looger LL (2009) Imaging neural activity in worms, flies and mice with improved GCaMP calcium indicators. *Nat Methods* 6(12):875–881. doi: [10.1038/nmeth.1398](https://doi.org/10.1038/nmeth.1398)
7. Zhao Y, Araki S, Wu J, Teramoto T, Chang YF, Nakano M, Abdelfattah AS, Fujiwara M, Ishihara T, Nagai T, Campbell RE (2011) An expanded palette of genetically encoded Ca^{2+} indicators. *Science* 333(6051):1888–1891. doi: [10.1126/science.1208592](https://doi.org/10.1126/science.1208592)
8. McCombs JE, Palmer AE (2008) Measuring calcium dynamics in living cells with genetically encodable calcium indicators. *Methods* 46(3): 152–159. doi: [10.1016/j.ymeth.2008.09.015](https://doi.org/10.1016/j.ymeth.2008.09.015)
9. Kim TD, Eddlestone GT, Mahmoud SF, Kuchtey J, Fewtrell C (1997) Correlating Ca^{2+} responses and secretion in individual RBL-2H3 mucosal mast cells. *J Biol Chem* 272(50): 31225–31229
10. Crivellato E, Baldini G, Basa M, Fusaroli P (1993) The three-dimensional structure of interdigitating cells. *Ital J Anat Embryol* 98(4): 243–258

11. Demitsu T, Kiyosawa T, Kakurai M, Murata S, Yaoita H (1999) Local injection of recombinant human stem cell factor promotes human skin mast cell survival and neurofibroma cell proliferation in the transplanted neurofibroma in nude mice. *Arch Dermatol Res* 291(6): 318–324
12. Metcalfe DD, Baram D, Mekori YA (1997) Mast cells. *Physiol Rev* 77(4):1033–1079
13. Blank U (2011) The mechanisms of exocytosis in mast cells. *Adv Exp Med Biol* 716:107–122. doi:[10.1007/978-1-4419-9533-9_7](https://doi.org/10.1007/978-1-4419-9533-9_7)
14. Chapman, E. R. (2008). “How does synaptotagmin trigger neurotransmitter release?” *Annual review of biochemistry* 77:615–641
15. Naal RM, Tabb J, Holowka D, Baird B (2004) In situ measurement of degranulation as a bio-sensor based on RBL-2H3 mast cells. *Biosens Bioelectron* 20(4):791–796. doi:[10.1016/j.bios.2004.03.017](https://doi.org/10.1016/j.bios.2004.03.017)
16. Gadi D, Wagenknecht-Wiesner A, Holowka D, Baird B (2011) Sequestration of phosphoinositides by mutated MARCKS effector domain inhibits stimulated Ca(2+) mobilization and degranulation in mast cells. *Mol Biol Cell* 22(24): 4908–4917. doi:[10.1091/mbc.E11-07-0614](https://doi.org/10.1091/mbc.E11-07-0614)
17. Hohman RJ, Dreskin SC (2001) Measuring degranulation of mast cells. In: John E. Coligan et al (eds). *Current protocols in immunology*. Chapter7:Unit7;26.doi:[10.1002/0471142735.im0726s08](https://doi.org/10.1002/0471142735.im0726s08)
18. Kawasaki Y, Saitoh T, Okabe T, Kumakura K, Ohara-Imaizumi M (1991) Visualization of exocytotic secretory processes of mast cells by fluorescence techniques. *Biochim Biophys Acta* 1067(1):71–80
19. Williams RM, Webb WW (2000) Single granule pH cycling in antigen-induced mast cell secretion. *J Cell Sci* 113(Pt 21):3839–3850
20. Jaiswal JK, Fix M, Takano T, Nedergaard M, Simon SM (2007) Resolving vesicle fusion from lysis to monitor calcium-triggered lysosomal exocytosis in astrocytes. *Proc Natl Acad Sci U S A* 104(35):14151–14156. doi:[10.1073/pnas.0704935104](https://doi.org/10.1073/pnas.0704935104)
21. Williams RM, Shear JB, Zipfel WR, Maiti S, Webb WW (1999) Mucosal mast cell secretion processes imaged using three-photon microscopy of 5-hydroxytryptamine autofluorescence. *Biophys J* 76(4):1835–1846. doi:[10.1016/S0006-3495\(99\)77343-1](https://doi.org/10.1016/S0006-3495(99)77343-1)
22. Barsumian EL, Isersky C, Petrino MG, Siraganian RP (1981) IgE-induced histamine release from rat basophilic leukemia cell lines: isolation of releasing and nonreleasing clones. *Eur J Immunol* 11(4):317–323. doi:[10.1002/eji.1830110410](https://doi.org/10.1002/eji.1830110410)
23. Posner RG, Lee B, Conrad DH, Holowka D, Baird B, Goldstein B (1992) Aggregation of IgE-receptor complexes on rat basophilic leukemia cells does not change the intrinsic affinity but can alter the kinetics of the ligand-IgE interaction. *Biochemistry* 31(23): 5350–5356
24. Collins TJ (2007) ImageJ for microscopy. *Biotechniques* 43(1 Suppl):25–30
25. Bonifacino JS, Yuan L, Sandoval IV (1989) Internalization and recycling to serotonin-containing granules of the 80K integral membrane protein exposed on the surface of secreting rat basophilic leukaemia cells. *J Cell Sci* 92(Pt 4):701–712
26. Cohen R, Corwith K, Holowka D, Baird B (2012) Spatiotemporal resolution of mast cell granule exocytosis reveals correlation with Ca²⁺ wave initiation. *J Cell Sci* 125(Pt 12): 2986–2994. doi:[10.1242/jcs.102632](https://doi.org/10.1242/jcs.102632)

Chapter 23

Flow Cytometry-Based Monitoring of Mast Cell Activation

Glenn Cruse, Alasdair M. Gilfillan, and Daniel Smrz

Abstract

Mast cell activation is a central process in the initiation of allergic disorders. As described elsewhere in this volume, this process can be readily monitored by biochemical, antibody-based, and enzyme-based formats when the cell population examined is homogenous. When dealing with mixed and transfected cell populations however, such approaches may not be appropriate. Hence alternative methods are required. Here we describe flow-cytometry-based assays that can be utilized to examine signaling processes and degranulation in both pure mast cell populations and, following appropriate selection, in populations where the mast cells of interest may only represent a fraction of the total cell population.

Key words Mast cell, Signaling, Protein phosphorylation, Calcium signal, Actin polymerization/depolymerization, Degranulation, Flow cytometry

Abbreviations

Fc ϵ RI	High-affinity IgE receptor
IP ₃	Inositol trisphosphate
F actin	Filamentous actin
GFP	Green fluorescent protein
rhSCF	Recombinant human stem cell factor
dH ₂ O	Distilled or deionized H ₂ O
BSA	Bovine serum albumin
PFA	Paraformaldehyde
PBS	Phosphate-buffered saline
DNP	Dinitrophenol
HSA	Human serum albumin
APC	Allophycocyanin
DMSO	Dimethylsulfoxide
BMMC	Bone marrow-derived mast cell
FITC	Fluorescein isothiocyanate
PE	Phycoerythrin

1 Introduction

Receptor-mediated mast cell activation occurs through a complex cascade of intracellular signaling processes culminating in degranulation and the generation and release of eicosanoids, cytokines, chemokines, and growth factors [1]. With regard to antigen/IgE-induced mediator release, the initiating response is aggregation of the high-affinity receptors for IgE (Fc ϵ RI) with resulting phosphorylation of critical tyrosine residues contained within the immunoreceptor-based tyrosine activation motifs (ITAMs) of the Fc ϵ RI β and γ chains [2]. These events result in the recruitment and subsequent activation of the ZAP-70-related tyrosine kinase Syk which, in turn, phosphorylates a series of adaptor molecules and other signaling proteins critical for propagation of the signals required for the release of the various classes of inflammatory mediators [3]. Thus, phosphorylation of key signaling molecules within the mast cell activation cascade has been used as an index of their activation. The advent of the generation of antibodies which uniquely recognize the phosphorylated, but not non-phosphorylated, forms of these signaling proteins has allowed monitoring of specific signaling events by immunoblot analysis. The efficacy of this approach is however dependent on the affinity and selectivity of the antibody, the abundance of the protein, and the purity of the cell populations. Nevertheless, this approach has proved to be a relatively sensitive and effective technique for assessing critical intracellular signaling events.

Downstream of these events, an increase in the cytosolic calcium concentration is essential for subsequent events leading to the release of the inflammatory mediators [4]. This calcium signal is primarily produced as a consequence of liberation of calcium from the endoplasmic reticulum in response to inositol trisphosphate (IP₃) liberated from phosphatidylinositol 4,5 bisphosphate by the action of phospholipase C. As a consequence of emptying of these intracellular stores, a secondary, more prolonged elevation of cytosolic calcium is produced via store-operated calcium entry. The calcium signal can be either monitored in cell populations or in single cells using calcium-chelating fluorescence probes such as Indo-1, Fura-2, Fluo-3, and Fluo-4.

For exocytosis of the cytoplasmic granules to proceed, rearrangement of the cytoskeleton through actin depolymerization/repolymerization is required [5, 6]. The toxin phalloidin, isolated from the death cap mushroom, *Amanita phalloides*, has the ability to bind to polymerized filamentous (F)-actin allowing monitoring of changes in the polymerized state of actin, once the phalloidin is conjugated to a suitable fluorescent moiety. This can be done by both fluorescent/confocal microscopy and flow cytometry.

As discussed above, and elsewhere in this volume, the aforementioned signal transduction processes and events leading

to, and including, degranulation can readily be assessed in pure mast cell populations by immunoblot analysis and by a variety of biochemical approaches. However there are specific circumstances where these approaches need to be refined to increase sensitivity or selectivity of the assays, for example, where mast cells may represent only a fraction of the total cell population or where efficiency of transfection is such that only a fraction of cells are accordingly genetically modified. Examples of the former would be the mixed cell population in peritoneal lavage which normally would require purification and/or further culture prior to conducting appropriate studies, and of the latter, where a green fluorescent protein (GFP)-tagged signaling molecule is overexpressed, but only in a proportion of the total cells. In the aforementioned cases the mast cell population can be selected by flow cytometry based on KIT (CD117) or Fc ϵ RI expression or by expression of GFP, and then signaling processes or degranulation in these cells assessed.

In this chapter, we describe a number of flow cytometry-based assays to monitor mast cell activation that can be used to examine events in relatively pure cell populations or, following selection, relatively impure cell populations. These protocols can be adapted for mast cells from both rodent and human origin.

2 Materials

2.1 Monitoring Signaling in Mast Cells by PhosFlow

1. StemPro-34 complete medium (GIBCO, Grand Island, NY): 13 mL StemPro-34 Nutrient Supplement, L-glutamine (2 mM), penicillin G (100 IU/mL), streptomycin (100 μ g/mL) in StemPro-34 serum-free medium.
2. Recombinant human stem cell factor (rhSCF).
3. Biotin-conjugated human myeloma IgE (*see Note 1*).
4. Streptavidin.
5. HEPES buffer: 10 mM HEPES, 137 mM NaCl, 2.7 mM KCl, 0.4 mM Na₂HPO₄·7H₂O, 5.6 mM glucose, 1.8 mM CaCl₂·2H₂O, 1.3 mM Mg²⁺ (as MgCl₂ or MgSO₄) in distilled or deionized H₂O (dH₂O).
 - (a) To make 1 L: Dissolve components *except* the calcium and magnesium salts in 900 mL dH₂O (2.38 g HEPES, 8.00 g NaCl, 0.200 g KCl, 0.103 g Na₂HPO₄·7H₂O, 1.008 g glucose).
 - (b) Adjust pH to 7.4 using concentrated NaOH or HCl.
 - (c) Add 0.265 g of CaCl₂·2H₂O and 1.3 mL of a 1 M MgCl₂ solution.
 - (d) Adjust volume to 1 L with dH₂O.
 - (e) Sterilize by filtration (pore size: 0.22 μ M) and store at 4 °C.

6. HEPES buffer with bovine serum albumin (BSA): 0.04 % (w/v) BSA in HEPES buffer (prepare fresh). Add 0.04 g BSA (>96 % purity) to 100 mL HEPES buffer. Warm up to 37 °C and mix well.
7. Fixation solution #1 (prepare fresh): 4 % (w/v) paraformaldehyde (PFA) in PBS. Add 1 mL of a 20 % (w/v) PFA solution (200 mg/mL prepared in dH₂O) to 4 mL PBS.
8. Appropriately labeled phosphorylation-specific antibody (*see Note 2*).
9. 5 mL polystyrene round-bottom tubes.
10. Amaxa Nucleofector cell line Nucleofection kit V (Lonza, Switzerland).
11. Flow cytometer with 488 nm excitation laser and detector for green (filter: 530/30) and orange-red (filter: 585/42) emission.

2.2 Calcium Response Kinetics

1. Mouse anti-dinitrophenyl (DNP) IgE, clone SPE-7.
2. DNP-human serum albumin (HSA).
3. Allophycocyanin (APC) anti-mouse CD117 antibody, 0.2 mg/mL.
4. Fluo-is 4 solution (50× concentrated): 0.456 mM (0.5 mg/mL) in dimethyl sulfoxide (DMSO). Dissolve 50 µg Fluo-4, AM in 100 µL DMSO. Store in aliquots at -70 °C.
5. 125 mM Probenecid solution (50× concentrated) (pH 7.4): Dissolve 356.7 mg in 9 mL 0.2 M NaOH solution (in dH₂O). Adjust pH to 7.4 using concentrated HCl or NaOH solution. Adjust volume to 10 mL with dH₂O and then sterilize by filtration (0.22 µM pore size). Store at room temperature (RT).
6. Fluo-4 labeling solution: 9.12 µM (10 µg/mL) Fluo-4, 2.5 mM probenecid, and 0.25 µg/mL APC anti-mouse CD117 in HEPES/BSA. Add 20 µL 50× concentrated Fluo-4 solution, 40 µL 50× concentrated probenecid solution, and 1.2 µL APC anti-mouse CD117 to 939 µL HEPES/BSA.
7. Fluo-4 washing solution: 2.5 mM probenecid in HEPES/BSA (prepare fresh). Add 400 µL 50× concentrated probenecid solution to 9.6 mL HEPES/BSA.
8. 5 mL polystyrene round-bottom tubes.
9. Flow cytometer with 488 nm and 635 nm excitation lasers and detectors for green (filter: 530/30) and red (filter: 661/16) emission.

2.3 Actin Polymerization/ Depolymerization Kinetics

1. Materials for bone marrow-derived mast cell (BMMC) culture and sensitization (*see Note 3*).
2. Fluorescein isothiocyanate (FITC)-phalloidin.
3. APC anti-mouse CD117 antibody, 0.2 mg/mL.

4. HEPES/BSA buffer.
5. 0.2 M EGTA (pH 8): Add 7.6 g EGTA and ~6–7 mL 10 N NaOH solution to 90 mL ddH₂O. Adjust pH to 8 with conc. NaOH (or HCl). Once the EGTA is completely dissolved then top up to 100 mL volume.
6. 0.5 M EDTA (pH 8): Add 104.05 g Na₂EDTA ·2H₂O (disodium EDTA dihydrate) to 400 mL ddH₂O. Gradually add 9–10 g NaOH pellets (or ~50 mL 1 N NaOH solution) until the EDTA is dissolved. Adjust pH to 8.0 and top of volume to 500 mL.
7. Fixation solution #2 (prepare fresh): 4 % (w/v) PFA, 5 mM EGTA, 5 mM EDTA in PBS. Add 1 mL 20 % (w/v) PFA solution (prepared in dH₂O), 125 µL 0.2 M EGTA and 50 µL 0.5 M EDTA to 3.83 mL PBS.
8. Incubation solution: 5 mM EGTA, 5 mM EDTA, 2 % (w/v) BSA in PBS (prepare fresh). Dissolve 20 mg BSA in 945 µL PBS. Add 25 µL 0.2 M EGTA, 10 µL 0.5 M EDTA.
9. Saponin solution (50× concentrated): 20 mg saponin in 980 µL dH₂O (prepare fresh).
10. F-actin labeling solution: 1 µg/mL FITC-phalloidin, 0.25 µg/mL APC anti-mouse CD117 antibody, 0.01 % (w/v) saponin in incubation solution. Add 1 µL FITC-phalloidin PBS solution (1 mg/mL), 1.2 µL APC anti-mouse CD117, and 20 µL 50× concentrated saponin solution to 978 µL incubation solution.
11. Flow cytometer with 488 and 635 nm excitation lasers and detectors for green (filter: 530/30) and red (filter: 661/16) emission.

2.4 Degranulation Kinetics

1. Materials for LAD2 culture and sensitization in Subheading 2.1.
2. Materials for BMMC culture and sensitization (*see Note 3*).
3. Phycoerythrin (PE) anti-human LAMP-2 antibody [H4B4].
4. FITC anti-mouse IgE antibody, 0.5 mg/mL.
5. PE anti-mouse CD117 antibody, 0.2 mg/mL.
6. APC anti-mouse CD107b (LAMP-2) antibody, 0.1 mg/mL.
7. HEPES/BSA buffer.
8. Incubation solution: 20 mM EGTA, 20 mM EDTA, 0.2 % (w/v) BSA in PBS (prepare fresh). Add 100 µL 0.2 M EGTA, 40 µL 0.5 M EDTA, and 20 mg BSA to 860 µL PBS.
9. Labeling solution (for BM MCs): 1.25 µg/mL FITC anti-mouse IgE antibody, 0.5 µg/mL PE anti-mouse CD117 antibody, 1 µg/mL APC anti-mouse CD107b (LAMP-2) antibody prepared in incubation solution (prepare fresh).
10. Labeling solution (for LAD2): Dilute PE anti-human CD107b (LAMP-2) antibody 1:100 in incubation solution (prepare fresh).

11. 5 mL polystyrene round-bottom tubes.
12. Flow cytometer with 488 and 635 nm excitation lasers and detectors for green (filter: 530/30), orange (filter: 585/42), and red (filter: 661/16) emission.

3 Methods

3.1 PhosFlow

The analysis of mast cell signaling by flow cytometry can be utilized when transfection of a protein is desired. Mast cells are difficult to transfect and efficiency is generally too low for conventional immunoblots. Thus, flow cytometry can be utilized for the analysis of populations positive for a marker such as GFP. This protocol describes the method for the human mast cell line LAD2, but this method could be adapted for mast cells from other origins.

Transfection of LAD2 Cells with Constructs Labeled with GFP (See Note 4)

1. Remove 2×10^6 LAD2 cells from culture for each transfection and place into a 15 mL centrifuge tube (see Note 5).
2. Centrifuge at $90 \times g$ for 10 min at RT with the brake turned off and aspirate the supernatant.
3. Gently resuspend the pellet in 10 mL of pre-warmed (37 °C) PBS/0.1 % BSA and centrifuge at $90 \times g$ for 10 min at RT with the brake turned off.
4. Aspirate the supernatant and repeat step 3.
5. Aspirate the supernatant, ensuring that as much is removed as possible, and resuspend the cells in 100 μ L of pre-warmed (37 °C) nucleofection solution V with supplement added.
6. Add 2 μ g of high-concentration plasmid DNA to the cells and transfer to a nucleofector cuvette (see Note 6).
7. Run the appropriate nucleofector program (see Note 7).
8. Using a nucleofector pipette, transfer the cells to 4 mL of pre-warmed (37 °C) StemPro-34 medium containing supplement and 100 ng/mL rhSCF in a 6-well plate and transfer to the incubator (Note 8).

Analysis of Signaling in Transfected Cells

1. Sensitize the LAD2 cells with 100 ng/mL biotinylated human myeloma IgE overnight (16 h) in StemPro-34 medium plus supplement, but without rhSCF (see Note 8).
2. Following the incubation, wash the cells by centrifugation ($250 \times g$ for 5 min) with 2 mL of HEPES/BSA buffer pre-warmed to 37 °C and aspirate the supernatant.
3. Repeat step 2.
4. After the final wash, resuspend the cells in pre-warmed HEPES/BSA buffer to give a final concentration of $2-5 \times 10^5$ cells in 450 μ L (Note 9).

5. Transfer 450 μ L of cell suspension to separate 5 mL polystyrene round-bottom tube and place in a heating block or water bath set to 37 °C.
6. Allow the cells to equilibrate by incubating in the heating block for 5 min.
7. Add 50 μ L of 10 \times pre-warmed (37 °C) activation solution (streptavidin, rhSCF, etc.), start a timer, and quickly swirl the tube before placing it back into the heating block.
8. Incubate for the desired time.
9. Stop the reaction by removing the tube and plunging it directly into ice.
10. Immediately add 1 volume (500 μ L) of ice-cold fixative solution.
11. Incubate on ice for 40 min (*see Note 10*).
12. After fixation, centrifuge the cells at 300 \times g for 8 min at 4 °C and aspirate the supernatant.
13. Wash the cells with 2 mL of PBS/0.1 % BSA and centrifuge at 300 \times g for 5 min at 4 °C.
14. Aspirate the supernatant and repeat **step 13**.
15. Aspirate the supernatant and resuspend the cells in 1 mL of very cold 100 % methanol (stored at -20 °C and added directly).
16. Cap the tubes and place in the freezer (-20 °C) for >4 h.
17. Centrifuge the tubes at 300 \times g for 5 min at 4 °C and discard the supernatant.
18. Wash the cells with 2 mL of ice-cold PBS/0.5 % BSA and centrifuge at 300 \times g for 5 min at 4 °C.
19. Discard the supernatant and repeat **step 18**.
20. Discard the supernatant and resuspend the cells in 195 μ L of ice-cold PBS/0.5 % BSA.
21. Add 5 μ L of PhosFlow PE-conjugated antibody and incubate on ice for >1 h.
22. After the incubation, add 1.8 mL of PBS/0.5 % BSA to each tube and centrifuge at 300 \times g for 5 min at 4 °C.
23. Discard the supernatant and repeat **step 22** twice.
24. Discard the supernatant and resuspend the cells in 200 μ L of PBS/0.1 % BSA.
25. Run samples on the flow cytometer.

The analysis of phosphorylation by flow cytometry has been shown to correlate well with immunoblots [7]. For the analysis of results, a tight gate should be set on the mast cell population to

eliminate cell debris, and then a secondary gate should be set on the subpopulation of GFP-positive cells (FL1). The FL2 fluorescence can be plotted in the GFP-positive cell population. As an additional control, the FL2 fluorescence can be plotted in the GFP-negative cell population.

A typical example of the phosphorylation of the critical signaling molecules Akt and ERK responses to SCF challenge is shown in Fig. 1.

3.2 Calcium Response Kinetics

The flow cytometry analysis of the calcium response in antigen-stimulated mast cells can be utilized when the mast cell population represents only a fraction of the analyzed cells, or a population of mast cells transfected with a fluorogenic marker, such as GFP. This protocol describes the method for monitoring the calcium response of KIT⁺ (CD117⁺) population in IgE-sensitized and antigen-stimulated mouse peritoneal cells (*see Note 11*).

1. Sensitize mouse by peritoneal injection with 0.5 mL mouse anti-DNP IgE solution in PBS (2 µg/mL) at days 4 and 2 before peritoneal lavage.
2. Isolate mouse peritoneal cells by peritoneal lavage using 3–5 mL HEPES/BSA buffer and transfer the cell suspension into 5 mL polystyrene round-bottom tubes (*see Note 12*).
3. Centrifuge the cells (200–300 $\times g$ for 5 min at RT) and aspirate the supernatant.
4. Gently resuspend the cells in 0.5 mL of Fluo-4-labeling solution and incubate at RT for 30 min in the dark.
5. Centrifuge the cells (200–300 $\times g$ for 5 min at RT), aspirate the supernatant, and gently resuspend in 1–4 mL Fluo-4 washing solution (1 mL per sample).
6. Divide the suspension into 1–4 samples and keep at RT in the dark until further processed.
7. Spin the individual sample (200–300 $\times g$, 5 min, RT), aspirate the supernatant, and resuspend in 250 µL HEPES/BSA buffer; temperate the cells at 37 °C for 2–5 min.
8. Record FL1 fluorescence of the gated (CD117⁺) population on flow cytometer at 37 °C for 1 min, then quickly add 200 µL 2× activator (DNP-HSA) in HEPES/BSA buffer (pre-warmed to 37 °C), and continue recording the fluorescence at 37 °C for an additional 5 min (*see Note 13*).
9. Repeat steps 7 and 8 for the remaining samples.

A typical example of calcium responses is shown in Fig. 2.

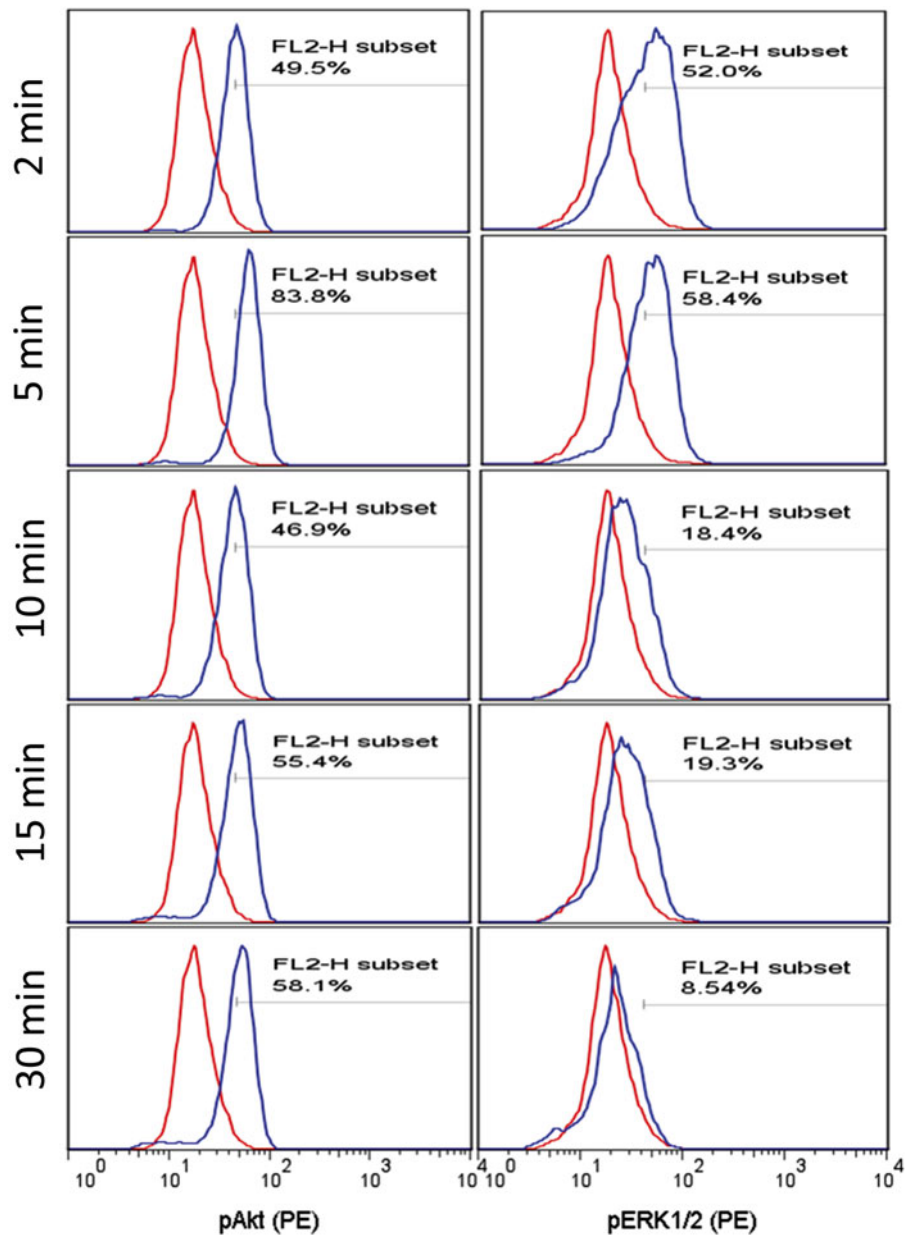


Fig. 1 Phosphorylation of Akt and ERK in LAD2 cells. A time course of phosphorylation in LAD2 cells following stimulation with SCF using phosphorylation flow cytometry demonstrating that Akt phosphorylation was sustained over 30 min, but ERK phosphorylation was more transient. Both Akt and ERK phosphorylation peaked at 5 min. The *red line* demonstrates staining with non-stimulated cells. The *blue line* overlays demonstrate staining at the indicated time point following SCF (100 ng/mL) stimulation

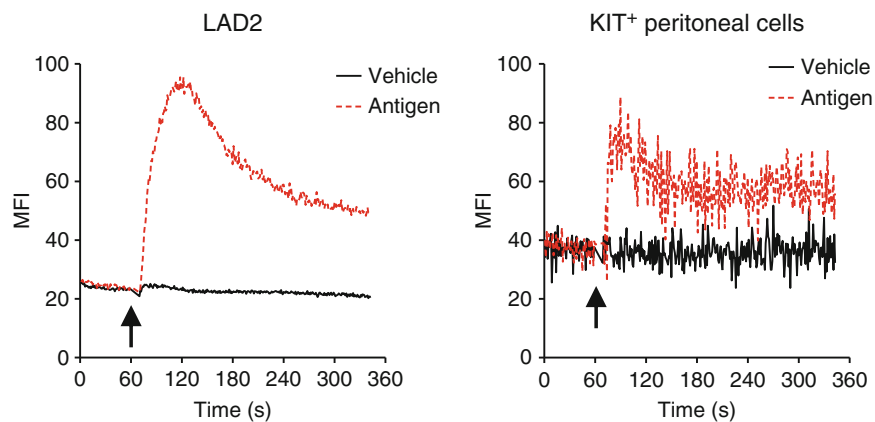


Fig. 2 Calcium response of activated mast cells. A calcium response of IgE-sensitized LAD2 mast cell line or KIT⁺ population of peritoneal cells to IgE cross-linkers (Antigen), respectively, streptavidin (100 ng/mL) or DNP-HSA (100 ng/mL). The cells were labeled by Fluo-4-AM and fluorescence intensity (MFI geometric mean fluorescence intensity) was monitored by flow cytometry before and after cell activation. The arrow indicates time of cell challenge

3.3 Actin Polymerization/Depolymerization Kinetics

The flow cytometry analysis of actin polymerization/depolymerization in antigen-stimulated mast cells can be utilized both in a homogeneous cell population and in mast cell population that represents only a fraction of the analyzed cells or a population of transfected mast cells with a fluorogenic marker. This protocol describes the method for monitoring actin polymerization/depolymerization in homogeneous cell populations of IgE-sensitized and antigen-stimulated BMMCs (see Note 14).

1. Centrifuge at least 1×10^5 IgE-sensitized cells ($200\text{--}300 \times g$, 5 min, RT) and remove the media by aspiration.
2. Gently resuspend the cells in 1–5 mL HEPES/BSA buffer.
3. Centrifuge the cells as in **step 1** and remove the buffer by aspiration.
4. Repeat **steps 2 and 3**.
5. Gently resuspend the cells in HEPES/BSA buffer to a concentration of $0.5\text{--}1.0 \times 10^6/\text{mL}$.
6. Transfer the cell suspension (defined as volume γ) to 5 mL polystyrene round-bottom tubes and temperate the cells at 37 °C for 2–10 min.
7. Add an equal volume (volume γ) of 2× activator (e.g., antigen) in HEPES/BSA buffer (pre-warmed to 37 °C) and activate at 37 °C for different period of times.
8. Stop activation by addition of $10 \times \gamma$ volume of the fixation solution and incubate at RT for 20 min. Gently agitate the cell suspension every 5 min to avoid formation of aggregates.

9. Centrifuge the cells ($400\text{--}600 \times g$, 5 min, RT).
10. Discard the supernatant, resuspend the cells in the incubation solution, and centrifuge ($400\text{--}600 \times g$, 5 min, RT).
11. Discard the supernatant, resuspend the cells in the F-actin-labeling solution, and incubate at RT for 1 h in the dark.
12. Centrifuge the cells ($400\text{--}600 \times g$, 5 min, RT).
13. Discard the supernatant and resuspend in the $10\times$ diluted incubation solution in PBS.
14. Repeat **steps 12 and 13**.
15. Analyze the cells in the suspension by flow cytometry within 60 min.

3.4 Degranulation Kinetics

The flow cytometry analysis of cell degranulation in antigen-stimulated mast cells can be utilized both in homogeneous cell populations and in mast cell populations that represent only a fraction of the analyzed cells, or in a population of transfected mast cells expressing a fluorogenic-tagged protein. This protocol describes the method for monitoring degranulation kinetics in a homogeneous cell population of IgE-sensitized and antigen-stimulated LAD2 cells and BMMCs.

1. Centrifuge at least 3×10^5 IgE-sensitized cells ($200\text{--}300 \times g$, 5 min, RT) and remove the media by aspiration.
2. Gently resuspend the cells in 1–5 mL HEPES/BSA buffer.
3. Centrifuge the cells as in **step 1** and remove the buffer by aspiration.
4. Repeat **steps 2 and 3**.
5. Gently resuspend the cells in HEPES/BSA buffer to a concentration of $0.5\text{--}1.0 \times 10^6$ cells/mL (the final volume of the cell suspension defined as volume Υ) (see **Note 15**).
6. Transfer the cell suspension to 5 mL polystyrene round-bottom tubes and temperate the cells at 37°C for 2–10 min.
7. Add an equal volume (volume Υ) of $2\times$ activator (DNP-HSA) in HEPES/BSA buffer (pre-warmed to 37°C) and activate at 37°C for different period of times.
8. Stop activation by addition of equal volume ($2 \times \Upsilon$) of the labeling solution and incubate at RT for 30–60 min.
9. Analyze the cells in the suspension by flow cytometry within 60 min (see **Note 16**).

A typical example of degranulation kinetics is shown in Fig. 3.

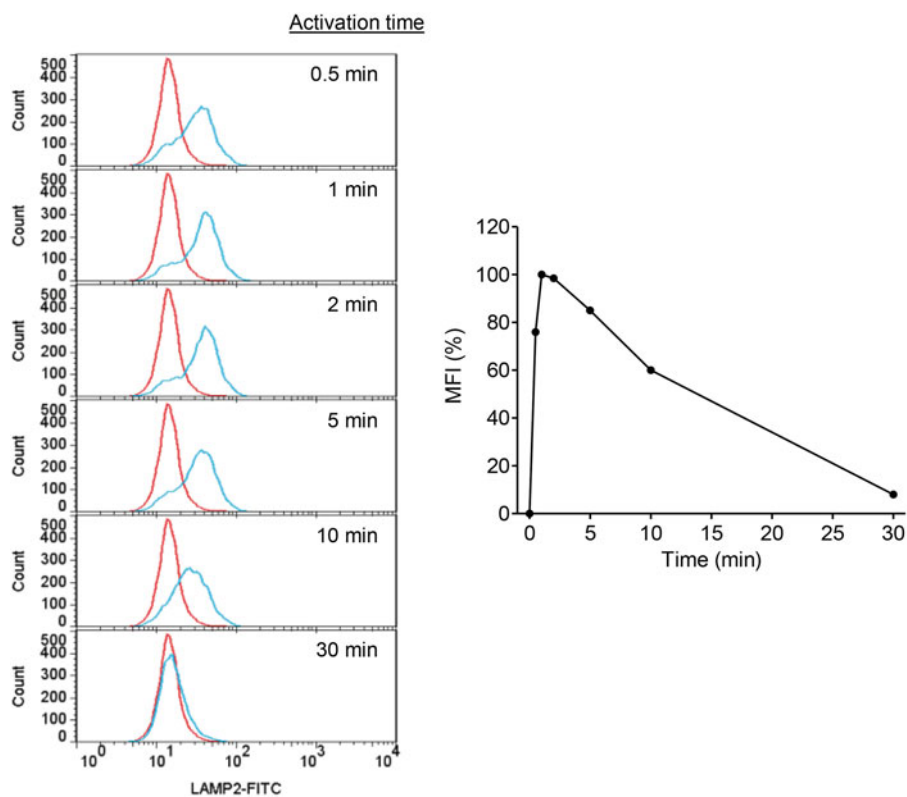


Fig. 3 LAMP-2 externalization kinetics in activated mast cells. A LAMP-2 externalization of gE-sensitized and antigen (streptavidin, 100 ng/mL)-activated LAD2 mast cell line. The externalization was detected by FITC-labeled LAMP-2-specific antibody and fluorescence intensities (*MFI* geometric mean fluorescence intensity) of non-activated (red) and activated cells (blue) were normalized to maximal response (*right*)

4 Notes

1. Biotinylation as described [8] or by use of an appropriate commercially available biotinylation kit.
2. In this chapter we describe the use of PE mouse anti-human phosphorylated ERK1/2 (pT202/Y204) and mouse anti-human phosphorylated Akt (pS473) PhosFlow antibodies. The antibodies used in this chapter represent well-characterized proteins in mast cell signaling. A variety of alternative antibodies are available for other signaling molecules. However, the specificity of the antibody is critical. Thus only well-characterized, highly specific, and validated antibodies should be used and adequate controls should always be included. Validation of the flow cytometry data with western blots should be carried out in control cells to establish the reliability of the antibodies prior to carrying out experiments with transfected populations.

3. Materials for BMMC culture and sensitization have been described previously [9].
4. The transfection of mast cells can be achieved using several approaches. This method describes the use of the Amaxa Nucleofector II. The process is quite harsh on the cells. Thus cells should be fed 24–48 h prior to transfection to ensure a healthy population. LAD2 cells should be cultured as described [10].
5. The optimal cell number for nucleofection may vary depending on the type of mast cells used. However, for LAD2 cells 2×10^6 is optimal.
6. The transfection of appropriate controls should always be included. For example, the empty GFP vector should be included. Extra tubes should be set up for each experiment to allow correct setting of the compensation for the flow cytometer. Unstained and untreated cells should be run as well as unstained tubes for each transfection (GFP positive but not stained for PE). Isotype controls and PE-stained GFP-negative cells should also be included. Each GFP construct will differ in fluorescence depending on the characteristics of the tagged protein. Thus each construct may need to be set up independently if fluorescence varies greatly.
7. The nucleofector program will vary according to the mast cell type used. For human mast cell lines, T-020, T-030, and X-001 have all been used. Optimization should be carried out for each cell type.
8. After transfection, it is recommended to culture the cells in complete medium to allow recovery from the procedure. It is not recommended to perform the cytokine withdrawal directly after nucleofection. Withdrawal of rhSCF is required for these assays since rhSCF induces significant signaling, but the cells should be given a minimum of 6 h in complete medium to recover before withdrawal of rhSCF.
9. The number of cells required for each condition will vary depending upon the efficiency of transfection for the different constructs. Each construct will differ in efficiency (even when using the same plasmid). Thus, to get enough cells in the GFP-positive population with a construct that transfests poorly, it will be necessary to increase the total number of cells. All of the transfections from each set of experiments should contain the same number of cells, so the number of cells per condition should be set from the construct with the lowest transfection efficiency.
10. Methanol will disrupt the conformation of GFP and consequently diminish fluorescence, so it should not be used to fix the cells. It is therefore necessary to adequately fix the cells with PFA (>30 min). This fixation will reduce the loss of fluorescence with methanol treatment. If the fluorescence is very

low, then other forms of permeabilization can be used, such as Triton X-100, which will not diminish fluorescence. However, these alternative permeabilization methods will reduce the signal on flow cytometry and do not work as well as methanol. If the cells are adequately fixed in PFA then loss of fluorescence with methanol is minimized.

11. In this example protocol we use KIT⁺ (CD117⁺) peritoneal cells as our mixed population. This method could also be applied to other various mast cell populations. All studies conducted in our laboratory mice and on mouse BMMCs are done so under a protocol (LAD2) approved by the Institutional Animal Care and Use Committee at NIH.
12. It is crucial to use the polystyrene tubes throughout the procedures as other polymers, such as polypropylene, cause strong attachment and possible activation of the processed cells. This leads to significant or even complete loss of the cells and their quality during the procedures.
13. The cell population of interest must be gated before the measurement and the basal fluorescence of the entire population must be on the scale. The wider the fluorescence peak of the population, the higher the basal level is required. As many flow cytometers are not equipped with a tempering system to keep the tube with cells at 37 °C, use a beaker or a thermo-beaker with 37 °C warm water instead to encase and temperate the tube with cells during the acquisition by flow cytometer.
14. In this example protocol, we use BMMCs, but this protocol could be modified for any mast cell type and can be used to study actin dynamics in mixed populations with the use of appropriate markers and gating.
15. The volume of cell suspension can vary depending on number of cells analyzed and number of cells available. The convenient volume is 50–200 µL.
16. The parameters of cell activation are sufficiently stable in the final suspensions. However, to ensure that there are no alterations in these parameters during the time of sample analysis, it is recommended to always re-measure the first measured sample also at the end of the measurement procedure.

Acknowledgement

Financial support for work in the authors' laboratory was provided by the Division of Intramural Research of NIAID within the National Institutes of Health.

References

1. Gilfillan AM, Tkaczyk C (2006) Integrated signalling pathways for mast-cell activation. *Nat Rev Immunol* 6(3):218–230
2. Kraft S, Kinet JP (2007) New developments in Fc ϵ RI regulation, function and inhibition. *Nat Rev Immunol* 7(5):365–378
3. Gilfillan AM, Rivera J (2009) The tyrosine kinase network regulating mast cell activation. *Immunol Rev* 228(1):149–169
4. Ma HT, Beaven MA (2009) Regulation of Ca $^{2+}$ signaling with particular focus on mast cells. *Crit Rev Immunol* 29(2):155–186
5. Pendleton A, Koffer A (2001) Effects of latrunculin reveal requirements for the actin cytoskeleton during secretion from mast cells. *Cell Motil Cytoskeleton* 48(1):37–51
6. Tolarová H, Dráberová L, Heneberg P, Dráber P (2004) Involvement of filamentous actin in setting the threshold for degranulation in mast cells. *Eur J Immunol* 34(6):1627–1636
7. Krutzik PO, Nolan GP (2003) Intracellular phospho-protein staining techniques for flow cytometry: monitoring single cell signaling events. *Cytometry A* 55(2):61–70
8. Kuehn HS, Rådinger M, Gilfillan AM (2010) Measuring mast cell mediator release. In: John E. Coligan et al (Eds). *Current protocols in immunology*. Chapter 7:Unit 7;38
9. Jensen BM, Swindle EJ, Iwaki S, Gilfillan AM (2006) Generation, isolation, and maintenance of rodent mast cells and mast cell lines. In: John E. Coligan et al (Eds). *Current protocols in immunology*. Chapter 3:Unit 3;23
10. Rådinger M, Jensen BM, Kuehn HS, Kirshenbaum A, Gilfillan AM (2010) Generation, isolation, and maintenance of human mast cells and mast cell lines derived from peripheral blood or cord blood. In: John E. Coligan et al (Eds). *Current protocols in immunology*. Chapter 7: Unit 7;37

Chapter 24

Measurement of Mast Cell Surface Molecules by High-Throughput Immunophenotyping Using Transcription (HIT)

D. James Haddon, Justin A. Jarrell, Michael R. Hughes, Kimberly Snyder, Kelly M. McNagny, Michael G. Kattah, and Paul J. Utz

Abstract

Here we describe the application of a highly multiplexed proteomic assay, called HIT (high-throughput immunophenotyping using transcription), to analyze human mast cell surface antigens at rest and during stimulation. HIT allows analysis of up to 100 analytes, including surface antigens and intracellular phosphoproteins, transcription factors, and cytokines, in a single experiment. Briefly, anti-mouse monovalent Fab fragments are covalently conjugated with barcoded oligonucleotides to generate a panel of conjugates. The oligonucleotide-Fab fragment conjugates are bound to monoclonal primary antibodies, creating a cocktail of up to 48 unique barcoded primary antibodies. As few as 100,000 mast cells are stained with the cocktail and the barcodes of the bound primary antibodies are amplified by in vitro transcription with fluorescently labeled NTPs. The resulting barcoded transcripts are quantified using a microarray spotted with oligonucleotides that are complementary to the barcoded transcripts. Differences in levels of the barcoded transcripts correlate well with actual protein levels and are capable of detecting stimulation-dependent changes in protein levels. HIT is an invaluable, broad-spectrum approach for characterizing mast cell surface antigens, signaling molecules, transcription factors, and cytokines.

Key words Mast cells, HMC-1, Microarray, Proteomics, Immunoassay, Multiplex, Surface marker profiling, Transcription, Monoclonal antibody

1 Introduction

Mast cells are innate immune effector cells, capable of releasing a wide variety of preformed and newly synthesized inflammatory and immunomodulatory molecules upon activation and degranulation. It is through the release of these mediators that mast cells provide protection against certain parasitic and bacterial infections, and also play a pathogenic role in allergy and anaphylaxis [1–3]. Mast cells are heterogeneous, expressing diverse phenotypes depending on their tissue of origin and microenvironment, and retain plasticity

between these phenotypes [4]. Further, the expression of mast cell mediators and surface molecules, response to stimuli, and level of activation are dependent on this heterogeneity [5]. Gene expression profiling of mast cells by microarray has been applied to evaluate these phenotypic differences [6]. This platform has the advantage of being highly multiplexed; however protein and transcript levels may differ significantly [6]. Traditional assays that measure protein levels directly have the disadvantage of only evaluating a few analytes. For example, analysis of mast cell cytokine production and signaling molecules by ELISA and western blot only measure a single analyte at a time. Conventional analysis of mast cell surface markers by flow cytometry measures a greater number of analytes in a single sample (~14 markers), but involves greater complexity in selection of compatible fluorescent dyes.

Our laboratory has developed a number of technologies that are directly applicable to proteomic analysis of mast cell biology, including reverse-phase protein lysate microarray, a technique that allows multiplexed analysis of hundreds of cell-signaling components in response to immune receptor signaling, and HIT (high-throughput immunophenotyping using transcription) [7–10]. HIT is a highly multiplexed, proteomic assay that allows analysis of up to 100 analytes, including surface antigens and intracellular phosphoproteins, transcription factors, and cytokines, in a single experiment. Here we have described the application of HIT to the analysis of human mast cell surface antigens at rest and during stimulation. Briefly, 5' amine-modified, barcoded oligonucleotides are modified to incorporate a formylbenzamide functional group at the 5' end of the oligonucleotides. Anti-mouse Fab fragments are concurrently treated with a linker to incorporate hydrazino-nicotinamide functional groups at lysine residues. The modified oligonucleotides and Fab fragments react to form antibody-oligonucleotide conjugates, covalently joined by a stable bis-arylhydrazone bond. Each unique antibody-oligonucleotide conjugate is bound to a monoclonal primary antibody, generating a cocktail of barcoded primary antibodies.

In our studies, a HIT cocktail of barcoded primary antibodies was used to stain stimulated HMC-1 cells, which were derived from a patient with mast cell leukemia [11]. The barcodes of the bound primary antibodies were amplified by in vitro transcription with fluorescently labeled NTPs. The resulting amplified barcoded transcripts were quantified using a microarray spotted with oligonucleotides complementary to each barcoded transcript. The markers identified by HIT were consistent with previously reported mast cell markers and were validated by flow cytometry. HIT represents an ideal approach for characterizing mast cell heterogeneity in surface antigens, signaling molecules, transcription factors, and cytokines.

2 Materials

Prepare all solutions using distilled-deionized water (ddH₂O) unless otherwise indicated.

2.1 *Fab-Oligonucleotide Conjugation Components*

1. Fab-oligonucleotide conjugation buffer: 25 mL of 100 mM sodium citrate (pH 5.75), 150 mM sodium chloride. Store at room temperature (RT).
2. Oligonucleotide annealing buffer: 5 mL of 10 mM sodium phosphate (pH 7.5), 100 mM sodium chloride. Store at RT.
3. Fab-oligonucleotide storage buffer: 25 mL of 50 % glycerol, 5 mM ethylenediaminetetraacetic acid (EDTA), 0.05 % sodium azide (NaAz).
4. 30-mer oligonucleotide containing the T7 promoter sequence 5'-ATGGAATTCTAATACGACTCACTATAGGG-3' with a 5' benzaldehyde modification (Trilink Biotechnologies, San Diego, CA).
5. 70-mer template strands containing barcode sequences flanked between T7 promoter and poly-adenylated tail sequences and 40-mer reverse complement sequences (Table 1) (Trilink Biotechnologies, San Diego, CA).
6. Goat anti-mouse monovalent Fab fragments.
7. PCR thermocycler.
8. Solulink Bioconjugation s-HyNic modification kit (Solulink).
9. Vivaspin 6–3,000 g/mol molecular weight (MW) Centrifugal Concentrator (Sartorius).
10. Zeba Spin Desalting columns (Thermo Scientific).

2.2 *Oligonucleotide Barcode Array Components*

1. Oligonucleotide barcode print solution: 25 mL of 50 mM sodium phosphate buffer (pH 8.5), 0.001 % sodium dodecyl sulfate (SDS) in phosphate-buffered saline (PBS) without Ca²⁺/Mg²⁺. Prepare fresh.
2. Sonication wash buffer: 525 mL of 0.1 % SDS, 1 mM EDTA. Prepare fresh.
3. Slide H blocking solution: 25 mL of 50 mM ethanolamine, 50 mM sodium tetraborate buffer (pH 9.0).
4. Nexterion® Slide H slides (Schott, catalog number 1070936).
5. Stealth Solid Microarray Printing Pins with 0.015" diameter tips (Arrayit, catalog number SSP015).
6. Bio-Rad VersArray Compact Microarrayer (Bio-Rad, Hercules, CA).
7. Bio-Rad VersArray Printing Software (Bio-Rad, Hercules, CA).

Table 1
List of primary antibodies and isotype controls with their respective oligonucleotide-Fab fragment and complementary array sequences

Tag	Antibody	Isotype	Array sequence	Template sequence
99	CD3	IgG2a	5'-TTCAACCTCATCCGAGTGGCTCCAATAGGA-3'	5'-AAAAAAAATTCAACCTCATCCGAGTGGCTCCAAT AGGACCCCTATAGTGAAGTCGTATTAGGAATTCCAT-3'
9802	CD86	IgG2b	5'-CTTCGGAGTGCATCTAAAGTAGCTGA-3'	5'-AAAAAAAACCTCGGGAGTGCATCTAAAGTAGA CTGACCCCTATAGTGAAGTCGTATTAGGAATTCCAT-3'
9640	CD18	IgG1	5'-GAAGTATTCCCTCGAGGGATCAGCGTGATA-3'	5'-AAAAAAAAGAAGTATTCCCTCGAGGGATCAGCG TGATACCCCTATAGTGAAGTCGTATTAGGAATTCCAT-3'
9494	CD44	IgG2b	5'-GTGGTTGCTTAATGCCAGAAATGACCCGCA-3'	5'-AAAAAAAAGTGGTTTGCTTAATGCCAGAAATGAC CGCACCCCTATAGTGAAGTCGTATTAGGAATTCCAT-3'
9207	CD25	IgG1	5'-AGGGATACTATGCCTCTGAGCAGCTAA-3'	5'-AAAAAAAAGGGATACTATGCCTCTGAGCAGC TCAACCCCTATAGTGAAGTCGTATTAGGAATTCCAT-3'
9182	CD45	IgG1	5'-AGCACAGGGAGTTACTAGCTAAGGGCTTCC-3'	5'-AAAAAAAAGCACAGGGAGTTACTAGCTAAGGC TTCCCCCCTATAGTGAAGTCGTATTAGGAATTCCAT-3'
9165	CD9	IgG1	5'-ATGCAGTACAAGGACAACGGGTCGGTCIT-3'	5'-AAAAAAAATGCAGTACAAGGACAACGGG TCTTCCCCCTATAGTGAAGTCGTATTAGGAATTCCAT-3'
8552	AI TR/GITR	IgG1	5'-GCGTAGGCCAGGGCCTGTAGAAAATATTGT-3'	5'-AAAAAAAAGCTAGGCCAGGGCCTGTAGAAAATA TTGTCCCCATAGTGAAGTCGTATTAGGAATTCCAT-3'
8430	CD11c	IgG1	5'-AGACGCTCAGGGTTGGGTGCATAGAATAC-3'	5'-AAAAAAAAGACGCCAGGGAGTCATTAG AATACCCCTATAGTGAAGTCGTATTAGGAATTCCAT-3'
8226	HLA-DR	IgG2b	5'-TCGGGAACGGAGTCATGTACAACATTIG-3'	5'-AAAAAAAATCGGGAACGGGAGTCATTAG TTTGGCCCTATAGTGAAGTCGTATTAGGAATTCCAT-3'
8122	CD1a	IgG1	5'-CGCGTTGCCAAGGGACCCGTTACCAATTAA-3'	5'-AAAAAAAACGCCGTTGCCAAGGGACCCGTTAC ATTAAACCCCTATAGTGAAGTCGTATTAGGAATTCCAT-3'
7794	CD38	IgG1	5'-TCTACTCAAGCAGAGACTGAGACGTTGGG-3'	5'-AAAAAAAATCTACTCAAGCAGAGACTGAGACG TGGGCCCTATAGTGAAGTCGTATTAGGAATTCCAT-3'

7553	CD34	IgG1	5'-GTCAGTTCCGCCGTAGCTAATGAAGCAGA-3'	5'-AAAAAAAAGTCAGTTCCGCCGTAGCTAATGAAGCAGA-3' GCAGACCCATAGTGAGTCGTATTAGGAATTCCAT-3'
7425	CD11b	IgG1	5'-GCTGATTTCAGTGATGCCAGAGATAGCCA-3'	5'-AAAAAAAAGCTGATTTCAGTGATGCCAGAGATA GCCACCCCTATAGTGAGTCGTATTAGGAATTCCAT-3'
7130	CXCR4	IgG2a	5'-ATGGCGAGAAATGCGAAGCTTCCCTATGTAG-3'	5'-AAAAAAAAGGCGAGAAATGCGAAGCTTCCCTAT GTAGCCCTATAGTGAGTCGTATTAGGAATTCCAT-3'
6991	CD45RB	IgG1	5'-AGGGCTCGATGATTACACAGAGCATTGGCC-3'	5'-AAAAAAAAGGCTCGATGATTACACAGAGCATT GGCCCTATAGTGAGTCGTATTAGGAATTCCAT-3'
6861	CD62L	IgG1	5'-TACACGATAACAGATTCAAGGTGCCGGC-3'	5'-AAAAAAAATACACGATAACAGATTCAAGGTGCCGGC CGGCCCTATAGTGAGTCGTATTAGGAATTCCAT-3'
6491	CD95	IgG1	5'-TCAGTTAACTAGCAGTCCGTCGGCAAGAC-3'	5'-AAAAAAAATCAGTTAACTAGCAGTCCGTCGGCA AGACCCCTATAGTGAGTCGTATTAGGAATTCCAT-3'
641	CD11a	IgG1	5'-TTAAAGTGTCTACAACCTGACCACCACTCGC-3'	5'-AAAAAAAATTAAAGTGTCTACAACCTGACCACCA TCGCCCTATAGTGAGTCGTATTAGGAATTCCAT-3'
5896	CD154	IgG1	5'-TGAAGTGGCGATAGATGATGGCACGTTGAG-3'	5'-AAAAAAAATGAACTGGCGATAGATGATGGCAC TGAGCCCTATAGTGAGTCGTATTAGGAATTCCAT-3'
5891	CD117	IgG1	5'-GTGATATAAAATCGGCCACATTTCGAGG-3'	5'-AAAAAAAATGATATAAAATCGGCCACATTTCG CAGGCCCTATAGTGAGTCGTATTAGGAATTCCAT-3'
5757	TWEAK	IgG2a	5'-CCAGAGGCATTGGGAACACTGCTGTAATT-3'	5'-AAAAAAAACCAGAGGCATTGGGAACACTGCTG TAATTCCCTATAGTGAGTCGTATTAGGAATTCCAT-3'
5509	CD2	IgG1	5'-CTCGAACCAACAACTGTGTCATG-3'	5'-AAAAAAAACACTCGAACCAACAACTGTGTCATG CATGCCCTATAGTGAGTCGTATTAGGAATTCCAT-3'
5104	CD43	IgG1	5'-TACCTATCAGAACAGATTCGGCTGGCGCTA-3'	5'-AAAAAAAATACCTATCAGAACAGATTCGGCTGGCG GCTACCCCTATAGTGAGTCGTATTAGGAATTCCAT-3'
5062	CD16	IgG1	5'-TGGTTATCAGAGCCCTAACCCCAATTAGC-3'	5'-AAAAAAAATGCGTTATCAGAGCCCTAACCCCA TAGGCCCTATAGTGAGTCGTATTAGGAATTCCAT-3'

(continued)

Table 1
(continued)

Tag	Antibody	Isotype	Array sequence	Template sequence
4820	CD45RO	IgG2a	5'-CAGGGATAATTCTCCCAAGGTCACTCACTGAG-3'	5'-AAAAAAAACAGGGATAATTCTCCCAAGGTCACTCAC TGAGCCCCATAAGTGAAGTCGTATTAGGAATTCCAT-3'
4810	CD124	IgG1	5'-CCTATGGACAGTCGGTAAAAGCTACCCCTGT-3'	5'-AAAAAAAACCTATGGACAGTCGGTAAAAGCTAC CTGTCCTATAGTGAAGTCGTATTAGGAATTCCAT-3'
4227	CD180	IgG1	5'-ACGTCATTAGGCAGGGCTGGATCAACTCC-3'	5'-AAAAAAAACGTCAATTAGGCAGGGCTGGATCAA CTTCCTCTATAGTGAAGTCGTATTAGGAATTCCAT-3'
3381	CD29	IgG1	5'-ATTCCGCCAGGTGACAGRTGCACTAAAGA-3'	5'-AAAAAAAATCCCCGCCAGGTGACAGRTGCACT AAGACCCCTATAGTGAAGTCGTATTAGGAATTCCAT-3'
3218	CD40	IgG1	5'-TGAATTACCCACACTAGGAGTCGGTAGTCG-3'	5'-AAAAAAAATGAATTACCCACACTAGGAGTCGGTA GTCGCCCTATAGTGAAGTCGTATTAGGAATTCCAT-3'
3171	CD54	IgG1	5'-GAAAGATGTTGCGAAATGTCCAGCCTGG-3'	5'-AAAAAAAAGAAAGATGTTGCGAAATGTCCAGC CTGGCCCTATAGTGAAGTCGTATTAGGAATTCCAT-3'
2233	CD28	IgG1	5'-GGAAAATTTCAGCCCATGGGATGGACGT-3'	5'-AAAAAAAAGGAAAATTTCAGCCCCATGGGATGG ACGTCCCTATAGTGAAGTCGTATTAGGAATTCCAT-3'
2186	TLR2	IgG1	5'-ATGCCCGGCCACTACTTGTGGTCGAGGGC-3'	5'-AAAAAAAATGCCCCGGCCACTACTTGTGGTCGA GGGCCCTATAGTGAAGTCGTATTAGGAATTCCAT-3'
1698	CD49d	IgG1	5'-GCTATGGGACCGGGGCAAATTATGAGAAC-3'	5'-AAAAAAAAGCTATGGACCCGGCCAAATTATGAA GAACCCCTATAGTGAAGTCGTATTAGGAATTCCAT-3'
1606	TRAIL	IgG1	5'-ATGTGAAGAGTGTTCAGCTCGACGGACTAC-3'	5'-AAAAAAAATGTAAGAGTGTCACTCGACGGACTAC CTACCCCTATAGTGAAGTCGTATTAGGAATTCCAT-3'
1064	CD45RA	IgG2b	5'-CAGAACAGATGTTCCGGACGTGAGC-3'	5'-AAAAAAAACAGAACAGATGTTTCGACGTAGC GAGCCCCCTATAGTGAAGTCGTATTAGGAATTCCAT-3'

For microarray printing, array sequences were synthesized with a 5' primary amine and six-carbon spacer

2.3 Mast Cell Stimulation Components

1. HMC-1 media: IMDM, 10 % fetal calf serum (FCS), 150 μ M monothioglycerol, 100 IU/mL penicillin, 100 μ g/mL streptomycin, 2 mM L-glutamine. Store at 4 °C.
2. Lipopolysaccharide (LPS) stock: 10 μ g/mL LPS in sterile H₂O. Aliquot and store at -20 °C.
3. Phorbol 12-myristate 13-acetate (PMA) stock: 5 mg/mL PMA in dimethyl sulfoxide (DMSO). Aliquot and store at -20 °C.
4. Ionomycin calcium salt stock: 1 mM ionomycin in DMSO. Aliquot and store at -20 °C.

2.4 HIT Cell Processing Components

1. HIT buffer: 500 mL of 15 mM EDTA, 1.5 % bovine serum albumin (BSA), 0.05 % NaAz in PBS without Ca²⁺/Mg²⁺. Filter with 500 mL, 0.2 μ m vacuum filter. Prepare fresh and store on ice or at 4 °C for all steps.
2. Cell fixation buffer: 0.4 % formaldehyde in PBS without Ca²⁺/Mg²⁺. Formaldehyde must be methanol free (e.g., 16 % formaldehyde; Polysciences, catalog number 18814-20). Prepare fresh.
3. 10 mg/mL mouse gamma globulin (Jackson Immunoresearch, catalog number 015-000-002) in HIT buffer.
4. Cy3- and Cy5-NTP mixtures: 2.5 mM NTP mix, 3:1 unlabeled:labeled cyanine-UTP. Add 100 μ L of 10 mM unlabeled ATP, CTP, and GTP and 75 μ L 10 mM unlabeled UTP to two 0.5 mL microfuge tubes. Add 25 μ L 10 mM Cyanine-3-UTP (Enzo Life Sciences, catalog number enz-42505) or 25 μ L 10 mM Cyanine-5-UTP (Enzo Life Sciences, catalog number enz-42506) to each tube (400 mL total). Mix by vortexing and store at -20 °C.
5. Cy3- and Cy5-amplification mixtures: 10 U/ μ L T7 RNA polymerase (Applied Biosystems), 1 \times transcription buffer (Ambion), 0.5 U/ μ L SUPERase-In™ (Applied Biosystems), 4 U/mL yeast pyrophosphatase (NEB), 0.5 mM Cy3-NTP, or Cy5-NTP mix. Prepare 30 μ L/reaction immediately before amplification. Mix by vortexing and store at -20 °C.
6. 20 \times SSC (saline-sodium citrate) buffer: 0.3 M sodium citrate (pH 7), 3 M sodium chloride. May also be purchased commercially.
7. Hybridization mixture: 2 \times SSC, 0.1 % SDS, 0.1 % salmon sperm DNA. Prepare 53 μ L/sample. Mix by vortexing and store on ice before use. Prepare fresh.
8. Post-hybridization wash buffers (PHWBs): Make 500 mL each.
 - (a) PHWB-1: 2 \times SSC, 0.1 % SDS.
 - (b) PHWB-2: 1 \times SSC.
 - (c) PHWB-3: 0.2 \times SSC.
 - (d) PHWB-4: 0.05 \times SSC.

9. RNeasy MinElute Cleanup Kit (QIAGEN).
10. RNaseZap Decontamination Solution (Applied Biosystems).
11. UltraPure DNase/RNase-Free Distilled Water.
12. Microarray Hybridization Cassette 4X16 (Arrayit, catalog number AHC4X16).
13. 4-Well dish, non-treated, sterile with lid (Thermo Scientific, catalog number 267061).
14. 96-Well, V-bottom plates.
15. Ethanol (EtOH) (200 proof).
16. Beta-mercaptoethanol (2-ME).

2.5 Microarray Scanning and Analysis Components

1. GenePix® 4000 Scanner (Molecular Devices, Sunnyvale, CA).
2. GenePix® Pro 6.0 Software (Molecular Devices, Sunnyvale, CA).
3. MeV: MultiExperiment Viewer v4.7 software (MeV, Boston, MA).
4. Microsoft Excel (Microsoft, Redmond, WA) or equivalent software for graphing and statistical analyses.

2.6 Flow Cytometry Components

1. FACS buffer: 2 % FCS, 1 mM EDTA, 0.05 % NaAz in PBS without Ca²⁺/Mg²⁺. Mix and store at 4 °C.
2. Alexa Fluor 488 goat-anti-mouse IgG (H+L) (Invitrogen).
3. 1.2 mL FACS cluster tubes (Corning Inc., Cat#4412).
4. FACScan flow cytometer (BD, Franklin Lakes, NJ).
5. Cell Quest Pro software (BD, Franklin Lakes, NJ).

3 Methods

Carry out all procedures at room temperature (RT) unless otherwise specified.

3.1 Fab-Oligonucleotide Synthesis

1. Concentrate goat anti-mouse monovalent Fab fragments to 10 mg/mL on Vivaspin 6 Centrifugal Concentrator spin columns.
2. Modify fragments with succinimidyl 6-hydrazinonicotinate acetone hydrazine (SANH) Solulink Bioconjugation s-HyNic modification kit according to the manufacturer's protocol.
3. Remove unbound SANH using Zeba Spin Desalting columns. Perform desalt three times.
4. Generate benzaldehyde-modified double-stranded oligonucleotide tags with T7 promoter and barcode sequences as follows:
 - (a) Mix 70-mer template strands containing barcode sequences flanked between T7 promoter and polyadenylated tail

sequences with 5' benzaldehyde-modified T7 promoter sequence and 40-mer reverse complement sequence in equimolar ratio (*see Table 1*).

- (b) Anneal samples with oligonucleotide annealing buffer in iCycler PCR machine by cooling from 95 °C to 4 °C, decreasing 0.5 °C every 30 s.
5. Mix aliquots of desalted hydrazine-modified Fab fragments with benzaldehyde-modified oligonucleotide tags at a molar ratio of 1:2 Fab to oligonucleotide in Fab-oligonucleotide conjugation buffer.
6. Incubate reaction for 12 h at 21–23 °C.
7. Transfer reaction to 4 °C and incubate for an additional 12 h.
8. Store conjugates in Fab-oligonucleotide storage buffer at –20 °C.
1. Resuspend 5'-amine-modified 30-mer array oligonucleotides (Table 1) to a final concentration of 50 µM in oligonucleotide barcode print solution (*see Note 1*).
2. Aliquot 12 µL of each tag per well in a 384-well plate (*see Note 2*).
3. Seal plates and store at –20 °C until ready to use (*see Note 3*).

Print Plate Preparation

Print Setup

During Print

4. When ready to print, thaw plates at RT and centrifuge at 200–300×*g* for 1 min.
5. Turn on VersArray Compact Microarrayer and open VersArray Printing Software on computer.
6. Click “Homing” icon to home pin printer head and load stealth solid microarray printing pins.
7. Fill sonication washbasin with 525 mL sonication wash buffer.
8. Fill water bath with 60 mL ddH₂O.
9. Set humidifier to 30–50 % humidity (*see Note 4*).
10. Go to toolbar and select “run & calibration”—modify program (specify the number of slides to print) and save file.
11. Go to toolbar, select “view” and then “console,” click “open a run,” and select program to run.
12. Click “Washing” on console to perform one wash cycle before printing (*see Note 5*).
13. Load slides and print plate #1.
14. Select “start” and run from “beginning” of program.
15. Check to make sure that printing pins dip properly in print plate wells. During wash cycles, check to make sure that pins are submerged in sonication wash buffer and ddH₂O (*see Note 6*).

Post-print

16. Switch print plates when necessary.
17. Add 5 mL ddH₂O to sonication washbasin every 1–2 h if necessary.
18. Add 1 mL ddH₂O to water bath every 1–2 h if necessary.
19. Increase humidity to 75 % and incubate slides in arrayer for an additional 2 h to immobilize DNA.
20. After immobilizing, click “Drain W1” to drain water bath.
21. Empty sonication washbasin manually.
22. Add 500 mL ddH₂O to sonication washbasin to rinse. Empty manually.
23. Remove pins and slides.
24. Turn off arrayer and computer.
25. Place slides in slide box and vacuum desiccate for at least 2 h to overnight at RT.
26. Vacuum seal slides and store at 4 °C (*see Note 7*).

3.3 Stimulation and Fixation of Human Mast Cells

1. Maintain HMC-1 cells (a kind gift from Dr. Joseph Butterfield, Mayo Clinic) between 2×10^5 and 2×10^6 cells/mL in HMC-1 media in a humidified 5 % CO₂ incubator at 37 °C. Passage cells every 3–5 days.
2. Centrifuge cells at $200 \times g$ and resuspend in fresh media at 10^6 cells/mL.
3. Stimulate cells with 1 µg/mL LPS, 50 ng/mL PMA, and 1 µM ionomycin, or stimuli of interest for 8 and 24 h (*see Note 8*). Keep unstimulated cells at each time point as controls.
4. Place cells on ice for 10 min to end stimulation. Assess cells for viability and perform live cell count (*see Note 9*).
5. Centrifuge cells at $200 \times g$. Aspirate supernatant and gently flick pellet to dislodge cells.
6. Add 10 mL cell fixation buffer and place at RT for 1 h, resuspending with pipette periodically to avoid cell clumping. If necessary, live cells can be analyzed instead (*see Note 10*).
7. Centrifuge cells at $200 \times g$. Aspirate supernatant, gently flick pellet, and add 5 mL FACS buffer. Gently pipette up and down to dislodge cell clumps. Repeat once more (*see Note 11*).
8. Resuspend fixed cells in 10 mL FACS buffer and perform cell count.
9. Keep fixed cells in FACS buffer on ice or at 4 °C (long term, ~1 week) until ready to stain.

3.4 Preparation of Staining Cocktails

1. Prepare each antibody-oligonucleotide conjugate (Table 1) in a 96-well, V-bottom cell culture plate on ice as follows: (0.2 µg × number of samples) monoclonal antibody or isotype

control per well with (0.2 μ g \times number of samples) Fab-oligonucleotide (e.g., 2 μ g mAb and 2 μ g Fab-oligonucleotide per well for a ten-sample experiment). This results in a 3:1 Fab:antibody molar ratio.

2. Allow conjugation to proceed for 2 h at 4 °C.
3. Add 5 μ g of mouse gamma globulin per μ g of Fab-oligonucleotide to each well and pipette up and down slowly to mix. Incubate for 10 min at 4 °C.
4. Quickly pool antibody-oligonucleotide conjugates together into a single 1.5 mL tube (1 mAb cocktail and 1 isotype cocktail) and dilute to a final concentration of 5 μ g/mL of each mAb with HIT buffer (*see Note 12*).
5. Keep cocktails on ice or at 4 °C until ready to stain cells.

3.5 Cell Staining

Keep cells on ice for stain.

1. Add 200 μ L HIT buffer/well to a 96-well, V-bottom plate to block for 1 h.
2. Flick “blocked” 96-well plate into sink to remove HIT buffer.
3. Add cells to blocked plate (1–3 \times 10⁵ cells/well).
4. Centrifuge plate at 200 \times *g* for 3 min.
5. Flick plate to discard supernatant. Keep cells on ice until ready to stain. If staining for intracellular antigens, permeabilize cells before staining (*see Note 13*).
6. Add 35 μ L cocktail per well with either mAb or isotype cocktail and gently pipette up and down.
7. Incubate for 45 min at 4 °C.
8. Centrifuge at 200 \times *g* for 3 min. Add 200 μ L ice-cold HIT buffer/well and gently pipette up and down to wash. Repeat three times (*see Note 14*).
9. Repeat **step 8** twice more with ice-cold PBS.
10. Flick plate to discard supernatant. Keep cells on ice.

Oligonucleotide Barcode Amplification

1. Add 30 μ L Cy3- or Cy5-amplification mix to cells and pipette to mix.
2. Add 1 μ L 1/100 dilution of mAb or isotype cocktail to 39 μ L Cy3- and Cy5-amplification mixes in separate wells as positive controls.
3. Amplify samples for 2 h at 37 °C on orbital shaker with gentle agitation.

RNA Purification

RNA purification protocol adapted from Qiagen Minelute RNA purification kit.

1. Prepare RLT solution: Add 10 μ L of 2ME per 1 mL RLT needed (*see Note 15*).

2. Add 140 μ L RLT solution to each sample (*see Note 16*).
3. Combine Cy3 and Cy5 samples in 5 mL tubes if experiment includes dye swaps. Otherwise, transfer samples directly to tubes (*see Note 17*).
4. Add 180 μ L 95 % EtOH per sample and pipette or vortex to mix.
5. Transfer samples to individual RNA Minelute spin columns.
6. Centrifuge for 15 s at 9,500 $\times g$.
7. Transfer spin column to new 2 mL collection tube.
8. Add 500 μ L RPE buffer to each column. Centrifuge for 15 s at 9,500 $\times g$. Repeat once more.
9. Transfer spin column to new 2 mL collection tube.
10. Centrifuge for 10 min at 9,500 $\times g$.
11. Transfer column to 2 mL elution tube and add 14 μ L RNase-free ddH₂O to the center of column (avoid touching filter).
12. Centrifuge column for 5 min at 16,000 $\times g$.
13. Store RNA on ice until ready to hybridize on array. Purification should yield 12–14 μ L/sample.

Pre-hybridization Blocking

14. Place printed slides in 4-well dish, printed side up.
15. Add 10 mL of slide H blocking solution per slide (*see Note 18*).
16. Block slides for 1 h at RT with rocking.
17. Aspirate slide H blocking solution and add 10 mL ddH₂O to slide until fully submerged. Repeat once more.
18. Centrifuge slides at 200 $\times g$ in a metal slide rack for 5 min to dry.
19. Wash 4X16 microarray hybridization cassette with RNaseZap and pat dry. Rinse with 95 % EtOH and dry completely. Place slides in chamber, print side up. Screw cassette tightly.

Hybridization

20. Adjust block heater to 95 °C.
21. Add 53 μ L hybridization buffer to each sample and place at 95 °C for 1 min.
22. Centrifuge for 5 min at 16,000 $\times g$.
23. Load 65 μ L of sample to each array (*see Note 19*) and seal arrays with foil tape to prevent evaporation.
24. Place hybridization cassette in humidified chamber (*see Note 20*) and hybridize arrays overnight at 42 °C with rocking.

Post-hybridization Washing

25. Prepare post-hybridization wash buffers (PHWB-1, -2, -3, -4) in Coplin jars.
26. Aspirate each well individually and wash 1 \times with 200 μ L PHWB-1 (*see Note 21*).
27. Flick cassette and add 200 μ L PHWB-1 per well.

28. Remove slides from cassette and quickly transfer to slide rack submerged in PHWB-1 (avoid drying). Cover Coplin jar with foil and shake for 5 min (*see Note 22*).
29. Remove slides and place in PHWB-2. Cover with foil and shake for 5 min.
30. Repeat **step 5** in PHWB-3.
31. Repeat **step 5** in PHWB-4.
32. Remove slides and centrifuge at $200 \times g$ for 5 min.
33. Place slides in slide box. Cover slide box with foil and scan immediately.

Scanning

34. Open GenePix Pro 6.1.
35. Open GenePix Scanner and place slide on platform, print side down. Close scanner.
36. Select “Hardware” Icon—select one or both excitation wavelengths (532, 635) and set “PMT Gain” to 500 to start. Set “Power” to 100 %, “Pixel size” to 10 μm , “Lines to Average” to 1, and “Focus Position” to 0 μm .
37. Click “double arrow” icon to preview image. Adjust PMT gain to obtain greatest signal:noise ratio and to ensure that spots are not saturated.
38. After selecting an optimal PMT, click “single arrow” icon to capture high-resolution image (Fig. 1a).
39. When scan is finished, click “Disk” icon and select “Save Image.” Select “multiple-image file” if scanning with both wavelengths. Choose “single-image file” and select 532 or 635 if scanning with a single wavelength.

Gridding

40. Open GenePix Pro 6.1.
41. Click “Disk” icon and select “Open Images.” Select image to grid (*see Note 23*).
42. Click “Disk” icon and select “Load Array List.” Select gal file. Grid will appear over selected image.
43. Move grids to fit arrays (*see Note 24*).
44. Click “Align Blocks” icon and select “Options.” Click “Alignment” tab. Select “Find irregular features” and “Resize feature during alignment.” Adjust “minimum diameter” to 33 % and “maximum diameter” to 300 %. Select “Estimate warping and rotation when finding blocks.” Adjust “Automated Image Registration, Max translation value” to 10.
45. Set Composite pixel intensity (CPI) to 1 and click “OK.”
46. Click “Align Blocks” icon and select “Align Features in All Blocks.”
47. Inspect each array to make sure that grids encircle features (*see Note 25*).

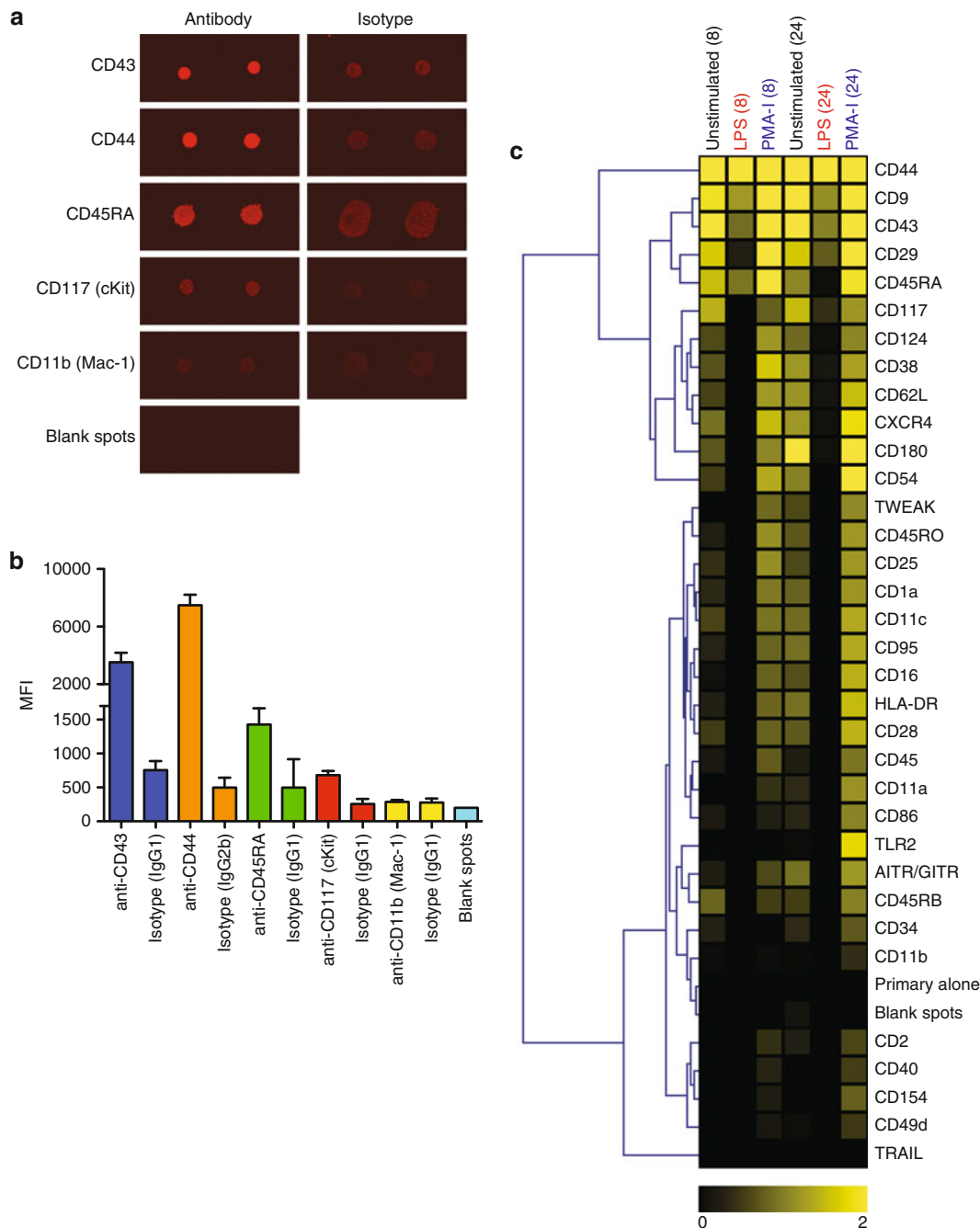


Fig. 1 Surface marker profiling of human mast cells by HIT. (a) Cy5 fluorescence of oligonucleotide barcode microarray stained with Cy5-labeled transcripts amplified from unstimulated HMC-1 cells stained with antibody or isotype cocktail. (b) Quantification of the MFI of the spots from A (bars represent SD of duplicate arrays; blank spots = barcode spots on the array for which a corresponding oligonucleotide was not included in the staining cocktail). (c) Unsupervised hierarchical clustering of \log_2 ratios (antibody/isotype) of 34 HMC-1 surface markers across stimulations and two time points (primary alone = cells stained with unconjugated primary antibody, to demonstrate stability of Fab/antibody complexes; length of stimulation in hours is shown in brackets)

48. Click “BCR” icon to extract data.

49. Click “Image” tab to return to image.

50. If arrays require additional flagging, click “Feature Mode” icon to highlight individual features. To flag manually, select feature and press “a.” An “X” will appear over manually flagged features (*see Note 26*).

51. To complete gridding, click “Disk” icon and select “Save Results.” Results will be saved as a GPR file.

Analysis

52. Using Excel, open the array’s GenePix GPR files and copy the F635 Median (for Cy5) or F532 Median (for Cy3) and Flags columns to a new sheet. Copy all three columns if performing a dye swap.

53. Reassign spots that were flagged as “bad” (-100) as empty. Set cells flagged as “not found” (-50), or below the baseline fluorescence (suggest 200 MFI) as 200.

54. If performing a dye swap, calculate the Log_2 Cy5/Cy3 ratio for each spot.

55. Average duplicate spots on each array and then average replicate arrays (using the reciprocal for dye-swap pairs) (Fig. 1b).

56. For single-color experiments, calculate a Log_2 ratio of antibody/isotype for each pair.

57. Export the results as a tab-delimited spreadsheet and load in MeV.

58. Perform hierarchical clustering with the following options: Gene Tree, Optimize Gene Leaf Order, Euclidean distance, and Complete linkage clustering.

59. Export an image of the heatmap (Fig. 1c).

3.6 Validation of Candidate Markers via Flow Cytometry

1. Prepare HMC-1 cells as described in Subheading 3.3 and aliquot cells into a 96-well, V-bottom plate at 10^5 cells/well.
2. Using one well per antibody, stain the cells with 50 μL of 2.5 $\mu\text{g}/\text{mL}$ primary antibody for 20 min on ice. Remember to include isotype, unstained, and secondary alone controls. Antibody staining concentrations may need to be titrated individually.
3. Centrifuge at $200 \times g$, flick plate to remove supernatant, and wash with 200 μL FACS buffer per well.
4. Stain cells with a 1/1,000 dilution of fluorescently labeled anti-mouse secondary antibody for 20 min on ice. Secondary antibody dilution may need to be titrated separately.
5. Centrifuge at $200 \times g$, flick plate to remove supernatant, and wash with 200 μL FACS buffer per well.
6. Resuspend in 100 μL of FACS buffer and transfer to a cluster tube.
7. Collect samples on a FACScan; typically 10,000 events per sample is sufficient for analysis (Fig. 2a, b).

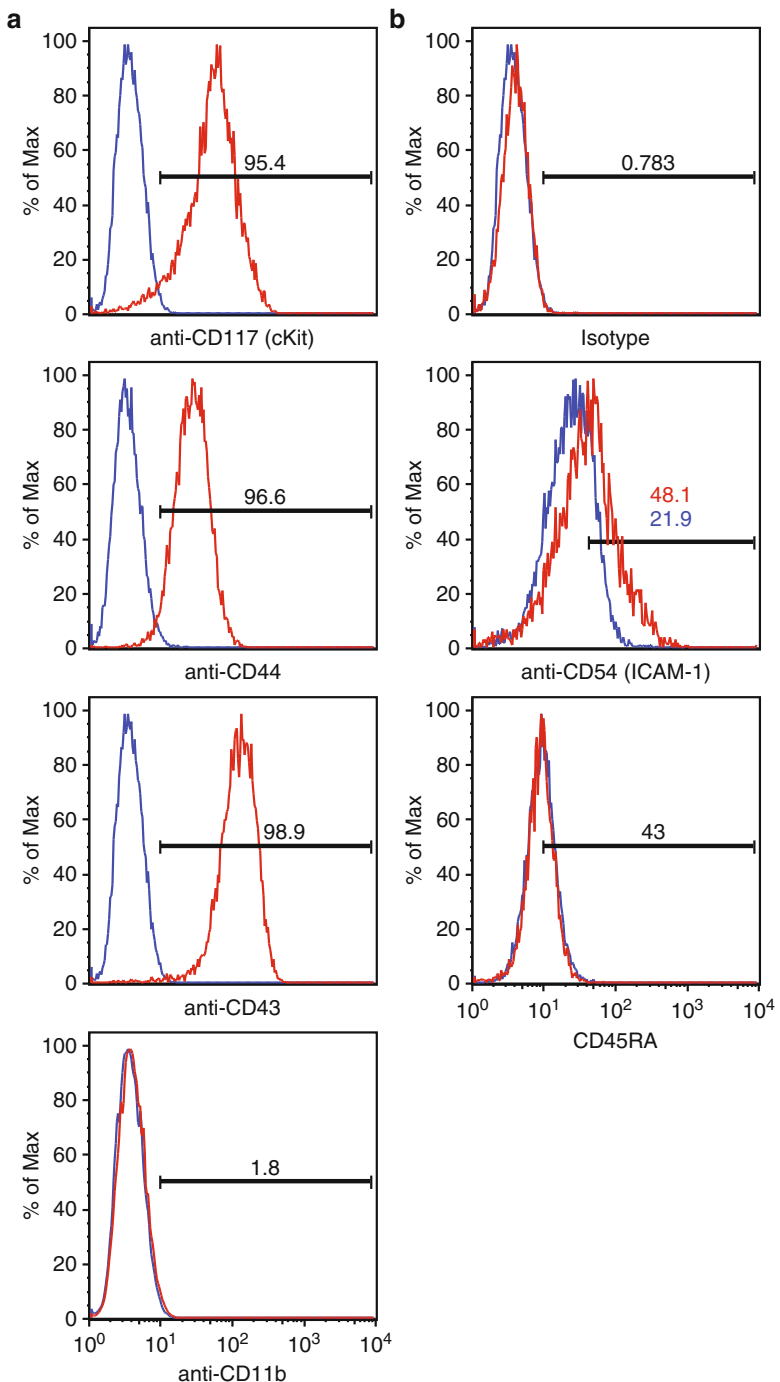


Fig. 2 HIT accurately measures mast cell surface marker levels at baseline and during stimulation. (a) FACS validation demonstrates that HIT correctly identified CD117 (cKit), CD44, and CD43, and the absence of CD11b on the surface of unstimulated mast cells, in agreement with previous reports (isotype = blue line, antibody = red line) [12]. (b) Further, FACS validation demonstrates that HIT correctly identified PMA-ionomycin stimulation-dependent upregulation of CD54 (ICAM-1), in agreement with previous reports (unstimulated = blue line, PMA-I = red line) [13].

4 Notes

1. For microarray printing, array sequences were synthesized with a 5' primary amine and six-carbon spacer.
2. Print plates can be stored for a long term (>1 year) at -20 °C. The print plate layout will need to be adapted for each specific printing setup. We recommend developing a 12-pin array printing program to print 12 arrays per slide. Before committing to a print run, perform a test print to make sure that arrays will fit microarray hybridization cassette.
3. 30 % humidity is optimal for longer print runs (>2 h).
4. Check pins to make sure that they are fully submerged in sonication buffer and wash buffer. Add more buffer if necessary. As pins hover in the vacuum platform, check to see that each pin enters a vacuum well. Pins will lift from the printer head if they are bent. After the wash cycle is complete, move printer head to door and replace pins. Repeat until all pins are flush with vacuum wells. If pins continue to lift from print head, arrayer may need to be recalibrated.
5. If an issue is encountered during a print run, immediately stop the program. Remedy the issue and modify print run program to start where it left off. Click “start” on print console and run from “middle” of program.
6. Printed slides can be stored in a sealed (airtight) slide box at 4 °C for at least 2 months.
7. Plan to stimulate more than the minimal amount of cells needed to perform experiment to accommodate cell loss during fixation.
8. Before fixing cells, it is important to assess cells for viability because significant amounts of dead cells can interfere with the assay. Remove dead cells via Ficoll gradient (GE Healthcare) or by using a MACS Dead Cell Removal Kit (Miltenyi Biotec).
9. Live cells can be analyzed; however the staining is long and traumatic. Nucleases can also decrease overall signal. If using live cells, it is critical to handle cells gently and work quickly.
10. Alternatively, postfix washes can also be performed using HIT buffer. Fixed cells can be stored in HIT buffer on ice or for a long term.

◀ **Fig. 2** (continued) This shift was not due to a change in autofluorescence, as the MFI of stimulated isotype controls and another surface marker (CD45RA) were not altered from baseline. *Horizontal bars* represent the percentage of antibody-stained cells within the gate and were set to capture ~1 % of isotype control-stained cells (except for the middle panel of **b**, where the percentages of stimulated and unstimulated are shown in *red* and *blue*, respectively)

11. We find it helpful to use a multichannel pipettor to pool tags in a single row, and then a single-channel pipettor to pool columns.
12. To prepare cells for intracellular staining, permeabilize fixed cells with 250 mL 100 % molecular grade ethanol (Sigma-Aldrich, Cat#02854) for 10 min on ice. Centrifuge at $200 \times g$ and wash cells with HIT buffer. Repeat 2x and proceed to stain.
13. Dye-swap experiments can be prepared as follows: unstimulated cells (Cy5) vs. stimulated cells (Cy3) on array 1, and unstimulated cells (Cy3) vs. stimulated cells (Cy5) on array 2. Alternatively, a common calibration sample can be used as follows: unstimulated cells (Cy5) vs. calibrator sample (Cy3) on array 1, and stimulated cells (Cy5) vs. calibrator sample (Cy3) on array 2. We suggest preparing aliquots of a 1/100 dilution of amplified antibody cocktail as a calibrator sample or aliquots of amplified cocktail from staining of a known cell line.
14. We find it helpful to wash cells using a multichannel pipette. To reduce cell loss, be sure to flick plate only once after each spin. Be gentle with cells and pipette up and down slowly.
15. Amount of RLT solution will vary with the number of experimental conditions. Determine the number of conditions and multiply by 0.140 to determine the total RLT (mL) required. Take RLT total and divide by 10 to determine the amount of 2ME (μ L) needed to add to RLT. Mix by vortexing and store on ice.
16. Samples can be frozen in RLT solution at -20°C . Processing can continue up to a week later.
17. We find it helpful to combine/transfer samples to 1.2 mL cluster tubes (Corning Inc., Cat#4412).
18. Blocking solution is somewhat hydrophobic. If needed, pipette additional blocking solution in well to cover the entire slide.
19. It is important to avoid touching the array surface (with pipette tip, fingers, etc.) to prevent smudging of printed oligonucleotides. Be sure to switch pipette tips between loading samples to avoid cross-contamination.
20. To construct the chamber, use a small TupperwareTM container that fits the hybridization cassette and line it with damp paper towels (with PBS or ddH₂O). This step is an additional precaution to prevent evaporation.
21. To prevent drying, aspirate and wash arrays individually with a single-channel pipette before moving on to the next array. Keeping arrays hydrated will help to reduce background fluorescence while scanning.
22. It is important to keep slides covered from this point forward to prevent bleaching of the fluorescent dye.
23. GenePix scanner saves scans as Tagged Image File Format Images (TIFFs). Although GenePix 6.1 will recognize JPEG

images, we recommend gridding high-resolution TIFF images for best results.

24. There are several approaches to aligning grids. We recommend the following: Click “Block Mode” and highlight all grids. Click “Zoom Mode” and zoom into a single array. Return to “Block Mode” and align grid with features as best as possible. Click “Undo Zoom” to zoom out. Return to “Block Mode” and select first array. Use “<” and “>” keys to move across single grids. Inspect each array individually and adjust individual grid spots over array features when necessary. To do this, click “Feature Mode,” highlight spot, and move spot in position over feature.
25. If grid spot does not outline the feature after initial alignment, further adjustments can be made. If spot appears larger than a given feature, increase the CPI value and realign feature (highlight feature and select “Aligned Selected Feature”). Repeat until spot outlines feature. If GenePix does not recognize a feature despite CPI adjustment, and the feature is visible above background, spot can be adjusted manually. We suggest using this feature sparingly. In “Feature Mode” select spot. Hold down “control” and adjust spot size using “up” and “down” arrow keys.
26. Empty/Blank features flagged by GenePix appear as circles bisected by a single line. These flags are distinguishable from manual flags. To override flags (empty or manual) select spot and press “L” key. Adjust spot accordingly.

Acknowledgements

P.J.U. is supported by NHLBI Proteomics Contract 268201000034C, Proteomics of Inflammatory Immunity and Pulmonary Arterial Hypertension; 5 U19-AI082719, National Institutes of Health; 2 OR-92141, Canadian Institutes of Health Research (CIHR); a gift from the Floren Family Trust; and a gift from the Ben May Trust. D.J.H. is supported by a CIHR postdoctoral fellowship.

References

1. Ierna MX, Scales HE, Saunders KL, Lawrence CE (2008) Mast cell production of IL-4 and TNF may be required for protective and pathological responses in gastrointestinal helminth infection. *Mucosal Immunol* 1:147–155
2. Piliponsky AM, Chen CC, Grimaldeston MA, Burns-Guydish SM, Hardy J, Kalesnikoff J, Contag CH, Tsai M, Galli SJ (2010) Mast cell-derived TNF can exacerbate mortality during severe bacterial infections in C57BL/6-KitW-sh/W-sh mice. *Am J Pathol* 176: 926–938
3. Martin TR, Galli SJ, Katona IM, Drazen JM (1989) Role of mast cells in anaphylaxis. Evidence for the importance of mast cells in the cardiopulmonary alterations and death induced by anti-IgE in mice. *J Clin Invest* 83: 1375–1383

4. Sonoda S, Sonoda T, Nakano T, Kanayama Y, Kanakura Y, Asai H, Yonezawa T, Kitamura Y (1986) Development of mucosal mast cells after injection of a single connective tissue-type mast cell in the stomach mucosa of genetically mast cell-deficient W/Wv mice. *J Immunol* 137:1319–1322
5. Moon TC, St Laurent CD, Morris KE, Marcet C, Yoshimura T, Sekar Y, Befus AD (2010) Advances in mast cell biology: new understanding of heterogeneity and function. *Mucosal Immunol* 3:111–128
6. Haddon D, Hughes M, Antignano F, Westaway D, Cashman N, McNagny K (2009) Prion protein expression and release by mast cells after activation. *J Infect Dis* 200:827–831
7. Chan SM, Ermann J, Su L, Fathman CG, Utz PJ (2004) Protein microarrays for multiplex analysis of signal transduction pathways. *Nat Med* 10:1390–1396
8. Qin H, Lee IF, Panagiotopoulos C, Wang X, Chu AD, Utz PJ, Priatel JJ, Tan R (2011) Natural killer cells from children with type 1 diabetes have defects in NKG2D-dependent function and signaling. *Diabetes* 60:857–866
9. Gulmann C, Sheehan KM, Conroy RM, Wulfkuhle JD, Espina V, Mullarkey MJ, Kay EW, Liotta LA, Petricoin EF (2009) Quantitative cell signalling analysis reveals down-regulation of MAPK pathway activation in colorectal cancer. *J Pathol* 218:514–519
10. Kattah MG, Coller J, Cheung RK, Oshidary N, Utz PJ (2008) HIT: a versatile proteomics platform for multianalyte phenotyping of cytokines, intracellular proteins and surface molecules. *Nat Med* 14:1284–1289
11. Nilsson G, Blom T, Kusche-Gullberg M, Kjellén L, Butterfield JH, Sundström C, Nilsson K, Hellman L (1994) Phenotypic characterization of the human mast-cell line HMC-1. *Scand J Immunol* 39:489–498
12. Füredér W, Bankl HC, Toth J, Walchshofer S, Sperr W, Agis H, Semper H, Sillaber C, Lechner K, Valent P (1997) Immunophenotypic and functional characterization of human tonsillar mast cells. *J Leukoc Biol* 61:592–599
13. Weber S, Babina M, Feller G, Henz BM (1997) Human leukaemic (HMC-1) and normal skin mast cells express beta 2-integrins: characterization of beta 2-integrins and ICAM-1 on HMC-1 cells. *Scand J Immunol* 45:471–481

Part V

Mouse Models of Disease to Study Mast Cell Function

Chapter 25

Cre/loxP-Based Mouse Models of Mast Cell Deficiency and Mast Cell-Specific Gene Inactivation

Katrin Peschke, Anne Dudeck, Anja Rabenhorst, Karin Hartmann, and Axel Roers

Abstract

Over the past decades, research on in vivo functions of mast cells has largely relied on *kit*-mutant mouse strains. Recently, new mouse models for investigation of mast cell functions based on the Cre/loxP recombination system have been published and results in these new models challenged findings of previous studies in *kit*-mutant mice. Herein we describe procedures central to mast cell-specific gene inactivation and the generation of mast cell-deficient mice based on the mouse strain Mcpt5-Cre, which expresses Cre recombinase selectively in connective tissue mast cells.

Key words Mast cell-specific conditional gene targeting, Cre/loxP-mediated recombination, Diphtheria toxin-induced cell ablation, Diphtheria toxin receptor, Mcpt5, Mcpt5-Cre, Single-cell PCR

1 Introduction

While the pathogenic role mast cells play in IgE-mediated allergies is well known, beneficial functions of these cells are less clear [1]. Over the past 30 years, research into mast cell functions largely relied on *kit*-mutant mouse strains as models of mast cell deficiency, like the strains WBBF1-Kit^{W/W^v} and C57BL/6 Kit^{W-sh/W-sh}. Experiments using these models provided evidence for important functions of mast cells in innate and adaptive immunity [2, 3]. Moreover, mast cells were shown to play critical roles in a broad spectrum of pathologic conditions, including inflammation, autoimmunity, cancer, and metabolic disease [4, 5]. However, in addition to their mast cell deficiency, *kit*-mutant mice feature complex alterations of the immune system and other organ systems, which could potentially confound the results obtained with these models [6, 7].

We and others have recently described new mouse models for the investigation of mast cell functions in vivo, most of which are based on the Cre/loxP recombination system [8–15].

Cre recombinase is a bacteriophage enzyme, which recombines DNA flanked by 34 bp long loxP recognition sequences resulting in deletion of the loxP-flanked (“floxed”) fragment. Cell type-specific or inducible expression of Cre in transgenic mice allows for conditional inactivation of floxed genes [16, 17]. Vast numbers of gene-targeted mouse lines carrying floxed genes are available to the community. We generated the BAC-transgenic mouse strain Mcpt5-Cre which expresses Cre selectively in connective tissue mast cells (i.e., the mast cell population in the peritoneal cavity, the skin, and in the connective tissue of most other organs) [9]. The Mcpt5-Cre transgene is not active in the intraepithelial subset of mast cells of the intestine, the so-called mucosal mast cells. Mcpt5-Cre mice were used to generate fluorescent mast cell reporter mice and mice with mast cell-specific “knockout” of various target genes [9, 10]. Of note, the latter represent mice, which are normal except for the lack of a particular gene of interest only in connective tissue mast cells. Furthermore, Mcpt5-Cre mice were used to generate novel mouse models of mast cell deficiency [10]. Using the new Mcpt5-Cre-based models, we investigated the role of mast cells in contact allergy and found that mast cells are essential promoters of contact hypersensitivity responses [10]. Similar results were reported in “MASTRECK” mice, which represent another novel *kit*-independent model of mast cell deficiency [11]. These findings are at conflict with a recent study in *kit*-mutant mice describing suppression of contact hypersensitivity by mast cells [18]. Results discrepant with published studies in *kit*-mutant mice were also obtained in studies using the “Cre-Master” mouse strain, an additional new model of constitutive mast cell deficiency [13]. These animals were tested in models of autoimmunity and the critical role for mast cells that experiments in *kit*-mutant mice had previously suggested could not be confirmed. We conclude that findings in *kit*-mutant strains should be interpreted with caution, even if validated by mast cell reconstitution, and rather recommend using one of the novel models, which are independent of *kit* mutations.

Herein, we describe experimental procedures central to the use of the Mcpt5-Cre-based mouse models. First, we describe a strategy that allows to quantitatively determine the extent to which Cre-mediated deletion of a gene of interest occurs in mast cells. Second, we outline induction of mast cell deficiency by injections of diphtheria toxin.

1.1 Protocols for Genotyping for the Mcpt5-Cre Transgene as well as the R-DTA and the iDTR Knock-In Alleles

Polymerase chain reaction (PCR) is the standard tool for the identification of genetically modified animals. DNA from tail biopsies of mice can be obtained following a simple protocol. We detail our protocol for the detection of the Mcpt5-Cre transgene. The R-DTA [19] and the iDTR [20] lines see (1.3) both represent a “knock-in” into the Rosa26 locus. Both contain a similar loxP-flanked stop cassette. The detection of this cassette by PCR as described below is sufficient in general. However, we recommend specific detection of

the R-DTA and the iDTR allele, in particular in situations where both strains are kept in the same facility to avoid mistakes.

1.2 Single-Cell Sorting and Single-Target PCR to Determine Efficiency and Cell Type Specificity of Gene Inactivation in Mast Cells

It is important to realize that different loxP-flanked loci undergo Cre-mediated recombination with different ease. Therefore, efficiency of deletion of individual target genes in connective tissue mast cells by the Mcpt5-Cre transgene (close to 100 % for all loci tested so far) and the frequency of ectopic deletion in non-mast cells (very low for the loci tested so far) may vary and have to be determined for each loxP-flanked locus [17]. For cell types that can readily be isolated in large numbers, this information can be obtained by Southern blot analysis of genomic DNA from purified cells. In the case of mast cells this approach is not possible due to the scarcity of these cells in mouse tissue or in the peritoneum. Quantification of deleted versus undeleted (floxed) alleles in DNA preparations from low numbers of cells by quantitative PCR is possible but technically challenging and does not yield information on the status of two alleles of a single cell. We therefore routinely FACS-sort single mast cells and non-mast cells (from peritoneal lavage fluid or single-cell suspensions obtained by tissue digest) into PCR tubes or microtiter plates. To this end, we stain peritoneal cell suspensions for CD117 (ckit), Fc ϵ RI, B220, CD19, and F4/80 to identify mast cells (CD117 $^+$ Fc ϵ RI $^+$), B cells (B220 $^+$ CD19 $^+$), and macrophages (F4/80 $^+$), respectively (Fig. 1).

In skin cell suspensions, we additionally include a staining for the leukocyte marker CD45. We amplify the locus of interest from each single deposited cell by two-round nested single-target PCR to determine whether the two alleles are in the floxed or the deleted state (Fig. 2).

This approach reliably yields quantitative information on the efficiency of deletion within the mast cell population. In order to exclude gross ectopic deletion in other cell types, we recommend standard Southern blot analysis of DNA from an array of tissues as well as abundant hematopoietic cell types, which can easily be isolated in high numbers by magnetic or flow cytometric sorting.

1.3 Mcpt5-Cre Mice Can Be Used to Generate Animals with Inducible or Constitutive Mast Cell Deficiency

Crossing Mcpt5-Cre mice to the iDTR (Cre-inducible diphtheria toxin receptor) strain [20] yields mice in which Cre-mediated excision of a loxP-flanked stop cassette in mast cells results in selective expression of a high-affinity receptor for diphtheria toxin (DT) in mast cells. While wild-type mouse cells are largely resistant to DT, mast cells of Mcpt5-Cre iDTR animals can selectively be killed by injections with DT, resulting in profound deficiency for connective tissue mast cells (Fig. 3).

Alternatively, crossing Mcpt5-Cre to the R-DTA strain [19] yields mice in which, upon deletion of a stop cassette, mast cells express DT and thereby are selectively eliminated. Mcpt5-Cre R-DTA mice are therefore constitutively deficient for connective tissue mast cells. We recommend breeding the R-DTA allele to

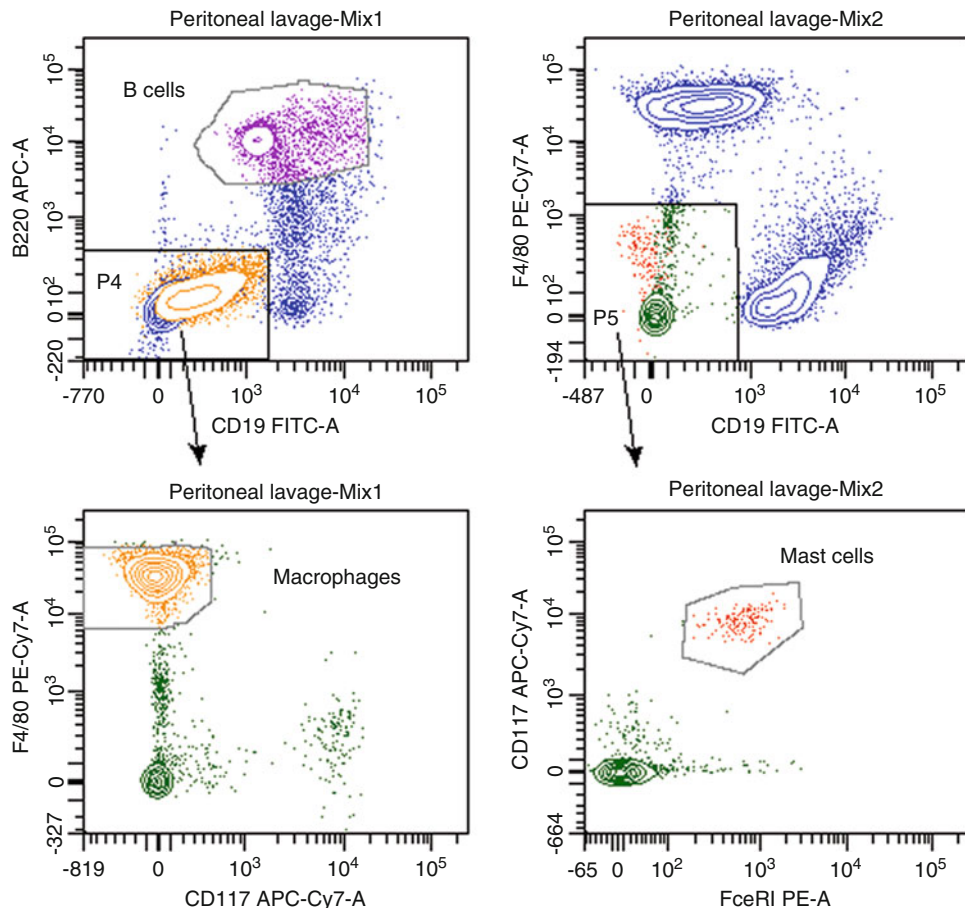


Fig. 1 Gating strategy for flow cytometric sorting of B cells (*left*) as well as mast cells (*right*) from peritoneal lavage fluid. Living cells after doublet exclusion are displayed

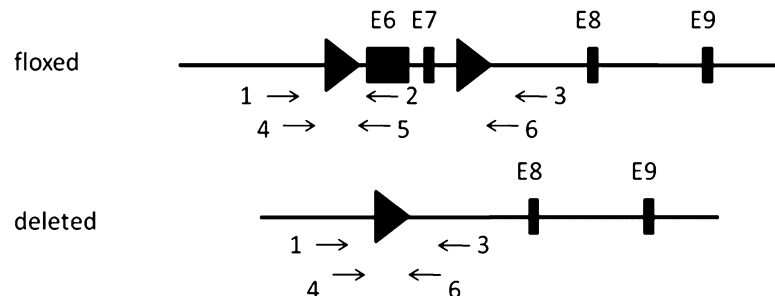


Fig. 2 Nested PCR strategy to detect loxP-flanked or deleted alleles of a floxed gene of interest in genomic DNA of single cells. A mix of primers 1, 2, and 3 are used for the first round of amplification. Second round is performed in two separate reactions containing either primers 4 and 5 or 4 and 6. In the loxP-flanked situation, a product amplified by primers 1 and 2 in the first round and primers 4 and 5 in the second round will be obtained, while primers 1 and 3 and primers 4 and 6 will amplify a product of different length from deleted alleles

Mcpt5-Cre/iDTR

DTR: diphtheria toxin receptor
DT : diphtheria toxin

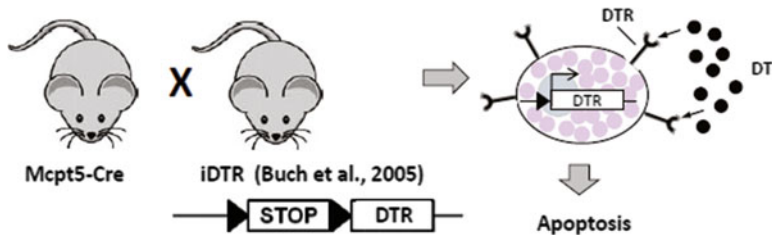


Fig. 3 The stop cassette, which prohibits DTR expression, is removed by crossing the iDTR strain to a tissue-specific Cre-expressing mouse strain. Crossing of the iDTR strain to the Mcpt5-Cre strain renders MCs sensitive to cell death induced by injection of diphtheria toxin

homozygosity. Two copies of the R-DTA knock in allele result in very low numbers of residual mast cells. The number of residual mast cells can vary in heterozygous animals. In aged Mcpt5-Cre R-DTA/R-DTA animals and in chronically inflamed skin of these mice, we occasionally observe individual groups of mast cells in the otherwise mast cell-deficient skin. Most likely, these represent local clonal expansions of single mast cells, which escaped the suicide mechanism e.g. by mutation. Herein, we describe procedures for DT-induced mast cell ablation.

2 Materials

2.1 Genotyping

1. Lysis buffer: 100 mM Tris, 200 mM NaCl, 5 mM ethylenediaminetetraacetic acid (EDTA), 0.2 % sodium dodecyl sulfate (SDS). Dissolve 12.1 g Tris, 11.7 g NaCl, 1.46 g EDTA, and 2 g SDS in 900 mL distilled water. Adjust pH to 8.5 with HCl and fill up to 1 L with additional distilled water.
2. Proteinase K (recombinant), PCR grade: Prepare Proteinase K at 20 mg/mL in DNase-free and RNase-free water.
3. Isopropanol.
4. 70 % Ethanol.
5. TE buffer: 10 mM Tris, pH 8.0, 1 mM EDTA. Dissolve 1.2 g Tris and 0.3 g EDTA in 900 mL distilled water. Adjust pH to 8.0 by adding 2 N HCl and adjust volume to 1 L with additional distilled water.
6. PCR primers (see Table 1).
7. DreamTaq DNA Polymerase (Fermentas).
8. 10× DreamTaq buffer.

Table 1
Primer used for animal genotyping

Allele	Primer name	Primer sequence 5' → 3'
Mcpt5-Cre	P1 Mcpt5-CreFor P3 Mcpt5-CreRev P4 Mcpt5-Ex1-DO3	ACA GTG GTA TTC CCG GGG AGT GT GTC AGT GCG TTC AAA GGC CA TGA GAA GGG CTA TGA GTC CCA
iDTR	P1 Mutant P2 Common P3 WT Rev	CAT CAA GGA AAC CCT GGA CTA CTG AAA GTC GCT CTG AGT TGT TAT GGA GCG GGA GAA ATG GAT ATG
ROSA-DTA	P1 R26F2 P2 R26F1	AAA GTC GCT CTG AGT TGT TAT TGC TAA AGC GCA TGC TCC AG
ROSA26-STOP	ROSA26-UP R26stopDO1 ROSA26-DO2	CCA AAG TCG CTC TGA GTT GTT ATC GCG AAG AGT TTG TCC TCA ACC GGA GCG GGA GAA ATG GAT ATG

2.2 Single-Cell Sort and PCR

2.2.1 Single-Cell Sort Components

9. dNTP (deoxyribonucleotide mix) stock (10 mM).
10. Agarose.
11. Scissors.
12. Thermocycler.
1. 1× Phosphate-buffered saline (PBS): Dissolve 8 g NaCl, 0.2 g KCl, 1.44 g Na₂HPO₄, and 0.24 g KH₂PO₄ in 800 mL distilled water. Adjust pH to 7.4 with 2 N HCl. Adjust volume to 1 L with additional distilled water. Sterilize by autoclaving or filter sterilization.
2. 5 mL syringes.
3. 18-gauge needles.
4. FACS buffer: 0.5 % BSA, 2 mM EDTA in PBS.
5. Skin digest medium: Dulbecco's modified Eagle's medium (DMEM + GlutaMAX™-I, Gibco), 20 mM HEPES (4-(2-hydroxyethyl)-1-piperazineethanesulfonic acid).
6. Enzyme mix: 0.1 mg/mL liberase (Roche), 738 U/mL DNase I (Roche), 1 mg/mL hyaluronidase (Sigma), prepare just before use.
7. Cell strainer, 40 µm.
8. FACS tubes (4.5 mL) with cell strainer cap.
9. 96-Well round-bottom plates.
10. Fluorochrome-labelled anti-mouse monoclonal antibodies for FACS staining: CD19-FITC (MB19-1, eBioscience), B220-APC (RA3-6B2, eBioscience), F4/80-PeCy7 (BM8, Biolegend), CD117-APC/Cy7 (2B8, Biolegend), Fc ϵ RI-PE

(MAR-1, eBioscience), CD45-eFluor 450 (30-F11, eBioscience), CD4-APC (GK1.5, eBioscience).

11. Fc-Block (anti-mouse CD16/32 unconjugated, clone 93, eBioscience).
12. Propidium iodide (PI) solution: 200 µg/mL PI in PBS.
13. Cell sorter with single-cell deposition module (e.g., FACSaria III, BD Biosciences).

2.2.2 Nested PCR Components

1. DreamTaq DNA Polymerase (Fermentas).
2. 10× DreamTaq buffer.
3. 25 mM MgCl₂ solution.
4. dNTP (deoxyribonucleotide mix) stock (10 mM).
5. Proteinase K (recombinant), PCR grade, 20 mg/mL.
6. First-round PCR primer, HPLC-purified.
7. Second-round nested PCR primer.
8. 96-Well PCR plates.
9. Thermocycler compatible with 96-well plates.
10. Agarose.

2.3 Diphtheria Toxin (DT)-Induced Mast Cell Depletion

2.3.1 Mast Cell Depletion in *Mcpt5-Cre iDTR* Mice

1. *Mcpt5-Cre + iDTR + C57BL/6* mice at 6–8 weeks of age and Cre-negative littermate control mice.
2. Diphtheria toxin (DT) reconstituted as 1 mg/mL stock solution in pyrogen-free deionized water. Aliquots should be stored at –80 °C.
3. 1 mL syringes.
4. 18-gauge needle.
5. 1× Phosphate-buffered saline (PBS) (prepare as in Subheading “Single- Cell Sort Components”).
6. Pyrilamine maleate salt.

2.3.2 Evaluation of Mast Cell Deficiency Using Histology and Flow Cytometry

1. Xylazine/ketamine anesthesia solution mix: Rompun/Ketanest solution: 5 % Rompun (v/v) (Bayer HealthCare) and 10 % Ketanest (v/v) (Pfizer) in sterile isotonic saline. Anesthesia dosage 5 mg/kg Rompun bodyweight and 100 mg/kg Ketanest bodyweight.
2. 5 mL syringes.
3. 18-gauge needles.
4. 4 mm biopsy punches (Stiefel, Wächtersbach).
5. 4 % formaldehyde solution.
6. Giemsa stain.
7. FACS buffer: 0.5 % bovine serum albumin (BSA) in PBS.

8. Skin digest medium: Dulbecco's modified Eagle's medium (DMEM + GlutaMAX™-I, Gibco), 20 mM HEPES (4-(2-hydroxyethyl)-1-piperazineethanesulfonic acid).
9. Enzyme mix: 0.1 mg/mL Liberase (Roche), 738 U/mL DNaseI (Roche), 1 mg/mL hyaluronidase (Sigma), prepare just before use.
10. Cell strainer, 40 μ m.
11. FACS tubes.
12. 96-Well round-bottom plates.
13. Fluorochrome-labelled anti-mouse monoclonal antibodies for FACS staining against mast cell surface markers: CD117-APC (2B8, eBioscience), Fc ϵ RI-PE (MAR-1, eBioscience), CD45-eFluor 450 (30-F11, eBioscience).
14. Fluorochrome-labelled anti-mouse monoclonal antibodies for FACS staining against cell surface markers of other immune cells if required, e.g., CD19, F4/80, CD3, CD4, CD8, CD11c, CD11b, and Gr-1.
15. Fc-Block (anti-mouse CD16/32 unconjugated, clone 93, eBioscience).
16. Propidium iodide (PI) solution (prepare as in Subheading "Single-Cell Sort Components").

3 Methods

3.1 Genotyping

3.1.1 Lysis of Tail-Tip Biopsy Tissue

1. Obtain tail biopsies from 3-week-old mice by holding mouse firmly at base of tail with one hand, and cut off approximately 0.5 cm of the tail tip with a scissor (see Note 1).
2. Add 500 μ L lysis buffer and 5 μ L proteinase K per sample.
3. Incubate overnight (8–24 h) at 55 °C in a thermal shaker.

3.1.2 DNA Isolation

1. Centrifuge for 5 min at 4 °C at >10,000 \times g.
2. Transfer supernatant to new tube and add 700 μ L ice-cold isopropanol.
3. Mix gently by inverting.
4. Centrifuge for 15 min at 4 °C at >10,000 \times g.
5. Discard supernatant.
6. Add 500 μ L 70 % ethanol to the DNA pellet.
7. Centrifuge for 5 min at 4 °C at >10,000 \times g.
8. Discard supernatant.
9. Dry DNA pellet for 15 min at room temperature and 15 min at 55 °C.
10. Resuspend DNA pellet in 50 μ L TE buffer.

11. Dissolve DNA overnight (8–24 h) at 55 °C in a thermal shaker.
12. Store at 4 °C.

3.1.3 Detection of the *Mcpt5-Cre* Transgene [9]

1. Prepare the master mix of specific primers (25 µL/sample) as in Table 2.
2. Perform thermal cycling program as in Table 3.
3. Run a 2 % agarose gel. The expected product sizes for the wt (Cre-negative) and the *Mcpt5-Cre*⁺ situation are 224 bp and 554 bp, respectively.

3.1.4 Detection of the *iDTR Rosa26* Knock-In Allele [20]

1. Prepare the R-DTA master mix (20 µL/sample) as in Table 4.
2. Perform thermal cycling as in Table 5.
3. Run a 2 % agarose gel. The expected product sizes for the wt and the knock-in alleles are 603 bp and 242 bp, respectively.

Table 2
PCR master mix for detection of the *Mcpt5-Cre* transgene

Reagent	[Final]	[Stock]	Volume (µL)
10× DreamTaq buffer	1×	10×	2.5
P1 <i>Mcpt5-Cre</i> For	0.2 µM	10 µM	0.5
P3 <i>Mcpt5-Cre</i> Rev	0.2 µM	10 µM	0.5
P4 <i>Mcpt5-Ex1-DO3</i>	0.2 µM	10 µM	0.5
dNTP	200 µM	10 mM	0.5
DreamTaq enzyme	0.05 U/µL	5 U/µL	0.25
DNA			1
ddH ₂ O			19.25

Table 3
PCR cycling profile for detection of the *Mcpt5-Cre* transgene

Cycling step #	Temp. (°C)	Time	Note
1	95.0	5 min	
2	95.0	45 s	
3	57.0	1 min	
4	72.0	45 s	Repeat steps 2–4 for 29 cycles
5	72.0	7 min	
6	10.0	Pause	

Table 4
PCR master mix for detection of the iDTR Rosa26 knock-in allele

Reagent	[Final]	[Stock]	Volume (μL)
10× DreamTaq buffer	1×	10×	2.5
Primer P1 Mutant	0.5 μM	10 μM	1.25
Primer P2 Common	1.0 μM	10 μM	2.5
Primer P3 WT Rev	1.0 μM	10 μM	2.5
dNTP	200 μM	10 mM	0.5
DreamTaq enzyme	0.05 U/μL	5 U/μL	0.25
DNA			1
ddH ₂ O			14.5

Table 5
PCR cycling profile for detection of the iDTR Rosa26 knock-in allele

Cycling step #	Temp. (°C)	Time	Note
1	94.0	3 min	
2	94.0	30 s	
3	61.0	1 min	
4	72.0	1 min	Repeat steps 2–4 for 35 cycles
5	72.0	2 min	
6	10.0	Pause	

3.1.5 Detection of the R-DTA Rosa26 Knock-In Allele [19]

1. Prepare the R-DTA master mix (20 μL/sample) as in Table 6.
2. Perform thermal cycling as in Table 7.
3. Run a 2 % agarose gel. The expected fragment size for the mutant locus is 446 bp. The wild-type locus does not yield a product.

3.1.6 Detection of the Stop Cassette Contained in the iDTR and the R-DTA Allele

1. Prepare the ROSA26-STOP master mix (25 μL/sample) as in Table 8.
2. Perform thermal cycling as in Table 9.
3. Run a 2 % agarose gel. The expected product sizes for both knock-in alleles and the wt Rosa26 locus are 300 bp and 600 bp, respectively.

Table 6
PCR master mix for detection of the R-DTA Rosa26 knock-in allele

Reagent	[Final]	[Stock]	Volume (μL)
10× DreamTaq buffer	1×	10×	2.0
Primer R26F2	0.5 μM	10 μM	1.0
Primer R26F1	0.5 μM	10 μM	1.0
dNTP	350 μM	10 mM	0.7
DreamTaq enzyme	0.125 U/μL	5 U/μL	0.5
DNA			1
ddH ₂ O			13.8

Table 7
PCR cycling profile for detection of the R-DTA Rosa26 knock-in allele

Cycling step #	Temp. (°C)	Time	Note
1	94.0	3 min	
2	94.0	30 s	
3	56.0	30 s	
4	72.0	1 min	Repeat steps 2–4 for 38 cycles
5	72.0	10 min	
6	4.0	Pause	

Table 8
PCR master mix for detection of the stop cassette contained in the iDTR and the R-DTA allele

Reagent	[Final]	[Stock]	Volume (μL)
10× DreamTaq buffer	1×	10×	2.5
ROSA26-UP	0.2 μM	10 μM	0.5
R26-stopDO1	0.2 μM	10 μM	0.5
ROSA26-DO2	0.2 μM	10 μM	0.5
dNTP	200 μM	10 mM	0.5
DreamTaq enzyme	0.05 U/μL	5 U/μL	0.25
DNA			1
ddH ₂ O			19.25

Table 9
PCR cycling profile for detection of the stop cassette contained in the iDTR and the R-DTA allele

Cycling step #	Temp. (°C)	Time	Note
1	95.0	5 min	
2	95.0	45 s	
3	54.0	1 min	
4	72.0	1 min	Repeat steps 2–4 for 11 cycles
5	95.0	45 s	
6	51.0	1 min	
7	72.0	1 min	Repeat steps 5–7 for 17 cycles
8	72.0	7 min	
9	4.0	Pause	

3.2 Single-Cell Sorting and PCR from Peritoneal Lavage

Keep all reagents and samples on ice unless indicated otherwise. Carry out centrifugation steps at 4 °C and 300 $\times g$. Single cells are sorted from the peritoneal lavage fluid and single-cell suspensions of ear skin, which is particularly rich in mast cells. Macrophages and B cells serve as controls for peritoneal lavage cells, while macrophages and T cells are sorted as controls from skin. Additional animals are included as donors for cells, which serve to set compensation of the cell sorter using single-stained samples. Cells stained with combinations of antibodies (see below) are used for test sorts. After sorting, these cells are reanalyzed to determine the purity of the isolated population. This information is important for the interpretation of the PCR results.

1. Lavage the peritoneal cavity using a 5 mL syringe and 5 mL ice-cold PBS.
2. Resuspend the cells for the single-cell sort in 300 μ L FACS buffer. Resuspend the cells of the additional control lavage in 1 mL.
3. Transfer 100 μ L of cell suspension for staining with mix 1 and 200 μ L for staining with mix 2 into a cavity of a 96-well round-bottom plate.
4. Transfer 100 μ L of lavage cell suspension from the additional control donors for each of the five single-stain controls, one unstained control, and test samples stained with mix 1 or 2.
5. Prepare the staining mixes in FACS buffer (100 μ L/animal) as in Table 10.

Table 10
Staining mixes for sorting cells from peritoneal lavages

Mix 1	Mix 2		
CD19-FITC	1:200	CD19-FITC	1:200
B220-APC	1:200	Fc ϵ RI-PE	1:300
F4/80-PeCy7	1:200	F4/80-PeCy7	1:200
CD117-APC/Cy7	1:1,600	CD117-APC/Cy7	1:1,600
CD16/32	1:200	CD16/32	1:200

6. Centrifuge 96-well plate.
7. Discard supernatant.
8. Resuspend cell samples in 100 μ L mix 1 or mix 2.
9. Single-antibody control stainings: Resuspend cells in 100 μ L FACS buffer and add single antibody.
10. Incubate for 30 min at 4 °C in the dark.
11. Add 100 μ L FACS buffer, centrifuge, and repeat this washing.
12. Resuspend cell pellet in 100 μ L FACS buffer.
13. Shortly before sorting, add 10 μ L of PI solution, filter cells into FACS tubes, and flush cell strainer once by adding 100 μ L FACS buffer.
14. Sort the following cell populations from samples stained with mix 1 (Table 10): B cells: F4/80 $^{-}$ CD117 $^{-}$ CD19 $^{+}$ B220 $^{+}$; macrophages: CD19 $^{-}$ B220 $^{-}$ CD117 $^{-}$ F4/80 $^{+}$.
15. Sort the following cell populations from samples stained with mix 2 (Table 10): mast cells CD19 $^{-}$ F4/80 $^{-}$ CD117 $^{+}$ Fc ϵ RI $^{+}$.
16. Perform the post-sort reanalysis for all populations sorted from the additional control cell donor (see Note 2).
17. Sort single cells into 96-well PCR plates containing 15 μ L H₂O per well (see Note 3).
18. Spin down sorted cells briefly.
19. Freeze cells and store at -20 °C.

3.3 Single-Cell Sorting and PCR from Skin Cell Suspensions

We usually use peritoneal lavage cells from one of the ear skin donors to set instrument compensations and one additional animal for the generation of skin cell suspensions for unstained controls and test sorts.

1. Perform peritoneal lavage from one animal with 5 mL PBS for single-stained compensation controls.

2. Take both ears from one animal and generate dermal sheets by tearing apart the dorsal from the ventral layer using forceps. Mince tissue into small pieces with a scalpel.
3. Transfer pieces into 2 mL tube containing 0.5 mL digest medium.
4. Add 0.5 mL enzyme mix.
5. Digest at 37 °C for 1 h in a thermal shaker. Do not extend incubation time as surface markers can be degraded.
6. From now on keep samples on ice.
7. Run samples through 40 µm cell strainer and rinse with 1 mL FACS buffer.
8. Wash cells by centrifugation at $300 \times g$, resuspend in 1 mL FACS buffer, and centrifuge again.
9. Resuspend skin and the peritoneal lavage cells in 200 µL and 1 mL FACS buffer, respectively. Transfer 200 µL of the cell suspension into a cavity of a 96-well round-bottom plate.
10. Transfer 100 µL/well of the peritoneal lavage cell suspension for each single staining into the 96-well plate.
11. Prepare the staining mix 3 in FACS buffer (100 µL/animal) as in Table 11.
12. Proceed as described in Subheading 3.2, steps 7–14.
13. Sort the following cell populations of mix 3: T cells CD45⁺ F4/80⁻ CD4⁺; macrophages CD45⁺ CD4⁻ F4/80⁺; and mast cells CD45⁺ CD4⁻ F4/80⁻ CD117⁺ FcεRI⁺.
14. Perform the reanalysis for all populations using the extra skin sample (see Note 2).
15. Sort single cells into 96-well PCR plate containing 15 µL H₂O per well (see Note 3).
16. Spin down sorted cells briefly.
17. Freeze cells and store at -20 °C.

Table 11
Staining mix for sorting cells from skin cell suspensions

Mix 3	
CD45-eFluor 450	1:500
FcεRI-PE	1:300
F4/80-PeCy7	1:200
CD4-APC	1:400
CD117-APC/Cy7	1:1,600
CD16/32	1:200

3.4 Nested PCR

3.4.1 Cell Lysis

1. Add 2 μ L 10 \times DreamTaq buffer, 2 μ L Proteinase K, and 1 μ L H₂O per well.
2. Perform cell lysis for 1.5 h at 50 °C.
3. Inactivate Proteinase K at 95 °C for 10 min.

3.4.2 PCR

For optimal results MgCl₂ concentration and primer annealing temperature should be titrated. PCR is performed in a total volume of 50 μ L. Keep all reagents on ice (*see Notes 4 and 5*).

1. Prepare PCR reaction mix for the first round of PCR as in Table 12.
2. Perform thermal cycling as in Table 13.
3. The PCR product is used as a template for the second round of nested PCR, and include positive and negative controls.

Table 12
PCR master mix for the first round of nested PCR

Reagent	[Final]	[Stock]	Volume (μ L)
10 \times DreamTaq buffer	1 \times	10 \times	3
Primer 1	0.2 μ M	10 μ M	1
Primer 2	0.2 μ M	10 μ M	1
Primer 3	0.2 μ M	10 μ M	1
dNTP	200 μ M	10 mM	1
DreamTaq enzyme	0.04 U/ μ L	5 U/ μ L	0.4
Single-cell mix			20
ddH ₂ O			22.6

Table 13
PCR cycling profile for nested PCR

Cycling step #	Temp. (°C)	Time	Note
1	95.0	2 min	
2	95.0	20 s	
3	50–60	30 s	Temp depends on Tm of specific primers
4	72.0	1 min	Repeat steps 2–4 for 35 cycles
5	72.0	10 min	

Table 14
PCR master mix for the second round of nested PCR

Reagent	[Final]	[Stock]	Volume (μL)
10× DreamTaq buffer	1×	10×	5
Primer 4	0.2 μM	10 μM	1
Primer 5	0.2 μM	10 μM	1
Primer 6	0.2 μM	10 μM	1
dNTP	200 μM	10 mM	1
DreamTaq enzyme	0.04 U/μL	5 U/μL	0.4
PCR product of first round of nested PCR			1
ddH ₂ O			39.6

Prepare PCR reaction mix for the second round of PCR as in Table 14.

3.5 Induced Depletion of Connective Tissue-type Mast Cells in *Mcpt5-Cre iDTR* Mice

3.6 Evaluation of Mast Cell Deficiency Using Histology and Flow Cytometry

3.6.1 Histology

4. Run PCR cycles using the same program as in step 2 (Table 13).

5. Load 10 μL of the second-round PCR product on a 1.5 % agarose gel.

1. Thaw DT stock solution (1 mg/mL) aliquots on ice and dilute to a working solution of 5 μg/mL in sterile PBS.
2. Inject both *Mcpt5-Cre⁺iDTR⁺* mice and Cre-negative iDTR⁺ littermate controls intraperitoneally (i.p.) with 25 ng DT/g bodyweight four times in weekly intervals. For first DT injection add 5 μg pyrilamine/g bodyweight (see Notes 6 and 7).

The efficiency of inducible or constitutive mast cell depletion in *Mcpt5-Cre iDTR* or *Mcpt5-Cre R-DTA* can be evaluated by histology of skin biopsies or by flow cytometric analysis of peritoneal lavage or skin cell suspensions. On one hand, the analysis of skin biopsies allows for the evaluation of mast cell numbers in living mice before the use of the respective mice in experimental models of interest. On the other hand, we usually assess the efficiency of mast cell depletion in each single mouse after performing the respective experiment by analyzing the mast cell numbers in peritoneal lavage or skin.

1. For evaluation of mast cell depletion in back skin biopsies, anesthetize mice by intraperitoneal injection of 10 μL/g bodyweight of a Rompun/Ketanest solution (see step 1, Subheading “Evaluation of Mast Cell Deficiency Using Histology and Flow Cytometry”).

2. Shave mice, lift a skin fold from the back, and fix this with two fingers on a sterile pad. Take a biopsy at the edge of the skin fold using a 4 mm biopsy punch.
3. Fix skin samples in 4 % formaldehyde solution overnight, process tissues (following standard histology protocols) and embed in paraffin. Stain 5 μ m sections with Giemsa following standard protocols. Mast cells can be identified in Giemsa-stained sections by means of their dark purple cytoplasmic granules.

3.6.2 Flow Cytometry

1. Perform peritoneal lavage and skin cell suspension as described in Subheadings 3.2 and 3.3.
2. Transfer 200 μ L of the single-cell suspension per well to a 96-well round-bottom plate.
3. Centrifuge the 96-well plate for 5 min at $300 \times g$, 4 °C. Discard the supernatant and resuspend the pellet in 100 μ L FACS buffer.
4. For detection of mast cells incubate cells with CD117-APC (1:500) and Fc ϵ RI-PE (1:200) for 30 min at 4 °C in the dark. We recommend to also stain for CD45 (e.g., CD45-eFluor 450, 30-F11, eBioscience (1:500)) in skin samples. Include the Fc-block CD16/CD32 (1:200) to avoid unspecific antibody binding.
5. Centrifuge the 96-well plate for 5 min at $300 \times g$, 4 °C. Discard the supernatant and resuspend the pellet in 100 μ L FACS buffer. Repeat this step to wash the cells.
6. Add 10 μ L of PI solution and analyze the cell suspension using a flow cytometer (*see Note 8*).

4 Notes

1. Genotyping of the animals should be performed upon weaning. Additionally, we recommend to reanalyze freshly isolated tail DNA after finishing the experiments.
2. Reanalysis of sorted cells before sorting single cells for PCR is crucial to determine efficiency and purity of the desired populations.
3. Analysis of multiple wells containing more than one cell (e.g. 10 cells) can facilitate the acquisition of a comprehensive data set. In this type of experiments, we include additional controls containing multiple mast cells plus two non-mast cells in order to make sure that we reliably detect only a few floxed alleles among a majority of deleted alleles.
4. Successful single-target PCR depends on optimal conditions during the first few cycles. Nonspecific binding of primers

results in competing nonspecific amplification, which can suppress the desired reaction. Therefore primer design is one critical step for the first round of PCR. Primers should be highly specific for their target. Check by blasting the sequence against the genome and exclude primers, which anneal nonspecifically with more than ten subsequent bases at the 3' end. For the same reason, HPLC-purified primers should be used in the first round. Non-purified oligos contain populations of oligos that lack one or several bases at the 3' end and may not be specific for the desired target.

5. Due to the extreme sensitivity (one single target) of the nested PCR, precautions against contamination with genomic DNA or, more importantly, PCR products determine the success of the experiment. The first-round reaction should be pipetted in a separated room distant to all post-first-round manipulations, preferentially in a different building. This room should be entered only with fresh cloths and a dedicated lab coat as well as bonnet and plastic overshoes. Pipetting can be done under a laminar flow. Decontamination by UV is recommended. The experimenter should shower before entering this first-round PCR area after working in post-amplification areas. After cycling is completed, never open first, never open first round PCR tubes PCR tubes in this room. Always include sufficient negative controls. In addition to standard PCR water controls, sorting controls should be included (i.e., wells in which no cell was deposited) but which are otherwise treated exactly as wells containing a cell.
6. To maintain mast cell deficiency for longer periods (several weeks) additional local treatment (e.g., by subcutaneous injections of 80 µL DT (5 ng/µL) once a week) may be required.
7. Pyrilamine maleate salt, a H₁ histamine receptor antagonist (antihistamine), was added to prevent possible anaphylactic reactions.
8. We find that stringent exclusion of doublets before and additionally after gating of the desired cell type increases the precision of the analysis.

Acknowledgments

This work was supported by research grants from the German Research Council to A.D. (DFG, Du1172/1; Du1172/2, Priority Program 1468), K.H. (DFG, CRC/SFB832, project A14; Ro2133/2), and A.R. (DFG, Ro2133/2; Ro2133/3; Ro2133/4, Priority Program 1394) and from the German-Israeli Foundation for Scientific Research and Development to K.H. (993/2008).

References

1. Galli SJ, Tsai M (2010) Mast cells in allergy and infection: versatile effector and regulatory cells in innate and adaptive immunity. *Eur J Immunol* 40:1843–1851
2. Galli SJ, Grimaldston M, Tsai M (2008) Immunomodulatory mast cells: negative, as well as positive, regulators of immunity. *Nat Rev Immunol* 8:478–486
3. Shelburne CP, Abraham SN (2011) The mast cell in innate and adaptive immunity. In: Gilfillan AM, Metcalfe DD (eds) *Mast cell biology*. Springer, USA, pp 162–185
4. Abraham SN, St. John AL (2010) Mast cell-orchestrated immunity to pathogens. *Nat Rev Immunol* 10:440–452
5. Wasiuk A, De Vries VC, Hartmann K, Roers A, Noelle RJ (2009) Mast cells as regulators of adaptive immunity to tumours. *Clin Exp Immunol* 155:140–146
6. Grimaldston MA, Chen C-C, Piliponsky AM, Tsai M, Tam S-Y, Galli SJ (2005) Mast cell-deficient W-sash c-kit mutant KitW-sh/W-sh mice as a model for investigating mast cell biology in vivo. *Am J Pathol* 167:835–848
7. Nigrovic PA, Gray DHD, Jones T, Hallgren J, Kuo FC, Chaletzky B, Gurish M, Mathis D, Benoist C, Lee DM (2008) Genetic inversion in mast cell-deficient Wsh mice interrupts Corin and manifests as hematopoietic and cardiac aberrancy. *Am J Pathol* 173:1693–1701
8. Müsch W, Wege AK, Männel DN, Hehlgans T (2008) Generation and characterization of alpha-chymase-Cre transgenic mice. *Genesis* 46:163–166
9. Scholten J, Hartmann K, Gerbaulet A, Krieg T, Müller W, Testa G, Roers A (2008) Mast cell-specific Cre/loxP-mediated recombination in vivo. *Transgenic Res* 17:307–315
10. Dudeck A, Dudeck J, Scholten J, Petzold A, Surianarayanan S, Köhler A, Peschke K, Vöhringer D, Waskow C, Krieg T, Müller W, Waisman A, Hartmann K, Gunzer M, Roers A (2011) Mast cells are key promoters of contact allergy that mediate the adjuvant effects of haptens. *Immunity* 34:973–984
11. Otsuka A, Kubo M, Honda T, Egawa G, Nakajima S, Tanizaki H, Kim B, Matsuoka S, Watanabe T, Nakae S, Miyachi Y, Kabashima K (2011) Requirement of interaction between mast cells and skin dendritic cells to establish contact hypersensitivity. *PLoS One* 6:e25538
12. Furumoto Y, Charles N, Olivera A, Leung WH, Dillahunt S, Sargent JL, Tinsley K, Odom S, Scott E, Wilson TM, Ghoreschi K, Kneilling M, Chen M, Lee DM, Bolland S, Rivera J (2011) PTEN deficiency in mast cells causes a mastocytosis-like proliferative disease that heightens allergic responses and vascular permeability. *Blood* 118:5466–5475
13. Feyerabend TB, Weiser A, Tietz A, Stassen M, Harris N, Kopf M, Radermacher P, Möller P, Benoist C, Mathis D, Fehling HJ, Rodewald H-R (2011) Cre-mediated cell ablation contests mast cell contribution in models of antibody- and T cell-mediated autoimmunity. *Immunity* 35:832–844
14. Katz HR, Austen KF (2011) Mast cell deficiency. A game of kit and mouse. *Immunity* 35:668–670
15. Lilla JN, Chen C-C, Mukai K, BenBarak MJ, Franco CB, Kalesnikoff J, Yu M, Tsai M, Piliponsky AM, Galli SJ (2011) Reduced mast cell and basophil numbers and function in Cpa3-Cre; Mcl-1fl/fl mice. *Blood* 118: 6930–6938
16. Rajewsky K, Gu H, Kühn R, Betz UA, Müller W, Roes J, Schwenk F (1996) Conditional gene targeting. *J Clin Invest* 98:600–603
17. Schmidt-Supplian M, Rajewsky K (2007) Vagaries of conditional gene targeting. *Nat Immunol* 8:665–668
18. Grimaldston MA, Nakae S, Kalesnikoff J, Tsai M, Galli SJ (2007) Mast cell-derived interleukin 10 limits skin pathology in contact dermatitis and chronic irradiation with ultraviolet B. *Nat Immunol* 8:1095–1104
19. Voehringer D, Liang H-E, Locksley RM (2008) Homeostasis and effector function of lymphopenia-induced “Memory-Like” T Cells in constitutively T cell-depleted mice. *J Immunol* 180:4742–4753
20. Buch T, Heppner FL, Tertilt C, Heinen TJAJ, Kremer M, Wunderlich FT, Jung S, Waisman A (2005) A Cre-inducible diphtheria toxin receptor mediates cell lineage ablation after toxin administration. *Nat Methods* 2:419–426

Chapter 26

Evaluation of Synovial Mast Cell Functions in Autoimmune Arthritis

Peter A. Nigrovic and Kichul Shin

Abstract

Mast cells are innate immune effector cells that reside in the healthy synovial sublining and expand in number with inflammation. These cells can play an important role in initiation of arthritis, but much about their biology and importance remains obscure. This chapter reviews the use of animal models for the study of mast cells in arthritis, with a particular focus on the K/BxN serum transfer model. We discuss tissue preparation and histological analysis for the assessment of joint inflammation, injury, and the presence and phenotype of synovial mast cells, as well as the use of bone marrow-derived mast cell (BMMC) engraftment into W/W^v mice as a tool to isolate the role of mast cells in joint inflammation and injury.

Key words K/BxN, Arthritis, Synovium, Synovial mast cells

1 Introduction

In the normal human joint, mast cells represent approximately 3 % of nucleated cells residing within 70 μ m of the joint lumen [1]. These cells do not co-compact directly with the fibroblasts and macrophages that make up the synovial lining, but rather cluster beneath it in the loose connective tissue of the synovial sublining, where they reside near blood vessels, fascial planes, and within nerves [2]. In autoimmune inflammatory arthritis and osteoarthritis, mast cells can expand in number by tenfold or more, most likely via maturation of resident or newly recruited mast cell progenitors originating from the bone marrow [2, 3]. Mast cells thereby become an impressive histological feature of the inflamed synovium (Fig. 1), and identifying their role is an important task for the synovial biologist.

Multiple systems are available for induction of experimental arthritis [4]. Most of these can be grouped into two categories. The first category consists of models in which mice develop systemic autoimmunity that then translates into joint inflammation. One example is K/BxN arthritis, in which KRN mice on the

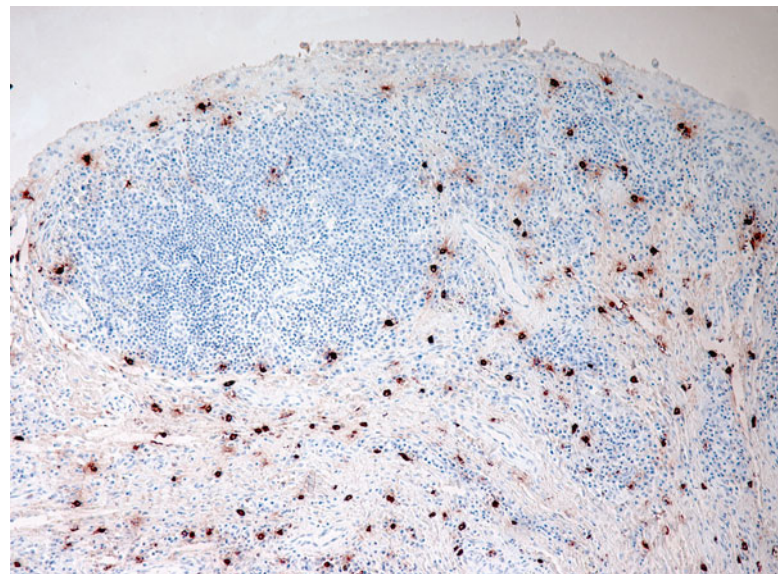


Fig. 1 Human RA synovium stained for tryptase (red) highlights abundance of mast cells in chronically inflamed joint tissue; reproduced from ref. 2

C57Bl/6 genetic background (therefore “K/B”) bearing a transgenic T cell receptor are crossed to NOD mice expressing a specific MHC II (I-A^{g7}). F1 mice from this cross (“K/BxN”) spontaneously develop high-titer IgG antibodies against the glyco-lytic enzyme glucose-6-phosphate isomerase (GPI), and arthritis develops principally through the action of these autoantibodies [5–7]. A similar sequence of events occurs in collagen-induced arthritis (CIA), a model in which DBA/1 mice immunized with type II collagen develop joint-specific autoimmunity [8]. Arthritis in these systems reflects both the formation of the adaptive immune response and the subsequent effector phase of joint inflammation. In most such models, antibodies represent a major pathogenic actor, a prominent exception being arthritis in the SKG mouse strain, which can develop through the activity of autoimmune T cells in the absence of antibody [9].

The second category of arthritis model reflects only the effector phase of disease, bypassing the generation of systemic autoimmunity via the adoptive transfer of arthritogenic autoantibodies. Examples are arthritis induced by anti-type II collagen antibodies (anti-collagen antibody-induced arthritis, CAIA), or by injection of autoantibody-containing serum from K/BxN mice (K/BxN serum transfer arthritis). In each of these experimental systems, a single monoclonal antibody is insufficient to cause disease. Rather, a cocktail of several different autoantibodies is required, likely reflecting the need for immune complex formation—i.e., both systems model IgG immune complex arthropathy [10]. These systems have several

advantages. First, formation of the autoimmune response can be taken out of the equation, affording a discrete focus on the effector phase of disease. Second, they are rapid, evolving within days of autoantibody transfer; an important corollary is that they may not model the pathogenic processes occurring in chronic, established disease such as human rheumatoid arthritis. Third, they can be induced in most strains of mice, enabling study of informative mutants, though since the intensity of resulting arthritis depends on the genetic background, care must be taken to match the background of experimental strains.

Given strong evidence implicating IgG immune complexes in human autoimmune arthritis, in particular rheumatoid-factor-positive rheumatoid arthritis, our studies have employed K/BxN serum transfer arthritis [11]. In this model, anti-GPI antibodies are believed to target the joints either through deposition of circulating immune complexes or by formation of immune complexes *in situ* on GPI deposited on the cartilage surface [12]. This chapter describes methods for the evaluation of the role of mast cells in murine K/BxN arthritis.

Distinct mast cell (MC) subpopulations are situated at specific microanatomic locations. MCs have historically been divided into two subpopulations based on histochemical staining properties: chondroitin sulfate proteoglycan-rich mucosal mast cells (MMCs) and heparan sulfate proteoglycan-rich connective tissue mast cells (CTMCs). As their names suggest, MMCs are generally found in mucosal tissue, while CTMCs are localized in connective tissue (e.g., skin, peritoneum, and synovium).

Subsequent analyses have refined the phenotypic characterization of murine MCs based on the proteases found in their cytoplasmic secretory granules. Although more than a dozen proteases are expressed in murine MCs, limited subsets are useful for defining MC subtypes. Specifically, murine MMCs express the chymases murine mast cell protease 1 (mMCP-1) and mMCP-2, whereas CTMCs express a different combination of the proteases, including the chymases mMCP-4 and mMCP-5 and the tryptases mMCP-6 and mMCP-7 [13]. Analyses using protease expression to define tissue MC subsets have revealed that MC subpopulations are quite variable, with identifiable distinctions in phenotype within the MMC and CTMC subsets at separate anatomic locations.

Murine synovial mast cells have been identified as CTMCs, therefore expressing mMCP-4, -5, -6, and -7 [13]. In contrast, human MCs can be divided into two subsets: MCs that are positive for tryptase only (MCT) and more MMC-like, and MCs that are positive for both tryptase and chymase (MCTC) and more CTMC-like. Healthy human synovial MCs are heterogeneously populated with both subsets, although MCTC outnumber MCT by 5:1 [2].

In 2002, Lee et al. demonstrated that mast cell-deficient W/Wv mice are relatively resistant to K/BxN serum transfer arthritis,

and that this resistance may be overcome by engraftment with cultured bone marrow-derived mast cells (BMMC) [14]. Analogous engraftment experiments have been conducted using Pretty2 mice, which like W/Wv animals lack mast cells through mutation in *Kit* and can be engrafted with BMMC [15]. Other mice deficient in mast cells are susceptible to antibody-mediated arthritis, including Wsh and *CPA3-Cre* (“CreMaster”) animals [16–18]. These conflicting results have been interpreted as demonstrating the shortcomings of *Kit* and *KitL* mutant mice as a model for mast cell deficiency, since mast cells are not the only lineage affected by these gene defects [19]. Yet such divergent findings could represent an interesting opportunity to understand conditions under which mast cells play a key role in joint inflammation. For example, the role of mast cells in arthritis may depend on the susceptibility of the background strain to disease and the strength of the arthritogenic stimulus. Thus, the wild-type control strain for W/Wv (WBB6) achieves a far lower intensity of arthritis than B6 or Balb/c, suggesting one explanation why mast cells might be particularly important in this background [14, 16]. Arthritis resistance in mMCP6^{-/-} mice emerges only at submaximal doses of K/BxN serum [20], while induction of arthritis in Wsh mice using lower serum doses also exposes partial arthritis resistance (PAN, unpublished data). To dissect the role of mast cells in the acute phase of K/BxN arthritis, we have used two approaches: (1) reconstitution of W/Wv mice with BMMC, and (2) study of mice genetically deficient in mediators specific for mast cells.

Mast cells are multifaceted effectors capable of both pro- and anti-inflammatory activity. Genetic deficiency ablates both facets of mast cell activity, as well as any potential effect of mast cells on neighboring cells such as fibroblasts and endothelial cells. Thus, while absence of mast cells helps to assess the “net” effect of mast cells upon a given system, alternate approaches are superior at identifying the specific contributions of individual mediators, for example as therapeutic targets. As examples of such studies, we have explored the role of mast cell mediators by inducing arthritis in animals deficient for the mast cell protease mMCP6, and more recently in mice lacking Ras guanyl nucleotide-releasing protein 4 (RasGRP4), expressed predominantly in mast cells and implicated in the modulation of signal transduction [20, 21].

2 Materials

Part I: K/BxN serum transfer arthritis

2.1 Mouse Strains and K/BxN Serum

1. KRN (K/B) mice (see Note 1).
2. NOD mice bearing H2 haplotype I^{Ag7} (e.g., NOD/ShiLtJ or NOD.Cg-*Prkdc*^{scid} *Il2rg*^{tm1Wjl}/SzJ).

3. Experimental mouse strains.
4. Non-heparinized glass pipettes (Fischer 22-260-943).
5. 1.5 mL microfuge tubes and microfuge.
6. Sterile syringes (0.3–1 cc volume) and needles (28–30G, 3/8" or 1/2" length).

2.2 Arthritis Assessment

1. Spring-loaded thickness gauge with range at least 10 mm with a resolution of ~0.01 mm and accuracy of ~15 μ m (e.g., Kafer Model J15 with 6 mm flat anvils, SPI Model 21-790-1, Long Island Indicator, Inc.).

2.3 ELISA for Anti-GPI IgG Quantitation

1. ELISA plate carbonate coating buffer: 0.1 M sodium bicarbonate buffer (pH 7.0). Dissolve 8.4 g sodium bicarbonate (NaHCO_3) in 1 L water and adjust pH to 7.0.
2. Recombinant glucose-6-phosphate isomerase (GPI) standard: 5 μ g/mL in carbonate coating buffer.
3. High-binding ELISA plates (96-well flat bottom).
4. ELISA wash buffer: Phosphate-buffered saline (PBS), 1 % Tween-20.
5. Super block: 4 % whey (w/v), 10 % fetal bovine serum (FBS), 0.5 % Tween-20, 0.05 % sodium azide (NaN_3) (w/v) in PBS. Add 40 g whey, 100 mL FBS, 5 mL Tween-20, and 0.5 g NaN_3 to 1 L PBS.
6. Detection antibody: Donkey anti-mouse IgG conjugated to horseradish peroxidase (HRP).
7. ELISA substrate: TMB (3,3',5,5'-tetramethylbenzidine) commercial stock (e.g., BD OptEIA®).
8. K/BxN serum.
9. Normal mouse serum (negative control).
10. Spectrophotometer capable of absorbance detection at 650 nm.

Part II: Histological assessment of K/BxN serum transfer arthritis

2.4 Tissue Harvest and Preparation

1. Scissors, serrated or toothed forceps, and scalpel.
2. 4 % (w/v) PFA (pH 7.2–7.4): 40 g paraformaldehyde (PFA) in PBS. Heat PFA and 900 mL PBS in large Erlenmeyer flask with magnetic agitation. Solution will go from cloudy to clear when ready. Do not allow solution boilover. If PFA does not dissolve, add a few chips of sodium hydroxide (NaOH). When PFA has dissolved, switch off heat and leave to stir while solution cools. Adjust pH to 7.2–7.4 using HCl. Add the remaining PBS to 1 L volume. Store at 4 °C.
3. Kristenson's decalcification solutions:

- (a) Stock "A" (40.5 % formic acid): Add 410 mL of 99 % formic acid to 590 mL distilled water.
- (b) Stock "B" (1 M sodium formate): Dissolve 68 g sodium formate in 1 L distilled water.
4. Kristenson's decalcification buffer (20 % A:80 % B): Mix 20 mL Stock "A," 80 mL Stock "B."

2.5 Frozen Sections

1. O.C.T. freezing medium (TissueTek®).
2. Tissue histology cryo-molds.

2.6 Histological and Immunohistochemical Staining

2.6.1 Histological Stains

1. Microscope slides and cover slips.
2. Toluidine blue
 - (a) Toluidine blue stock solution (1 %): 5 g Toluidine blue "O" (powder) in 500 mL dH₂O.
 - (b) Toluidine blue working solution (0.1 %): Dilute stock solution 1:10 in dH₂O.
3. Freshly filtered Harris' Hematoxylin (commercial).
4. Hematoxylin/eosin stain (commercial).
5. Xylene.
6. Naphthol AS-D chloroacetate (CAE) solution: Naphthol AS-D chloroacetate 100 mg in *N,N*-dimethyl formamide 50 mL (store at -20 °C).
7. 0.1 M phosphate buffer (pH 7.6): 6.5 mL of stock *A* + 43.5 mL of stock *B* (to make 50 mL).

Stock A. 0.2 M monobasic sodium phosphate (13.9 g NaH₂PO₄ in 500 mL H₂O).

Stock B. 0.2 M dibasic sodium phosphate (14.2 g Na₂HPO₄ in 500 mL H₂O).

8. 4 % sodium nitrite solution: 1 g sodium nitrite (NaNO₂) in 25 mL dH₂O.
9. New Fuchsin solution: 1 g New Fuchsin in 25 mL 2 N hydrochloric acid (HCl).
10. Lithium carbonate buffer: 1.54 g lithium carbonate (Li₂CO₃) in 100 mL dH₂O.
11. Absolute ethanol.
12. Nonaqueous mounting medium (e.g., CytoSeal 60): Use for H&E, CAE, and toluidine blue stains.

2.6.2 Immunohistochemical Staining Reagents

1. Hoechst #33258 (Sigma): Prepare 0.5 mg/mL in dH₂O, and store frozen aliquots. Dilute to 1:10,000 for inclusion in secondary antibody stain to visualize DNA.
2. VECTASTAIN® kit (Vector Labs): Contains Vectastain ABC-AP and FastRed.

3. Zenon® IgG labeling kit (Invitrogen).
4. Citrate buffer (pH 6.0) (e.g., Dako S236984-2).
5. Primary antibody to detect protein of interest.
6. Aqueous mounting medium (e.g., Biomeda Crystal/Mount)—for VECTASTAIN®.
7. Immunofluorescence mounting medium (“Vinol”): 15 % w/v polyvinyl alcohol, 33 % v/v glycerol, 0.1 % sodium azide.
 - (a) 5 g of Fisher “cold soluble” polyvinyl alcohol, P-8136-250G in 20 mL of PBS in a 50 mL tube. Mix by sonication, followed by tumbling overnight at RT.
 - (b) Add 5 mL (12.7 g) of absolute glycerol and 0.2 mL of 20 % sodium azide. Continue tumbling for 16 h at RT.
 - (c) Remove undissolved material by centrifugation at 20,000× $\times g$ for 20 min.
 - (d) Decant the syrupy supernatant and store in airtight vials at -20 °C; frozen aliquots last indefinitely.

Part III: In vivo assessment of the role of mast cells in K/BxN serum transfer arthritis

2.7 Adoptive Transfer of BMMCs into Recipient Mice

1. Donor mast cell strain.
2. Recipient mice, e.g., W/Wv (WBB6F1/J-Kit^W/Kit^{W-v}).
3. BMMC media: IMDM, 15 % FBS, 10 ng/mL interleukin 3 (IL-3), and 10–25 ng/mL Kit-L (cKit ligand, stem cell factor) with 150 μM monothioglycerol and antibiotics.

3 Methods

Part I: K/BxN serum transfer arthritis

3.1 Generation of K/BxN Serum

1. Generate donor arthritic mice by crossing the KRN strain with NOD mice bearing I-A^{g7}. All offspring develop arthritis, typically by 4–6 weeks. Both male and female mice are acceptable donors.
2. Harvest donor serum from mice between 9 and 11 weeks old.
3. Bleed animals by cardiac puncture immediately after CO₂ euthanasia. Eject blood gently (to avoid hemolysis) into 1.5 mL microfuge tubes into which small non-heparinized glass pipettes have been placed to nucleate the clot.
4. Allow blood to clot at room temperature (RT), typically 30 min.
5. Remove glass pipettes with adherent clot from the serum.
6. Centrifuge serum at maximum speed for 10 min in a microfuge.

7. Pool all serum and then split into 1 mL fractions. Store frozen at -20°C .
8. Serum remains active for at least 1 year and probably much longer.

3.2 K/BxN Serum Transfer and Assessment of Arthritis

1. Inspect paws and record baseline clinical scores and paw measurements of mice before administering K/BxN serum (see Subheading 3.3).
2. Inject experimental mice (intraperitoneal (i.p.)) with desired volume of K/BxN serum on day 0 (see Notes 2–4).
3. Inject mice with second K/BxN serum dose on day 2 if desired.

3.3 Assessment of Arthritis

K/BxN arthritis principally affects the paws, and is typically assessed in all four paws at each reading using both subjective (clinical index) and objective (paw swelling) measurements. In experienced hands, assessment can be done and recorded in less than 1 min per mouse.

1. Grade each mouse daily by scoring clinical index and measuring paw swelling. We typically grade mice daily starting with observations on day 0 before injecting the first serum dose.
2. *Clinical index*: Grade each paw on an arbitrary scale of 0–3 with a total possible of score of 12 (see Table 1). Normal ankles are scored 0; a point is given for swelling affecting the dorsal surface, ventral surface, toes, and ankle/wrist itself, capping at a maximum of 3 [14, 21] (see Note 5).
3. *Paw swelling*: Paws are measured in a standardized way at each reading using a spring-loaded thickness gauge (Fig. 2). Ankles are measured across the malleoli with the joint in dorsiflexion; the degree of dorsiflexion varies somewhat from examiner to examiner depending on preferred grip technique, but should be consistent among measurements. We prefer to measure wrists as well.

Table 1
Assessment of arthritis (clinical index)

Score for each paw	Description
0	Normal
1	Swelling isolated to one aspect of joint (toes, dorsal surface, ventral surface, or ankle/wrist)
2	Swelling evident in two aspects of joint (toes, dorsal surface, ventral surface, or ankle/wrist)
3	Swelling evident in three or more aspects of joint (toes, dorsal surface, ventral surface, or ankle/wrist)

Clinical index = sum of each paw score. Maximum score = 12

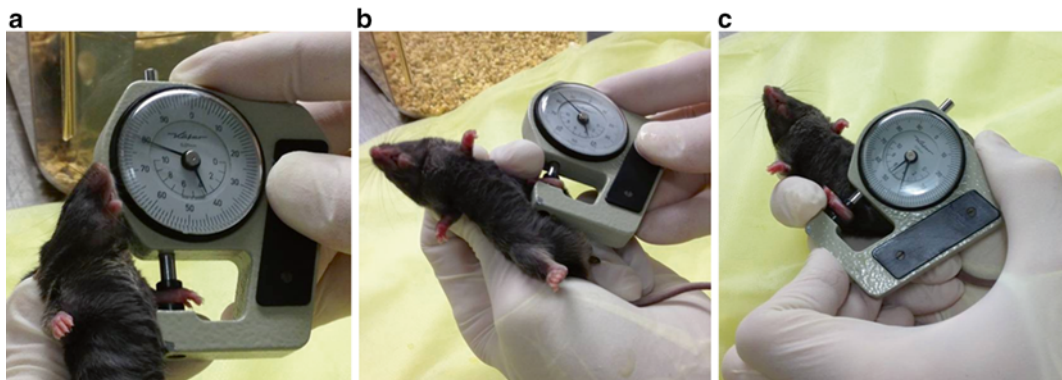


Fig. 2 Measurement of paw thickness in arthritis. **(a)** Forepaw measurement in dorsal-ventral axis. **(b)** Left hindpaw measurement. **(c)** Right hindpaw measurement. Note in **b** and **c** that a finger in the restraining hand is used to maintain the measured joint in a degree of flexion that must be maintained constant from measurement to measurement. The caliper must be held in each hand alternately

These are measured with the joint in neutral (straight) position (*see Note 6*).

4. The “flare”: Several groups have described the rapid entry of K/BxN serum into joints after injection [22, 23]. Binstadt et al. found that this entry reflected transient paw-restricted vascular leak that was dependent upon both mast cells and neutrophils [23]. We find that this acute edema can be readily assessed as transient swelling in the paws, peaking 20–30 min after i.p. injection [24] (*see Note 7*).

3.4 ELISA for Anti-GPI IgG Quantitation

In some situations, it may be useful to quantify anti-GPI IgG in treated mice, for example to justify exclusion of an extreme experimental outlier. Another situation in which this is useful is in the evaluation of new murine strains, where unusual susceptibility or resistance can occasionally result from aberrant clearance of administered IgG [25].

1. Coat high-binding ELISA plate overnight at 4 °C with 100 µl of 5 µg/mL recombinant GPI in 0.1 M sodium bicarbonate buffer (pH 7.0).
2. Wash plate twice with ELISA wash buffer, 5 min per wash at RT.
3. Add 100 µl Super Block and incubate for 1 h at RT.
4. Wash plate twice with ELISA wash buffer, 5 min per wash at RT.
5. Add 50 µL/well of K/BxN or normal mouse serum diluted in Super Block to plates and incubate for 1 h at RT (*see Note 8*). Positive control, KBN serum (diluted). Negative control, normal mouse serum.
6. Wash plate four times with ELISA wash buffer, 5 min per wash at RT (*see Note 9*).

7. Add 50 μ L per well HRP-conjugated detection antibody (1:400 in PBS). Incubate for 1 h at RT.
8. Wash plate four times with ELISA wash buffer, 5 min per wash at RT.
9. Add 100 μ l of TMB substrate per well and incubate for 5 min at RT.
10. Read absorbance using spectrophotometer with $\lambda = 650$ nm.

Part II: Histological assessment of K/BxN serum transfer arthritis

3.5 Tissue Harvest and Preparation

1. Following euthanasia, wet the skin with 70 % EtOH spray to control fur.
2. Make a single longitudinal incision through skin with a sharp scalpel from mid-shin to dorsal mid-foot.
3. Grasp edges of skin with toothed forceps and gently pull up and down to remove skin from deeper tissues (see Note 10).
4. Use scissors to cut lower leg just distal to the knee and cut off distal foot and attached skin.
5. The sample can be trimmed further after fixation by the histotechnologist to fit the cassette prior to embedding.

3.5.1 Paraffin

Paraffin sections are most generally used for standard histological analysis as well as for immunohistochemical study.

1. Fix joints in 4 % PFA for 24–48 h at RT.
2. Transfer to Kristenson's decalcification buffer (20 % A:80 % B) for 48 h at RT (see Notes 11 and 12).
3. Dehydrate in 70 % EtOH and then process to embed in paraffin.

3.5.2 Frozen Sections

Frozen sections are used where antigens are unavailable for staining after paraffin or where immunofluorescence studies are desired.

1. Embed whole ankles in O.C.T. freezing medium (Tissue-Tek[®]) in specially designed plastic receptacles (e.g., histology cryomolds) (see Note 13).
2. Samples are stored at -80 °C in Bitran[®] freezer bags to avoid desiccation.

3.6 General Histological Assessment of Joint Injury

Multiple aspects of arthritis pathophysiology can be assessed by histology using standard hematoxylin and eosin (H&E)-stained slides of joint synovial sections. Typically, we begin by grading H&E-stained paraffin sections of ankle tissue for inflammation, bone erosion, and cartilage injury using the system described in Table 2. The importance of blinding the investigator to the sample identifications during assessment to guarantee objectivity cannot be overstated.

Table 2
Histological scoring of arthritis severity

Score	Inflammation	Bone erosion	Cartilage damage
0	Normal	Normal	Normal
1	Minimal infiltration of inflammatory cells and/or mild edema	Small areas of resorption, not readily apparent on low magnification, in trabecular or cortical bone	Synovial adherence to margins of cartilage in <3 sites
2	Mild infiltration	More numerous areas of resorption, not readily apparent on low magnification, in trabecular or cortical bone	Synovial adherence to margins of cartilage in three or more sites
3	Moderate infiltration	Obvious resorption of trabecular and cortical bone, without full-thickness defects in the cortex; loss of some trabeculae; lesions apparent on low magnification	Synovial adherence to cartilage not limited to margins but no full thickness
4	Marked infiltration	Full-thickness defects in the cortical bone and marked trabecular bone loss, without distortion of the profile of the remaining cortical surface	Full-thickness injury in <3 sites
5	Severe infiltration	Full-thickness defects in the cortical bone and marked trabecular bone loss, with distortion of the profile of the remaining cortical surface	Full-thickness injury in three or more sites

Adapted from ref. [29], based on original scoring system from Pettit et al. [30]

3.7 Specific Stains and Protocols for Synovial Tissue Staining

3.7.1 Proteoglycan Staining of Paraffin-Embedded Sections

3.7.2 Toluidine Blue

Proteoglycans in the cartilage can be stained using toluidine blue or by immunohistochemical staining using an anti-aggreccan polyclonal antibody [20] (see Note 14).

1. Deparaffinize and hydrate slide to distilled water.
2. Expose tissue for 15–20 s to 0.1 % toluidine blue solution (adjusted according to desired staining intensity).
3. Rinse briefly with distilled water (too long will “decolor” extensively)—this step is empiric and tissue dependent.
4. Immediately place in 95 % EtOH followed by 3–4 quick changes of 100 % EtOH.
5. Allow to air-dry completely.
6. Coverslip with nonaqueous mounting medium (e.g., Cytoseal 60). Mast cells and cartilage proteoglycan stain violet (Figs. 3 and 4).

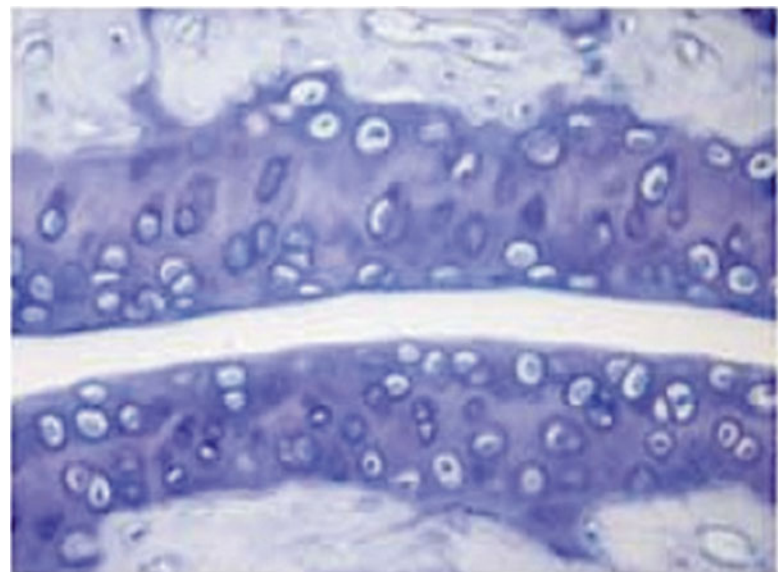


Fig. 3 Cartilage proteoglycan staining with toluidine blue. This murine tibiotalar joint was sectioned and stained with toluidine blue. Proteoglycan within cartilage is stained as *darker bluish-purple*

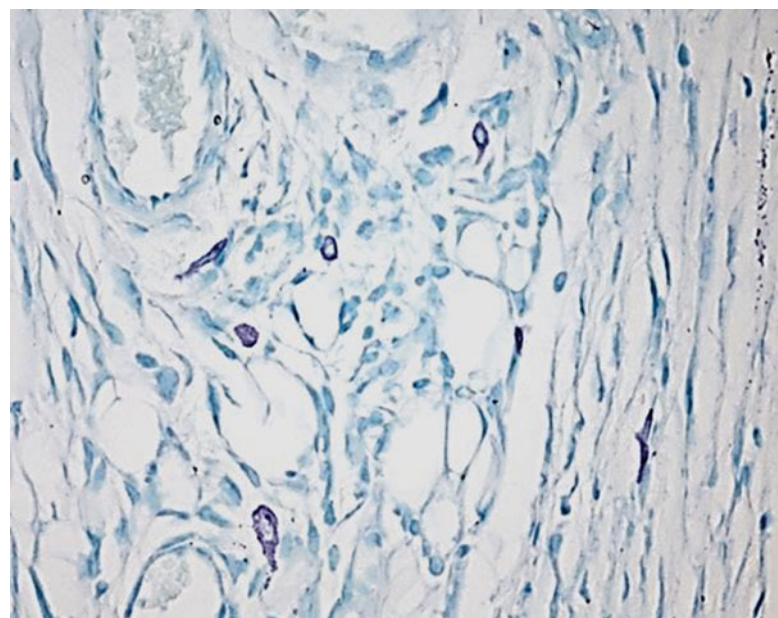


Fig. 4 Toluidine blue staining of synovial mast cells. Note *purple* color of mast cells compared to *blue* background

3.7.3 Chloroacetate Esterase (CAE) Staining

1. Deparaffinize and hydrate slide to distilled water.
2. Mix 5 μ L 4 % sodium nitrite solution and 5 μ L New Fuchsin solution: wait for ~1 min.
3. Add 2 mL phosphate buffer (0.1 M, pH 7.6) and mix with reagents in **step 2**. Wait for ~3 min (turns to pinkish color).
4. Add 100 μ L naphthol AS-D chloroacetate to reagents in **step 3** (gives red turbid color).
5. Add 100–150 μ L of mixture per slide and stain for 10–15 min. Wash with dH₂O.
6. Counterstain with hematoxylin for approximately 20–60 s (adjust hematoxylin staining duration to desired color intensity). Wash with dH₂O.
7. Wash with lithium carbonate
8. Dehydrate in EtOH series: 95 % EtOH (two changes), absolute EtOH (two changes), then xylene (two changes).
9. Coverslip with nonaqueous mounting medium (e.g., Cytoseal 60).

A sample CAE stain of synovial tissue is shown in Figure 5. This stain has the advantage of rendering mast cells bright and easy to identify and photograph.

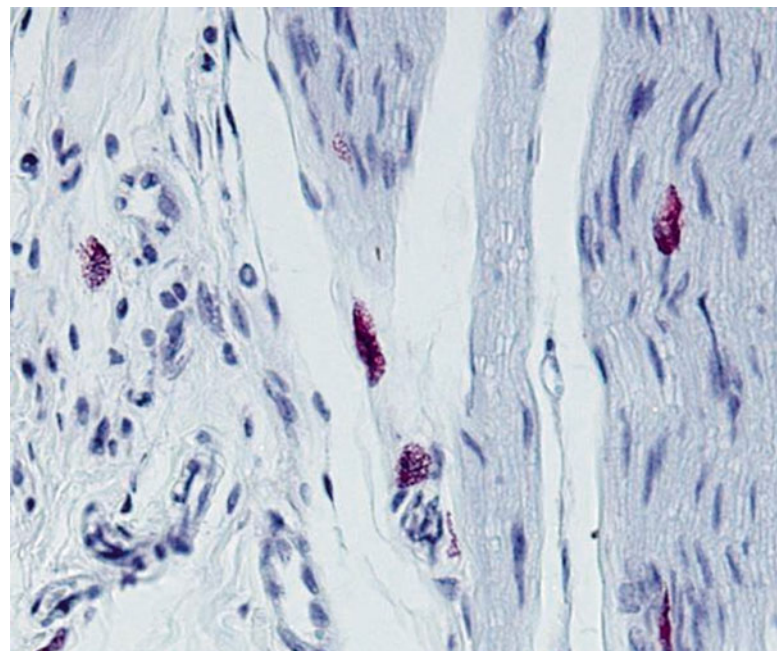


Fig. 5 CAE staining of synovial mast cells

3.7.4 Immunohistochemical Staining of Mouse Mast Cell Proteases or Human Tryptase

1. Deparaffinize and hydrate slide to distilled water.
2. Perform antigen retrieval:
 - (a) Immerse slide in preheated citrate buffer (pH 6.0) in 86 °C water bath for 15 min.
 - (b) Cool to room temperature (RT) for 10 min.
 - (c) Rinse with water (RT).
 - (d) Immerse in PBS for 5 min (RT).
3. Incubate slide in blocking serum for 30 min, and then blot excess serum (*see Note 15*).
4. Incubate in 150 µL primary antibody diluted in PBS for 60 min at RT (*see Note 16*). Wash three times with PBS.
5. Incubate in 500 µL biotinylated secondary antibody for 30 min. Wash three times with PBS.
6. Incubate in 500 µL VECTASTAIN ABC-AP reagent (*see Note 17*) for 30 min. Wash three times with PBS.
7. Incubate in 200 µL FASTRED until desired stain intensity develops (~15 min) and then rinse with water.
8. Counterstain lightly with hematoxylin for 30 s. Wash three times with water.
9. Dip in lithium carbonate. Wash 1× with water.
10. Coverslip with aqueous mounting media (e.g., Biomeda Crystal/Mount).

Sample of immunohistology stain of synovial tissue using primary antibody to mMCP6 is shown in Fig. 6.

3.7.5 Immunofluorescence Staining of Murine Mast Cell Proteases

1. Deparaffinize and hydrate slide to distilled water.
2. Perform antigen retrieval:
 - (a) Immerse slide in preheated citrate buffer (pH 6.0) in 86 °C water bath for 15 min.
 - (b) Cool to room temperature (RT) for 10 min.
 - (c) Rinse with water (RT).
 - (d) Immerse in PBS for 5 min (RT).
3. Incubate slide in blocking serum for 30 min, and then blot excess serum (*see Note 15*).
4. Prepare 1 µg of primary antibody in PBS (volume < 20 µL) (*see Notes 16 and 18*).
5. Add 5–10 µL (3:1 or 6:1) of Zenon® IgG labeling reagent (Component A) to antibody solution and incubate for 5 min in RT.
6. Add 5 µL of Zenon® blocking reagent (Component B) to mixture and incubate for 5 min in RT (use within 30 min).

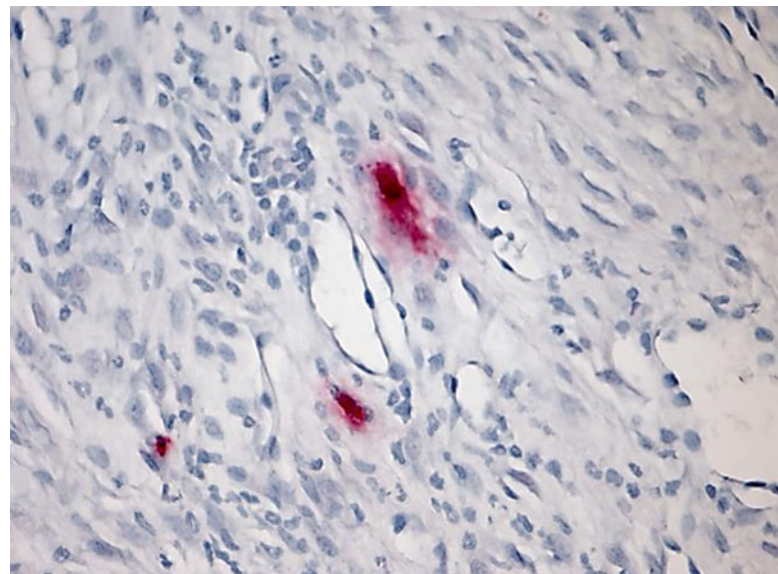


Fig. 6 Immunohistochemistry of murine synovial mast cells for mMCP-6

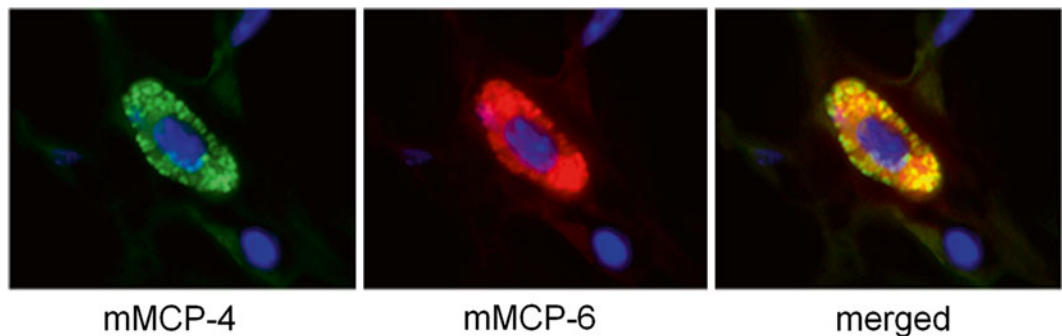


Fig. 7 Immunofluorescence staining of murine synovial mast cells for mMCP4 (green) and -6 (red). Merged figure (yellow) shows that both proteases are expressed in the synovial mast cell

7. Add 100 μ L of final mixture diluted in PBS for 60 min.
8. Wash twice with PBS (or wash once for 10–15 min).
9. Add 300 μ L of 4 % PFA and incubate for 15 min in RT.
10. Wash three times with PBS.
11. Counterstain with Hoechst 1:10,000 in PBS for 10 min.
12. Wash once more with PBS.
13. Mount with Vinol mounting medium (*see Note 19*).

Direct conjugation of antibodies permits multicolor immunofluorescence microscopy [13] (Fig. 7).

Part III: In vivo assessment of the role of mast cells in K/BxN serum transfer arthritis

3.8 Mast Cell Engraftment

1. Culture bone marrow-derived mast cells (BMMC):
 - (a) Flush bone marrow from tibias and femurs of a donor mouse.
 - (b) Cultured in media supplemented in BMMC media for approximately 4 weeks. Change media weekly.
 - (c) After approximately 4 weeks in culture, culture conditions yield a population of $50\text{--}80 \times 10^6$ cells that is $>97\%$ cKit $^+$ Fc ϵ RI $^+$.

By employing mast cells genetically deficient in specific molecules of interest, the role of these factors can be identified [16, 24].

2. Adoptive transfer of BMMCs:
 - (a) At 4 weeks, inject 1×10^7 BMMC (in 200 μL volume) by tail vein into W/Wv mice.
 - (b) Allow 8–10 weeks for engraftment before conducting serum-transfer experiments (see Notes 20 and 21).
 - (c) Engraftment can be confirmed using the histological methods described in Subheadings 3.5–3.7.

4 Notes

1. KBN mice are available only by permission of INSERM (Institut National de la Santé et de la Recherche Medicale).
2. *Batch effect.* K/BxN serum is a biological product and exhibits batch-to-batch variability in potency. This effect is relatively minor, such that inter-experimental comparison is usually possible. However, if a subtle effect is expected, it is helpful to generate a common serum stock for use in replicate experiments. In every case, all animals within any experiment should receive aliquots of the same serum pool.
3. *Titrate K/BxN serum dose.* The intensity of arthritis depends on the background strain [26]. For C57BL/6 (B6) mice, we find that a dose of 150 μL K/BxN serum on days 0 and 2 usually elicits a maximal response. Balb/c mice are more susceptible to disease and can be rendered vigorously arthritic at a dose of 50–75 $\mu\text{L} \times 2$. However, maximal arthritis is not always the desired outcome. For example, reduction in arthritis intensity due to deficiency of mouse mast cell protease 6 (mMCP6, B6 background) is seen at 50 μL but not 150 $\mu\text{L}/\text{dose}$ [20]. Similarly, an increase in the intensity of arthritis cannot be observed if all mice are maximally arthritic. Therefore, arthritis of mid-range intensity (mean clinical index of 6–8) is often optimal. Where such a mid-range of arthritis intensity is required, it

can be helpful to prepare a serum pool sufficient for all experimental replicates and titered it to identify an optimal dose.

4. *Serum administration regimen.* K/BxN serum may be administered either by intravenous (i.v.) or intraperitoneal (i.p.) routes. For convenience we typically employ the latter. Repeat doses on days 0 and 2 are employed both to achieve maximal arthritis and to provide a safeguard in case one of the doses is inadvertently administered into a hollow viscus such as gut or bladder, which can occur as often as 1 in 5 blind lower quadrant injections. To further minimize this consequence, we commonly divide each injection (e.g., 75 μ L) into each lower quadrant on both days 0 and 2 for B6 mice.
5. Where the clinical examination is ambiguous, a change in measured paw thickness (*see* below) can help at assignment of a final score. Trauma to the toes is fairly common; in particular, swelling of the great toes is of limited specificity, particularly if there is evident nail injury.
6. Thickness should be noted at the point where the dial gauge first arrests, since continued compression will result from the pressure of the caliper spring, especially in the edematous paw. A typical adult mouse ankle measures around 3 mm and wrist about 2 mm. Inter-observation measurement consistency should be in the range of 0.1 mm. Maximum swelling is typically in the range of 0.5–1.5 mm per paw. Swelling is typically reported as change from baseline summed across all measured joints.
7. Flare is quantitated by clinical index, caliper measurement of paw swelling, or both. Recognizing that i.p. injections sometimes enter a hollow viscus, where serum is biologically unavailable, we monitor all animals for flare as a proxy measure for satisfactory serum delivery. Note that (1) flare occurs only after the *first* serum injection and (2) mice lacking mast cells or depleted of neutrophils do not flare [24, 27]. Given the role of mast cells in the flare, observing this phenomenon can be informative about the status and behavior of synovial mast cells.
8. Where large differences in arthritis intensity become evident between test and control animals, it is important to assess serum anti-GPI IgG concentration to determine whether the effect represents accelerated IgG clearance [21, 25]. Similarly, absence of detectable anti-GPI IgG is an objective basis to exclude from the analysis a mouse that failed to develop arthritis, since in some cases the serum injected i.p. ends up in a hollow viscus such as gut or bladder. The ELISA is very sensitive. Use multiple serial dilutions (e.g., 1:3 dilution steps) to ensure that the results fall within the linear range of the ELISA.
9. Extensive washing is required to eliminate potential inactivation of HRP in detection antibody by azide present from Super Block reagent.

10. Skin removal allows fixative to penetrate the tissues and removes the fur that interferes with processing.
11. Although a 50 % Stock A+50 % Stock B mixture reduces the time necessary to adequately decalcify tissues this is *not* recommended.
12. Tissues should remain in working solution for 24–48 h as Kristenson's is slower than commercial decalcification solutions. If bone samples are large, change solution after the first 24 h and continue with new solution for a full 48 h. Decalcification can be repeated or resumed even after tissue dehydration in 70 % EtOH.
13. Be careful to avoid air bubbles and ensure that the specimen floats horizontally (long axis parallel to floor of cassette) in the freezing medium in order to permit optimal sectioning.
14. Aggrecan (cartilage-specific proteoglycan core protein) is the major protein constituent of proteoglycan in cartilage.
15. Always use a humidified staining chamber to prevent desiccation of stain onto tissue, and prepare buffers and other reagents immediately before staining.
16. Primary antibodies against a range of targets can be identified from the published literature (e.g., *see* ref. 13).
17. Note that an alkaline phosphatase (AP)-based system is preferable to horseradish peroxidase (HRP) owing to abundant endogenous peroxidase in mast cells. The red-colored substrate also helps to better distinguish mast cells within tissues.
18. Buffers can affect immunofluorescence staining intensity. While the protocols here are optimized for PBS, some antigens stain better in PHEM buffer (pH 6.9) (60 mM Pipes, 25 mM HEPES, 10 mM EGTA, 2 mM MgCl₂). Both should be tried when optimizing a new staining protocol.
19. When applying Vinol, place a small drop of the medium and press down gently without sliding the cover slip. Where feasible, such as with cytospin preparations, consider spinning cells on the cover slip rather than the slide for highest resolution, but this is not possible for tissue sections. Blot off excess Vinol with laboratory wipes (e.g., Kimwipes), rinse very briefly with distilled water from a squirt bottle, and immediately re-blot. Slides may be viewed immediately but should be allowed to set overnight (protected from light) at room temperature before viewing with oil immersion. Store fluorescent slides in the dark.
20. By this time point, mast cells are histologically visible in ankle tissue at levels of approximately 50 % that observed in WBB6 controls [16]. Mast cells are also abundant in spleen, though splenectomy experiments suggest that these cells are not relevant for the arthritis phenotype [16]. Studies in our hands using CD45.1 congenic donors have not identified co-engraftment

of hematopoietic lineages aside from mast cells, as determined by flow cytometry of circulating blood, spleen, or marrow (PAN, unpublished data). Similar purity of engraftment has been recently found for BMMC transfer into Pretty2 mice [15]. Thus, phenotypic changes observed after mast cell transfer can, to the best of our knowledge, justifiably be attributed to the engrafting mast cells. However, limitations include failure to achieve normal numbers of mast cells in joint tissues and, potentially, differences in distribution and effector phenotype compared with endogenous mast cells, though in general engrafted mast cells are believed to assume the phenotype dictated by their new environment [28].

21. While W/Wv mice will “accept” mast cells from many B6-derived donor strains, some fail to engraft, perhaps because of rejection of non-B6 elements. Therefore, the success of engraftment must be determined in each experiment, for example by tissue staining of ankle tissue with toluidine blue. Of note, we have been unsuccessful at achieving engraftment of B6 mast cells into ankle tissues of Wsh mice, despite the appearance of mast cells in recipient spleens (PAN, unpublished data).

Acknowledgements

This work was funded in part through the support of the Cogan Family Foundation (to P.A.N.). We are grateful to Dr. Altan Ercan for the K/BxN IgG ELISA protocol, to Ms. Theresa Bowman for histotechnical guidance, and to Dr. Nancy Kedersha for the immunofluorescence mounting medium protocols.

References

1. Castor W (1960) The microscopic structure of normal human synovial tissue. *Arthritis Rheum* 3:140–151
2. Nigrovic PA, Lee DM (2007) Synovial mast cells: role in acute and chronic arthritis. *Immunol Rev* 217:19–37
3. Crisp AJ, Chapman CM, Kirkham SE, Schiller AL, Krane SM (1984) Articular mastocytosis in rheumatoid arthritis. *Arthritis Rheum* 27(8): 845–851
4. Monach PA, Benoist C, Mathis D (2004) The role of antibodies in mouse models of rheumatoid arthritis, and relevance to human disease. *Adv Immunol* 82:217–248
5. Kouskoff V, Korganow AS, Duchatelle V, Degott C, Benoist C, Mathis D (1996) Organ-specific disease provoked by systemic autoimmunity. *Cell* 87(5):811–822
6. Korganow AS, Ji H, Mangialao S, Duchatelle V, Pelanda R, Martin T et al (1999) From systemic T cell self-reactivity to organ-specific autoimmune disease via immunoglobulins. *Immunity* 10(4):451–461
7. Matsumoto I, Staub A, Benoist C, Mathis D (1999) Arthritis provoked by linked T and B cell recognition of a glycolytic enzyme. *Science* 286(5445):1732–1735
8. Courtenay JS, Dallman MJ, Dayan AD, Martin A, Mosedale B (1980) Immunisation against heterologous type II collagen induces arthritis in mice. *Nature* 283(5748):666–668
9. Sakaguchi N, Takahashi T, Hata H, Nomura T, Tagami T, Yamazaki S et al (2003) Altered thymic T-cell selection due to a mutation of the ZAP-70 gene causes autoimmune arthritis in mice. *Nature* 426(6965):454–460

10. Maccioni M, Zeder-Lutz G, Huang H, Ebel C, Gerber P, Hergueux J et al (2002) Arthritogenic monoclonal antibodies from K/BxN mice. *J Exp Med* 195(8):1071–1077
11. Nigrovic PA, Lee DM (2006) Immune complexes and innate immunity in rheumatoid arthritis. In: Firestein GS, Panayi GS, Wollheim FA (eds) *Rheumatoid arthritis: new frontiers in pathogenesis and treatment*, 2nd edn. Oxford University Press, Oxford, pp 135–156
12. Matsumoto I, Maccioni M, Lee DM, Maurice M, Simmons B, Brenner M et al (2002) How antibodies to a ubiquitous cytoplasmic enzyme may provoke joint-specific autoimmune disease. *Nat Immunol* 3(4):360–365
13. Shin K, Gurish MF, Friend DS, Pemberton AD, Thornton EM, Miller HR et al (2006) Lymphocyte-independent connective tissue mast cells populate murine synovium. *Arthritis Rheum* 54(9):2863–2871
14. Lee DM, Friend DS, Gurish MF, Benoist C, Mathis D, Brenner MB (2002) Mast cells: a cellular link between autoantibodies and inflammatory arthritis. *Science* 297(5587):1689–1692
15. Guma M, Kashiwakura J, Crain B, Kawakami Y, Beutler B, Firestein GS et al (2010) JNK1 controls mast cell degranulation and IL-1 β production in inflammatory arthritis. *Proc Natl Acad Sci U S A* 107(51):22122–22127
16. Nigrovic PA, Binstadt BA, Monach PA, Johnsen A, Gurish M, Iwakura Y et al (2007) Mast cells contribute to initiation of autoantibody-mediated arthritis via IL-1. *Proc Natl Acad Sci U S A* 104(7):2325–2330
17. Zhou JS, Xing W, Friend DS, Austen KF, Katz HR (2007) Mast cell deficiency in Kit(W-sh) mice does not impair antibody-mediated arthritis. *J Exp Med* 204(12):2797–2802
18. Feyerabend TB, Weiser A, Tietz A, Stassen M, Harris N, Kopf M et al (2011) Cre-mediated cell ablation contests mast cell contribution in models of antibody- and T cell-mediated autoimmunity. *Immunity* 35(5):832–844
19. Katz HR, Austen KF (2011) Mast cell deficiency, a game of kit and mouse. *Immunity* 35(5):668–670
20. Shin K, Nigrovic PA, Crish J, Boilard E, McNeil HP, Larabee KS et al (2009) Mast cells contribute to autoimmune inflammatory arthritis via their tryptase/heparin complexes. *J Immunol* 182(1):647–656
21. Adachi R, Krilis SA, Nigrovic PA, Hamilton MJ, Chung K, Thakurdas SM et al (2012) Ras guanine nucleotide-releasing protein-4 (RasGRP4) involvement in experimental arthritis and colitis. *J Biol Chem* 287(24):20047–20055
22. Wipke BT, Wang Z, Kim J, McCarthy TJ, Allen PM (2002) Dynamic visualization of a joint-specific autoimmune response through positron emission tomography. *Nat Immunol* 3(4):366–372
23. Binstadt BA, Patel PR, Alencar H, Nigrovic PA, Lee DM, Mahmood U et al (2006) Particularities of the vasculature can promote the organ specificity of autoimmune attack. *Nat Immunol* 7(3):284–292
24. Nigrovic PA, Malbec O, Lu B, Markiewski MM, Kepley C, Gerard N et al (2010) C5a receptor enables participation of mast cells in immune complex arthritis independently of Fc γ receptor modulation. *Arthritis Rheum* 62(11):3322–3333
25. Akilesh S, Petkova S, Sproule TJ, Shaffer DJ, Christianson GJ, Roopenian D (2004) The MHC class I-like Fc receptor promotes humorally mediated autoimmune disease. *J Clin Invest* 113(9):1328–1333
26. Ohmura K, Johnsen A, Ortiz-Lopez A, Desany P, Roy M, Besse W et al (2005) Variation in IL-1 β gene expression is a major determinant of genetic differences in arthritis aggressivity in mice. *Proc Natl Acad Sci U S A* 102(35):12489–12494
27. Wang J-X, King S, Bair A, Shnayder R, Hsieh Y-F, Shieh C-C et al (2012) Ly6G ligation blocks recruitment of neutrophils via a beta 2 integrin-dependent mechanism. *Blood* 120(7):1489–1498
28. Gurish MF, Pear WS, Stevens RL, Scott ML, Sokol K, Ghildyal N et al (1995) Tissue-regulated differentiation and maturation of a v-abl-immortalized mast cell-committed progenitor. *Immunity* 3(2):175–186
29. Chen M et al (2006) Neutrophil-derived leukotriene B4 is required for inflammatory arthritis. *J Exp Med* 203:837–842
30. Pettit AR et al (2001) TRANCE/RANKL knockout mice are protected from bone erosion in a serum transfer model of arthritis. *Am J Pathol* 159:1689–1699

Chapter 27

Methods for the Study of Mast Cells in Cancer

Nichole R. Blatner, FuNien Tsai, and Khashayarsha Khazaie

Abstract

Tumor growth requires interactions of tumor cells with a receptive and inductive microenvironment. Two major populations of tumor-infiltrating cells are considered to be essential for producing such a microenvironment: (1) proinflammatory cells that nurture the tumor with growth factors and facilitate invasion and metastasis by secreting proteases and (2) immune suppressive leukocytes including T-regulatory cells (Treg) that hinder tumor-specific CD8 T-cell responses, which otherwise could potentially reject the tumor. Among the proinflammatory cells, accumulation of mast cells (MCs) in human tumors is frequently recorded and was recently linked with poor prognosis. Causative links between mast cell infiltration and tumor progression can be deduced from animal studies. There is an interesting link between mast cells and Treg. The adoptive transfer of Treg from healthy syngeneic mice to mice susceptible to colon cancer suppresses focal mastocytosis and hinders tumor progression. Furthermore, T-cell-deficient mice susceptible to colon cancer show enhanced focal mastocytosis and tumor invasion. Here, we describe methods to assess MCs in mouse models of cancer and to investigate how MCs affect tumor epithelium. Additionally, we will detail methods used to investigate how T cells influence MCs and how MCs influence T cells.

Key words Polyposis, Colon cancer, Mast cell, Treg

1 Introduction

Inflammation in the gastrointestinal tract can be protective or pathogenic. A certain level of inflammation is necessary to maintain intestinal homeostasis and protect against gut microbiota [1]. However, chronically elevated inflammation predisposes to colon cancer, and inflammation in response to cancer is an inherent component of tumor progression. MC infiltration in tumors, which can be detected by immunohistochemistry of MC-specific products, in many instances correlates with poor prognosis [2]. We have provided evidence for a tumor-promoting role of MC. In mice prone to polyposis, MC progenitors (MCp) migrated from the bone marrow (BM) to seed and accumulate in newly arising dysplastic lesions comprised of aberrant crypts and adenomatous polyps; BM reconstitution with MC-deficient BM resulted in attenuation of polyposis [3]. Once in the tumor microenvironment, tumor

promotion by MC is linked with their ability to release mediators that stimulate angiogenesis and recruitment of additional proinflammatory cells [2]. MC mediator release can also directly facilitate tumor proliferation and invasion, which we have demonstrated in vitro [4, 5].

Our lab and others have shown that healthy Treg can suppress MC function [1, 6–8]. Both effector T cells and Treg can be isolated and then tested for their ability to inhibit MCp differentiation/expansion (mouse T cells [1, 6, 8]) or MC degranulation (mouse and human T cells [1, 6]) in vitro. We have found that Treg isolated from healthy B6 mice are able to suppress the differentiation and expansion of MCp, while Treg from polyp-ridden mice were unable to do this [1, 9]; effector T cells were also unable to suppress the MCp irrelevant of the source of T cells. Treg isolated from healthy B6 mice or healthy humans are also capable of suppressing MC degranulation, while Treg isolated from polyp-ridden mice or colon cancer patients are unable to suppress MC degranulation [1, 6]. Additionally, we have been able to detect degranulated MC in human tumors [6]. In vivo, we have shown that adoptive transfer of Treg into polyp-bearing mice induces active regression of polyposis and hinders MC infiltration into the remaining polyps [8]. A similar strategy to access Treg influence on MC in the tumor microenvironment could be utilized in other models of cancer where MC infiltration into tumors is prevalent.

1.1 *Mouse Models to Study Mast Cell Function in Polyposis and Cancer*

1.1.1 *APC^{Min}*

This multiple intestinal neoplasia (Min) mouse was the first mouse model of colon cancer described [9] (see Note 1). These mice have a single point mutation at codon 850 in the adenomatous polyposis coli (APC) gene and develop multiple adenomas in the intestine. It was found that this mutation was analogous to mutations found in patients with familial adenomatous polyposis (FAP) and colorectal cancer.

1.1.2 *APC^{Δ468} Mice*

These mice contain a truncated APC gene downstream of exon 10 at APC-codon 468 [10, 11] (see Note 2). A 53 kDa protein is expected from this truncated gene that lacks all β -catenin binding sites. These mice show early and more severe polyposis in comparison to Min mice. On the C57Bl/6J background, visible adenomatous polyps accumulate in the small and large intestine starting from 2 months of age, due to loss of heterozygosity of the APC allele. Polyps increase in number and diameter with the age of the mice. At 4 months of age, these mice typically harbor 80–120 small intestine polyps and 5–10 large intestine polyps. Mice do not survive much past 4 months of age due to cachexia and anemia. The small intestine polyps are typically sessile/villous and increased infrequency distally, being highest in the ileum. The colonic polyps were almost exclusively pedunculated/tubular and larger but fewer in numbers as compared with the lesions in the small intestine.

All adenomas are restricted to the mucosa and remain completely benign as the mice age. On the BALB/c background, visible adenomas are not seen until 4–5 months of age and are smaller and fewer in number by more than one order of magnitude.

1.1.3 *TS4CreER* × *Ctnb*^{lox(ex3)} Mice

These mice are used to observe early events in polyposis. To generate these mice, the intestine-specific promoter, TS4, derived from the liver-specific fatty acid binding gene promoter [12] was used to drive expression of Cre-ERT2, a fusion of Cre recombinase and a mutated form of the mouse estrogen receptor that responds to tamoxifen and not estrogen [13]. The double transgenic TS4 × Cre-ERT2 mice were then crossed with *Ctnb*^{lox(ex3)} mice [14], in which exon 3 of β -catenin is flanked by loxP sequences. Oral gavage of lactating female *TS4CreER* × *Ctnb*^{lox(ex3)} with 2 mg tamoxifen per day for 5 days leads to rapid initiation of extensive intestinal polyposis in the parents as well as the nursing pups. Polyposis in the pups is visible as early as 2.5–3.5 weeks following termination of the treatment. Morphogenetic analysis of intestinal polyps in the *TS4CreER* × *Ctnb*^{lox(ex3)} mice reveals early enlargement and migration by the crypt proliferative zone cells across the crypt-villus boundary followed by extension of the aberrant crypt into the inner side of adjoining villi. To study initiation of polyposis with the appearance of intraepithelial MC, triple mutant mice are euthanized 3 weeks after termination of 5-day course of treatment with tamoxifen. Histological analysis of paraffin-embedded intestines shows extensive polyposis, including multiple aberrant crypt foci.

Utilizing the *TS4CreER* × *Ctnb*^{lox(ex3)} mice, staining with CAE revealed intraepithelial MC within aberrant crypts that were beginning to invade the crypt-villus boundary and in the mass of early adenomas [3]. Intraepithelial mast cells can also be detected in the periphery of newly arising aberrant crypts and villi. A similar frequency of MC infiltrating polyps can be observed in *APC*^{Δ468} mice, and these cells are also typically intraepithelial [3, 8]. When staining for protease content, the polyps contain both chymase (mMCP2) and tryptase (mMCP6), but mMCP2 is more prevalent [3]. Very few mast cells are visible in the healthy tissue surrounding the polyp or in the intestine of healthy B6 mice. The data indicates that the induction of intraepithelial MC is strictly related to polyposis and is an early and persistent event common to adenomas arising through the mutagenesis of β -catenin or of the APC gene.

1.1.4 *Min* × *Rag*^{−/−} or *APC*^{Δ468} × *Rag*^{−/−} Mice

These mice are generated by crossing the *Min* or *APC*^{Δ468} mice to *Rag*^{−/−} mice. These mice are then used to observe the impact of T cells and B cells on polyposis and also MC infiltration into polyps. Utilizing the *Min*-*Rag*^{−/−} mice, staining with CAE detected intraepithelial MC within the aberrant epithelium of the polyps and apparently healthy tissue immediately neighboring the adenomas. Hence the appearance of MC in adenomas does not require T or B cells.

2 Materials

2.1 Mouse Bone Marrow-Derived Mast Cells (BMMC)

1. All procedures should be performed in a biosafety cabinet (Class II) with sterile equipment as the harvest cells will be maintained in long-term culture.
2. Bone marrow-derived mast cell (BMMC) media: 15 % heat-inactivated fetal bovine serum (FBS), 1 % penicillin/streptomycin (10,000 U/mL stock), 2 mM L-glutamine (200 mM stock), 1 mM sodium pyruvate, 3.5 µL β-mercaptoethanol in 500 mL RPMI. Supplement with 10 ng/mL stem cell factor (SCF) and/or 20 ng/mL IL-3.
3. Leg bones harvested from mouse strain of interest.

2.2 Human LAD2 Mast Cells

1. LAD2 cells.
2. StemPro®-34 serum-free medium (1×) (Life Technologies™ #10639-011).
3. Recombinant human SCF.

2.3 Reagents for Immunohistochemistry

1. 10 % neutral buffered formalin.
2. Xylene.
3. 100 % ethanol (EtOH).
4. Paraffin for embedding.
5. Positively charged microscope slides.
6. Target Retrieval Solution (Dako #S1699).
7. PAP pen.
8. Background Buster (Innovex Biosciences #NB306).
9. Wash Buffer (Dako #S3006).
10. Antibody Diluent (Dako #S0809).
11. Anti-Mast Cell Tryptase Antibody (Thermo Scientific Lab Vision #MS-1216).
12. ABC kit Alkaline Phosphatase Mouse IgG (Vectastain #AK-5002).
13. SIGMAFAST™ Fast Red TR/Naphthol AS-MX tablets (Sigma #F4523).
14. Gill's II Hematoxylin.
15. CC/Mount™ (Sigma #C9368).
16. Coverslips.
17. Toluidine blue stock: Dissolve 1 g of toluidine blue O in 100 mL 70 % EtOH.
18. 1 % sodium chloride solution: Mix 0.5 g NaCl with 50 mL distilled water and adjust pH to 2.0–2.5 using glacial acetic

acid (AcCOOH) or hydrochloric acid (HCl). This solution needs to be made fresh each time.

19. Toluidine blue working solution: Combine 5 mL of toluidine blue stock solution with 45 mL 1 % NaCl solution and mix well. Recheck the pH. The pH should be around 2.3–2.5. A higher pH will result in less contrast.
20. Slide mounting medium compatible with toluidine blue stain: Permount® (Fisher Scientific #SP15-100).

2.4 Reagents for Tumor Epithelium Assays

1. ^3H -thymidine.
2. BD BioCoat™ Matrigel™ Invasion Chamber (BD Biosciences #354480). Follow the manufacturer's instructions for rehydration of the chambers before use.
3. Diff-Quik staining kit (Allegiance #B4132-1A).

2.5 Reagent for Human T-Cell Isolation

1. EDTA blood collection tubes.
2. Biocoll Separating Solution (density 1.077 g/mL; Cedarlane Laboratories Ltd #L6155).
3. Working media (for isolation of mononuclear cells (MNC) from tissue): 100 IU/mL penicillin, 100 $\mu\text{g}/\text{mL}$ streptomycin, and 10 $\mu\text{g}/\text{mL}$ gentamicin sulfate in 500 mL RPMI.
4. DNase solution: Make a 5 mg/mL stock of DNase (Sigma #DN25) in PBS.
5. 5 \times digestion media for isolation of mononuclear cells (MNC) from tissue:
 - (a) Dissolve 1,500 U/mL of collagenase (type IV) (Worthington Biochemical #4188) into 50 mL of working media.
 - (b) Dissolve 1,000 U/mL hyaluronidase (Sigma #H3506) into 50 mL of working media.
 - (c) Combine collagenase solution and hyaluronidase solutions in equal portions, i.e., 10 mL each to a final volume of 20 mL.
 - (d) Add 0.5 μL of DNase solution to each aliquot for a final concentration of 125 ng/mL.
 - (e) These aliquots can be frozen at -20°C .
6. 1 oz Whirl-Pak sample bags (Nasco #B01067N).
7. Percoll solutions: Percoll (GE Healthcare #17-0891-09) is mixed with 1 \times Hank's balanced salt solution (HBSS) to make a 40 % solution and an 80 % solution.
8. 40 μm cell strainer.
9. Transfer pipette.
10. Isolation buffer: 1 \times PBS, 2 % human AB serum, 2 mM EDTA.

11. Dynabeads® Untouched™ Human T Cells Kit (Life Technologies™ #113-44D).
12. DynaMag™-15 Magnet (Life Technologies™ #123-01D).
13. CD4⁺CD25⁺ Regulatory T Cell Isolation Kit, human (Miltenyi Biotec #130-091-301).
14. MS columns (Miltenyi Biotec #130-042-201).
15. OctoMACS Separator (Miltenyi Biotec #130-042-109).

2.6 Reagents for Mouse T-Cell Isolation

1. Isolation buffer: 2 % FBS, 2 mM EDTA in PBS.
2. Antibodies: CD4 (BD Bioscience, clone RM4-5), CD25 (BD Bioscience, clone 7D4), CD45Rb (BD Bioscience, clone 16A), Foxp3 (eBioscience, clone FJK-16s).
3. Dynal® Mouse T Cell Negative Isolation Kit (Life Technologies™ #114-13D).
4. DynaMag™-15 Magnet (Life Technologies™ #123-01D).
5. CD4⁺CD25⁺ Regulatory T Cell Isolation Kit, mouse (Miltenyi Biotec #130-091-041).
6. MS columns (Miltenyi Biotec #130-042-201).
7. OctoMACS Separator (Miltenyi Biotec #130-042-109).

2.7 Reagents for MC Degranulation

1. Mouse BMMC or human LAD2 cells.
2. Tyrode's buffer (pH 7.3): 135 mM NaCl, 5 mM KCl, 5.6 mM glucose, 1 mM MgCl₂, 1.8 mM CaCl₂ and 20 mM HEPES, 0.5 mg mL BSA (fraction V). Prepared in distilled water. Filter solution and store at 4 °C.
3. Quenching buffer: sodium carbonate or glycine buffer.
 - (a) Sodium carbonate buffer (pH 10.0): 1.06 g Na₂CO₃, 0.84 g NaHCO₃ in 100 mL distilled water.
 - (b) Glycine buffer (pH 10.7): 0.2 M glycine prepared in distilled water.
4. Citrate buffer (pH 4.5): Make a 50 mM citric acid solution and a 50 mM sodium citrate solution. Mix 49.5 mL of 50 mM citric acid with 50.5 mL 50 mM sodium citrate. Adjust pH to 4.5 and store at room temperature (RT).
5. 1 mM *p*-nitrophenyl N-acetyl- β -D-glucosamide (pNAG): Dissolve 3.42 mg in 10 mL citrate buffer. Warm to 37 °C and vortex to dissolve. Store aliquots at -20 °C.
6. Triton X-100.
7. DNP-HSA.
8. IgE: monoclonal anti-dinitrophenyl (DNP) antibody (for BMMC experiments, Sigma #D8406) or Chimaeric Human IgE anti-NP (for LAD2 experiments, AbD Serotec #MCA333S).
9. Ionomycin (or other Ca²⁺ ionophore), used for positive control of degranulation.

3 Methods

3.1 Enumerating Mast Cells in Human Tissue: Tryptase Staining

1. To detect tissue mast cells in human colon [6] and pancreas [6] tumors and healthy tissue, fix fresh surgical samples in 10 % neutral buffered formalin for 16–24 h.
2. Transfer to 70 % EtOH and then embed in paraffin.
3. Section tissues at 4 μ m.
4. Deparaffinize with xylene (two changes, 5 min each).
5. Rehydrate in as follows:
 - (a) Tap off excess xylene.
 - (b) Place slides in 100 % EtOH (three times, 3 min each).
 - (c) Place slides in 95 % EtOH (twice, 3 min each).
 - (d) Place slides in 70 % EtOH (once for 3 min).
 - (e) Transfer slides to distilled water to complete the hydration.
6. Perform heat-mediated antigen retrieval using a pressure cooker and Dako Target Retrieval Solution as follows:
 - (a) Add approximately 500 mL of distilled water to the pressure cooker so that there is a few inches of liquid in the bottom of the cooker.
 - (b) Place slides in the staining jar filled with Dako Target Retrieval Solution and then set jar with the lid off into the pressure cooker.
 - (c) Tightly close pressure cooker as per manufacturer's instructions. Set the pressure cooker to cook for 10 min at 100 °C and then start the heat-mediated antigen retrieval.
 - (d) After cooking has finished and pressure has been released, remove the staining jar from the cooker.
 - (e) Allow solution to cool to RT (approximately 30 min).
 - (f) Rinse slides with running tap water for 5 min.
7. To minimize background and nonspecific binding, block tissue with Background Buster prior to primary antibody staining. Start by drawing a circle with a PAP pen around the tissue of interest. Add sufficient amount of Background Buster to the encircled area (amount needed will depend on size of tissue to be stained) and block for 15 min at RT.
8. To stain with the primary antibody, flick off the Background Buster and directly add the diluted anti-Mast Cell Tryptase Antibody (1:200 in Dako Antibody Diluent).
9. Incubate tissue with primary antibody solution for 1 h at RT or overnight at 4 °C.

10. After primary antibody incubation is complete, flick off the slides and wash three times with Dako Wash Buffer (2 min each wash).
11. To detect tryptase use an ABC alkaline phosphatase kit. Dilute the provided biotinylated secondary antibody according to the manufacturer's instructions and then apply to the slides for 30 min at RT.
12. Wash slides three times with Dako Wash Buffer (2 min each wash).
13. Add the ABC-AP reagent to the tissue slide for 30 min at RT. This reagent is made up ahead of time according to manufacturer's instructions and needs to sit for 30 min prior to use.
14. After the ABC-AP reagent has reacted, wash slides three times with Dako Wash Buffer (2 min each wash).
15. While slides are being washed, prepare a sufficient amount of SIGMAFAST™ detection reagent (see Note 3).
16. Take the slides covered in the Wash Buffer, the prepared diluted SIGMAFAST™, and an additional slide box containing distilled water to the microscope (see Note 4).
17. Take the slides out of the Wash Buffer and add alkaline phosphatase substrate (SIGMAFAST) and watch spots develop. Development can take 2–15 min.
18. Flick off solution once color has developed to desired intensity and place slides in water to stop the reaction.
19. Counterstain in hematoxylin for approximately 10–15 s. Rinse excess hematoxylin from slides with running warm water for 1–2 min. Quickly check under the microscope that desired intensity has been obtained.
20. Add aqueous base CC/Mount™ dropwise to the stained slides and mount with a coverslip.
21. Mast cells will appear pink and background is purple (Fig. 1).
22. Blind the slide identifications with a piece of opaque masking tape to avoid investigator bias. Enumerate tissue MC by counting the number of positive (pink-stained cells) in a high-powered field of vision (typically 200×). Total cell number within that field of vision is then assessed using ImageJ analysis software with nuclease counter plug-in. Calculate the frequency of MC relative to fields of view (FOV) or tissue area.

3.2 *Enumerating Mast Cells in Human Tissue: Toluidine Blue Staining to Detect MC Degranulation*

1. Prepare dehydration solutions in five slide jars before proceeding (step 5):
 - (a) One chamber containing 95 % EtOH.
 - (b) Two chambers containing 100 % EtOH.
 - (c) Two chambers containing xylene.

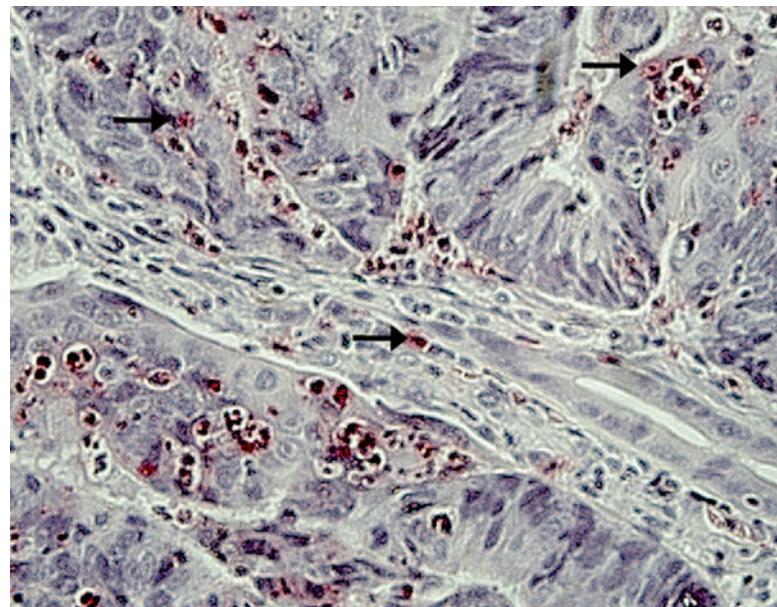


Fig. 1 Detecting MC with tryptase staining. Tryptase+ MS are *pink* and are indicated with *arrow*

2. Tissue is prepared for staining, including deparaffinization and hydration, as described in Subheading 3.1, steps 4 and 5.
3. Add hydrated slides to toluidine blue working solution (prepare fresh) for 3 min.
4. Immediately remove and wash three times in distilled water (1 min each).
5. As soon as washing is complete, quickly move to dehydration as stain will fade quickly.
6. To dehydrate, dip slides ten times in each slide chamber (prepared as in step 1) sequentially (a → 2 × b → 2 × c).
7. Mount with toluidine-based mounting media (Permount®) and add coverslip.
8. Mast cells will appear purple and on a blue background (Fig. 2).
9. Quantification of MCs in the tissues is described in Subheading 3.1, step 22.

3.3 Enumerating Mast Cells in Human Tissue: Chloracetate Esterase (CAE) Staining

1. Tissue is prepared for staining, including deparaffinization and hydration, as described in Subheading 3.1, steps 4 and 5.
2. CAE staining is performed as described in Chapter 5 of this volume (*editor's note: see Chapter 5 Methods for the study of mast cell recruitment and accumulation in different tissues*).
3. Quantification is done as described in Subheading 3.1, step 22.

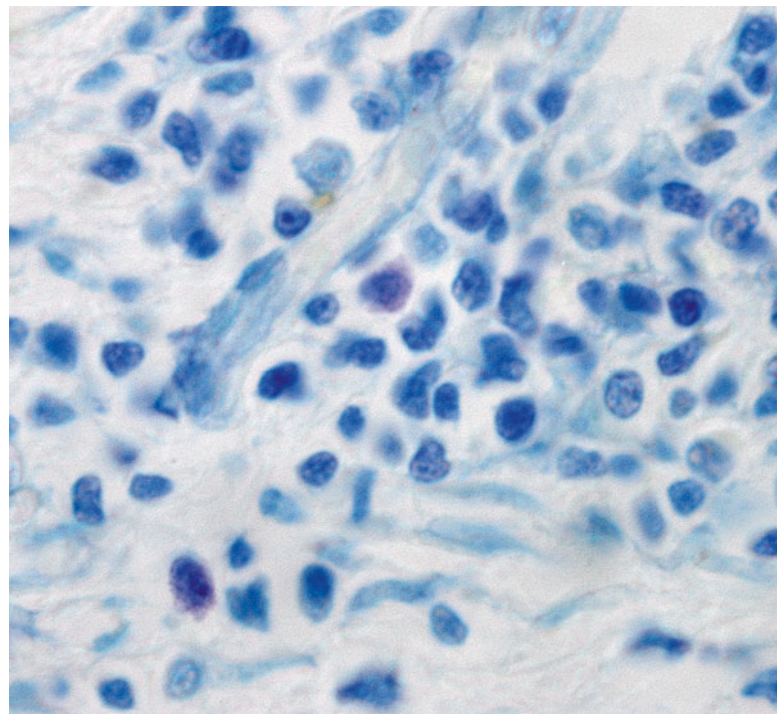


Fig. 2 Detecting MC with toluidine blue staining. MC granules will appear *purple* (arrows) while the background will stain blue

3.4 MCp and Mature Mast Cell Frequency with Limiting Dilution Assay in Mouse Models of Polyposis

The frequency of MCp throughout the intestine of each type of mouse model described in Subheading 1.1 can be determined as described in Chapter 5 of this volume (*editor's note: see Chapter 5 Methods for the study of mast cell recruitment and accumulation in different tissues*). This method can be used to determine frequency of MCp at different time points during polyp development. Differences in the frequency of MC progenitors found within tumor tissue versus surrounding healthy tissue can be determined by first microdissecting the polyps from either the small or large bowel. Isolation of mononuclear cells (MNC) from polyp tissue is performed separately from MNC isolation from the surrounding healthy tissue. Mice can be treated with various inhibitors or neutralizing antibodies, reconstituted with BM deficient in a gene of interest, or crossed to additional transgenes, and then MCp frequency can be determined from these mice and compared to age matched un-manipulated mice [3]. These methods will reveal the impact of the manipulation on MCp homing to intestinal tissue.

3.5 Mature Mast Cell Frequency in Mouse Intestinal Tissue

Both CAE staining and MC protease staining as described in Chapter 5 can be utilized to quantify the frequency of MC that infiltrate polyp tissue in each type of mouse model described in Subheading 1.1. For best visualization of the MC in the polyp,

“jelly rolls” of the harvested tissue should be made. After tissue has been isolated and flushed as described in Chapter 5, the tissue is laid onto bibulous (blotting) paper.

1. Divide the small intestine into four equal parts and cut at the turn of each section, taking note as to which end is the duodenum and which is the ileum.
2. Using blunt-ended scissors, cut along the top of the intestine.
3. Dip your finger into the PBS and gently run your finger along the cut intestine to flay it open.
4. Place the paper with opened tissue into a tray containing a block of dissecting wax large enough to fit the paper.
5. Using small insect pins, pin the ends of the tissue to the wax.
6. The four ends and two places in the middle can be pinned quickly, and then 10 % neutral buffered formalin can be added to maintain the integrity of the tissue.
7. Once in fixative, additional pinning can be done. Enough pins need to align each side so that the tissue does not curl under itself.
8. After sufficient time has passed (16–24 h), remove the formalin and add 70 % EtOH to the tray. Remove all pins.
9. Using non-serrated tissue forceps, pick up the start of the duodenum and begin to roll the tissue on top of itself so as to keep the villi on the inside and the muscle layer on the outside of the roll.
10. Once the rolling is complete, set the roll into an embedding cassette so that you can see the spiral created.
11. To remove the tissue from the forceps, ever so slightly release your hold on the forceps so that they open just a little, and then, using additional forceps, hold the tissue in place as you pull the forceps used to roll the tissue out from the tissue.
12. Sectioning the tissue rolled in this manner will allow for proper visualization of the intestinal architecture.

3.6 Assessing How MCs Influence Tumor Epithelium

3.6.1 Preparation of Mouse Bone Marrow-Derived Mast Cells (BMMCs)

1. Euthanize mouse and then spray liberally with 70 % EtOH.
2. Remove the skin and muscle from the entire length of the leg.
3. Using surgical scissors, remove the leg from the body by cutting above the hipbone, being careful not to cut the femur. Then cut at the knee to separate the femur and tibia.
4. Hold the femur with forceps and cut a small piece of bone off from the top and bottom to reveal the BM.
5. Hold the opened bone over a 15 mL tube, and using a 25G needle and 3 cc syringe, insert the needle into the top of the bone and flush out BM with RPMI. Flip bone over and repeat flushing to ensure all BM is removed.

6. Fill tube to 15 mL with RPMI and centrifuge at $400 \times g$ for 10 min.
7. Resuspend pellet in 1 mL of RPMI and filter through a 40 μm cell strainer and then wash twice with RPMI.
8. After final wash, resuspend BM cells in BMMC media (start with 5 mL per mouse for counting).
9. Count nucleated cells using a hemacytometer or automated method.
10. Place 5×10^5 cell per mL into a 25 cm^2 cell culture flask with a canted neck and culture at 37 °C, 5 % CO₂.
11. Every 2 days, add 5 mL BMMC media to a max of 15 mL.
12. On day 6 or 7, pellet the BMMC culture at $200 \times g$ for 10 min and then resuspend in a fresh 5 mL of BMMC media and transfer into a new cell culture flask.
13. It will take 4–6 weeks for the BM to differentiate and mature into a BMMC culture. MC purity should be checked by flow cytometry for purity. Cultures by week 6 should be >95 % cKit⁺Sca1⁺FcεRI⁺.

3.6.2 Mast Cell-Conditioned Media

1. Supernatant from BMMC or LAD2 MC is used to assess whether MC can stimulate tumor cell proliferation and/or invasion.
2. To generate MC-conditioned supernatant, culture MC at high density for 1 week.
3. Pellet the cells by centrifugation and collect the supernatant for the assays listed below.
4. In a separate flask, incubate MC media *without* MC for 1 week. This media serves as the control unconditioned media.

3.6.3 Mast Cell-Induced Tumor Cell Proliferation

1. Tumor cells of interest are plated at a concentration of 1×10^5 cells per well in a 96-well plate.
2. The cells are centrifuged at $400 \times g$ force for 10 min and the media is removed.
3. The media is replaced with either MC-conditioned media or non-conditioned control media.
4. The cells are then grown for 24, 48, and 72 h (a different 96-well plate is needed for each condition).
5. Proliferation is then assayed by adding 0.5 μCi of ^3H -thymidine per well for 6 h and thymidine uptake is then measured with a scintillation counter.

3.6.4 Mast Cell-Induced Tumor Cell Invasion

1. Tumor cells of interest are plated at a concentration of 1×10^5 cells per well in the upper chamber of an 8 μm Matrigel-coated 12-well Boyden chamber.

2. The lower chamber is filled with 750 μ L of MC-conditioned media or non-conditioned media.
3. The cells are then incubated for 48 h at 37 °C, 5 % CO₂.
4. After 48 h, the membrane inserts are removed (follow manufacturers' instructions), fixed, and stained with Diff-Quik.
5. The number of invading cells is then manually counted at a 200 \times magnification in at least three random areas of the membrane and each condition should be tested in triplicate.
6. The number of invaded cells/high-powered field is then plotted.

3.7 Isolation of Human Mononuclear Cells from Blood

1. Peripheral blood is collected into an EDTA blood collection tube and then mononuclear cells are freshly isolated.
2. Add 15 mL of Biocoll to two 50 mL tubes (only need one tube for 30 mL of peripheral blood).
3. Slowly add 5 mL of RPMI + 1 % HEPES + 1 % Pen/Step on top of the Biocoll. Be careful to maintain the two layers. Blood will not separate well if you do not.
4. Slowly add blood sample onto the RPMI, using a 5 mL syringe attached with a 16G needle. Blood will mix with RPMI but should not mix with Biocoll.
5. Disperse blood equally to each of the 50 mL tubes.
6. Centrifuge 1,160 \times g for 20 min. Make sure break is off.
7. Mononuclear cells are found as a white/cloudy band at the interphase of the Biocoll and plasma solutions.
8. Remove the interface with a transfer pipette and put cells into new 50 mL tube and then add RPMI + 1 % HEPES + 1 % Pen/Step to bring volume up to 50 mL.
9. Centrifuge 400 \times g for 10 min.
10. Pour off supernatant and resuspend the pellet in 1 mL of PBS + 2 % AB + 2 mM EDTA.
11. Cells are ready to be counted and used.

3.8 Isolation of Human Mononuclear Cells from Colonic Tissue

1. After surgical removal of the tissue, the tissue is stored and transported in working media on ice.
2. Thaw an aliquot of 5 \times digestion media and dilute to a 2.5 \times solution with 20 mL working media.
3. Total volume is now 40 mL: 20 mL for isolation of cells from tumor tissue and 20 mL for isolation of cells from normal mucosa.
4. To two Petri dishes, add 5 mL of working media and to a third Petri dish add 5 mL of the 2.5 \times digestion media.
5. Remove tissue from transporting tube with long forceps and add to the first dish containing working media. Swish around the tissue to remove debris.

6. Do the same in the second dish.
7. In the last dish containing digestion media, mince the tissue using two surgical blades.
8. The tissue pieces need to be small enough to fit though a 25 mL pipette.
9. Once finished mincing, suck up the tissue solution with the 25 mL pipette and put mix in a 50 mL tube. Wash out the dish with the remaining 15 mL of digestion media and add to the 50 mL tube.
10. Put entire 20 mL of tissue solution into sample bag (1 oz. Whirl-Pak sample bag).
11. Put the sample bag into a bigger bag to make sure the digestion mix does not leak out onto workspace.
12. “Stomach” bag for approximately 2 min (i.e., squeeze the bag lightly with fingers).
13. Incubate for 1 h at 37 °C with shaking.
14. “Stomach” bag for an additional 2 min.
15. Transfer mix, including tissue, into a 50 mL tube using a 25 mL pipette.
16. Add an additional 15 mL of working media to the mix, invert a couple of times and place on ice for 5 min. Remove most of the supernatant and transfer into a 50 mL tube.
17. Filter the remaining undigested tissue through a 40 µm cell strainer using the plunger of a 5 cc syringe to push the tissue and solution through the filter.
18. Add the filtered solution to the supernatant collected in **step 16**.
19. Centrifuge the supernatant for 10 min at $400 \times g$.
20. Pour off all supernatant.
21. Watch the pellet carefully. The tissue will not always adhere to the tube and you will lose your cells if you are not cautious.
22. Resuspend the pellet in 4 mL 40 % Percoll and transfer to a 15 mL tube.
23. Underlay with ~2.5 mL 80 % Percoll using a transfer pipette. Be very careful not to disrupt the layer. Add slowly to avoid bubbles.
24. Centrifuge for 20 min at $3,000 \times g$ with **no brake**.
25. Mononuclear cells are found as a white/cloudy band at the interphase of the Percoll gradient.
26. Remove the cells to a new 15 mL tube and add working media for a total volume of 15 mL.
27. Spin in a centrifuge at $1,810 \times g$ for 10 min to remove any Percoll.

28. Pour off supernatant and resuspend the pellet in 1 mL of PBS + 2 % AB human serum + 2 mM EDTA.
29. Cells are ready to be counted and used.

3.9 Isolation of Human T Cells from PB or Tissue MNC

1. T cells are first separated from all other contaminating cells using the Dynabeads® Untouched™ Human T Cells isolation kit.
2. Follow all manufacturers' instructions with one exception: Use AB serum instead of FBS (i.e., PBS with 2 % AB and 2 mM EDTA).
3. Treg can then be separated from effector T cells and each tested separately, using Miltenyi Biotec's human CD4⁺CD25⁺ Regulatory T cell Isolation Kit.
4. Follow all manufacturers' instructions with one exception: Use AB serum instead of FBS (i.e., PBS with 2 % AB and 2 mM EDTA).

3.10 Isolation of Mouse T Cells

Separating effector T cells from Treg can be done in one of three ways (see Note 5):

1. Using Foxp3-GFP reporter mice (Jackson Laboratories), total MNCs are immunostained with antibodies toward CD4 and CD25, DAPI is added to gate out dead cells, and then the cells are FACS sorted for live, CD4⁺CD25⁺Foxp3⁻ effector T cells and CD4⁺CD25⁺Foxp3⁺ Treg.
2. If reporter mice are not available, total MNC are immunostained with antibodies toward CD4, CD25, and CD45Rb, DAPI is added to gate out dead cells, and then the cells are FACS sorted for live, CD4⁺CD25⁺CD45Rb^{high} effector T cells and CD4⁺CD25⁺CD45Rb^{lo} Treg. A small aliquot of each sorted population should then be fixed and intracellular stained with a Foxp3 antibody to check for purity.
3. When FACS sorting is not an option, total T cells can first be separated from all other contaminating cells using the Dynabeads® Untouched™ Mouse T Cells isolation kit and then Treg can be separated from effector T cells using Miltenyi Biotec's CD4⁺CD25⁺ Regulatory T Cell Isolation Kit. Follow all manufacturers' instructions.

3.11 Assessing How T Cells Influence Mast Cell Function: MCp Assay in the Presence of T Cells

1. This assay is a modified version of the MCp limiting dilution assay described in Chapter 5.
2. MNC should be isolated from Rag^{-/-} mice so no endogenous T cells are present. MNC and T cell are added at a 1:1 ratio.
3. The cells should be mixed together at the starting concentration and then serially diluted twofold together. The number of γ -irradiated feeder cells and concentration of IL-3 and SCF are as previously described.

4. IL-2 (50 U/mL) is also added to this mixture since T cells are present. A control plate of MNC without T cells should be included for the baseline standard.
5. The MCp concentration is expressed as previously described in Chapter 5.
6. Experimental conditions with T cells are then compared to ones without T cells.

3.12 Assessing How T Cells Influence Mast Cell Function: MC Degranulation in the Presence of T Cells

1. MCs of interest are treated overnight at 37 °C, 5 % CO₂ with 0.5 µg/mL of appropriate IgE in cytokine-free medium. Be sure to calculate sufficient number of cells to assay each condition in triplicate and to account for loss of cells during procedure.
2. Before beginning procedure the following day, isolate T cells of interest and warm Tyrode's buffer to 37 °C. T cells should be resuspended in Tyrode's buffer before use in this assay.
3. After overnight stimulation, cells are centrifuged at 200 ×*g* for 10 min and then washed three times with warmed Tyrode's buffer. After final wash, resuspend MC in 1 mL of Tyrode's buffer and recount.
4. Aliquot 5 × 10⁴ MC into a 96-well round bottom plate in a volume of 45 µL.
5. Add 5 × 10⁴ T cells in a volume of 45 µL to the appropriate wells containing MC.
6. 9 wells without T cells will be needed for additional controls:
 - (a) 3 wells for MC without DNP-HSA.
 - (b) 3 wells with DNP-HSA.
 - (c) 3 wells with ionomycin.
7. Incubate the cells at 37 °C for 10 min.
8. Add 10 µL of DNP-HSA (or ionomycin) so that the final concentration is 100 ng/mL. Gently pipette to mix. Return the cells to 37 °C and incubate for an additional 30 min.
9. To stop the reaction, place the cells on ice for 5 min and centrifuge 200 ×*g* for 10 min.
10. Transfer the supernatant to a new 96-well bottom plate. Avoid transferring any cells.
11. To the remaining cell pellets, add 150 µL of 0.5 % Triton X-100 prepared in Tyrode's buffer to lyse the cells, pipette to mix, and then incubate on ice for 15 min.
12. Re-centrifuge both the supernatant and the cell pellet lysis at 200 ×*g* for 10 min. This will ensure that in the next step no cells are transferred, which could result in a higher than actual degranulation value.

13. Transfer 50 μ L of each supernatant and cell lysates to new 96-well flat bottom plate.
14. Add 100 μ L of 1 mM pNAG solution to each well and incubate at 37 °C for 90 min.
15. After incubation, add 50 μ L carbonate (or glycine) buffer to quench the reaction. The solution should change yellow to indicate β -hexosaminidase activity.
16. Read the plate absorbance at 405 nm with a reference filter of 630 nm.
17. To calculate percentage of β -hexosaminidase release: [absorbance of the supernatant/(absorbance of supernatant+absorbance of pellet)] \times 100 = % release.

3.13 Adoptive T-Cell Transfer into Polyp-Bearing Mice to Access Influence on MC In Vivo

1. 1×10^6 purified T cells are retro-orbitally transferred into an anesthetized mouse. Mice can then be examined for tumor load 3 and 6 weeks after transfer.
2. Tumor-bearing tissue would then be fixed and analyzed for MC infiltration as described in Subheading 3.5 of this chapter.

3.14 Assessing How MC Influence T-Cell Function

1. Purified MC and T cells are co-incubated together, and phenotypic and functional changes are then assayed.
2. For this assay, the cell culture media consists of RPMI with 100 U/mL IL-2 and 10 ng/mL SCF.
3. Resuspend the purified T cells and MC in this media and then add 1×10^6 T cells, and MCs are added to a 24-well plate.
4. Bring up to a final volume of 2 mL.
5. A well of T cells alone should also be plated as a control. Cells can be incubated for up to 5 days.
6. Phenotypic changes in T cells can be accessed by flow cytometry: both surface cell activation markers and intracellular cytokines.
7. We have seen that, after 5 days, Treg that have been cocultured with MC stop producing the anti-inflammatory cytokine IL-10 and instead begin to produce the proinflammatory cytokine IL-17 [6].
8. Functional changes in the T cells can be accessed by separating the T cells from the MC via magnetic methods described in Subheading 3.9 of this chapter.
9. These re-purified T cells are then added to new MCs that have been cultured overnight with IgE.
10. The T cells cultured with or without MC are then tested for their ability to suppress MC degranulation as described in Subheading 3.12 of this chapter.

4 Notes

1. C57BL/6J-ApcMin/J (Jackson Laboratory Stock# 002020).
2. APC^{Δ468} mice are not commercially available but can be obtained on request.
3. Approximately 200 µL substrate per slide, but this will vary depending on size of the tissue.
4. To visualize development and thereby minimize overdevelopment/excess background of the substrate.
5. In a healthy C57Bl/6 mouse, Treg constitute 2–5 % of the total CD4 T-cell population and therefore yield is typically low. Pooling cells from multiple mice can alleviate this problem. T cells can be isolated from any organ of interest (our lab typically uses lymph nodes or spleen T cells).

References

1. Blatner NR et al (2012) Expression of ROR γ t marks a pathogenic regulatory T cell subset in human colon cancer. *Sci Transl Med* 4(164):164ra159
2. Khazaie K et al (2011) The significant role of mast cells in cancer. *Cancer Metastasis Rev* 30(1):45–60
3. Gounaris E et al (2007) Mast cells are an essential hematopoietic component for polyp development. *Proc Natl Acad Sci U S A* 104(50):19977–19982
4. Strouch MJ et al (2010) Crosstalk between mast cells and pancreatic cancer cells contributes to pancreatic tumor progression. *Clin Cancer Res* 16(8):2257–2265
5. Khan MW et al (2013) PI3K/AKT signaling is essential for communication between tissue-infiltrating mast cells, macrophages, and epithelial cells in colitis-induced cancer. *Clin Cancer Res* 19(9):2342–2354
6. Blatner NR et al (2010) In colorectal cancer mast cells contribute to systemic regulatory T-cell dysfunction. *Proc Natl Acad Sci U S A* 107(14):6430–6435
7. Piconese S et al (2009) Mast cells counteract regulatory T-cell suppression through interleukin-6 and OX40/OX40L axis toward Th17-cell differentiation. *Blood* 114(13):2639–2648
8. Gounaris E et al (2009) T-regulatory cells shift from a protective anti-inflammatory to a cancer-promoting proinflammatory phenotype in polyposis. *Cancer Res* 69(13):5490–5497
9. Su LK et al (1992) Multiple intestinal neoplasia caused by a mutation in the murine homolog of the APC gene. *Science* 256(5057):668–670
10. Gounari F et al (2005) Loss of adenomatous polyposis coli gene function disrupts thymic development. *Nat Immunol* 6(8):800–809
11. Gounaris E et al (2008) Live imaging of cysteine-cathepsin activity reveals dynamics of focal inflammation, angiogenesis, and polyp growth. *PLoS One* 3(8):e2916
12. Saam JR, Gordon JI (1999) Inducible gene knockouts in the small intestinal and colonic epithelium. *J Biol Chem* 274(53):38071–38082
13. Indra AK et al (1999) Temporally-controlled site-specific mutagenesis in the basal layer of the epidermis: comparison of the recombinase activity of the tamoxifen-inducible Cre-ER(T) and Cre-ER(T2) recombinases. *Nucleic Acids Res* 27(22):4324–4327
14. Harada N et al (1999) Intestinal polyposis in mice with a dominant stable mutation of the beta-catenin gene. *EMBO J* 18(21):5931–5942

Chapter 28

Studying Mast Cells in Peripheral Tolerance by Using a Skin Transplantation Model

Victor C. de Vries, Isabelle Le Mercier, Elizabeth C. Nowak, and Randolph J. Noelle

Abstract

Mast cells (MCs) play an important role in both inflammatory and immunosuppressive responses [1]. The importance of MCs in maintaining peripheral tolerance was discovered in a FoxP3⁺ regulatory T-cell (T_{reg})-mediated skin transplant model [2]. MCs can directly mediate tolerance by releasing anti-inflammatory mediators (reviewed in ref. 3) or by interacting with other immune cells in the graft. Here we will present protocols used to study the role of MCs in peripheral tolerance with the emphasis on how MCs can regulate T-cell functionality. First we will introduce the skin transplant model followed by reconstitution of mast cell-deficient mice (B6.Cg-*Kit*^{W-sh}). This includes the preparation of MCs from the bone marrow. Finally the methods used to study the influence of MCs on T-cell responses and T_{reg} functionality will be presented by modulating the balance between tolerance and inflammation.

Key words Peripheral tolerance, Transplantation, Skin, Mast cells, Degranulation, Inflammation, Regulatory T cells

1 Introduction

Mast cells (MCs) play an important role in both inflammatory and immunosuppressive responses [1]. The importance of MCs in maintaining peripheral tolerance was discovered in a skin transplant model. In this model tolerance is furthermore mediated by FoxP3⁺ regulatory T cell (T_{reg}) [2] and dendritic cells [4]. The graft-derived MCs retain their plasticity and can become proinflammatory by environmental cues. We showed that in the presence of an allergy, allergen-specific IgE-mediated degranulation of MCs leads to acute T-cell-dependent graft rejection [5]. This is independent of the route of administration of the allergen. Under steady-state conditions of acquired immune tolerance, MCs can directly mediate tolerance by releasing anti-inflammatory mediators (reviewed in ref. 3). However, MCs can also interact and modulate other

immune cells important for graft tolerance, such as T_{reg} (reviewed in ref. 6) and dendritic cells [4].

Here we will discuss the protocols used to study the role of MCs in peripheral tolerance by using a skin graft model. This includes the induction of tolerance, grafting of the mice, and reconstitution of mast cell-deficient mice (B6.Cg-*Kit*^{W-sh}) with in vitro-cultured bone marrow-derived mast cells. This will be followed by protocols used to study the balance of proinflammatory “allergic” and immunosuppressive “graft” MCs and the impact this has on regulatory T-cell function.

2 Materials

2.1 Donor Splenocyte Transfusion (DST) and Tolerance Induction

1. CB6F1 donor mice at 6–8 weeks of age (use one donor spleen per recipient) (see Note 1).
2. 70 % ethanol (EtOH).
3. Hank’s balanced salt solution (HBSS).
4. Anti-Thy-1/CD90 antibody (hybridoma supernatant clone: HO13-4; used at 1:5,000, need to be optimized for each lot).
5. Rabbit complement (rabbit 3/4-week complement, Invitrogen, Catalog #31038-100, use at 1:20, 250 μ L/spleen).
6. HBSS supplemented with 10 % fetal bovine serum (FBS).
7. Anti-CD154 monoclonal antibody (anti-CD40L, clone MR-1).
8. 40 μ m nylon mesh cell strainers.
9. Small (60 \times 15 mm) sterile Petri dishes.
10. Syringes (1 cc) and 25G-5/8" and 30G-1/2" needles.

2.2 Donor Skin Harvest

1. C57Bl/6 or CB6F1 (see Note 1) donor mice at 6–8 weeks of age.
2. Sterile phosphate buffered saline (PBS).
3. Large (150 \times 25 mm) Petri dishes.
4. Sterile 4" \times 4" gauze pads.
5. Knife handle and surgical blades or disposable scalpel.
6. Tissue and suture forceps with side grasping teeth.
7. Curved forceps.
8. Aluminum foil.

2.3 Skin Grafting

1. Recipient C57Bl/6 or B6.Cg-*Kit*^{W-sh} (see Note 2) mice at 6–8 weeks of age.
2. Mouse anesthesia cocktail: 5.4 mL ketamine (100 mg/mL) and 0.6 mL xylazine (100 mg/mL) in 14 mL saline (final concentrations 27 mg/mL ketamine and 3 mg/mL xylazine).

3. Hair clippers.
4. Pharmaderm Puralube Petrolatum Vet ophthalmic ointment.
5. Povidone-iodine prep pads.
6. Alcohol prep pads.
7. Sterile latex surgical gloves.
8. Autoclaved surgery pack containing:
 - (a) One curved scissors with one serrated blade for skin removal.
 - (b) One hemostatic forceps.
 - (c) One thin curved forceps.
 - (d) One small straight scissors.
9. Disposable surgical JorVet drapes.
10. Dermalon™ suture cuticular needles for reverse cutting (C-1 3/8 Circle, 12 mm, size 5-0, Covidien, code 8886174121).
11. Hot glass bead dry sterilizer.
12. Plastic bandages 3/4" width.
13. Adhesive tape such as autoclave tape.
14. Heating table for recovery.
15. Stitch scissors.
16. Bandage scissors.

2.4 BMMC Derivation and Culture

1. Donor C57BL/6 mice at 6–8 weeks of age.
2. Hank's balanced salt solution (HBSS).
3. 70 % ethanol.
4. Complete RPMI 1640 media (cRPMI): 10 % FBS, 0.050 mM 2-mercaptoethanol, 100 IU/mL penicillin, 100 µg/mL streptomycin, 2 mM L-glutamine, 10 mM HEPES, 100 µM nonessential amino acids, and 100 mM sodium pyruvate. Use a 0.22 µm filter unit to sterilize.
5. Recombinant murine interleukin 3 (IL-3).
6. Recombinant murine stem cell factor (SCF).
7. Small (60×15 mm) Petri dishes.
8. Razor blade or disposable scalpel.
9. 40 µm nylon mesh cell strainer.
10. Cell culture Petri dishes 100 mm (BD tissue culture dish, Catalog 353003) (*see Note 3*).
11. 5 cc syringes and 25G-5/8" needles.
12. Antibodies for purity check: anti-mouse CD117-APC (cKit, clone: 2B8) and anti-mouse FcεRI-PE (clone Mar-1).

2.5 Adoptive Transfer of BMMCs

1. Bone marrow-derived mast cells (BMMCs) from strain of interest.
2. Recipient B6.Cg-Kit^{W-sh} mice (*see Note 2*) or other recipient mice at 6–8 weeks of age.
3. Sterile PBS.
4. Mouse anesthesia cocktail: 5.4 mL ketamine (100 mg/mL) and 0.6 mL xylazine (100 mg/mL) in 14 mL normal saline (final concentrations 27 mg/mL ketamine and 3 mg/mL xylazine). Use 0.1 mL per ~30 g mouse body weight (90 mg/kg ketamine, 10 mg/kg xylazine).
5. Digestion cocktail: DNase, Liberase (both at 4 mg/mL), Collagenase D (or IV) (10 mg/mL).
6. HBSS supplemented with 10 % FBS.
7. Hair clippers.
8. Straight scissors.
9. 40 µm nylon mesh cell strainer.
10. 1 cc syringes.
11. 25G-5/8" needles.
12. 37 °C water bath.
13. 24-well plates.
14. 50 mL tubes.
15. Antibodies for purity check: anti-mouse CD117-APC (cKit, clone: 2B8) and anti-mouse FcεRI-PE (clone: MAR-1).

2.6 Degranulation of MCs to Mimic Allergy

1. Grafted C57BL/6 mice or grafted and reconstituted B6.Cg-Kit^{W-sh} mice (*see Note 2*).
2. Isoflurane vaporizer with small rodent chamber.
3. Compound 40/80 solution: prepared at 1 mg/mL in PBS.
4. Aluminum hydroxide (Imject Alum Adjuvant).
5. Ovalbumin (OVA grade V).
6. Bovine serum albumin (BSA).
7. IgE (OVA specific, clone 2C6) (*see Note 4*).
8. Cromolyn sodium salt solution (39 mM): prepared at 20 mg/mL in PBS.
9. 1.5 mL microfuge tubes.
10. Syringes (1 cc) with 25G-5/8" needles.

2.7 Induction of Inflammation

1. C57BL/6 mice and/or reconstituted B6.Cg-Kit^{W-sh} mice (*see Note 2*).
2. Phosphate buffered saline (PBS).
3. Acetone.

4. Dibutyl phthalate (DBPT).
5. Complete Freund's adjuvant.
6. TLR4 agonist (LPS, *E. coli* 055:B5).
7. TLR9 agonist (CpG; ODN-1826).
8. FITC:DBPT paint:
 - (a) Mix 1 volume of DBPT with 1 volume of acetone.
 - (b) Weigh 5 mg of FITC powder (fluorescein isothiocyanate) into a microfuge tube.
 - (c) Add 1 mL of the DBPT:acetone to the FITC.
 - (d) Vortex until the solution becomes clear (should be bright yellow).
 - (e) If FITC does not dissolve completely, warm the solution in a 37 °C water bath.
9. Murine anti-CD40 antibody (clone: FGK.45).
10. Microfuge tubes (1.5 mL).
11. Syringes (1 cc) with 25G-5/8" needles.

2.8 Cytokine Profile in the Graft

1. Grafted C57Bl/6 mice. Grafting protocol is described in Subheading 3.1.
2. IgE (OVA specific, clone 2C6).
3. Ovalbumin (OVA grade V).
4. Isoflurane vaporizer with small rodent chamber.
5. HBSS.
6. Bent-tip forceps.
7. Straight scissors.
8. 24-well plate.
9. 37 °C incubator with 5 % CO₂.
10. Microcentrifuge tubes (1.5 mL).
11. Syringes (1 cc) with 25G-5/8" needles.

2.9 Antibody-Mediated Depletion of T Cells

1. Grafted C57Bl/6 mice. Grafting protocol is described in Subheading 3.1.
2. Isoflurane vaporizer with small rodent chamber.
3. Anti-CD4 (clone GK1.5).
4. Anti-CD8 (clone 2.43).
5. IgE (OVA specific, clone 2C6) (*see Note 4*).
6. Ovalbumin (OVA grade V).
7. Syringes (1 cc) fitted with 25G-5/8" needles.

2.10 Adaptive Transfer of Tolerance Using Total Lymphocytes

1. Grafted C57Bl/6 mice as described in Subheading 3.1.
2. CB6F1 (*see Note 1*) grafted C57BL/6-*Rag2^{tm1Cgn}*/J (*see Note 5*).
3. Isoflurane vaporizer with small rodent chamber.
4. IgE (OVA specific, clone 2C6) (*see Note 4*).
5. Ovalbumin (OVA grade V).
6. Straight scissors.
7. Straight and bent-tip forceps.
8. Digestion solution: 4 mg/mL each of DNase I and Liberase.
9. 37 °C water bath.
10. 24-well plates.
11. 40 µm cell strainers.
12. 50 mL conical tubes.
13. Syringes (1 cc volume) with 25G-5/8" needles.

2.11 Systemic Decay of Tolerance After Local MC Degranulation

1. Dual-grafted C57Bl/6 mice (*see Subheading 2.1* and additional comments in Subheading “Decay of Tolerance After Local MC Degranulation”).
2. Degranulating agents and antibodies (*see Subheading 2.6*).

2.12 Adoptive Transfer of Tregs

1. Grafted Ly5.1⁺ B6.Cg-FoxP3^{tm2Tch}/J mice (*see Note 6*). Grafting protocol is described in Subheading 3.1.
2. CB6F1 grafted C57BL/6-*Rag2^{tm1Cgn}*/J mice (*see Note 5*). Grafting protocol is described in Subheading 3.1.
3. Degranulating agents as described in Subheading 3.1.
4. Bent-tip and straight forceps.
5. Straight scissors.
6. Antibodies: CD4 (clone: L3T4), CD25 (clone: 3C7).
7. Biotin selection kit (EasySep® Mouse Biotin Positive Selection Kit, STEMCELL Technologies Inc.) or equivalent.
8. Syringes (1 cc) with 25G-5/8" needles.

2.13 Enumeration of Tregs in Skin Graft by Fluorescent Microscopy

1. Grafted mice as described in Subheading 3.1.
2. Degranulating agents as described in Subheading 2.6.
3. 1:1 mixture of acetone:methanol.
4. Straight scissors and forceps.
5. 10 % normal serum in PBS (*see Note 7*).
6. 100 % EtOH.
7. 10 % normal buffered formalin.
8. Sucrose.
9. Antibodies: CD4 (clone: L3T4) and FoxP3 (clone: FJK-16s).

10. Hoechst 33342 (1 μ g/mL final concentration) or DAPI (2.86 μ M final concentration).
11. Aqueous mounting media with anti-fading properties.
12. Cryo-molds.
13. Optimal Cutting Temperature (OCT) embedding medium.
14. Dry ice.
15. Cryostat.
16. Superfrost/Plus[®] slides.
17. Cover slips.
18. Nail polish (clear/transparent).

2.14 Enumeration of Tregs in Skin Graft by Flow Cytometry

1. Grafted mice as described in Subheading 3.1.
2. Degranulating agents as described in Subheading 2.6.
3. Straight scissors and forceps.
4. Digestion cocktail: DNase, Liberase (both 4 mg/mL), Collagenase D (or IV) (10 mg/mL).
5. 38 % Percoll or Percoll+ (add 1 mL of 10 \times PBS to the pure Percoll to make 100 % and dilute further with 1 \times PBS).
6. HBSS containing 10 % FBS.
7. FACS buffer (5 % FBS, 2 mM EDTA in PBS).
8. Antibodies directed against: CD4 (clone: L3T4), CD25 (clone: 3C7), FoxP3 (clone: FJK-16s), CD16/CD32 (clone: 2.4G2).
9. Fix/Perm buffer set (commercially available from various vendors).
10. 24-well plates.
11. 40 μ m cell strainers.
12. 15 mL and 50 mL conical tubes.
13. Syringes (1 cc).
14. Transfer pipettes.
15. Centrifuge with a no brake option.
16. Trypan blue (0.4 % stock solution used at 0.1 % final concentration).
17. Hemocytometer.

2.15 Ex Vivo Analysis of Treg Function

1. Grafted Ly5.1 $^{+}$ B6.Cg-FoxP3^{tm2Tch}/J (see Subheading 3.1).
2. Degranulating agents (see Subheading 2.6).
3. Straight and bent-tip forceps.
4. Straight scissors.

2.16 Preparation of Naïve CFSE-Labeled T Cells

1. Graft-derived Ly5.1⁺ regulatory T cells, naïve CSFE-labeled Ly5.2⁺ splenic T cells, irradiated T-cell-depleted splenocytes:
 - (a) Ly5.2⁺ C57Bl/6 mice and/or Ly5.2⁺ donor skin graft (see Note 8).
 - (b) B6.SJL-*Ptprc^a* *Pep3^b*/BoyJ (Ly5.1⁺ C57Bl/6) donor skin graft (see Note 9).
2. Straight forceps and scissors.
3. Carboxyfluorescein diacetate succinimidyl ester (CSFE): 5 µM in PBS.
4. FBS.
5. 37 °C humidified incubator, 5 % CO₂.

2.17 Treg Cell Suppressor Assay

1. Treg assay complete medium (TCM): RPMI containing 10 % FBS, 50 µM β-mercaptoethanol, 100 IU/mL penicillin, 100 µg/mL streptomycin.
2. CD3 positive selection kit (MACS®, Miltenyi Biotec).
3. Magnetic separation columns: LD columns (MACS®, Miltenyi Biotec).
4. MACS® separators.
5. Mark I 137-cesium irradiator or equivalent.
6. Antibodies: CD4 (clone: L3T4), Ly5.2 (CD45.2, clone 104).
7. Round bottom 96-well plate.
8. Hemocytometer.
9. Trypan blue (0.4 % stock solution used at 0.1 % final concentration).
10. 37 °C humidified incubator, 5 % CO₂.

3 Methods

3.1 Skin Grafting

3.1.1 Donor Splenocyte Transfusion and Tolerance Induction

1. Euthanize the donor mice by CO₂ inhalation (or another approved humane method).
2. Harvest the spleens and place them in a small Petri dish containing HBSS (see Note 10).
3. In a biosafety cabinet, transfer the spleens into a sterile 40 µm nylon mesh cell strainer placed in new Petri dishes containing 5 mL of HBSS.
4. Mash the spleens through the cell strainer into the Petri dish with a 1 cc syringe plunger, transfer the cells to a sterile 15 mL tube, and spin down at 400 × g for 5 min at 4 °C.
5. Resuspend the cells in 5 mL of HBSS per spleen with anti-Thy-1/CD90 antibody (hybridoma supernatant used at

1:5,000, need to be optimized for each lot) and incubate for 30 min at 4 °C.

6. Wash cells once with 5 mL HBSS.
7. Resuspend the cells in 5 mL of HBSS containing rabbit complement (use at 1:20, 250 µL/spleen). Follow the manufacturer's instructions and incubate for 30 min at 37 °C.
8. Stop the complement action by adding an excess volume of HBSS with 10 % FBS.
9. Wash cells once with HBSS + 10 % FBS and then once again with HBSS.
10. Count cells and resuspend in HBSS at 10×10^7 cells/mL.
11. Inject the graft-recipient mice (intravenous (iv), tail vein) with 2×10^7 T-cell-depleted splenocytes (200 µL) 1 week *before* planned surgery (i.e., Day 7).
12. Inject the recipient mice (intraperitoneal (ip)) with 250 µg of anti-CD154 mAb (CD40L) on Days 7, 5, and 3 before surgery (*see Note 11*).

3.1.2 Donor Skin Harvest (Surgery Day 1)

1. Harvest donor skin on Day 1 (*see Note 12*).
2. Prepare one or more Petri dishes per strain of donor skin.
3. Place a sterile gauze pad on the dish and soak it with 15–20 mL PBS.
4. Euthanize skin donor mice by CO₂ inhalation (or another approved method).
5. Perform a continuous incision around the circumference of the tail (near the top of the tail) using a scalpel. Be careful to incise the skin only and not to damage the deeper tissue of the tail.
6. Lie the mouse down on its back and perform a midline incision of the ventral side of the tail starting from the circular incision. Try to incise in one single gesture without raising the blade.
7. Grab the skin at the junction of the two incisions using the serrated forceps and tear it away while maintaining the mouse body with the other hand.
8. Place the tail skin on its backside on the cover of a Petri dish. Cut perpendicularly the first two-thirds of the length in four or five square pieces of 0.5–1 cm² and discard the narrow end of the tail skin.
9. Grab the grafts delicately with thin forceps and place them inside down on the PBS-soaked gauze. A dark vertical median line (dorsal side of the tail skin) should be visible on each graft.
10. Drape the dish in foil and keep it overnight at 4 °C (Fig. 1a) (*see Note 13*).

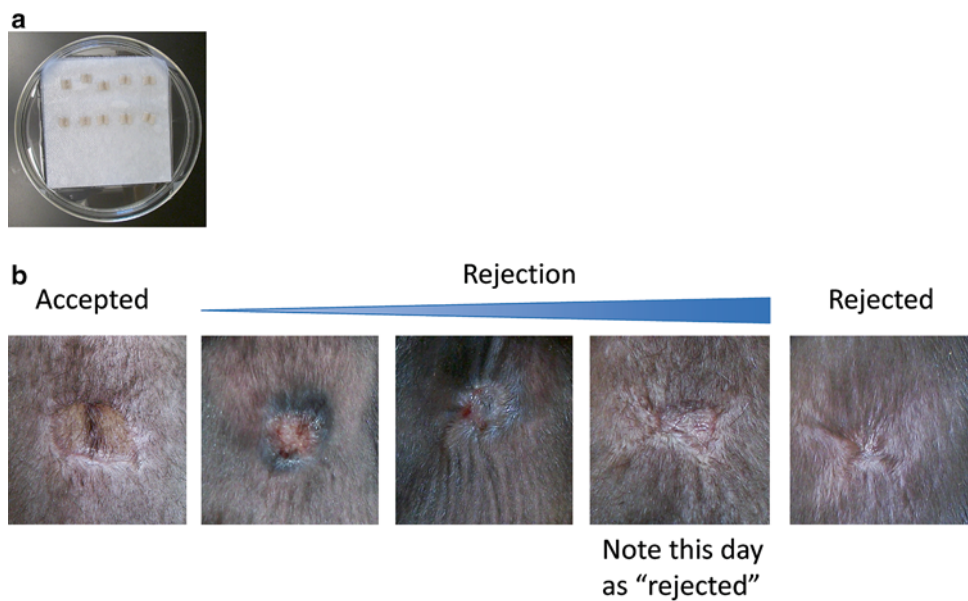


Fig. 1 (a) Preparation of the skin grafts for transplantation. In order to stretch the grafts and prevent them from rolling, place them on sterile gauze soaked in sterile PBS and store them overnight at 4 °C. (b) Different stages of graft acceptance (left) to graft rejection (right) can be monitored visually. Initial signs of rejection should be noted however. In some cases only the upper dermis of the graft will fall off and the graft bed will stay intact. Rejection as end point should only be noted when rejection progresses to the final picture (right)

3.1.3 Skin Grafting Surgery (Surgery Day 0)

1. Transplant skin graft onto recipient mice on Day 0 (*see Note 14*).
2. Prepare the surgery area within a functioning changing hood or a safety cabinet by performing the following:
 - (a) Plug in the heating table and set it to 35 °C.
 - (b) Place as many clean and dry cages as needed on its surface and cover the bedding with a piece of paper towel to prevent the recovering mice from suffocating.
 - (c) Plug in the hot glass bead sterilizer.
 - (d) Cover the surgery area with autoclaved drapes.
3. Place the instruments, several gauze pads, and the suture on the drapes, opening the packages without contaminating the content.
4. In a separate area, anesthetize the recipient mice, four mice at a time, by intraperitoneal (i.p.) injection of the mouse anesthesia cocktail (100 µL/30 g mouse body weight).
5. Shave the upper back of the mice between the shoulder blades.
6. Apply lubricating eye ointment to both eyes and gently massage the eye area.
7. Disinfect the shaved back of the mice by alternating swabs of povidone-iodine scrub with alcohol wipes a total of three times ending with povidone-iodine.

8. Bring the mice to the side of the surgical area and place them to wait for surgery on a drape or gauze to prevent them from cooling (*see Note 15*).
9. Put on the sterile surgical gloves.
10. Transfer the first mouse using a sterile gauze pad and place it in the surgical area.
11. Cut a 0.5–1 cm² incision on the shaved area using the curved serrated scissors. Make the initial cut small and enlarge as needed.
12. Using the curved forceps, place the donor tail skin graft on the hole keeping the median dark line vertical.
13. Suture the graft with a small stitch at each of the four corners using the hemostatic forceps to hold the needle and the curved forceps to maintain the graft in position (*see Note 13*).
14. Put the mouse aside while grafting the next three (*see Note 15*).
15. Sterilize the instrument in the bead sterilizer for 15 s between each mouse.
16. Cover the grafted skin areas with a bandage.
17. Lie the mice down on their back and secure the bandage with a second stripe of adhesive tape.
18. Place the grafted mice in a clean cage on the heated table until anesthesia recovery. Mice should be awake and moving approximately 1 h after administering anesthesia; at this time, mice can be removed from the heat pad.

3.1.4 Rejection Monitoring

1. Monitor the mice daily for the first week to ensure they do not catch their mouth on the bandage (*see Note 16*).
2. After 7 days, remove the bandage and stitches by using a stitch scissor to prevent damaging the graft.
3. Monitor the mice every other day for rejection. An accepted graft should be square or slightly rounded off. The dark median line of the skin graft is most often visible. The upper part of the skin can sometimes become dry and rip-off; however, the underlying graft bed should still be intact. A rejecting graft is shrinking until no donor skin is left and the recipient skin surrounds a small hole or replaces the graft. Without a tolerizing treatment, an allogeneic skin graft rejects within 2 weeks (Fig. 1b and **Note 17**).

3.2 Adoptive Transfer of Mast Cells

3.2.1 Preparing BMMC Donor Cultures

1. Perform the following steps at least 6 weeks before planned adoptive transfer of BMMCs to recipient mice.
2. Euthanize mice by CO₂ inhalation (or another approved method). When looking at the effects of specific MC-derived products on peripheral tolerance, a second culture needs to be

set up along with the WT MCs with the MCs of interest (e.g., GFP expressing cells, knockout mice or transgenic mice).

3. Remove both femora and tibia bones, trying to cut at joints. Place into cold HBSS in a small Petri dish.
4. Using a razor blade or scalpel, scrape off any large pieces of muscle until the bones are clean. A KimWipe can also be used to clean the bones. Perform the rest of the cell culture work in a hood to maintain sterility.
5. Place the bones in 5 mL of 70 % ethanol for 2 min and then transfer to a small Petri dish with 5 mL of HBSS.
6. Take the bones one by one and cut off ends. Flush the bones well with HBSS using a 5 cc syringe with a 25G-5/8" needle.
7. Using the syringe, transfer the bone marrow into a 15 mL tube and break up any large cell aggregates.
8. Add complete RPMI medium to the 15 mL tube (12–14 mL final volume) and spin down at $400 \times g$ for 5 min at 4 °C.
9. Resuspend cells in 5 mL of HBSS and run through a cell filter to removes any residual bone and aggregates.
10. Count lymphocytes, being sure to exclude red blood cells in the count.
11. For each 100 mm cell culture Petri dish, culture 5×10^6 bone marrow cells in 10 mL of complete RPMI supplemented with IL-3 at a final concentration of 20 ng/mL.
12. Every 3–4 days (when media starts to yellow), remove all media and cells in suspensions, spin down ($400 \times g$ for 5 min at 4 °C), and replate the cells into new Petri dishes (see Note 18). Around 3 weeks from the start of the culture, the number of mast cell progenitors should double to triple, and each dish can be split keeping the number of live cells at about 5×10^6 in 10 mL of complete RPMI. At this time, in addition to IL-3 (20 ng/mL), add SCF (50 ng/mL). Expect to split the cells once a week thereafter.
13. After week 5 (post bone marrow harvest), all the cells should have a mast cell phenotype. To check purity, stain cells with CD117 and FcεRI and analyze by flow cytometry. Mast cells can be maintained in culture for up to 12 weeks by refreshing media and splitting cells as necessary.

3.2.2 Reconstitution of *B6.Cg-Kit^{W-sh}* Mice

1. Collect the cultured MCs prepared in Subheading “Preparing BMMC Donor Cultures” at week 6 of culture and spin them down at $300 \times g$ for 5 min at room temperature (RT).
2. Wash 1× with PBS and spin down at $300 \times g$ for 5 min at RT.
3. Resuspend the pellet at a density of 20×10^6 live BMMCs/mL in PBS.

4. Fill a 1 cc syringe with ~850 mL, which is enough to transplant four mice (4×10^6 BMMC/mouse). Install needle after loading the syringe and remove dead air space to yield at least 800 mL final volume in loaded syringe (see Note 19).
5. Anesthetize the B6.Cg-*Kit*^{W-sh} mice by i.p. injection of the anesthesia cocktail (0.1 mL/30 g body weight).
6. Shave the back of the mice at the location of the future skin transplant.
7. Inject 50 μ L (1×10^6) BMMC intradermal into each corner of the future graft bed (200 μ L total for each recipient) using 25G-5/8" needle with 1 cc syringe. To do this gently tent up skin at site and inject away from the graft bed area (see Note 20).
8. Wait at least 8 weeks from the last set of BMMC injections to start with the induction of tolerance as described in Subheading 3.1.
9. At the end of the grafting experiment or when grafts are rejected during the experiment, the skin should be taken and assessed for reconstitution.

3.2.3 Assessment of Reconstitution

1. Take a small piece of skin including the graft if still present.
2. Mince with straight scissors in a 24-well plate.
3. Spin down at $400 \times g$ for 10 min at RT.
4. Remove the supernatant carefully since the pellet dislodges easily.
5. Add digestion cocktail and incubate for 45 min at 37°C (water bath).
6. Transfer to 40 μ m cell strainer on a 50 mL tube and press through while rinsing regularly with ice-cold HBSS containing 10 % FBS.
7. Neutralize the digestion cocktail by filling up the tube with ice-cold HBSS containing 10 % FBS.
8. Spin down at $400 \times g$ for 10 min at 4 °C (see Note 21).
9. Stain the cells with anti-CD117-APC and Fc ϵ RI-PE and analyze for the presence of MCs by flow cytometry (see Notes 22 and 23).

3.3 Breaking Tolerance Inducing Mast Cell Degranulation

In order to study the effect of mast cell-mediated inflammation on the maintenance of peripheral tolerance, one of the approaches is to induce degranulation. The most robust but also the least physiological is by using chemicals like compound 40/80. When doing translational research, it is better to choose an active immunization protocol in which the antigen is administered together with an adjuvant to induce IgE production by endogenous B cells. However, this is more time consuming, and the potential impact of

the generated B cells on the MC function needs to be taken into consideration. If it is required to bypass the B-cell compartment, a passive immunization by transferring antigen-specific IgE could be used. Both active and passive immunizations require a challenge with the relevant antigen in order to cross-link IgE bound to the Fc ϵ RI on mast cells to induce degranulation. Protocols for all three possibilities of degranulation will be discussed.

3.3.1 Chemically Induced Degranulation

1. Sedate the grafted mice at Day 10 post grafting by isoflurane inhalation (see Note 24).
2. Inject 50 μ L (50 μ g/mouse) of compound 40/80 directly under the graft with a 1 cc syringe and 25G-5/8" needle.
3. In order to block degranulation, subcutaneous injection of 100 μ L of a 39 mM cromolyn should be given 30–60 min prior to degranulation of the MCs near the graft (see Note 25).
4. Monitor graft rejection as described in Subheading “Rejection Monitoring” or harvest the graft tissue for further analysis.

3.3.2 IgE-Mediated Degranulation

Active Immunization with OVA/Alum

1. Prepare a 2 mg/mL solution of ovalbumin (OVA) in PBS.
2. Shake the Imject Alum vigorously to resuspend well before use.
3. Add an equal volume of Imject Alum to the OVA solution. Rotate for 1 h at RT before use.
4. Inject (i.p.) 100 μ L of the Alum/OVA suspension.
5. Repeat steps 1–5 1 week after the first immunization.
6. After 30 days, check the IgE levels in the serum by ELISA. The amount of OVA-specific IgE should be minimal and total IgE should be reduced to baseline levels. For ELISA, follow the instructions provided by the manufacturer (see Note 26).
7. Tolerize and graft mice as described in Subheading 3.1 and proceed with steps 9–13 below.

Passive Immunization with Antigen-Specific IgE

8. Optional: in place of steps 1–6 above, after tolerization and skin grafting (step 7). Prepare a 20 μ g/mL OVA-specific IgE in PBS and inject 100 μ L intravenously (i.v.) 24 h prior to challenge (step 10) at Day 10 when rejection controls are needed or at Day 30 when tolerance is established.

IgE-Mediated Degranulation

9. In order to block degranulation, subcutaneous injection (near the graft) of 100 μ L of a 39 mM cromolyn sodium salt solution should be given 30–60 min prior to OVA challenge (see Note 25).

10. Administer the allergen (OVA) to challenge the mice. Controls should be treated with an equal volume and concentration of an irrelevant protein (e.g., BSA):
 - (a) Systemic: 500 μ L of 1 mg/mL OVA in PBS.
 - (b) Local: 50 μ L of 1 mg/mL OVA in PBS.
11. Follow graft rejection as described in Subheading “Rejection Monitoring” or harvest the grafted tissue for further analysis.

3.4 Induction of Inflammation in the Absence of Degranulation

The following methods are a list of possible ways to induce either systemic or local inflammation. There are many other ways to induce inflammation, but the following methods have been tested in our hands and do not induce graft rejection of syngeneic grafts (negative controls) except for the use of anti-CD40 (positive control). These controls are needed to separate the effects of degranulation-induced inflammation from non-IgE-mediated inflammation. Induction of inflammation without inducing graft rejection can be used to find potential effector molecules involved in mast cell-mediated loss of tolerance. For all injections, use a 1 cc syringe with a 25G-5/8" needle and pre-tolerized grafted mice as described in Subheading 3.1. The use of pre-tolerized mice is important since it has been shown that i.p. administration of TLR4 agonist during the tolerization phase (Day 7 to Day 0) leads to a reduction in graft acceptance in this model [7].

1. Non-specific Th1-type systemic inflammation:
 - (a) Inject (i.p.) 200 μ L of complete Freund’s adjuvant.
 - (b) Proceed to **step 5**.
2. TLR-mediated Th1-type systemic inflammation:
 - (a) Inject (i.p.) 200 μ L of a TLR4 agonist (LPS, *E. coli* 055:B5; 250 μ g/mL) OR TLR9 agonist (CpG; ODN-1826; 250 μ g/mL).
 - (b) Proceed to **step 5**.
3. Graft-localized Th2 type of inflammation:
 - (a) Gently pipette 8 μ L of FITC:DBPT paint (*see step 2*) onto the center of the skin graft. Controls will receive the solvent without the FITC. *Important: Do not repeat application of FITC (see Notes 27 and 28).*
 - (b) Proceed to **step 5**.
4. CD40-induced systemic inflammation (positive control):
 - (a) Inject (i.p.) 200 μ L agonistic anti-CD40 (clone: FGK.45; 250 μ g/mL).
 - (b) Proceed to **step 5**.
5. After induction of inflammation grafts, monitor for skin graft rejection as described in Subheading “Rejection Monitoring”.

3.5 Analysis of the Cytokine Profile in the Graft

1. Treat grafted mice with OVA-specific IgE 24 h prior to challenge with OVA as described in Subheading “IgE-Mediated Degranulation.”
2. At 18 h, post-challenge mice will be euthanized by CO₂ inhalation.
3. Carefully remove the grafts by cutting along side of the graft. Lift the graft and detach it from the back by moving bent-tip forceps under the hypodermis. Remove the graft by cutting along the other edges while holding it up with forceps.
4. Collect the grafts in a 24-well plate.
5. Weigh the grafts individually and place them back in their respective wells.
6. Add HBSS (1 mL HBSS per 500 mg wet weight of graft tissue).
7. Cut the graft in small pieces.
8. Incubate for 1 h at 37 °C in an incubator.
9. Collect the graft tissue and supernatant in 1.5 mL microfuge tubes.
10. Spin down for 10 min at 400×*g* and 4 °C.
11. Remove the supernatant and place in a clean 1.5 mL microfuge tube and discard the tissue.
12. Spin down for 10 min at 1,000×*g* and 4 °C to remove the last cell debris.
13. Collect and fractionate the supernatant into separate 1.5 mL microfuge tubes (see Note 29).
14. Analyze the cytokines of interest the same day or store the supernatant at –80 °C for further analysis (see Note 30).

3.6 Studies on T Cells After Mast Cell Degranulation

The induction of tolerance by blocking CD40L is based on the suppression of alloreactive T cells and the induction of allograft-specific regulatory T cells (reviewed in ref. 8). Therefore, it is important to study the impact of MCs on both effector T cells and regulatory T cells *in vivo*. Several approaches to study either one of them will be described here. First, we will focus on the role of the effector T cell after degranulation of the MCs. This will include proving that the observed rejection is T cell mediated and whether the break in tolerance is a local or systemic event. The second part will address changes in regulatory T-cell numbers *in vivo* and functionality *ex vivo* as a result of degranulation.

For clarity the use of cromolyn to block degranulation and mice in which MC will not be degranulated at all is omitted. However, these controls need to be included when performing these types of experiments (see Subheading 3.3).

3.6.1 Antibody-Mediated Depletion of T Cells

1. Anesthetize grafted mice (described in Subheading 3.1) by isoflurane inhalation at Day 27 post graft.
2. Inject 300 μ L of a mixture of anti-CD4 (clone GK1.5; 500 μ g/mouse) and anti-CD8 (clone 2.43; 500 μ g/mouse) i.p. The amount of antibodies needed varies per strain and should be tested before use.
3. Additionally inject 50 μ L of the CD4/CD8 antibody cocktail used in the previous step directly into the graft bed.
4. At Day 29, inject 100 μ L of a 20 μ g/mL OVA-specific IgE in PBS i.v. (see Note 31).
5. At Day 30, anesthetize the mice by isoflurane inhalation and challenge by local injection of 50 μ L OVA (1 mg/mL in PBS) (see Note 32).
6. At Day 35, anesthetize the mice by isoflurane inhalation.
7. Inject 300 μ L of anti-CD4 (clone GK1.5; 250 μ g/mouse) and anti-CD8 (clone 2.43; 250 μ g/mouse) i.p. and 50 μ L locally.
8. Monitor graft rejection as described in Subheading “Rejection Monitoring.”

3.6.2 Adoptive Transfer of Tolerance Using Total Lymphocytes

1. Graft WT C57Bl/6 mice with either CB6F1 skin after tolerizing the host (tolerant) or C57Bl/6 skin (syngeneic) as described in Subheading 3.1.
2. At Day 21, graft C57BL/6-*Rag2^{tm1Cgn}*/J with CB6F1 donor skin (see Note 1). This can be done without prior DST and anti-CD40L treatment. Start the grafting protocol at Subheading 3.1.
3. At Day 33, inject the WT mice with 100 μ L of a 20 μ g/mL OVA-specific IgE in PBS intravenously.
4. At Day 34, anesthetize the WT mice by isoflurane inhalation and challenge by local injection of 50 μ L OVA (1 mg/mL in PBS).
5. At Day 35, euthanize the WT mice by CO₂ inhalation.
6. Collect the graft draining lymph nodes in 24-well plates containing 0.5 mL of PBS (see Note 33).
7. Add 0.5 mL of DNase/Liberase solution (8 mg/mL for each; final concentration will be 4 mg/mL).
8. Cut the lymph nodes at least once to break the surrounding capsula.
9. Incubate for 30 min in a 37 °C water bath.
10. Transfer the lymph nodes and digestion cocktail to a 40 μ m cell strainer placed on a 50 mL conical tube and dilute with 10 mL of cold PBS.

11. Mash the lymph nodes with 1 cc syringe plunger and spin down at $400 \times g$ for 5 min at 4 °C.
12. Completely remove the supernatant and resuspend in 1 mL of cold PBS. Sample 10 μ L to perform a cell count.
13. Fill the tube with at least 20 mL of cold PBS to wash the cells. Spin down at $400 \times g$ for 5 min at 4 °C.
14. Resuspend the pellet to 10×10^6 cells/mL in PBS (warm to RT) and inject 100 μ L (i.v.) into experimental mice (e.g., Day 14 post-graft C57Bl/6.RAG2^{-/-} recipient mice).
15. Follow graft rejection as described in Subheading “Rejection Monitoring.”

3.6.3 Decay of Tolerance After Local MC Degranulation

In studies that pursue the question of whether regional loss of tolerance induces a global effect, the introduction of two skin grafts may be necessary. This is a deviation from the protocol described in Subheading 3.1. In this case all mice need to be pre-tolerized with DST and anti-CD40L, i.e., also the mice that will receive a syngeneic graft.

1. Graft WT pre-tolerized C57Bl/6 mice on the dorsal side of the mouse, close to the base of the tail (see Note 34).
2. At Day 1, after grafting, inject (i.p.) 250 μ g of anti-CD154.
3. Mice that successfully engrafted will receive a second graft at Day 14 post grafting. This graft will be placed at the dorsal side, between the shoulder blades, and is transplanted as described in Subheadings “Donor Skin Harvest (Surgery Day 1)” and “Skin Grafting Surgery (Surgery Day 0).” This second graft will drain into the axillary and brachial lymph nodes.
4. At Day 30 post grafting of the first graft, degranulate the MC by using one of the previously discussed methods in Subheading 3.3 (see Note 35).
5. Monitor graft rejection of the second graft as described in Subheading “Rejection Monitoring.”

3.7 The Role of Treg After MC Degranulation

3.7.1 Adoptive Transfer of Tolerance Using Tregs

1. Graft Ly5.1⁺ B6.Cg-FoxP3^{tm2Tch}/J mice “FoxP3-GFP mice” with either CB6F1 skin after tolerization (tolerant) or C57Bl/6 skin (syngeneic) as described in Subheading 3.1.
2. At Day 14, graft C57BL/6-*Rag2^{tm1Cgn}*/J mice with CB6F1 skin (see Note 1). Start the grafting protocol at Subheading “Donor Skin Harvest (Surgery Day 1).”
3. At Day 30 post grafting, degranulate the graft of the FoxP3-GFP mice by using one of the previously described methods (see Subheading 3.3).
4. Euthanize the mice by CO₂ and collect the draining lymph nodes 24 h later. Also euthanize a WT untreated mice and collect the spleen.

5. Process the spleen and the lymph nodes as described in Subheadings “Donor Splenocyte Transfusion and Tolerance Induction” and “Adoptive Transfer of Tolerance Using Total Lymphocytes,” respectively.
6. Purify the regulatory T cells by sorting for GFP⁺, i.e., FoxP3⁺, cells.
7. Pre-enrich the splenocytes for CD4⁺CD25⁻ cells using a CD4-negative selection (e.g., biotin selection kit, STEMCELL Tech.) and then stain the cells for CD4-APC and CD25-PE prior to sorting the CD4⁺/CD25⁻ T cells.
8. Mix the sorted GFP⁺ regulatory T cells with the sorted naïve polyclonal T cells at different ratios.
9. Transfer 1×10^6 mixed T cells to the pre-grafted C57Bl/6. RAG2^{-/-} by tail vein injection.
10. Monitor the C57Bl/6.RAG2^{-/-} for graft rejection as described in Subheading “Rejection Monitoring.”

3.7.2 Quantifying Tregs in the Skin Graft by Fluorescent Microscopy

1. Graft mice as described in Subheading 3.1 and degranulate at Day 30 by using one of the described methods in Subheading 3.3.
2. Euthanize mice at different time points after degranulation to evaluate changes in the cellular composition of the graft over time.
3. Collect the grafts by carefully cutting it from the back of the mice (see Subheading 3.5).
4. Place the graft in cryo-molds containing OCT.
5. Freeze the tissue by placing them on a mixture of dry ice and ethanol. The frozen blocks can be stored at -80°C for up to 3 months or continue with step 11.

Alternative Freezing Protocol to Increase Cryo-protection

6. Fix the grafts in 10 % normal buffered formalin for 12–24 h.
7. Place the grafts in 10 % sucrose in PBS for 1 h at RT.
8. Transfer the grafts to 20 % sucrose in PBS for 1 h at RT.
9. Transfer the grafts to 30 % sucrose in PBS. Leave the graft in 30 % sucrose until they sink to the bottom of the tube or store them at 4°C overnight.
10. Place the graft in OCT containing cryo-molds and freeze them on a dry ice/ethanol mixture. The blocks can be stored at -80°C for up to 3 months or continue with step 11.
11. Cut the blocks on a cryostat at 8 μm thickness and collect the sections on Superfrost slides. This will allow for analysis on conventional fluorescent microscopes as well as confocal microscopy. In the case that confocal microscopy will be used, the thickness of the cuts can be increased.

12. Fix the tissue by placing them in a 1:1 acetone:methanol mixture for 7 min at RT.
13. Wash twice in PBS at RT (5 min each wash).
14. Place the slides in a humidified chamber.
15. To block non-specific binding, incubate the slides with 10 % serum (*see Note 6*).
16. Flick off the blocking buffer and apply the primary antibody mix containing anti-FoxP3 and anti-CD4. Incubate overnight at 4 °C.
17. Wash stringently with PBS: minimum of three times on a shaker (30 min each).
18. Apply the secondary antibody if required and incubate for 4–6 h at RT.
19. Wash stringently with PBS: minimum of three times on a shaker (30 min each).
20. Add either Hoechst 33342 or DAPI to stain the nuclei. Incubate for 10 min at RT.
21. Wash three times in PBS (5 min each wash).
22. Mount with a cover slip using an aqueous mounting media, preferably one that protects the fluorescence.
23. After the slides have dried, seal the edges of the cover slip with nail polish.
24. Scan and photograph the skin grafts and count the number of FoxP3⁺CD4⁺ T cells and express as number of cells per surface area of the graft tissue.

3.7.3 *Enumerating Graft-Infiltrating Tregs by Flow Cytometry*

1. Graft mice as described in Subheading 3.1 and degranulate at Day 30 by using one of the described methods in Subheading 3.3.
2. Euthanize mice at different time points after degranulation to evaluate changes in the cellular composition of the graft over time.
3. Collect the grafts by carefully cutting grafted skin from the back of the mice (*see* Subheading 3.5).
4. Mince with straight scissors in a 24-well plate.
5. Spin down at 400 $\times g$ for 10 min at RT.
6. Remove the supernatant carefully since the pellet dislodges easily.
7. Add digestion cocktail and incubate for 45 min at 37 °C (water bath).
8. Transfer to 40 m cell strainer placed atop a 50 mL tube and press and rinse cells through the strainer.

9. Neutralize the pellet with excess of ice-cold HBSS containing 10 % FBS.
10. Spin down at $400 \times g$ for 10 min at 4 °C (see Note 10).
11. Resuspend the pellet in 3 mL of PBS at RT.
12. Prepare 38 % Percoll in PBS by first adding 1/10th of a volume of 10× PBS to the Percoll (100 %) and further dilute the resulting 90 % Percoll with 1× PBS. Add 4 mL 38 % Percoll to a 15 mL conical polystyrene tube for each graft. *Important: Percoll should be at RT before use.*
13. Carefully layer the cell suspension on top of the Percoll and spin down for 30 min without brake.
14. Remove the interphase first with a transfer pipette in order to minimize the chance of contaminating the pellet.
15. Pipette off and discard the remaining solution.
16. Add at least 10 mL of cold PBS (4 °C) to the pellet.
17. Spin down at $400 \times g$ for 10 min at 4 °C.
18. Resuspend the pellet in 200 µL and take a small aliquot for cell counts.
19. Stain the cells for CD4-APC and CD25-PE for 30 min in the dark on ice.
20. Wash with PBS (4 °C) and spin down (5 min at $400 \times g$ at 4 °C).
21. Resuspend the pellet in Fix/Perm solution and incubate for 30 min in the dark on ice.
22. Wash twice with permeabilization buffer (10 min each at 4 °C in the dark).
23. Block with 100 µL of anti-CD16/32 antibody in permeabilization buffer for 15 min at 4 °C in the dark.
24. Add the anti-FoxP3-FITC antibody (2× concentrated antibody solution in permeabilization buffer). Incubate for 30 min at 4 °C in the dark.
25. Wash 2× with permeabilization buffer and then spin down ($400 \times g$ for 5 min at 4 °C).
26. Wash once with FACS buffer (4 °C) and spin down ($400 \times g$ for 5 min at 4 °C).
27. Resuspend the cells in FACS buffer and analyze for CD4⁺CD25⁺FoxP3⁺ cells within the lymphocyte gate by flow cytometry (see Note 36).

3.7.4 Ex Vivo Analysis of Treg Function

Harvest Graft-Associated Tregs

1. Graft tolerized Ly5.1⁺ B6.Cg-FoxP3^{tm2Tch}/J mice with either CB6F1 skin or C57Bl/6 skin (syngeneic) as described in Subheading 3.1 (see Notes 1 and 6).

2. Degranulate the mast cells at Day 30 by using any method described in Subheading 3.3.
3. Collect the draining lymph nodes at different time points after degranulation and process as described in Subheading “Adoptive Transfer of Tolerance Using Total Lymphocytes” (see Note 33).
4. Isolate the regulatory T cells by sorting for the GFP⁺, i.e., FoxP3⁺, cells.

Prepare Naïve CFSE-Labeled Splenic T Cells

5. For each time point, sacrifice a WT Ly5.2⁺ mouse (see Note 8) and purify the naïve splenic T cells as described in Subheading 3.7.1.
6. Label the naïve T cells by adding a 50 µL of 5 µM CFSE solution in PBS.
7. Incubate for 7 min in a 37 °C incubator.
8. Add 1 mL of 100 % FBS to bind the residual CFSE and let it stand for 5 min at RT. Add 9 mL of PBS and spin down at 400×*g* for 5 min. The pellet should have a yellowish color.

Prepare T-Cell-Depleted Splenocytes

9. For each time point, sacrifice a WT Ly5.1⁺ B6.SJL-*Ptprc^a* *Pep3^b*/BoyJ mouse (see Note 9) and process the spleen as described in Subheading “Donor Splenocyte Transfusion and Tolerance Induction.”
10. Remove the T cells by CD3-positive selection using MACS separation column (follow manufacturer’s protocol). Collect the flow through and repeat the selection with a new column. Check the flow through for the presence of CD3⁺ cells by flow cytometry.
11. Irradiate (3,000 rad (30 Gy)) the T-cell-depleted splenocytes.

Set Up the Treg Suppressor Assay

12. Plate 5 × 10⁴ irradiated splenocytes per well in a round bottom 96-well plate.
13. Spin down splenocytes in plate (400×*g* for 5 min) and aspirate the supernatant.
14. Add 50 µL TCM containing 5 × 10⁴ CFSE-labeled Ly5.2⁺ naïve T cells to the culture and resuspend.
15. Add 50 µL TCM containing Ly5.1⁺ regulatory T cells at different ratios to the wells and resuspend (see Note 37).
16. Place the plate in a 37 °C incubator with 5 % CO₂.

After 3 days analyze the Ly5.2⁺CD4⁺ cells for CSFE dilution as measure of suppression/proliferation (see Note 38).

4 Notes

1. These mice are the first-generation offspring of Balb/C × C57Bl/6 breeding pairs.
2. B6.Cg-*Kit*^{W-sh}/H_{Nihr}JaeBsmJ (JAX Stock#005051). By using B6.Cg-Kit^{W-sh} mice, the role of MCs or MC products can be confirmed by reconstituting these mice. The method is described in Subheading “Reconstitution of B6.Cg-KitW-sh Mice.”
3. It is important to use this type of Petri dish since not all plastics give the same growth pattern and final yield. If contamination of cultures is a problem, 25 cm² vented tissue culture flasks (Corning 430639) can be used instead of dishes. Please note that BMMC grow more slowly in these flasks.
4. Instead of OVA-specific IgE, any other IgE/allergen combination can be used but the quantities of the IgE and OVA may require specific optimization. In our studies we also used TNP (trinitrophenol)-specific IgE (clone A3B1; 100 µL of a 50 µg/mL solution) with nitrophenol (NP)-conjugated allergens NP₁₇-OVA or NP₂₃-BSA. Challenge with 50 µL intragraft injection of a 400 µg/mL solution in PBS. It is important to know that there is cross-reactivity between this clone and the hapten NP.
5. C57BL/6-*Rag2*^{tm1Cgn}/J (JAX Stock#008309).
6. B6.Cg-FoxP3^{tm2Tch}/J (JAX Stock#006772).
7. When using only directly conjugated antibodies, any serum will provide reduction of background staining. However, when using secondary antibodies, the serum should ideally match the host species of the secondary antibody.
8. Ly5.2/CD45.2 is a B-cell antigen present on C57Bl/6 mice, among other congenic strains. Currently, the designation of this antigen has been changed to Ptprc^b.
9. B6.SJL-*Ptprc^a* *Pep3^b*/BoyJ is a congenic strain carrying the Ly5.1/CD45.1/ Ptprc^a B-cell antigen.
10. For DST, one spleen of the donor mouse is used to tolerize one recipient mouse.
11. The induction of tolerance by blocking CD40L is based on the suppression of alloreactive T cells and the induction of allograft-specific regulatory T cells (reviewed in ref. 8).
12. Initially grafting might take up to 20–30 min per mouse, but with practice around six mice per hour can be achieved.
13. Although skin grafts can be collected on the day of transplantation, the donor tail skin has a tendency to roll up making it hard to suture. Moreover, it induces additional tension on the

corners of the graft and is thus likely to result in tearing at the point of needle entry. Keeping the grafts overnight on PBS-soaked gauze at 4 °C in the dark will prevent the skin from rolling.

14. The surgery is performed according to the “Aseptic Non-Touch Technique” or “Sterile-Tip Technique.” With this method, the hands never touch the incision or sterile field; only the instrument tips enter the surgical field.
15. Due to the rapid cooling of anesthetized mice, it is advised to perform the surgery on a heat pad for beginning surgeons.
16. During the first week following surgery, we have observed that both the use of fabric and plastic Band-Aids can lead to the mice getting their teeth stuck in the Band-Aid. Putting an extra layer of autoclave tape over the Band-Aid can reduce the incidence of this happening. When mice get stuck, carefully cut the Band-Aid to free them. If needed, replace the Band-Aid with a new one.
17. Scoring the grafts for rejection is rather subjective and should preferably be done by two independent observers.
18. You are deliberately removing the adherent cells. During the first 3 weeks of culture, it is expected that there will be some cell death, but mast cell progenitors will continue to differentiate and grow. As the cultures continue and you no longer have growth of adherent cells, the plates can be reused with just a media change.
19. It is advised to draw up the cells into the syringe without the needle attached to prevent cell death due to sheer stress.
20. In order to inject around the same location, a square can be drawn with a permanent marker at the spot where the graft will be introduced. To increase success rate of reconstitution, injection of the BMMC can be repeated once a week for an additional two times. This means maintaining the original cultures for two more weeks.
21. In order to increase the yield of cell recovery (or if digestion was not complete), the digestion, straining, and neutralization steps can be repeated with the tissue remaining in the cell strainer. Tubes of the same mouse can be pooled afterwards.
22. A dump (exclusion) gate can be included during flow cytometric analysis or sorting using murine anti-CD4, anti-CD11b, and anti-CD11c antibodies coupled to an appropriate fluorochrome.
23. Reduced numbers of total mast cells in locally reconstituted mice can be expected when compared to WT controls. Mice should be excluded when no CD117⁺/FceRI⁺ cells are detected (i.e., unsuccessful reconstitution). Expect around 20 % of the mice to be excluded at the end of the experiment and thus adjust the initial number of mice to cover this loss.

24. The mice should be immobilized but reflexes can still be there. Using mice at Day 10 or earlier is required when acute rejection controls (allogeneic graft without prior tolerization) are needed. For effects of degranulation at later time points, this group should not be included.
25. We have found that cromolyn sodium salt solution is best given in two injections of 50 μ L each on opposing sides of the graft.
26. IgE ELISA requires about 100 μ L of blood yielding about 40 μ L of serum which can be obtained by either tail vein or cheek bleed of live mice. This is enough to have duplicate wells with a minimum dilution of 2.5 times (50 μ L end volume/well). Both total and OVA-specific IgE ELISA kits are available from various vendors.
27. Due to the nature of the solvent, the FITC will spread over the graft and enter the skin. For a 0.25 mm² graft, 8 μ L FITC paint will lead to minimal spillover to the surrounding tissue.
28. Application of FITC should not be repeated since FITC induces an IgE-mediated contact allergy. Reintroducing FITC to the graft will induce degranulation of the graft resident MCs and subsequent rejection.
29. Aliquot size will depend on further analysis but for standard ELISA 50 μ L aliquot will suffice, whereas for Luminex analysis 200 μ L aliquots are recommended.
30. Some cytokines are very unstable (e.g., IL1 β) and we recommend analyzing culture supernatants for these on the same day of collection.
31. The protocols described for the studies on MC and T cells all use a passive immunization. However, active immunization as well as chemical degranulation can be used (*see* Subheading 3.3 for methods).
32. This late time point is to ensure tolerance is established.
33. Both axillary and brachial lymph nodes can be pooled and thus in total you can collect four draining lymph nodes from one mouse.
34. This location will drain to the inguinal lymph nodes. As such, the graft should be placed as close to the tail as possible. Extra mice should be grafted since grafts in this location are prone to be ripped off by the mice. Single mouse housing is recommended to increase success rate.
35. To control for potential systemic distribution of the antigen used to degranulate, one cohort of mice should first receive a syngeneic graft followed by a second CB6F1 graft. If there is undesired systemic distribution, the second graft will reject and the dosing of the degranulating agent (compound 40/80 or OVA) should be lowered.

36. Alternatively, the B6.Cg-FoxP3^{tm2Tch}/J mice can be used as recipient. In this case, intracellular staining for FoxP3 is not required resulting in higher yields and more accurate numbers of graft-derived regulatory T cells.
37. Functional regulatory T cells will fully suppression proliferation of the naïve T cells at a 2:1 ratio of regulatory T cell to naïve T cell.
38. Each peak will present one division and in the absence of regulatory T cells a maximum of seven peaks can be observed.

References

1. Galli SJ, Grimaldeston M, Tsai M (2008) Immunomodulatory mast cells: negative, as well as positive, regulators of immunity. *Nat Rev Immunol* 8(6):478–486
2. Lu LF et al (2006) Mast cells are essential intermediaries in regulatory T-cell tolerance. *Nature* 442(7106):997–1002
3. de Vries VC, Noelle RJ (2010) Mast cell mediators in tolerance. *Curr Opin Immunol* 22(5):643–648
4. de Vries VC et al (2011) Mast cells condition dendritic cells to mediate allograft tolerance. *Immunity* 35(4):550–561
5. de Vries VC et al (2009) Mast cell degranulation breaks peripheral tolerance. *Am J Transplant* 9(10):2270–2280
6. de Vries VC et al (2009) The enigmatic role of mast cells in dominant tolerance. *Curr Opin Organ Transplant* 14(4):332–337
7. Miller DM et al (2009) TLR agonists prevent the establishment of allogeneic hematopoietic chimerism in mice treated with costimulation blockade. *J Immunol* 182(9):5547–5559
8. Elgueta R et al (2009) Molecular mechanism and function of CD40/CD40L engagement in the immune system. *Immunol Rev* 229(1):152–172

Chapter 29

The Function of Mast Cells in Autoimmune Glomerulonephritis

Renato C. Monteiro, Walid Beghdadi, Lydia Celia Madjene, Maguelonne Pons, Michel Peuchmaur, and Ulrich Blank

Abstract

Immune-mediated glomerulonephritis is caused by deposition of immune complexes on the glomerular basement membrane or of autoantibodies directed against the glomerular basement membrane. Depositions lead to an inflammatory response that can ultimately destroy renal function and lead to chronic kidney disease. However, the pathological processes leading to the development of renal injury and disease progression remain poorly understood. To investigate the mechanisms of disease development in glomerulonephritis various animal models have been developed, which include as the most popular one the induction of glomerulonephritis by the injection of heterologous antibodies directed to the glomerular basement membrane. The role of mast cells and mast cell-derived mediators has been evaluated in these models. In this chapter we describe the methods that allow to set up and study the disease parameters of immune-mediated glomerulonephritis development.

Key words Glomerulonephritis, Kidney, Mast cell, Renal injury, Mast cell protease

1 Introduction

Immune-mediated glomerulonephritis (GN) can be induced by autoantibodies reacting with glomerular antigens or by the deposition of (“structurally altered”) circulating antibodies or antibody complexes [1]. Renal injury has been found to involve activation of complement as well as of Fc receptors on inflammatory cells leading to the development of proteinuria and inflammatory responses with leukocyte infiltration [2, 3]. Disease progression then promotes formation of crescents, glomerulosclerosis, interstitial inflammation and fibrosis, and loss of renal function. However, the pathological processes leading to the development of renal injury and disease progression still remain poorly understood.

To better understand the mechanism of immune-mediated glomerulonephritis experimental animal models have been developed and characterized starting during the 1930s with the groundbreaking

work of Masugi [4, 5]. His model was based on the injection of antibodies directed to the glomerular basement membrane inducing anti-GBM GN, sometimes also called Masugi nephritis [6]. Two distinct experimental models for anti-GBM disease have been used routinely [6, 7]. The first consists in the injection of heterologous anti-GBM antibodies without preimmunization. The disease develops slowly with an initial heterologous phase leading to renal injury, which is mediated by neutrophils followed by an autologous phase characterized by the development of host antibodies to the injected anti-GBM. The latter involves the action of macrophages and T cells. However, large amounts of antibodies are required to induce disease. The second consists in an accelerated model in which mice are first preimmunized with heterologous IgG in the presence of complete Freund's adjuvant followed by the injection of anti-GBM antibodies leading to a more rapid development of the autologous effector phase. Early experimental studies have mainly used rat models, although recently mouse models with genetic deficiency have been increasingly used to dissect the underlying mechanisms and pathological features of anti-GBM disease. It should be noted that in mice disease development largely depends on the mouse strain with commonly used C57Bl/6 and Balb/c strains being less susceptible than for example 129/svJ or DBA/1 J. However, some of the strains, like C57Bl/6, may become susceptible to immune nephritis if the dosage of the administered anti-GBM sera is increased [8, 9].

We have applied the anti-GBM glomerulonephritis model to test the involvement of mast cells and the mast cell produced mediator mouse mast cell protease-4 (mMCP-4) in the development of disease. These investigations have shown that mast cell-deficient *W/W^v* mice showed increased susceptibility to the development of glomerulonephritis due to the absence of repair and remodeling functions [10]. Another group reported similarly a protective effect of mast cells that was explained by their capacity to reduce influx of pathogenic T cells and macrophages by affecting the absence of a mast cell coordinated action on regulatory T cells [11]. Surprisingly, a third study using a non-accelerated model reported an aggravating role of mast cells in disease development by enhancing glomerular expression of adhesion molecules and promotion of $T_{H}1$ -dependent effector mechanisms [12]. Although these studies arrived at somewhat different conclusions they may actually reveal the delicate balance of the inflammatory reactions coordinated by mast cells in a given pathological context that can depend on many additional parameters such as the kinetics of disease development [7]. In agreement with this notion we found that examination of a single mediator, the mMCP-4 chymase, rather showed a deleterious effect, which at least partly depended on the capacity of this protease to increase glomerular expression of disease-promoting Ang II [13]. In the following we provide a

description of the methods used to analyze glomerulonephritis in mast cell-deficient mice by focusing on those particularly relevant to the model.

2 Materials

2.1 Mouse Strains

1. WBB6F_{1/J}-Kit^W/Kit^{W-v} mast cell-deficient mice (*see Note 1*).
2. mMCP-4 knockout (C57Bl/6-congenic).
3. C57Bl/6 J mice.

2.2 Nephrotoxic Serum

1. Kidney glomeruli isolated from Wistar rats (*see Note 2*).
2. Rabbit anti-GBM serum (*see Note 3*).

2.3 Purification of Rat Glomeruli for Immunization of Rabbits

1. Scissors, scalpel, glass beaker.
2. Phosphate-buffered saline (PBS).
3. 5 and 50 cc syringes.
4. Needles (25G×7 mm).
5. 0.22 µm filters.
6. Petri dishes.
7. 50 ml sterile conical tubes (polypropylene).
8. Stainless steel mesh sieves 60 (pore size 250 µm), 100 (pore size 100 µm), and 200 (pore size 75 µm).
9. Collecting stainless steel trays.
10. Sonicator.

2.4 Immuno-fluorescence Analysis

1. Antibodies:
 - (a) Goat anti-rabbit IgG-FITC (Jackson Immunoresearch).
 - (b) Goat anti-mouse IgG-FITC (Jackson Immunoresearch).
 - (c) Goat anti-rat IgG FITC (Jackson Immunoresearch).
 - (d) Donkey anti-guinea-pig-Rhodamine (Jackson Immunoresearch).
 - (e) Donkey anti-goat-FITC (Jackson Immunoresearch).
 - (f) Anti-fibrin-FITC (Nordic Immunological Laboratories).
 - (g) Anti-CD11b (Mac1) (AbD Serotec).
 - (h) L3T4 rat anti-CD4 (Southern Biotechnology Associates).
 - (i) Goat anti-type I collagen (Southern Biotechnology Associates).
 - (j) Guinea-pig anti-angiotensin II (Peninsula laboratories).
2. Superfrost Plus microscope slides.
3. Acetone (-20 °C).
4. PBS-Tween 20: PBS containing 0.1 % Tween-20.

2.5 Evaluation of Cellular and Humoral Immune Responses to Injected Rabbit Anti-GBM Antibodies

5. PBS-5 % BSA: PBS containing 5 % bovine serum albumin (BSA).
6. Fluorescence microscope.

1. 96-Well ELISA plates.
2. Rabbit IgG (Southern Biotechnologies Associates).
3. F(ab')2 goat anti-rabbit IgG (Jackson Immunoresearch).
4. Biotinylated donkey-anti-rabbit IgG (Jackson Immunoresearch).
5. Biotinylated donkey-anti-mouse IgG (Jackson Immunoresearch).
6. Streptavidin-HRP (Southern Biotechnologies Associates).
7. 3,3',5,5'-Tetramethylbenzidine (TMB) substrate solution (Interchim).
8. 1 N hydrochloric acid (HCl).
9. PBS-1 % BSA: PBS containing 1 % BSA.
10. ELISA plate reader.
11. Thickness gage (Mitutoyo).

3 Methods

3.1 Generation of Nephrotoxic Anti-GBM Rabbit Serum

1. Euthanize ~10 rats with intraperitoneal (i.p.) injection of pentobarbital (120 mg/kg).
2. Spray fur of the abdomen thoroughly with alcohol to disinfect.
3. Open abdomen and collect kidneys. Decapsulate kidneys and immediately place in ice-cold PBS.
4. Dissect kidneys under the culture hood. Collect the outer cortex layers containing the glomeruli (distinguishable from the medulla by their lighter color).
5. Cut the cortex layers into small slices with a scalpel and then transfer them into ice-cold sterile PBS.
6. Force cortex slices with the bulb of a syringe through three successive sieves with decreasing pore sizes (250 µm → 100 µm → 75 µm) (*see Note 4*).
7. Collect the material that emerges through the first sieve into ice-cold PBS in a receiving pan containing ice.
8. Shake the sieved material gently and then pour on top of the second mesh sieve.
9. Collect the flow through as before and push through the third sieve.
10. Wash the third sieve extensively with ice-cold PBS (*see Note 4*). This time, discard the flow through and keep the captured material.
11. Invert the third mesh and place in a new Petri dish. Using a syringe, rinse the mesh three times with 10 ml PBS.

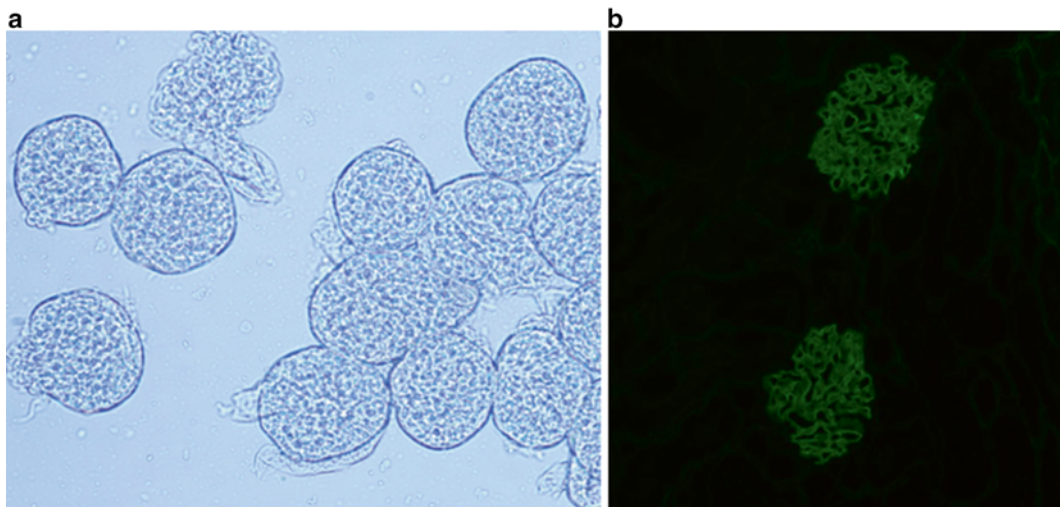


Fig. 1 Evaluation of purified glomeruli and anti-GBM serum. (a) Light microscopic picture of purified glomeruli from rat kidneys retained on mesh 200. (b) Binding of produced rabbit anti-GBM antiserum to mouse glomeruli. Mice were injected i.v. with 200 µl of anti-GBM antiserum. After 3 days, mice were sacrificed and frozen kidney sections were examined for the presence of anti-GBM antibodies using anti-rabbit IgG-FITC. Objective magnification 20×

12. Pass the collected material through a 25G×7 mm needle and transfer into a 50 ml conical polypropylene tube.
13. Centrifuge the cells for 10 min at 1,800× g . Aspirate the PBS and retain the cell pellet.
14. Resuspend the pellet in 3 ml PBS.
15. Examine the purified glomeruli under a light microscope to evaluate contamination with tubular fractions (Fig. 1a).
16. Break the glomeruli by sonication (80 W, two bursts of 30 s each) (Branson Ultrasonic processor 750 W, Sigma Aldrich).
17. Centrifuge for 20 min at 1,800× g and discard the supernatant. Wash twice with PBS.
18. Resuspend the pellet in 3 ml PBS. Store aliquots (50 µl) at -80 °C.
19. Use aliquots (50 µl or ~300 µg) to immunize rabbits to generate nephrotoxic serum (using classical immunization protocols with complete Freund's adjuvant).

3.2 Induction of Anti-GBM Glomerulonephritis

1. An accelerated model of anti-GBM glomerulonephritis is described below.
2. Day -5: Pre-immunize male mice using purified normal rabbit IgG (Southern Biotechnology Associates). Inject 0.5 mg IgG per 20 g body weight emulsified in complete Freund's adjuvant.
3. Day 0: Administer nephrotoxic serum through the tail vein at a dose of 50–200 µl per 20 g body weight (see Note 5). Routinely, normal rabbit serum is used as a control (see Note 6).

4. Except for mortality studies, mice are sacrificed at day 3 to evaluate early changes and at day 14 to evaluate late changes.
5. Euthanize mice by anesthetic overdose.
6. For optimal histological staining and to avoid contamination by blood cells perfuse anesthetized mice according to established protocols.
7. Examine a minimum of three to six mice per experimental group.

3.3 Assessment of Renal Function

1. Evaluate proteinuria, blood urea nitrogen (BUN), and blood creatinine levels in experimental glomerulonephritis models.
2. Collect spot samples of urine on day 0 before the induction of anti-GBM glomerulonephritis, day 3 (to evaluate early changes), day 9 or 10, and day 14 before sacrifice (to evaluate late changes).
3. Alternatively, place mice into metabolic cages to determine 24-h proteinuria.
4. Collect blood samples at day 14 before sacrifice.
5. Proteinuria, BUN, and blood and urinary creatinine concentrations are determined using commercially available kits (Olympus Diagnostica) and an AU400 Autoanalyzer (Olympus Diagnostica) (see Note 7).
6. Urinary protein is normalized to the urinary creatinine and expressed as urinary protein per creatinine [13] (see Notes 8 and 9).

3.4 Histological Assessment of Glomerulonephritis

1. After perfusion, some portions of the kidney (usually one half cut longitudinally) are immediately frozen in Tissue-Tek OCT compound for immunohistochemical analysis.
2. For the remaining kidneys, decapsulate and fix (both capsules and kidneys) in 10 % formalin and embed in paraffin.
3. Stain paraffin-embedded sections with periodic acid Schiff's (PAS reagent), Masson Trichrome (Fig. 2), as well as toluidine blue staining to enumerate mast cells.
4. Evaluate the pathological features of kidney sections in a blinded fashion. Score glomerular deposits and intracapillary cellular proliferation [10, 13]. Evaluate interstitial infiltration, fibrosis, and tubular necrosis. All determinations are ranked using a semiquantitative score of 1–4 as described [10, 13].

3.5 Immuno-fluorescence Staining of Frozen Kidney Sections

Pathological parameters of anti-GBM kidneys, such as glomerular deposited rabbit anti-GBM IgG (Fig. 1b), mouse anti-rabbit IgG (during the autologous phase), fibrin, angiotensin, as well as glomerular and interstitial type I collagen, are assessed by immuno-fluorescence using frozen kidney sections. Kidney cryosections of mice injected with normal mice serum are used as a control.

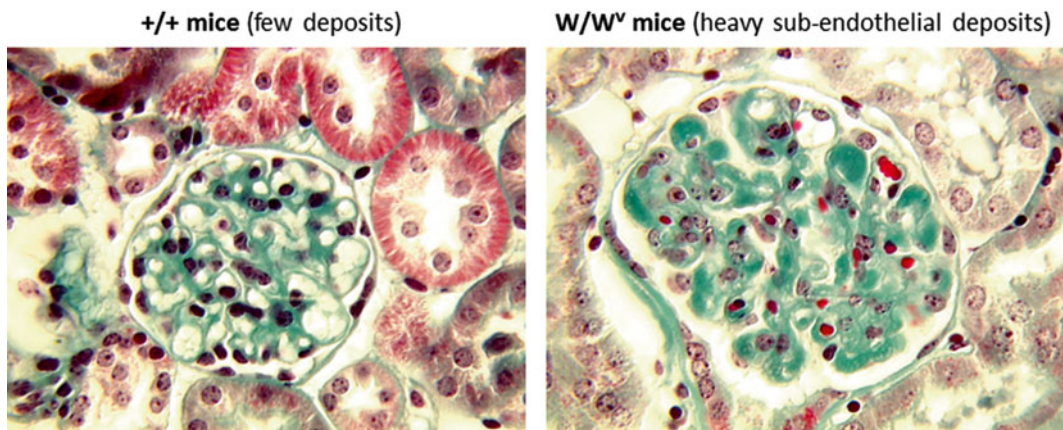


Fig. 2 Evaluation of glomerulonephritis by renal histology. Micrographs taken after light microscopic examination of Massons Trichrome-stained kidney section from WBB6F_{1/J}-Kit^W/Kit^{W-v} (W/W^v) (*left panel*) and wild-type +/+ (*right panel*) subjected to anti-GBM glomerulonephritis and sacrificed at day 3. The micrographs show the heavy deposits that become apparent in mast cell-deficient W/W^v mice. Objective magnification 63×

1. Cut decapsulated kidneys in half longitudinally and embed in OCT. Freeze in liquid nitrogen. Blocks can be kept at -80 °C for long-term storage.
2. Mount kidney cryosections (5 µm) on Superfrost Plus slides. Fix in ice-cold acetone. Fixed cryosections can be kept at -80 °C for long-term storage.
3. When ready to stain, allow frozen sections to come to RT in a humidified chamber.
4. Rinse sections with PBS-Tween 20 and then block by incubation in PBS-5 % BSA for 20 min.
5. After rinsing with PBS-Tween 20, incubate tissue sections with primary antibody for 2 h at RT or overnight at 4 °C. Optimal antibody concentration is usually in the range of 1–10 µg/ml in PBS-1 % BSA.
6. After rinsing with PBS-Tween 20, sections are incubated with fluorescent secondary antibody. Optimal antibody concentration is usually in the range of 5–10 µg/ml in PBS-1 % BSA.
7. At this step and in subsequent steps, protect slides from light by covering slides with aluminum foil.
8. Slides are examined with a fluorescence microscope using appropriate filters.
9. Finally, quantitative analysis of images is performed on a minimum of 30 high-powered fields (hpf) using NIH ImageJ software.

3.6 Evaluation of Cellular and Humoral Immune Responses to Injected Rabbit Anti-GBM Antibodies

1. Evaluate the concentration of injected rabbit anti-GBM antibodies by ELISA (*see Note 11*).
2. Coat 96-well plates overnight at 4 °C with 1 µg/ml F(ab')2 goat anti-rabbit IgG in PBS (100 µl/well).
3. After washing in PBS, block wells with PBS-BSA for 1 h at room temperature (RT).
4. To generate a standard curve, incubate wells with defined concentrations of rabbit IgG (concentration range is determined empirically in preliminary experiments) in PBS-1 % BSA for 1 h at RT.
5. In parallel, add mouse serum samples to test wells (dilution range 1/100 to 1/10,000). Incubate for 1 h at RT.
6. After washing biotinylated donkey-anti-rabbit IgG (1/100) is added 2 h before the addition of streptavidin-HRP (1/200) for 20 min at RT.
7. After a final washing step develop the ELISA by adding 150 µl TMB substrate solution.
8. Stop the reaction with 50 µl 1 N HCl.
9. Determine the OD₄₅₀ of each well using an ELISA plate reader. The concentration of rabbit IgG in mouse serum is interpolated from the standard curve (*see Note 10*).
10. To detect mouse-anti-rabbit IgG that develops in the autologous phase, 96-well plates were coated overnight at 4 °C with rabbit IgG at 1 µg/ml.
11. Block plates with PBS-1 % BSA. Wash once with PBS.
12. Incubate with mouse serum samples (100 µl/well) diluted in PBS-1 % BSA (dilutions evaluated empirically, range of 1/200 to 1/1,000) for 1 h at RT. Wash plates with PBS-1 % BSA.
13. Add biotinylated donkey-anti-mouse IgG and incubate for 2 h at RT. Wash once with PBS-1 % BSA.
14. Add streptavidin-HRP (1/200) and then substrate as above.
15. Determine OD₄₅₀ values with an ELISA plate reader.

3.7 Dermal Delayed-Type Hypersensitivity Responses to Rabbit IgG

1. Challenge mice 13 days after induction of anti-GBM glomerulonephritis by injecting 250 µg purified normal rabbit IgG or control mouse IgG into the right and left hind footpad, respectively (*see Note 12*).
2. After 24 h, measure swelling of right and left footpads using a thickness gauge.
3. The magnitude of the hypersensitivity reaction is the difference in the swelling response between the right and left footpads.

4 Notes

1. Mast cell-deficient mice were bred by mating WB/Re-kit^{W/+} and C57BL6/kit^{W/+} F1 hybrids to obtain mast cell-deficient WBB6F₁/Kit^W/Kit^{W-v} (W/W^v) and wild-type +/+ littermates identified by coat color (W/W^v white; +/+ black). Previously generated mMCP-4 knockout mice [14] in the C57BL/6J background were provided by G. Pejler (Uppsala) and C57/BL/6J mice were used as controls. Mice were housed under strictly controlled pathogen-free conditions at the mouse facilities of IFR02 at the Bichat Medical School. Male mice were used between 8 and 12 weeks of age.
2. Inbred male Wistar rats (Charles River, France) weighing 100–150 g were used for the preparation of glomeruli from kidneys. Rats were housed under strictly controlled pathogen-free conditions at the mouse facilities of IFR02 at the Bichat Medical School.
3. Several sources of rabbit anti-GBM antibody (nephrotoxic serum) have been used for our studies. For initial studies anti-GBM was provided from Tanabe Co., Ltd. (Tokyo, Japan). We also produced our own anti-GBM by immunizing rabbits with preparation of glomeruli from rats. A commercial sheep anti-rat glomeruli (GBM) serum can also be purchased from Probetex Inc (San Antonio, Texas 78229-6020, USA) for the induction of non-accelerated anti-GBM GN. However, at present we have not tested the potential of this antiserum to induce disease in mice.
4. The large tubular fragments are retained on the first two sieve while cells and smaller debris pass through the last sieve. Intact glomeruli are retained on the third mesh (75 µm) sieve.
5. The antibody dose depends on the individual anti-GBM anti-serum and needs to be established in pilot experiments; as mentioned above we also noted strain differences as for example in our hands WBB6F₁ +/+ mice showed higher sensitivity as compared to C57BL/6 mice.
6. Normal (pre-immune) rabbit serum does not induce any apparent renal glomerular disease.
7. All determinations are outsourced to biochemical technological platform at the IFR02 at the Bichat Medical School.
8. The latter ratio is unaffected by urine volume and concentration and usually correlates well with 24-h urine sampling in metabolic cages.
9. High urinary creatinine indicates renal damage.

10. We noticed that levels were higher during the early heterologous phase as compared to the late autologous phase due to catabolism of the exogenous antibody.
11. This assures that equivalent amounts of antibody have been injected.
12. Besides humoral immunity cell-mediated immunity has also been implicated in glomerulonephritis development [15] and can be evaluated by measurement of DTH responses.

References

1. Couser WG (1999) Glomerulonephritis. *Lancet* 353:1509–1515
2. Tang T, Rosenkranz A, Assmann KJ, Goodman MJ, Gutierrez-Ramos JC, Carroll MC, Cotran RS, Mayadas TN (1997) A role for Mac-1 (CD11b/CD18) in immune complex-stimulated neutrophil function in vivo: Mac-1 deficiency abrogates sustained Fc_γ receptor-dependent neutrophil adhesion and complement-dependent proteinuria in acute glomerulonephritis. *J Exp Med* 186:1853–1863
3. Suzuki Y, Shirato I, Okumura K, Ravetch JV, Takai T, Tomino Y, Ra C (1998) Distinct contribution of Fc receptors and angiotensin II-dependent pathways in anti-GBM glomerulonephritis. *Kidney Int* 54:1166–1174
4. Masugi M (1935) Zur Pathogenese der Diffusen Glomerulonephritis als allergischer Erkrankung der Niere. *Klin Wschr* 14(11): 361–400
5. Wilson C (1996) Renal response to glomerular injury, 5th edn. WB Saunders, Philadelphia, pp 1253–1391
6. Unanue ER, Dixon FJ (1967) Experimental glomerulonephritis: immunological events and pathogenetic mechanisms. *Adv Immunol* 6:1–90
7. Blank U, Essig M, Scanduzzi L, Benhamou M, Kanamaru Y (2007) Mast cells and inflammatory kidney disease. *Immunol Rev* 217:79–95
8. Xie C, Rahman ZS, Xie S, Zhu J, Du Y, Qin X, Zhou H, Zhou XJ, Mohan C (2008) Strain distribution pattern of immune nephritis—a follow-up study. *Int Immunol* 20:719–728
9. Xie C, Sharma R, Wang H, Zhou XJ, Mohan C (2004) Strain distribution pattern of suscep-
10. tibility to immune-mediated nephritis. *J Immunol* 172:5047–5055
11. Kanamaru Y, Scanduzzi L, Essig M, Brochetta C, Guerin-Marchand C, Tomino Y, Monteiro RC, Peuchmaur M, Blank U (2006) Mast cell-mediated remodeling and fibrinolytic activity protect against fatal glomerulonephritis. *J Immunol* 176:5607–5615
12. Hochegger K, Siebenhaar F, Vielhauer V, Heininger D, Mayadas TN, Mayer G, Maurer M, Rosenkranz AR (2005) Role of mast cells in experimental anti-glomerular basement membrane glomerulonephritis. *Eur J Immunol* 35:3074–3082
13. Timoshanko JR, Kitching R, Semple TJ, Tipping PG, Holdsworth SR (2006) A pathogenetic role for mast cells in experimental crescentic glomerulonephritis. *J Am Soc Nephrol* 17:150–159
14. Scanduzzi L, Beghdadi W, Daugas E, Abrink M, Tiwari N, Brochetta C, Claver J, Arouche N, Zang X, Pretolani M, Monteiro RC, Pejler G, Blank U (2010) Mouse mast cell protease-4 deteriorates renal function by contributing to inflammation and fibrosis in immune complex-mediated glomerulonephritis. *J Immunol* 185:624–633
15. Tchougounova E, Pejler G, Abrink M (2003) The chymase, mouse mast cell protease 4, constitutes the major chymotrypsin-like activity in peritoneum and ear tissue. A role for mouse mast cell protease 4 in thrombin regulation and fibronectin turnover. *J Exp Med* 198:423–431
16. Kitching AR, Holdsworth SR, Tipping PG (2000) Crescentic glomerulonephritis—a manifestation of a nephritogenic Th1 response? *Histol Histopathol* 15:993–1003

Chapter 30

A Mouse Model of Atopic Dermatitis

Yuko Kawakami and Toshiaki Kawakami

Abstract

Atopic dermatitis (AD) is a chronic or chronically relapsing, pruritic inflammatory skin disease. The incidence of AD has dramatically increased for the past three decades in industrialized countries. We established a highly efficient method to induce AD-like skin lesions using repeated epicutaneous treatments with house dust mite allergen and staphylococcal enterotoxin B (SEB). The dermatitis-induced mice showed increased serum IgE levels that were similar to human AD patients and also treatable with dexamethasone. This mouse AD model has been used in a vaccinia virus infection study. It will also be useful to study pathogenic processes of AD and to evaluate the efficacy of a drug candidate. In this chapter, we describe the detailed method that can induce AD-like skin inflammation in multiple mouse strains.

Key words Atopic dermatitis, Mouse model, Staphylococcal enterotoxin B, House dust mite, NC/Nga, C57BL/6, BALB/c

1 Introduction

The incidence of allergic diseases such as asthma and atopic dermatitis (AD) has been dramatically increasing in industrialized countries for the past three decades. AD is a chronic or chronically relapsing, pruritic inflammatory skin disease [1, 2]. Skin lesions infiltrated by T cells, eosinophils, mast cells, and other cells imply underlying complex immune dysfunctions. The etiology of this disease is multifactorial, and involves complex interactions between genetic and environmental factors. The skin in a pre-AD state has been postulated to have hypersensitivity to environmental triggers, resulting from a defective skin barrier that allows the penetration of allergens and microbial pathogens [3]. The acute phase of AD is characterized by eczematous skin lesions with an infiltration of Th2 cells. The chronic phase is characterized by lichenification of skin and an infiltration of Th1 cells. However, the pathogenic processes of AD seem much more complex than this clear-cut picture and our understanding of this disease is far from complete. Several mouse models of human AD have been developed over the

last decade, and have provided insights into the pathogenesis of human AD [4–10]. For example, an OVA epicutaneous sensitization model mimicked skin lesions of human AD in terms of infiltration of CD3⁺ T cells, eosinophils, and neutrophils and local expression of mRNAs for IL-4, IL-5, and IFN- γ [5]. Differential roles of IL-4, IL-5, and IFN- γ in skin lesion development and leukocyte infiltration in this model were demonstrated using gene-manipulated mice, whereas IgE was not required for skin lesion development in this model [11]. However, some models suffer from low efficiency or unpredictable nature and have not been extensively characterized yet. For example, NC/Nga mice develop AD-like skin lesions under conventional (nonspecific pathogen-free) conditions [4]. However, the incidence of skin lesions in these mice drastically varies from facility to facility (<5 % in our facility). Therefore we still need an animal model that mimics human AD and allows the analysis of disease processes, particularly the involvement of cell types and genes, in a highly reliable and speedy fashion [12, 13]. Using dust mite allergen and bacterial superantigen, we established an accelerated protocol to induce AD-like skin lesions in NC/Nga mice [14], whose skin lesions and high serum IgE levels occurring under conventional (nonspecific pathogen-free) conditions have been extensively shown to be similar to human AD. The same allergen/superantigen topical treatment was more recently found to be applicable to other mouse strains. This is an efficient, accelerated method to induce AD-like skin lesions and to probe into cellular and genetic requirements of the skin lesion development.

2 Materials

2.1 Reagents for Induction of Atopic Dermatitis (AD)

1. Isoflurane (liq.).
2. *Dermatophagoides farinae* extract (Der f) (Greer Laboratories, Lenoir, NC): Prepare at a concentration of 100 μ g/mL in sterile phosphate-buffered saline (PBS). Make aliquots and freeze them for later use.
3. Staphylococcal enterotoxin B (SEB) stock: Prepare at a concentration of 10 μ g/mL in sterile phosphate-buffered saline (PBS). Make aliquots and freeze them for later use.

2.2 Equipment

1. Anesthesia machine (isoflurane).
2. First-Aid gauze pads.
3. Tegaderm™ Transparent Dressing (3M).
4. Nexcare Durable Cloth Tape (3M).
5. Flexible fabric adhesive bandages.
6. Pipetman and autoclaved tips.

3 Methods

Day 1

1. Anesthetize mice with isoflurane.
2. Shave approximately a 3 cm^2 dorsal area at the level of the shoulder blades with an electric shaver.

Day 2

3. Anesthetize mice with isoflurane.
4. Adhere and detach shaved back skin with durable cloth tape to remove the remaining fur. Repeat this tape stripping several times to thoroughly clean the skin of fur.
5. Place a 1 cm^2 square of gauze pad on the area of application. This will serve as the reservoir for the antigens.
6. Pipette 500 ng of SEB in 50 μl of PBS onto the gauze pad.
7. Pipette 10 μg of Der f (house-dust mite antigen) in 100 μl PBS onto the gauze pad.
8. Occlude the gauze and antigens onto the skin using a 2 cm^2 piece of Tegaderm™ transparent dressing, completely covering the gauze. This prevents loss of the antigens due to ingestion or rubbing off.
9. Keep the entire system in place using $8 \times 2 \text{ cm}$ flexible fabric adhesive bandages. Cut one bandage lengthwise down the center. Tightly wrap the mouse with a resulting $8 \times 1 \text{ cm}$ bandage strip, covering the upper half of the underlying dressing. With the other bandage strip, wrap the mouse just below the first strip, covering the lower half of the dressing. Make sure that bandage wrapping is so tight that the mouse does not remove it. The mouse should appear as if dressed in a thoracic “body cast” (Fig. 1). Leave the system in place for 3–4 days.



Fig. 1 NC/Nga mouse under the Der f/SEB treatment

Day 5 or 6

10. Remove the first set of bandages and dressing and replace it with a fresh set to occlude the antigens and gauze for another 3–4 days.

Day 9

11. Remove the dressings and keep the mice without treatment for a week.

Day 16

12. Repeat the procedures of day 2 to day 6 (*see Note 1*).

Day 23

13. Remove all the dressings.

Day 24

14. Anesthetize and shave the mice as on day 1.

Day 25

15. Score skin lesions (Fig. 2) for the severity of *each* of the four parameters: redness, bleeding, eruption, and scaling. Use the following severity scale:

0—no symptoms

1—mild

2—intermediate

3—severe

The total possible score for each mouse is 12 (*see Notes 2 and 3*).

16. The mice are now ready for the further experiments such as infection or evaluation of the efficacy of drugs (*see Note 4*).



Fig. 2 Der f/SEB-induced dermatitis in NC/Nga mice. A representative mouse (*left*) with skin lesions of clinical score of 12 is shown along with a mouse (*right*) with healthy skin

4 Notes

4.1 Repetitive Induction

1. You may repeat one more round of induction when you cannot get high scores. However, too many (>4) repetitive treatments may lead to lower skin scores possibly due to anergy induction.

4.2 Clinical Scoring for AD Mouse Model

2. To obtain reliable results, scoring must be done in a blind fashion. The investigator performing the scoring requires some training and experience to become proficient.
3. Clinical scores widely vary depending on the strain of mice. In the case of NC/Nga mice, more than 90 % of the mice score higher than 7. The average score in C57BL/6 (B6) mice is about 6 but that in BALB/c mice is around 3. If you need to use AD-induced mice for evaluation of efficacy of drug treatment, it is advisable to use NC/Nga or B6 mice, but not BALB/c. If your purpose of the experiment is to find the condition that exacerbates AD, you may want to use BALB/c mice. The NC/Nga mice with clinical score of 7 or higher (or 5+ in B6 mice) can be used for experiments such as infection or testing the efficacy of treatment. See our successful example to establish and characterize a mouse model of eczema vaccinatum [15].
4. The induced skin lesions will disappear after 4 weeks without any treatment. We found that the best timing for virus or bacteria infection on the AD-induced skin is 7–8 days after the last Der f/SEB treatment. To test the efficacy of the treatment drug, start treatment right after the scoring.

References

1. Bieber T (2008) Atopic dermatitis. *N Engl J Med* 358:1483–1494
2. Leung AK, Hon KL, Robson WL (2007) Atopic dermatitis. *Adv Pediatr* 54:241–273
3. Leung DYM (2006) New insights into the complex gene-environment interactions evolving into atopic dermatitis. *J Allergy Clin Immunol* 118:37–39
4. Matsuda H, Watanabe N, Geba GP, Sperl J, Tsudzuki M, Hiroi J, Matsumoto M, Ushio H, Saito S, Askenase PW, Ra C (1997) Development of atopic dermatitis-like skin lesion with IgE hyperproduction in NC/Nga mice. *Int Immunol* 9:461–466
5. Spergel JM, Mizoguchi E, Brewer JP, Martin TR, Bhan AK, Geha RS (1998) Epicutaneous sensitization with protein antigen induces localized allergic dermatitis and hyperresponsiveness to methacholine after single exposure to aerosolized antigen in mice. *J Clin Invest* 101:1614–1622
6. Chan LS, Robinson N, Xu L (2001) Expression of interleukin-4 in the epidermis of transgenic mice results in a pruritic inflammatory skin disease: an experimental animal model to study atopic dermatitis. *J Invest Dermatol* 117:977–983
7. Yamanaka K, Tanaka M, Tsutsui H, Kupper TS, Asahi K, Okamura H, Nakanishi K, Suzuki M, Kayagaki N, Black RA, Miller DK, Nakashima K, Shimizu M, Mizutani H (2000) Skin-specific caspase-1-transgenic mice show cutaneous apoptosis and pre-endotoxin shock condition with a high serum level of IL-18. *J Immunol* 165:997–1003

8. Konishi H, Tsutsui H, Murakami T, Yumikura-Futatsugi S, Yamanaka K, Tanaka M, Iwakura Y, Suzuki N, Takeda K, Akira S, Nakanishi K, Mizutani H (2002) IL-18 contributes to the spontaneous development of atopic dermatitis-like inflammatory skin lesion independently of IgE/stat6 under specific pathogen-free conditions. *Proc Natl Acad Sci U S A* 99: 11340–11345
9. Klement JF, Rice NR, Car BD, Abbondanzo SJ, Powers GD, Bhatt PH, Chen CH, Rosen CA, Stewart CL (1996) IkappaBalpha deficiency results in a sustained NF-kappaB response and severe widespread dermatitis in mice. *Mol Cell Biol* 16:2341–2349
10. Barton D, HogenEsch H, Weih F (2000) Mice lacking the transcription factor RelB develop T cell-dependent skin lesions similar to human atopic dermatitis. *Eur J Immunol* 30: 2323–2332
11. Spergel JM, Mizoguchi E, Oettgen H, Bhan AK, Geha RS (1999) Roles of TH1 and TH2 cytokines in a murine model of allergic dermatitis. *J Clin Invest* 103:1103–1111
12. Kawakami T, Ando T, Kimura M, Wilson BS, Kawakami Y (2009) Mast cells in atopic dermatitis. *Curr Opin Immunol* 21:666–678
13. Jin H, He R, Oyoshi M, Geha RS (2009) Animal models of atopic dermatitis. *J Invest Dermatol* 129:31–40
14. Kawakami Y, Yumoto K, Kawakami T (2007) An improved mouse model of atopic dermatitis and suppression of skin lesions by an inhibitor of tec family kinases. *Allergol Int* 56:403–409
15. Kawakami Y, Tomimori Y, Yumoto K, Hasegawa S, Ando T, Tagaya Y, Crotty S, Kawakami T (2009) Inhibition of NK cell activity by IL-17 allows vaccinia virus to induce severe skin lesions in a mouse model of eczema vaccinatum. *J Exp Med* 206:1219–1225

Chapter 31

Mouse Models of Allergic Asthma

Matthew Gold, David Marsolais, and Marie-Renee Blanchet

Abstract

In the last 20 years, the development of murine models of allergic asthma has provided researchers with a means to explore the mechanisms of this T-helper type 2 (Th2)-driven inflammatory disease. While systemic sensitization and airway challenge with ovalbumin has been the most widely used model, recent emphasis has been placed on the development of models using more naturally occurring antigens. However, the diversity of models currently available makes it hard for investigators new to this field to choose to use the most effective and appropriate model to test their hypothesis. Here we describe three different mouse models of allergic asthma, including the classical ovalbumin model, a modified ovalbumin model that has been shown to be mast-cell dependent, as well as a house dust mite antigen-induced model. We also discuss briefly their characterization and differences, in the aim to facilitate the choice of the appropriate model when working on this intricate Th2 inflammatory disease.

Key words Asthma, Mouse, Ovalbumin, House dust mite, Bronchoalveolar lavage, Inflammation, Intranasal

1 Introduction

Asthma is an inflammatory disease characterized by airway inflammation, airway hyperresponsiveness, and remodelling (reviewed in Barnes [1]). The complex pathophysiology of this disease (including important contributions from various inflammatory cell types such as eosinophils [2–5], lymphocytes [6], and mast cells [7, 8]) leads to an urgent need in the development of mouse models of allergic asthma. In the early 1990s, the first attempts to mimic the allergic reaction leading to airway inflammation and responsiveness were made using IgE receptor cross-linking techniques [9, 10], quickly followed by models using allergens which are still used nowadays, such as the ovalbumin (OVA) mouse model of asthma [11]. In these models, mice are actively immunized against various proteins (such as ovalbumin) using the parallel administration of adjuvant such as alum or Al(OH)_3 .

As our understanding of the pathogenesis of asthma improved, it became obvious that there was a need to alter these models to allow their use in the study of the complex mechanisms leading to the development of asthma. Therefore, various versions of these models made their appearance in the literature. Here, we discuss the two most used mouse models of asthma: the OVA model of asthma and the house dust mite (HDM) model of asthma. We will try to elucidate the differences between these models, and discuss the role of mast cells in their development.

1.1 Ovalbumin-Induced Allergic Asthma Model

In the mouse model of OVA-induced asthma, active sensitization is achieved either by concurrent administration of Al(OH)_3 as an adjuvant or via repetitive exposure to low doses of ovalbumin [8]. In the case of the use of Al(OH)_3 , a second administration of OVA coupled to the adjuvant is needed to achieve a degree of sensitization which will ensure the development of the inflammatory reaction in response to the airway challenges with OVA. When trying to induce an asthmatic-like airway inflammatory response without adjuvant, the sensitization period comprises repetitive exposure to small doses of OVA (either intraperitoneally or via the airways), followed by a period of time where mice are not exposed to the protein. Then, independently of the use of adjuvant, mice are challenged via the airways using either aerosolized or intranasal administration of ovalbumin to develop pulmonary eosinophilia, a major hallmark of the inflammatory asthmatic response. Of interest is the fact that as long as the sensitization and challenge steps are respected and that 7 days are allowed for the formation of antibodies against ovalbumin (sensitization period), the timing of the challenge period can vary [12, 13].

However, it is important to note here that the use of adjuvant has been reported to induce a mast cell-independent form of airway inflammation in the mouse model of asthma, led mostly by a strong lymphocyte-driven induced Th2 inflammation and eosinophilia. Models not using an adjuvant, such as Al(OH)_3 , are reportedly dependant on the presence of mast cells for the development of airway inflammation [8, 14–16]. Of importance is the fact that independently of the use of adjuvant, airway hyper-responsiveness was shown to be strongly dependant on the presence of mast cells.

However, these two models (with and without adjuvant) are not recognized to induce airway remodelling, which is an important hallmark of asthma and is closely related to the development of airway hyper-responsiveness in humans (reviewed in Barnes [1]). In order to induce remodelling of the airways, mice need chronic post-sensitization low-intensity exposure to OVA (over 8–12 weeks) [17, 18]. Although the level of airway inflammation after 12 weeks is lower than what is observed with the acute models, collagen deposition, basement membrane thickening, as well as alterations in the pulmonary function are observed in these mice.

1.2 House Dust Mite Mouse Model of Asthma

As the OVA mouse model of asthma grew in popularity, so did the criticizing of its strengths and limits. The main criticism of the OVA mouse model of asthma is the use of a normally nonantigenic protein, and the development of an artificial immune response to this protein via the use of adjuvant. The need for a model using a “natural antigen” (i.e., found in the environment of asthmatic patients), which would cause an asthmatic-like response in mice without the use of adjuvant, became quickly obvious. Also, there was a lot of pressure towards developing a model that would use a natural route of exposure to the allergens (i.e., via the airways, compared to intraperitoneal sensitization in the mouse model of OVA).

As a result, the house dust mite (HDM) model of asthma was originally characterized in 1996 [19], and well described recently by Cates et al. [20]. The latest studies report that administration of HDM extract once a day for 10 days causes an asthmatic response characterized by increased IgE, airway and parenchymal eosinophilia, a Th2 cytokine response, as well as the development of an increased response to methylcholine as a measure of airway hyper-responsiveness.

The exact antigenic epitopes of the HDM extract are yet to be fully characterized; however, the fact that sensitization to HDM can be achieved via a natural route of delivery is likely due to the intrinsic protease activity of the antigenic preparation [21, 22], creating a breach in the epithelial barrier and the subsequent activation of airway antigen-presenting cells. So far, there is no solid proof in the literature of the involvement of mast cells in the development of the asthmatic response in this model; however, the high levels of IgE, histamine, and airway hyper-responsiveness (which is known to be dependant of mast cells independently of the use of adjuvant) all indicate that mast cells are likely to play a major role in the development of the asthma-like response in this disease.

In this chapter, we describe the material and methods necessary to develop these two major mouse models of asthma (OVA and HDM), and the methods used to assess airway inflammation in both models.

2 Materials

2.1 Ovalbumin (OVA)-Induced Allergic Asthma

1. C57BL/6J mice (minimum of 6 weeks old at the start of experiment and age and sex matched): All animal experiments must be conducted according to your institution guidelines (*see Notes 1 and 2*).
2. Albumin from chicken egg white, grade III or higher (*see Note 3*).
3. Imject Alum adjuvant (Thermo Scientific, 40 mg/mL aluminum hydroxide and 40 mg/mL magnesium hydroxide).

4. Phosphate-buffered saline (PBS).
5. 1 mL tuberculin syringes.
6. 26–28G needles.
7. Isoflurane (Abbott Laboratories).

2.2 House Dust Mite (HDM)-Induced Allergic Asthma

1. House dust mite lyophilized extract, *Dermatophagoides pteronyssinus* (Greer Labs), resuspended to 2.5 mg/mL in sterile PBS (see Note 4).

2.3 Assessment of Airway Inflammation

1. Avertin: Dissolve 10 g of 2,2,2-tribromoethanol with 10 mL of *tert*-amyl alcohol for a stock solution. Prior to use, dilute stock solution 1:40 with PBS, adding stock solution dropwise in PBS that is at 37 °C with constant stirring to avoid formation of a precipitate. Store both solutions at 4 °C protected from light (see Note 5).
2. Surgical scissors and forceps.
3. 70 % ethanol (EtOH).
4. Catheters, 22G (BD Insite) (see Note 6).
5. Suture thread.
6. 1 mL tuberculin syringe.
7. PBS.
8. 15 mL conical tubes.
9. 10 % neutral buffered formalin.
10. Red cell lysis buffer: 150 mM NH₄Cl, 10 mM KHCO₃, 0.1 mM EDTA (pH 7.3).
11. Hemocytometer.
12. 0.4 % Trypan blue solution in PBS.
13. Microscope slides.
14. Shandon Filter Cards (Thermo Scientific).
15. Cytospin 4 Cytocentrifuge (Thermo Scientific).
16. Wright-Giemsa stain:
 - (a) Fixative (100 % MeOH).
 - (b) Solution I: PROTOCOL HEMA-3 (Fisher Scientific).
 - (c) Solution II: PROTOCOL HEMA-3 (Fisher Scientific).
17. Permount mounting medium.

2.4 Enumeration and Differentiation of BALF Leukocytes

1. Flow cytometry buffer: 2 % FBS, 2 mM EDTA, 0.05 % sodium azide in PBS.
2. 96-Well V-bottom plates.
3. Latex counting beads (Invitrogen, cat #: C37259, 10 µm, approximately 1 × 10⁸ beads/mL).

4. Normal goat serum.
5. Purified anti-CD16/32 antibody (clone 2.4G2).
6. Fluorochrome-conjugated antibodies:
 - (a) FITC anti-7/4.
 - (b) PE anti-Siglec-F.
 - (c) PE-Cy7 anti-CD3e.
 - (d) APC anti-CD11c.
 - (e) Pacific Blue anti-CD45.
 - (f) APC-Cy7 anti-B220/CD45R.

2.5 Lung Cell Isolation for Leukocyte Differentiation

1. Dulbecco's modified eagle medium (DMEM).
2. Fetal bovine serum (FBS).
3. 100× penicillin/streptomycin.
4. 12-Well tissue-culture plate.
5. Collagenase, type IV.
6. 70 μ m cell strainer.
7. 10 mL pipette.
8. 3 mL syringe.
9. 50 mL conical tube.
10. Red cell lysis buffer: 150 mM NH₄Cl, 10 mM KHCO₃, 0.1 mM EDTA, pH 7.3.
11. Percoll.
12. 10× Hanks' balanced salt solution (HBSS).

2.6 Lung Inflation and Fixation for Histology

1. 30 mL Luer-Lok syringe.
2. 18 gauge (18G) needle.
3. 250 mL volume Erlenmeyer Filter Flask (Büchner flask).
4. 10 mL polystyrene serological pipet.
5. Male Luers (Bio-Rad).
6. Female-to-Female Luer (Bio-Rad).
7. Tubing, 1.6 mm internal diameter (ID) (Bio-Rad).

3 Methods

3.1 OVA/Alum Model Disease Induction

1. Dilute OVA in PBS to make a 4 mg/mL solution.
2. Shake the inject alum solution well before use. Dilute the 4 mg/mL OVA solution 1:1 with the alum for a final OVA concentration of 2 mg/mL.
3. Mix the OVA/alum mixture for 30 min at RT in order for the alum to effectively adsorb the OVA antigen.

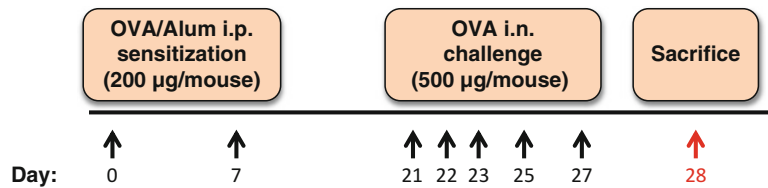


Fig. 1 Mast cell-*independent* OVA/alum model of allergic asthma. The “traditional” allergic asthma model requires systemic sensitization by intraperitoneal (i.p.) administration of 200 µg ovalbumin (OVA) complexed with alum adjuvant (per mouse) at day 0 and day 7. Two weeks later, mice are lightly anesthetized and then challenged with OVA (500 µg/mouse) delivered in a small volume (~40–50 µL) through the nares (intranasal, i.n.) using the dose schedule shown. On day 28, 1 day after the final i.n. OVA challenge, mice are sacrificed for analysis or otherwise treated experimentally

4. Immunize mice intraperitoneally on days 0 and 7 with 100 µL of the OVA/alum mixture using a 1 mL syringe and 26G needle (Fig. 1).
5. For intranasal challenges on days 21, 22, 23, 25, and 27, dilute OVA in PBS to make a 10 mg/mL solution (*see Note 7*) (Fig. 1).
6. Anesthetize mice until breathing rate reduces to approximately 1 per second (oxygen 1.5 L/min with 3.5 % isoflurane).
7. Once mice are appropriately sedated, intranasally administer 50 µL of 10 mg/mL OVA solution, adding dropwise through the nares (*see Notes 8 and 9*).
8. Monitor the mice until they recover from anesthesia (approximately 5 min).

3.2 Adjuvant-Free OVA Model Disease Induction

1. Dilute OVA in PBS to make a 100 µg/mL solution.
2. Immunize mice intraperitoneally on days 0, 2, 4, 6, 8, 10, and 12 with 100 µL of OVA solution (10 µg OVA/mouse) (Fig. 2).
3. For intranasal challenges on days 40, 43, and 46, dilute OVA in PBS to make a 4 mg/mL solution (Fig. 2).
4. Anesthetize mice until breathing rate reduces to approximately 1 per second (oxygen 1.5 L/min with 3.5 % isoflurane).
5. Once mice are appropriately sedated, intranasally administer 50 µL of 4 mg/mL OVA solution, adding dropwise through the nares.
6. Monitor the mice until they recover from anesthesia (approximately 5 min).

3.3 House Dust Mite Model Disease Induction

1. Reconstitute lyophilized house dust mite extract to a stock concentration of 2.5 mg/mL in PBS.
2. For HDM challenges on days 0, 1, and 2, dilute stock HDM solution to 2 mg/mL in PBS, and intranasally administer 50 µL dropwise through the nares (Fig. 3).

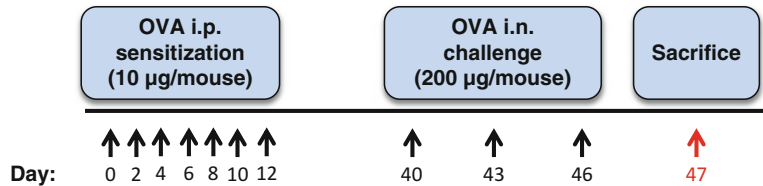


Fig. 2 Mast cell-dependent OVA model of allergic asthma. By excluding the alum adjuvant and altering the OVA-sensitization schedule, the OVA allergic asthma model can be rendered mast cell dependent. In this experimental mode, mice are systemically sensitized by intraperitoneal (i.p.) administration of 10 µg ovalbumin (OVA) every 2 days for a total of seven treatments as shown. Four weeks later (day 40), mice are lightly anesthetized and then challenged with OVA (200 µg/mouse) delivered in a small volume (~40–50 µL) through the nares (intranasal, i.n.) using the dose schedule shown. On day 47, 1 day after the final i.n. OVA challenge, mice are sacrificed for analysis or otherwise treated experimentally. The OVA sensitization and challenge doses and the depicted administration schedule were adapted from Nakae et al. [8]

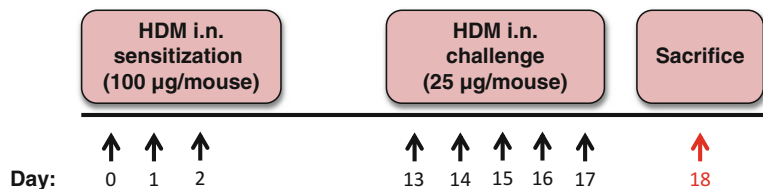


Fig. 3 House dust mite (HDM) model of allergic asthma. House dust mite (HDM) antigen (*Dermatophagoides pteronyssinus*, Der p) prepared in PBS is administered HDM (100 µg/mouse) through the nares (i.n.) of lightly anesthetized mice daily for the first 3 days. Starting on day 13, mice are treated daily with 25 µg/mouse HDM antigen (i.n.). One day after the fifth and final HDM dose, mice are sacrificed for analysis or otherwise treated experimentally. The HDM sensitization and challenge doses and the depicted administration schedule were adapted from Phipps et al. [23]

3. For HDM challenges on days 13–17, dilute stock HDM solution to 500 µg/mL in PBS and intranasally administer 50 µL dropwise through the nares (Fig. 3).

1. Anesthetize mice with avertin (500 µL injected intraperitoneally per 20 g body weight).
2. Place mice ventral side up and pin down forepaws and hindpaws.
3. Using scissors and forceps, remove skin above the neck area. Carefully pull the parotid and submaxillary gland laterally, taking care not to rupture the jugular vein.
4. Upon visualization of the trachea, remove the muscle layer surrounding it, and then make a pinhole partial cut of the trachea just inferior of the larynx and thyroid. Carefully insert

3.4 Collection of Bronchoalveolar Lavage Fluid (BALF) and Lung Specimens

the flexible 22G catheter into the trachea, using the suture thread to secure the catheter.

5. Prepare three 1 mL slip-tip syringes and fill them each with 1 mL of PBS. Lavage the lungs three times with 1 mL of PBS, slowly advancing and recovering the PBS lavage liquid. Pool the collected lavages into a 15 mL conical tube and store on ice until further use (*see Notes 10 and 11*).
6. *Important:* For improved lung histology morphometry, *skip steps 6 and 7* and continue with Subheading 3.5 for lung inflation and fixation.
7. After collecting the BAL, dissect open the thoracic cavity, exposing the left lung and the four lobes of the right lung (superior, middle, inferior, and postcaval).
8. Dissect out some lung specimens for histology, and place in 10 volumes of 10 % buffered formalin. Store specimens at 4 °C for 24 h, and then replace the formalin with 70 % EtOH for long-term storage at 4 °C before paraffin embedding and histology.

3.5 Lung Inflation and Fixation for Histology

1. Before sacrificing mice, assemble apparatus for lung inflations.
 - (a) In a 250 mL Erlenmeyer filter flask, add distilled H₂O until it is about two-thirds full.
 - (b) Take a 10 mL pipette, remove the cotton plug, using a black rubber plug on top of the filter flask, and insert the pipette into the flask until the tip is a few centimeters below the water line.
 - (c) Using a ruler, measure 20 and 25 cm from the top of the water line towards the top of the pipette. Mark the level with a felt pen.
 - (d) Pierce a 30 mL syringe with an 18G needle at around the 10 mL mark. Bond the needle to the syringe with an epoxy or other adhesive, making sure to produce an airtight seal.
 - (e) Connect the hose barb on the side of the flask to the 1.6 mm ID tubing and then add a male-luer adaptor to the end of the tubing in order to connect it to the syringe side port. It will be necessary to step down from the wide tubing connected to the hose barb protruding from the flask to the thinner tubing. Use a female-to-female luer connected to the original tubing and then use a male luer with a 1.6 mm barb to connect to the small-diameter tubing.
2. Once apparatus is assembled, sacrifice mice as mentioned in Subheading 3.5.
3. After collecting the BAL, fill up the 30 mL syringe with 10 % formalin (there should be a fair amount of air in the syringe).

Connect the tip of the syringe to the catheter in the trachea, and connect the tubing from the filter flask to the side port of the syringe.

4. Instill formalin into the lungs until the water inside the filter flask reaches the 25 cm mark on the pipette (indicating a pressure of 25 cm H₂O).
5. Tie off the trachea with the suture thread and remove the catheter.
6. Dissect out the lung and trachea en bloc being careful not to puncture the lung, and place in a 50 mL tube with more 10 % formalin to fix overnight at 4 °C.

3.6 Enumeration and Differentiation of BALF Leukocytes

1. Record collected BALF volume and then spin down at 453×*g* for 5 min.
2. Resuspend cell pellet in 1 mL of red cell lysis buffer, incubate for 3–5 min, then dilute with PBS, and spin down at 453×*g* for 5 min.
3. Resuspend cell pellet in 1 mL of PBS or media. Collect aliquot of cells for dilution with trypan blue and enumeration on hemocytometer.
4. Prepare aliquots of cells for cytocentrifugation. Dilute aliquots to 5.0–7.5×10⁵ cells/mL, and cytocentrifuge 100 µL of cell dilutions to each slide for 3 min at 55–60×*g* (approximately 50,000–75,000 cells/slide, *see Note 12*).
5. Allow slides to dry for 2 h to overnight, before staining.
6. Insert slides for 30 s each into 100 % MeOH, solution I and solution II of the PROTOCOL HEMA-3 staining set. Allow excess MeOH/stain to drip down in between solutions.
7. Allow slides to air-dry, and then, if desired mount with cover slip using Permount.
8. Perform differential cell counts from a minimum of 400 cells/slide using standard morphological criteria of macrophages, lymphocytes, neutrophils, and eosinophils (*see Table 1* and *Note 13*).

3.7 BALF Leukocyte Cell Population Analysis by Flow Cytometry

1. Record collected BALF volume. Spin down at 453×*g* for 5 min.
2. Resuspend cell pellet in 1 mL of FACS buffer, and aliquot 200 µL into a well of a 96-well v-bottom plate. Pool some of the remaining cells and aliquot into seven individual wells for the single-stained controls needed for FACS setup.
3. Spin down cells for 3 min at 453×*g*, aspirate supernatant, and resuspend cells in 50 µL of blocking buffer (FACS buffer with 10 % goat serum and 5 µg/mL anti-CD16/32 to block Fc receptors, *see Note 14*).

Table 1
Morphological criteria of HEMA-3-stained leukocyte lineages from BALF

Cell type	Color of nucleus	Color of cytoplasm	Color of granules	Nucleus morphometry
Macrophages	Violet	Sky blue	No granules	Round, indented, or kidney shaped
Lymphocytes	Violet	Sky blue	No granules	Round, occupies majority of cells with narrow ring of cytoplasm
Neutrophils	Dark blue	Pale pink	Reddish-lilac	Multilobed connected by thin strands
Eosinophils	Blue	Blue	Red/red-orange	Segmented, usually two lobes

4. Incubate cells for 20 min at 4 °C, then spin down cells at $453 \times g$ for 5 min, and aspirate supernatant.
5. In FACS buffer, make up antibody mix containing fluorochrome-conjugated antibodies to 7/4, Siglec-F, CD3e, CD11c, CD45, and B220/CD45R. In addition, make up dilutions of each antibody individually for single-stained controls (*see Note 15*).
6. Add 50 µL of antibody mix or single-stained controls to the appropriate samples. Incubate samples protected from light at 4 °C for 20 min.
7. Add 150 µL of FACS buffer to each well, spin down cells at $453 \times g$ for 5 min, and aspirate supernatant.
8. Wash samples one more time with 200 µL of FACS buffer, then spin down cells at $453 \times g$ for 5 min, and aspirate supernatant.
9. Dilute latex beads 1:100 in FACS buffer to obtain a bead concentration of 1×10^6 beads/mL (*see Notes 16 and 17*).
10. Resuspend samples in 100 µL of diluted beads and resuspend single-stained controls in 100 µL of FACS buffer. Acquire samples on BD LSRII cytometer using FACS Diva software. Ensure that you can differentiate between leukocyte and bead populations on the FSC vs. SSC graph (*see Note 18*).
11. Analyze results using FlowJo software. On FSC vs. SSC graph, gate the beads and leukocyte populations. Using the count function of the analysis software, enumerate the events in both populations and quantitate the total number of cells using the following formula:
 - (a) Number of leukocytes counted \times (number of beads loaded \div number of beads counted) \times dilution factor: In this example, the dilution factor is 5 (200 µL of BALF cells were used out of a total volume of 1 mL, i.e., 1/5th of total BALF cells were used).

Table 2
Cell surface antigen profile of leukocyte lineages in BALF and lung tissue

Lineage	Cell surface antigen profile
Alveolar macrophages	CD11c ⁺ , Siglec-F ⁺ , auto-fluorescence ^{hi}
Dendritic cells	CD11c ^{+/lo} , Siglec-F ⁻ , auto-fluorescence ^{neg}
Eosinophils	Siglec-F ⁺ , CD11c ⁻
Neutrophils	7/4 ⁺
T-cells	CD3e ⁺ , B220 ⁻
B-cells	B220 ⁺ , CD3e ⁻

3.8 Lung Leukocyte Isolation for Flow Cytometry

(b) Determine the number of BALF cells/mL by dividing the total number of cells by the recorded BALF volume collected.

12. Using the FlowJo FACS analysis software, determine the different leukocyte populations based on their surface staining markers (*see Table 2 and Notes 19 and 20*).

1. Lung lobes can be stored in culture media on ice in a 12-well tissue culture plate during animal harvest.
 - (a) Culture media (DMEM with 2–10 % FBS, 100 IU/mL penicillin, 100 µg/mL streptomycin, *see Note 21*).
2. After animal harvest, aspirate culture media from each well and mince lungs with scissors into small pieces (roughly 1 mm³).
3. Add 2 mL of collagenase solution to each well, and incubate for 30–120 min at 37 °C (200 U/mL of collagenase, type IV, diluted in culture media, *see Note 22*).
4. After digestion, collect digested lung tissue and media with a 10 mL pipette and transfer to a 70 µm cell strainer on top of a 50 mL conical tube. Pass tissue pieces through strainer using the plunger end of a 3 mL syringe. Wash cells through strainer using extra culture media.
5. Spin down cells for 5 min at 453 $\times g$.
6. Aspirate supernatant, resuspend cells in 3 mL of red cell lysis buffer, incubate at 37 °C for 5 min, then dilute with 10 mL of PBS or culture media, and spin down cells for 5 min at 453 $\times g$.
7. Make up 30 % Percoll solution.
 - (a) Dilute stock Percoll 9:1 with 10 \times HBSS to obtain a 90 % Percoll solution with a balanced salt concentration.
 - (b) Dilute 90 % Percoll solution with culture media to make a 30 % Percoll solution.

8. Aspirate supernatant from cells, resuspend cells in 3–5 mL of 30 % Percoll, and spin down cells for 10 min at $290 \times g$ with the brake turns off (see Note 23).
9. Aspirate supernatant, resuspend purified leukocytes in 1 mL of culture media, and proceed for any downstream application.
 - (a) Isolated cells can be diluted with trypan blue and counted on a hemocytometer to obtain total lung leukocyte counts and cytospun for differentials, following the same protocol for BALF leukocytes in Subheading 3.6.
 - (b) Isolated cells can be enumerated and differentiated by FACS as in Subheading 3.7.
 - (c) Isolated cells can be utilized for in vitro antigen re-stimulation cultures. Plate 1×10^6 to 8×10^6 cells/mL of isolated lung cells in culture media into tissue-culture-treated plates containing various amounts of antigen (1–100 $\mu\text{g}/\text{mL}$ of OVA or HDM) and place in 37 °C TC-incubator for 24–96 h. Collect cell-free supernatant after incubation for cytokine analysis by ELISA (see Note 24).

3.9 Lung Specimen Histopathology

1. Paraffin-embed lung specimens, section 3–6 μm thick, and then stain with H&E.
2. Under microscopic examination, score disease severity based on the following criteria (Table 3A–C). Score four to five airway sections per mouse for each criterion and take the average of the sum for a final score. Therefore maximum possible score is 12.

4 Notes

1. Most methods mentioned above are tailored for mice on the C57Bl/6J background. Due to the increased Th2 bias of the immune response in other inbred strains (Balb/cJ or 129S1/SvImJ for example) it would be advisable to titrate down the antigen concentration for both the OVA and HDM asthma models.
2. It is important to use only age- and sex-matched mice for all asthma experiments due to the reported sex differences in asthma susceptibility in mice [24, 25].
3. It is important to keep the stock OVA and aluminum hydroxide sterile; only open inside a biosafety cabinet. We also notice that the aluminum hydroxide tends to lose potency after a while and we discard unused adjuvant 1 year after opening.
4. Reconstituted house dust mite extract should be kept at 4 °C for use within 1 month. HDM extract can be reconstituted

Table 3
Infiltration

Score	Criteria (appearance of tissue section, H&E stain)
A. Perivascular infiltration	
0	No cells
1	A few cells
2	Entire encirclement of vessel with infiltrate 1–2 cells deep
3	Entire encirclement of vessel with infiltrate 3–5 cells deep
4	Entire encirclement of vessel with infiltrate >5 cells deep
B. Peribronchiolar infiltration	
0	No cells
1	A few cells
2	Entire encirclement of bronchiole with infiltrate 1–2 cells deep, slight loss of uniformity of airway epithelium
3	Entire encirclement of bronchiole with infiltrate 3–5 cells deep, with a more pronounced hyperplasia and metaplasia of the airway epithelium
4	Entire encirclement of vessel with infiltrate >5 cells deep, complete loss of airway epithelial structure including tissue damage leading to rupture of the bronchiole
C. Parenchymal infiltration	
0	No cells
1	A few scattered cells throughout the lung
2	One quadrant of the lung with a high degree of infiltration
3	Two quadrants of the lung with a high degree of infiltration
4	More than two quadrants of the lung with a high degree of infiltration

and aliquoted for long-term storage at -20°C , but thawed aliquots should not be refrozen. Make note of the Certificate of Analysis values for Derp1 and endotoxin as there is sometimes considerable batch-to-batch variation. Endotoxin should be less than 100 EU per mg of protein; significantly higher endotoxin contamination will result in a model more similar to LPS-induced acute lung injury and will not induce a Th2 response.

5. Use only anesthetics approved by your local animal care committees. Anesthetics such as a combination of ketamine and xylazine can be used in place of avertin.
6. It is important to have a tight seal with the catheter inside the trachea. For 6–8-week-old C57Bl/6 mice a 22G catheter

works well; for older and larger mice a lower gauge catheter, such as an 18G, would be recommended.

7. The OVA dosage for immunizations and challenges has been modified for use with C57Bl/6 mice that are more Th1 biased than other strains. When utilizing Th2-biased strains such as Balb/c or 129/Sv it would be advisable to titre down the dosage of OVA and/or alum. Additionally, we have found that irradiated mice from bone marrow transplantations develop more severe disease symptoms and the amount of OVA and/or adjuvant should be titrated down accordingly.
8. For intranasal challenges, the volume of solution administered can be modified but should not exceed 50 μ L.
9. For intranasal administration, it is imperative to treat the mice at the optimal sedation point. We normally find this to be when the mice have a breathing rate of one breath every second.
10. To avoid the entrance of blood in the BAL, avoid performing cardiac punctures until after the collection of the BAL. After collection of the BAL, a cardiac puncture can be performed with a 1 mL syringe and 25G needle. Collected blood can then be allowed to clot and serum collected for measurement of serum antibodies (i.e., IgE and IgG₁) or cytokines.
11. If interested in measuring cytokines or protein in the BAL fluid (BALF) it is advised to collect the first lavage in a small volume of PBS (i.e., 0.5 mL) and collected into a 1.5 mL microfuge tube. Follow this with two subsequent instillations of 1 mL that are pooled into a 15 mL conical tube. Spin down the microfuge tube and collect the supernatant noting its volume. Resuspend the pellet in an equal volume of PBS and pool with the other two washes. Freeze the BALF immediately for downstream ELISA measurements.
12. It is important to normalize the number of cells cytospun onto the glass slides. Too high a cell density makes it difficult to accurately differentiate and count the leukocytes, whereas too low a density will slow the counting on 400 individual events.
13. Accurately performing differential cell counts visually from stained cytopsins can take a fair amount of training and cannot identify between different myeloid or lymphoid populations (i.e., macrophages and dendritic cells or T-cells, B-cells, and NK-cells). Performing differentials using flow cytometry, as in Subheading 3.7 or as performed by van Rijt et al. [26], allows for rapid, accurate, and reproducible differentials between different researchers or research sites.
14. The use of V-bottom plates makes it easier to identify the cell pellet and remove the supernatant. For larger sample sizes, after centrifugation plates can be inverted and carefully “flicked” to remove supernatant rather than aspirating individual

wells. Check for cell pellets before and after to ensure no loss of cells during this procedure.

15. This protocol is optimized for a BD LSRII cytometer equipped with 405, 488, and 633 nm excitation lasers. The fluorochromes and antibodies listed are suggested and can be modified depending on the instrumentation available. For example, CD19 can easily be substituted for B220 in order to mark B-cells depending on antibodies available. If FACS detectors are at a premium, CD45 can be omitted and CD3e and B220 antibodies can be used conjugated to the same fluorochrome, as in the protocol by van Rijt et al. [26], reducing the number of different fluorochromes to four from six. Conversely, other antibodies can be added, such as NK1.1, to differentiate NK- and NKT-cells from other lymphocytes, and CD4 and CD8 to differentiate the different T-cell subsets, depending on available detectors on the accessible cytometers.
16. After diluting latex beads, remove aliquot and confirm bead concentration using a hemocytometer.
17. We find that the use of a viability marker, such as propidium iodide (PI), helps clean up the FACS results if there are unused detectors. If using PI, dilute latex beads in FACS buffer containing PI and add to cells. Allow cells to sit for 5–10 min protected from light at RT and then analyze on a flow cytometer. The PI stain needs to be with the cells during acquisition; *do not* wash PI out after staining.
18. When acquiring samples, setting FSC to linear scale and SSC to log scale will make it easier to differentiate between cell and bead populations.
19. Alveolar macrophages are highly autofluorescent and can bleed into several FACS channels. It is advised to gate them on their autofluorescent properties and expression of both CD11c and Siglec-F, and then remove them from the population for the analysis of other leukocyte subsets.
20. It should be noted that the staining parameters provide a rough differential. For instance, there are multiple different dendritic cell subsets present in the inflamed alveolar space or lung. Additional markers, such as CD11b and CD103, can also be used to further classify the infiltrating leukocyte cells.
21. IMDM and RPMI can be substituted for DMEM. In addition, media can be supplemented with HEPES (25 mM final concentration) to buffer pH.
22. This isolation protocol is tailored for isolation of leukocyte cells from lung tissue (approximately >95 % CD45⁺). If endothelial or epithelial cells are also desired, dispase should be added to the collagenase solution (to a concentration of 1.5–3.0 mg/mL), and the Percoll step should be omitted.

23. If aiming to isolate both leukocytes, endothelial cells and epithelial cells, omit the Percoll step and instead add dispase and/or DNase into the digestion mixture along with collagenase. Samples may need to be passed through another 40 or 70 μ m cell strainer to obtain a single-cell suspension before downstream applications.
24. If interested in culturing isolated lung cells, perform **steps 4–9** in a biosafety cabinet to maintain a sterile work environment.

References

1. Barnes PJ (2008) Immunology of asthma and chronic obstructive pulmonary disease. *Nat Rev Immunol* 8:183–192. doi:[10.1038/nri2254](https://doi.org/10.1038/nri2254)
2. Lee JJ et al (2004) Defining a link with asthma in mice congenitally deficient in eosinophils. *Science* 305:1773–1776. doi:[10.1126/science.1099472](https://doi.org/10.1126/science.1099472)
3. Fulkerson PC et al (2006) A central regulatory role for eosinophils and the eotaxin/CCR3 axis in chronic experimental allergic airway inflammation. *Proc Natl Acad Sci U S A* 103:16418–16423. doi:[10.1073/pnas.0607863103](https://doi.org/10.1073/pnas.0607863103)
4. Walsh ER et al (2008) Strain-specific requirement for eosinophils in the recruitment of T cells to the lung during the development of allergic asthma. *J Exp Med* 205:1285–1292. doi:[10.1084/jem.20071836](https://doi.org/10.1084/jem.20071836)
5. Fattouh R et al (2011) Eosinophils are dispensable for allergic remodeling and immunity in a model of house dust mite-induced airway disease. *Am J Respir Crit Care Med* 183:179–188. doi:[10.1164/rccm.200905-0736OC](https://doi.org/10.1164/rccm.200905-0736OC)
6. Corry DB et al (1998) Requirements for allergen-induced airway hyperreactivity in T and B cell-deficient mice. *Mol Med* 4: 344–355
7. Becker M et al (2011) Genetic variation determines mast cell functions in experimental asthma. *J Immunol* 186:7225–7231. doi:[10.4049/jimmunol.1100676](https://doi.org/10.4049/jimmunol.1100676)
8. Nakae S et al (2007) Mast cell-derived TNF contributes to airway hyperreactivity, inflammation, and TH2 cytokine production in an asthma model in mice. *J Allergy Clin Immunol* 120:48–55. doi:[10.1016/j.jaci.2007.02.046](https://doi.org/10.1016/j.jaci.2007.02.046)
9. Desquand S, Lefort J, Liu FT, Mencia-Huerta JM, Vargaftig BB (1989) Antigen-induced bronchopulmonary alterations in the guinea pig: a new model of passive sensitization mediated by mouse IgE antibodies. *Int Arch Allergy Appl Immunol* 89:71–77
10. Sertl K, Kowalski ML, Slater J, Kaliner MA (1988) Passive sensitization and antigen challenge increase vascular permeability in rat airways. *Am Rev Respir Dis* 138:1295–1299
11. Van Oosterhout AJ et al (1993) Effect of anti-IL-5 and IL-5 on airway hyperreactivity and eosinophils in guinea pigs. *Am Rev Respir Dis* 147:548–552
12. Lopez E et al (2011) Gene expression profiling in lungs of chronic asthmatic mice treated with galectin-3: downregulation of inflammatory and regulatory genes. *Mediators Inflamm* 2011:823279. doi:[10.1155/2011/823279](https://doi.org/10.1155/2011/823279)
13. Yu M et al (2011) Identification of an IFN-gamma/mast cell axis in a mouse model of chronic asthma. *J Clin Invest* 121:3133–3143. doi:[10.1172/jci43598](https://doi.org/10.1172/jci43598)
14. Kung TT et al (1995) Mast cells modulate allergic pulmonary eosinophilia in mice. *Am J Respir Cell Mol Biol* 12:404–409
15. Takeda K et al (1997) Development of eosinophilic airway inflammation and airway hyperresponsiveness in mast cell-deficient mice. *J Exp Med* 186:449–454
16. Williams CM, Galli SJ (2000) Mast cells can amplify airway reactivity and features of chronic inflammation in an asthma model in mice. *J Exp Med* 192:455–462
17. Cho JY et al (2010) Chronic OVA allergen challenged Siglec-F deficient mice have increased mucus, remodeling, and epithelial Siglec-F ligands which are up-regulated by IL-4 and IL-13. *Respir Res* 11:154. doi:[10.1186/1465-9921-11-154](https://doi.org/10.1186/1465-9921-11-154)
18. Cho JY et al (2004) Inhibition of airway remodeling in IL-5-deficient mice. *J Clin Invest* 113:551–560. doi:[10.1172/jci19133](https://doi.org/10.1172/jci19133)
19. O'Brien R, Ooi MA, Clarke AH, Thomas WR (1996) Immunologic responses following respiratory sensitization to house dust mite allergens in mice. *Immunol Cell Biol* 74:174–179. doi:[10.1038/icb.1996.24](https://doi.org/10.1038/icb.1996.24)
20. Cates EC et al (2004) Intranasal exposure of mice to house dust mite elicits allergic airway inflammation via a GM-CSF-mediated mechanism. *J Immunol* 173:6384–6392
21. Jacquet A (2011) The role of innate immunity activation in house dust mite allergy. *Trends*

Mol Med 17:604–611. doi:[10.1016/j.molmed.2011.05.014](https://doi.org/10.1016/j.molmed.2011.05.014)

22. Thomas WR, Smith WA, Hales BJ, Mills KL, O'Brien RM (2002) Characterization and immunobiology of house dust mite allergens. *Int Arch Allergy Immunol* 129:1–18

23. Phipps S et al (2009) Toll/IL-1 signaling is critical for house dust mite-specific helper T cell type 2 and type 17 [corrected] responses. *Am J Respir Crit Care Med* 179:883–893. doi:[10.1164/rccm.200806-974OC](https://doi.org/10.1164/rccm.200806-974OC)

24. Melgert BN et al (2010) Macrophages: regulators of sex differences in asthma? *Am J Respir* Cell Mol Biol 42:595–603. doi:[10.1165/rcmb.2009-0016OC](https://doi.org/10.1165/rcmb.2009-0016OC)

25. Melgert BN et al (2005) Female mice are more susceptible to the development of allergic airway inflammation than male mice. *Clin Exp Allergy* 35:1496–1503. doi:[10.1111/j.1365-2222.2005.02362.x](https://doi.org/10.1111/j.1365-2222.2005.02362.x)

26. van Rijt LS et al (2004) A rapid flow cytometric method for determining the cellular composition of bronchoalveolar lavage fluid cells in mouse models of asthma. *J Immunol Methods* 288:111–121. doi:[10.1016/j.jim.2004.03.004](https://doi.org/10.1016/j.jim.2004.03.004)

Chapter 32

Methods in Assessment of Airway Reactivity in Mice

Matthew Gold and Marie-Renee Blanchet

Abstract

Due to the wealth of reagents and transgenic strains available, mice have become one of the most commonly used model organisms for the study of allergic airway inflammation. One of the major hallmarks of the asthma phenotype in humans is reversible airflow obstruction, or airway hyper-responsiveness. However, the ability to confidently obtain useful physiological responses from such a small animal has presented a large technological challenge in murine studies. Recent advances have provided the technology to obtain lung mechanics through either the forced oscillation technique or plethysmography. Here we describe the utility of these measurements in mouse models of allergic airway inflammation and anaphylaxis.

Key words Asthma, Mouse, Airway responsiveness, Airway resistance, Methylcholine, flexiVent

1 Introduction

One of the major characteristics of the asthmatic response in humans is reversible airflow obstruction, or airway hyper-responsiveness (AHR). AHR is defined by an increased sensitivity of the airways to a constrictor agonist [1]. It is a phenomenon well described in asthmatic patients, and can be caused by stimulation of the airway smooth muscle by a variety of molecules such as histamine, prostaglandins, and leukotrienes [2, 3]—all released by inflammatory cells present in the lung environment. In humans, AHR is normally measured using the PC₂₀ (provocative dose challenge causing a 20 % decrease of the FEV₁ (forced expiratory volume in 1 s)). In this test, increasing doses of either methacholine (MCh) or allergens are administered via nebulization to a patient. After each dose, the FEV₁ is determined: The MCh dose causing a 20 % decrease of the FEV₁ (PC₂₀) is then calculated and used in the diagnosis of mild, moderate, or severe airway responsiveness or asthma.

While techniques used for testing AHR in humans are widespread, fairly straightforward, and well described, testing of lung functions in mice is more challenging. In the aim to obtain a

valid measurement of the response of airways to bronchoconstrictors, the first tests done on rodents were made using whole-body plethysmographs in the 1970s [4]. Plethysmography has become popular for evaluating lung function in mice, mainly due to its ease of use and noninvasive nature, which allows the monitoring of animals throughout disease and treatment regimens. However, this noninvasive approach cannot accurately measure lung mechanics in small rodents such as mice. Instead, these methods yield an arbitrary quantity called the enhanced pause (Penh) [5, 6]. Although Penh is a measure of the shape and duration of expiratory flows, it is not a true measure of lung mechanics. Although Penh may be proportional to airway resistance, invasive procedures are required to accurately calibrate the Penh in each experimental setup and design. In recent years, more accurate testing of the pulmonary functions of rodents became available, notably through the development of complete systems designed for lung function analysis in small rodents including the flexiVent (SCIREQ, Montreal, Canada) and Buxco instrument (Buxco Research Systems, Wilmington, NC, USA). These instruments are capable of measuring a variety of parameters such as airway resistance, compliance, and elastance [7, 8]. In mouse models of asthma and mast cell-dependant airway hyper-responsiveness, the parameter most widely used to determine airway responsiveness is airway resistance.

1.1 Airway Resistance in Mice

Airway resistance is undoubtedly the gold standard for measurement of AHR in mouse models of asthma. Using the flexiVent or Buxco apparatus, airway resistance is easily measurable at baseline (naïve mice without respiratory challenge). For the purpose of measuring an increase in reactivity of the lung in mouse models of asthma, resistance measurements can also be obtained in response to increasing doses of methacholine (MCh), administered either intravenously (IV) or via nebulization. In this technique, mice are anesthetized, paralyzed to block any skeletal muscle interference with the measurements, and tracheotomized with an 18-gauge(G) solid catheter (such as a blunt 18G needle). The flexiVent or Buxco apparatus provides for a set breathing rate and tidal volume. Following the intravenous administration of MCh, the airway resistance is measured every 10 s until the maximum resistance is obtained and noted. Results are typically expressed as an increase in resistance compared to baseline for each dose of MCh and these data can be compared between genotypes or experimental mice groups. This technique is sensitive enough to detect differences in airway resistance between genetically modified mice and their wild-type littermates [9, 10] and also sensitive enough to detect the effect of potential anti-inflammatory or bronchodilator drugs [11]. Increases in airway resistance have also been utilized to measure direct activation of lung-resident mast cells in a model of passive anaphylaxis [12].

Here we provide an overview of the technique used to measure airway resistance in mice. This technique can be used on naive mice as well as on mice that have undergone treatment with ovalbumin or house dust mite antigen to detect increases in airway responsiveness.

2 Materials

2.1 Surgical Preparation, Anesthesia, and Paralysis

1. C57Bl/6J, Wsh (Kit^{W-sh}/HNihrJaeBsmJ (JAX Stock#005051)), W/Wv (WBB6F1/J-Kit^W/Kit^{W-v} (JAX Stock#100410)), or other mouse strains. All experiments must be conducted in accordance with the institutional and national guidelines (*see Note 1*).
2. Injectable anesthesia:
 - (a) Avertin stock solution: Dissolve 10 g of 2,2,2-tribromo ethanol with 10 mL of *tert*-amyl alcohol for a stock solution. Store at 4 °C protected from light.
 - (b) 2.5 % working avertin solution: Prior to use, dilute stock solution 1:40 with PBS. Add the avertin stock solution dropwise to pre-warmed PBS (37 °C) with constant stirring to avoid formation of a precipitate. Store at 4 °C protected from light.
 - (c) Institutional guidelines will influence the choice of anesthetic. Avertin can be replaced with other drugs such as ketamine/xylazine or pentobarbital/xylazine.
3. Pancuronium bromide (stock 10 mg/mL in PBS or saline, stored at 4 °C).
4. Tracheal catheter.
 - (a) Prepare the tracheal catheter using an 18G needle.
 - (b) Saw off the bevel until the needle is approximately 1.2–1.4 cm long.
 - (c) Sand down the tip until it is dull to the touch (*see Note 2*).
5. Surgical scissors, forceps, laboratory tape, and suture thread.
6. 70 % ethanol.

2.2 Jugular Vein Cannulation or Aerosolized Delivery of Methylcholine

1. 30G1/2" needles.
2. Polyethylene tubing, 0.28 mm internal diameter (ID) (Becton Dickinson PE10).
 - (a) Create catheter by cutting the tubing into lengths approximately 40 cm. Cut a 30G needle away from its plastic fitting (approx. 1 cm), and carefully insert the blunt end into the catheter.
 - (b) In the other end, insert a Hamilton syringe (50–100 µL capacity) charged with PBS.

- (c) Slowly expel the PBS until it reaches the bevel of the needle, record volume, and trim the tubing until its total volume is 30 μ L.
- 3. Hamilton 50 μ L syringe, model 1705RN without needle (*see Note 3*).
- 4. Removable needles for Hamilton syringe, 30G-2".
- 5. Acetyl- β -methylcholine chloride (MCh): prep volume and diluent.
- 6. Aeroneb attachment to flexiVent (for aerosolized drug delivery, *see Note 4*).

3 Methods

3.1 Surgical Preparation, Anesthesia, and Paralyzation

1. Before anesthetizing the first mouse, make sure that the flexiVent instrument is calibrated and ready for ventilation (*see Subheading 3.2*).
2. Anesthetize mice with 2.5 % avertin, i.p. or an alternative method (500 mg/kg, or 200 μ l/10 g body weight).
3. Secure mouse with its ventral side up to a styrofoam dissection board using laboratory tape (*see Note 5*).
4. Using an elastic band drawn across the dissection board, secure the head by placing elastic band underneath the upper incisors.
5. Make sure to calibrate the flexiVent machine with the catheter before inserting into the mouse (*see Note 6*).
6. Using scissors and forceps, remove skin and tissue above the neck area, exposing the trachea.
7. Make a pinhole cut in the trachea just inferior of the larynx and thyroid, carefully insert the 18G catheter into the trachea, and secure using suture thread.
8. Connect the mouse to the flexiVent machine and begin default ventilation (Subheading 3.2, step 5).

3.2 flexiVent Instrument Setup, Calibration, and Operation

1. Open up the flexiVent application on the desktop.
2. Select module 1 (FV-M1, 1.7 mL) and then start a new experiment from a template.
3. For jugular vein administration of MCh, select "Mouse EKG v5.2.1," create a new experiment folder, and perform the system calibrations for airway pressure, cylinder pressure, and the EKG (*see Note 7*).
4. After calibration, select the TLC (total lung capacity) and SnapShot-150 perturbation signals, connect the 18G catheter to the machine, and perform the dynamic tube calibration.

Ensure that the resulting values are within the acceptable limits (*see Note 8*).

5. Disconnect the catheter from the machine, insert it into the trachea of surgically prepared mouse, and then connect the catheter and mouse back to machine to begin default ventilation.
6. Immediately after connecting the mouse to the ventilator, inject 100 μ L of pancuronium bromide (0.5–1.0 mg/kg, 100 μ L i.p. of 200 μ g/mL for a 20 g mouse) intraperitoneally (or intramuscularly) to prevent efforts against the ventilation of the machine (*see Note 9*).
7. Allow 5 min for the muscle relaxant to take effect before beginning data acquisition. Connect the three EKG leads to the right forepaw and right and left hind paw.
8. While waiting for the pancuronium to take effect, prepare the mouse for insertion of the jugular vein catheter.
 - (a) Surgically expose the external jugular vein and carefully dissect the connective tissue surrounding it.
 - (b) Ensure that the catheter is filled with solution (either PBS/saline or MCh), and then insert into the external jugular vein.
 - (c) Secure the tubing to dissection board using laboratory tape.
9. Acquire snapshot readings at baseline, then administer 30 μ L of PBS/saline via the jugular vein catheter, and immediately begin acquiring snapshot readings to monitor any increase in resistance. Perform a deep-lung inflation (TLC manoeuvre) before each PBS or MCh drug delivery to return respiratory system to baseline [7] (*see Notes 10 and 11*).
10. Once the resistance readings have returned to baseline, continue with the MCh doses (30 μ L volume, 30–2,000 μ g/kg). Immediately after administration of each MCh dose, begin taking snapshot acquisitions every 5 s until the peak of the response curve has been reached. Then, decrease the acquisition rate and monitor airway resistance until it again returns to baseline.
11. Repeat **step 10** with the successively higher MCh doses (*see Notes 12 and 13*).
12. After completion of the final MCh dose, humanely euthanize the mouse via institutional guidelines. Lung tissue and other biological samples can be collected and used for other analyses. We typically collect bronchoalveolar lavage fluid (BALF), peripheral blood by cardiac puncture, and lung tissue for gene expression, flow cytometric, and ELISA assays.
13. Results can be plotted as either raw resistance values or as a % increase over baseline.

4 Notes

1. The degree of airway hyper-responsiveness depends greatly on the mouse strain and the disease model. In models of OVA/alum-induced allergic asthma, C57Bl/6J mice develop milder responses than other strains. For example, Balb/c or 129/Sv strains typically provide more robust AHR readouts [13, 14].
2. It is important to carefully sand down the edges of the tracheal catheter; any remaining edge will cut the tracheal wall when inserted.
3. Alternatively a small volume insulin syringe (i.e., 3/10 cc with a 29G needle) can be used in place of a Hamilton syringe.
4. We find that the jugular vein administration route for MCh gives a more robust response than the nebulized delivery method. To use the nebulizer, connect the Aeroneb attachment to the flexiVent machine and use the “Mouse AN-EKG” template.
5. To reduce stress and injury, use masking or laboratory tape to secure mouse limbs rather than pinning down with needles. Mice can also be placed on heating pads or warmed with heat lamps.
6. It is important to calibrate the machine with the same catheter used for that mouse. Any difference in length between different catheters will affect the readouts.
7. If using the Aeroneb attachment for nebulized drug delivery, select the “Mouse AN-EKG” file.
8. The snapshot perturbation performs a single frequency forced oscillation manoeuvre that obtains the resistance and elastance measurements of the entire respiratory system (i.e., airways and chest wall). The Quick Prime-3 or Prime-8 perturbations perform a series of frequency oscillations and are able to obtain segregate resistance from the central airways and lung tissue.
NB: To perform the quick prime and prime-8 manoeuvres, make sure that they are selected when performing the calibrations.
9. Do not administer pancuronium bromide until the animal is connected to the ventilator; otherwise the paralytic will impair their respiration.
10. Administration of MCh will cause a spike in the heart rate observed from the EKG leads. Make sure that the heart rhythm returns to baseline before performing the subsequent MCh challenge.
11. Delivery of MCh via the jugular vein provides a rapid increase in airway resistance. Therefore perform snapshot analyses (data

acquisition takes approximately 1.2 s per manoeuvre) immediately after delivery of MCh. The Quickprime-3 and Prime-8 manoeuvres take much longer to acquire (3 s and 8 s, respectively), so it is advised not to use these in conjunction with intravenous delivery of MCh. Nebulized delivery of MCh provides a broader response curve and is better suited for the Quickprime-3 or Prime-8 perturbations.

12. If collecting multiple doses you will have to readminister the injectable anesthetic to maintain an appropriate surgical plane (a single dose of avertin will last for approximately 15–20 min).
13. There are pre-programmed command scripts that will run various perturbations automatically, negating the need to manually perform snapshot or Quickprime manipulations. There are several default scripts pre-loaded onto the software (flexiWare), which can be modified to fit any experimental requirements.

References

1. O'Byrne PM, Inman MD (2003) Airway hyperresponsiveness. *Chest* 123:411S–416S
2. Liu MC et al (1990) Evidence for elevated levels of histamine, prostaglandin D₂, and other bronchoconstricting prostaglandins in the airways of subjects with mild asthma. *Am Rev Respir Dis* 142:126–132
3. Cockcroft DW, Davis BE (2006) Mechanisms of airway hyperresponsiveness. *J Allergy Clin Immunol* 118:551–559
4. Fairchild GA (1972) Measurement of respiratory volume for virus retention studies in mice. *Appl Microbiol* 24:812–818
5. Lundblad LK, Irvin CG, Adler A, Bates JH (2002) A reevaluation of the validity of unrestrained plethysmography in mice. *J Appl Physiol* 93:1198–1207
6. Bates JH, Irvin CG (2003) Measuring lung function in mice: the phenotyping uncertainty principle. *J Appl Physiol* 94:1297–1306
7. Shalaby KH, Gold LG, Schuessler TF, Martin JG, Robichaud A (2010) Combined forced oscillation and forced expiration measurements in mice for the assessment of airway hyperresponsiveness. *Respir Res* 11:82
8. Vanoirbeek JA et al (2010) Noninvasive and invasive pulmonary function in mouse models of obstructive and restrictive respiratory diseases. *Am J Respir Cell Mol Biol* 42:96–104
9. Blanchet MR et al (2007) CD34 facilitates the development of allergic asthma. *Blood* 110: 2005–2012
10. Naus S et al (2010) The metalloprotease-disintegrin ADAM8 is essential for the development of experimental asthma. *Am J Respir Crit Care Med* 181:1318–1328
11. Blanchet MR, Israel-Assayag E, Cormier Y (2005) Modulation of airway inflammation and resistance in mice by a nicotinic receptor agonist. *Eur Respir J* 26:21–27
12. Cyphert JM, Kovarova M, Koller BH (2011) Unique populations of lung mast cells are required for antigen-mediated bronchoconstriction. *Clin Exp Allergy* 41:260–269
13. Takeda K, Haczku A, Lee JJ, Irvin CG, Gelfand EW (2001) Strain dependence of airway hyperresponsiveness reflects differences in eosinophil localization in the lung. *Am J Physiol Lung Cell Mol Physiol* 281: L394–L402
14. Whitehead GS, Walker JK, Berman KG, Foster WM, Schwartz DA (2003) Allergen-induced airway disease is mouse strain dependent. *Am J Physiol Lung Cell Mol Physiol* 285:L32–L42

INDEX

A

Acidophilic/eosinophilic granule 14
Acridine orange staining 317, 320, 321
Actin
 filamentous actin 219
 microfilaments 220
 polymerization/depolymerization
 kinetics 368–369, 374–375
 polymerization inhibitors
 cytochalasin D 220
 latrunculin B 220
Activation of mast cells
 Aeromonas salmonicida 14, 15, 31, 37
 compound 48/80 14, 15, 17, 21, 31, 37, 53, 54, 124, 125, 127, 128, 134, 220
 with pathogen products 179–196
Acute viral infection 181
Adenomatous polyps
 adenomatous polyposis coli (APC) 444
 familial adenomatous polyposis (FAP) 444
 mouse models
 APC^{Δ468} mice 444, 445
 APC^{Min} (Min) mouse 444
 Min-Rag^{-/-} mice 445
Adoptive transfer
 of BMMCs into recipient mice 429
 of mast cells 488
 of T cells into polyp bearing mice to assess mast cell
 function in vivo 459
 of total lymphocytes to induce tolerance 482
Akt and Erk phosphorylation in LAD2 cells 373
Alcian blue–safranin reaction 126
Allergic disease 20, 56, 61, 145, 179, 205, 291, 326, 497
Allergic disorders 239, 308
Allergic enteritis 164
Allergic inflammation 60, 291
Allergic lung inflammation
 airway challenge 504
 airway hyperresponsiveness (AHR) 503
 airway inflammation 100, 504
 airway remodeling 504
 airway resistance 522
 allergic airway constriction 148
Amperometry 351
Analysis and quantification of Ca²⁺ imaging
 ImageJ
 functions 361
 plug-ins 356, 357, 361, 362
Analysis of skin graft cytokine profile 476
Anaphylatoxin 12
Anaphylaxis 7, 8, 21, 30, 94, 98, 272, 274, 280–282, 307, 381, 522
Ancestral leukocyte 59
Angiogenesis 11, 13, 60, 106, 205, 283, 444
Angiotensin II
 angiotensin converting enzyme (ACE)-independent
 angiotensin II 133
 angiotensin II type 1 (AT1) receptor 132
 AT1 receptor antagonist 133
Animal models
 of arthritis 104
 of cardiomyopathy
 chronic cardiac volume overload 127
 experimentally induced hypertension 122
 myocardial infarction 104, 122
Annexin V 328, 330, 331
 and propidium iodide staining 261
Antagonomir 293, 294, 299–300, 302
 antagonomir design 299–300
Antibody
 complexes 394, 487
 mediated depletion of T cells 465
Antigenic markers 60
Antigen-induced bronchoconstriction 149
Anti-human Fc_εRI_γ antibody 50
Anti-oxidants
 diphenyleneiodonium 126
 ebselen 126
Anti-parasite immunity by mast cells in the intestine
 collection of infective larvae 86
 mouse infection 86
 rescue of mast-cell deficient mice 87
 Strongyloides venezuelensis infection 86
Aortocaval fistula 122, 123
Apoptosis
 BH3-domain 258
 cell death cascade 258

Arthritis

- assessment 427
- clinical index 430
- histological assessment of joint injury 432–433
- paw swelling 430

Arthropathy 424

Assay

- of chemokine/cytokine production 145, 165, 171–174, 188, 189, 195, 275, 281, 292, 293, 382
- of mast cell mediators 307–322
- of mast cell signaling pathways 131

Assessing Fc ϵ R1 expression on
BMCMC 243–245, 248, 253Assessing how mast cells influence tumor
epithelium 453–455

Assessment of airway reactivity in mice

- allergic airway inflammation 100
- anaphylaxis 522
- asthma phenotype 522
- Buxco instrument 522
- compliance 522
- elastance 522
- enhanced pause (Penh) 522
- flexiVent instrument 524–525
- forced expiratory volume (FEV) 521
- forced oscillation 526
- jugular vein cannulation 523–524
- lung mechanics 522
- nebulization 521, 522
- plethysmography 522
- provocative dose challenge (PC20) 521

Assessment of mast cell reconstitution 473

Assessment of mature mast cells

- by histology
 - in intestine 77
 - in lung 77
 - in trachea 77

- by immunohistochemistry 77
- mMCP-2,4,5,6,7 and CPA3 77

Assessment of renal function 492

Asthma 7, 8, 56, 61, 99–100, 147, 148, 291, 307, 322, 326, 497, 503–518, 521, 522, 526

Autoimmune disease 20, 60, 95, 107, 111, 205

- autoantibodies 424, 425

Autoimmune glomerulonephritis 107, 487–496

Autoimmune inflammatory arthritis and
osteoarthritis 423**B**

Basement membrane thickening 504

Basophil 7, 23, 59–66, 145, 162, 182, 183, 292

B cell receptor 219, 271

Bone marrow derived/cultured mast cells

- (BMCMC) 8, 106, 129, 147, 206–213, 215, 220–222, 224–226, 228–231, 233–235, 241, 243–245, 247–253, 270–280, 282, 292, 294, 308–311, 313–321, 327, 353, 368, 369, 374, 375, 377, 378, 426, 438, 441, 446, 448, 453–454, 462–464, 471–473, 483, 484

Bone marrow reconstitution 289

Breaking tolerance by mast cell degranulation

- active immunization with OVA/Alum 474
- chemically induced degranulation 474
- IgE mediated degranulation 474–475

Bromophenol blue 37, 52, 259, 329

Bronchoalveolar lavage 509–510, 525

CCa $^{2+}$. *See* Calcium (Ca $^{2+}$)CAE. *See* Chloroacetate esterase (CAE)Ca $^{2+}$ -induced calcium release (CICR) 350

Calcitonin gene related peptide (CGRP) 148

Calcium (Ca $^{2+}$)

- chelators 350
- clearance mechanisms 350
- flux indicator dyes
 - Ca $^{2+}$ elevation 348
 - oscillation amplitude and frequency 350
 - oscillation rise and decay times 350
 - region of origin 350
 - wave velocity 350
- influx 270, 347–348, 350, 357
 - TRPC1-mediated Ca $^{2+}$ influx 348
 - intracellular stores 347, 348
 - ionophore 185, 353, 448
 - mobilization and entry in mast cells 348
 - PI(4,5)P₂ complex 351
 - release from endoplasmic reticulum (ER) 348, 349
 - response kinetics 368, 372–374
 - sensors 348–349, 356
 - Fluo-4 368
 - Fura-2 349, 366
 - Indo-1 349, 366

signaling dynamics

- Ca $^{2+}$ oscillations 350, 355
- Ca $^{2+}$ puffs 350
- Ca $^{2+}$ waves 350

Calcium-release activated calcium channels

- (CRAC) 349

Canine heart 131, 132

Capsaicin-sensitive C-fibers 148

Carboxypeptidases

- carboxypeptidase A3 (CPA3) 99
- carboxypeptidase A5 (CPA5) 30, 38, 47

Cardiac fibroblasts response to histamine

- PGE₂ 133

- PGI₂ and 6-keto-PGF_{1 α} 133

Cardiac mast cell
 biology 28, 131
 density 123, 124, 127, 129, 130, 135
 isolation 122–126
 phenotype 123–126
 secretagogues 122–126

Cardiac volume overload 122, 127, 130, 132

Cardioprotection by estrogen 135

Cardiovascular disease
 abdominal aortic aneurysm 102, 103
 atherosclerosis 102–103
 cardiomyopathy 103–104
 chronic heart failure 103–104
 coronary artery disease 102–103

Caspases 257, 334
 caspase-3 activation assay 327, 328, 333–334

β-Catenin 444, 445

Cathelicidin peptide 18

Cathepsin G 12, 21, 103, 104, 123

Cbl ubiquitin ligase 240

CD117 (c-Kit) 6, 8, 59, 71, 104, 105, 108, 122, 127, 128, 166, 168, 174, 182, 208, 215, 221, 269, 270, 272, 276, 277, 279, 280, 396, 405

CD34⁺ and HuMC culture 159–160

CD34⁺ cell selection and enrichment 158
 magnetic separation 158

CD34⁺ hematopoietic cells 155–162

C2 domain 351

Cellular protrusions 348

CGRP. *See* Calcitonin gene related peptide (CGRP)

Chemokine arrays 185–186

Chemokines 12, 19, 97, 98, 108, 147, 164, 172, 179, 181, 183, 185, 186, 188–196, 206, 240, 291, 308–310, 313–315, 318, 322, 366

Chloroacetate esterase (CAE) 69, 71, 76, 428, 435, 445, 451, 452

Cholecystokinin (CCK) receptors 144

Cholinergic activation of mast cells 145–146

Cholinergic and inhibitory NANC
 neurons 142–146, 148, 149

Cholinergic anti-inflammatory pathway 144–145

Chondroitin sulfate proteoglycan-rich connective tissue
 mast cells 425

Chronic inflammation 102, 110, 164

Chronic kidney disease 492–493

Chronic phase atopic dermatitis 497

Chymase
 big ET-1 133
 chymase activation of 133
 latent TGF-β 133, 134
 MMP-2 and MMP-9 133
 stem cell factor (SCF) 133

Chymase and tryptase positive mast cells (MCCT) 164

Chymase/renin/angiotensin II 133

Clathrin-mediated endocytosis 241

Clonogenic assay 74

Co-immunoprecipitation 206, 208, 214–215

Collagen
 collagen antibody induced arthritis 424
 degradation 122, 123, 126, 130–135
 deposition 128, 129, 504
 synthesis 131, 133

Colon cancer 443, 444

Complement 17, 18, 32, 66, 180, 322, 383, 389, 462, 469, 487

Complement receptors 18, 180

Compound 48/80 14, 15, 17, 21, 24, 31, 37, 53, 54, 124, 125, 127, 128, 130, 134, 147, 220, 322

Compound E (γ-secretase inhibitor) 46

Connective tissue 5, 6, 12, 16, 79, 94, 123, 125, 133, 164, 215, 404, 418, 423, 425, 525

Connective tissue type mast cells
 (CTMC) 69, 76, 94, 164, 418, 425
 T_H2-conditioned 87

Cord blood
 cord-blood derived mast cells 183
 culture 187
 derivation 183, 341

CPA3-Cre mice 426

Cre/loxP-mediate recombination 403

Cre-Master mouse strain 109, 404

Cryopreservation of CD34⁺ cells 158–159

Crypt proliferative zone 445

CTMC proteases (mMCP-4,5,6,7) 80, 425

Culture of intestinal mast cells 166, 170–171

Cysteine cathepsin activity 328, 331, 333

Cytokine/chemokine expression by qPCR 310
 isolation of total RNA from mast cells 313–314
 measuring gene expression by qPCR 315

Cytokine profile in the skin graft 465, 476

Cytokines and growth factors 12, 164, 240, 308, 366
 involved in mast cell growth and differentiation 61

Cytokine secretion assay by ELISA 311

Cytosolic Ca²⁺ concentration 348

D

DAF-FM diacetate assay
 fibronectin matrix 342
 fluorescent plate reader 342, 343
 phenol red interference 342
 stimulation of mast cells to generate NO 344

Decay of tolerance after local mast cell
 degranulation 466, 478

Degranulation
 assay 210
 degranulation and T cell dependent
 graft rejection 461
 kinetics 313, 369–370, 375–376
 role of allergens 461
 role of IgE 461

De novo synthesized mast cell mediators

- eicosanoids 94, 308
- leukotriene C₄ (LTC4) 308
- lipid-derived inflammatory mediator 308
- prostaglandin D₂ (PGD₂) 308

Derivation of human mast cells

- from bone marrow 182
- from cord blood 182, 183
- from peripheral blood 182

Dermal delayed-type hypersensitivity response to rabbit IgG 494

Detection of miRNA 294, 297

Diphtheria toxin (DT)-induced mast cell depletion

- Cre-inducible diphtheria toxin receptor
- iDTR mice 405
- loxP-flanked stop cassette 405
- R-DTA mice 405
- diphtheria toxin receptor (DTR) 405
- DTR-induced gene expression in mice 405

DsRNA 98, 184, 185

- poly inosinic:cytidylic (I:C) 184

Dual specific PTPs 281

Dynamic remodeling of the cytoskeleton

- adhesion 219
- migration 219
- morphology 219

E

Eczematous skin lesions 467

- infiltration of T_H2 cells 497

Effect of protease inhibitors on apoptosis 329, 335–336

Effects of Notch signaling

- localization of mast cells in small intestine 85–86
- mMCP-1 and -2 expression in CMCs 85

Efficiency and specificity of gene inactivation

- in mast cells 405

Eicosanoid generation assay

- measuring eicosanoids in cell-free supernatants 319–320
- preparing sample supernatants for eicosanoid measurement 318–319

Electron microscopy 14, 15, 17, 31

End-binding (EB) family proteins 221

Endocytosis 240, 241, 329, 352

Endoplasmic reticulum (ER) 242, 348, 349, 366

Endothelin-1 (ET1) 99

Enumerating mast cells in human tissue

- chloroacetate esterase (CAE) 451–452
- toluidine blue staining to detect degranulation 450–451
- tryptase staining 449–450

Enumeration

- and differentiation of BALF leukocytes
- by cytospin/morphology 511
- by flow cytometry 511–513

of intestinal mast cells 492

of mast cells by flow cytometry 511–513

of Tregs in skin graft

- by flow cytometry 467
- by fluorescent microscopy 466–467

Enzyme-linked immunosorbent assay (ELISA) 33, 85, 166, 172, 186, 188, 190, 192–194, 308, 309, 311, 316–317, 382, 427, 431–432, 439, 474, 484, 490, 494, 514, 516, 525

Eosinophilia 8, 14, 55, 122, 291, 504, 505

Evaluation of cellular responses 494

Evaluation of humoral immune responses 490

Evaluation of mast cell deficiency

- by flow cytometry 409–410, 418–419
- genotyping 407, 410–414
- by histology 409–410, 418–419
- tissue preparation 418

Evolutionary history

- fish
- Danio rerio* H 14
- zebrafish 21, 29–56
- cartilaginous 13, 20
- primitive jawless fish 13
- frog 16
- invertebrates 15–18, 20, 23, 24
- mammals 12, 14–19, 21
- phylogenesis 13
- reptiles 12, 14, 21, 22
- vertebrates 11–13, 16–18, 20, 23, 24

Exocytosis of secretory granules 347, 352

Ex vivo analysis of Treg function 467, 481–482

Ezrin, radixin, moesin (ERM) family 220

F

Fc epsilon receptor I (Fc ϵ RI)

- complex 240, 253, 269, 282
- recycling assay 242, 244, 249–250, 253
- signalling intermediates
- Bruton's tyrosine kinase (Btk) 213
- c-Jun kinase (JNK) 279
- Fyn 205
- Lyn 205, 240
- protein kinase B, Akt 279
- protein kinase C (PKC) 214–215
- Src 205, 206
- Syk 206, 279
- Tec family 206

 stability assay 244, 247–248

 stimulation 207, 209–210

 surface expression dynamics

- internalization 240, 241
- membrane trafficking 240, 241
- recycling 240–242, 244, 249–250
- stabilization 240, 244

Fc receptor activation 258

Fc receptors 219, 487, 511
 Fc ϵ RI. *See* Fc epsilon receptor I (Fc ϵ RI)
 Fc ϵ RI γ 31, 36, 50
 Fc ϵ RI α half-life 248
 Fc γ RII/III 60
 Fibrillar collagen 121, 123
 Fibrosis 11, 13, 95, 104, 109–111, 122, 123, 129–132, 134, 292, 487, 492
 Fibrotic process in volume overloaded heart 132
 Flow cytometry
 enumeration of mast cells 467
 monitoring of mast cell activation
 by phospho-flow 365–378
 surface staining of mast cells
 bone marrow 62–63
 cord blood 62–63
 peripheral blood 62–63
 sputum 63, 65–66
 Fluorescence activated cell sorting (FACS)
 Fluorimeter 348, 352, 357, 358
 Fractalkine (CX3CL1) 147

G

Ganglia 125, 142, 143
 Gastrointestinal inflammation 100
 Generation of recombinant retrovirus 210–211
 Genetically encoded Ca $^{2+}$ indicators for optical (GECO)
 imaging proteins
 fused with calmodulin (CaM) 358
 GCaMP2 349, 352, 354–359
 GCaMP3 349, 352, 358
 GCaMP5 349, 358
 Glomerulonephritis (GN)
 glomerular basement membrane (GBM) 488, 495
 histological assessment of glomerulonephritis 492
 immune-mediated glomerulonephritis 487
 generating nephrotoxic serum 489
 generating nephrotoxic serum: anti-GBM rabbit serum 490–491
 induction of anti-GBM glomerulonephritis 491–492
 Glucocorticoid treatment of asthma 61
 Graft tolerance
 graft-localized T H 2 type inflammation 475
 non-specific T H 1-type inflammation 475
 role of mast cells 475
 TLR-mediated T H 1-type systemic inflammation 475
 Gut microbiota 61, 443

H

Heart failure 102–104, 127, 128, 130
 Hemacytometer 73, 454
 Hematopoietic cell differentiation 79, 279, 289
 Hematopoietic stem cell (HSC)
 basophil progenitor 59–66
 common myeloid progenitor 59
 eosinophil progenitor 59–66
 erythromyeloid progenitor (EMP) 30
 Hemolymph 15, 16, 23
 Heparan sulphate proteoglycan-rich connective tissue mast cells 425
 β -Hexosaminidase assay (degranulation assay) 311
 H2 haplotype IAg7 426
 H1 histamine antagonist (ketotifen) 14
 Highly sulfated glycosaminoglycan (GAG) 16
 High-throughput immunophenotyping based on transcription (HIT) assay
 Fab-oligonucleotide conjugation 383, 388–389, 391
 HIT processing 388–396
 validation of candidate markers identified by HIT 395–396
 Histamine
 histamine-induced myocardial edema 130
 receptors 8, 56, 101, 104, 132
 release 101, 104, 125, 126, 145, 146, 148, 175, 308
 HMC-1 cell line 183, 341
 Host defense 18, 22, 94–96, 151, 164, 179–181, 183
 House dust mite model of asthma 505, 506
 Dermatophagoides pteronyssinus (Der p1) 506, 509
 natural antigen 505
 H $_2$ receptor antagonist 8, 133
 famotidine 133
 5-HT2A and 5HT2 receptors 149
 Human airway mast cells 147, 148
 Human basophil growth and differentiation 59–61
 Human LAD2 mast cell line 37, 56, 446, 448
 Human mast cell activation
 bacterial 180–182
 fungal 184
 parasites 180
 viruses 179–196
 Human mast cell differentiation 60, 61
 Human mast cells (HuMCs) 6, 8, 59–66, 97, 147, 151, 155–164, 171, 175, 179–196, 257–259, 261, 283, 308–311, 313–322, 370, 377, 382, 390, 394
 Human rheumatoid arthritis 425
 Human synovial mast cells 425
 Human systemic mastocytosis 30, 31, 46
 KIT D816V mutation 30, 46
 Human T cell isolation 447–448, 457
 HuMC histochemical staining
 acidic toluidine blue 159–161
 cytospin 160
 Mota's fixative 156, 160
 Wright-Giemsa 159, 160
 HuMCs. *See* Human mast cells (HuMCs)
 Hypersensitivity 6, 7, 182, 205, 239, 283, 404, 494, 497

Hypertensive heart 127, 130
 Hypertrophy 130, 132, 133, 180

I

IgE-independent activation of mast cells
 anaphylatoxins (C3a and C5a) 12
 c-Kit 12, 83, 269
 fibrinogen 12
 fibronectin 12
 IgY-G-antigen receptors 12
 FcgRIII 12
 toll-like receptors (TLRs) 12

IgE-like receptor 21, 31
 IgE receptor (FcεR1) 94, 258, 350, 503
 IgE receptor crosslinking (IgER-CL) 258, 261, 503
 IgE sensitization and stimulation of mast cells 309
 IL-1 receptors 142, 291
 Imaging single cell degranulation events using
 FITC-dextran 359, 360
 Immunoassay 172, 185, 186, 311, 318
 Immunofluorescence staining of frozen
 kidney sections 492–493
 Immunofluorescence staining of murine mast cell
 proteases 436–438
 Immunoglobulin E (IgE) 8, 12, 31, 81, 82, 94, 239
 Immunohistochemical staining of mouse mast cell proteases
 or human tryptase 436–438
 Immunohistochemistry and histochemistry
 antigen retrieval 49, 77, 436
 chloroacetate esterase (CAE) 61, 79, 435
 chromogenic tryptase assay 31
 Eosin Y 35, 49
 Fast Red stain 36, 41–43
 hematoxylin and eosin
 Gill's hematoxylin 35, 71
 Harris hematoxylin solution 35
 Mayer's hematoxylin 36, 51
 McManus periodic acid-Schiff (PAS) 36, 49
 toluidine blue 35, 48
 Wright Giemsa 44
 Immunoprecipitation 206, 208, 213
 Immunoreceptors 206, 219, 240, 270, 366
 Immunoreceptor tyrosine-based activation motif
 (ITAM) 206, 240, 270, 278, 280, 366
 Induced depletion of CTMC in Mcpt5-Cre iDTR
 mice 418
 Induction of mast cell apoptosis 261, 325–336
 Induction of mast cell differentiation using Notch ligands
 immobilization of Delta1-Fc or Jagged1-Fc 83
 isolation of myeloid progenitors 84–85
 Induction of mast cell survival 170, 174, 258–261, 276
 Induction of secretory granule
 permeabilization 327, 329–330, 332

L-leucyl-L-leucine methyl ester (LLME) 327
 Infection of mast cells 187, 189–191, 210–213
 Inflammatory axon reflex 142
 Inflammatory bowel disease (IBD)
 Crohn's disease (CD) 100
 ulcerative colitis (UC) 100
 Inflammatory response 8, 14, 16, 19, 59, 101, 144, 240, 291, 487, 504
 Inhibition of mast cell intracellular proteins 173
 Innate immunity 13, 16–20, 23, 59, 94, 205
 Inositol-1,4,5-trisphosphate (IP₃) receptor (IP₃R) 345
 inositol 1,4,5-trisphosphate (IP₃) 345
 Interleukin 4 (IL-4) 19, 81, 87, 95, 99, 106, 110, 130, 147, 164, 166, 170, 171, 175, 180, 278, 340, 344, 498
 Interleukin 8 (IL-8) 19, 105, 310
 Interleukin 9 (IL-9) 80, 81, 85
 Interleukin 25 (IL-25) 59
 Interleukin 33 (IL-33) 59, 129, 151
 Intestinal motility 101, 146, 164
 Intestinal mucosal mast cells 95, 143, 144
 Intestinal permeability 101, 148, 164
 Intracellular delivery of antibodies into mast cells using
 Streptolysin O (SLO) 167, 173
 In vitro kinase assay 213–214, 216
 Ionophore 124, 125, 147, 185, 353, 448
 Ca²⁺ ionophore A23187 124, 125, 147, 185
 Ion-transporters 349
 IP₃ receptor inhibitors
 adenophostin A 350
 2-aminoethoxydiphenyl borate (2-APB) 350
 xestospongin C 350
 Ischemia-reperfusion injury
 ischemia-reperfusion myocardial
 infarction 123, 128–129
 ischemic rat heart 126
 Isolation
 and analysis of peritoneal mast cells 86
 of cardiac mast cells 126–128
 of human mononuclear cells from colonic
 tissue 455–457
 of human T cells from PB or tissue MNC 457
 of intestinal mast cells 163–175
 of mononuclear cells by Percoll
 gradient 70, 72, 73
 of mononuclear cells from mouse tissues
 lungs 72
 small intestine 72
 spleen 73
 of mononuclear cells from polyp tissue 452
 of plasma membrane sheets 228

J

Jejunal mucosa 143
Joint inflammation 423, 424, 426

K

K/BxN mice
 ELISA for anti-GPI IgG
 quantitation 427, 431–432
 glucose-6-phosphate isomerase (GPI) 424, 427
 K/BxN serum 424–427, 429–432, 438, 439
 KRN mice 423
 MHC II (I-Ag7) 424
K/BxN serum-induced arthritis
 adoptive transfer of arthritogenic
 autoantibodies 424
 histological assessment 427, 432
Key PTPs affecting mast cell biology 271, 282
Kidney disease
 crescents 487
 kidney glomeruli 489
 proteinuria 487, 492
Kinase assays 207–208, 213–217
KIT (c-Kit) 6, 8, 59, 60, 71, 75, 104, 105,
 108, 122, 127, 128, 166, 168, 174, 182, 208, 215,
 221, 269, 270, 272, 276, 277, 280
Kit-mutant mice 108, 403, 404
KU812 cells 182–184, 187, 188, 190, 195
Kymograph 357, 360, 361

L

Lactate dehydrogenase activity assay 328
LAD2 mast cell line 37, 56, 374, 376, 446
Lamellipodia 219, 220
Lamina propria 163, 164
LAMP2 externalization kinetics in activated
 mast cells 376
Laser-scanning confocal microscopy
 of microtubules 224, 229–231
Lectin-like receptors 180
Left ventricular hypertrophy
 brain natriuretic peptide (BNP) 133
 H₂ receptor antagonists 133
Leukocyte differential assay 507
Leukocyte infiltration 487, 498
Leukotriene B4 (LTB₄) 19, 181, 187, 189,
 191, 194, 196
Leukotriene production 185, 187, 189, 191, 195
 LTC₄ and LTB₄ assays 187, 196
 sulfidoleukotriene C4 (sLTC₄) ELISA 308
Lichenification of skin 497
 infiltration of T_H1 cells 497
Ligand-induced internalization 240, 241
Limiting dilution assay 71, 77, 78, 452, 457
Lineage commitment 60, 69, 290

Lineage (Lin) markers 71, 75
Lipid rafts 241, 282
Lipopeptides 184
 di- and tri-acyl lipopeptides 184
 FSL-1 and Pam3CSK4 184
Live cell
 imaging 223, 232, 353, 355
 microscopy 348
Low-density lipoprotein receptor (*Ldlr*^{-/-})-deficient
 mice 123
Lung cell isolation 507
Lung fibroblast response to histamine 133
 upregulation of connective tissue
 growth factor 133
Lung inflammation 272, 277
Lung leukocyte isolation for flow cytometry 513–514
Lung parenchyma 148
Lung specimen histopathology
 assessment of inflammation (scoring) 506
 inflation and fixation 507, 510–511
 lung morphometry 510, 512
Lymph node hypertrophy 180
Lyn 205, 206, 222, 240, 270–272, 274–279
Lysosome 241, 329, 332, 351

M

Magnetic cell separation 158, 165, 168–170
 MACS enrichment 168
Major development of understanding of mast
 cell biology 7–8
Marker of intestinal mast cells 60, 80
 mMCP-1 80
Mast cell(s)
 activation 127, 144, 164, 171, 179–196,
 219–236, 242, 274, 275, 277–280, 292, 293, 308,
 319, 320, 360, 365–378
 adaptive immunity 19–21, 403
 allergy 205
 apoptosis
 extrinsic pathway 257
 intrinsic pathway 257–259
 in cancer 104–107, 443–460
 conditioned media 454
 deficient mice 87, 88, 123, 128–130, 132,
 136, 193, 277, 407, 425, 462, 489, 493, 495
 degranulation 8, 31, 56, 122, 125–128,
 130, 145, 146, 186, 188, 190, 220, 221, 272, 278,
 281, 308, 309, 351–352, 473–478
 degranulation in the presence of T cells 458–459
 depletion in Mctp5-Cre iDTR mice 409, 418
 derived cytokines 179
 differentiation 59–61, 82–83, 87, 274
 distribution in the intestine 80
 endogenous secretagogues 122–126
 engraftment 438

Mast cell(s) (*cont.*)

- evolutionary history (*see* Evolutionary history)
- exocytosis
 - compound 21, 360
 - full 360
 - kiss and run 360
- functions in grafts/transplant
 - immune suppressive tolerance 461
 - pro-inflammatory rejection 94, 96
- generation in methylcellulose 85
- in glomerulonephritis 487–496
- granules 6, 146, 240, 308, 352
- heterogeneity 12, 125, 215
- histochemical staining 35–36, 79, 436
- in human hearts with dilated cardiomyopathy 122
- induced tumor cell invasion 454–455
- induced tumor cell proliferation 454
- innate immunity 17–19, 205
- interaction with other immune cells
 - dendritic cells 270
 - regulatory T cells (Treg) 270
- mediators
 - mast cell mediator release assay 131–134, 307–322
 - mast cell mediators and myocardial remodeling 270
- membrane-cytoskeleton dynamics 219–236
- membrane stabilization
 - nedocromil 126, 127, 130, 135
 - sodium cromolyn 105
- membrane topography using electron microscopy
 - actin filaments 226
 - oxidized phosphatases 228
- morphology
 - angle 351
 - length 351
 - volume 351
- numbers increased in heart disease 128
- phenotype heterogeneity 60, 123–126, 134–136, 175, 216, 272, 472
- plasticity 150, 381, 461
- production of NO 142, 147–148
- production of VIP 146–148, 150
- protease 80, 99, 135, 426, 436–437
- response to virus
 - CCL5 production by mast cells
 - in response to virus 181
 - CXCL8 responses 181
 - reovirus 185, 189
- secretagogues 123–126, 136
- signaling 219, 269–283, 347, 370, 376
- surface marker profiling 182, 382, 394, 396, 397, 410
- survival 170, 174, 257–266, 276
- tissue homing 69–78
- in tissue remodeling 5, 164, 180
- and tumor epithelium 453–455
- and vagus nerve 143
- viability measurement 174, 259, 328, 330, 341

Mast cell-dependent asthma 509

Mast cell-induced collagen synthesis

- and degradation 131

Mast cell-induced degradation of heart collagen 132

- mast cell-induced heart fibrosis 129, 131

Mast cell-like cells in invertebrates 15–17

Mast cell-nerve interaction 142, 149

- mediation of bronchoconstriction 148

Mast cell progenitors (MCp)

- 71, 74–75, 78, 95, 272, 276, 278, 423, 443, 444, 452, 457–458, 472
- assay in the presence of T cells 457–459
- assessment by limiting dilution analysis 74–75, 78, 452, 457
- differentiation 444
- and mature mast cell frequency with limiting dilution assay 452–453

Mast cell secretion of vascular endothelial growth factor (VEGF)

- 16, 59
- in response to substance P 125

Mast cell-specific conditional gene targeting 206

Mastocytosis

- human disease 46
- in zebrafish 31

MASTRECK mice 404

Masugi nephritis 488

Matrix metalloproteinase (MMP)

- MMP-2 123, 126, 130, 133, 134
- MMP-9 133

Mature cardiac mast cells 124

Mature mast cell frequency in mouse intestinal tissue 452–453

MC/9 mast cell line 134

MCp. *See* Mast cell progenitors (MCp)

Mcp4 knock out mice 99, 110, 437

Mcpt5-Cre mice 404–409, 411, 418

Measurement of mast cell

- apoptosis 330–332
- surface molecules 381–399

Measurement of nitric oxide (NO) in mast cells

- diaminofluorescein (DAF) 339–345
- flow cytometry 339
- fluorescent indicators 339–345
- half-life 339
- live animal imaging 339
- live cell imaging 339
- nitrate (NO³) 339
- nitrite (NO²) 339
- NO detection limit 340
- NO synthesis 339–341
- western blot 340

Measurement of protease activity in cytosolic extracts 328, 333

Mediator release and cytokine production 165, 171–173

Membrane migration 219, 220

Membrane spreading 220, 227, 230

Metastasis 33, 105, 106, 283

Methylcellulose colony assay

- bone marrow 62, 63
- cord blood 62, 63
- peripheral blood 62, 63

Microarray 106, 185, 293, 382, 383, 386, 388, 389, 392, 394, 397

Microfilaments 220, 224–228

Microtubule nucleation 221

MiRNA in hematopoietic development 289–291

MiRNA profiling 292, 294, 298–299

MMC. *See* Mucosal mast cell (MMC)

MMC proteases (mMCP-1 and -2) 22, 71, 77, 80, 85, 425

MMPs in volume overloaded heart 122

MNC. *See* Mononuclear cell (MNC)

Modulating the tolerance and inflammation balance 461–486

Modulation of cardiac mast cell phenotype

- by estrogen 134–135

Monitoring signaling in mast cells

- by phospho-flow 367–368

Mononuclear cell (MNC) 15, 17, 63, 66, 70, 72–77, 82, 155, 158, 161, 183, 291, 447, 452, 455–458

Morpholino oligonucleotides

- miRNA blocking 55
- splice blocking 55
- translation blocking 55

Mouse mast cell proteases

- mMCP-1 22, 71, 77, 80, 85, 425
- mMCP-4 22, 80, 425, 488, 489, 495
- mMCP-5 22, 80, 425
- mMCP-6 22, 80, 425
- mMCP-7 22, 80, 425

Mouse model

- of allergic asthma 503–518
- of atopic dermatitis

 - clinical scoring for atopic dermatitis
 - mouse model 497–501
 - Der f/SEB-induced dermatitis 499–501
 - NC/Nga (Derm1) mice 498–501
 - OVA epicutaneous sensitization model 498
 - of cancer 444–445
 - of disease 96, 106, 150, 444, 503, 504, 522
 - of polyposis 452

- Mouse T cell isolation 448
- Mucosa 13, 31, 100, 102, 105, 123, 143, 163, 165, 167–168, 174, 445, 455
- Mucosal mast cell (MMC) 69, 79, 80, 94, 143, 144, 215, 404, 425
- Multiple intestinal neoplasia (Min) mouse 444
- Multiple sclerosis 107–108
- experimental autoimmune encephalomyelitis (EAE) 108–110
- Multiplex cytokine bead array 310
- T_H1/T_H2 cytokine profile 310, 317
- Muscarinic cholinergic receptors 142
- Mx-Cre (Mx1-Cre) conditional knockout mouse model 81, 85, 87, 88
- Myocardial infarction 104, 122, 123, 128–129
- Myocardial remodeling 121–136
- Myocytes 125, 131

N

- NAChR expression on mast cells 145
- Nerve fiber 125, 142
- Neuroimmune communication 141
- Neuro-immune functional units 142
- Neuropeptide 22, 125, 142, 146, 148, 150
- Neurotransmitters 101, 141, 142, 146, 147, 150
- Neutralizing antibodies 167, 173, 452
- Neutrophil extracellular traps (NETs) 18
- Nicotinic acetylcholine receptors (nAChR) 144, 145
- Nicotinic receptors 144–146, 150
- Nitric oxide (NO) 8, 142, 147–148, 339–345
- Nitric oxide synthase (NOS)

 - isoforms 340
 - mast cell expression 271
 - NOS2 340

- NK-1 receptor antagonists 127
- L732138 127
- NOD-like receptors (NLR) 180
- NO donor

 - NOR-3 340–342, 344
 - sodium nitroprusside 147

- NO effect on mast cells 170, 292
- Nonyl-acridine orange (NAO) staining 328, 332
- Norepinephrine-induced arrhythmias 133
- NO scavenger 340, 342, 345
- PTIO 340, 342, 345
- Notch

 - mucosal cell fate determination 29, 40, 44
 - notch1b in zebrafish 30
 - Notch2 signaling in mast cell development 79–87

- Novel secretory granule-mediated pathway 325–336
- Nuclear condensation 258

O

- Oligonucleotide barcode

 - amplification 391
 - array 383–386, 389–390

- Opsonins 18
- Organization of microtubules in resting and activated mast cells 230

Ovalbumin (OVA) induced allergic asthma model
 adjuvant (alum) 100, 464, 503–505, 509
 chicken egg albumin (OVA) 505

Oxidative regulation of mast cell PTPs 282

P

Parasites 17, 18, 21, 95–96, 180

Parasympathetic
 nervous system 141–151
 neurotransmitters
 acetylcholine 142
 nitric oxide 142
 vasoactive intestinal peptide (VIP) 142, 146

Pathogenic progress of atopic dermatitis
 acute phase 497
 chronic phase 497

Pattern recognition receptor 17, 18, 180, 184

Paul Ehrlich
 mast cell discovery 6, 7
 Mastzellen 3–8, 107
 Nobel Prize 7
 Westphal 6, 107

Peptidoglycan 94, 184

Percoll gradient
 density gradient 70
 for isolation of mononuclear cells 70

Peripheral blood 6, 62–63, 69, 142, 155–160,
 163, 164, 182, 187, 291, 309, 341, 455, 525
 leukapheresis 155

Peritoneal lavage 367, 372, 405, 406, 414–416, 418, 419

Pharmacological tools to study Ca^{2+} signaling
 dynamics 349–350

Phosphatidylserine (PS) 258, 277, 330

Phosphohistone H3 30

Phospholipase C 206, 366
 phospholipase C-gamma (PLC γ) 348

Phosphoprotein 265, 382

Phosphotyrosine 270, 276, 277

PI(4,5)P₂ (phosphatidyl inositol-4,5-bisphosphate) 366

Piscidins 15, 181

Plasma membrane (PM) 124, 219, 220, 224–228,
 233, 235, 241, 258, 282, 330, 347, 349, 351, 352

Plasma membrane integrity 258

Plasmid linearization 38

Plate reader 52, 312, 343, 348, 352, 490, 494

Pleurocidins 15, 18

Pluripotent hematopoietic cells 155–162

Polyposis 443–445, 452

Preparation of naive CFSE labeled T cells 468

Preparing BMMC donor cultures 471–472

Pre-synthesized mast cell mediators
 β -hexosaminidase 308
 cytoplasmic granules 308
 exocytosis 308
 histamine 308

Pro-apoptotic Bcl-2 family members 258

Progressive kidney disease 109–110

Pro-inflammatory cells 283

Propidium iodide (PI) 243–246, 250, 258,
 259, 261, 325, 328, 330, 331, 409, 410, 517

Pro-survival Bcl-2 family members 258

Protease inhibitors 329, 335–336

Proteases 5, 12, 16, 21, 22, 69, 77, 80, 94–96,
 98, 99, 103–106, 108–110, 122, 135, 146, 164,
 179, 180, 326, 327, 332, 333, 335, 425, 436–437

Protein tyrosine kinase (PTKs) 207

Protein tyrosine phosphatase (PTP) superfamily
 PTP-deficient mast cell phenotypes 272
 PTP α -null mice 275

PTP expression in mast cells
 PTP α 274–276, 282
 PTP ϵ 274–276, 282

receptor-like PTPs in mast cells
 CD45 (*Ptprc*) 271

SH2-domain-containing intracellular PTPs in mast cells
 Fc ϵ R1 signaling and responses 277–279
 motheaten phenotype 276–277
 SHP-1 276–277
 SHP-2 276–280

Pruritic inflammatory skin disease 497

Pulmonary function 504, 522

Purification of rat glomeruli for immunization
 of rabbits 489

R

Rabaptin-5 240

Rab family of small GTPases 240

RabGEF1 240

RasGRP4-deficient mice 426

Rat basophilic leukemia (RBL)-2H3 cell line 219

Rat hearts, mast cell enumeration 125, 126, 135

Rat mast cell protease II (RMCP II) 143, 144

Real-time imaging of Ca^{2+}
 acridine orange 351
 Ca^{2+} red asanate 352
 FITC-dextran loading 352
 Fura-Red 352, 358
 GECI plasmids 352, 354
 red-shifted GECO (R-GECO) 358

Regulation of mast cell granule exocytosis 351

Release of anti-inflammatory mediators 461

Renal function 487, 492

Renal injury 487, 488

Resting mast cell Ca^{2+} concentration 347

Retroviral transduction
 of BMMCs 210–213, 215–216

Retrovirus-mediated gene transfer into myeloid progenitors
 Gata3 84
 Hes1 84
 human NGFR 84

RNA-induced silencing complex (RiSC) 288

RNA probe preparation 38–39

RNA purification 391

Role of mast cells in K/BxN serum transfer
 arthritis 429, 438

S

Sarcoplasmic reticulum (SR)
 sacro-endoplasmic reticulum Ca^{2+} -ATPase
 (SERCA) 349

SCF. *See* Stem cell factor (SCF)

Secretagogue 14, 17, 24, 122–127, 135, 136

Selection of transgene-expressing cells 210–213

Separation of lineage-negative cells and myeloid progenitors
 anti-lineage marker (Lin) antibodies 82
 common myeloid progenitors (CMPs) 83
 granulocyte-macrophage progenitors (GMPs) 83

Serglycin proteoglycan 69, 326, 331

Serine/threonine kinases 206, 213, 270

Serosal mast cell 60, 145

Serotonin receptors 149

Signaling networks in mast cells 206

Simulation of intestinal mast cells 80, 166–167

Single cell sorting and PCR
 from peritoneal lavage 414–415
 from skin 415–416

Skin lesion infiltrates 497

Skin transplantation model
 adoptive transfer of BMMCs 464
 bone marrow mast cell derivation and culture 464
 degranulation of mast cells *in vivo* 464
 donor skin harvest 462
 donor splenocyte transfusion (DST) 462, 468
 induction of inflammation 464–465
 skin grafting 462–463
 surgery 469–470
 tolerance induction 468–469

Soluble NSF attachment protein receptors (SNAREs)
 N-ethyl-maleimide-sensitive factor (NSF) 351

Source of cardiac mast cells 126–128

Species heterogeneity of mast cells 340, 382

Sputum processing 62, 64

Src family kinases (SFK) 280

Staining vesicle associated membrane protein
 (VAMP)-3 after SLO-treatment 173

Stem cell factor (SCF). *See* Transforming growth factor-beta 1 (TGF β 1)

74, 78, 81, 83–85, 93, 103–105, 107, 122, 127, 128, 133, 135, 162, 164, 166, 168, 170, 171, 174, 175, 183, 184, 188–191, 206, 207, 211–213, 215, 216, 221, 222, 225, 233, 257, 259, 269, 270, 272–274, 276, 277, 282, 322, 340, 344, 372, 373, 429, 446, 457, 459, 463, 472

Stimulation-induced internalization of Fc ϵ R1-bound IgE 243–244

Store-operated Ca^{2+} entry (SOCE) 348

SOCE inhibitors
 2-APB 350
 lanthanides 350
 nickel 350

Strongyloides venezuelensis 80, 86

Studies on T cells after mast cell degranulation 476–478

Studying mast cells in peripheral tolerance
 adoptive transfer of tolerance 478–479, 482
 FoxP3 $^{+}$ regulatory T-cells (T_{reg}) 461
 inflammatory and immune-suppressive responses 461
 regulation of T cell functionality 476

Substance P 15, 100, 125, 127, 136, 148, 150, 322

Super oxide dismutase mimetic 126
 M40403 126

Syk 206, 222, 270, 272, 275, 277–280, 366

Sympathectomy 127

Synaptotagmins 351

Synovial lining 109, 423

Synovial mast cells 423–441

Synovial tissue staining
 anti-aggreccan polyclonal antibody 433
 chloroacetate esterase (CAE) staining 435
 proteoglycan staining 433, 434
 toluidine blue 433–434

Synovium 423–425

Systemic sensitization 508

T

Tachykinins 148

Tamoxifen inducible mouse gene 108

Targeting miRNA with antagonists 294, 299–300

T cell and mast cell interactions
 T cell receptor 219
 T helper type 1 (TH_1) cells 497
 T helper type 2 (TH_2) cells 497

TGF β 1. *See* Transforming growth factor-beta 1 (TGF β 1)

$\text{T}_{\text{H}1}$ -dependent effector mechanisms 488

$\text{T}_{\text{H}2}$ inflammation 504

Thymic stromal lymphoprotein (TSLP) 59

Tissue culture 62, 71, 74, 156, 169, 190, 212, 221, 225, 245, 247–249, 343, 353, 463, 483, 507, 513, 514

Tissue harvest and preparation
 frozen sections 432
 histological stains 428
 immunohistological staining 428–429

Tissue remodeling 5, 60, 134, 164, 180

TNF α . *See* Tumor necrosis factor alpha (TNF α)

Toll-like receptors (TLR) 8, 12, 14, 18, 59, 94, 180, 194, 291, 475

Toluidine blue staining 44, 48, 159, 434, 450–452, 492

Total internal reflection fluorescence microscopy
 (TIRFM) 231–235
 TIRFM time-lapse imaging in living cells 234

Toxic shock 143

Transcriptional regulation 60

Transcription factors 30, 206, 290, 291, 382
 gata2, pu.1 in zebrafish 30

Transfection of LAD2 cells 370

Transforming growth factor-beta 1 (TGF β 1) 80, 81,
 85, 109, 124, 292

Transgenesis
 bacterial artificial chromosome (BAC) 32

 to generate mast cell reporter line 32

Transient receptor potential channels (TRPC)
 Ca $^{2+}$ dynamics and temperature 360

 optimization of Ca $^{2+}$ loading 360

 optimization of cell density in single
 cell imaging 361

Treg suppressor assay 468, 482

Tri-nitrophenyl (TNP) and di-nitrophenyl
(DNP) 54, 222, 223

Tryptase
 activation of
 proMMP3 134

protease-activated receptor 2 (PAR-2) 134

mMCP1 95, 96

 substrate 56

Tryptase positive mast cells (MCT) 94, 102, 104,
 106, 109, 123, 164, 182, 425

TS4CreER x Ctnb $^{llox(ex3)}$ mice 445
 liver specific fatty acid binding gene promoter
 (*TS4*) 445

Tubulin
 $\alpha\beta$ -tubulin microtubules 220, 232

γ -tubulin 221, 222, 230, 232, 235

Tumor epithelium
 assay for intraepithelial mast cells 445, 447

 tumor growth 5, 60, 106

 tumor invasion 444, 447
 tumor microenvironment 106, 443, 444

Tumor necrosis factor alpha (TNF α) 19, 94, 96,
 97, 100, 106, 109, 110, 122, 124, 125, 131, 132,
 134, 135, 272, 273, 278–280, 291, 310

Types of mast cells for NO analysis
 HMC-1 cell line 183, 341, 382, 390, 394, 395

LAD2 cell line 341

 primary BMMCs 294

 primary human cord blood and peripheral blood-derived
 MCs 341

 rat peritoneal mast cells 147, 220, 281, 341, 344

Tyrosine kinases 105, 269–271, 275, 277–280, 366

Tyrosine-specific PTPs in mast cells 270, 276, 280–281

U

Ubiquitination 241, 242

V

Vagal stimulation 143, 144, 146, 148

Vagus nerve 142–146

Vasoactive intestinal peptide (VIP) receptors 146
 VPAC1 and *VPAC2* 146

Ventricular dilatation 123, 126, 128, 130,
 131, 134, 135

Viability dye
 7-AAD 83, 84, 86

propidium iodide 243

trypan blue 64, 73, 161

Viruses 18, 94, 97–98,
 179–196, 210

Virus infection of mast cells 189–191

Visualization of microfilaments
 electron microscopy 225–228

 immunofluorescence microscopy 229–231

 interactions with the plasma
 membrane 224–228

 visualization of microfilaments 224–228

Visualizing and quantifying Ca $^{2+}$
 oscillations 357

 puffs and waves 350

W

Western blot
 Bradford protein assay 328

 Western blot analysis 259, 329, 334–336

Whole mount RNA in situ hybridization (WISH)
 in zebrafish
 carboxypeptidase a5 (cpa5) 44

co-localization (double WISH) 42–43

mast cell specific marker in zebrafish 44

Wistar kyoto rats 124

X

Xenotransplantation 32, 33

Z

Zebrafish embryos
 dechorionation 37

dissociation buffer 35

egg water 34

fixation 37–38